THE DYNAMICS OF GENERIC KUPERBERG FLOWS

STEVEN HURDER AND ANA RECHTMAN

Abstract. In this work, we study the dynamical properties of Krystyna Kuperberg's aperiodic flows on 3-manifolds. We introduce the notion of a "zippered lamination", and with suitable generic hypotheses, show that the unique minimal set for such a flow is an invariant zippered lamination. We obtain a precise description of the topology and dynamical properties of the minimal set, including the presence of non-zero entropy-type invariants and chaotic behavior. Moreover, we show that the minimal set does not have stable shape, yet satisfies the Mittag-Leffler condition for homology groups.

2010 *Mathematics Subject Classification.* Primary 57R30, 37C55, 37B45; Secondary .
Preprint date: June 19, 2013; Revised October 14, 2015; minor edits February 22, 2016.
AR supported in part by CONACyT Postdoctoral Research Fellowship.

Contents

List of Figures

1. Introduction

The "Seifert Conjecture", as originally formulated in 1950 by Seifert in [44], asked: "Does every non-singular vector field on the 3-sphere $\mathbb{S}^3$ have a periodic orbit?" The partial answers to this question have a long history. F.W. Wilson constructed in the 1966 work [50] a smooth flow on a *plug* with exactly two periodic orbits, which was used to modify a given flow on a 3-manifold to obtain one with only isolated periodic orbits. Paul Schweitzer showed in the 1974 work [43], that for any closed 3-manifold M, there exists a non-singular C^1-vector field on M without periodic orbits. Schweitzer's result suggested a modified version of Seifert's question: "Does every non-vanishing C^∞ vector field on a closed 3-manifold have a periodic orbit?" Krystyna Kuperberg showed in her celebrated 1994 work [26], that the smooth Seifert Conjecture is also false by inventing a construction of aperiodic plugs which is renowned for its simplicity, beauty and subtlety.

THEOREM 1.1 (K. Kuperberg)**.** *On every closed oriented 3-manifold M, there exists a C^∞ non-vanishing vector field without periodic orbits.*

The goal of this work is to understand the dynamical properties of such "Kuperberg flows", especially the structure of their minimal sets. In the exploration of these properties, we reveal their beauty and discover the hidden complexity of the Kuperberg dynamical systems.

Let us recall the strategy of the proofs of the results cited above. A *plug* is a compact 3-manifold with boundary in $\mathbb{R}^3$, equipped with a flow satisfying additional conditions. The flow in a plug is assumed to be parallel to the "vertical" part of the boundary, so that it may be inserted in any coordinate chart of a 3-manifold M to modify the given flow on M, and changes only those orbits entering and leaving the "horizontal" faces of the plug. Another assumption on the flow in a plug is that there are orbits, which are said to be *trapped*, which enter the plug and never exit. The closure of such an orbit limits to a compact invariant set contained entirely within the interior of the plug, thus the plug must contain at least one minimal set. In the case of the Wilson Plug, the two periodic orbits are the minimal sets.

A plug is said to be *aperiodic* if it contains no closed orbits. Schweitzer observed in [43] that the role of the periodic orbits in a Wilson Plug could be replaced by Denjoy minimal sets, resulting in an aperiodic plug, which could then be used to "open up" the isolated closed orbits provided by Wilson's result. The flow in the Schweitzer Plug is only C^1, due to the topology of the minimal set contained in the plug, around which all trapped orbits for the flow must accumulate. Harrison constructed in [19] a modified "non-flat" embedding of the Denjoy continuum into a 3-ball, which she used to construct an aperiodic plug with a C^2-flow. In contrast, Handel showed in [18] that if the trapped orbits of a plug accumulate on a minimal set whose topological dimension is one and is the only *invariant* set for the flow in the plug, then the minimal set is *surface-like*: the flow restricted to the minimal set is topologically conjugated to the minimal set of a flow on a surface.

Kuperberg's construction in [26] of aperiodic smooth flows on plugs introduced a fundamental new idea, that of "geometric surgery" on a modified version of the Wilson Plug $\mathbb{W}$, to obtain the *Kuperberg Plug* $\mathbb{K}$ as a quotient space, $\tau\colon \mathbb{W} \to \mathbb{K}$. The Wilson vector field $\mathcal{W}$ on $\mathbb{W}$ is modified to provide a smooth vector field $\mathcal{K}$ on the quotient. The flow of $\mathcal{K}$ is denoted by Φ_t. This is said to be a *Kuperberg flow* on $\mathbb{K}$.

The periodic orbits for the Wilson flow on $\mathbb{W}$ get "cut-open" when they are mapped to $\mathbb{K}$, and there they become trapped orbits for Φ_t. The essence of the novel strategy behind the aperiodic property of Φ_t is perhaps best described by a quote from the paper by Matsumoto [33]:

> We therefore must demolish the two closed orbits in the Wilson Plug beforehand. But producing a new plug will take us back to the starting line. The idea of Kuperberg is to *let closed orbits demolish themselves*. We set up a trap within enemy lines and watch them settle their dispute while we take no active part.

The images in $\mathbb{K}$ of the cut-open periodic orbits from the Wilson flow Ψ_t on $\mathbb{W}$, generate two orbits for the Kuperberg flow Φ_t on $\mathbb{K}$, which are called the *special orbits* for Φ_t. These two special orbits play an absolutely central role in the study of the dynamics of a Kuperberg flow.

There followed after Kuperberg's seminal work, a collection of three works explaining in further detail the proof of the aperiodicity for the Kuperberg flow, and investigating its dynamical properties:

- the Séminaire Bourbaki lecture [17] by Étienne Ghys;
- the notes by Shigenori Matsumoto [33] in Japanese, later translated into English;
- the joint paper [27] by Greg Kuperberg and Krystyna Kuperberg.

It was observed in these works that the special orbits in $\mathbb{K}$ each limit to the other, and that a Kuperberg flow has a unique minimal set, which we denote by Σ. The topological and dynamical properties of the minimal sets for the Wilson, Schweitzer and Harrison Plugs are fundamental aspects of the constructions of the flows in these plugs. For the Kuperberg flow, the minimal set Σ is not specified by the construction, but rather its topological properties are a consequence of the strong interaction of the special orbits. We will see that with the proper geometric assumptions in the construction of $\mathbb{K}$, we are able to obtain a detailed understanding of the topological and dynamical properties of the minimal set Σ as a result.

The *Radius Inequality*, stated as hypothesis (K8) in Section 3, is a topological property of the insertion maps used to construct the quotient space $\mathbb{K}$ from the Wilson Plug $\mathbb{W}$. It is an absolutely remarkable aspect of Kuperberg's construction, that the Radius Inequality is essentially all that is required to show that the quotient flow Φ_t is aperiodic. Moreover, the smooth insertion maps which satisfy hypothesis (K8) admit many variations in their local behavior near the special orbits for the Wilson flow, with each choice yielding an aperiodic "Kuperberg flow".

In order to describe the *generic hypotheses* that we introduce, we require some notions which are described more precisely in Sections 2, 3 and 4. The *modified Wilson Plug* $\mathbb{W}$, as defined in Section 2, contains a cylinder set $\mathcal{R} \subset \mathbb{W}$ which is invariant under the Wilson flow Ψ_t on $\mathbb{W}$, and the boundary of $\mathcal{R}$ consists of the periodic orbits for the flow. There is a "notched" subset $\mathcal{R}' \subset \mathcal{R}$, illustrated in Figure 18, which maps to a closed subset $\tau(\mathcal{R}') \subset \mathbb{K}$ by the quotient map $\tau \colon \mathbb{W} \to \mathbb{K}$, as illustrated in Figure 24. The Φ_t-flow of $\tau(\mathcal{R}')$ is a non-compact, embedded surface, $\mathfrak{M}_0 \subset \mathbb{K}$, with boundary consisting of the special orbits in $\mathbb{K}$. Thus, the closure $\mathfrak{M} = \overline{\mathfrak{M}_0}$ is a flow invariant, compact connected subset of $\mathbb{K}$, which contains the closure of the special orbits, hence as observed in [17, 27, 33], the minimal set $\Sigma \subset \mathfrak{M}$. The existence of this compact subset $\mathfrak{M}$ which is invariant for the Kuperberg flow Φ_t is a remarkable consequence of the construction, and is the key to a deeper understanding of the dynamical properties of the flow Φ_t.

This work introduces several new concepts and techniques which are used in the study of the space $\mathfrak{M}_0$ and its closure $\mathfrak{M}$. The first is the notion of *propellers*, which are surfaces with boundary, possibly minus a point at infinity, embedded in $\mathbb{W}$ so that they wrap around the core cylinder $\mathcal{R}$ in the Wilson Plug $\mathbb{W}$, as illustrated in Figure 19. The projections of these surfaces to $\mathbb{K}$ are assembled according to the dynamics of the Kuperberg flow, to yield the embedded surface $\mathfrak{M}_0$ as partially illustrated in Figure 28.

The study of the topological structure of $\mathfrak{M}_0$ reveals the fundamental role played by the local dynamics of the flow Φ_t in a small open neighborhood of the core cylinder $\tau(\mathcal{R}') \subset \mathbb{K}$, and especially in sufficiently small open ϵ-neighborhoods of the special orbits along the boundary of $\tau(\mathcal{R}')$. In fact, we show in Proposition 9.16 that the return times of a Kuperberg flow to these ϵ-neighborhoods form a syndetic set, so that the global dynamics of Φ_t is essentially determined by its local dynamics in ϵ-neighborhoods of $\tau(\mathcal{R}')$. The local dynamics of Φ_t depend on the choices made constructing the Wilson vector field $\mathcal{W}$ on $\mathbb{W}$ and the Kuperberg vector field $\mathcal{K}$ on $\mathbb{K}$. We formulate generic conditions on the choice of $\mathcal{W}$ and the construction of $\mathcal{K}$, in order to eliminate pathologies in the dynamics of the flows for $\mathcal{W}$ and $\mathcal{K}$ that may otherwise be possible.

The first type of generic condition is given by Hypothesis 12.2. In brief, this states that the vertical component of the Wilson vector field $\mathcal{W}$ has quadratic vanishing along the periodic orbits. The anti-symmetry imposed on the modified Wilson vector field $\mathcal{W}$ forces the generic case to be a quadratic vanishing condition.

The second type of generic condition is imposed on the insertion maps σ_i for $i = 1, 2$ which are introduced in Section 3 as part of the construction of the space $\mathbb{K}$. These maps are required to satisfy the Radius Inequality, in order to obtain an aperiodic flow on $\mathbb{K}$, but the smooth properties of these maps also control many other aspects of the global dynamics of Φ_t. For example, the propellers associated to the flow Φ_t which form $\mathfrak{M}_0$ are

generated by the images of curves under the embedding maps σ_i and their inverses, and without assumptions on the geometries of these curves, it seems impossible to control the geometry of the space $\mathfrak{M}_0$. The precise statements of the "generic hypotheses" we impose requires various preliminary notations, and are formally given in Definition 17.3. In brief, they assert that the insertion maps σ_i are "uniformly quadratic" in an open neighborhood of each periodic orbit.

We say that a Kuperberg flow Φ_t is *generic* if it satisfies the conditions of Definition 17.3, which includes the quadratic hypotheses on the Wilson flow in Hypothesis 12.2. The goal of this work is then to make a complete investigation of the dynamical properties of *generic Kuperberg flows*.

We next discuss the results of this work. First, two natural problems concerning the topological dynamics of the flow Φ_t are to identify its wandering set $\mathfrak{W}$ and its non-wandering set Ω, which are defined in Section 8. The minimal set Σ is always contained in the non-wandering set, and we show in Theorem 16.1 that:

THEOREM 1.2. *Let Φ_t be a Kuperberg flow of $\mathbb{K}$ which satisfies Hypothesis 12.2. Then the non-wandering set Ω is a subset of the closure $\mathfrak{M}$ of the embedded manifold $\mathfrak{M}_0$, and thus the complement of $\mathfrak{M}$ consists of wandering points for the flow.*

With the additional hypothesis that the flow is generic, then Theorem 17.1 shows that the minimal set Σ equals the non-wandering set Ω, and we have:

THEOREM 1.3. *Let Φ_t be a generic Kuperberg flow of $\mathbb{K}$, then $\Sigma = \Omega = \mathfrak{M}$.*

The papers [17] and [27] gave examples where the minimal set Σ equals the space $\mathfrak{M}$, and suggested that the inclusion $\Sigma \subset \mathfrak{M}$ may be an equality in more generality than the examples they gave. The proof of Theorem 1.3 is inspired by the examples and related remarks in these works.

It was remarked above that the topological properties of the minimal set Σ are a consequence of the "strong interaction" of the special orbits. The identification $\Sigma = \mathfrak{M}$ for a generic flow Φ_t allows to make this remark precise, using the structure theory for the space $\mathfrak{M}$ that we develop in this work. In fact, a notable aspect of this work is the precise description of $\mathfrak{M}$ that is developed, which is possibly the first detailed description of an exceptional minimal set of topological dimension 2 for a flow.

Consider the submanifold $\mathfrak{M}_0 \subset \mathbb{K}$ as a stratified space, with the interior being a stratum of topological dimension 2, and the boundary curves (the *special orbits*) being a stratum of topological dimension 1. Thus, the closure $\mathfrak{M}$ of $\mathfrak{M}_0$ inherits a type of stratified structure, where the 2-dimensional stratum of $\mathfrak{M}$ are the leaves of a laminated structure on a subset of $\mathfrak{M}$, obtained from the closure in $\mathbb{K}$ of the interior of $\mathfrak{M}_0$. The 1-dimensional stratum of $\mathfrak{M}$ can be described as the boundaries of the "leaves" of the "lamination" $\mathfrak{M}$. Difficulties arise from this description though, as the special orbits for Φ_t are the two boundary components of the manifold $\mathfrak{M}_0$, which are dense in $\mathfrak{M}$ for a generic flow. That is, the 1-stratum of $\mathfrak{M}$ is dense in the 2-stratum, which is not a normal property for a lamination.

In fact, we show in Theorem 19.1 that for a generic Kuperberg flow, the space $\mathfrak{M}$ has a stronger property than these informal observations, in that it satisfies the conditions in Definition 19.3 which gives it a local product structure, which is analogous to that of a lamination. We call this type of structure a *zippered lamination*, as it is "sewn together" along the special boundary orbits.

THEOREM 1.4. *For a generic Kuperberg flow, the space $\mathfrak{M}$ has the structure of a zippered lamination with 2-dimensional leaves.*

The basis of many of our results concerning $\mathfrak{M}$, including the proof of Theorem 1.4 above, is a detailed structure theory for $\mathfrak{M}_0$ based on the properties of *finite* or *infinite*, *simple* or *double propellers*, arising from either *boundary* or *interior notches* in $\mathfrak{M}_0$. The amazing complexity of these aspects of the embedding of $\mathfrak{M}_0$ in $\mathbb{K}$ are organized using the level function on $\mathfrak{M}_0$, which is introduced in this work.

The notion of the *relative level* of two points along the same orbit of the Kuperberg flow was introduced by Kuperberg in [26], and is a key technique for showing that the flow obtained is aperiodic. It is defined by

equations (12) and (13) in Section 4 below. Further properties of the concept of relative level were developed by Ghys and Matsumoto in [17, 33]. In Section 12, we show that the relative level function along orbits induces a well-defined level function on $\mathfrak{M}_0$, for which the Reeb cylinder $\tau(\mathcal{R}')$ is at level 0. The level function on $\mathfrak{M}_0$ is used to decompose this space into an infinite union of propellers $\mathfrak{M}_\ell$ for $\ell \geq 1$, where $\mathfrak{M}_\ell$ consists of sets at level ℓ: for $\ell = 1$ this set is composed by two non-compact propellers attached to $\tau(\mathcal{R}')$, while $\mathfrak{M}_\ell$ for $\ell \geq 2$ is formed by 2^ℓ families of compact propellers. The level decomposition of $\mathfrak{M}_0$ is used to analyze its geometry and dynamics, and consequently also that of $\mathfrak{M}$.

One of the original motivations for this work was a question posed by Krystyna Kuperberg concerning the *topological shape* of the minimal set Σ for the flow Φ_t. Section 23 gives a very brief introduction to shape theory, including the definitions of "stable shape" in Definition 23.3 and for a continua to be "movable" in Definition 23.5. It is a simple observation that the subspaces $\mathfrak{M}$ and its dense subset $\mathfrak{M}_0$ have the same topological shape, and thus for a generic flow, we can use the level decomposition of $\mathfrak{M}_0$ to study the shape properties of the minimal set Σ. As a cumulation of the results in this work, we show in Section 23 the following results:

THEOREM 1.5. *For a generic Kuperberg flow, the minimal set Σ does not have stable shape.*

The Mittag-Leffler condition for homology groups, as introduced in Proposition 23.6, is a homology version of the movable condition. Proposition 23.7 yields the following consequence:

THEOREM 1.6. *For a generic Kuperberg flow, the minimal set Σ satisfies the Mittag-Leffler condition for homology groups.*

Theorems 1.5 and 1.6 follow from three fundamental properties of the minimal set Σ. First, that for the generic Kuperberg flow, the minimal set Σ equals $\mathfrak{M}$, which is the closure of the non-compact, embedded surface $\mathfrak{M}_0$ obtained from the flow of the Reeb cylinder $\tau(\mathcal{R}') \subset \mathbb{K}$. Second, that the topology of a sufficiently fine open neighborhood approximation $\mathfrak{M} \subset U_k$ – as occurs in a shape approximation of $\mathfrak{M}$ – has increasing topological complexity as the index k tends to infinity. Third, for any finite time, the trace of the flow of the cylinder $\tau(\mathcal{R}')$ retracts to the cylinder $\tau(\mathcal{R}')$, which implies that for k sufficiently large, the topological complexity of the approximating spaces U_k are contained in an arbitrarily small open neighborhood of a space $\mathfrak{M}_0^1$ introduced here, from which the Mittag-Leffler condition is shown to follow.

Thus, our study of the shape properties of Σ uses and combines almost all of the results of this paper. The details of these arguments are often quite subtle and tedious, and begin with the construction in Section 23 of a decreasing nested sequence of compact domains $\mathfrak{N}_\ell \subset \mathbb{K}$ for $\ell \geq 0$, such that each $\mathfrak{N}_\ell$ satisfies $\mathfrak{M} \subset \mathfrak{N}_\ell$ and has the homotopy type of a finite CW-complex. The spaces $\mathfrak{N}_\ell$ are constructed using the level function on $\mathfrak{M}_0$ and the observation in Section 13 that the double propellers introduced there are nested. That is, the double propellers at level $\ell + 1$ are contained in the closures of the interiors of double propellers at level ℓ. We show that the first homology groups of the spaces $\mathfrak{N}_\ell$ have ranks which grow without bound with ℓ, and yet for an appropriate choice of a subsequence of these spaces, the ranks of the maps induced on homology from the bonding maps have constant rank 3. We use this to conclude that the shape of Σ is not stable, but does satisfy the Mittag-Leffler condition.

Our final collection of results concern the entropy invariants and dynamical complexity of a Kuperberg flow Φ_t. The topological entropy of a Kuperberg flow is zero, for as noted by Ghys in [17], this follows as a consequence of a result of Katok on C^2-flows on 3-manifolds in [23], which implies that the entropy of an aperiodic smooth flow on a 3-manifold must be zero. Katok's proof in [23] uses the *Pesin Theory* for smooth flows, for example as given in [1], to conclude from $h_{top}(\Phi_t) > 0$ that Φ_t must have a periodic orbit.

Note that Theorem 1.2 above shows that the non-wandering set of Φ_t is contained in $\mathfrak{M}$, and hence the flow entropy $h_{top}(\Phi_t) = h_{top}(\Phi_t|\mathfrak{M})$, where the latter is the entropy for the flow restricted to $\mathfrak{M}$. This naturally suggests the question, whether some geometric property of $\mathfrak{M}$ may directly imply that $h_{top}(\Phi_t|\mathfrak{M}) = 0$?

It is a standard technique for the study of the dynamics of flows, to choose a section to the flow and study the dynamics of the induced return maps. There is a natural choice of "section" for the Kuperberg flow Φ_t,

given by the rectangle $\mathbf{R}_0 \subset \mathbb{K}$ defined by (25) in Section 9. There is a well-defined "return map" $\widehat{\Phi}$ to $\mathbf{R}_0$ for the flow Φ_t. However, the vector field $\mathcal{K}$ is tangent to $\mathbf{R}_0$ along the center horizontal line, which complicates the study of the dynamics for $\widehat{\Phi}$. For this reason, we introduce in Section 9 the pseudogroup $\mathcal{G}_K$ generated by the return map $\widehat{\Phi}$ restricted to open subsets of $\mathbf{R}_0$ on which the map is continuous.

We show in Section 9 that the global dynamics of the Kuperberg flow is determined by the actions of the generators for $\mathcal{G}_K$. In particular, the compact set $\mathfrak{M}_{\mathbf{R}_0} = \mathfrak{M} \cap \mathbf{R}_0$ is locally invariant under the return map $\widehat{\Phi}$, and so is invariant under the local actions of elements of $\mathcal{G}_K$. The space $\mathfrak{M}_{\mathbf{R}_0}$ is the closure of the set $\mathfrak{M}_0 \cap \mathbf{R}_0$, and it turns out that for the collection of special generating maps $\mathcal{G}_K^{(1)} \subset \mathcal{G}_K$ as defined in (146), the action of these generators on $\mathfrak{M}_0 \cap \mathbf{R}_0$ has a systematic description in terms of the level decomposition for the propellers in $\mathfrak{M}_0$. This is discussed in Section 13.

Even more is true. The action of the set $\mathcal{G}_K^{(1)}$ on the space $\mathfrak{M}_0 \cap \mathbf{R}_0$ has a description in terms of a Cayley graph for the pseudogroup, as described in Section 14. Choosing a Riemannian metric on the Kuperberg plug, induces a metric on $\mathfrak{M}_0$ for which this space is quasi-isometric to a tree $\mathbf{T}_\Phi$ with valence at most 4. The notation system for the level decomposition of $\mathfrak{M}_0$ also labels the vertices of the embedded tree $\mathbf{T}_\Phi \subset \mathfrak{M}_0$. The properties of the tree model for the dynamics of $\mathcal{G}_K$ are discussed further in Sections 14 and 22.

Section 20 introduces the entropy associated to a *finite symmetric set of generators* for a pseudogroup, following the ideas introduced by Ghys, Langevin and Walczak in [16]. To obtain entropy invariants of Φ_t, it is necessary to choose a finite symmetric generating set in $\mathcal{G}_K$. We work with two such choices:

- The collection $\mathcal{G}_{\widehat{\Phi}}^{(1)}$ defined in (135), with associated entropy $h_{GLW}(\mathcal{G}_{\widehat{\Phi}}^{*}|\mathfrak{M}_{\mathbf{R}_0})$.
- The collection $\mathcal{G}_K^{(1)}$ defined in (146), with associated entropy $h_{GLW}(\mathcal{G}_K^{*}|\mathfrak{M}_{\mathbf{R}_0})$.

The results in Section 20 yield the implications:

$$h_{top}(\Phi_t|\mathfrak{M}) > 0 \implies h_{GLW}(\mathcal{G}_{\widehat{\Phi}}^{*}|\mathfrak{M}_{\mathbf{R}_0}) > 0 \implies h_{GLW}(\mathcal{G}_K^{*}|\mathfrak{M}_{\mathbf{R}_0}) > 0 \ . \tag{1}$$

The structure theory of $\mathfrak{M}_0$ and the subexponential growth estimate Corollary 14.6, are used in the proof of Theorem 20.14 to show that $h_{GLW}(\mathcal{G}_K^{*}|\mathfrak{M}_{\mathbf{R}_0}) = 0$. We thus conclude:

THEOREM 1.7. *Let Φ_t be a generic Kuperberg flow, then $h_{top}(\Phi_t|\mathfrak{M}) = 0$.*

One of the intriguing aspects of the dynamics of the $\mathcal{G}_K$-action associated to a Kuperberg flow, is the presence of families of "horseshoe-like" structures, as illustrated in Figure 46, which show that the Φ_t-orbits have a form of chaotic behavior. However, the rate of contraction for the return maps of the flow Φ_t near the special orbits is "too slow" for this chaotic behavior to yield positive entropy, as is seen in the calculations we make in Section 20 for the proof of Theorem 1.7. We say that the flow Φ_t has "slow chaos" near $\mathfrak{M}$.

We show in the work [21], that by varying the embeddings σ_i for $i = 1, 2$ so they no longer satisfy the *Radius Inequality*, then the "slow chaos" for the Kuperberg flow, becomes "rapid chaos" associated with a hyperbolic attractor for the perturbed flow. These observations imply that the construction of the Kuperberg flow Φ_t places it at "the boundary of hyperbolicity", in the manner of partially hyperbolic systems [2].

Another pseudogroup model for the dynamics of Φ_t is introduced in Section 21, which is the pseudogroup $\mathcal{G}_{\mathfrak{M}}$ acting on the *simple curves* in $\mathfrak{M}_{\mathbf{R}_0}$. This action on curves induces an action on a Cantor set $\mathfrak{C} \subset \mathfrak{M}_{\mathbf{R}_0}$ which is transverse to the leaves of the lamination $\mathfrak{M}$. The action of $\mathcal{G}_{\mathfrak{M}}$ on $\mathfrak{C}$ can be thought of as the "essential model" for the chaotic behavior on the flow Φ_t.

The "slow chaos" property of Φ_t is quantified by introducing the *slow lamination entropy* for $\mathcal{G}_{\mathfrak{M}}$, denoted by $h_{GLW}^{\alpha}(\mathcal{G}_{\mathfrak{M}})$ for $0 < \alpha < 1$. This invariant for a pseudogroup action, is the analog of the *slow flow entropy* introduced in the works of Katok and Thouvenot [24] and Cheng and Li [8]. Our main result in this section is Theorem 21.10, which relates the growth of orbits for the pseudogroup with the dynamics of the insertion maps used in the construction of $\mathbb{K}$.

THEOREM 1.8. *Let Φ_t be a generic Kuperberg flow. If the insertion maps σ_j have "slow growth" in the sense of Definition 21.11, then $h_{GLW}^{1/2}(\mathcal{G}_{\mathfrak{M}}) > 0$.*

REMARK 1.9. Let Φ_t be a generic Kuperberg flow satisfying Definition 21.11. The works [10, 11] suggests that $h^{1/2}_{GLW}(\mathcal{G}_{\mathfrak{M}}) > 0$ implies the Cantor set $\mathfrak{C}$ has Hausdorff dimension at least $1/2$.

One of the conclusions of the calculations in Sections 20 and 21 of the entropy for the pseudogroups associated to Φ_t, is that the quadratic vanishing of the vertical component of the Wilson vector field, as specified in Hypothesis 12.2, is a key to showing that $h_{top}(\Phi_t|\mathfrak{M}) = 0$. Remark 1.9 is a speculation that it may be possible to show a more direct relationship between the rate of vanishing for the Wilson field $\mathcal{W}$ along its periodic orbits and the Hausdorff dimension of the closure $\mathfrak{M}$ of $\mathfrak{M}_0$.

If the Kuperberg vector field $\mathcal{K}$ is constructed using a *piecewise smooth* Wilson vector field, with hyperbolic contracting singularities along its periodic orbits, then Theorem 21.18 states that $h_{GLW}(\mathcal{G}^*_{\mathfrak{M}}) > 0$, as a consequence of the preceding calculations, suitably adapted. Question 21.19 then poses the problem of showing that $h_{top}(\Phi_t|\mathfrak{M}) > 0$ for such flows.

It was remarked in [17, 26] that Kuperberg Plugs can also be constructed for which the manifold $\mathbb{K}$ and its flow $\mathcal{K}$ are real analytic. Details of this construction are given in the Ph.D. Thesis [41] of the second author. The authors expect that for real analytic flows, many of the results of this work remain valid without the generic hypotheses in Definition 17.3.

In general, there are many further questions about the dynamics of flows formed by a "Kuperberg surgery", which is the colloquial name for the construction described in Section 3.

To conclude this introduction to our work, we explain how the paper is organized, and at the same time we summarize the properties of the dynamics of a Kuperberg Plug, making the distinction between the results which were known for a general Kuperberg flow, and those results obtained in this work.

Of course, the fundamental result is Kuperberg's theorem, which is Theorem 1.1 above: For any choice of modified Wilson flow on $\mathbb{W}$ as constructed in Section 2, and any pair of insertion maps σ_i which satisfy the Radius Inequality from Section 3, the Kuperberg flow Φ_t constructed on $\mathbb{K}$ is aperiodic. Sections 2 to 8 give a self-contained and very detailed proof of this result, which is based on a synthesis of the results of the papers [26], [17] and [33].

The papers by Ghys [17] and Matsumoto [33] include further results on the dynamics of the Kuperberg flow Φ_t. In particular, they show that it has a unique minimal set Σ contained in the interior of $\mathbb{K}$. Also, Matsumoto showed that the Kuperberg Plug traps a set with non-empty interior. These results are also discussed and proved in Sections 2 to 8 of this work, which also establish notations and fundamental techniques required for the remaining parts of the work.

The pseudogroup $\mathcal{G}_K$ acting on a rectangle $\mathbf{R}_0 \subset \mathbb{K}$ is introduced in Section 9. We choose five maps among the generators of this pseudogroup that reflect the flow dynamics near the minimal set Σ: the pseudogroup orbits are syndetic in the flow orbits of points in Σ. The choice of the rectangle is not arbitrary, as it takes advantages of the symmetries in the construction of the plugs $\mathbb{W}$ and $\mathbb{K}$. One unavoidable consequence of the anti-symmetry property of the Kuperberg flow, is that there must be discontinuities for the return map of the flow. The nature of these discontinuities is described in Section 9, and again later in Section 20 where they enter into the calculation of the entropy for various pseudogroups.

The set $\mathfrak{M}_0$ that is dense in $\mathfrak{M}$ is described in Sections 11 and 12, giving the definition of propeller and the decomposition of $\mathfrak{M}_0$ in level sets. The relation of this decomposition with the pseudogroup $\mathcal{G}_K$ is explained in Section 13, with the introduction of the notion of double propellers. Double propellers play a fundamental role in the proofs of Theorem 1.5.

To complete the description of $\mathfrak{M}_0$ we introduce in Section 14 a graph $\mathbf{T}_\Phi \subset \mathfrak{M}_0$, which is a tree with an additional loop added at the root point $\omega_0 \in \mathbf{T}_\Phi$. The vertices of $\mathbf{T}_\Phi$ are in fact defined by the action of the five special generators of $\mathcal{G}_K$ acting on the root point ω_0. We call $\mathcal{G}^*_K$ the set of words obtained by composition of the special generators. The geometric interpretation suggests an algebraic decomposition of words in $\mathcal{G}^*_K$ as *normal* words: a composition of two level monotone words, that is words along which the level is only increasing or only decreasing. This simplification is described in Section 14 and is a key tool for the

entropy calculations in Sections 20 and 21. It is also used to calculate in Section 22 the area growth rate of the special leaf $\mathfrak{M}_0$ in $\mathfrak{M}$.

In the approach to the set $\mathfrak{M}_0$ described in Section 12 we introduce and discuss two types of irregular behaviors that can arise in the description of the structure of $\mathfrak{M}_0$, and that depend on the choices made in the construction of the Kuperberg Plug (Remark 12.4). Each type of irregularity results in the existence of "double propellers" attached to $\mathfrak{M}_0$, that change the embedding of $\mathfrak{M}_0$ in a uniformly bounded way, without affecting the dynamical invariants of $\mathfrak{M}$. One type of irregularity is studied in Section 15. The second type is more subtle and the generic hypothesis is needed to control it, hence the description and boundedness of this phenomena is discussed later in the text, in Section 18. Neither of these types of irregularities have been considered previously in the study of the Kuperberg flow.

Theorem 1.3 is proved in Section 17. The key to the proof are the estimates established in Section 17 for the orbit behavior of the return map $\widehat{\Phi}$ near the critical line $r = 2$ in $\mathbf{R}_0$. The proofs of these inequalities are based on the generic assumptions on the insertion maps. It is to be expected that some form of strong regularity hypotheses is required to prove Theorem 1.3, as its conclusion is a type of "Denjoy Theorem" for a smooth flow on a surface lamination. In fact, [27, Theorem 3] gives an example of a PL flow for which the minimal set is 1-dimensional, hence not all of $\mathfrak{M}$. It seems reasonable to conjecture that a smooth example, not satisfying the generic hypotheses, can also be constructed for which the inclusion $\Sigma \subset \mathfrak{M}$ is proper.

Section 16 uses the notion of double propellers to prove that the set $\mathfrak{M}$ is the non-wandering set of the Kuperberg Plug. This result allows us to restrict the entropy calculation for the flow to $\mathfrak{M}$, as discussed in Section 20. The calculations in this section use almost all the results of the study of the geometry and dynamical properties of the flow established in previous sections. In particular, the calculations show the usefulness of the pseudo$\star$group $\mathcal{G}_K^*$ defined by the nice set of generators for $\mathcal{G}_K$ mentioned above. The computation of the entropy that we present uses the results and techniques from Sections 9, 14 and 16, but avoids the use of Pesin Theory for flows.

The definition of a zippered lamination is given in Definition 19.3, and Theorem 19.1 shows that for a generic flow, the space $\mathfrak{M}$ is a zippered lamination. The holonomy pseudogroup $\mathcal{G}_{\mathfrak{M}}$ of the zippered lamination $\mathfrak{M}$ is introduced in Section 21, and its generators are related to the five special generators of the pseudogroup $\mathcal{G}_K$ induced by the return map of the flow Φ_t to the section $\mathbf{R}_0$. The notable properties of $\mathcal{G}_{\mathfrak{M}}$ is that it collapses the symmetry built into the Kuperberg flow, and also that the holonomy induced by a leafwise path can give a more efficient representation of the action of words in $\mathcal{G}_K$. These two properties suggest the possibility of the entropy of the lamination being positive, even if the flow has zero topological entropy. In Section 21 we show that the entropy of the action of $\mathcal{G}_{\mathfrak{M}}$ vanishes as well, but under extra hypothesis on the insertion maps, we prove Theorem 1.8, implying that some chaotic behavior exist in its orbit structure anyway. In Section 22, we use normal forms of words in $\mathcal{G}_{\mathfrak{M}}$ to establish the growth type of the leaves of $\mathfrak{M}$.

Finally, Theorems 1.5 and 1.6 are proved in Section 23, using the double propellers of Section 13 to build a suitable sequence of neighborhoods of $\mathfrak{M}$ which are used to study its shape properties.

The reader will quickly observe one of the significant contributions of this work, which is an extensive collection of illustrations which accompany the text. Many of the dynamical properties that we discuss here are difficult to grasp without these illustrations, which we hope will aid the reader to a full understanding of the beauty and complexity of the dynamics of Kuperberg flows. The approach in this paper invokes four perspectives on the dynamics of the Kuperberg flow, and the illustrations help to understand the relationship between the dynamics as analyzed using each of these viewpoints. The models of the dynamical behavior illustrated in each case are related by non-linear transformations, so that it often requires some effort to visualize the correspondence between each approach.

This paper owes a profound debt to the authors of the works [17, 26, 27, 33, 41] whose text and pictures provided many insights to the Kuperberg dynamics during the development of this work, and inspired many of the illustrations in this paper.

This work was made possible by the help of many colleagues and institutions. We thank our colleagues Alex Clark, Étienne Ghys and Krystyna Kuperberg for their insights and suggestions during the development of this work. We also thank the funding agency CONACyT of Mexico for its postdoctoral Research Fellowship support, the Mathematics Department of UIC, and the Mathematics Department of University of Chicago for its welcoming support of the second author, and the University of Strasbourg for its welcoming support of the first author. We gave numerous talks on this work during the preparation of this manuscript, we thank the colleagues that contributed with comments and questions.

Finally, the authors owe many thanks to the referee, who provided many and repeated helpful comments to improve the presentation, and to improve and correct the proofs of various results in this text through the multiple revisions of this manuscript.

2. The modified Wilson Plug

A 3-dimensional plug is a manifold P endowed with a vector field $\mathcal{X}$ satisfying the following characteristics: The manifold P is of the form $D \times [-2,2]$, where D is a compact 2-manifold with boundary ∂D. Set

$$\partial_v P = \partial D \times [-2,2] \quad , \quad \partial_h^- P = D \times \{-2\} \quad , \quad \partial_h^+ P = D \times \{2\}$$

Then the boundary (with corners) of P has a decomposition

$$\partial P \;=\; \partial_v P \cup \partial_h P \;=\; \partial_v P \cup \partial_h^- P \cup \partial_h^+ P \;.$$

Let $\frac{\partial}{\partial z}$ be the *vertical* vector field on P, where z is the coordinate on $[-2,2]$.

The vector field $\mathcal{X}$ on P must satisfy the conditions:

(P1) *vertical at the boundary*: $\mathcal{X} = \frac{\partial}{\partial z}$ in a neighborhood of ∂P; thus, $\partial_h^- P$ and $\partial_h^+ P$ are the entry and exit regions of P for the flow of $\mathcal{X}$, respectively;
(P2) *entry-exit condition*: if a point $(x,-2)$ is in the same trajectory as $(y,2)$, then $x = y$. That is, an orbit that traverses P, exits just in front of its entry point;
(P3) *trapped orbit*: there is at least one entry point whose entire *forward* orbit is contained in P; we will say that its orbit is *trapped* by P;
(P4) *tameness*: there is an embedding $i\colon P \to \mathbb{R}^3$ that preserves the vertical direction on the boundary ∂P.

A plug is *aperiodic* if there is no closed orbit for $\mathcal{X}$.

Note that conditions (P2) and (P3) imply that if the forward orbit of a point $(x,-2)$ is trapped, then the backward orbit of $(x,2)$ is also trapped.

A *semi-plug* is a manifold P endowed with a vector field $\mathcal{X}$ as above, satisfying conditions (P1), (P3) and (P4), but not necessarily (P2). The concatenation of a semi-plug with an inverted copy of itself, that is a copy where the direction of the flow is inverted, is then a plug. Note that we can generalize the above definition to higher dimensions: just take the manifold D to have dimension $n-1$, where n is the dimension of the ambient manifold of the flow.

Condition (P4) implies that given any open ball $B(x,\epsilon) \subset \mathbb{R}^3$ with $\epsilon > 0$ and x a point, there exists a modified embedding $i'\colon P \to B(x,\epsilon)$ which preserves the vertical direction again. Thus, a plug can be used to change a vector field $\mathcal{Z}$ on any 3-manifold M inside a flowbox, as follows. Let $\varphi\colon U_x \to (-1,1)^3$ be a coordinate chart which maps the vector field $\mathcal{Z}$ on M to the vertical vector field $\frac{\partial}{\partial z}$. Choose a modified embedding $i'\colon P \to B(x,\epsilon) \subset (-1,1)^3$, and then replace the flow $\frac{\partial}{\partial z}$ in the interior of $i'(P)$ with the image of $\mathcal{X}$. This results in a flow $\mathcal{Z}'$ on M.

The entry-exit condition implies that a periodic orbit of $\mathcal{Z}$ which meets $\partial_h P$ in a non-trapped point, will remain periodic after this modification. An orbit of $\mathcal{Z}$ which meets $\partial_h P$ in a trapped point never exits the plug P, hence after modification, limits to a closed invariant set contained in P. A closed invariant set contains a minimal set for the flow, and thus, a plug serves as a device to insert a minimal set into a flow.

We next introduce the "modified Wilson Plug", which is the first step in the construction of the Kuperberg Plug. Consider the rectangle

$$\mathbf{R} = [1,3] \times [-2,2] = \{(r,z) \mid 1 \leq r \leq 3 \;\&\; -2 \leq z \leq 2\}.$$

Choose a C^∞-function $g\colon \mathbf{R} \to [0,g_0]$ for $g_0 > 0$, which satisfies the "vertical" symmetry condition $g(r,z) = g(r,-z)$. The value of $g_0 > 0$ is arbitrary; to be definite, we fix $g_0 = 1$ throughout this work. Also, require that $g(2,-1) = g(2,1) = 0$, that $g(r,z) = 1$ for (r,z) near the boundary of $\mathbf{R}$, and that $g(r,z) > 0$ otherwise. Later, in (44) we will specify that $g(r,z) = 1$ for all points outside of an ϵ_0-neighborhood of the vanishing points $(2,-1)$ and $(2,1)$.

Define the vector field $\mathcal{W}_v = g \cdot \frac{\partial}{\partial z}$ which has two singularities, $(2,\pm 1)$ and is otherwise everywhere vertical, as illustrated in Figure 1.

Next, choose a C^∞-function $f\colon \mathbf{R} \to [-1,1]$ which satisfies the following conditions:

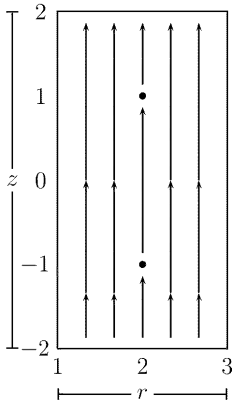

FIGURE 1. Vector field $\mathcal{W}_v$

(W1) $f(r,-z) = -f(r,z)$ [*anti-symmetry in* z].
(W2) $f(\xi) = 0$ for ξ near the boundary of $\mathbf{R}$.
(W3) $f(r,z) \geq 0$ for $-2 \leq z \leq 0$, and $f(r,z) > 0$ for $5/4 \leq r \leq 11/4$ and $-7/4 \leq z < 0$.
(W4) $f(r,z) \leq 0$ for $0 \leq z \leq 2$, and $f(r,z) < 0$ for $5/4 \leq r \leq 11/4$ and $0 < z \leq 7/4$.
(W5) $f(r,z) = 1$ for $5/4 \leq r \leq 11/4$ and $-7/4 \leq z \leq -1/4$.
(W6) $f(r,z) = -1$ for $5/4 \leq r \leq 11/4$ and $1/4 \leq z \leq 7/4$.

Condition (W1) implies that $f(r,0) = 0$ for all $1 \leq r \leq 3$, and that Conditions (W5) and (W6) are equivalent. Note that Conditions (W5) and (W6) are stated more precisely than in the works [26, 17, 33], as it is convenient to specify the values of f on the specified domain in later considerations.

Next, define the manifold with boundary

$$\mathbb{W} = [1,3] \times \mathbb{S}^1 \times [-2,2] \cong \mathbf{R} \times \mathbb{S}^1 \tag{2}$$

with cylindrical coordinates $x = (r, \theta, z)$. That is, $\mathbb{W}$ is a solid cylinder with an open core removed, obtained by rotating the rectangle $\mathbf{R}$, considered as embedded in $\mathbb{R}^3$, around the z-axis.

Extend the functions f and g above to $\mathbb{W}$ by setting $f(r,\theta,z) = f(r,z)$ and $g(r,\theta,z) = g(r,z)$, so that they are invariant under rotations around the z-axis. The *modified Wilson vector field* $\mathcal{W}$ on $\mathbb{W}$ is defined by

$$\mathcal{W} = g(r,\theta,z)\frac{\partial}{\partial z} + f(r,\theta,z)\frac{\partial}{\partial \theta} \ . \tag{3}$$

Let Ψ_t denote the flow of $\mathcal{W}$ on $\mathbb{W}$. Observe that the vector field $\mathcal{W}$ is vertical near the boundary of $\mathbb{W}$, and is horizontal for the points $(r,\theta,z) = (2,\theta,\pm 1)$. Also, $\mathcal{W}$ is tangent to the cylinders $\{r = const.\}$. The flow Ψ_t on the cylinders $\{r = const.\}$ is illustrated (in cylindrical coordinate slices) by Figures 2 and 3.

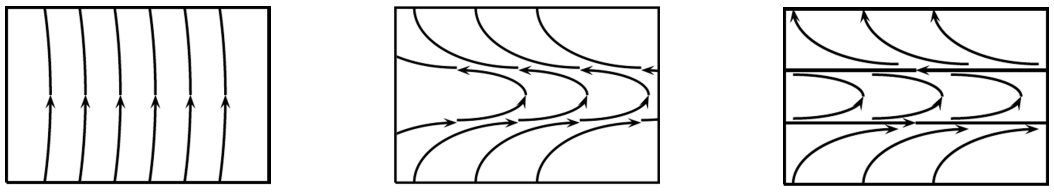

FIGURE 2. $\mathcal{W}$-orbits on the cylinders $\{r = const.\}$

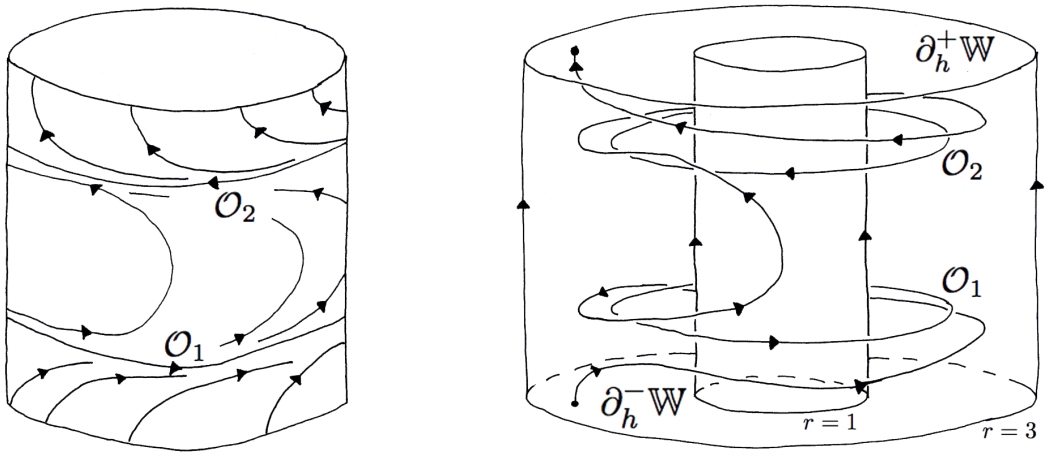

FIGURE 3. $\mathcal{W}$-orbits in the cylinder $\mathcal{C} = \{r = 2\}$ and in $\mathbb{W}$

We give some of the basic properties of the Wilson flow. Let $R_\varphi \colon \mathbb{W} \to \mathbb{W}$ be rotation by the angle φ. That is, $R_\varphi(r, \theta, z) = (r, \theta + \varphi, z)$. Define the closed subsets:

$$\begin{aligned} \mathcal{C} &\equiv \{r = 2\} \quad [\textit{The Full Cylinder}] \\ \mathcal{R} &\equiv \{(2, \theta, z) \mid -1 \le z \le 1\} \quad [\textit{The Reeb Cylinder}] \\ \mathcal{A} &\equiv \{z = 0\} \quad [\textit{The Center Annulus}] \\ \mathcal{O}_i &\equiv \{(2, \theta, (-1)^i)\} \quad [\textit{Periodic Orbits, i=1,2}] \end{aligned}$$

Then $\mathcal{O}_1$ is the lower boundary circle of the Reeb cylinder $\mathcal{R}$, and $\mathcal{O}_2$ is the upper boundary circle.

PROPOSITION 2.1. *Let Ψ_t be the flow on $\mathbb{W}$ defined above, then:*

(1) $R_\varphi \circ \Psi_t = \Psi_t \circ R_\varphi$ for all φ and t.
(2) The flow Ψ_t preserves the cylinders $\{r = const.\}$ and in particular preserves the cylinders $\mathcal{R}$ and $\mathcal{C}$.
(3) $\mathcal{O}_i$ for $i = 1, 2$ are the periodic orbits for Ψ_t.
(4) For $x = (2, \theta, -2)$, the forward orbit $\Psi_t(x)$ for $t > 0$ is trapped.
(5) For $x = (2, \theta, 2)$, the backward orbit $\Psi_t(x)$ for $t < 0$ is trapped.
(6) For $x = (r, \theta, z)$ with $r \neq 2$, the orbit $\Psi_t(x)$ terminates in the top face $\partial_h^+\mathbb{W}$ for some $t \ge 0$, and terminates in $\partial_h^-\mathbb{W}$ for some $t \le 0$.
(7) The flow Ψ_t satisfies the entry-exit condition (P2) for plugs.

Proof. The only assertion that needs a comment is the last, which follows by (W1) and the symmetry condition imposed on the functions g and f. □

Observe that for the choice of $g_0 = 1$ for the maximum value of the function g, the typical orbit of $\mathcal{W}$ rises from $z = -2$ to $z = 2$ in less than one revolution around the circle parameter θ. A smaller choice of g_0 much closer to 0 will result in a flow which climbs much slower, and so will possibly make many more revolutions before transiting the cylinder. This observation will be used in the discussion of the pseudogroup dynamics in Section 9, and also in the discussion of propellers in Sections 11, 13.

3. The Kuperberg plug

The construction of the Kuperberg Plug begins with the modified Wilson Plug $\mathbb{W}$ with vector field $\mathcal{W}$. The first step is to re-embed the manifold $\mathbb{W}$ in $\mathbb{R}^3$ as a *folded figure-eight*, as shown in Figure 4, preserving the vertical direction. A simple but basic point is that the embeddings of the faces of the plug are not "planar".

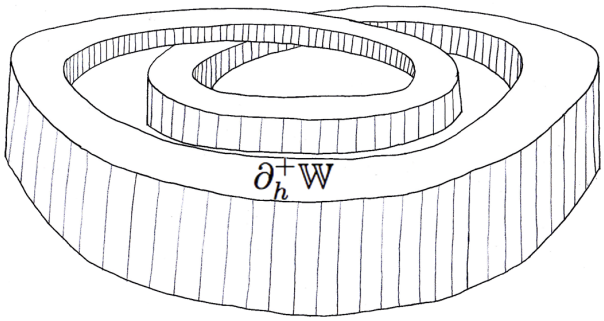

FIGURE 4. Embedding of Wilson Plug $\mathbb{W}$ as a *folded figure-eight*

The fundamental idea of the Kuperberg Plug is to construct two insertions of $\mathbb{W}$ into itself, in such a way that the two periodic orbits will be trapped by these self-insertions. Moreover, the insertions are made so that the resulting space $\mathbb{K}$ is again embedded in $\mathbb{R}^3$. A key subtlety of the construction arises in the precise requirements on these self-insertions. As with the construction of the modified Wilson Plug, the description of this construction in the works [26, 17, 33] is qualitative, as this suffices to prove the aperiodicity of the resulting flow. As will be seen in later sections of this work, other properties of the dynamics of the flow Φ_t in the resulting plug $\mathbb{K}$ are strongly influenced by the precise nature of these maps, so we specify the definitions and some properties of the insertion maps more carefully in this section. Later in the manuscript, we formulate additional "generic" requirements on the insertion maps, in order to obtain further properties about the dynamics of the flow Φ_t.

The construction begins with the choice in the annulus $[1, 3] \times \mathbb{S}^1$ of two closed regions L_i, for $i = 1, 2$, which are topological disks. Each region has boundary defined by two arcs: for $i = 1, 2$, α_i' is the boundary contained in the interior of $[1, 3] \times \mathbb{S}^1$ and α_i in the outer boundary contained in the circle $\{r = 3\}$, as depicted in Figure 5.

We fix these curves precisely. Let $\zeta_1 = \pi/4$ and $\zeta_2 = -\pi/4$, then define the arcs

$$\alpha_1 \ = \ \{(3, \theta) \mid \ |\theta - \zeta_1| \leq 1/10\} \quad , \quad \alpha_2 \ = \ \{(3, \theta) \mid \ |\theta - \zeta_2| \leq 1/10\} \ .$$

Let α_i' be the curves in the interior of L_i which in polar coordinates (r, θ) are parabolas with minimum values $r = 3/2$ and base the line segment α_i, as depicted in Figure 5. We choose an explicit form for the embedded curves, for example, given by $\alpha_i' \equiv \{r = 3/2 + 300/2 \cdot (\theta - \zeta_i)^2\}$.

Consider the closed sets $D_i \equiv L_i \times [-2, 2] \subset \mathbb{W}$, for $i = 1, 2$. Note that each D_i is homeomorphic to a closed 3-ball, that $D_1 \cap D_2 = \emptyset$ and each D_i intersects the cylinder $\{r = 2\}$ in a rectangle. Label the top and bottom faces of these regions by

$$L_1^{\pm} = L_1 \times \{\pm 2\} \ , \ L_2^{\pm} = L_2 \times \{\pm 2\} \ . \tag{4}$$

The next step is to define insertion maps $\sigma_i \colon D_i \to \mathbb{W}$, for $i = 1, 2$, in such a way that the periodic orbits $\mathcal{O}_1$ and $\mathcal{O}_2$ for the Ψ_t-flow intersect $\sigma_i(L_i^-)$ in points corresponding to $\mathcal{W}$-trapped entry points for the modified Wilson Plug. Consider the two disjoint arcs β_i' in the inner boundary circle $\{r = 1\}$,

$$\begin{aligned} \beta_1' \ &= \ \{(1, \theta) \mid \ |\theta - (\zeta_1 + \pi)| \leq 1/10\} \\ \beta_2' \ &= \ \{(1, \theta) \mid \ |\theta - (\zeta_2 + \pi)| \leq 1/10\} \ . \end{aligned}$$

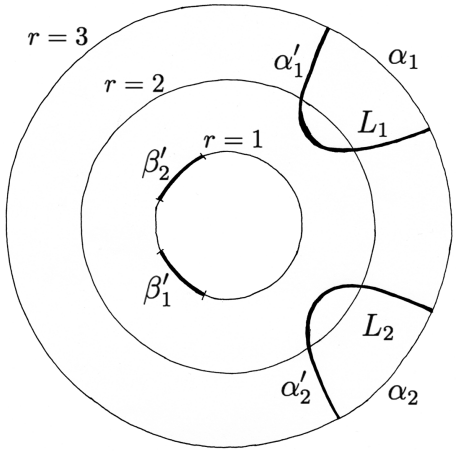

FIGURE 5. The disks L_1 and L_2

For $i = 1, 2$, choose orientation preserving diffeomorphisms $\sigma_i \colon \alpha_i' \to \beta_i'$, and extend these maps to smooth embeddings $\sigma_i \colon D_i \to \mathbb{W}$, as illustrated in Figure 6, which satisfy the conditions:

(K1) $\sigma_i(\alpha_i' \times z) = \beta_i' \times z$ for $z \in [-2, 2]$, and the interior arc α_i' is mapped to a boundary arc β_i';
(K2) $\mathcal{D}_i = \sigma_i(D_i) \subset \{(r, \theta, z) \mid 1 \leq r \leq 5/2\ ,\ |\theta - (\zeta_i + \pi)| \leq 1/10\}$, thus $\mathcal{D}_1 \cap \mathcal{D}_2 = \emptyset$;
(K3) $\sigma_1(L_1^-) \cap \{r \geq 2\} \subset \{z < 0\}$ and $\sigma_2(L_2^-) \cap \{r \geq 2\} \subset \{z > 0\}$;
(K4) For every $x \in L_i$, the image $\mathcal{I}_{i,x} \equiv \sigma_i(x \times [-2, 2])$ is an arc contained in a trajectory of $\mathcal{W}$;
(K5) Each slice $\sigma_i(L_i \times \{z\})$ is transverse to the vector field $\mathcal{W}$, for all $-2 \leq z \leq 2$;
(K6) $\mathcal{D}_i$ intersects the periodic orbit $\mathcal{O}_i$ and not $\mathcal{O}_j$, for $i \neq j$.

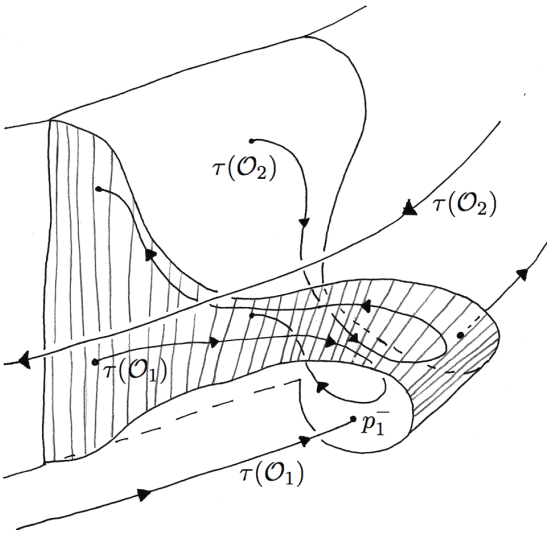

FIGURE 6. The image of $L_1 \times [-2, 2]$ under σ_1

The "horizontal faces" of the embedded regions $\mathcal{D}_i = \sigma_i(D_i) \subset \mathbb{W}$ are labeled by

$$\mathcal{L}_1^{\pm} = \sigma_1(L_1^{\pm})\ ,\ \mathcal{L}_2^{\pm} = \sigma_2(L_2^{\pm})\ . \tag{5}$$

Note that the arcs $\mathcal{I}_{i,x}$ in condition (K4) are line segments from $\sigma_i(x \times \{-2\})$ to $\sigma_i(x \times \{2\})$ which follow the $\mathcal{W}$-trajectory and traverse the insertion from the bottom face to the top face. Since $\mathcal{W}$ is vertical near

the boundary of $\mathbb{W}$, and horizontal in the two periodic orbits, we have that the arcs $\mathcal{I}_{i,x}$ are vertical near the inserted curve $\sigma_i(\alpha_i')$ and horizontal at the intersection of the insertion with the periodic orbit $\mathcal{O}_i$. Thus, the embeddings of the surfaces $\sigma_i(L_i \times \{z\})$ make a *half turn* upon insertion, for each $-2 \leq z \leq 2$, as depicted in Figure 6. The turning is clockwise for the bottom insertion $i = 1$ as illustrated in Figure 6 and counter-clockwise for the upper insertion $i = 2$, which is not illustrated.

The image of the first insertion $\sigma_1(D_1)$ in Figure 6 intersects the first periodic orbit of $\mathcal{W}$ and is disjoint of the second periodic orbit. The image of the second insertion $\sigma_2(D_2)$ is disjoint from the first insertion and the first periodic orbit, and intersects the second periodic orbit.

The embeddings σ_i are also required to satisfy two further conditions, which are the key to showing that the resulting Kuperberg flow Φ_t is *aperiodic*:

(K7) For $i = 1, 2$, the disk L_i contains a point $(2, \theta_i)$ such that the image under σ_i of the vertical segment $(2, \theta_i) \times [-2, 2] \subset D_i \subset \mathbb{W}$ is an arc $\{r = 2\} \cap \{\theta_i^- \leq \theta \leq \theta_i^+\} \cap \{z = (-1)^i\}$ of the periodic orbit $\mathcal{O}_i$ of $\mathcal{W}$.

(K8) *Radius Inequality*: For all $x' = (r', \theta', z') \in L_i \times [-2, 2]$, let $x = (r, \theta, z) = \sigma_i(r', \theta', z') \in \mathcal{D}_i$, then $r < r'$ unless $x' = (2, \theta_i, z')$ and then $r = r' = 2$.

The Radius Inequality (K8) is one of the most fundamental concepts of Kuperberg's construction. The condition (K4) and the fact that the flow of the vector field $\mathcal{W}$ on $\mathbb{W}$ preserves the radius coordinate on $\mathbb{W}$, allows restating (K8) in the more concise form for points in the faces $\mathcal{L}_i^-$ of the insertion regions $\mathcal{D}_i$. For $x = (r, \theta, z) = \sigma_i(r', \theta', z') \in \mathcal{D}_i$ we have

$$r(\sigma_i^{-1}(x)) \geq r \text{ for } x \in \mathcal{L}_i^- \ , \text{ with } r(\sigma_i^{-1}(x)) = r \text{ if and only if } x = \sigma_i(2, \theta_i, -2) \ . \tag{6}$$

The Radius Inequality (K8) is illustrated in Figure 7 below. This is an "idealized" case, as it implicitly assumes that the relation between the values of r and r' is "quadratic" in a neighborhood of the special points $(2, \theta_i)$, which is not required in order that (K8) be satisfied. Later in this work, this "quadratic condition" will be added as part of the generic hypotheses on the construction.

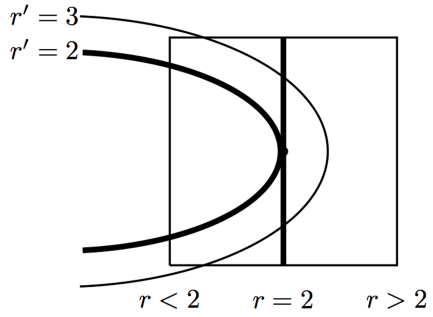

FIGURE 7. The radius inequality illustrated

The embeddings $\sigma_i \colon L_i \times [-2, 2] \to \mathbb{W}$, for $i = 1, 2$, can be constructed by first choosing smooth embeddings of the faces $\sigma_i \colon L_i^- \times \{-2\} \to \mathbb{W}$ so that the image surfaces are transverse to the vector field $\mathcal{W}$ on $\mathbb{W}$, and satisfy the conditions (K1), (K3), (K7) and (K8). Then we extend the embeddings of the faces $L_i^- \times \{-2\}$ to the cylinder sets $L_i \times [-2, 2]$ by flowing the images using a reparametrization of the flow of $\mathcal{W}$, so that we obtain embeddings of $L_i \times [-2, 2]$ satisfying conditions (K1) to (K8), and as pictured in Figure 6.

Finally, define $\mathbb{K}$ to be the quotient manifold obtained from $\mathbb{W}$ by identifying the sets D_i with $\mathcal{D}_i$. That is, for each point $x \in D_i$ identify x with $\sigma_i(x) \in \mathbb{W}$, for $i = 1, 2$. This is illustrated in Figure 8.

The restricted Ψ_t-flow on the inserted disk $\mathcal{D}_i = \sigma_i(D_i)$ is not compatible with the image of the restricted Ψ_t-flow on D_i. Thus, to obtain a smooth vector field $\mathcal{X}$ from this construction, it is necessary to modify $\mathcal{W}$ on each insertion $\mathcal{D}_i$. The idea is to replace the vector field $\mathcal{W}$ on the interior of each region $\mathcal{D}_i$ with the image

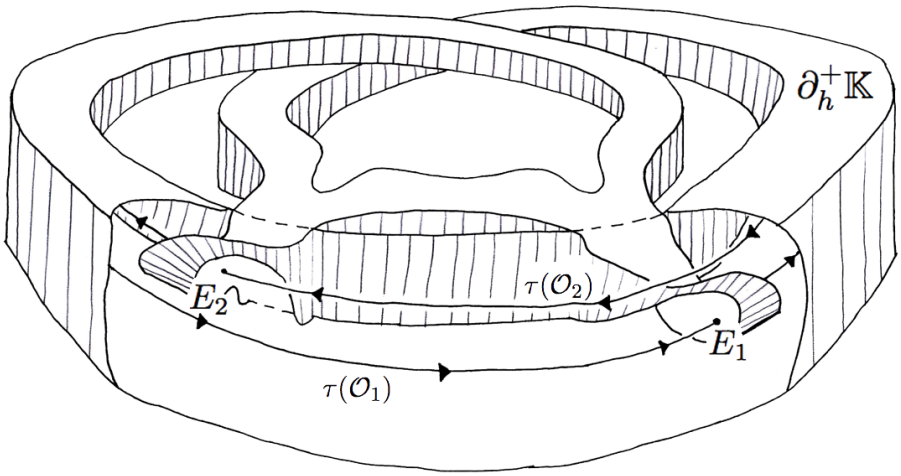

FIGURE 8. The Kuperberg Plug $\mathbb{K}$

vector field, so that the dynamics of Φ_t in the interior of each insertion region $\mathcal{D}_i$ reverts back to the Wilson dynamics on D_i. This requires a minor technical step first.

Smoothly reparametrize the image of $\mathcal{W}|_{D_i}$ under σ_i on an open neighborhood of the boundary of $\mathcal{D}_i$ so that it agrees with the restriction of $\mathcal{W}$ to the same neighborhood. This is possible since the vector field $\mathcal{W}$ is vertical on a sufficiently small open neighborhood of the boundary of D_i so is mapped by σ_i to an orbit segment of $\mathcal{W}$ by (K4). We obtain a vector field $\mathcal{W}'_i$ on $\mathcal{D}_i$ with the same orbits as the image of $\mathcal{W}|_{D_i}$. The case of $\mathcal{D}_1$ is illustrated in Figure 6.

Then modify $\mathcal{W}$ on each insertion $\mathcal{D}_i$, replacing it with the modified image $\mathcal{W}'_i$. Let $\mathcal{W}'$ denote the vector field on $\mathbb{W}$ after these modifications and note that $\mathcal{W}'$ is smooth. By the modifications made above, the vector field $\mathcal{W}'$ descends to a smooth vector field on $\mathbb{K}$ denoted by $\mathcal{K}$. Let Φ_t denote the flow of the vector field $\mathcal{K}$ on $\mathbb{K}$. The *Kuperberg Plug* is the resulting space, $\mathbb{K} \subset \mathbb{R}^3$.

4. Transition points and the radius function

In this section, we introduce notations that will be used throughout this work and also some basic concepts which are fundamental for relating the dynamics of the two vector fields $\mathcal{W}$ and $\mathcal{K}$. These results are contained in the literature [17, 27, 26, 33], though in a variety of differing notations and presentations.

Recall that $\mathcal{D}_i = \sigma_i(D_i)$ for $i = 1, 2$ are solid 3-disks embedded in $\mathbb{W}$. Introduce the sets:

$$\mathbb{W}' \equiv \mathbb{W} - \{\mathcal{D}_1 \cup \mathcal{D}_2\} \quad , \quad \widehat{\mathbb{W}} \equiv \overline{\mathbb{W} - \{\mathcal{D}_1 \cup \mathcal{D}_2\}} \ . \tag{7}$$

The closure $\widehat{\mathbb{W}}$ of $\mathbb{W}'$ is the *piège de Wilson creusé* as defined in [17, page 292]. The compact space $\widehat{\mathbb{W}} \subset \mathbb{W}$ is the result of "drilling out" the interiors of $\mathcal{D}_1$ and $\mathcal{D}_2$, as the terminology *creusé* suggests.

For $x, y \in \mathbb{K}$, we say that $x \prec_{\mathcal{K}} y$ if there exists $t \geq 0$ such that $\Phi_t(x) = y$. Likewise, for $x', y' \in \mathbb{W}$, we say that $x' \prec_{\mathcal{W}} y'$ if there exists $t \geq 0$ such that $\Psi_t(x') = y'$.

Let $\tau\colon \mathbb{W} \to \mathbb{K}$ denote the quotient map, which for $i = 1, 2$, identifies a point $x \in D_i$ with its image $\sigma_i(x) \in \mathcal{D}_i$. Then the restriction $\tau'\colon \mathbb{W}' \to \mathbb{K}$ is injective and onto. Let $(\tau')^{-1}\colon \mathbb{K} \to \mathbb{W}'$ denote the inverse map, which followed by the inclusion $\mathbb{W}' \subset \mathbb{W}$, yields the (discontinuous) map $\tau^{-1}\colon \mathbb{K} \to \mathbb{W}$, where $i = 1, 2$, we have:

$$\tau^{-1}(\tau(x)) = x \text{ for } x \in D_i \ , \text{ and } \sigma_i(\tau^{-1}(\tau(x))) = x \text{ for } x \in \mathcal{D}_i \ . \tag{8}$$

For $x \in \mathbb{K}$, let $x = (r, \theta, z)$ be defined as the $\mathbb{W}$-coordinates of $\tau^{-1}(x) \subset \mathbb{W}'$. In this way, we obtain (discontinuous) coordinates (r, θ, z) on $\mathbb{K}$. In particular, let $r \colon \mathbb{W}' \to [1, 3]$ be the restriction of the radius coordinate on $\mathbb{W}$, then the function is extended to the *radius function* of $\mathbb{K}$, again denoted by r, where for $x \in \mathbb{K}$ set $r(x) = r(\tau^{-1}(x))$.

The flow of the vector field $\mathcal{W}$ on $\mathbb{W}$ preserves the radius function on $\mathbb{W}$, so $x' \prec_{\mathcal{W}} y'$ implies that $r(x') = r(y')$. However, $x \prec_{\mathcal{K}} y$ need not imply that $r(x) = r(y)$. The points of discontinuity for the function $t \mapsto r(\Phi_t(x))$ play a fundamental role in the study of the dynamics of Kuperberg flows.

Let $\partial_h^- \mathbb{K} \equiv \tau(\partial_h^- \mathbb{W} \setminus (L_1^- \cup L_2^-))$ and $\partial_h^+ \mathbb{K} \equiv \tau(\partial_h^+ \mathbb{W} \setminus (L_1^+ \cup L_2^+))$ denote the bottom and top horizontal faces of $\mathbb{K}$, respectively. Note that each of the surfaces $\partial_h^- \mathbb{K}$ and $\partial_h^+ \mathbb{K}$ are closed homeomorphic to a twice-punctured torus, as can be seen in Figure 8 and have boundary which is the union of two circles. By the choice of $\mathcal{K}$, the vertical boundary component $\partial_v \mathbb{K} \equiv \tau(\widehat{\mathbb{W}} \cap \partial_v \mathbb{W})$ is tangent to $\mathcal{K}$.

Points $x' \in \partial_h^- \mathbb{W}$ and $y' \in \partial_h^+ \mathbb{W}$ are said to be *facing*, and we write $x' \equiv y'$, if $x' = (r, \theta, -2)$ and $y' = (r, \theta, 2)$ for some r and θ. The entry/exit property of the Wilson flow is then equivalent to the property that $x' \equiv y'$ if $[x', y']_{\mathcal{W}}$ is an orbit from $\partial_h^- \mathbb{W}$ to $\partial_h^+ \mathbb{W}$ whenever $r(x') \neq 2$. There is also a notion of facing points for $x, y \in \mathbb{K}$, if either of two cases are satisfied:

- For $x = \tau(x') \in \partial_h^- \mathbb{K}$ and $y = \tau(y') \in \partial_h^+ \mathbb{K}$, if $x' \equiv y'$ then $x \equiv y$.
- For $i = 1, 2$, with $x = \sigma_i(x')$ and $y = \sigma_i(y')$, if $x' \equiv y'$ then $x \equiv y$.

The context in which the notation $x \equiv y$ is used dictates which usage applies.

Consider the embedded disks $\mathcal{L}_i^{\pm} \subset \mathbb{W}$ defined by (5), which appear as the faces of the insertions in $\mathbb{W}$. Their images in the quotient manifold $\mathbb{K}$ are denoted by:

$$E_1 = \tau(\mathcal{L}_1^-) \ , \ S_1 = \tau(\mathcal{L}_1^+) \ , \ E_2 = \tau(\mathcal{L}_2^-) \ , \ S_2 = \tau(\mathcal{L}_2^+) \ . \tag{9}$$

Note that $\tau^{-1}(E_i) = L_i^-$, while $\tau^{-1}(S_i) = L_i^+$. Also, introduce the notation:

$$\mathcal{T}_{\mathcal{K}} \ = \ E_1 \cup E_2 \cup S_1 \cup S_2 \ . \tag{10}$$

Then by the formulation (6) of the Radius Inequality, the points of discontinuity along $\mathcal{K}$-orbits for the radius function $r \colon \mathbb{K} \to [1, 3]$ are contained in the set $\mathcal{T}_{\mathcal{K}}$.

The set $\mathcal{T}_{\mathcal{K}} \subset \mathbb{K}$ is transverse to the flow $\mathcal{K}$. The *transition points* of an orbit of $\mathcal{K}$ are those points where the orbit intersects the transversal $\mathcal{T}_{\mathcal{K}}$, or terminate in a boundary component $\partial_h^- \mathbb{K}$ or $\partial_h^+ \mathbb{K}$. They are then either *primary* or *secondary* transition points, where $x \in \mathbb{K}$ is:

- a *primary entry point* if $x \in \partial_h^- \mathbb{K}$;
- a *primary exit point* if $x \in \partial_h^+ \mathbb{K}$;
- a *secondary entry point* if $x \in E_1 \cup E_2$;
- a *secondary exit point* $x \in S_1 \cup S_2$.

If a $\mathcal{K}$-orbit contains no transition points, then it lifts to a $\mathcal{W}$-orbit in $\mathbb{W}$ flowing from $\partial_h^- \mathbb{W}$ to $\partial_h^+ \mathbb{W}$.

The *special points* for the flow Φ_t are the images, for $i = 1, 2$,

$$p_i^- = \tau(\mathcal{O}_i \cap \mathcal{L}_i^-) \in E_i \ , \ p_i^+ = \tau(\mathcal{O}_i \cap \mathcal{L}_i^+) \in S_i \ . \tag{11}$$

Note that by definitions and the Radius Inequality, we have $r(p_i^{\pm}) = 2$ for $i = 1, 2$.

A $\mathcal{W}$-*arc* is a closed segment $[x, y]_{\mathcal{K}} \subset \mathbb{K}$ of the flow of $\mathcal{K}$ whose endpoints $\{x, y\}$ lie in $\mathcal{T}_{\mathcal{K}}$, while the interior $(x, y)_{\mathcal{K}}$ of the arc is disjoint from $\mathcal{T}_{\mathcal{K}}$. The open interval $(x, y)_{\mathcal{K}}$ is then the image under τ of a unique $\mathcal{W}$-orbit segment in $\mathbb{W}'$, denoted by $(x', y')_{\mathcal{W}}$ where $\tau(x') = x$ and $\tau(y') = y$ (see Figure 9.) Let $[x', y']_{\mathcal{W}}$ denote the closure of $(x', y')_{\mathcal{W}}$ in $\widehat{\mathbb{W}}$, then we say that $[x', y']_{\mathcal{W}}$ is the *lift* of $[x, y]_{\mathcal{K}}$. Note that the radius function r is constant along $[x', y']_{\mathcal{W}}$.

The properties of the Wilson flow $\mathcal{W}$ on $\widehat{\mathbb{W}}$ determine the endpoints of lifts $[x', y']_{\mathcal{W}}$. We state the six cases which arise explicitly, as they will be cited in later arguments. Figure 9 helps in visualizing these cases.

LEMMA 4.1. *Let $[x,y]_{\mathcal{K}} \subset \mathbb{K}$ be a $\mathcal{W}$-arc, and let $[x',y']_{\mathcal{W}} \subset \widehat{\mathbb{W}}$ denote its lift.*

(1) **(p-entry/entry)** *If x is a primary entry point, then $x' \in \partial_h^- \mathbb{W} \setminus (L_1^- \cup L_2^-)$ and if y is a secondary entry point, we have $y' \in \mathcal{L}_i^-$ for $i = 1$ or 2.*

(2) **(p-entry/exit)** *If x is a primary entry point, then $x' \in \partial_h^- \mathbb{W} \setminus (L_1^- \cup L_2^-)$ and if y is an exit point, then $y' \in \partial_h^+ \mathbb{W}$ is a primary exit point, and by the entry/exit condition on $\mathbb{W}$ we have $x \equiv y$.*

(3) **(s-entry/entry)** *If x is a secondary entry point, then $x' \in L_i^-$ for $i = 1$ or 2, and if y is an entry point, then we have $y' \in \mathcal{L}_j^-$ where $j = 1, 2$ is not necessarily equal to i.*

(4) **(s-entry/exit)** *If x is a secondary entry point, then $x' \in L_i^-$ for $i = 1$ or 2, and if y is an exit point, then $y' \in L_i^+$ and $x \equiv y$ by the entry/exit condition of $\mathbb{W}$.*

(5) **(s-exit/entry)** *If x is a secondary exit point, then $x' \in \mathcal{L}_i^+$ for $i = 1$ or 2, and if y is an entry point, so that $y' \in \mathcal{L}_j^-$ then $j = 2$ if $i = 2$, and $j = 1, 2$ if $i = 1$.*

(6) **(s-exit/exit)** *If x is a secondary exit point, then $x' \in \mathcal{L}_i^+$ for $i = 1$ or 2, and if y is a primary exit point, $y' \in \{\partial_h^+ \mathbb{W} \setminus (L_1^+ \cup L_2^+)\}$. If y is a secondary exit point, then $y' \in L_j^+$, where $j = 1$ or 2 is not necessarily equal to i.*

Figure 9 illustrates some of the notions discussed in this section. The disks L_1^- and L_2^- contained in $\partial_h^- \mathbb{W}$ are drawn in the bottom face, though they are partially obscured by the cylinder $\{r = 1\}$. The image of L_1^- under σ_1 is the entry face of the insertion region in the lower half of the cylinder, while the image of L_2^- under σ_2 is the entry face of the insertion region in the upper half of the cylinder. Analogously, the disks L_1^+ and L_2^+ in $\partial_h^+ \mathbb{W}$ are mapped to the exit region of the insertion regions. The intersection of the $\mathcal{W}$-periodic orbits $\mathcal{O}_1$ and $\mathcal{O}_2$ with $\widehat{\mathbb{W}}$ is illustrated, as well as two $\mathcal{W}$-arcs in $\mathbb{W}'$ that belong to the same orbit. One $\mathcal{W}$-arc goes from $\partial_h^- \mathbb{W}$ to $\mathcal{L}_1^-$, hence from a principal entry point to a secondary entry point (as in Lemma 4.1.1). The second $\mathcal{W}$-arc goes from $\mathcal{L}_1^+$ to $\mathcal{L}_1^-$, thus from a secondary exit point to a secondary entry point (as in Lemma 4.1.5).

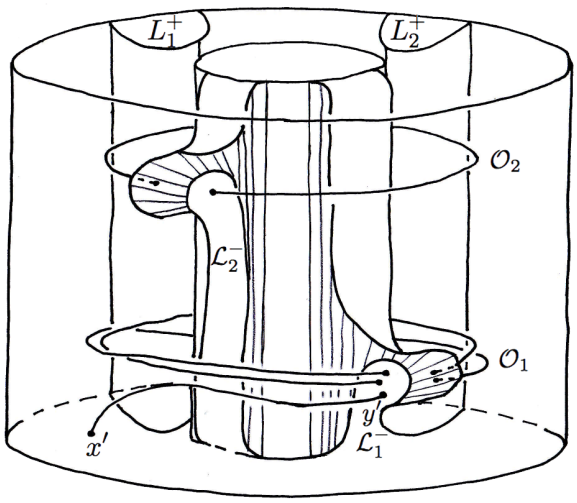

FIGURE 9. $\mathcal{W}$-arcs lifted to $\widehat{\mathbb{W}}$

Introduce the radius coordinate function along $\mathcal{K}$-orbits. For $x \in \mathbb{K}$ set $\rho_x(t) \equiv r(\Phi_t(x))$. Note that if $\Phi_t(x) \notin \mathcal{T}_{\mathcal{K}}$ then the function $\rho_x(t)$ is locally constant at t, and thus we have:

LEMMA 4.2. *If the $\mathcal{K}$-arc $\{\Phi_t(x) \mid t_0 \le t \le t_1\}$ contains no transition point, then $\rho_x(t) = \rho_x(t_0)$ for all $t_0 \le t \le t_1$.* □

The *level function* along an orbit indexes the discontinuities of the radius function. Given $x \in \mathbb{K}$, set $n_x(0) = 0$ and for $t > 0$ define

$$n_x(t) = \#\left\{(E_1 \cup E_2) \cap \Phi_s(x) \mid 0 < s \leq t\right\} - \#\left\{(S_1 \cup S_2) \cap \Phi_s(x) \mid 0 < s \leq t\right\}. \tag{12}$$

That is, $n_x(t)$ is the total number of secondary entry points, minus the total number of secondary exit points, traversed by the flow of x over the interval $0 < s \leq t$. For example, suppose that $x_1 = \Phi_{t_1}(x)$ is the first transition point for $t > 0$. If x_1 is a secondary entry point, then $n_x(t_1) = 1$, while $n_x(t_1) = -1$ if x_1 is a secondary exit point. Thereafter, $n_x(t)$ changes value by ± 1 at each $t > t_1$ such that $\Phi_t(x) \in \mathcal{T}_{\mathcal{K}}$ and whether the value increases or decreases, indicates whether the transition point is an entry or exit point.

The function can be extended to negative time by setting, for $t < 0$,

$$n_x(t) = \#\left\{(S_1 \cup S_2) \cap \Phi_s(x) \mid t < s \leq 0\right\} - \#\left\{(E_1 \cup E_2) \cap \Phi_s(x) \mid t < s \leq 0\right\}. \tag{13}$$

Endow the manifold $\mathbb{K}$ with a Riemannian metric, induced from the natural coordinates on $\widehat{\mathbb{W}}$. Along the boundaries $\partial_h^{\pm}\widehat{\mathbb{W}}$ it is necessary to make a small adjustment to the Riemannian metric so that it becomes smooth on the quotient space $\mathbb{K}$. We can assume that the vector field $\mathcal{K}$ on $\mathbb{K}$ has unit length, and so the adjustments are made to the metric transverse to $\mathcal{K}$ in a small open neighborhood of these boundaries. Let $d_{\mathbb{K}}$ denote the resulting path length metric on $\mathbb{K}$.

Let $d_{\mathbb{W}}$ be the path length metric in $\mathbb{W}$. By the assumption that $\mathcal{K}$ is unit length, the metric $d_{\mathbb{W}}$ is just the same as that derived from the time coordinate along the flow Φ_t. For example, by this convention, the length of the circles $\{(r, \theta, 0) \mid 0 \leq \theta \leq 2\pi\} \subset \mathbb{K}$ is $2\pi r$.

For $x' \prec_{\mathcal{W}} y'$ in $\mathbb{W}$, let $d_{\mathcal{W}}(x', y')$ denote the path length of the $\mathcal{W}$-orbit segment $[x', y']_{\mathcal{W}}$ between them. Similarly, for $x \prec_{\mathcal{K}} y$ in $\mathbb{K}$, let $d_{\mathcal{K}}(x, y)$ denote the path length of the $\mathcal{K}$-orbit segment $[x, y]_{\mathcal{K}}$. Note that if $[x, y]_{\mathcal{K}}$ is a $\mathcal{W}$-arc with lift $[x', y']_{\mathcal{W}}$, then $d_{\mathcal{K}}(x, y) = d_{\mathcal{W}}(x', y')$.

We establish some basic length estimates which are used in later sections.

LEMMA 4.3. *Let $0 < \epsilon < 1$. There exists $L(\epsilon) > 0$ such that for any $\xi \in \mathbb{W}$ with $|r(\xi) - 2| \geq \epsilon$, the total $\mathcal{W}$-orbit segment $[x', y']_{\mathcal{W}}$ through ξ has length bounded above by $L(\epsilon)$.*

Proof. Since $r(\xi) \neq 2$, the orbit of $\mathcal{W}$ containing ξ is finite, hence there exists $x'_\xi \in \partial_h^- \mathbb{W}$ such that $x'_\xi = \Phi_t(\xi)$ for some $t \leq 0$. Likewise, there exists $s \geq 0$ such that $y'_\xi = \Phi_s(\xi) \in \partial_h^+ \mathbb{W}$. Then $[x'_\xi, y'_\xi]_{\mathcal{W}}$ is the complete $\mathcal{W}$-orbit containing ξ. In particular, $d_{\mathcal{W}}(x'_\xi, y'_\xi) < \infty$.

The function $\xi \mapsto d_{\mathcal{W}}(x'_\xi, y'_\xi)$ is continuous on the open domain $r(\xi) \neq 2$. Since the flow in $\mathbb{W}$ is rotationally invariant, this function depends only on $r(\xi)$. Let $L(\epsilon)$ denote the maximum of this length function on the compact domain $|r(\xi) - 2| \geq \epsilon$. □

LEMMA 4.4. *There exists $0 < d_{min} < d_{max}$ such that if $[x', y']_{\mathcal{W}} \subset \widehat{\mathbb{W}}$ is the lift of a $\mathcal{W}$-arc $[x, y]_{\mathcal{K}}$, then we have the uniform estimate*

$$d_{min} \leq d_{\mathcal{W}}(x', y') \leq d_{max} \ . \tag{14}$$

Proof. First, suppose that $x' \in \partial_h^- \mathbb{W}$ and so either $y' \in \mathcal{L}_i^-$ for $i = 1, 2$ or $y' \in \partial_h^+ \mathbb{W}$. The set of points $x' \in \partial_h^- \mathbb{W}$ whose forward orbit has first transition point in $\mathcal{L}_i^-$ is a compact set containing the circle $\{(2, \theta, -2) \mid 0 \leq \theta \leq 2\pi\} \subset \mathbb{W}$ in its interior. Thus, there is a lower and upper bound for the length $d_{\mathcal{W}}(x', y')$.

Away from the core circle in $\partial_h^- \mathbb{W}$, the $\mathcal{W}$-orbit for a point $x' \in \partial_h^- \mathbb{W}$ with $r(x') \neq 2$ is not trapped, so terminates in $y' \in \partial_h^+ \mathbb{W}$. Moreover, the set of x' whose $\mathcal{W}$-orbit does not intersect the compact set $\mathcal{L}_i^-$ has $r(x')$ value bounded away from 2 by the previous case, and thus there exists $\epsilon > 0$ so $|r(x') - 2| \geq \epsilon$. Then by Lemma 4.3 the length $d_{\mathcal{W}}(x', y')$ is then bounded above by $L(\epsilon)$. The lower bound on $d_{\mathcal{W}}(x', y')$ follows from the compactness of the set $\{x' \in \partial_h^- \mathbb{W} \mid \ |r(x') - 2| \geq \epsilon\}$.

The analysis of the cases where $x' \in \mathcal{L}_i^+$, for $i = 1, 2$, proceeds similarly. □

COROLLARY 4.5. *Let $[x, y]_{\mathcal{K}} \subset \mathbb{K}$ be a $\mathcal{W}$-*arc*. Then there is a uniform length estimate*

$$d_{min} \leq d_{\mathcal{K}}(x, y) \leq d_{max} \ . \tag{15}$$

These results then combine to give the observation:

COROLLARY 4.6. *The Wilson orbit through $x' \in \mathbb{W}$ with $r(x') \neq 2$ contains at most a finite number of lifts of distinct $\mathcal{W}$-arcs, partially-ordered by the relation $\prec_{\mathcal{W}}$.*

We summarize the dynamical properties of orbits for Φ_t which follow from the above results.

For each $x \in \mathbb{K}$ the $\mathcal{K}$-orbit $\{\Phi_t(x) \mid a \leq t \leq b\}$, where $-\infty \leq a < b \leq \infty$, can be decomposed in a finite or infinite family of $\mathcal{W}$-arcs $\left\{[x'_i, y'_{i+1}]_{\mathcal{W}}\right\} \subset \mathbb{W}$. These $\mathcal{W}$-arcs are indexed relative to the initial point x by the level function $n_x(t)$ and the radius function $\rho_x(t)$, both functions are constant along $(x_i, y_{i+1})_{\mathcal{K}}$. Thus, the $\mathcal{W}$-arcs can be grouped according to the values $\rho_x(t)$ and so grouped, lie in orbits of the Wilson flow in disjoint cylinders $\{r = const.\}$.

The $\mathcal{K}$-orbit of x is then determined by understanding when two segments $[x'_i, y'_{i+1}]_{\mathcal{W}}$ and $[x'_j, y'_{j+1}]_{\mathcal{W}}$ have the same r-value and so lie in a common cylinder. Then whether they are contained in a common $\mathcal{W}$-orbit within that cylinder, so that $x'_i \prec_{\mathcal{W}} x'_j$ or $x'_j \prec_{\mathcal{W}} x'_i$. By Corollary 4.6 there can be only a finite number of segments in each finite $\mathcal{W}$-orbit.

Once the arcs have been grouped according to their "$\mathcal{W}$-orbit type", it then remains to understand how these $\mathcal{W}$-arcs are assembled to give the full $\mathcal{K}$-orbit, while satisfying the constraints imposed by the Radius Inequality (K8).

5. Semi-local dynamics

In this section, we establish a variety of properties of the level function and how it relates the dynamical behavior of the Wilson flow Ψ_t with the much more complicated dynamical behavior of the Kuperberg flow Φ_t. This relationship is one of the main themes in the understanding of the dynamics of the flow Φ_t as developed in this work.

We first consider the properties of finite length segments of $\mathcal{K}$-orbits. The results presented below are formulations, in our notation, of results which are contained in the works [17, 27, 26, 33] and are the most basic techniques used in the analysis of the dynamics of the Kuperberg flow.

We say that the $\mathcal{K}$-orbit of $x \in \mathbb{K}$ is *trapped in forward time* if the forward orbit is defined for all $t \geq 0$, so that the segment $\{\Phi_t(x) \mid t \geq 0\} \subset \mathbb{K}$. In particular, this forward orbit never intersects $\partial_h^+\mathbb{K}$. Likewise, the $\mathcal{K}$-orbit of $x \in \mathbb{K}$ is *trapped in backward time* if the segment $\{\Phi_t(x) \mid t \leq 0\} \subset \mathbb{K}$. When it is clear whether forward or backward time is meant, such as for points on the faces $\partial_h^{\pm}\mathbb{K}$, we simply refer to a *trapped orbit*.

The $\mathcal{K}$-orbit of x is *infinite* if it is trapped in both forward and backward time.

For a $\mathcal{K}$-orbit segment $[x, y]_{\mathcal{K}}$, we define its "lift" to $\widehat{\mathbb{W}}$, which is a union of lifts of $\mathcal{W}$-orbit segments. This is a fundamental technical construction and introduces another useful notational convention. Let $0 \leq t_0 < t_1 < \cdots < t_n$ be such that $x_\ell = \Phi_{t_\ell}(x)$ are the successive transition points in $[x, y]_{\mathcal{K}}$ so that

$$[x, y]_{\mathcal{K}} = [x, x_0]_{\mathcal{K}} \cup [x_0, x_1]_{\mathcal{K}} \cup \cdots \cup [x_\ell, x_{\ell+1}]_{\mathcal{K}} \cup \cdots \cup [x_{n-1}, x_n]_{\mathcal{K}} \cup [x_n, y]_{\mathcal{K}} \subset \mathbb{K} \ . \tag{16}$$

By convention, $[x, x_0]_{\mathcal{K}}$ is defined to be empty if $x = x_0$, and otherwise has a well-defined lift $[x', x'_0]_{\mathcal{W}} \subset \widehat{\mathbb{W}}$. The case for y is analogous. Each $\mathcal{W}$-arc $[x_\ell, x_{\ell+1}]_{\mathcal{K}}$ for $0 \leq \ell < n$ lifts to a $\mathcal{W}$-orbit segment $[x'_\ell, y'_{\ell+1}]_{\mathcal{W}} \subset \widehat{\mathbb{W}}$, where $\tau(x'_{\ell+1}) = \tau(y'_{\ell+1}) = x_{\ell+1}$ though $y'_{\ell+1} \neq x'_{\ell+1}$. The lift of $[x, y]_{\mathcal{K}}$ to $\mathbb{W}$ is defined to be the collection of orbit segments in $\mathbb{W}$,

$$\left\{[x', y'_0]_{\mathcal{W}}, [x'_0, y'_1]_{\mathcal{W}}, \cdots, [x'_\ell, y'_{\ell+1}]_{\mathcal{W}}, \cdots, [x'_{n-1}, y'_n]_{\mathcal{W}}, [x'_n, y']_{\mathcal{W}}\right\} \ . \tag{17}$$

The lift of a $\mathcal{K}$-orbit segment is closely related to the behavior of the level function $n_x(t)$ along an orbit. Given a $\mathcal{K}$-orbit segment $[x_0, x_n]_{\mathcal{K}}$, where $x_0 = \Phi_0(x)$, decompose it into $\mathcal{W}$-arcs as in (16). The orbit $\Phi_t(x)$ for $t > 0$

flows from x until it hits a transition point x_1. This initial $\mathcal{W}$-arc $[x_0, x_1]_{\mathcal{K}}$ is the image under τ of a $\mathcal{W}$-orbit segment $[x'_0, y'_1]_{\mathcal{W}} \subset \widehat{\mathbb{W}}$ as in (17). After this first transition point, it then follows the image of the vector field $\mathcal{W}$ under an insertion map σ_i, which is again the image of a $\mathcal{W}$-orbit segment $[x'_1, y'_2]_{\mathcal{W}} \subset \widehat{\mathbb{W}}$. At the next transition point, the flow $\Phi_t(x)$ either exits the insertion and reverts back to the same orbit of $\mathcal{W}$ in $\widehat{\mathbb{W}}$; or, it flows into another insertion, and thus the orbit is the image of a $\mathcal{W}$-arc into an insertion within the first insertion. This process continues along the entire $\mathcal{K}$-orbit segment. The level function $n_x(t)$ counts the number of such insertions within insertions along the $\mathcal{K}$-segment $[x_0, x_n]_{\mathcal{K}}$, so measures the "depth of penetration" of the orbit into the self-insertion process used to construct the plug $\mathbb{K}$.

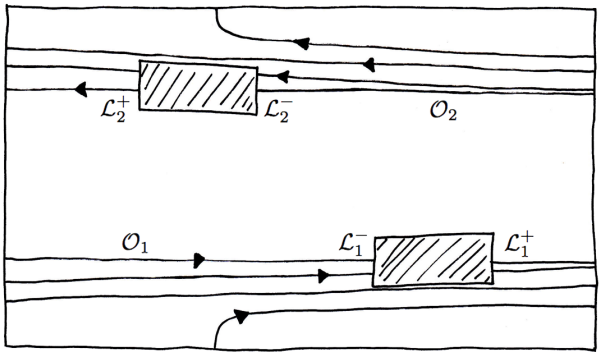

FIGURE 10. Decomposition into $\mathcal{W}$-arcs in the cylinders $\{r = 2\} \subset \widehat{\mathbb{W}}$

We illustrate this orbit decomposition in Figure 10, that represents the cylinder $\{r = 2\}$ in $\widehat{\mathbb{W}}$. Consider the first periodic orbit and its intersection with $\widehat{\mathbb{W}}$, which is pictured as the lower horizontal line in the drawing. Flowing in forward time, the lift of the $\mathcal{K}$-orbit first intersects the entry face $\mathcal{L}_1^-$ of the lower insertion in a "special point". The flow then continues to a point in the lower boundary of the same cylinder $\{r = 2\}$ where it enters. Thus the next $\mathcal{W}$-arc in this orbit is in the same cylinder. It starts climbing and turning, until hits the first insertion and exits the cylinder $\{r = 2\}$ through $\mathcal{L}_1^-$. We prove, in Proposition 6.7, that after a certain time this orbit comes back to the cylinder $\{r = 2\}$ in the facing point. Thus the $\mathcal{K}$-orbit will eventually pass the insertion and continue in the same $\mathcal{W}$-orbit for another turn before hitting the insertion again. This pattern then repeats infinitely many times. Flowing in backward time, the lift of the $\mathcal{K}$-orbit containing the arc $\mathcal{O}_1 \cap \widehat{\mathbb{W}}$, first intersects the exit face $\mathcal{L}_1^+$ in a special point. The orbit then continues to a point in the upper bound of the cylinder. It thus descends turning until it hits the exit face $\mathcal{L}_2^+$. Proposition 6.7 applies, implying that after a certain time this backward orbit comes back to the cylinder and continues descending and turning. This process repeats infinitely many times. Remark that the $\mathcal{K}$-orbit containing the arc $\mathcal{O}_1 \cap \widehat{\mathbb{W}}$ accumulates in forward time on $\mathcal{O}_1 \cap \widehat{\mathbb{W}}$ and in backward time on $\mathcal{O}_2 \cap \widehat{\mathbb{W}}$. Applying the same analysis to the $\mathcal{K}$-orbit containing $\mathcal{O}_2 \cap \widehat{\mathbb{W}}$, we obtain the same conclusion. This argument is explained again in the proof of Proposition 7.1.

We next give a sequence of technical results concerning the properties of the lift (17) of a path as in (16), beginning with the very simple concept of a *short-cut*, which was introduced in [26], and developed in more detail in [17, 27, 33].

LEMMA 5.1 (Short-cut)**.** *Suppose that $x \in E_i$ and $y \in S_i$ are facing. Then there exists $x', y' \in \mathbb{W}$ such that $\tau(x') = x$, $\tau(y') = y$ and $x' \prec_{\mathcal{W}} y'$. That is, there is a $\mathcal{W}$-orbit segment $[x', y']_{\mathcal{W}} \subset \mathbb{W}$ (the short-cut) between x' and y'.*

Proof. Let $x' \in \mathcal{L}_i^-$ with $\tau(x') = x$ and $y' \in \mathcal{L}_i^+$ with $\tau(y') = y$. Consider $x'' \in L_i^-$ with $\sigma_i(x'') = x'$ and $y'' \in L_i^+$ with $\sigma_i(y'') = y'$. Then $x \equiv y$ implies $x'' \equiv y''$ by definition. By (K4) the image $\sigma_i(\mathcal{I}_{i,x''})$ is a $\mathcal{W}$-orbit segment in $\mathcal{D}_i$ with endpoints x', y'. Thus, $x' \prec_{\mathcal{W}} y'$. □

Note that the short-cut path $[x', y']_{\mathcal{W}} \subset \mathbb{W}$ has endpoints in $\mathcal{L}_i^{\pm}$ and "bridges the gap" between these two faces in $\mathbb{W}$. In Figure 10, this may be viewed as filling in with a flow line across any of the insertion boxes, from an entry point to an exit point.

Note that for a short-cut, the length of the path segment $[x', y']_{\mathcal{W}}$ is bounded above by Lemma 4.4, independent of the choice of the points x, y. On the other hand if we are only given that $x \prec_{\mathcal{K}} y$, then no such a priori bound exists. Thus, the $\mathcal{W}$-path $[x', y']_{\mathcal{W}}$ is truly a "short-cut" between x' and y' when compared to the length of the $\mathcal{K}$-path between x and y.

The next result shows that given a pair of $\mathcal{W}$-arcs in $\mathbb{K}$ whose *inner endpoints* are facing, there is a $\mathcal{W}$-orbit segment in $\mathbb{W}$ containing the lifts of both $\mathcal{W}$-arcs.

LEMMA 5.2. *Let $x, y, z, u \in \mathbb{K}$ be successive transition points on a $\mathcal{K}$-orbit, such that $x' \prec_{\mathcal{W}} y'$, $z' \prec_{\mathcal{W}} u'$, y is an entry point, z is an exit point and $y \equiv z$. Then $x' \prec_{\mathcal{W}} u'$ and hence $r(x') = r(u')$.*

Proof. Observe that $x' \prec_{\mathcal{W}} y'$ implies y must be a secondary entry point, thus by Lemma 4.1, the endpoint y' of the $\mathcal{W}$-orbit segment $[x', y']_{\mathcal{W}}$ must lie in $\mathcal{L}_i^-$ for some $i = 1, 2$. Similarly, z must be a secondary exit point, thus the endpoint z' of the $\mathcal{W}$-orbit segment $[z', u']_{\mathcal{W}}$ must lie in $\mathcal{L}_j^+$ for some j. The assumption $y \equiv z$ implies that $i = j$. Then by Lemma 5.1, there is a $\mathcal{W}$-arc in $\mathbb{W}$ between y' and z', a short-cut. Thus, $y' \prec_{\mathcal{W}} z'$, and so $x' \prec_{\mathcal{W}} y' \prec_{\mathcal{W}} z' \prec_{\mathcal{W}} u'$ which implies $x' \prec_{\mathcal{W}} u'$ and so $r(x') = r(u')$. □

The following result gives a criteria for when a pair of $\mathcal{W}$-arcs, whose inner endpoints lift to points which can be joined by a $\mathcal{W}$-orbit segment in $\mathbb{W}$, are themselves contained in a $\mathcal{W}$-orbit segment and have facing endpoints.

LEMMA 5.3. *Suppose that $x \in \mathbb{K}$ is an entry point, $u \in \mathbb{K}$ is an exit point, $[x, y]_{\mathcal{K}}$ and $[z, u]_{\mathcal{K}}$ are $\mathcal{W}$-arcs with lifts $[x', y']_{\mathcal{W}}$ and $[z', u']_{\mathcal{W}}$. If $y' \prec_{\mathcal{W}} z'$, then $x' \prec_{\mathcal{W}} u'$ and $x \equiv u$.*

Proof. Let $[x', y']_{\mathcal{W}} \subset \widehat{\mathbb{W}}$ be the lift of $[x, y]_{\mathcal{K}}$. The fact that x is an entry point implies that $x' \in \partial_h^- \mathbb{W}$ and so either $y' \in \mathcal{L}_i^-$ for $i = 1, 2$, or $y' \in \partial_h^+ \mathbb{W}$. The assumption that $y' \prec_{\mathcal{W}} z'$ implies there is a $\mathcal{W}$-orbit segment from y' to z' so the case $y' \in \partial_h^+ \mathbb{W}$ is impossible. Similarly, let $[z', u']_{\mathcal{W}} \subset \mathbb{W}$ be the lift of $[z, u]_{\mathcal{K}}$, then u is an exit point implies that $u' \in \partial_h^+ \mathbb{W}$ and so $z' \in \mathcal{L}_j^+$ for $j = 1, 2$ as $y' \prec_{\mathcal{W}} z'$ is given. Thus, concatenating the $\mathcal{W}$-orbits segments from x' to y' to z' to u' yields $x' \prec_{\mathcal{W}} u'$. The entry/exit property for the Wilson flow on $\mathbb{W}$ implies that x' and u' are facing, hence $x \equiv u$. □

The next result gives a criteria using the level function, for when a sequence of three $\mathcal{K}$-arcs admit a lift to a segment of the Ψ_t-flow.

LEMMA 5.4. [33, Corollary 4.2] *Let $x \in \mathbb{K}$. Given successive transition points $x_\ell = \Phi_{t_\ell}(x)$ where $0 = t_0 < t_1 < t_2 < t_3$, suppose that $n_{x_0}(t) \geq 0$ for all $0 \leq t < t_3$, and that $n_{x_0}(t_2) = 0$. Then $x_1 \equiv x_2$, $x_0' \prec_{\mathcal{W}} y_3'$ and hence $r(x_0') = r(y_3')$.*

Proof. For $0 \leq \ell < 3$, let $[x_\ell', y_{\ell+1}']_{\mathcal{W}} \subset \widehat{\mathbb{W}}$ be the lift of the $\mathcal{W}$-arc $[x_\ell, x_{\ell+1}]_{\mathcal{K}}$. The fact that $n_{x_0}(t_0) = 0$ and the assumption $n_{x_0}(t_1) \geq 0$ implies that $n_{x_0}(t_1) = 1$. Then x_1 is a secondary entry point, with $y_1' \in \mathcal{L}_i^-$ for $i = 1$ or $i = 2$. Similarly, the assumption $n_{x_0}(t_2) = 0$ implies that x_2 is a secondary exit point, with $x_2' \in \mathcal{L}_j^+$ for $j = 1$ or $j = 2$.

For the middle $\mathcal{W}$-arc $[x_1', y_2']_{\mathcal{W}} \subset \widehat{\mathbb{W}}$, we must then have $x_1' \in L_i^-$ and $y_2' \in L_j^+$. By the entry/exit assumption on $\mathbb{W}$, we have $x_1' \equiv y_2'$ so that $i = j$ and $x_1 \equiv x_2$. It follows that there exist a short-cut $[y_1', x_2']_{\mathcal{W}} \subset \mathcal{D}_i$ between y_1' and x_2'. Thus we have $x_0' \prec_{\mathcal{W}} y_3'$. □

In geometric terms, the lifts of the $\mathcal{W}$-arcs in Lemma 5.4 to $\widehat{\mathbb{W}}$ do not form a continuous $\mathcal{W}$-orbit segment, due to the discontinuity of the map τ, but by replacing the middle segment $[x_1', y_2']_{\mathcal{W}}$ with a short-cut $[y_1', x_2']_{\mathcal{W}}$ through $\mathcal{D}_i$ we obtain a $\mathcal{W}$-orbit segment $[x_0', y_3']_{\mathcal{W}}$. This is illustrated in Figure 11.

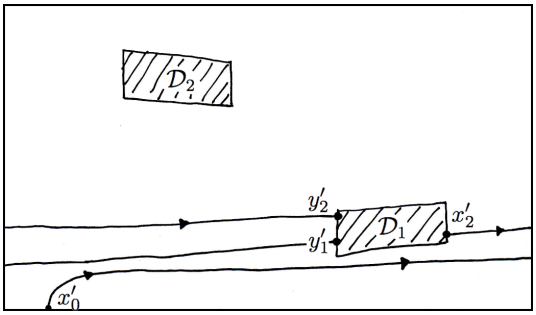

FIGURE 11. Three step curves

Next, we use Lemmas 5.1 to 5.4 to obtain a general form of Lemma 5.4, which is one of the fundamental results concerning the finite orbits of the Kuperberg flow.

PROPOSITION 5.5. [17, Lemme p.297] *Let $x \in \mathbb{K}$. For $n \geq 3$, assume there are given successive transition points $x_\ell = \Phi_{t_\ell}(x)$ for $0 = t_0 < t_1 < \cdots < t_{n-1} < t_n$. Suppose that $n_{x_0}(t) \geq 0$ for all $0 \leq t < t_n$ and that $n_{x_0}(t_{n-1}) = 0$. Then $x'_0 \prec_{\mathcal{W}} y'_n$, and hence $r(x'_0) = r(y'_n)$. Moreover, if x_0 is an entry point and x_n is an exit point, then $x_0 \equiv x_n$.*

Proof. For $0 \leq \ell < n$, let $[x'_\ell, y'_{\ell+1}]_{\mathcal{W}} \subset \widehat{\mathbb{W}}$ be the lift of the $\mathcal{W}$-arc $[x_\ell, x_{\ell+1}]_{\mathcal{K}}$. The fact that $n_{x_0}(t_0) = 0$ and the assumption $n_{x_0}(t_1) \geq 0$ implies that $n_{x_0}(t_1) = 1$. Then x_1 is a secondary entry point, with $y'_1 \in \mathcal{L}_i^-$ for $i = 1$ or $i = 2$. Similarly, the assumption $n_{x_0}(t_{n-1}) = 0$ and $n_{x_0}(t_{n-2}) \geq 0$ implies that x_{n-1} is an exit point. Then x_{n-1} must be a secondary exit point and thus $x'_{n-1} \in \mathcal{L}_j^+$ for $j = 1$ or $j = 2$. The case $n = 3$ then follows from Lemmas 5.3 and 5.4.

For the case $n > 3$, we proceed by induction. Assume that the result holds for all $\mathcal{K}$-segments containing at most n transition points. We will now prove the result for a segment with $n + 1$ transition points x_ℓ for $0 \leq \ell \leq n$. Observe that by hypothesis, $n_{x_0}(t_1) = 1 = n_{x_0}(t_{n-2})$. If there exists $3 \leq \ell \leq n - 2$ such that $n_{x_0}(t_{\ell-1}) = 0$, then consider the least such ℓ. By the inductive hypothesis, we have that $x'_0 \prec_{\mathcal{W}} y'_\ell$, and as $n_{x_0}(t_{\ell-1}) = 0$, we also have that $x'_{\ell-1} \prec_{\mathcal{W}} y'_n$. Both $\mathcal{W}$-segments contain the arc $[x'_{\ell-1}, y'_\ell]_{\mathcal{W}} \subset \widehat{\mathbb{W}}$. Thus, the last arc of the $\mathcal{W}$-orbit segment $[x'_0, y'_\ell]_{\mathcal{W}}$ and the first arc of the $\mathcal{W}$-orbit segment $[x'_{\ell-1}, y'_n]_{\mathcal{W}}$ must agree, hence $x'_0 \prec_{\mathcal{W}} y'_n$ as claimed.

If in addition, x_0 is an entry point and x_n is an exit point, then $x'_0 \prec_{\mathcal{W}} y'_n$ implies $x_0 \equiv x_n$ by Lemma 5.3.

If $n_{x_0}(t) \geq 1$ for all $t_1 \leq t < t_{n-1}$, then apply the inductive hypothesis to the segment $[x_1, x_{n-1}]_{\mathcal{K}}$ to obtain $x'_1 \prec_{\mathcal{W}} y'_{n-1}$. Using the induction, we have that since x_1 is an entry point and x_{n-1} is an exit point, hence $x_1 \equiv x_{n-1}$. Then, Lemma 5.2 implies that $x'_0 \prec_{\mathcal{W}} y'_n$ and $r(x'_0) = r(y'_n)$. If in addition, x_0 is an entry point and x_n is an exit point, then again, $x'_0 \prec_{\mathcal{W}} y'_n$ implies that $x_0 \equiv x_n$. □

Proposition 5.5 implies that the flow Φ_t on $\mathbb{K}$ satisfies the entry/exit condition.

PROPOSITION 5.6. [33, Proposition 5.2] *Let $x \in \partial_h^- \mathbb{K}$ be a primary entry point and suppose $x_\ell = \Phi_{t_\ell}(x)$ for $0 = t_0 < t_1 < \cdots < t_{n-1} < t_n$ are successive transition points. If $y = x_n$ is a primary exit point, then $x \prec_{\mathcal{W}} y$ and hence $x \equiv y$. Moreover, $n_x(t) \geq 0$ for $0 \leq t < t_n$.*

Proof. If $n = 1$, then $[x_0, x_1]_{\mathcal{K}}$ is a $\mathcal{W}$-arc, and the conclusion follows by the entry/exit condition for $\mathbb{W}$. The case $n = 2$ is impossible by Lemma 4.1.

If $n = 3$, note that x_1 must be a secondary entry point, hence $n_x(t_1) = 1$. The case $n_x(t_2) = 2$ is impossible, as x_3 is a primary exit point, hence x_2 must be a secondary exit point, contrary to assumption. Thus $n_x(t_2) = 0$. Then by Lemma 5.4 we have $x'_1 \equiv y'_2$ and $x'_0 \prec_{\mathcal{W}} y'_3$. As x'_0 is a primary entry point, and y'_3 is a primary exit point of $\mathbb{W}$, they must be facing, or $x \equiv y$.

Now assume that $n > 3$. As before, x_1 must be a secondary entry point with $n_x(t_1) = 1$, so it suffices to prove that $n_x(t_{n-1}) = 0$ and $n_x(t) \geq 0$ for all $0 \leq t \leq t_{n-1}$, and then apply Proposition 5.5. This will imply that $x'_0 \prec_{\mathcal{W}} y'_n$ and as $x_0 = x$ is a primary entry point and $x_n = y$ is a primary exit point, then $x \equiv y$.

We claim that $n_x(t) \geq 0$ for all $0 \leq t < t_n$. Suppose not, then there exists a least $2 < \ell < n$ such that $n_x(t_\ell) = -1$. Then $n_x(t) \geq 0$ for all $0 \leq t < t_\ell$ and $n_x(t_{\ell-1}) = 0$. By Proposition 5.5 we have $x'_0 \prec_{\mathcal{W}} y'_\ell$, and since x_ℓ is an exit point, we have $x_0 \equiv x_\ell$. This implies that x_ℓ is a primary exit point, which is a contradiction as $\ell < n$. We can thus assume that $n_x(t) \geq 0$ for all $t_0 \leq t \leq t_n$ and that $n_x(t_1) = 1$.

If $n_x(t_{n-1}) = k > 0$, consider the greatest integer $0 < \ell < n$ such that $n_x(t_\ell) = k$ and $n_x(t_{\ell-1}) = k - 1$. Then the $\mathcal{K}$-orbit segment $[x_\ell, x_n]_{\mathcal{K}}$ satisfies the conditions of Proposition 5.5 with x_ℓ an entry point, so that $x'_\ell \prec_{\mathcal{W}} y'_n$ and $x_\ell \equiv x_n$. As x_n is a primary exit point and $x_\ell \equiv x_n$, the entry/exit property of the Wilson flow implies that x_ℓ is a primary entry point. This is a contradiction as we have that $\ell > 0$. Then $n_x(t_{n-1}) = 0$ and the proof is finished. □

In summary, the proofs of Propositions 5.5 and 5.6 show that, given a $\mathcal{K}$-orbit segment $[x, y]_{\mathcal{K}}$ in $\mathbb{K}$ with x an entry point, y a facing exit point, the condition $n_x(t) \geq 0$ for the $\mathcal{K}$-orbit between the two points, then there exists a $\mathcal{W}$-orbit segment $[x'_0, y'_n]_{\mathcal{W}}$ in $\mathbb{W}$ between lifts x'_0 of x and y'_n of y. The $\mathcal{W}$-orbit segment $[x'_0, y'_n]_{\mathcal{W}}$ is obtained by an inductive "short-cut" procedure, which replaces the "dynamics" of the Kuperberg flow with that of the Wilson flow.

6. Dynamics and level

In this section, we consider when it is possible to perform an inverse of the short-cut reduction used in Section 5, which replaces a $\mathcal{W}$-arc with a suitable $\mathcal{K}$-orbit segment that spans the gap between the endpoints of a $\mathcal{W}$-orbit segment. The solution to this problem depends on the relations between the functions $\rho_x(t)$, $n_x(t)$, and the lengths of $\mathcal{W}$-orbit segments in $\mathbb{W}$ as will be shown below. An important application of this analysis gives criteria for when the $\mathcal{K}$-orbit of a point $x \in \mathbb{K}$ must necessarily escape through a face of $\mathbb{K}$, either in forward or backward time.

Recall that $\mathcal{D}_i = \sigma_i(D_i) \subset \mathbb{W}$ is the inserted compact region. Define

$$R_* = \max\{R_1, R_2\} \ , \ R_i = \max\{r(x) \mid x \in \mathcal{D}_i\} > 2 \tag{18}$$

Note that for any $x \in \mathbb{W}$ with $r(x) > R_*$, the $\mathcal{W}$-orbit of x in $\mathbb{W}$ does not intercept the inserted regions $\mathcal{D}_i$, but it might intersect the regions D_i. Hence the $\mathcal{K}$-orbit of $\tau(x) \in \mathbb{K}$ escapes through the top face $\partial_h^+\mathbb{K}$ of $\mathbb{K}$ or intersects the secondary exit regions S_i for $i = 1$ or 2 in forward time, and escapes through the bottom face $\partial_h^-\mathbb{K}$ or intersects the secondary entry regions E_i for $i = 1$ or 2 in backward time. Also, for the case where $r(x) = R_*$, the orbit of $\tau(x)$ in $\mathbb{K}$ behaves in the same way as the flow on the boundary of $\mathcal{D}_i$ agrees with the Wilson flow on $\mathbb{W}$.

Let $\mathcal{C}(r) = \{x \in \mathbb{W} \mid r(x) = r\}$ denote the cylinder in $\mathbb{W}$ of radius r, with $\mathcal{C}(2) = \mathcal{C}$ as defined in Section 2. Observe that the entry regions E_i, for $i = 1, 2$ intersect the cylinders $\mathcal{C}(r)$ for $1 \leq r \leq R_*$ in lines. Then for $1 < r \leq R_*$, the radius inequality and the compactness of $\mathcal{C}(r)$ imply there exists a lower bound

$$\delta(r) = \min\{r(\sigma_i^{-1}(x)) \mid x \in \mathcal{C}(r) \cap E_i \ , \ i = 1, 2\} \ \geq \ r \tag{19}$$

with equality only for $r = 2$. Note that $\delta(2) = 2$ and $\delta(R_*) = 3$, and that $\delta(r)$ is an increasing function of r. The graph of $r \mapsto \delta(r)$ is illustrated in Figure 12.

Fix $r_0 > 2$, set $r_1 = \delta(r_0)$ and define $r_k = \delta(r_{k-1})$ recursively, if $r_{k-1} \leq R_*$. By the compactness of the regions $\mathcal{D}_i$ there exists $N(r_0) \geq 0$ such that $r_k \leq R_*$ for $k < N(r_0)$, but $r_k > R_*$ for $k = N(r_0)$. Note that r_k is not defined for $k > N(r_0)$.

We make an observation concerning the hypothesis "x is not a secondary exit point" which is often imposed in the statements of the following results. Consider the level function $n_x(t)$ for the case where $x \in \mathbb{K}$ is a secondary exit point. For $\epsilon > 0$ sufficiently small so that the orbit segment $\{\Phi_t(x) \mid 0 < t \leq \epsilon\}$ contains no

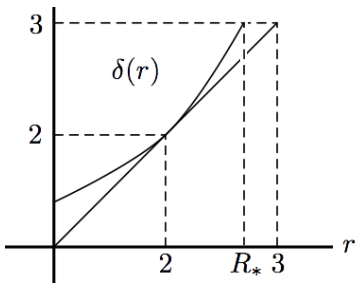

FIGURE 12. The function $\delta(r)$

transition point, then we have that $n_x(t) = 0$ for $0 \leq t < \epsilon$ by the definition (12). Recall that the radius function $r(x) = r(\tau^{-1}(x))$ on $\mathbb{K}$ has a discontinuity at a secondary exit point, where $r(x) = r(x')$ for $x' \in D_i$ with $\tau(x') = x$. As x is a secondary exit point, we have that $\rho_x(t) = r(\Phi_t(x)) = r(x'')$ for $0 < t < \epsilon$ where $x'' = \sigma_i(x')$ as in (8). By the Radius Inequality (K8), we have $r(x'') < r(x')$ unless $r(x') = r(x'') = 2$ where x is a special point. Thus, if x is a secondary exit point with $r(x) > 2$, we have that $\rho_x(t) < r(x)$ for $0 < t < \epsilon$. The assumption x is not a secondary point eliminates this possibility.

We now give a sequence of results relating the level function with the properties of the orbits of Φ_t. First, we show that $N(r_0)$ gives a uniform bound on the level function for forward $\mathcal{K}$-orbits. In what follows, when we say "for all t" we mean "for all t such that $\Phi_t(x)$ is defined".

LEMMA 6.1. *Let $r_0 > 2$. Suppose that $x \in \mathbb{K}$ with $r(x) \geq r_0$ and that $n_x(t) \geq 0$ for all $t \geq 0$. If x is not a secondary exit point, then $n_x(t) \leq N(r_0)$ for all $t \geq 0$.*

Proof. Suppose there exists $t_* > 0$ such that $n_x(t_*) > N(r_0)$. We show this leads to a contradiction. Let $x_\ell = \Phi_{t_\ell}(x)$ with $0 \leq t_0 < t_1 < \cdots < t_m < t_*$ be the transition points for $\{\Phi_t(x) \mid 0 \leq t \leq t_*\}$.

Suppose there exists $k > 1$ such that $n_x(t_{k-1}) = n_x(t_0) = 0$. Then the segment $[x_0, x_k]_{\mathcal{K}}$ satisfies the hypotheses of Proposition 5.5, so we have $x'_0 \prec_{\mathcal{W}} y'_k$ and thus $r(x'_{k-1}) = r(x) \geq r_0$. The length of the $\mathcal{W}$-orbit containing the segment $[x'_0, y'_k]_{\mathcal{W}}$ is bounded above by $L(\epsilon)$ for $\epsilon = r_0 - 2$, from Lemma 4.3. Hence there can exist at most a finite number of values $k > 1$ for which $n_x(t_{k-1}) = n_x(t_0) = 0$.

Let $k \geq 0$ be the largest index such that $n_x(t_{k-1}) = n_x(t_0) = 0$. Set $\ell_1 = k$. Then the segment $[x_0, x_{\ell_1}]_{\mathcal{K}}$ satisfies the hypotheses of Proposition 5.5, so we have $x'_0 \prec_{\mathcal{W}} y'_{\ell_1}$ and thus $r(x'_{\ell_1 - 1}) = r(x) \geq r_0$. As $n_x(t) \geq 0$ for all $t \geq 0$, we must have $1 = n_x(t_{\ell_1}) > n_x(t_{\ell_1 - 1})$ and thus x_{ℓ_1} is a secondary entry point, and so $r(x'_{\ell_1}) \geq r_1$.

The assumption that ℓ_1 is maximal implies that $n_x(t) > 0$ for $t_{\ell_1} \leq t \leq t_*$. If $n_x(t_{\ell_1}) = 1 < N(r_0)$, then repeat the above process to choose ℓ_2 to be the largest index such that $n_x(t_{\ell_2 - 1}) = 1$.

Continuing in this way for $j < N(r_0)$, choose the sequence $0 = \ell_0 < \ell_1 < \cdots < \ell_n$ where $n \leq N(r_0)$ as long as possible, such that ℓ_j is the largest index satisfying $n_x(t_{\ell_j - 1}) = j - 1$ and $n_x(t_{\ell_j}) = j$, for $0 < j \leq n$. Then $r(x'_{\ell_j}) \geq \delta(r(x'_{\ell_j - 1})) \geq \delta(r_{j-1}) = r_j$ since x_{ℓ_j} is a secondary entry point and $r(x'_{\ell_j - 1}) = r(x'_{\ell_{j-1}}) \geq r_{j-1}$.

The assumption $n_x(t_*) > N(r_0)$ implies it is possible to choose an index ℓ_n with $n_x(t_{\ell_n}) = N(r_0)$. By the choice of $N(r_0)$ we have $r_n > R_*$ and $n_x(t) \geq N(r_0)$ for all $t \geq t_{\ell_n}$, and hence the forward $\mathcal{K}$-orbit $\{\Phi_t(x) \mid t \geq t_{\ell_n}\}$ does not contain a transition point. Thus, $\rho_x(t)$ is constant for $t \geq t_{\ell_n}$ and hence the maximum value of $n_x(t)$ is achieved at $t = t_{\ell_n}$, where the value is $N(r_0)$. This contradicts the assumption that $n_x(t_*) > N(r_0)$. □

COROLLARY 6.2. *Suppose that $x \in \mathbb{K}$ satisfies $\rho_x(t) \geq r_0 > 2$ for all $t \geq 0$. Then there exists $n(r_0)$ such that $n(r_0) \leq n_x(t) \leq N(r_0)$ for all $t \geq 0$.*

Proof. Suppose no such lower bound on $n_x(t)$ exists. Let $x_\ell = \Phi_{t_\ell}(x)$ with $0 \leq t_0 < t_1 < \cdots < t_n < \cdots$ be the transition points in $\mathcal{K}$-orbit $\{\Phi_t(x) \mid t \geq 0\}$ and $\{\ell_k \mid k = 1, 2, \ldots\}$ be an increasing subsequence such that $n_x(t_{\ell_k}) = -k$.

Consider the flow $\Xi_t^k(x) = \Phi_{t_{\ell_k}-t}(x)$ on $\mathbb{K}$, then $\Xi_0^k(x) = x_{\ell_k}$ and $\Xi_{t_{\ell_k}}^k(x) = x$. Moreover, $r(\Xi_t^k(x)) \geq r_0$ for all $0 \leq t \leq t_{\ell_k}$. Then the level with respect to the flow Ξ_t^k starting at x_{ℓ_k} increases to k for $0 \leq t \leq t_{\ell_k}$. We can then apply the method of proof of Lemma 6.1 to conclude that the level is bounded above by $N(r_0)$, independent of the choice of k, which contradicts the above. □

These results combine to yield an "escape" result for $\mathcal{K}$-orbits.

PROPOSITION 6.3. *Let $x \in \mathbb{K}$ satisfy $r_0 = r(x) > 2$, assume that x is not a secondary exit point and suppose that $n_x(t) \geq 0$ for all $t \geq 0$. Then the forward $\mathcal{K}$-orbit of x is not trapped.*

Proof. Suppose that the forward orbit of x is trapped, then there exists $0 \leq t_0 < t_1 < \cdots < t_n < \cdots$ so that the points $x_\ell = \Phi_{t_\ell}(x)$ are the forward transition points for the $\mathcal{K}$-orbit $\{\Phi_t(x) \mid t \geq 0\}$. By Lemma 6.1 and our assumption, we have that $0 \leq n_x(t_\ell) \leq N(r_0)$ for all $\ell \geq 0$.

Let $0 \leq n_0 < N(r_0)$ be the least integer such that there exists $0 \leq \ell_0 < \ell_1 < \cdots < \ell_k < \cdots$ such that $n_x(t_{\ell_j}) = n_0$. That is, $n_0 = \liminf_{\ell>0} n_x(t_\ell)$. Since n_0 is the least such integer, there exists $k \geq 0$ such that $n_x(t) \geq n_0$ for all $t \geq t_{\ell_k}$. Then for each integer $\alpha \geq 1$, the segment $[x_{\ell_k}, x_{\ell_{k+\alpha}+1}]_{\mathcal{K}}$ satisfies the hypotheses of Proposition 5.5, so we have $x'_{\ell_k} \prec_{\mathcal{W}} y'_{\ell_{k+\alpha}+1}$. Then by Lemma 4.3 and Corollary 4.5, considering the lengths of the lifted $\mathcal{W}$-orbit segments $[x'_{\ell_k}, y'_{\ell_{k+\alpha}+1}]_{\mathcal{W}}$ yields the estimate $d_{min} \cdot (\ell_{k+\alpha} - \ell_k) \leq L(r_0 - 2)$ for all α. However, we can choose $\ell_{k+\alpha}$ arbitrarily large and hence also $(\ell_{k+\alpha} - \ell_k)$, which yields a contradiction. □

COROLLARY 6.4. *Let $x \in \mathbb{K}$ satisfy $\rho_x(t) > 2$ for all $t \geq 0$, and suppose that $\liminf_{t>0} n_x(t) > -\infty$. Then the forward $\mathcal{K}$-orbit of x is not trapped.*

Proof. Let $t_0 \geq 0$ be such that $x_0 = x_{t_0} = \Phi_{t_0}(x)$ is a transition point with $n_x(t_0) = \liminf_{t>0} n_x(t)$. Then $n_{x_0}(t) \geq 0$ for all $t \geq t_0$ and we have $r(x_0) > 2$. Then apply Proposition 6.3 for $x = x_0$. □

Ghys remarks in [17, Lemme, page 300], that for an entry point $x \in \mathbb{K}$ which escapes to its facing exit point y, so that $x \equiv y$, "the $\mathcal{K}$-orbit of x contains the image under τ of all the $\mathcal{W}$-arcs that lie in $\mathbb{W}'$ between x' and y', where y' is the exit point such that $x' \equiv y'$." Propositions 6.5 and 6.7 below give a precise formulation of this assertion. Figure 13 illustrates these lifts.

PROPOSITION 6.5. *Let $x' \in \mathbb{W}$ such that $x = \tau(x')$ is a primary entry point in $\mathbb{K}$ with $r(x) > 2$. Then the $\mathcal{K}$-orbit of x escapes from $\mathbb{K}$ at some primary exit point w, we have that $\rho_x(t) \geq r(x)$ for all t and the collection of lifts of the $\mathcal{W}$-arcs in $[x, w]_{\mathcal{K}}$ contains all the $\mathcal{W}$-arcs of the $\mathcal{W}$-orbit of x' that are in $\widehat{\mathbb{W}}$.*

Proof. Suppose that the forward orbit of x is trapped, then there exists $0 = t_0 < t_1 < \cdots < t_n < \cdots$ with $x_\ell = \Phi_{t_\ell}(x)$ the transition points for the $\mathcal{K}$-orbit $\{\Phi_t(x_0) \mid t \geq 0\}$. We claim that $n_{x_0}(t) \geq 0$ for all $t \geq 0$, then the result follows from Proposition 6.3 and Proposition 5.6.

Suppose $n_{x_0}(t) < 0$ for some $t > 0$, then there is a least $k > 0$ such that $n_{x_0}(t_k) = -1$, and thus $n_{x_0}(t_{k-1}) = 0$ and x_k is an exit point. Proposition 5.5 then implies that $x'_0 \prec_{\mathcal{W}} x'_k$ and $x_0 \equiv x_k$. Since x_0 is a primary entry point, we must have that x_k is a primary exit point, which is a contradiction. Thus, $n_{x_0}(t) \geq 0$ for all $t \geq 0$.

Next, note that as x_0 is a primary entry point, $[x'_0, y'_1]_{\mathcal{K}} \subset \widehat{\mathbb{W}}$ is the initial $\mathcal{W}$-arc in the intersection of the $\mathcal{W}$-orbit of x' with $\widehat{\mathbb{W}}$. Then let $\ell_1, \ell_2, \ldots, \ell_m$ be the collection of all the indices such that $n_{x_0}(t_{\ell_k - 1}) = 0$ for all $k = 1, 2, \ldots, m$. Proposition 5.5 implies that $x'_0 \prec_{\mathcal{W}} y'_{\ell_1}$ and $x_1 \equiv x_{\ell_1 - 1}$, hence the subsequent lift $[x'_{\ell_1 - 1}, y'_{\ell_1}]_{\mathcal{K}} \subset \widehat{\mathbb{W}}$ is the second arc in the intersection of $\mathcal{W}$-orbit of x'_0 with $\widehat{\mathbb{W}}$. Continuing by induction, we obtain that all the $\mathcal{W}$-arcs for x'_0 lying in $\widehat{\mathbb{W}}$ are contained in the $\mathcal{K}$-orbit of x_0. □

There is an important consequence of this result.

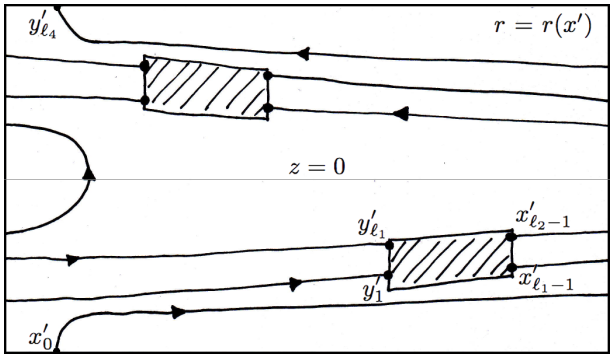

FIGURE 13. The arcs of the lifted $\mathcal{K}$-segment $[x, y]$ on the cylinder $r = r(x')$ with $x = x_0$ and $y = x_{\ell_4}$

COROLLARY 6.6. *Let $z \in \mathbb{K}$ satisfy $r(z) > 2$ and $n_z(t) \geq 0$ for all $t \geq 0$. Then the forward $\mathcal{K}$-orbit of z exits $\mathbb{K}$ in a point $y = \Phi_T(z)$ at which $n_z(T) = 0$. Furthermore, z is contained in a bounded orbit of Φ_t, starting at a primary entry point x of $\mathbb{K}$, where $x \equiv y$.*

Proof. Proposition 6.3 implies that the flow Φ_t has a primary exit point y at time T. Note that $n_z(T) \geq 0$ implies $r(y) \geq r(z) > 2$ by Proposition 5.5.

Then apply Proposition 6.5 to the reverse flow $\Xi_t^T(\xi) \equiv \Phi_{T-t}(\xi)$ to deduce that there exists $t_* \geq T$ such that $x = \Xi_{t_*}^T(y)$ is a primary *exit* point for Ξ_t^T and hence a primary *entry* point for Φ_t. Moreover, the proof of Proposition 6.5 shows that $n_x(t) \geq 0$ for all $t \geq 0$. Note that $y = \Phi_T(z) = \Phi_{t_*}(x)$ so we also have $n_x(t_*) = 0$.

The fact $n_z(T) = 0$ follows form the equality $n_z(t) = n_x(t_* - T + t) - n_x(t_* - T)$ for all $t \geq 0$. Thus $n_z(T) = n_x(t_*) - n_x(t_* - T) = -n_x(t_* - T) \leq 0$. Since $T \geq 0$ and $n_z(T) \geq 0$ by hypothesis, $n_z(T) = 0$ as claimed. □

The conclusion of Corollary 6.6 has a simple geometric interpretation. Given a *primary* entry point $x \in \mathbb{K}$ with $r(x) > 2$, the points $z = \Phi_t(x)$ along the $\mathcal{K}$-orbit of x for which $n_x(t) = 0$ are *exactly* those points on the Wilson flow of x' which lie in $\widehat{\mathbb{W}}$. Proposition 6.5 implies that each such $\mathcal{W}$-arc of the $\mathcal{W}$-orbit of x' is contained in the $\mathcal{K}$-orbit of x. Observe that by taking $z \in \mathbb{K}$ with $r(z) > 2$ and $n_z(t) \geq 0$ for all $t \geq 0$, we assume that $z' \in \mathbb{W}$ such that $\tau(z') = z$ belongs to a $\mathcal{W}$-orbit whose entry point is in $\partial_h^- \mathbb{W} - (L_1^1 \cup L_2^-)$.

Note that Proposition 6.5 implies that the endpoints of the $\mathcal{K}$-orbit through z are facing, so that $x \equiv y$. The following result is valid for secondary entry points, and is used repeatedly in subsequent arguments.

PROPOSITION 6.7. *Let $x \in \mathbb{K}$ be a secondary entry point with $r(x) > 2$, let y be a secondary exit point and suppose that $x \equiv y$. Then $x \prec_{\mathcal{K}} y$ and the collection of lifts of the $\mathcal{W}$-arcs in $[x, y]_{\mathcal{K}}$ contains all the $\mathcal{W}$-arcs of the $\mathcal{W}$-orbit of x' that are in $\widehat{\mathbb{W}}$, where $\tau(x') = x$. Hence, if $[\xi', x']_{\mathcal{W}}$ and $[y', z']_{\mathcal{W}}$ are $\mathcal{W}$-arcs, then their images under τ are both contained in the $\mathcal{K}$-orbit through x.*

Proof. Corollary 6.6 implies there exists a maximal $t_* > 0$ such that $n_x(t) \geq 0$ for $0 \leq t < t_*$ as x is assumed to be a secondary entry point. Then $x_* = \Phi_{t_*}(x)$ must be an exit point.

Let $0 = t_0 < t_1 < \cdots < t_n = t_*$ with $x_\ell = \Phi_{t_\ell}(x)$ be the transition points for the $\mathcal{K}$-orbit $\{\Phi_t(x) \mid 0 \leq t \leq t_n\}$. Then $n_x(t) \geq 0$ for all $0 \leq t < t_n$, and $n_x(t_{n-1}) = 0$. Hence x_{n-1} and x_n are exit points. By Proposition 5.5, $x'_0 \prec_{\mathcal{W}} y'_n$ and $x_0 \equiv x_n$. The point facing x is unique, so we must have $y = x_n = \tau(y'_n)$ and $x \prec_{\mathcal{K}} y$.

The proof that the segment $[x, y]_{\mathcal{K}}$ contains all the $\mathcal{W}$-arcs on the $\mathcal{W}$-orbit of x' that are in $\widehat{\mathbb{W}}$ follows as in the proof of Proposition 6.5. The first transition point x_1 must be a secondary entry as $n_x(t_1) \geq 0$, thus $n_x(t_1) = 1$. If $n_x(t_2) = 0$ then x_2 is a secondary exit, so by Proposition 5.5 we have that $x' \prec_{\mathcal{W}} x'_3$ and so

$x_1 \equiv x_2$. Thus the lift of the $\mathcal{W}$-arc $[x_2, x_3]_{\mathcal{K}}$ is contained in the $\mathcal{W}$-orbit of x'. Otherwise, $n_x(t_2) = 2$ and we continue the analysis of cases, until we obtain the first instance where $n_x(t_{\ell-1}) = 0$. We can then apply Proposition 5.5 to conclude that $x'_0 \prec_{\mathcal{W}} y'_\ell$. Thus the lift of the $\mathcal{W}$-arc $[x_{\ell-1}, x_\ell]_{\mathcal{K}}$ is contained in the $\mathcal{W}$-orbit of x'. The rest follows as in the proof of Proposition 6.5. □

Let $x' \in \partial_h^- \mathbb{W}$ with $r(x') > 2$ and let $y' \in \partial_h^+ \mathbb{W}$ be the unique facing point. Let $x = \tau(x')$ and $y = \tau(y')$. If x is a primary entry point, then $x \prec_{\mathcal{K}} y$ by Proposition 6.5. If x is a secondary entry point, then $x \prec_{\mathcal{K}} y$ by Proposition 6.7. Thus, in both cases there exists $T_x > 0$ such that $\Phi_{T_x}(x) = y$.

COROLLARY 6.8. *The function $x' \mapsto T_{x'}$ is well-defined and continuous for $x' \in \partial_h^- \mathbb{W}$ with $r(x') > 2$. Moreover, $T_{x'}$ tends to infinity as $r(x')$ tends to 2.* □

7. Trapped and infinite orbits

In this section, we begin the analysis of the trapped orbits of the flow Φ_t. We first consider the orbits of points $x = \tau(x')$ with $r(x') = 2$. The following result is a general formulation of an observation of Kuperberg, which provided the original insight leading to her construction [28] and was sketched in Figure 10.

PROPOSITION 7.1. *Let $x' \in \mathbb{W}'$ with $r(x') = 2$ and set $x = \tau(x')$. Then the $\mathcal{K}$-orbit of x is trapped in either forward or backward time, or both. Moreover, the collection of $\mathcal{W}$-arcs for the $\mathcal{K}$-orbit of x contains every $\mathcal{W}$-arc lying in $\widehat{\mathbb{W}}$ of the $\mathcal{W}$-orbit of x' and there is a subsequence $\{x'_{\ell_j} \mid j = 1, 2, \ldots\}$ of transition points with $r(x'_{\ell_j}) = 2$ such that $\{x_{\ell_j} = \tau(x'_{\ell_j}) \mid j = 1, 2, \ldots\}$ converges to a special point p_i^- for $i = 1, 2$.*

Proof. Assume without loss of generality that x is not a transition point and let $x_\ell = \Phi_{t_\ell}(x)$, for $0 < t_0 < t_1 < \cdots < t_n < \cdots$, be the transition points for the $\mathcal{K}$-orbit $\{\Phi_t(x) \mid t \geq 0\}$. There are five cases to consider:

(1) $z(x') = -1$;
(2) $z(x') = 1$;
(3) $-2 \leq z(x') < -1$;
(4) $-1 < z(x') < 1$;
(5) $1 < z(x') \leq 2$;

Consider first the case of the forward $\mathcal{K}$-orbit of a point $x = \tau(x')$ with $x' \in \mathbb{W}'$, $r(x') = 2$ and $z(x') = -1$. Then $x_0 \in E_1$ is the special point p_1^- of (11) and for the $\mathcal{W}$-arc $[x'_0, y'_1]_{\mathcal{W}} \subset \mathbb{W}'$ we have $x'_0 \in L_1^- \subset \partial_h^- \mathbb{W}$. Then $r(x'_0) = 2$ by Condition (K7) so that $r(y'_1) = 2$ also. The $\mathcal{W}$-arc $[x'_0, y'_1]_{\mathcal{W}}$ flows upward from $z(x'_0) = -2$ until it intersects at $y'_1 \in \mathcal{L}_1^-$ with $z(y'_1) < -1$, as in Figure 10. Let $x'_1 \in L_1^-$ satisfy $\tau(x'_1) = \tau(y'_1)$, then the Radius Inequality implies that $r(x'_1) > 2$. Let $\overline{x}_1 \in S_1$ be the facing point to x_1. Then by Proposition 6.7, we have $x_1 \prec_{\mathcal{K}} \overline{x}_1$ and so $\overline{x}_1 = x_{\ell_1 - 1}$ for some $\ell_1 > 2$. Then $r(x'_{\ell_1 - 1}) = 2$, $z(y'_1) < z(x'_{\ell_1 - 1}) < -1$ and $[x'_{\ell_1 - 1}, y'_{\ell_1}]_{\mathcal{W}}$ is the subsequent $\mathcal{W}$-arc. Thus $x_{\ell_1} = \tau(y'_{\ell_1})$ must be a secondary entry point again and we can repeat this argument inductively to obtain a subsequence $\{y'_{\ell_i} \mid i = 1, 2, \ldots\}$ in $\mathcal{L}_1^-$ with $x_{\ell_i} = \tau(y'_{\ell_i})$ in E_1 converging to p_1^-, so that the forward orbit of x is trapped. The assertion about the collection of lifts of $\mathcal{W}$-arcs in $\widehat{\mathbb{W}}$ follows from Proposition 6.7. A similar analysis for the backward orbit of x yields a subsequence of transition points converging to p_2^-.

For the case of $x = \tau(x')$ with $x' \in \widehat{\mathbb{W}}$, $r(x') = 2$ and $z(x') = 1$, note that the first forward transition point $x_0 \in E_2$ is the special point p_2^- of (11) and so for the $\mathcal{W}$-arc $[x'_0, y'_1]_{\mathcal{W}} \subset \mathbb{W}'$ we have $x'_0 \in L_2^- \subset \partial_h^- \mathbb{W}'$. Then again $r(x'_0) = 2$ by Condition (K7) and the rest of the analysis proceeds similarly to the previous case. Note that the forward orbits of a point $x = \tau(x')$ in the two cases where $r(x') = 2$ and $z(x') = \pm 1$ limit to p_1^-, while their backward orbits tend to p_2^-.

There are three remaining cases: either $-2 \leq z(x') < -1$, $-1 < z(x') < 1$, or $1 < z(x') \leq 2$. All three cases proceed in a manner analogous to the two cases above.

If $-2 < z(x') < -1$, then the forward $\mathcal{W}$-orbit of x' is asymptotic to the periodic orbit $\mathcal{O}_1$, so in particular is trapped for the Wilson Plug and each time the $\mathcal{W}$-orbit enters an insertion region $\mathcal{D}_i \subset \mathbb{W}$, it subsequently exits through the facing point. Thus, the forward $\mathcal{K}$-orbit of the point $x = \tau(x')$ has first transition point $x_0 \in E_1$. As x' is not in a periodic orbit, we have $x'_0 = \tau^{-1}(x_0) \in L_1^-$ with $r(x'_0) > 2$. Let $x_{\ell_1 - 1} \in S_1$ be the facing point, by Proposition 6.7 $x_0 \prec_{\mathcal{K}} x_{\ell_1 - 1}$. We then proceed as above, to obtain a subsequence $\{x_{\ell_i} \mid i = 0, 1, 2, \ldots\}$ in E_1 with x_{ℓ_i} converging to p_1^-.

Note that the backward $\mathcal{W}$-orbit of x' is not trapped and so exits $\mathbb{W}$ at a point y'. The backward $\mathcal{K}$-orbit of x contains the point $y = \tau(y')$. If $y \notin L_i^-$ for $i = 1, 2$, then the backward $\mathcal{K}$-orbit of x is not trapped. If $y \in L_i^-$ for $i = 1, 2$, then the process continues in the backward direction.

For the case $-1 < z(x') < 1$, the forward $\mathcal{W}$-orbit of x' in $\mathbb{W}$ is asymptotic to the periodic orbit $\mathcal{O}_2$, and each time the $\mathcal{W}$-orbit enters an insertion region $\mathcal{D}_i$ it subsequently exits the same region. The rest of the analysis proceeds similarly to the case when $-2 \leq z(x') < -1$, yielding a subsequence of secondary entry points for the forward $\mathcal{K}$-orbit which converge to p_2^-. The backward $\mathcal{W}$-orbit of x' in $\mathbb{W}$ is asymptotic to the periodic orbit $\mathcal{O}_1$, yielding in the same manner a subsequence of secondary entry points for the reverse $\mathcal{K}$-orbit converging to p_1^-.

The last case, for $1 < z(x') \leq 2$, reduces to the case for $-2 \leq z(x') < -1$ by reversing the flow Φ_t. Thus, the forward $\mathcal{K}$-orbit of x may escape through $\partial_h^+ \mathbb{K}$ or may be trapped for all forward time. The backward $\mathcal{W}$-orbit of x' always converges to $\mathcal{O}_2$ and so yields a subsequence of secondary entry points for the reverse flow converging to p_2^-. □

We observe two additional consequences of Proposition 7.1 and its proof.

COROLLARY 7.2. *Let $x \in \mathbb{K}$ and suppose that either x is a primary entry point with $r(x) = 2$, or $x = \tau(x')$ where $x' \in \mathcal{O}_i \cap \mathbb{W}'$ for $i = 1, 2$. Then the level function based at x satisfies $n_x(t) \geq 0$ for all $t \geq 0$. Moreover, if $\Phi_t(x)$ is not a transition point for $t \geq 0$, then $n_x(t) = 0$ if and only if $\rho_x(t) = 2$.* □

COROLLARY 7.3. *Let $x \in \mathbb{K}$ and suppose there exists $t_* \in \mathbb{R}$ such that $y = \Phi_{t_*}(x)$ is a secondary entry point with $\rho_x(t_*) = 2$. Then for all $t > t_*$ we have that $\rho_y(t) \geq 2$. Moreover, the forward orbit of x contains an infinite sequence of secondary entry points that limit to $p_i^- \in E_i^-$ for $i = 1$ or $i = 2$.* □

We next consider the $\mathcal{K}$-orbits of points $x \in \mathbb{K}$ for which $r(x) < 2$. We recall results by Ghys [17] and Matsumoto [33], which give conditions such that the orbit of x is trapped in forward time and that the closure of the $\mathcal{K}$-orbit of x contains a special point. Hence the closure of the $\mathcal{K}$-orbit of x contains the closures of the orbits of both special points p_1^- and p_2^-.

Fix $i = 1, 2$ and consider the restriction of the insertion map $\sigma_i \colon L_i^- \to \mathcal{D}_i \subset \mathbb{W}$. Express this map in polar coordinates (r', θ') on the domain L_i^- and (r, θ, z) on the image. The image under σ_i of the curve $\{r' = 2\} \cap L_i^-$ is a "parabolic curve" Υ which is tangent to the vertical line $\{r = 2\}$. For each $i = 1, 2$, we define two regions (see Figure 14) contained in the image of the region $\mathcal{L}_i^- \cap \{r < 2\}$:

- $\mathcal{E}_i^{-,-} = \sigma_i(\{r' < 2\} \cap L_i^-) \cap \{r < 2\}$ with outer boundary Υ
- $\mathcal{E}_i^{-,+} = \sigma_i(\{r' > 2\} \cap L_i^-) \cup \{r < 2\}$ with inner boundary Υ.

We make two basic observations, as used in the proof of [33, Proposition 7.1]. First, the tangency of Υ with the vertical line $\{r = 2\}$ and Taylor's Theorem implies that for $\delta > 0$ sufficiently small, the vertical line segment $\mathcal{E}_i^{-,-} \cap \{r = 2 - \delta\}$ has length at least $C' \cdot \sqrt{\delta}$ for some fixed $C' > 0$.

The second observation is that the Wilson vector field $\mathcal{W}$ is horizontal along the periodic orbits $\mathcal{O}_i$ as the vertical component $g(r, \theta, z)\frac{\partial}{\partial z}$ in (3) vanishes at the points $(2, \theta, \pm 1)$. Thus, there exists $C'' > 0$ so that for $\delta > 0$ sufficiently small, the flow $\Psi_t(x')$ of a point $x' \in \mathbb{W}$ with $r(x') = 2 - \delta$ intersects the face $\mathcal{L}_i^-$ in a sequence of points whose vertical spacing near the planes $\{z = \pm 1\}$ is bounded above by $C'' \cdot \delta$. A more precise estimate can be obtained using the method of proof for Lemma 17.5, but these approximate results suffice for the proof of Proposition 7.5 below.

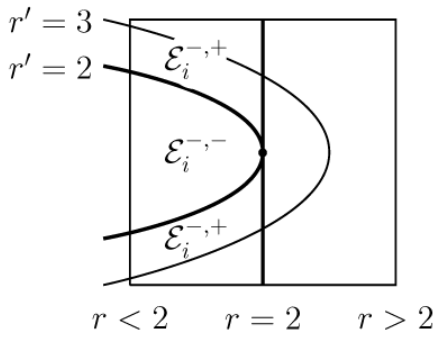

FIGURE 14. The regions $\mathcal{E}_i^{-,-}$ and $\mathcal{E}_i^{-,+}$ of $\mathcal{L}_i^-$

DEFINITION 7.4. *We say that $\delta_M > 0$ is a Matsumoto constant if for all $0 < \delta \leq \delta_M$ and C', C'' as above, then*

$$C'' \cdot \delta < C' \cdot \sqrt{\delta} \tag{20}$$

The Matsumoto region *for δ_M is the set $\mathcal{U}(\delta_M) = \tau(\{2 - \delta_M < r < 2\}) \subset \mathbb{K}$.*

PROPOSITION 7.5. [33, Proposition 7.1] *Let $\delta_M > 0$ be a Matsumoto constant, and $x = \tau(x') \in \mathcal{U}(\delta_M)$.*

1. *If $z(x') = -2$, then the* forward orbit *of x is trapped. Moreover, there exists a subsequence of transition times, $0 < t_0 < t_{\ell_1} < \cdots < t_{\ell_i} < \cdots$, such that $r(x'_{\ell_i}) \leq 2$ for $i \geq 0$ with $\lim_{i\to\infty} r(x'_{\ell_i}) = 2$.*
2. *If $z(x') = 2$, then the backward orbit of x is trapped. Moreover, there exists a subsequence of transition times, $0 > t_0 > t_{\ell_1} > \cdots > t_{\ell_i} > \cdots$, such that $r(x'_{\ell_i}) \leq 2$ for $i \geq 0$ with $\lim_{i\to\infty} r(x'_{\ell_i}) = 2$.*
3. *If $z(x') = 0$, then the orbit of x is infinite and there exists a bi-infinite subsequence of transition times such that $r(x'_{\ell_i}) \leq 2$ for all i, with $\lim_{i\to\pm\infty} r(x'_{\ell_i}) = 2$.*

Proof. We consider first the case $z(x') = -2$. The case $z(x') = 2$ follows analogously, by reversing the flow Φ_t. Figure 15 illustrates the following construction.

Given $x'_0 = (r_0, \theta, -2)$ which satisfies $2 - \delta_M < r_0 < 2$, the $\mathcal{W}$-orbit of x'_0 has increasing z-coordinate in $\mathbb{W}$ and intersects the face $\mathcal{L}_1^-$ in the set $\mathcal{E}_1^{-,+}$, possibly repeatedly, until it first intersects either the curve Υ or the region $\mathcal{E}_1^{-,-}$. If $\Psi_{t_*}(x'_0) \in \Upsilon$ for some $t_* > 0$, then $r(\tau(\Psi_{t_*}(x'_0))) = 2$ and the analysis of the forward orbit reduces to the case of Corollary 7.3.

Otherwise, the assumption that $2 - \delta_M < r_0 < 2$ implies the initial segment of the $\mathcal{K}$-orbit of $x_0 = \tau(x'_0)$ contains a sequence of $\mathcal{W}$-arcs which coincide with the initial $\mathcal{W}$-arcs of the $\mathcal{W}$-orbit of x'_0, up until the initial point of the $\mathcal{W}$-arc that is contained in $\mathcal{E}_1^{-,-}$. Then the $\mathcal{K}$-orbit jumps to a radius r_1 with $\delta_M < r_0 < r_1 < 2$ and this pattern repeats itself. We make this sketch of proof precise.

Let $x_\ell = \Phi_{t_\ell}(x_0)$ with $0 = t_0 < t_1 < \cdots < t_n < \cdots$ be the transition points for the $\mathcal{K}$-orbit $\{\Phi_t(x_0) \mid t \geq 0\}$. Denote the corresponding lifts to $\mathbb{W}$ of the $\mathcal{W}$-arcs in this forward orbit by $[x'_\ell, y'_{\ell+1}]_{\mathcal{W}}$. As remarked above, we can assume that $r(x'_\ell) \neq 2$ for all ℓ. The orbit of x_0 is then described by an iterative process, as follows.

Note that $x'_0 \in \partial_h^- \mathbb{W}$ implies that $y'_1 \in \mathcal{L}_1^-$, so $n_{x_0}(t_1) = 1$. If $x_1 \in \mathcal{E}_1^{-,-}$, set $\lambda_1 = 1$, $\eta_1 = x_1$ and $r_1 = r(\eta_1)$. Then note that $r(y'_1) = r(x'_0) = r_0$ while $r_0 < r(\eta'_1) < 2$ by the definition of the region $\mathcal{E}_1^{-,-}$.

Otherwise, we have $x_1 \in \mathcal{E}_1^{-,+}$ and so $r(y'_1) = r_0$ while $r(x'_1) > 2$ by definition. Proposition 6.7 implies that there is a least $\ell_1 > 1$ such that $n_{x_0}(t_{\ell_1 - 1}) = 0$, so that x_0 and x_{ℓ_1} satisfy $x'_0 \prec_{\mathcal{W}} x'_{\ell_1 - 1}$ by Proposition 5.5 and $r(x'_{\ell_1 - 1}) = r_0$. Then x_{ℓ_1} is a secondary entry point.

If $x_{\ell_1} \in \mathcal{E}_i^{-,-}$ then set $\lambda_1 = \ell_1$, $\eta_1 = x_{\ell_1}$ and $r_1 = r(\eta_1)$. Otherwise, $x_{\ell_1} \in \mathcal{E}_i^{-,+}$ and so $r(x'_{\ell_1}) > 2$, and we repeat this process. By Corollary 4.6 and the choice of δ, this inductive process can be repeated at most a

finite number of times, until we obtain $\{0 = \ell_0 < \ell_1 < \cdots < \ell_{k_0}\}$ with $r(x'_{\ell_i - 1}) = r_0$, $r(x'_{\ell_i}) > 2$ for $1 \leq i < k_0$ and $r_0 < r(x'_{\ell_{k_0}}) < 2$. Thus $x_{\ell_{k_0}} \in \mathcal{E}_i^{-,-}$. Then set $\lambda_1 = \ell_{k_0}$, $\eta_1 = x_{\lambda_1}$ and $r_1 = r(\eta_1)$.

We thus obtain the secondary entry points $\{y'_{\ell_i} \mid 0 \leq i < k_0\} \subset \{r = r_0\} \cap \mathcal{L}_1^-$ all contained in a vertical line $r = r_0$, plus a new point $\eta_1 \in E_1$ with lifts $y'_{\lambda_1} \in \{r = r_0\} \cap \mathcal{L}_1^-$ and $x'_{\lambda_1} = \eta'_1$ and $r_0 < r_1 = r(\eta'_1) < 2$. We can then repeat the above process by considering the $\mathcal{K}$-orbit of η_1, which yields an ascending finite sequence of secondary entry points $\{x_{\ell_i}\}$ with $\{y'_{\ell_i}\}$ contained in the vertical line segment $\mathcal{E}_1^{-,+} \cap \{r = r_1\}$, until they reach the point $\eta_2 = x_{\lambda_2} \in \mathcal{E}_1^{-,-}$ with radius $r_0 < r_1 < r_2 = r(\eta_2) < 2$.

This process then continues recursively, so that the sequence of transition points $\{x_i \mid i \geq 0\}$ contains an infinite collection of finite subsequences lying on the lines $\{r = r_j\} \cap \mathcal{L}_1^-$ with $r_0 < r_1 < r_2 < \cdots < 2$, where the initial points η_j for each such "finite stack of points" is defined as the secondary entry points where the sequence transitions from the region $\mathcal{E}_1^{-,+}$ to the region $\mathcal{E}_1^{-,-}$. Moreover, the sequence of radii $r_j \to 2$ by the Radius Inequality. Finally, note that the forward $\mathcal{K}$-orbit of x_0 satisfies $r(\eta_\ell) < r(\eta_{\ell+1})$ so the orbit cannot be recurrent.

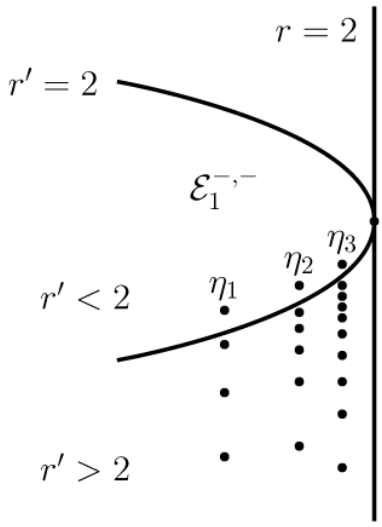

FIGURE 15. Trapped orbits intersecting $\mathcal{E}_1^{-,-}$ infinitely often

As noted above, if $x'_0 = (r_0, \theta, 2)$ with $2 - \delta_M < r_0 < 2$, then we obtain a similar conclusion using the reverse time flow and the z-symmetry of the flow $\mathcal{W}$ on $\mathbb{W}$.

If $x'_0 = (r_0, \theta, 0)$ with $2 - \delta_M < r_0 < 2$, then the forward $\mathcal{W}$-orbit of x'_0 has increasing z-coordinate in $\mathbb{W}$, and intersects the face $\mathcal{L}_2^-$ in the set $\mathcal{E}_2^{-,+}$, possibly repeatedly, until it first intersects either the curve Υ, or the region $\mathcal{E}_2^{-,-}$. The analysis then proceeds as above. The backward $\mathcal{W}$-orbit of x'_0 has decreasing z-coordinate in $\mathbb{W}$, and we obtain a similar conclusion using the z-symmetry of the Wilson flow. □

Suppose that $r(x) < 2$ and assume there exists $t_0 > 0$ such that $\rho_x(t_0) = 2$. Then by Corollary 7.3, the forward orbit $\{\Phi_t(x) \mid t \geq t_0\}$ is trapped in the region $\{r \geq 2\}$.

For $r(x) < 2$, it remains to consider the case where $\rho_x(t) \neq 2$ for all $t \geq 0$. The proof of the next result is adapted from the proof of the Théorème in [17, page 301].

PROPOSITION 7.6. *Let $x \in \mathbb{K}$ satisfy $r(x) < 2$ and assume that its forward orbit is trapped and satisfies $\rho_x(t) \neq 2$ for all $t \geq 0$. Then there exists an infinite subsequence of transition points $\{x_{\ell_i} \mid i = 1, 2, \ldots\}$ with $r(x'_{\ell_i}) < 2$ such that $\lim_{i \to \infty} r(x'_{\ell_i}) = 2$.*

Proof. Let $x_\ell = \Phi_{t_\ell}(x)$ with $0 < t_0 < t_1 < \cdots < t_n < \cdots$ be the transition points for $\{\Phi_t(x) \mid t \geq 0\}$, with associated lifts of $\mathcal{W}$-arcs $[x'_\ell, y'_{\ell+1}]_{\mathcal{W}}$.

We first show that $r(x'_\ell) < 2$ for an infinite number of indices ℓ. If not, then there exists $\ell_0 \geq 0$ which is the least index such that $r(x'_\ell) \geq 2$ for all $\ell \geq \ell_0$. As $r(x'_\ell) \neq 2$ for all $\ell \geq 0$, thus $r(x'_\ell) > 2$ for all $\ell \geq \ell_0$. In particular, the choice of ℓ_0 implies that $r(x'_{\ell_0-1}) < 2$. Then $x_{\ell_0} \in E_i$ for $i = 1$ or $i = 2$, and let $\overline{x}'_{\ell_0} \in L_i^+$ be the facing point to $x'_{\ell_0} \in L_i^-$. As $r(x'_{\ell_0}) > 2$, Proposition 6.7 implies that $x_{\ell_0} \prec_{\mathcal{K}} \overline{x}_{\ell_0}$ where $\overline{x}_{\ell_0} = \tau(\overline{x}'_{\ell_0})$. Thus there exists $\ell_1 > \ell_0$ such that $x_{\ell_1} = \overline{x}_{\ell_0}$. Then $x'_{\ell_0-1} \prec_{\mathcal{W}} x'_{\ell_1}$ by Lemma 5.2 and so $r(x'_{\ell_1}) = r(y'_{\ell_0}) = r(x'_{\ell_0-1}) < 2$. This contradicts the choice of ℓ_0, and thus the set of indices ℓ for which $r(x'_\ell) < 2$ must be infinite.

Next, we show that there exists a subsequence $\{x'_{\ell_i} \mid i = 1, 2, \ldots\}$ with $r(x'_{\ell_i}) < 2$ such that $\lim_{i\to\infty} r(x'_{\ell_i}) = 2$. Set $r_* = \limsup\{r(x'_\ell) \mid \ell \geq 0 \text{ such that } r(x'_\ell) < 2\}$ and let $\epsilon_* = 2 - r_* \geq 0$ and $r'_* = 2 - \epsilon_*/2 \leq 2$. Assume that $\epsilon_* > 0$, then we show this yields a contradiction.

Note that for all $0 < \epsilon < \epsilon_*$ the collection $\{x'_\ell \mid 2 - \epsilon \leq r(x'_{\ell_i}) < 2\}$ is finite by the definition of r_*. We can thus choose $\ell_* \geq 0$ so that $r(x'_{\ell_*}) < 2$ and satisfying the condition that for all $\ell \geq \ell_*$, if $r(x'_\ell) < 2$ then $r(x'_\ell) < r'_*$. Set $t_* = t_{\ell_*}$.

Observe that Radius Inequality (K8) implies that there exists $\delta_*^+ > 0$ so that if $r(x'_\ell) \leq r'_*$ and $x_{\ell+1}$ is a secondary entry point, then $r(x'_{\ell+1}) > r(x'_\ell) + \delta_*^+$. Conversely, the Radius Inequality also implies there exists $\delta_*^- > 0$ such that if $r(x'_\ell) \leq r'_*$ and $x_{\ell+1}$ is a secondary exit point, then $r(x'_{\ell+1}) < r(x'_\ell) - \delta_*^-$.

LEMMA 7.7. *There exists a greatest lower bound N_* such that $n_x(t) \geq N_*$ for all $t \geq 0$.*

Proof. The set of values $\{n_x(t) \mid 0 \leq t \leq t_*\}$ is finite, so it suffices to show there is a lower bound on $n_x(t)$ when $t \geq t_*$.

If no such bound exists, then there exists an increasing subsequence of indices $\{\ell_i > \ell_* \mid i \geq 1\}$ with $n_x(t_{\ell_1}) = n_x(t_*) - 1$ and $n_x(t_{\ell_i}) = n_x(t_*) - i$ for all $i > 1$. Moreover, we can assume that ℓ_i is the least index $\ell > \ell_i$ such that $n_x(t_\ell) = n_x(t_{\ell_i}) - 1$. Consequently, each point x_{ℓ_i} must be a secondary exit point.

If $\ell_{i+1} > \ell_i + 1$, then $n_x(t_k) \geq n_x(t_{\ell_i})$ for $\ell_i \leq k < \ell_{i+1}$, so by Proposition 5.5 we have $x'_{\ell_i} \prec_{\mathcal{W}} y'_{\ell_{i+1}}$ and $r(x'_{\ell_i}) = r(y'_{\ell_{i+1}})$. For $i = 1$, this yields

$$r(x'_{\ell_1}) < r(x'_{\ell_1-1}) - \delta_*^- = r(x'_{\ell_*}) - \delta_*^- < r'_*$$

so that $r(x'_{\ell_1}) < 2$. Then by induction, we have that $r(x'_{\ell_i}) < r(x'_{\ell_*}) - i\,\delta_*^- < r'_* - i\,\delta_*^-$ and in particular $r(x'_{\ell_i}) < 2$.

As $r(x'_{\ell_i}) \geq 1$ and $r'_* < 2$, the value of the index i is bounded by $i \leq 1/\delta_*^-$, contradicting our assumption that the subsequence is infinite. □

Let $N_* = \min\{n_x(t) \mid t \geq 0\}$, and let $0 < t_{\ell_1} < t_{\ell_2} < \cdots < t_{\ell_k}$ be the sequence of times such that $n_x(t_{\ell_i}) = N_*$. Note that the sequence $t_{\ell_i} < t_{\ell_i+1} < \cdots < t_{\ell_{i+1}+1}$ satisfies the hypotheses of Proposition 5.5 for each $i \geq 1$, and thus $x'_{\ell_i} \prec_{\mathcal{W}} x'_{\ell_{i+1}}$ so $r(x'_{\ell_i}) = r(x'_{\ell_{i+1}})$. Then as in the proof of Proposition 6.3, this implies that $x'_{\ell_1} \prec_{\mathcal{W}} x'_{\ell_i}$ for all $i > 1$. However, $r(x'_{\ell_1}) < r'_* < 2$ so by Lemma 4.3 the length of the $\mathcal{W}$-orbit through x'_{ℓ_1} has an upper bound. This implies there is an upper bound on the number of $\mathcal{W}$-segments $[x'_{\ell_i}, y'_{\ell_{i+1}+1}]_{\mathcal{W}}$ which implies that k is bounded above by a constant k_1 depending only on $r(x'_{\ell_1})$.

Then note that $n_x(t) \geq N_* + 1$ for all $t \geq t_{\ell_{k_1}+1}$. Repeat the above arguments inductively, to conclude that for each $i \geq 0$, there exists only a finite number of transition points $\{t_\ell \mid \ell > 0\}$ with $r(x'_\ell) < 2$ and $n_x(t_\ell) = N_* + i$. It follows that for some index $\ell > \ell_*$, we have that $r(x'_\ell) \geq r'_*$. However, $r'_* \leq r(x'_\ell) \leq 2$ is forbidden, so we obtain that $r(x'_\ell) > 2$ for all $\ell \geq \ell_k$ for k sufficiently large. By Corollary 6.6 it follows that the orbit of x_{ℓ_k} escapes from $\mathbb{K}$, contrary to assumption.

Therefore, $r_* = 2$ and so there exists an infinite subsequence of transition points $\{x_{\ell_i} \mid i = 1, 2, \ldots\}$ with $r(x'_{\ell_i}) < 2$ such that $\lim_{i\to\infty} r(x'_{\ell_i}) = 2$.

Finally, note that the above proof shows that $\liminf_{k\to\infty} \{r(x'_\ell) \mid \ell \geq k\} = 2$. □

We point out a corollary of the proof of Proposition 7.6.

COROLLARY 7.8. *Suppose that $x \in \mathbb{K}$ satisfies $\rho_x(t) < 2$ for all t, then x is not trapped.* □

Finally, consider the case where $x \in \mathbb{K}$ with $\rho_x(t) > 2$ for all $t \geq 0$. Sections 5 and 6 developed various criteria for when the orbit of x is not trapped. For example, if the level function $n_x(t) \geq 0$ for all $t \geq 0$, then by Proposition 6.3 the $\mathcal{K}$-orbit escapes. The techniques used above yield the following result for such trapped orbits. Note that later in this work, in Proposition 16.10 with the assumption of Hypotheses 12.1 and 12.2, we obtain a stronger conclusion about such orbits.

PROPOSITION 7.9. *Let $x \in \mathbb{K}$ be trapped in forward time. If $\rho_x(t) > 2$ for all $t \geq 0$, then there exists a special point p_j^- as in (11) and a subsequence $\{x_{\ell_i} \mid i = 1, 2, \ldots\}$ of forward transition points such that $\lim_{i\to\infty} x'_{\ell_i} = p_j^-$. The analogous result holds if x is trapped in backward time.*

Proof. By assumption, $r(x'_\ell) > 2$ for all transition points $x_\ell = \Phi_{t_\ell}(x)$ with $t_\ell \geq 0$. Suppose that $n_x(t)$ admits a minimum value, then consider the least ℓ such that $n_x(t_\ell)$ is equal to this minimum. Then, $r(x'_\ell) > 2$ and $n_{x_\ell}(t) \geq 0$ for all $t \geq 0$ and by Proposition 6.3 the $\mathcal{K}$-orbit of x escapes.

Hence, there is an infinite sequence $t_{\ell_0} < t_{\ell_1} < \cdots$ where ℓ_i is the least index with $n_x(t_{\ell_i}) = -i$, and all x_{ℓ_i} must be secondary exit points. We claim that $r(x'_{\ell_i}) > r(x'_{\ell_{i+1}}) > 2$ for all i. Observe that $r(x'_\ell) \geq r(x'_{\ell_0})$ for all $\ell_0 \leq \ell < \ell_1$ and $r(x'_{\ell_1-1}) = r(x'_{\ell_0})$ by Proposition 5.5, so that $2 < r(x'_{\ell_1}) < r(x'_{\ell_1-1}) = r(x_{\ell_0})$ by the Radius Inequality.

Continue in this way, to obtain a sequence of points x_{ℓ_i} for which

$$2 < \cdots < r(x'_{\ell_{i+1}}) < r(x'_{\ell_i}) < \cdots < r(x'_{\ell_1}) < r(x'_{\ell_0}).$$

It follows that $\lim_{i\to\infty} \{r(x'_{\ell_{i+1}}) - r(x'_{\ell_i})\} \to 0$ and $\lim_{i\to\infty} r(x'_{\ell_i}) = r_* \geq 2$. The Radius Inequality implies that for each $j = 1, 2$, there is a unique fixed point for the radius coordinate on the range and domain of the inverse σ_j^{-1} of the insertion map, which is the point $r = 2$ and $z = (-1)^j$. Thus, $\lim_{i\to\infty} r(x_{\ell_i}) = 2$ and there is a subsequence of this subsequence converging to one of the special points. □

COROLLARY 7.10. *Suppose that the $\mathcal{K}$-orbit of $x \in \mathbb{K}$ is forward trapped, then there is a sequence of times $0 < t_1 < t_2 < \cdots$ such that $\rho_x(t_\ell) \to 2$ and $z(\Phi_{t_\ell}(x)) \to \pm 1$. The analogous conclusion holds when the $\mathcal{K}$-orbit of $x \in \mathbb{K}$ is backward trapped.*

Proof. Assume that the $\mathcal{K}$-orbit of x is forward trapped.

If $\rho_x(t) > 2$ for $t \geq 0$, then the claims follow from Proposition 7.9.

If $\rho_x(t) = 2$ for some $t \geq 0$, then the claims follow from Proposition 7.1.

If $r(x) < 2$ and $\rho_x(t) \neq 2$ for $t \geq 0$ then the claims follow from Proposition 7.6

If the $\mathcal{K}$-orbit of $x \in \mathbb{K}$ is backward trapped, consider the reverse $\mathcal{K}$-orbit to obtain the claims. □

8. The Kuperberg minimal set

In this section, we give the proof that the flow Φ_t has no periodic orbits in the plug $\mathbb{K}$, and then discuss some of the properties of the minimal set Σ for the flow. We also state some results on the non-wandering set of the flow.

THEOREM 8.1. *The flow Φ_t in the Kuperberg Plug is aperiodic.*

Proof. Suppose there exist a periodic orbit $x \in \mathbb{K}$ for the flow Φ_t. We show that this leads to a contradiction.

Let $x_\ell = \Phi_{t_\ell}(x)$ with $0 \leq t_0 < t_1 < \cdots < t_n < \cdots$ be the forward transition points in $\{\Phi_t(x) \mid t \geq 0\}$ and suppose that x_n is the first transition point with $x_n = \Phi_{t_n}(x_0) = x_0$ for $t_n > 0$. Note that we then have $\Phi_{t+t_n}(x) = \Phi_t(x)$ for all t.

Let $[x'_\ell, y'_{\ell+1}]_{\mathcal{W}} \subset \widehat{\mathbb{W}}$ be the lift of the $\mathcal{W}$-arc $[x_\ell, x_{\ell+1}]_{\mathcal{K}} \subset \mathbb{K}$ for $0 \leq \ell \leq n$. Then $[x'_0, y'_1]_{\mathcal{W}} = [x'_n, y'_{n+1}]_{\mathcal{W}}$. Recall that the r-coordinate is constant on each $\mathcal{W}$-arc $[x'_\ell, y'_{\ell+1}]_{\mathcal{W}}$ and define $r_0 = \min\{r([x'_\ell, y'_{\ell+1}]_{\mathcal{W}}) \mid 0 \leq \ell < n\}$. We may assume this minimum occurs for $[x'_0, y'_1]_{\mathcal{W}}$.

If $r([x'_\ell, y'_{\ell+1}]_{\mathcal{W}}) = 2$ for some $0 \leq \ell < n$, then the $\mathcal{K}$-orbit of x_ℓ is either trapped or infinite by Proposition 7.1. The same is true for x, which contradicts the assumption that x is a periodic point. Thus $r(x'_\ell) \neq 2$ for all ℓ. If $r([x'_\ell, y'_{\ell+1}]_{\mathcal{W}}) < 2$ for some $0 \leq \ell < n$, then by Proposition 7.6 the orbit of x contains a special orbit in its closure, which contradicts the assumption that the orbit is periodic. Thus $r_0 > 2$.

As $r([x'_1, y'_2]_{\mathcal{W}}) \geq r_0 > 2$, we have that $r(x'_1) > r(y'_1)$ and then Condition (K8) implies that x_1 must be a secondary entry point. Thus, $n_{x_0}(t_1) = 1$.

Next, observe that if $n_{x_0}(t) < 0$ for some $t > 0$, then there is a least $\ell > 0$ such that $n_{x_0}(t_\ell) < 0$. Hence $n_{x_0}(t_{\ell-1}) = 0$, and both $x_{\ell-1}$ and x_ℓ are secondary exit points by the minimality of ℓ. Then by Proposition 5.5, we have $x'_0 \prec_{\mathcal{W}} y'_\ell$. Thus $r(x'_{\ell-1}) = r(x'_0) = r_0$. As $r(x'_\ell) \neq 2$ and x_ℓ is a secondary exit point, it follows that $r(x'_\ell) < r(x'_{\ell-1}) = r_0$, which is a contradiction. Thus, we have $n_{x_0}(t) \geq 0$ for all $t \geq 0$.

Next, suppose that $n_{x_0}(t_n) = 0$, we can then apply Proposition 5.5 to the orbit segment $[x_0, x_{n+1}]_{\mathcal{K}}$ to conclude that $x'_0 \prec_{\mathcal{W}} y'_{n+1}$. Hence, $x'_0 \prec_{\mathcal{W}} y'_1 \prec_{\mathcal{W}} x'_n \prec_{\mathcal{W}} y'_{n+1}$, but since $x_0 = x_n$ we conclude $x'_0 \prec_{\mathcal{W}} y'_1 \prec_{\mathcal{W}} x'_0$. Hence, the $\mathcal{W}$-arc $[x'_0, y'_1]$ is contained in one of the $\mathcal{W}$-periodic orbits, in particular $r(x_0) = 2$ which is a contradiction.

The only possibility left is that $n_x(t_n) > 0$, but this is impossible by considering the reversed flow and then it becomes the forbidden case $n_x(t_n) < 0$ considered above. □

The above proof is essentially that given by Kuperberg in [26]. Proposition 5.5 is not formally stated in her paper, though it is stated explicitly in the subsequent treatments [17, 27, 33].

We now give a summary of general properties of the minimal set for the Kuperberg flow, as observed in [17, 27, 33]. These are based on Theorem 8.1 and results of previous sections. Recall that $p_i^- = \tau(\mathcal{L}_i^- \cap \mathcal{O}_i)$ for $i = 1, 2$ are the special entry points. Define the orbit closures in $\mathbb{K}$,

$$\Sigma_1 \equiv \overline{\{\Phi_t(p_1^-) \mid -\infty < t < \infty\}} \quad , \quad \Sigma_2 \equiv \overline{\{\Phi_t(p_2^-) \mid -\infty < t < \infty\}} \, . \tag{21}$$

THEOREM 8.2. *For the closed sets Σ_i for $i = 1, 2$ we have:*

(1) Σ_i is Φ_t-invariant;
(2) $r(x) \geq 2$ for all $x \in \Sigma_i$;
(3) $\Sigma_1 = \Sigma_2$ and we set $\Sigma = \Sigma_1 = \Sigma_2$;
(4) $\Sigma \subset \mathcal{Z}$, where $\mathcal{Z} \subset \mathbb{K}$ is any closed invariant set for Φ_t.
(5) Σ is the unique minimal set for Φ_t;

Proof. For 1) note that the closure of any Φ_t-orbit is a Φ_t-invariant set.

For 2) note that for any point $x \in \tau(\mathcal{O}_1 \cap \widehat{\mathbb{W}})$, Corollary 7.2 shows that $n_x(t) \geq 0$ for all $t \geq 0$, hence $\rho_x(t) \geq r(x) = 2$. Thus all points $y \in \Sigma_i$ in the closure of the orbit also satisfy $r(y) \geq 2$.

For 3) first observe that the proof of Proposition 7.1 for p_1^- implies that Σ_1 contains p_2^-, and thus $\Sigma_2 \subset \Sigma_1$. It likewise implies that $\Sigma_1 \subset \Sigma_2$, and thus $\Sigma_1 = \Sigma_2$.

For 4) let $x \in \mathcal{Z}$ then $\mathcal{Z}$ is invariant implies that x has an infinite orbit. By Theorem 8.1 the orbit of x is not periodic.

If $\rho_x(t) = 2$ for some $t \in \mathbb{R}$, then Proposition 7.1 shows that the Φ_t-orbit of x contains a special point in its closure, hence $\Sigma \subset \mathcal{Z}$. If $r(x) < 2$ and $\rho_x(t) \neq 2$ for all $t \in \mathbb{R}$, then Proposition 7.6 shows that the Φ_t-orbit of x contains a special point in its closure, hence $\Sigma \subset \mathcal{Z}$. If $r(x) > 2$ and $\rho_x(t) \leq 2$ for some t, then we are reduced to the above cases. Otherwise, if $\rho_x(t) > 2$ for all t, then Proposition 7.9 shows that the Φ_t-orbit of x again contains a special point in its closure. Thus, in all cases, the closure of an infinite orbit must contain Σ in its closure.

For 5) note that the closure of the Φ_t-orbit of any $x \in \Sigma$ contains Σ, so the set is minimal. Suppose that $\mathcal{Z}$ is a minimal set for Φ_t then given any $x \in \mathcal{Z}$, by 4) we have $\Sigma \subset \mathcal{Z}$, so they must be equal. □

We conclude this discussion of the Kuperberg minimal set, with some observations concerning other aspects of the topological dynamics of a Kuperberg flow, which follow from the results of the previous sections. Recall that the orbits of the Kuperberg flow are divided into those which are finite, forward or backward trapped, or trapped in both directions and so infinite. Correspondingly, the asymptotic properties of the orbits must be considered within this restraint, as the asymptotic behavior outside of the plug $\mathbb{K}$ of an orbit which escapes is not known.

First, we recall some standard definitions from topological dynamics. The *forward limit set* of a forward trapped point $x \in \mathbb{K}$ is the Φ_t-invariant set

$$\alpha(x) \equiv \bigcap_{T \to \infty} \overline{\{\Phi_t(x) \mid t \geq T\}}, \tag{22}$$

and x is *forward recurrent* if $x \in \alpha(x)$. The *backward limit set* of a backward trapped point $x \in \mathbb{K}$ is the Φ_t-invariant set

$$\omega(x) \equiv \bigcap_{T \to -\infty} \overline{\{\Phi_t(x) \mid t \leq T\}} \tag{23}$$

and x is *backward recurrent* if $x \in \omega(x)$.

COROLLARY 8.3. *Let x be forward trapped, then $\Sigma \subset \alpha(x)$. Likewise, if x is backward trapped, then $\Sigma \subset \omega(x)$.*

Proof. Theorem 8.2.4 yields the inclusions $\Sigma \subset \alpha(x)$ and $\Sigma \subset \omega(x)$. □

Next, consider the opposite extreme from recurrent points. A point $x \in \mathbb{K}$ is *forward wandering* if there exists an open set $x \in U \subset \mathbb{K}$ and $T_U > 0$ so that for all $t \geq T_U$ we have $\Phi_t(U) \cap U = \emptyset$. Similarly, x is *backward wandering* if there exists an open set $x \in U \subset \mathbb{K}$ and $T_U < 0$ so that for all $t \leq T_U$ we have $\Phi_t(U) \cap U = \emptyset$. A point x with infinite orbit is *wandering* if it is forward and backward wandering.

Define the following subsets of $\mathbb{K}$:

$$\begin{aligned}
\mathfrak{W}^0 &\equiv \{x \in \mathbb{K} \mid x \text{ orbit is finite}\} \\
\mathfrak{W}^+ &\equiv \{x \in \mathbb{K} \mid x \text{ orbit is forward wandering}\} \\
\mathfrak{W}^- &\equiv \{x \in \mathbb{K} \mid x \text{ orbit is backward wandering}\} \\
\mathfrak{W}^\infty &\equiv \{x \in \mathbb{K} \mid x \text{ is wandering}\}
\end{aligned}$$

Note that $x \in \mathfrak{W}^0$ if and only if the orbit of x escapes through $\partial_h^+ \mathbb{K}$ in forward time, and escapes though $\partial_h^- \mathbb{K}$ in backward time. Define

$$\mathfrak{W} = \mathfrak{W}^0 \cup \mathfrak{W}^+ \cup \mathfrak{W}^- \cup \mathfrak{W}^\infty \quad ; \quad \Omega = \mathbb{K} - \mathfrak{W}. \tag{24}$$

The set Ω is called the *non-wandering* set for Φ_t. A point x with forward trapped orbit is characterized by the property: $x \in \Omega$ if for all $\epsilon > 0$ and $T > 0$, there exists y and $t > T$ such that $d_{\mathbb{K}}(x, y) < \epsilon$ and $d_{\mathbb{K}}(x, \Phi_t(y)) < \epsilon$, where $d_{\mathbb{K}}$ is a distance function defined in Section 4. There are obvious corresponding statements for points which are backward trapped or infinite.

We now give some of the properties of the wandering and non-wandering sets.

LEMMA 8.4. *Ω is a closed, Φ_t-invariant subset, with $\Sigma \subset \Omega$.*

Proof. The fact that each of the sets $\mathfrak{W}^0$, $\mathfrak{W}^+$, $\mathfrak{W}^-$ and $\mathfrak{W}^\infty$ is open follows directly from the definition of wandering, as does their invariance under the flow Φ_t. For $x \in \Sigma$, its orbit is recurrent so is not wandering, hence $x \in \Omega$. □

LEMMA 8.5. *If $x \in \mathbb{K}$ is a primary entry or exit point, then $x \in \mathfrak{W}$.*

Proof. Let $x \in \partial_h^- \mathbb{K}$ be a primary entry point. Then for some $\epsilon > 0$, the choice of the vector field $\mathcal{W}$ on $\mathbb{W}$ implies that the coordinate function $z(\Phi_t(z))$ is strictly increasing for $0 \leq t \leq \epsilon$. For $0 < \delta < \epsilon$, let $B(x, \delta)$ be the closed ball of radius δ centered at x. Then for δ sufficiently small, the image $\Phi_t(B(x, \delta))$ is disjoint from $B(x, \delta)$ for all $t > \epsilon$. Thus, $x \in \mathfrak{W}^0$ if its orbit is not trapped and $x \in \mathfrak{W}^+$ if its orbit is trapped. Similar considerations apply for a primary exit point $x \in \partial_h^+ \mathbb{K}$, to show that either $x \in \mathfrak{W}^0$ or $x \in \mathfrak{W}^-$. □

COROLLARY 8.6. *For each $x \in \Omega$, the Φ_t-orbit of x is infinite.*

We can also restrict the radius coordinates of the non-wandering orbits.

PROPOSITION 8.7. $\Omega \subset \{x \in \mathbb{K} \mid r(x) \geq 2\}$.

Proof. Let $x \in \Omega$ and suppose that $r(x) = r_0 < 2$. Note that x is an infinite orbit implies that $r(x) > 1$ and x cannot be contained in the orbit of a special point as $r(x) < 2$. Moreover, it follows as in the proof of Lemma 7.7, that the level function $n_x(t)$ has a greatest lower bound $N_* \leq 0$ for all $t \in \mathbb{R}$. Let $x_* = \Phi_{t_*}(x)$ be a transition point with $n_x(t_*) = N_*$. As Ω is Φ_t-invariant, it will suffice to show that x_* is wandering, which is a contradiction. Thus, we may assume that $x = x_*$ and the level function satisfies $n_x(t) \geq 0$ for $t \geq 0$.

Let $x_\ell = \Phi_{t_\ell}(x)$ with $0 = t_0 < t_1 < \cdots < t_\ell < \cdots$ be the forward transition points in $\{\Phi_t(x) \mid t \geq 0\}$. Let $[x'_\ell, y'_{\ell+1}]_{\mathcal{W}} \subset \widehat{\mathbb{W}}$ be the lift of the $\mathcal{W}$-arc $[x_\ell, x_{\ell+1}]_{\mathcal{K}}$, for $\ell \geq 0$.

The proof of Proposition 7.6 shows that there are only a finite number of indices $\ell \geq 0$ such that x_ℓ is a transition point with level $n_x(t_\ell) = 0$. Let $\ell_0 \geq 1$ be the greatest index for which $n_x(t_{\ell_0 - 1}) = 0$. Then $n_x(t_\ell) \geq 1$ for all $\ell \geq \ell_0$, which implies that both x_{ℓ_0} and x_{ℓ_0+1} are secondary entry points and thus $x'_{\ell_0} \in L_i^-$ for $i = 1$ or $i = 2$ and $y'_{\ell_0+1} \in \mathcal{L}_j^-$ for $j = 1$ or $j = 2$.

We have $r_0 = r(x'_0) = r(x'_{\ell_0 - 1})$ and set $r_1 = r(x'_{\ell_0})$. As x is not on a special orbit, the Radius Inequality (K8) implies that $r_1 > r_0$. By the geometry of the insertion maps σ_i it follows that $x'_{\ell_0} \in L_i^-$ must be an interior point for the compact region L_i^-. The flow Φ_t is transverse to the section $\mathcal{T}_{\mathcal{K}}$ defined in (10), so it follows that there exists $\delta_0 > 0$ such that, for each $0 \leq \ell \leq \ell_0$, the ball $B(x_\ell, \delta_0)$ intersects just one component of $\mathcal{T}_{\mathcal{K}}$ and is disjoint from its boundary.

By the continuity of the flow, we can choose $0 < \epsilon \leq \delta_0$ sufficiently small so that $\Phi_{t_\ell}(B(x, \epsilon)) \subset B(x_\ell, \delta_0)$ for each $0 \leq \ell \leq \ell_0$. Moreover, for $r'_0 = r_0 + (r_1 - r_0)/3$ and $r'_1 = r_1 - (r_1 - r_0)/3$ we require that $r(y) \leq r'_0$ for each $y \in B(x, \epsilon) \cap \mathcal{T}_{\mathcal{K}}$ and $r(z) \geq r'_1$ for each $z \in B(x_{\ell_0}, \delta_0) \cap \mathcal{T}_{\mathcal{K}}$.

For $y \in B(x, \epsilon)$, it then follows that for each $0 \leq \ell \leq \ell_0$, $\Phi_{t'_\ell}(y)$ is an interior point of $\mathcal{T}_{\mathcal{K}}$ for some t'_ℓ close to t_ℓ. In particular, $\Phi_{t'_{\ell_0}}(y)$ is a secondary entry point with $n_y(t'_{\ell_0}) = n_x(t_{\ell_0}) = 1$. As in the proof of Proposition 7.6, it follows that $n_y(t) \geq 1$ for all $t \geq t_{\ell_0}$ and $r(\Phi_t(y)) \geq r(\Phi_{t'_{\ell_0}}(y)) \geq r'_1$ for all $t \geq t'_{\ell_0}$. Thus, $\Phi_t(B(x, \epsilon)) \cap B(x, \epsilon) = \emptyset$ for all $t \geq t_{\ell_0}$, so that x is forward wandering, as was to be shown. □

9. The Kuperberg pseudogroup

In this section, we define a pseudogroup $\mathcal{G}_K$ acting on a rectangle $\mathbf{R}_0 \subset \mathbb{K}$ which captures the dynamics of the flow Φ_t. The study of the action of $\mathcal{G}_K$ leads to a deeper understanding of the geometry and topology of the minimal set Σ, and gives a framework for the rest of the paper. The analysis of the dynamical properties of the action of $\mathcal{G}_K$ on $\mathbf{R}_0$ uses many of the results and techniques developed in the previous sections and provides an interpretation of these results in a pseudogroup setting.

Choose a value of θ_0 such that the rectangle $\mathbf{R}_0$ as defined in cylindrical coordinates,

$$\mathbf{R}_0 \equiv \{\xi = (r, \theta_0, z) \mid \ 1 \leq r \leq 3 \ , \ -2 \leq z \leq 2\} \subset \mathbb{W}' \ , \tag{25}$$

is disjoint from both the regions D_i and their insertions $\mathcal{D}_i$ for $i = 1, 2$, as defined in Section 3. For example, for the curves α_i and β_i' defined in Section 3, we can take $\theta_0 = \pi$, so that $\mathbf{R}_0$ is between the embedded regions $\mathcal{D}_i$ for $i = 1, 2$ as illustrated in Figure 16.

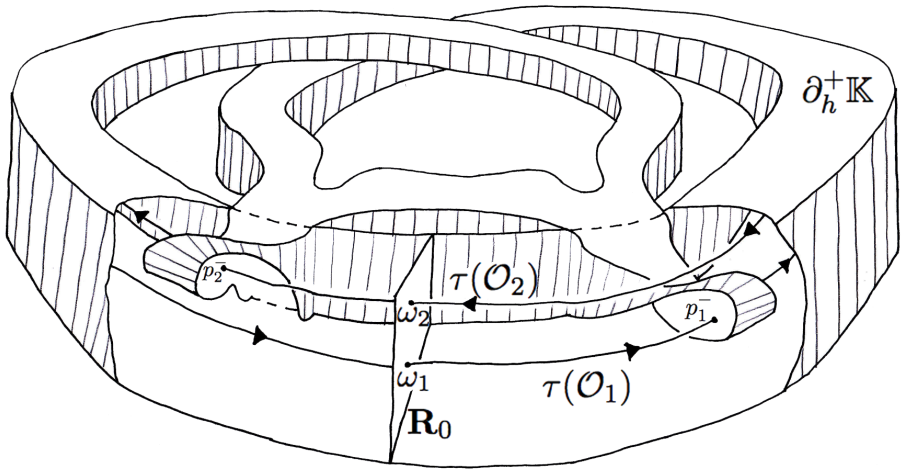

FIGURE 16. The rectangle $\mathbf{R}_0$ in the Kuperberg plug $\mathbb{K}$

As $\mathbf{R}_0 \subset \mathbb{W}'$, the quotient map $\tau \colon \mathbb{W} \to \mathbb{K}$ is injective on $\mathbf{R}_0$ and we denote its image in $\mathbb{K}$ also by $\mathbf{R}_0$ with coordinates $r = r(\xi)$ and $z = z(\xi)$ for $\xi \in \mathbf{R}_0$. The metric on $\mathbf{R}_0$ is given by

$$d_{\mathbf{R}_0}(\xi, \xi') = \sqrt{(r' - r)^2 + (z' - z)^2} \quad \text{for } \xi = (r, \pi, z) \ , \ \xi' = (r', \pi, z') \ . \tag{26}$$

Introduce the special points $\omega_i \in \mathbf{R}_0$, given by

$$\omega_1 = \mathcal{O}_1 \cap \mathbf{R}_0 = (2, \pi, -1) \quad , \quad \omega_2 = \mathcal{O}_2 \cap \mathbf{R}_0 = (2, \pi, 1) \ . \tag{27}$$

The first transition point of the forward orbit of ω_i is the special entry point $p_i^- = \tau(\mathcal{L}_i^- \cap \mathcal{O}_i) \in E_i$. The first transition point of the backward orbit of ω_i is the special exit point $p_i^+ = \tau(\mathcal{L}_i^+ \cap \mathcal{O}_i) \in S_i$.

We next give a basic result concerning the behavior of $\mathcal{K}$-orbits with respect to $\mathbf{R}_0$.

PROPOSITION 9.1. *Let $x \in \mathbb{K}$ be such that its forward (or backward) $\mathcal{K}$-orbit is trapped, then the orbit intersects $\mathbf{R}_0$. Hence, if the $\mathcal{K}$-orbit of x does not intersect $\mathbf{R}_0$, it escapes from $\mathbb{K}$ in both forward and backward time.*

Proof. Both the forward and the backward $\mathcal{K}$-orbit of a special point p_i^- limits to each special point p_j^- by Proposition 7.1, and thus intersects $\mathbf{R}_0$ repeatedly. It follows that there is an open neighborhood of each of the special points $\{\omega_1, \omega_2\}$ consisting of points whose forward and backward $\mathcal{K}$-orbit intersects $\mathbf{R}_0$. Suppose that $r(x) < 2$, then by Proposition 7.6 the assumption that the forward orbit of x is trapped implies that it contains a special point in its closure, hence must intersect $\mathbf{R}_0$ infinitely often. The case where $r(x) \geq 2$ follows

similarly by Propositions 7.1 and 7.9. The case when the backward orbit is trapped follows by reversing the flow and applying the above case. □

COROLLARY 9.2. *If $x \in \mathbb{K}$ belongs to an infinite $\mathcal{K}$-orbit, then it intersects $\mathbf{R}_0$ in an infinite sequence of points in both forward and backward time.* □

The first return map $\widehat{\Phi}$ on $\mathbf{R}_0$ for the Kuperberg flow Φ_t is defined at $\xi \in \mathbf{R}_0$ if there is a $\mathcal{K}$-orbit segment $[\xi, \eta]_{\mathcal{K}}$ with $\eta \in \mathbf{R}_0$ and its interior $(\xi, \eta)_{\mathcal{K}}$ is disjoint from $\mathbf{R}_0$. We then set $\widehat{\Phi}(\xi) = \eta$. The domain of $\widehat{\Phi}$ is the set:

$$Dom(\widehat{\Phi}) \equiv \{\xi \in \mathbf{R}_0 \mid \exists\ t > 0 \ \text{ such that } \Phi_t(\xi) \in \mathbf{R}_0 \text{ and } \Phi_s(\xi) \notin \mathbf{R}_0 \text{ for } 0 < s < t\}\,. \tag{28}$$

Corollary 9.2 implies that every $x \in \mathbf{R}_0$ with infinite orbit is in the domain of $\widehat{\Phi}$, and thus the dynamical behavior of the map $\widehat{\Phi}$ reflects the dynamical behavior of the infinite orbits for Φ_t. We also note that the map $\widehat{\Phi}\colon Dom(\widehat{\Phi}) \to \mathbf{R}_0$ has many points of discontinuity, as will be shown.

Recall the formal definition of a pseudogroup modeled on a space X:

DEFINITION 9.3. *A pseudogroup $\mathcal{G}$ modeled on a topological space X is a collection of homeomorphisms between open subsets of X satisfying the following properties:*

1. *For every open set $U \subset X$, the identity $Id_U\colon U \to U$ is in $\mathcal{G}$.*
2. *For every $\varphi \in \mathcal{G}$ with $\varphi\colon U_\varphi \to V_\varphi$ where $U_\varphi, V_\varphi \subset X$ are open subsets of X, then also $\varphi^{-1}\colon V_\varphi \to U_\varphi$ is in $\mathcal{G}$.*
3. *For every $\varphi \in \mathcal{G}$ with $\varphi\colon U_\varphi \to V_\varphi$ and each open subset $U' \subset U_\varphi$, then the restriction $\varphi \mid U'$ is in $\mathcal{G}$.*
4. *For every $\varphi \in \mathcal{G}$ with $\varphi\colon U_\varphi \to V_\varphi$ and every $\varphi' \in \mathcal{G}$ with $\varphi'\colon U_{\varphi'} \to V_{\varphi'}$, if $V_\varphi \subset U_{\varphi'}$ then the composition $\varphi' \circ \varphi$ is in $\mathcal{G}$.*
5. *If $U \subset X$ is an open set, $\{U_\alpha \subset X \mid \alpha \in \mathcal{A}\}$ are open sets whose union is U, $\varphi\colon U \to V$ is a homeomorphism to an open set $V \subset X$ and for each $\alpha \in \mathcal{A}$ we have $\varphi_\alpha = \varphi \mid U_\alpha\colon U_\alpha \to V_\alpha$ is in $\mathcal{G}$, then φ is in $\mathcal{G}$.*

We apply this definition to the first return map $\widehat{\Phi}$ on $\mathbf{R}_0$ to obtain:

DEFINITION 9.4. *Let $\mathcal{G}_K$ be the pseudogroup generated by the map $\widehat{\Phi}$ acting on $X = \mathbf{R}_0$. That is, if $U \subset Dom(\widehat{\Phi})$ is an open set with $V = \widehat{\Phi}(U)$ and the restriction $\widehat{\Phi} \mid U$ is a homeomorphism, then both $\widehat{\Phi}|U$ and $\widehat{\Phi}^{-1}|V$ are in $\mathcal{G}_K$. The remaining elements of $\mathcal{G}_K$ are given by adding maps as required so that the conditions of Definition 9.3 are satisfied.*

In the rest of this section, we consider the basic dynamical properties of the action of $\mathcal{G}_K$ on $\mathbf{R}_0$ and begin developing the relationship between the dynamics of the flow Φ_t on $\mathbb{K}$ and that of the induced action of $\widehat{\Phi}$. We first consider the relation between the actions of the maps $\widehat{\Phi}$ and $\widehat{\Psi}$ on $\mathbf{R}_0$, where $\widehat{\Psi}$ denotes the return map to $\mathbf{R}_0$ for the Wilson flow Ψ_t. The dynamical properties of Ψ_t on $\mathbb{W}$ are described in Proposition 2.1, and illustrated in Figures 2 and 3.

The first return map $\widehat{\Psi}$ on $\mathbf{R}_0$ for the Wilson flow Ψ_t is defined at $\xi \in \mathbf{R}_0$ if there is a $\mathcal{W}$-orbit segment $[\xi, \eta]_{\mathcal{W}}$ with $\eta \in \mathbf{R}_0$ and its interior $(\xi, \eta)_{\mathcal{W}}$ is disjoint from $\mathbf{R}_0$. We then set $\widehat{\Psi}(\xi) = \eta$. The domain of $\widehat{\Psi}$ is the set:

$$Dom(\widehat{\Psi}) \equiv \{\xi \in \mathbf{R}_0 \mid \exists\ t > 0 \ \text{ such that } \Psi_t(\xi) \in \mathbf{R}_0 \text{ and } \Psi_s(\xi) \notin \mathbf{R}_0 \text{ for } 0 < s < t\}\,. \tag{29}$$

The radius function is constant along the orbits of the Wilson flow, so that $r(\widehat{\Psi}(\xi)) = r(\xi)$ for all $\xi \in Dom(\widehat{\Psi})$. Also, note that the points ω_i for $i = 1, 2$ defined in (27) are fixed-points for $\widehat{\Psi}$. For all other points $\xi \in \mathbf{R}_0$ with $\xi \neq \omega_i$, it was assumed in Section 2 that the function $g(r, \theta, z) > 0$, so the $\mathcal{W}$-orbit of ξ has a "vertical drift" arising from the term $g(r, \theta, z)\frac{\partial}{\partial z}$ in the formula (3) for $\mathcal{W}$.

For $\xi \in \mathbf{R}_0$ sufficiently close to the vertical boundary $\partial_v \mathbb{W}$, function $f(r, \theta, z) = 0$ and hence the vector field $\mathcal{W}$ is tangent to $\mathbf{R}_0$. Then the Ψ_t-flow of ξ is contained in $\mathbf{R}_0$ and hence $\xi \notin Dom(\widehat{\Psi})$.

For $\xi \in \mathbf{R}_0$ such that $\mathcal{W}$ is not vertical at ξ, then the Ψ_t-flow of ξ exits $\mathbf{R}_0$ and has increasing z-coordinate, and so flows upward until it either returns to $\mathbf{R}_0$, or exits through $\partial_h^+ \mathbb{W}$ without intersecting $\mathbf{R}_0$, in which case it fails to make a complete revolution around the cylinder. In the latter case, $\xi \notin Dom(\widehat{\Psi})$. If $z(\xi) \geq 0$, then whether its forward Ψ_t-flow returns to $\mathbf{R}_0$ or not, depends strongly on the choices of the functions $g(r, \theta, z)$ and $f(r, \theta, z)$ and the minimum distance from the forward orbit of ξ to the fixed-point ω_2.

On the other hand, let $\xi = (r, \pi, z) \in \mathbf{R}_0$ with $z < 0$ and suppose that $\mathcal{W}$ is not vertical at ξ. Then as before, the forward Ψ_t-orbit of ξ exits $\mathbf{R}_0$ and has increasing z-coordinate, so must intersect the annular region $\mathcal{A} = \{z = 0\}$. If the forward orbit does not intersect $\mathbf{R}_0$ before crossing $\mathcal{A}$, then by the anti-symmetry hypothesis on the Wilson flow, the Ψ_t-orbit of ξ returns to $\mathbf{R}_0$ at the point $\eta = (r, \pi, -z)$, and so $\widehat{\Psi}(\xi) = \eta$.

Note that these remarks imply that for all $\xi \in \mathbf{R}_0$ with $z(\xi) < 0$ and such that $\mathcal{W}$ is not vertical at ξ, then $\xi \in Dom(\widehat{\Psi})$. However, which of the two cases above occurs again depends strongly on the choices of the functions $g(r, \theta, z)$ and $f(r, \theta, z)$ and the minimum distance from the forward orbit of ξ to the fixed-points ω_i.

Finally, we consider the domain of $\widehat{\Psi}$ in an open neighborhood of the vertical segment $\{r = 2\}$. For $\xi \in \mathbf{R}_0$ sufficiently close to one of the fixed points ω_i the function $g(r, \theta, z)$ is arbitrarily small, so the forward $\mathcal{W}$-orbit of ξ must intersect $\mathbf{R}_0$, and thus $\xi \in Dom(\widehat{\Psi})$. In particular, for each ω_i the set $Dom(\widehat{\Psi})$ contains a open neighborhood of ω_i. The return map for $\widehat{\Psi}$ at other points close to $\{r = 2\}$ is considered in three cases, which are illustrated in Figures 2 and 3.

First, the Ψ_t-flow of the points in the open segment

$$\mathcal{I}_0 = \{(2, \pi, z) \mid -1 < z < 1\} \subset \{r = 2\} \cap \mathbf{R}_0$$

always return to the same segment, so we have $\mathcal{I}_0 \subset Dom(\widehat{\Psi})$ with $\widehat{\Psi} \colon \mathcal{I}_0 \to \mathcal{I}_0$. Moreover, $\widehat{\Psi}$ is bijective when restricted to $\mathcal{I}_0$. However, $\widehat{\Psi}$ is not continuous on $\mathcal{I}_0$ as we will discuss further below.

The conditions (W5) and (W6) in Section 2 imply there exists a least $0 < \epsilon_f < 1/4$ such that the function $f(2, \theta, z) > 0$ for $-2 + \epsilon_f < z < 0$. Thus, for the open segment

$$\mathcal{J}_0 = \{(2, \pi, z) \mid -2 + \epsilon_f \leq z < -1\} \subset \{r = 2\} \cap \mathbf{R}_0$$

we have $\mathcal{J}_0 \subset Dom(\widehat{\Psi})$ and $\widehat{\Psi}(\mathcal{J}_0) \subset \mathcal{J}_0$. By the anti-symmetry condition (W1) for the function f, we also have that $f(2, \theta, z) < 0$ for $0 < z < 2 - \epsilon_f$. Thus, for the open segment

$$\mathcal{K}_0 = \{(2, \pi, z) \mid 1 < z \leq 2 - \epsilon_f\} \subset \{r = 2\} \cap \mathbf{R}_0$$

we have $\mathcal{K}_0 \subset Dom(\widehat{\Psi}^{-1})$ and $\widehat{\Psi}^{-1}(\mathcal{K}_0) \subset \mathcal{K}_0$. Thus, $\mathcal{I}_0$, $\mathcal{J}_0$ and $\widehat{\Psi}^{-1}(\mathcal{K}_0)$ are in the interior of $Dom(\widehat{\Psi})$.

In order to illustrate the regions in the domain of $\widehat{\Psi}$ as described above, assume that $0 \leq g(r, \theta, z) \leq 1/10$ and that $g(r, \theta, z) = 1/10$ when allowed. Thus, the flow of Ψ_t rises at an approximate rate of $1/10$ in $\mathbb{W}$, and $z(\widehat{\Psi}(\xi)) \approx z(\xi) + r(\xi)/10$. Figure 17.(A) pictures the three regions of the domain in this case.

We next consider the continuity properties of the return map $\widehat{\Psi}$. Recall that the Wilson flow reverses direction at the annulus $\mathcal{A} = \{z = 0\} \subset \mathbb{W}$, and is anti-symmetric with respect to the annulus $\mathcal{A}$ by Condition (W1) in Section 2, so that $\mathcal{W}$ is tangent to $\mathbf{R}_0$ along the line $\mathcal{T} = \mathcal{A} \cap \mathbf{R}_0$.

Let $\xi = (r, \pi, z) \in Dom(\widehat{\Psi})$ and $\eta = \widehat{\Psi}(\xi) = (r, \pi, 0)$. Then there exists a $\mathcal{W}$-orbit segment $[\xi, \eta]_{\mathcal{W}}$ which intersects $\mathbf{R}_0$ only in its endpoints, and the Ψ_t flow of ξ is tangent to $\mathbf{R}_0$ at $\eta \in \mathcal{T}$. Let $\xi' = (r, \pi, z')$ with $z - \epsilon' < z' < z$, for $\epsilon' > 0$ sufficiently small, then $\eta' = \widehat{\Psi}(\xi')$ is defined and satisfies $z(\widehat{\Psi}(\xi')) < 0$, with value depending continuously on z'. On the other hand, for $\xi'' = (r, \pi, z'')$ with $z < z'' < z + \epsilon''$, with $\epsilon'' > 0$ sufficiently small, then the point $\eta'' = \widehat{\Psi}(\xi'')$ is again well-defined. But the $\mathcal{W}$-orbit segment $[\xi'', \eta'']_{\mathcal{W}}$ is no longer tangent to $\mathbf{R}_0$ near η, as it traverses $\mathbb{W}$ in a counter-clockwise direction in the region $\{z < 0\}$, until it crosses the plane $\{z = 0\}$ before reaching the surface $\mathbf{R}_0$, and then afterwards reverses direction and subsequently intersects $\mathbf{R}_0$ from the opposite direction in the region $\{z > 0\}$, at a point close to $\widehat{\Phi}^2(\xi)$. Consequently, the map $\widehat{\Psi}$ has a discontinuity at ξ, and so $\mathcal{L}_1 = \widehat{\Psi}^{-1}(\mathcal{T})$ is a curve of discontinuities for $\widehat{\Psi}$.

There is another type of discontinuity for $\widehat{\Psi}$ that arises for $\xi = (r, \pi, 0) \in \mathcal{T}$. For $\epsilon' > 0$ sufficiently small, then for $\xi' = (r, \pi, -z')$ with $0 < z' < \epsilon'$, we have $\widehat{\Psi}(\xi') = (r, \pi, z')$ due to the anti-symmetry of Ψ_t. On the other hand, for $\xi'' = (r, \pi, z'')$ with $0 < z'' < \epsilon'$, suppose that $\eta'' = \widehat{\Psi}(\xi'')$ is well-defined then the $\mathcal{W}$-orbit segment $[\xi'', \eta'']_{\mathcal{W}}$ traverses $\mathbb{W}$ in a clockwise direction in the region $\{z > 0\}$, and so the value $z(\widehat{\Psi}(\xi''))$ is much larger than 0. Thus, $\mathcal{T} \cap Dom(\widehat{\Psi})$ is a set of discontinuities for $\widehat{\Psi}$.

Define the three domains of continuity for the induced return map $\widehat{\Psi}$ on $\mathbf{R}_0$, as illustrated in Figure 17.(A).

$$\begin{aligned} D(\widehat{\Psi})^-_- &= \{\xi \in Dom(\widehat{\Psi}) \mid z(\xi) < 0 \text{ and } z(\widehat{\Psi}(\xi)) \leq 0\} \\ D(\widehat{\Psi})^+_- &= \{\xi \in Dom(\widehat{\Psi}) \mid z(\xi) < 0 \text{ and } z(\widehat{\Psi}(\xi)) > 0\} \\ D(\widehat{\Psi})^+_+ &= \{\xi \in Dom(\widehat{\Psi}) \mid z(\xi) \geq 0 \text{ and } z(\widehat{\Psi}(\xi)) > 0\} \ , \end{aligned}$$

Restriction of the map $\widehat{\Psi}$ thus yields three continuous maps with disjoint domains, denoted by

$$\widehat{\Psi}_- = \widehat{\Psi}|D(\widehat{\Psi})^-_- \quad , \quad \widehat{\Psi}_0 = \widehat{\Psi}|D(\widehat{\Psi})^+_- \quad , \quad \widehat{\Psi}_+ = \widehat{\Psi}|D(\widehat{\Psi})^+_+ \ . \tag{30}$$

A comparable analysis of the domains of continuity for the return map $\widehat{\Phi}$ for the flow Φ_t is far more complicated, and will be postponed until Section 20, when techniques have been introduced which are sufficient for describing these domains. Our strategy here is to define a collection of special maps in $\mathcal{G}_K$, obtained by the restriction of $\widehat{\Phi}$ to particular domains of continuity, and which correspond to key aspects of the dynamics of the flow Φ_t. We show that these special elements and all their compositions in $\mathcal{G}_K$ capture all of the essential dynamical properties of the flow Φ_t. We first consider elements of $\mathcal{G}_K$ corresponding to the entry and exit dynamics of the two insertions.

For $i = 1, 2$, let $U_{\phi_i^+} \subset Dom(\widehat{\Phi})$ be the subset of $\mathbf{R}_0$ consisting of points $\xi \in Dom(\widehat{\Phi})$ with $\eta = \widehat{\Phi}(\xi)$, such that the $\mathcal{K}$-arc $[\xi, \eta]_{\mathcal{K}}$ contains a single transition point x, with $x \in E_i$. Note that for such ξ, we see from Figures 9 and 16, that its $\mathcal{K}$-orbit exits the surface E_i as the $\mathcal{W}$-orbit of a point $x' \in L_i^-$ with $\tau(x') = x$, flowing upwards from $\partial_h^- \mathbb{W}$ until it intersects $\mathbf{R}_0$ again. If the $\mathcal{K}$-orbit of ξ enters E_i but exits through S_i before crossing $\mathbf{R}_0$, then it is not considered to be in the domain $U_{\phi_i^+}$ as it contains more than one transition point.

Let $\phi_i^+ \colon U_{\phi_i^+} \to V_{\phi_i^+}$ denote the element of $\mathcal{G}_K$ defined by the restriction of $\widehat{\Phi}$. As the $\mathcal{K}$-arcs $[\xi, \eta]_{\mathcal{K}}$ defining ϕ_i^+ do not intersect $\mathcal{A}$, the restricted map ϕ_i^+ is continuous. The inverse map $(\phi_i^+)^{-1} \colon V_{\phi_i^+} \to U_{\phi_i^+}$ is also in $\mathcal{G}_K$ for $i = 1, 2$. The sets $U_{\phi_i^+}$ and $V_{\phi_i^+}$ are sketched in the center illustration in Figure 17.

For $i = 1, 2$, let $U_{\phi_i^-} \subset Dom(\widehat{\Phi})$ be the subset of $\mathbf{R}_0$ consisting of points $\xi \in Dom(\widehat{\Phi})$ with $\eta = \widehat{\Phi}(\xi)$, such that the $\mathcal{K}$-arc $[\xi, \eta]_{\mathcal{K}}$ contains a single transition point x, with $x \in S_i$. Then let $\phi_i^- \colon U_{\phi_i^-} \to V_{\phi_i^-}$ denote the element of $\mathcal{G}_K$ defined by the restriction of $\widehat{\Phi}$. Again, as the $\mathcal{K}$-arcs $[\xi, \eta]_{\mathcal{K}}$ defining the maps ϕ_i^- do not intersect $\mathcal{A}$, the restricted map ϕ_i^- is continuous. The inverse map $(\phi_i^-)^{-1} \colon V_{\phi_i^-} \to U_{\phi_i^-}$ is also in $\mathcal{G}_K$ for $i = 1, 2$. The sets $U_{\phi_i^-}$ and $V_{\phi_i^-}$ are sketched in the right hand side illustration in Figure 17.

We comment on some details of the regions in Figures 17.(B) and (C). For the map ϕ_i^+, $i = 1, 2$, the domain contains a neighborhood of the point ω_i. Flowing the domain $U_{\phi_i^+}$ forward to E_i and then applying the map σ_i^{-1} we obtain a set $\widetilde{U_{\phi_i^+}} \subset L_i^-$ containing points with r-coordinate equal to 2. Observe that the Radius Inequality implies that the maximum radius of points in $\widetilde{U_{\phi_i^+}}$ is bigger than the maximum radius of points in $U_{\phi_i^+}$. The first intersection of the $\mathcal{W}$-orbits of points in $\widetilde{U_{\phi_i^+}}$ with $\mathbf{R}_0$ is thus a region containing points with r-coordinate equal to 2 and since these points climb slower than other points, the region folds at $\{r = 2\}$. By the choice of $\mathbf{R}_0$, the points coming from L_2^- are farther than the ones coming from L_1^- and thus $V_{\phi_2^+}$ is above $V_{\phi_1^+}$. Similar considerations apply to the maps ϕ_i^- for $i = 1, 2$.

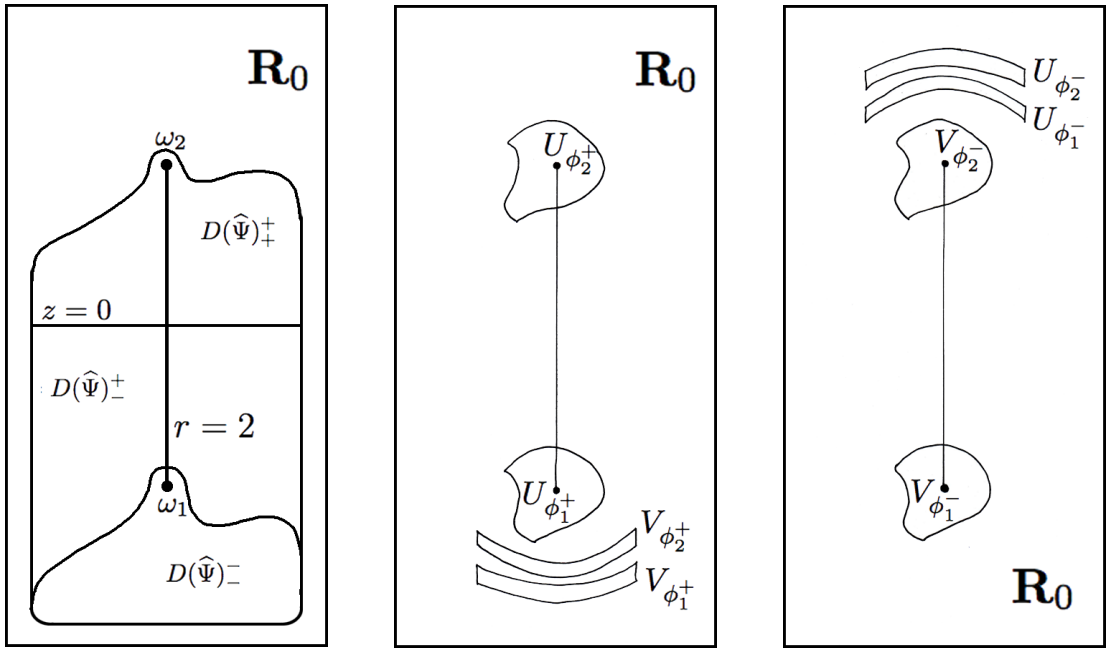

(A) Domains of $\widehat{\Psi}$ (B) Domains of ϕ_1^+, ϕ_2^+ (C) Domains of ϕ_1^-, ϕ_2^-

FIGURE 17. Domains and ranges for the maps $\{\widehat{\Psi}, \phi_1^+, \phi_2^+, \phi_1^-, \phi_2^-\}$

Observe that each generator ϕ_i^+ for $i = 1, 2$ corresponds to a flow through a transition point which increases the level function $n_x(t)$ by $+1$, so the inverse of ϕ_i^+ decreases the level function by 1. The map ϕ_i^- decreases the level by -1 and its inverse increases the level by $+1$.

Next, we develop a relation between the action of the return map $\widehat{\Psi}$ for the Wilson flow and the action of the pseudogroup $\mathcal{G}_K$. Define subsets of $\mathbf{R}_0$ contained in the domain of the Wilson map $\widehat{\Psi}$:

$$\begin{aligned} U^*_\psi &= \{(r, \pi, z) \in Dom(\widehat{\Psi}) \mid r > 2\} \subset \mathbf{R}_0 \cap \{r > 2\} \\ \mathbf{R}^*_0 &= \{(r, \pi, z) \in Dom(\widehat{\Psi}) \mid r \geq 2\} \setminus \{\omega_1, \omega_2\} \end{aligned}$$

Consider $\xi, \eta \in \mathbf{R}^*_0$ such that η is contained in the forward $\mathcal{W}$-orbit of ξ, then if $r(\xi) > 2$, Propositions 6.5 and 6.7 imply that η is in the forward $\mathcal{K}$-orbit of ξ. Thus, there exists some $k > 0$ such that $\eta = \widehat{\Phi}^k(\xi)$. The following result is a pseudogroup version of this observation.

LEMMA 9.5. *The continuous maps defined by restriction,*

$$\psi_- = \widehat{\Psi}_-|\{U^*_\psi \cap D(\widehat{\Psi})^-_-\} \quad , \quad \psi_0 = \widehat{\Psi}_0|\{U^*_\psi \cap D(\widehat{\Psi})^+_-\} \quad , \quad \psi_+ = \widehat{\Psi}_+|\{U^*_\psi \cap D(\widehat{\Psi})^+_+\} \ , \tag{31}$$

each belong to $\mathcal{G}_K$ after restricting to the interiors of their domains.

Proof. Consider first the case of ψ_-. We show that for each $\xi \in U^*_\psi \cap \text{int}(D(\widehat{\Psi})^-_-)$ there is an open neighborhood $\xi \in U_\xi \subset U^*_\psi \cap \text{int}(D(\widehat{\Psi})^-_-)$ such that the restriction $\widehat{\Psi} \mid U_\xi$ is in $\mathcal{G}_K$, then the claim that $\psi_-|\text{int}(D(\widehat{\Psi})^-_-) \in \mathcal{G}_K$ follows by the gluing condition Condition 9.3.5. Let $[\xi, \eta]_\mathcal{W}$ be the $\mathcal{W}$-orbit segment from ξ to $\eta = \widehat{\Psi}(\xi)$.

If $[\xi, \eta]_\mathcal{W}$ contains no transition point, then it is also a $\mathcal{K}$-orbit segment, so $\widehat{\Psi}(\xi) = \widehat{\Phi}(\xi)$. As the insertion regions $\mathcal{D}_i$ are closed, the continuity of the flows implies there is an open neighborhood $U_\xi \subset U^*_\psi \cap D(\widehat{\Psi})^-_-$ of ξ such that $\widehat{\Psi}|U_\xi = \widehat{\Phi}|U_\xi$. By Condition 9.3.3, $\widehat{\Psi}|U_\xi$ is in $\mathcal{G}_K$.

If $[\xi,\eta]_{\mathcal{W}} \cap \mathcal{D}_i$ is non empty, which for this case implies $i = 1$, then the first intersection with $\mathcal{D}_1$ is a point $x' \in \mathcal{L}_1^-$. This is followed along the $\mathcal{W}$-orbit segment $[\xi,\eta]_{\mathcal{W}}$ by a point $y' \in \mathcal{L}_1^+$ before returning to $\eta \in \mathbf{R}_0$. Thus, the first transition point in the $\mathcal{K}$-orbit of ξ must be the secondary entry point $x = \tau(x') \in E_1$.

As $\xi \prec_{\mathcal{W}} \eta$ with $x \equiv y$, and $r(\xi) > 2$ is given, Proposition 6.7 implies that $\xi \prec_{\mathcal{K}} \eta$. Moreover, from its proof we have that $n_\xi(t) \geq 0$ for $0 \leq t \leq t_\eta$ where $\eta = \Phi_{t_\eta}(\xi)$, and so also $\rho_\xi(t) > 2$ for $0 \leq t \leq t_\eta$. Let $\xi = \xi_0 \prec_{\mathcal{K}} \xi_1 \prec_{\mathcal{K}} \cdots \prec_{\mathcal{K}} \xi_k = \eta$ be the points of intersection of $\mathcal{K}$-arc $[\xi,\eta]_{\mathcal{K}}$ with $\mathbf{R}_0$, then $\eta = \widehat{\Phi}^k(\xi)$ and $r(\xi_\ell) > 2$ for each $0 \leq \ell \leq k$. By the transversality of the flow $\mathcal{K}$ with the faces E_1 and S_1, it follows that there is an open neighborhood $\xi \in U_\xi \subset U_\psi^*$ such that $\widehat{\Phi}^k | U_\xi$ is defined, and thus is the composition of elements in $\mathcal{G}_K$. Thus $\widehat{\Psi}|U_\xi = \widehat{\Phi}^k|U_\xi \in \mathcal{G}_K$.

The claim for the cases ψ_0 and ψ_+ is shown in the same way. □

Next we show that the maps in $\mathcal{G}_K$ defined in Lemma 9.5 admit continuous extensions to open neighborhoods of the space $\mathbf{R}_0^*$. This technical result is fundamental for many subsequent applications of the pseudogroup approach to the study of dynamics for the flow Φ_t.

LEMMA 9.6. *There exists an open set $U_\psi \subset \mathbf{R}_0$ containing $\mathbf{R}_0^*$ such that the restrictions of $\widehat{\Psi}$ to the domains of continuity in U_ψ define elements of $\mathcal{G}_K$.*

Proof. We first consider the case of the restriction $\widehat{\Psi}_-|\{U_\psi^* \cap D(\widehat{\Psi})_-^-\}$.

For $\xi \in \mathbf{R}_0^* \cap \mathrm{int}(D(\widehat{\Psi})_-^-)$ with $r(\xi) > 2$, Lemma 9.5 shows there is an open neighborhood $\xi \in U_\xi \subset U_\psi^*$ such that the restriction $\widehat{\Psi}|U_\xi$ defines an element $\psi \in \mathcal{G}_K$.

For $\xi \in \mathbf{R}_0^* \cap \mathrm{int}(D(\widehat{\Psi})_-^-)$ with $r(\xi) = 2$, the return map $\widehat{\Psi}$ is defined on a sufficiently small open neighborhood of ξ. Set $\eta = \widehat{\Psi}(\xi)$ and note that $r(\eta) = 2$. Let $[\xi,\eta]_{\mathcal{W}}$ be the $\mathcal{W}$-orbit segment from ξ to η. If $[\xi,\eta]_{\mathcal{W}}$ contains no transition point, then this is also a $\mathcal{K}$-orbit segment, so $\widehat{\Psi}(\xi) = \widehat{\Phi}(\xi)$ and there is an open neighborhood $U_\xi \subset \mathbf{R}_0$ such that $\widehat{\Psi}|U_\xi = \widehat{\Phi}|U_\xi$. Thus, $\widehat{\Psi}|U_\xi \in \mathcal{G}_K$ defines an extension of the map ψ defined by Lemma 9.5 to the open neighborhood U_ξ of ξ.

Now assume that $[\xi,\eta]_{\mathcal{W}} \cap \mathcal{D}_i$ is non empty, and so $i = 1$ in this case. Then the first intersection with $\mathcal{D}_1$ is a point $x' \in \mathcal{L}_1^-$. This is followed along the $\mathcal{W}$-orbit segment $[\xi,\eta]_{\mathcal{W}}$ by a point $y' \in \mathcal{L}_1^+$ before returning to $\eta \in \mathbf{R}_0$. Thus, the first transition point in the $\mathcal{K}$-orbit of ξ must be the secondary entry point $x = \tau(x') \in E_1$. As $\xi \prec_{\mathcal{W}} \eta$ with $x \equiv y$, and $r(\xi) = 2$ is given, and $\xi \neq \omega_i$, the Radius Inequality implies that $r(x') > 2$. Then as above, Proposition 6.7 implies that $\xi \prec_{\mathcal{K}} \eta$.

Let $\xi = \xi_0 \prec_{\mathcal{K}} \xi_1 \prec_{\mathcal{K}} \cdots \prec_{\mathcal{K}} \xi_k = \eta$ be the points of intersection of $\mathcal{K}$-arc $[\xi,\eta]_{\mathcal{K}}$ with $\mathbf{R}_0$, then $\eta = \widehat{\Phi}^k(\xi)$. As before, we have that $n_\xi(t) \geq 0$ for $0 \leq t \leq t_\eta$ where $\eta = \Phi_{t_\eta}(\xi)$ and so also $\rho_\xi(t) \geq 2$ for $0 \leq t \leq t_\eta$.

Then there is an open neighborhood $\xi \in U_\xi \subset \mathbf{R}_0$ such that $\widehat{\Phi}^k|U_\xi$ is defined and is the composition of elements in $\mathcal{G}_K$. It follows that $\widehat{\Psi}|U_\xi = \widehat{\Phi}^k|U_\xi$, and so $\widehat{\Psi}|U_\xi \in \mathcal{G}_K$. The vertical line segments $\{r = 2; z \neq \pm 1\} \cap \mathrm{int}(D(\widehat{\Psi})_-^-)$ thus admit coverings by open sets $U_\xi \subset \mathbf{R}_0$ such that $\widehat{\Phi}|U_\xi$ is the restriction of an element of $\mathcal{G}_K$. Thus by the gluing condition Condition 9.3.5, there exists an open set $U_{\psi_-} \subset \mathbf{R}_0 \cap \mathrm{int}(D(\widehat{\Psi})_-^-)$ containing $\mathbf{R}_0^* \cap \mathrm{int}(D(\widehat{\Psi})_-^-)$ for which $\widehat{\Psi}_-|U_{\psi_-}$ is continuous, and the restriction of $\psi_- = \widehat{\Psi}_-|U_{\psi_-}$ defines a map in $\mathcal{G}_K$.

The proofs for the other two cases in (31) follow similarly, yielding domains denoted by U_{ψ_0} and U_{ψ_+} such that $\widehat{\Psi}_0|U_{\psi_0} \in \mathcal{G}_K$ and $\widehat{\Psi}_+|U_{\psi_+} \in \mathcal{G}_K$. □

We thus obtain the following maps in $\mathcal{G}_K$

$$\psi_- = \widehat{\Psi}_-|U_{\psi_-} \quad , \quad \psi_0 = \widehat{\Psi}_0|U_{\psi_0} \quad , \quad \psi_+ = \widehat{\Psi}_+|U_{\psi_+} \ . \tag{32}$$

REMARK 9.7. *For convenience of notation in subsequent discussions, we will use the notation ψ for the union of the three maps ψ_-, ψ_0 and ψ_+ in* (32)*. The domains of these three maps are disjoint, so $\psi \in \mathcal{G}_K$ by*

the gluing condition Condition 9.3.5. Moreover, for ξ in the domain of ψ the meaning of $\psi(\xi)$ is then clear, as it is defined by exactly one of these maps.

We have established the existence of five special elements, $\{\phi_1^+, \phi_1^-, \phi_2^+, \phi_2^-, \psi\} \subset \mathcal{G}_K$, each of which reflects aspects of the dynamics of the flow Φ_t which played key roles in analyzing the dynamics of the flow Φ_t in the previous sections of this work. Also, let Id denote the identity map on $\mathbf{R}_0$. We introduce the subset of $\mathcal{G}_K$ generated by the compositions of these words:

DEFINITION 9.8. *Let $\mathcal{G}_K^* \subset \mathcal{G}_K$ denote the collection of all maps formed by compositions of the maps $\{Id, \phi_1^+, \phi_1^-, \phi_2^+, \phi_2^-, \psi\}$ and their restrictions to open subsets in their domains.*

Note that $\mathcal{G}_K^*$ need not satisfy the condition Definition 9.3.5 on unions of maps, so that $\mathcal{G}_K^*$ is not a sub-pseudogroup of $\mathcal{G}_K$. The reason for not imposing this condition, is that many dynamical properties for flows admit corresponding versions for local maps defined by compositions of maps in a generating set, but not if we allow for arbitrary unions as in condition (5). This issue is discussed further in Hurder [20] and Matsumoto [34]. Following the convention of [34], we say that $\mathcal{G}_K^*$ is a pseudo$\star$group, where the "$\star$" refers to the definition as the composition of maps.

A set $\mathcal{S} \subset \mathbb{R}$ is *syndetic* if there exists $\nu_{\mathcal{S}} > 0$ such that for all $a \in \mathbb{R}$ the interval $[a, a + \nu_{\mathcal{S}}]$ satisfies $\mathcal{S} \cap [a, a + \nu_{\mathcal{S}}] \neq \emptyset$. The set $\mathcal{S}$ has *bounded gaps* if there exists $\mu_{\mathcal{S}} > 0$ so that $|\mathcal{J}| \leq \mu_{\mathcal{S}}$ for all intervals $\mathcal{J} \subset \mathbb{R}$ with $\mathcal{J} \cap \mathcal{S} = \emptyset$. These two notions are clearly the same.

Let $x \in \mathbb{K}$ have forward trapped orbit and let $x_\ell = \Phi_{t_\ell}(x) \in \mathcal{T}_{\mathcal{K}}$, where $0 \leq t_0 < t_1 < \cdots$, be the sequence of transition points. Corollary 4.5 implies that there is an upper bound on the lengths $|t_{\ell+1} - t_\ell|$, so the set of transition times has bounded gaps and is a syndetic subset of $\{t \geq 0\}$. The study of the dynamical properties of the $\mathcal{K}$-orbit in previous sections used this property repeatedly.

The dynamics of the pseudogroup $\mathcal{G}_K$ acting on $\mathbf{R}_0$ provides a second discrete model for the dynamics of the flow Φ_t. The following result shows that the $\mathcal{G}_K$-pseudogroup dynamics is an accurate model of the $\mathcal{K}$-orbit dynamics along the infinite orbits in the region $\{r \geq 2\}$.

PROPOSITION 9.9. *Let $\xi \in \mathbf{R}_0$ have infinite orbit for the flow Φ_t with $\rho_\xi(t) \geq 2$ for all t. Then the set $\mathcal{S}_\xi = \{s \mid \Phi_s(\xi) \in \mathbf{R}_0\}$ is syndetic, for a constant $\nu_{\mathcal{K}}$ which is independent of ξ.*

Proof. We first make some observations about transition points and the rectangle $\mathbf{R}_0$. Recall that Lemma 4.1 lists the possible cases for a $\mathcal{W}$-arc $[x, y]_{\mathcal{K}} \subset \mathbb{K}$ with lift $[x', y']_{\mathcal{W}}$ in $\widehat{\mathbb{W}}$ and transition points $\{x, y\}$. Figures 9 and 16 help to visualize these possible cases. Note that there does not exists a $\mathcal{W}$-arc $[x, y]_{\mathcal{K}}$ for the case where $x \in S_2$ and $y \in E_1$. Also, for $x \in E_1$ and $y \in S_2$ or for $x \in E_2$ and $y \in S_1$, again no such $\mathcal{W}$-arc exists by the facing property of the Ψ_t-flow.

The following results describe the cases where a $\mathcal{W}$-arc $[x, y]_{\mathcal{K}} \subset \mathbb{K}$ intersects the rectangle $\mathbf{R}_0$.

CASES 9.10. *There are 7 cases where a $\mathcal{W}$-arc $[x, y]_{\mathcal{K}}$ always intersects $\mathbf{R}_0$:*

(1) $x \in E_i$ for $i = 1, 2$ and $y \in E_1$
(2) $x \in S_1$ and $y \in E_j$ for $j = 1, 2$
(3) $x \in S_1$ and $y \in S_j$ for $j = 1, 2$
(4) $x \in S_2$ and $y \in E_2$.

CASES 9.11. *There are 6 cases where a $\mathcal{W}$-arc $[x, y]_{\mathcal{K}}$ may not intersect $\mathbf{R}_0$:*

(1) $x \in E_i$ for $i = 1, 2$ and $y \in E_2$
(2) $x \in E_i$ for $i = 1, 2$ and $y \in S_i$ (with $x \equiv y$)
(3) $x \in S_2$ and $y \in S_i$ for $i = 1, 2$.

The cases where $x \in E_i$ for $i = 1, 2$ and $y \in E_2$ are notable, for they represent "entry/entry" transitions. Similarly, the cases where $x \in S_2$ and $y \in S_i$ for $i = 1, 2$, represent "exit/exit" transitions. These $\mathcal{W}$-arcs will

intersect $\mathbf{R}_0$ if $r(x)$ is sufficiently close to 2, but may not intersect $\mathbf{R}_0$ for $r(x)$ near the upper limit R_* defined in (18).

To prove Proposition 9.9, let $\xi_0 \in \mathbf{R}_0$ such that $\xi_1 = \widehat{\Phi}(\xi_0) = \Phi_{s_1}(\xi_0) \in \mathbf{R}_0$ and $[\xi_0, \xi_1]_{\mathcal{K}}$ is a $\mathcal{K}$-orbit segment containing no interior intersections with $\mathbf{R}_0$. We show that there is a uniform upper bound, independent of the point ξ_0, on the length of $[\xi_0, \xi_1]_{\mathcal{K}}$.

First, suppose that $[\xi_0, \xi_1]_{\mathcal{K}}$ contains no transition point, then it is a $\mathcal{W}$-orbit segment and so $\xi_1 = \psi(\xi_0)$. If $[\xi_0, \xi_1]_{\mathcal{K}}$ does not contain an interior point with $z = 0$, then the segment $[\xi_0, \xi_1]_{\mathcal{K}}$ makes one complete revolution in $\mathbb{W}$ from its start to finish in $\mathbf{R}_0$ and so admits a uniform upper and lower bound on its length. Otherwise, if $[\xi_0, \xi_1]_{\mathcal{K}}$ intersects the annulus $\mathcal{A} = \{z = 0\}$, the point ξ_0 must lie below $\mathcal{A}$ and flow counterclockwise until it meets $\mathcal{A}$. This half of the flow traverses less than one revolution, and then flows clockwise to the point ξ_1 which must be symmetric with ξ_0 with respect to $\mathcal{A}$. Thus, there is again a uniform upper bound on the length of the orbit segment between ξ_0 and ξ_1. Note that, as ξ_0 can be arbitrarily close to $\mathcal{A}$, there is no lower bound on this length.

If $[\xi_0, \xi_1]_{\mathcal{K}}$ contains transition points, label them $\{x_1, \ldots, x_k\}$ where $x_i = \Phi_{t_i}(\xi_0)$ for $0 < t_1 < \cdots < t_k < s_1$ with $k \geq 1$. Note that by assumption, $r(x_i) \geq 2$ for all $1 \leq i \leq k$. The lengths of the segments $[\xi_0, x_1]_{\mathcal{K}}$ and $[x_k, \xi_1]_{\mathcal{K}}$ in $\mathbb{K}$ admit a uniform upper (and lower) bound as the subsets $\mathbf{R}_0$, E_i and S_i for $i = 1, 2$, are compact.

If $[\xi_0, \xi_1]_{\mathcal{K}}$ contains exactly one transition point x_1, the above discussion shows that its length is bounded, as it is a union of two $\mathcal{K}$-orbit segments, both with an endpoint in $\mathbf{R}_0$. Moreover, if x_1 is a secondary entry point in E_i then $\xi_1 = \phi_i^+(\xi_0)$ and if x_1 is a secondary exit point in S_i then $\xi_1 = \phi_i^-(\xi_0)$.

For the remaining cases where $k \geq 2$, note that by Corollary 4.5, the lengths of the arcs $[x_i, x_{i+1}]_{\mathcal{K}}$ for $1 \leq i < k$ admit uniform upper (and lower) bounds. Thus, it suffices to show there is an upper bound on the index k, independent of the initial point ξ_0. Also, note that the assumption $[x_i, x_{i+1}]_{\mathcal{K}}$ does not intersect $\mathbf{R}_0$ limits the possibilities for these $\mathcal{K}$-arcs to the cases listed in Cases 9.11. We obtain an upper bound estimate on the number of such $\mathcal{K}$-arcs which can occur.

LEMMA 9.12. *There exists N_* such that if $[x_1, x_k]_{\mathcal{K}}$ is a segment of the $\mathcal{K}$-orbit in $\mathbb{K}$ with transition points $\{x_1, \ldots, x_k\}$ for $k \geq 2$, each x_i a* secondary entry point *with $r(x_i) \geq 2$ and $[x_1, x_k]_{\mathcal{K}} \cap \mathbf{R}_0 = \emptyset$, then $k \leq N_*$.*

Proof. By assumption, x_i is a secondary entry point for each $1 \leq i < k$, so there exists $x_i' \in L_i^-$ and $y_i' \neq x_i'$ satisfying $\tau(x_i') = \tau(y_i') = x_i$. Moreover, $y_{i+1}' \in \mathcal{L}_2^-$ for $1 \leq i < k$, for $y_{i+1}' \in \mathcal{L}_1^-$ implies $\mathcal{W}$-arc $[x_i', y_{i+1}']_{\mathcal{W}} \cap \mathbf{R}_0 \neq \emptyset$, contrary to assumption. Thus, each $\mathcal{W}$-arc $[x_i', y_{i+1}']_{\mathcal{W}}$ flows from the point $x_i' \in \partial_h^- \mathbb{W}$ to the point $y_{i+1}' \in \mathcal{L}_2^-$ as so misses the surface $\mathcal{L}_1^-$.

In fact, the $\mathcal{W}$-orbit of each x_i' must rise sufficiently fast vertically so that it crosses the annulus $\mathcal{A}$ before intersecting $\mathbf{R}_0$, where it reverses direction and then flows until it terminates at $y_{i+1}' \in \mathcal{L}_2^-$. We note that this is an *exceptional* condition, in that with some choices of embeddings σ_1 and σ_2 it may be impossible to satisfy.

Note that there exists $\epsilon'' > 0$ such that for all $x' \in \partial_h^- \mathbb{W}$ with $2 \leq r(x') \leq 2 + \epsilon''$, the $\mathcal{W}$-orbit of x' intersects $\mathbf{R}_0$ before intersecting $\mathcal{L}_2^-$. Thus, $r(x_i') \geq 2 + \epsilon''$ for $1 \leq i < k$. In particular, $r(x_1') \geq 2 + \epsilon''$.

As $n_{x_1}(t_{i+1}) = n_{x_1}(t_i) + 1$ for $1 \leq i < k$, we apply the Radius Inequality recursively to obtain that $r(x_{i+1}') > r(x_i') > r(x_1') \geq 2 + \epsilon''$. By Lemma 6.1, the number k of successive secondary entry transitions in the $\mathcal{K}$-orbit segment $[x_1, x_k]_{\mathcal{K}}$ is bounded above by the constant $N(2 + \epsilon'')$ introduced in its proof. Set $N_* \equiv N(2 + \epsilon'')$ and the result follows. □

LEMMA 9.13. *There exists $N^* > 0$ so that if $[x_1, x_k]_{\mathcal{K}}$ is a $\mathcal{K}$-orbit segment with transition points $\{x_1, \ldots, x_k\}$ for $k \geq 2$, each x_i is a* secondary exit point *with $r(x_i) \geq 2$ and $[x_1, x_k]_{\mathcal{K}} \cap \mathbf{R}_0 = \emptyset$, then $k \leq N^*$.*

Proof. For $1 \leq i < k$, x_i is a secondary exit point so there exists $x_i' \in \mathcal{L}_i^+$ satisfying $\tau(x_i') = x_i$. A $\mathcal{W}$-arc from $\mathcal{L}_1^+$ to L_j^+ for $j = 1, 2$ must intersect $\mathbf{R}_0$ as noted previously, so we must have $x_i' \in \mathcal{L}_2^+$ for $1 \leq i < k$ and thus $y_{i+1}' \in L_2^+$ for $1 \leq i < k - 1$ as well. Note that $y_k' \in L_j^+$ for either $j = 1$ or $j = 2$ is allowed.

There exists $\epsilon''' > 0$ such that for all $x' \in \mathcal{L}_2^+$ with $2 < r(x') \leq 2 + \epsilon'''$, the $\mathcal{W}$-orbit of x' must intersect $\mathbf{R}_0$ before it exits $\mathbb{W}$ through $\partial_h^- \mathbb{W}$. Thus, we must have $r(x'_i) > 2 + \epsilon'''$ for $1 \leq i < k$.

Let $0 < t_1 < \cdots < t_k$ be such that $x_i = \Phi_{t_i}(x)$ for $1 \leq i \leq k$. Then the level function satisfies $n_{x_1}(t_i) = 1 - i$ for $0 \leq i \leq k$ and thus $2 < r(x'_{i+1}) < r(x'_i)$ for all $0 \leq i < k$. By the Radius Inequality, using the same argument as in the proof of Lemma 6.1, there exists N^* such that $i \geq N^*$ implies that $r(x'_i) \leq 2 + \epsilon'''$. By the choice of ϵ''' this implies that $[x'_i, y'_{i+1}]_{\mathcal{K}}$ intersects $\mathbf{R}_0$. Thus, we must have $k \leq N^*$ and the result follows. □

We now conclude the proof of Proposition 9.9, for the cases $k \geq 2$, which involves an analysis of the possible cases which can arise for the $\mathcal{K}$-arcs $[x_i, x_{i+1}]_{\mathcal{K}}$ for $1 \leq i < k$.

• If $x_i \in E_1$ then $x_{i+1} \in E_2$ is possible though "exceptional", while $x_{i+1} \in S_j$ implies $j = 1$ and $x_i \equiv x_{i+1}$.

• If $x_i \in E_2$ then $x_{i+1} \in S_1$ is not possible, while if $x_{i+1} \in S_2$ then $x_i \equiv x_{i+1}$. The case $x_{i+1} \in E_2$ is possible, although exceptional and then Lemma 9.12 implies that we can repeat this case at most N_* times to yield consecutive secondary entry points in E_2, before there is a transition point in S_2.

Combining these two cases, it follows that if $x_i \in E_j$ then after at most $N_* + 1$ transition points, there follows a secondary exit point.

• If $x_i \in S_1$ then the $\mathcal{K}$-arc $[x_i, x_{i+1}]_{\mathcal{K}}$ must intersect $\mathbf{R}_0$ for all x_{i+1}.

• If $x_i \in S_2$ and $x_{i+1} \in S_1$, then the $\mathcal{K}$-arc $[x_i, x_{i+1}]_{\mathcal{K}}$ must be followed by a $\mathcal{K}$-arc which intersects $\mathbf{R}_0$. If $x_i \in S_2$ and $x_{i+1} \in S_2$, then by Lemma 9.13, this case can be repeated successively at most N^* times before the path must intersect $\mathbf{R}_0$.

Combining all possible cases above, starting with x_1, the number of possible cases which can occur is bounded by $k \leq 3 + N^* + N_*$. Thus, there is a uniformly bounded number of transition points $\{x_1, \ldots, x_k\}$ which can arise in a $\mathcal{K}$-orbit segment $[x_1, x_k]_{\mathcal{K}}$ which does not intersect $\mathbf{R}_0$. □

The following consequence of Proposition 9.9 shows that, in essence, the dynamical properties of Φ_t restricted to the non-wandering set Ω are determined by the action of the pseudogroup $\mathcal{G}_K$ restricted to the compact invariant subset $\Omega \cap \mathbf{R}_0$.

COROLLARY 9.14. *Let $x \in \Omega$, then there exists $-\nu_{\mathcal{K}} \leq t_x \leq \nu_{\mathcal{K}}$ such that $\Phi_{t_x}(x) \in \mathbf{R}_0$.*

Recall that the pseudo⋆group $\mathcal{G}_K^*$ is the subset of $\mathcal{G}_K$ generated by compositions of maps in the collection $\{\phi_1^+, \phi_1^-, \phi_2^+, \phi_2^-, \psi\}$. It is natural to ask if the actions of $\mathcal{G}_K$ and $\mathcal{G}_K^*$ on $\mathbf{R}_0$ are equivalent, which leads to the consideration of induced maps in $\mathcal{G}_K$ which are not products of these generators. These maps are related to the maps appearing in the list Cases 9.11. In the next result, we show that the dynamics of $\mathcal{G}_K$ and $\mathcal{G}_K^*$ restricted to the non-wandering set Ω agree, at least for points $\xi \in \mathbf{R}_0$ with $2 \leq r(\xi) \leq r_e$ where r_e is the "exceptional radius" as defined in (33) below.

Consider the $\mathcal{K}$-arcs as in Cases 9.11.1. Given $x' \in L_i^-$ with $2 < r(x') \leq 2 + \epsilon''$ the $\mathcal{W}$-orbit of x' intersects the rectangle $\mathbf{R}_0$ before intersecting the surface $\mathcal{L}_2^-$, as in the proof of Lemma 9.12. Then this case does not arise if $2 \leq r(x) < 2 + \epsilon''$ for $x = \tau(x')$.

Consider next the $\mathcal{K}$-arcs as in Cases 9.11.3. Recall from the proof of Lemma 9.13 that for $x' \in \mathcal{L}_2^+$ with $2 < r(x') \leq 2 + \epsilon'''$, the $\mathcal{W}$-orbit of x' intersects $\mathbf{R}_0$ before intersecting the exit region $\partial_h^- \mathbb{W}$. Then set

$$r_e = \min\{2 + \epsilon'', 2 + \epsilon'''\}. \tag{33}$$

PROPOSITION 9.15. *Let $\xi \in \mathbf{R}_0$ and suppose $\eta = \widehat{\Phi}(\xi)$, with $\eta = \Phi_{t_\eta}(\xi)$. Assume that $2 \leq \rho_\xi(t) \leq r_e$ for $0 \leq t \leq t_\eta$, then there exists $\phi \in \mathcal{G}_K^*$ such that $\phi(\xi) = \eta$.*

Proof. If the $\mathcal{K}$-segment $[\xi, \eta]_{\mathcal{K}}$ contains no transition points, then $\widehat{\Phi}(\xi) = \widehat{\Psi}(\xi) = \psi(\xi)$ and the claim follows. So consider the case when the $\mathcal{K}$-segment $[\xi, \eta]_{\mathcal{K}}$ contains at least one transition point and let $x_1 = \Phi_{t_1}(\xi)$ with $0 < t_1 < t_\eta$ be the first transition point in the $\mathcal{K}$-segment $(\xi, \eta)_{\mathcal{K}}$. Then x_1 is a secondary entry or exit point and we consider the possible cases.

Suppose that x_1 is a secondary entry point, so the $\mathcal{W}$-orbit of ξ intersects one of the surfaces $\mathcal{L}_i^-$ in a point y_1' with $\tau(y_1') = x_1$. Note that $r(y_1') = r(\xi) \leq r_e$. Let $x_1' \in L_i^-$ be such that $\tau(x_1') = x_1$, then $r(x_1') \leq 2 + \epsilon''$. Let x_2 be the next transition point in the $\mathcal{K}$-orbit of ξ, we have the three following cases:

- If $x_2 \in E_1$, then the $\mathcal{W}$-arc $[x_1, x_2]_{\mathcal{K}}$ intersects $\mathbf{R}_0$ at η and thus $\eta = \phi_i^+(\xi)$.
- If $x_2 \in E_2$, then η belongs also to the $\mathcal{W}$-arc $[x_1, x_2]_{\mathcal{K}}$ since $r(x_1') \leq 2 + \epsilon''$. Then $\eta = \phi_i^+(\xi)$.
- If $x_2 \in S_i$ for $i = 1, 2$, then $x_1 \equiv x_2$ and x_2' is in the $\mathcal{W}$-orbit of $\tau^{-1}(\xi)$. In this case it might happen that $[x_1, x_2]_{\mathcal{K}}$ does not intersects the rectangle $\mathbf{R}_0$. If this is the case, we have to consider more transitions points. Let $x_i = \Phi_{t_i}(\xi)$ with $0 < t_1 < t_2 < t_3 < t_\eta$ and $1 \leq i \leq 3$, be the first three transition points.

  According to Cases 9.10 if x_3 is a secondary entry point, the $\mathcal{W}$-arc $[x_2, x_3]_{\mathcal{K}}$ must intersect $\mathbf{R}_0$. Thus $\eta \in [x_2, x_3]_{\mathcal{K}}$ and since x_2 is in the Wilson orbit of ξ, Proposition 6.7 implies that $\eta = \psi(\xi)$. If x_3 is a secondary exit point, the choice of r_e implies that $[x_2, x_3]_{\mathcal{K}}$ must intersect $\mathbf{R}_0$ at η. Again we conclude that $\eta = \psi(\xi)$.

Next, suppose that x_1 is a secondary exit point, then the $\mathcal{W}$-orbit of ξ exits through $\partial_h^+\mathbb{W}$ in a point $y_1' \in L_i^+$ with $\tau(y_1') = x_1$, for $i = 1, 2$. Let $x_1' \in \mathcal{L}_i^+$ be such that $\tau(x_1') = x_1$.

Assume first that $x_1 \in S_1$. Let x_2 be the following transition point in the $\mathcal{K}$-orbit of ξ. Cases 9.10 imply that the $\mathcal{W}$-arc $[x_1, x_2]_{\mathcal{K}}$ must intersect $\mathbf{R}_0$, and thus $\eta = \phi_1^-(\xi)$.

We are left with the case $x_1 \in S_2$. If x_2 is a secondary entry point, then $x_2 \in E_2$ and the $\mathcal{W}$-arc $[x_1, x_2]_{\mathcal{K}}$ must intersect $\mathbf{R}_0$. We conclude that $\eta = \phi_2^-(\xi)$. If x_2 is a secondary exit point, then by the choice or r_e we have that $r(x_1') < 2 + e'''$ and thus the $\mathcal{W}$-arc $[x_1, x_2]_{\mathcal{K}}$ must intersect $\mathbf{R}_0$, implying that $\eta = \phi_2^-(\xi)$.

These cases exhaust the possibilities for the $\mathcal{K}$-orbit segment $[\xi, \eta]_{\mathcal{K}}$ so we have $\phi(\xi) = \eta$ where ϕ is one of the generators of $\mathcal{G}_K^*$. □

PROPOSITION 9.16. *Let $\xi \in \mathbf{R}_0$ have infinite orbit for the flow Φ_t with $r(\xi) < r_e$ and $\rho_\xi(t) \geq 2$ for all t. Then the set $\mathcal{S}_\xi^* = \{s \mid \Phi_s(\xi) \in \mathcal{G}_K^*(\xi) \subset \mathbf{R}_0 \ , \ r(\Phi_s(\xi)) < r_e\}$ is syndetic, for a constant $\nu_{\mathcal{K}}^*$ which is independent of ξ.*

Proof. Let $s_0 \in \mathcal{S}_\xi^*$ and let $s_1 \in \mathcal{S}_\xi^*$ satisfy $s_0 < s_1$, such that s_1 is the least such value. We need to show that there exists a value $\nu_{\mathcal{K}}^*$ independent of s_0 such that $s_1 - s_0 \leq \nu_{\mathcal{K}}^*$.

It is given that $\xi \in \mathbf{R}_0$ has infinite orbit with $\rho_\xi(t) \geq 2$ for all t, so the set $\mathcal{S}_\xi = \{s \mid \Phi_s(\xi) \in \mathbf{R}_0\}$ is syndetic in $\mathbb{R}$ with constant $\nu_{\mathcal{K}}$ by Proposition 9.9. Also, by definition there is an inclusion $\mathcal{S}_\xi^* \subset \mathcal{S}_\xi$. Consider successive points $s_0, s_1 \in \mathcal{S}_\xi^*$ with $s_0 < s_1$. It suffices to show that there exists $C(r_e) > 0$, depending on r_e but independent of ξ, so that $[s_0, s_1] \cap \mathcal{S}_\xi$ contains at most $C(r_e)$ points. We show this first for the case $s_0 \geq 0$.

Suppose that for all $s_0 \leq t \leq s_1$ we have $2 \leq \rho_\xi(t) \leq r_e$. Then by Proposition 9.15, the intersection $\mathcal{S}_\xi \cap (s_0, s_1)$ is empty.

If $\rho_\xi(t) \leq r_e$ for all $t \geq 0$, then the above argument shows that $[0, \infty) \cap \mathcal{S}_\xi = [0, \infty) \cap \mathcal{S}_\xi^*$. Otherwise, let $t_1 > 0$ be the least time for which $\rho_\xi(t_1) \geq r_e$. Then $x_1 = \Phi_{t_1}(\xi)$ is a secondary entry point. By Proposition 6.7 there exists $T_{x_1} > 0$ such that $\overline{x}_1 = \Phi_{t_1 + T_{x_1}}(\xi)$ is the secondary exit point facing x_1. Thus for $s = T_{x_1} + \epsilon$ and $\epsilon > 0$ small, $\rho_\xi(t_1 + s) < r_e$.

Consider the backwards flow of the secondary entry point x_1 to the first intersection of the orbit with $\mathbf{R}_0$ to obtain a point $\xi_1 = \Phi_{u_1}(\xi) \in \mathbf{R}_0$ where $0 \leq u_1 < t_1$. By the choice of t_1 and the remarks above, we have that $\xi_1 \in \mathcal{G}_K^*(\xi)$ and so $u_1 \in \mathcal{S}_\xi^*$. Also, note that $t_1 - u_1 < \nu_{\mathcal{K}}$ as $\mathcal{S}_\xi$ is syndetic for the constant $\nu_{\mathcal{K}}$.

Next, let $\xi_2 = \Phi_{u_2}(\xi)$ be the first intersection with $\mathbf{R}_0$ of the forward orbit of $\overline{x}_1 = \Phi_{t_1 + T_{x_1}}(\xi)$, so that $t_1 + T_{x_1} < u_2$ and $u_2 - (t_1 + T_{x_1}) < \nu_{\mathcal{K}}$. Since $\rho_\xi(t_1 + T_{x_1} + \epsilon) < r_e$ for $\epsilon > 0$ sufficiently small, by the choice of r_e in (33), there are no transition points in the $\mathcal{K}$-orbit segment between $\Phi_{t_1 + T_{x_1}}(\xi)$ and ξ_2. Then by Lemma 5.1, we have that $\xi_1 \prec_{\mathcal{W}} \xi_2$, which implies that $\xi_2 = \psi(\xi_1)$ for the generator $\psi \in \mathcal{G}_K^*$. Thus, $\xi_2 \in \mathcal{G}_K^*(\xi)$ with $r(\xi_2) < r_e$. Observe that $u_2 - u_1 < 2\nu_{\mathcal{K}} + T_{x_1}$.

Lemma 6.1 and Corollary 6.8 imply that there exists $T_{r_e} > 0$ such that $T_{x_1} \leq T_{r_e}$ for all x_1 with $r(x_1) \geq r_e$.

Define $\nu^*_{\mathcal{K}} = 2\nu_{\mathcal{K}} + T_{r_e}$. We can then apply the above process recursively along the forward $\mathcal{K}$-orbit of ξ to obtain that $[0,\infty) \cap \mathcal{S}^*_\xi$ is syndetic in $[0,\infty)$ for the constant $\nu^*_{\mathcal{K}}$. The conclusion for the backward flow follows by reversing the time parameter as usual. □

10. The level decomposition

We now begin the study of the dynamics of the Kuperberg flow Φ_t from a more topological point of view. Many of the results of the previous sections are given topological interpretations in this approach, which culminates in Section 19 with a description of the dynamics of the flow in terms of the structure of the "zippered lamination" $\mathfrak{M}$ containing the minimal set Σ.

Recall that the periodic orbits $\mathcal{O}_i$ of the Wilson flow are the boundary circles for the Reeb cylinder $\mathcal{R} \subset \mathbb{W}$. We introduce the *notched Reeb cylinder*, $\mathcal{R}' = \mathcal{R} \cap \mathbb{W}'$, which has two closed "notches" removed from $\mathcal{R}$ where it intersects the closed insertions $\mathcal{D}_i \subset \mathbb{W}$ for $i = 1, 2$. Figure 18 illustrates the cylinder $\mathcal{R}'$ inside $\mathbb{W}$.

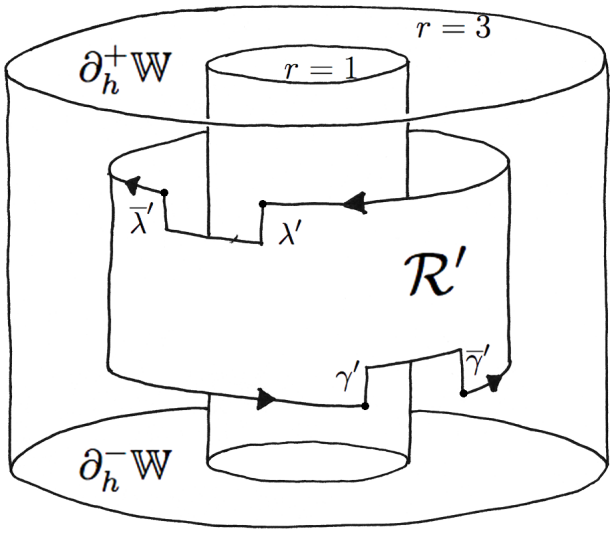

FIGURE 18. The notched cylinder $\mathcal{R}'$ embedded in $\mathbb{W}$

Consider the $\mathcal{K}$-orbit of the image $\tau(\mathcal{R}') \subset \mathbb{K}$ and its closure

$$\mathfrak{M}_0 \equiv \{\Phi_t(\tau(\mathcal{R}')) \mid -\infty < t < \infty\} \quad , \quad \mathfrak{M} \equiv \overline{\mathfrak{M}_0} \subset \mathbb{K} \, . \tag{34}$$

Note that since the special points $p_i^- = \tau(\mathcal{L}_i^- \cap \mathcal{O}_i)$ for $i = 1, 2$ are contained in $\mathfrak{M}_0$, we have $\Sigma \subset \mathfrak{M}$. Moreover, the flow Φ_t restricts to a flow on $\mathfrak{M}$, so the dynamics of Φ_t on Σ is defined by the restricted dynamics of the flow on $\mathfrak{M}$.

The horizontal segments of the boundary of $\mathcal{R}'$ which are not in the notches, are the orbit segments $\mathcal{O}_i \cap \mathbb{W}$ of $\mathcal{W}$, while the vertical segments labeled γ', $\overline{\gamma}'$, λ' and $\overline{\lambda}'$ in Figure 18 are transverse to the flow of $\mathcal{W}$. If $x \in \tau(\gamma')$ or $x \in \tau(\lambda')$ is on a vertical segment, the $\mathcal{K}$-orbit of x points into the notch. If in addition $z(x) \neq \pm 1$, then by Proposition 6.7, the forward $\mathcal{K}$-orbit of x returns in finite time to the opposite vertical boundary $\tau(\overline{\gamma}')$, or $\tau(\overline{\lambda}')$ respectively, of the notch. For each $0 < \epsilon < 1$, introduce the compact set $\mathfrak{M}_0^\epsilon$ as follows. Observe that for $x \in \gamma'$ with $z(x) > -1$ Proposition 6.7 implies that there is a finite time T_x such that $\Phi_{T_x}(\tau(x)) \in \tau(\overline{\gamma}')$. Analogously, for $x \in \lambda'$ with $z(x) < 1$ there is a finite time T_x such that $\Phi_{T_x}(\tau(x)) \in \tau(\overline{\lambda}')$. Let

$$\mathfrak{M}_0^\epsilon = \tau(\mathcal{R}') \cup \{\Phi_t(x) \,|\, x \in \tau(\gamma') \, , \; z(x) \geq -1 + \epsilon \, , \; 0 \leq t \leq T_x\} \cup \{\Phi_t(x) \,|\, x \in \tau(\lambda') \, , \; z(x) \leq 1 - \epsilon \, , \; 0 \leq t \leq T_x\}.$$

The regions added to $\tau(\mathcal{R}')$ "fill the gap" made by the notches in $\tau(\mathcal{R}')$, and yield the compact surface with boundary $\mathfrak{M}_0^\epsilon$ embedded in $\mathbb{K}$ (the embedding τ of $\mathcal{R}'$ in $\mathbb{K}$ is illustrated in Figure 24). The time $T_x \to \infty$ as x tends to the endpoint of γ' or λ', and the boundary curves of the compact surface $\mathfrak{M}_0^\epsilon$ become increasing complicated, though the surface remains embedded at all times. The limit of these compact surfaces gives approximations to the set $\mathfrak{M}_0$.

The properties of the level function $n_x(t)$ for the $\mathcal{K}$-orbit of $x \in \mathbb{K}$ were fundamental for the analysis of the orbital dynamics of the Kuperberg flow in previous sections. We next show that the level function along orbits yields a well-defined function on $\mathfrak{M}_0$ and use it to introduce the *level decomposition* of $\mathfrak{M}_0$. The geometry of $\mathfrak{M}_0$ is quite complicated to visualize. Beginning in Section 11, we formulate the structure of each of the components in the level decomposition in terms of *propellers* and develop a precise description of these sets.

For each $x \in \mathfrak{M}_0$ there exists some $y' \in \mathcal{R}'$ for which $y \in \tau(\mathcal{R}')$ such that $x = \Phi_t(y)$ for some $t \in \mathbb{R}$. The point y is not unique, but as any such choice satisfies $r(y) = 2$, the proof of Proposition 7.1 implies that $r(x) \geq 2$. The following result is a consequence of this observation and previous results.

PROPOSITION 10.1. *There is a well-defined level function*

$$n_0 \colon \mathfrak{M}_0 \to \mathbb{N} = \{0, 1, 2, \ldots\}. \tag{35}$$

Proof. First, for $x \in \tau(\mathcal{R}')$ set $n_0(x) = 0$.

Let $x \in \mathfrak{M}_0$, then there exists $y \in \tau(\mathcal{R}')$ such that $x = \Phi_{s_0}(y)$. Define $n_0(x) = n_y(s_0)$. Note that we allow both positive and negative values for s_0, using either formulas (12) or (13).

Let $w \in \tau(\mathcal{R}')$ be another point such that $x = \Phi_{s_1}(w)$. Assume without loss of generality that $y \prec_{\mathcal{K}} w$ so that there exists $T > 0$ with $w = \Phi_T(y)$. Note that $n_y(s + T) = n_w(s) + n_y(T)$, so it suffices to show that $n_y(T) = 0$.

Suppose that $y \in \tau(\mathcal{R}')$ where $y = \tau(y')$ with $z(y') = \pm 1$, so that y is on a special orbit. Then for $w \in \tau(\mathcal{R}')$ with $y \prec_{\mathcal{K}} w$ we must have $w = \tau(w')$ where $z(w') = z(y')$. This implies there are no transition points in the $\mathcal{W}$-orbit between y' and w', thus $n_y(T) = 0$.

Now suppose that $z(y') \neq \pm 1$, and let $0 \leq t_0 < t_1 < \cdots < t_k \leq T$ with $x_\ell = \Phi_{t_\ell}(y)$ be the transition points for the $\mathcal{K}$-orbit between y and w, for $k \geq 0$. The case $k = 0$ is again immediate, so assume that $k \geq 1$. We show that $n_y(T) = 0$, which will follow using an inductive argument on the number of transition points k between y and w.

Note that $y' \in \mathcal{R}'$ and $z(y') \neq \pm 1$ implies that the first transition point $x_0 \in E_i$ for $i = 1, 2$, so $n_y(t_0) = 1$ and satisfies $r(x_0') > 2$. Let $\ell > 0$ be the least integer such that $n_y(t_\ell) = 0$, which exists by the proof of Proposition 6.7. Then x_ℓ is an exit point with $x_0 \equiv x_\ell$ and so $x_\ell \in \tau(\mathcal{R}')$. Choose $u = \Phi_{t'}(y)$ on the $\mathcal{K}$-orbit between x_ℓ and $x_{\ell+1}$, so that $n_y(t') = n_y(0) = 0$ and we have reduced the problem to showing that $n_u(T - t') = 0$, where the $\mathcal{K}$-orbit segment $[u, w]_{\mathcal{K}}$ now has $k - \ell - 1$ transition points. The claim now follows by induction. □

Define the *level sets* of $\mathfrak{M}_0$ as follows:

$$\mathfrak{M}_0^n \;=\; \{x \in \mathfrak{M}_0 \mid n_0(x) \leq n\}\ ,\ n = 0, 1, 2, \ldots \tag{36}$$

The set $\mathfrak{M}_0^0$ contains the notched Reeb cylinder $\tau(\mathcal{R}')$ and the level 0 points in the boundary of the notches in $\tau(\mathcal{R}')$. The descriptions of the sets $\mathfrak{M}_0^n$ for $n > 0$ is more subtle and will follow from a detailed study of the $\mathcal{K}$-orbit of the vertical segments γ' and λ' in Section 12.

11. Embedded surfaces and propellers

The invariant set $\mathfrak{M}_0$ is the union of its level sets, as defined in (36). While the set $\mathfrak{M}_0^0$ as described in the last section is rather simple, the description of the level sets $\mathfrak{M}_0^n$ for $n > 0$ leads to the introduction of one of the main ideas of this work, the notion of *finite* and *infinite* propellers, which are obtained from the flow

Ψ_t of selected arcs in $\mathbb{W}$. These are defined and studied in this section. For example, $\mathfrak{M}_0^1$ is obtained from $\mathfrak{M}_0^0$ by attaching two non-compact surfaces which are infinite propellers, while the level sets $\mathfrak{M}_0^n$ for $n > 1$ are obtained by attaching finite propellers to $\mathfrak{M}_0^{n-1}$, where the complexity of these added finite propellers at level n increases as $n \to \infty$.

Consider a curve in the entry region, $\gamma \subset \partial_h^- \mathbb{W}$, with a parametrization $w(s) = (r(s), \theta(s), -2)$ for $0 \leq s \leq 1$, and assume that the map $w \colon [0,1] \to \partial_h^- \mathbb{W}$ is a homeomorphism onto its image. We use the notation $w_s = w(s)$ when convenient, so that $w_0 = w(0)$ denotes the initial point and $w_1 = w(1)$ the terminal point of γ. For $\epsilon > 0$, assume that $r(w_0) = 3$, $r(w_1) = 2 + \epsilon$ and $2 + \epsilon < r(w_s) < 3$ for $0 < s < 1$.

The $\mathcal{W}$-orbits of the points in γ traverse $\mathbb{W}$ from $\partial_h^- \mathbb{W}$ to $\partial_h^+ \mathbb{W}$ and hence the flow of γ generates a compact invariant surface $P_\gamma \subset \mathbb{W}$. The surface P_γ is parametrized by $(s,t) \mapsto \Psi_t(w(s))$ for $0 \leq s \leq 1$ and $0 \leq t \leq T_s$, where T_s is the exit time for the $\mathcal{W}$-orbit of $w(s)$. Observe that as $s \to 1$ and $\epsilon \to 0$, Corollary 6.8 implies that the exit time $T_s \to \infty$.

The surface P_γ is called a *propeller*, due to the nature of its shape in $\mathbb{R}^3$. It takes the form of a "tongue" wrapping around the core cylinder $\mathcal{C}(2+\epsilon)$ which contains the orbit of w_1. To visualize the shape of this surface, consider the case where γ is topologically transverse to the cylinders $\mathcal{C}(r_0) = \{r = r_0\}$ for $2 + \epsilon \leq r_0 \leq 3$. The transversality assumption implies that the radius $r(w_s)$ is *monotone decreasing* as s increases. Figure 19 illustrates the surface P_γ as a "flattened" propeller on the right and its embedding in $\mathbb{W}$ on the left. As $\epsilon \to 0$ the surface approaches the cylinder $\mathcal{C} = \{r = 2\}$ in an infinite spiraling manner.

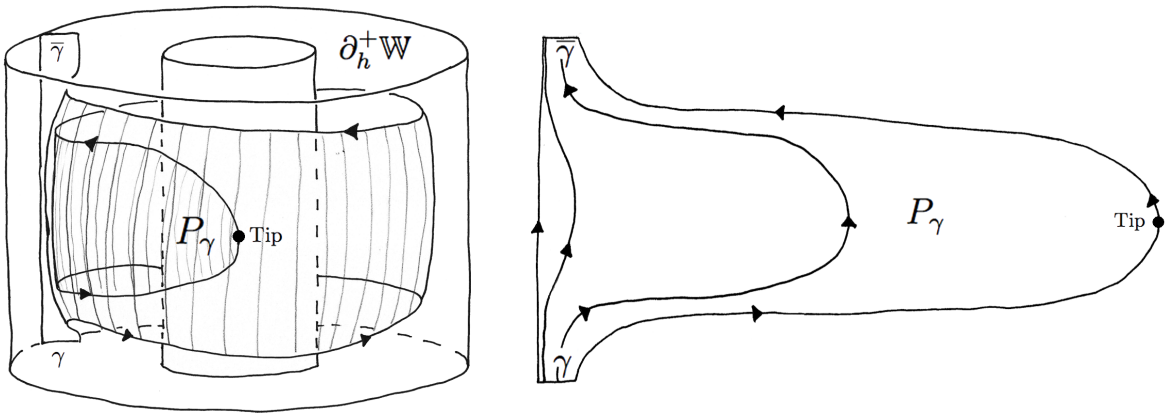

FIGURE 19. Embedded and flattened finite propeller

We comment on the details in Figure 19. The horizontal boundary $\partial_h P_\gamma$ is composed of the initial curve $\gamma \subset \partial_h^- \mathbb{W}$ and its mirror image $\overline{\gamma} \subset \partial_h^+ \mathbb{W}$ via the entry/exit condition on the Wilson Plug. The vertical boundary $\partial_v P_\gamma$ is composed of the vertical segment $w_0 \times [-2, 2]$ in $\partial_v \mathbb{W}$ and the orbit $\{\Psi_t(w_1) \mid 0 \leq t \leq T_1\}$ which is the inner (or long) edge in the interior of $\mathbb{W}$. One way to visualize the surface, is to consider the product surface $\gamma \times [-2, 2]$ and then start deforming it by an isotopy which follows the flow lines of $\mathcal{W}$, as illustrated in Figure 19. In the right hand side of the figure, some of the orbits in the propeller are presented, while in the left hand side, just the boundary orbit is presented.

Consider the orbit $\{\Psi_t(w_1) \mid 0 \leq t \leq T_1\}$ of the endpoint w_1 with $r(w_1) = 2 + \epsilon$. The path $t \mapsto \Psi_t(w_1)$ makes a certain number of turns in the positive $\mathbb{S}^1$-direction before reaching the core annulus $\mathcal{A}$ at $z = 0$. The Wilson vector field $\mathcal{W}$ is vertical on the plane $\mathcal{A}$, so the flow of w_1 then crosses $\mathcal{A}$, after which the orbit $\Psi_t(w_1)$ starts turning in the negative direction and ascending until it reaches $\partial_h^+ \mathbb{W}$. The point where the flow $\Psi_t(w_1)$ intersects $\mathcal{A}$ is called the *tip* of the propeller P_γ.

The anti-symmetry of the vector field $\mathcal{W}$ implies that the number of turns in one direction (considered as a real number) equals the number of turns in the opposite direction. To be precise, for $w_1 = (r_1, \theta_1, -2)$, let

$\Psi_t(w_1) = (r_1(t), \theta_1(t), z_1(t))$ in coordinates. The function $z_1(t)$ is monotone increasing and by the symmetry, we have $z_1(T_1/2) = 0$. Thus, the tip is the point $\Psi_{T_1/2}(w_1)$.

Set $\Theta(2+\epsilon) = \overline{\theta_1}(T_1/2) - \overline{\theta_1}(0)$, where $\overline{\theta_1}(t)$ is a *continuous* function with $\theta_1(t) = \overline{\theta_1}(t) \mod (2\pi)$. The function $\Theta(2+\epsilon)$ measures the total angle advancement of the curve $t \mapsto \Psi_t(w_1)$ between the initial point w_1 and the tip $\Psi_{T_1/2}(w_1)$. The number $\Theta(2+\epsilon)$ depends only on the radius $2+\epsilon$ of the point w_1, as the flow Ψ_t is rotationally symmetric by Proposition 2.1. Note that $\Theta(2+\epsilon) \to \infty$ as $\epsilon \to 0$. Also, introduce the notation

$$\Delta(2+\epsilon) = \lfloor \Theta(2+\epsilon)/2\pi \rfloor \ . \tag{37}$$

for the integer part of $\Theta(2+\epsilon)/2\pi$, which is the number of times that the curve $\Psi_t(w_1)$for $0 \leq t \leq T_1/2$ makes a complete circuit around the cylinder $\mathcal{C}(2+\epsilon)$.

Next, for fixed $0 \leq a < 2\pi$, consider the intersection of P_γ with a slice

$$\mathbf{R}_a \equiv \{\xi = (r, a, z) \mid \ 1 \leq r \leq 3 \ , \ -2 \leq z \leq 2\} \ . \tag{38}$$

The rectangle $\mathbf{R}_0$ defined by (25) in Section 9 corresponds to the value $a = \pi$. Each rectangle $\mathbf{R}_a$ is tangent to the Wilson flow along the annulus $\mathcal{A}$ and also near the boundary $\mathbb{W}$, but is transverse to the flow at all other points. The case when $a = \Theta(2+\epsilon) \mod (2\pi)$ is special, as the tip of the propeller is tangent to $\mathbf{R}_a$.

Assume that $a \neq \Theta(2+\epsilon) \mod (2\pi)$, then the flow $\Psi_t(w_1)$ intersects $\mathbf{R}_a$ in a series of points on the line $\mathcal{C}(2+\epsilon) \cap \mathbf{R}_a$ that are paired, as illustrated in Figure 20. Moreover, the intersection $P_\gamma \cap \mathbf{R}_a$ consists of a finite sequence of arcs between the symmetrically paired points of $\Psi_t(w_1) \cap \mathbf{R}_a$. The number of such arcs is equal to $\Delta(2+\epsilon) \pm 1$.

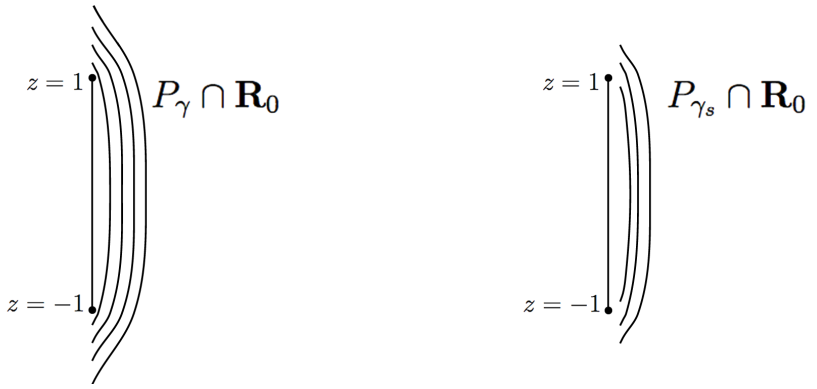

(A) Infinite propeller P_γ (B) Finite propeller P_{γ_s}

FIGURE 20. Trace of propellers in $\mathbf{R}_0$

We comment on the details of Figure 20. The vertical line between the points $(2, a, -1)$ and $(2, a, 1)$ (marked in the figure simply by $z = -1$ and $z = 1$, respectively) is the trace of the Reeb cylinder in $\mathbf{R}_a$. The trace of a propeller in $\mathbf{R}_a$ is a collection of arcs that have their endpoints in the vertical line $\{r = 2+\epsilon\}$. In the left hand figure, $r(w_1) = 2$ and the propeller in consideration is infinite. The curves form an infinite family, here just four arcs are shown, accumulating on the vertical line. The right hand figure illustrates the case $r(w_1) > 2$ and the propeller is finite.

Let us now describe the intersection of P_γ with the annulus $\mathcal{A} = \{z = 0\}$, which traces out the midpoints of the curves $t \mapsto \Psi_t(w(s))$ for $0 \leq s \leq 1$. That is, the intersection is the curve $s \mapsto \Psi_{T_s/2}(w(s)) \in \mathcal{A}$, which is a spiral, turning in the positive $\mathbb{S}^1$ direction $\Delta(2+\epsilon)$ times around the core circle, as in Figure 22. The point of the curve on the boundary of $\mathcal{A}$ in Figure 22 corresponds to the orbit $\Psi_t(w_0)$ and the point at the end of the spiral closest to the circle $\{r = 2\}$ corresponds to the tip of P_γ. If we change $\mathcal{A}$ for another annulus $\mathcal{A}_b = \{z = b\}$ where $b \neq 0$, the intersection $P_\gamma \cap \mathcal{A}_b$ will be a spiral turning in the positive $\mathbb{S}^1$-direction that is strictly shorter than the one in $\mathcal{A}$. By symmetry, the traces of P_γ on $\mathcal{A}_{-b}$ and $\mathcal{A}_b$ are the same.

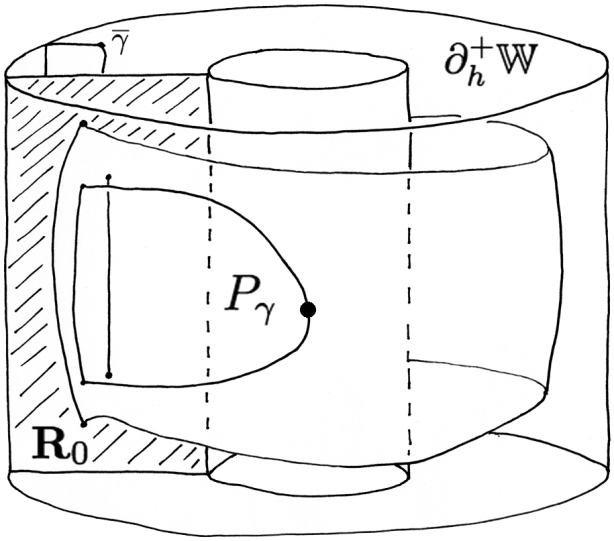

FIGURE 21. Intersection of finite propeller P_γ with $\mathbf{R}_0$

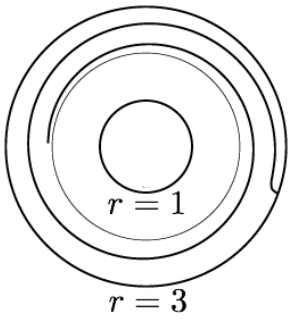

FIGURE 22. Intersection of a finite propeller P_γ with $\mathcal{A}$

Finally, consider the case where $\epsilon = 0$, so that the endpoint w_1 of γ lies in the cylinder $\mathcal{C}$. Then for $0 \leq s < 1$, we have $r(w(s)) > 2$, so the $\mathcal{W}$-orbit of $w_s \in \partial_h^-\mathbb{W}$ escapes from $\mathbb{W}$. Define the curve $\overline{\gamma}$ in $\partial_h^+\mathbb{W}$ to be the trace of these facing endpoints in $\partial_h^+\mathbb{W}$, parametrized by $\overline{w}(s)$ for $0 \leq s < 1$, where $w(s) \equiv \overline{w}(s)$. Define $\overline{w}_1 = \lim_{s\to 1} \overline{w}(s)$ so that $\overline{w}_1 \equiv w_1$ also.

Note that the forward Ψ_t-orbit of w_1 is asymptotic to the periodic orbit $\mathcal{O}_1$, while the backward Ψ_t-orbit of $\overline{w}_1$ is asymptotic to the periodic orbit $\mathcal{O}_2$. Introduce their "pseudo-orbit",

$$\mathcal{Z}_\gamma = \mathcal{Z}_\gamma^- \cup \mathcal{Z}_\gamma^+ \ , \ \mathcal{Z}_\gamma^- = \{\Psi_t(w_1) \mid t \geq 0\} \text{ and } \mathcal{Z}_\gamma^+ = \{\Psi_t(\overline{w}_1) \mid t \leq 0\} \tag{39}$$

Each curve $\mathcal{Z}_\gamma^\pm$ traces out a semi-infinite ray in $\mathcal{C}$ which spirals from the bottom or top face to a periodic orbit, and thus $\mathcal{Z}_\gamma$ traces out two semi-infinite curves in $\mathcal{C}$ spiraling to the periodic orbits $\mathcal{O}_1 \cup \mathcal{O}_2$.

For $0 < \epsilon \leq 1$, denote by γ^ϵ the curve with image $w([0, \epsilon])$, parametrized by

$$w^\epsilon(s) = w(\epsilon \cdot s). \tag{40}$$

DEFINITION 11.1. *Let γ be a curve parametrized by $w\colon [0,1] \to \mathbb{W}$ as above, with $r(w_0) = 3$ and $r(w_1) = 2$. Introduce the* infinite propeller *and its closure in $\mathbb{W}$:*

$$P_\gamma \equiv \mathcal{Z}_\gamma \cup \bigcup_{\epsilon>0} P_{\gamma^\epsilon} \quad , \quad \overline{P}_\gamma \equiv \overline{\bigcup_{\epsilon>0} P_{\gamma^\epsilon}} \tag{41}$$

PROPOSITION 11.2. *The closure $\overline{P}_\gamma$ of an infinite propeller contains the Reeb cylinder $\mathcal{R}$, with*

$$\overline{P}_\gamma \;=\; P_\gamma \;\cup\; \mathcal{R}\;. \tag{42}$$

In particular, the periodic orbits $\mathcal{O}_1$ and $\mathcal{O}_2$ are contained in $\overline{P}_\gamma$.

Proof. The endpoints of the arcs in $P_{\gamma^\epsilon} \cap \mathbf{R}_a$ tend to points in $\mathcal{C} \cap \mathbf{R}_a$ as $\epsilon \to 0$, as illustrated in Figure 20, so the closure $\overline{P}_\gamma$ contains the set $\mathcal{Z}_\gamma$. Thus, the intersection $\{\Psi_t(w_s) \mid 0 \leq t \leq T_s\} \cap \mathbf{R}_a$ for $s \to 1$ contains pairs of points arbitrarily close to the intersections $\mathcal{O}_i \cap \mathbf{R}_a$ for $i = 1, 2$. The family of arcs connecting these points is nested with the vertical line $\mathcal{R} \cap \mathbf{R}_a$ as the inner boundary. Thus, $P_\gamma \cap \mathbf{R}_a$ contains arcs joining these points which are arbitrarily close to $\mathcal{R} \cap \mathbf{R}_a$ and so $\mathcal{R} \cap \mathbf{R}_a \subset \overline{P}_\gamma \cap \mathbf{R}_a$. □

Note that the first-half $\mathcal{W}$-orbit segments $\{\Psi_t(w_s) \mid 0 \leq t \leq T_s/2\}$ for $s \to 1$ have $\mathcal{O}_1$ in their closure and the second-half $\mathcal{W}$-orbit segments $\{\Psi_t(w_s) \mid T_2/2 \leq t \leq T_s\}$ for $s \to 1$ have $\mathcal{O}_2$ in their closure.

12. Propellers and the level decomposition

In this section, we analyze the structure of the level decomposition of $\mathfrak{M}_0 \subset \mathbb{K}$ introduced in Section 10, using the concepts of propellers introduced in the last section. A key point is the introduction of an "intuitive" labeling system for the collection of propellers generated by the flow of the notched Reeb cylinder. This labeling gives order to the propellers at each level, which grow in number at an exponential rate. A second key point is the beginning of the study of the dynamics of the $\mathcal{K}$-orbit in terms of the action of the pseudogroup $\mathcal{G}_K$ on $\mathbf{R}_0$. In order to eliminate various pathologies that can arise in the study of this action, we first impose "generic" properties of the choices made in the construction of the Wilson flow $\mathcal{W}$ and on the insertions σ_i for $i = 1, 2$. For this purpose, we formulate additional assumptions on the insertions σ_i for $i = 1, 2$, which yield a stronger form of the Radius Inequality (K8) introduced by Kuperberg in [26].

Let $(r', \theta', z') = \sigma_i(x) \in \mathcal{D}_i$ for $i = 1, 2$, where $x = (r, \theta, z) \in D_i$ is a point in the domain of σ_i. Let $\pi_z(r', \theta', z') = (r', \theta', -2)$ denote the projection of $\mathbb{W}$ along the z'-coordinate. We assume that σ_i restricted to the bottom face, $\sigma_i \colon L_i^- \to \mathbb{W}$, has image transverse to the vertical fibers of π_z. Then $\pi_z \circ \sigma_i \colon L_i^- \to \mathbb{W}$ is a diffeomorphism into the face $\partial_h^- \mathbb{W}$, with image denoted by $\mathfrak{D}_i \subset \partial_h^- \mathbb{W}$. Given this assumption, let $\vartheta_i = (\pi_z \circ \sigma_i)^{-1} \colon \mathfrak{D}_i \to L_i^-$ denote the inverse map, so we have:

$$\vartheta_i(r', \theta', -2) = (r(\vartheta_i(r', \theta')), \theta(\vartheta_i(r', \theta')), -2) = (R_{i,r'}(\theta', -2), \Theta_{i,r'}(\theta', -2), -2)\;. \tag{43}$$

We formalize the assumptions on the insertion maps σ_i that are intuitively implicit in Figure 6. Set

HYPOTHESIS 12.1 (*Strong Radius Inequality*)**.** *For $i = 1, 2$, assume that:*

1. *$\sigma_i \colon L_i^- \to \mathbb{W}$ is transverse to the fibers of π_z;*
2. *$r' = r(\sigma_i(r, \theta, z)) < r$, except for $(2, \theta_i, z)$ and then $z(\sigma_i(2, \theta_i, z)) = (-1)^i$;*
3. *$\Theta_{i,r'}(\theta') = \theta(\vartheta_i(r', \theta', -2))$ is an increasing function of θ' for each fixed r';*
4. *$R_{i,r'}(\theta') = r(\vartheta_i(r', \theta', -2))$ has non-vanishing derivative for $r' = 2$, except for the case of θ_i' defined by $\vartheta_i(2, \theta_i', -2) = (2, \theta_i, -2)$;*
5. *For r' sufficiently close to 2, we require that the θ' derivative of $R_{i,r'}(\theta')$ vanish at a unique point denoted by $\theta'(i, r')$.*

Consequently, each surface $\mathcal{L}_i^-$ is transverse to the coordinate vector fields $\partial/\partial\theta$ and $\partial/\partial z$ on $\mathbb{W}$.

Recall from (3) that we have $\mathcal{W} = g(r, z)\frac{\partial}{\partial z} + f(r, z)\frac{\partial}{\partial \theta}$, where $g \colon \mathbf{R} \to [0, 1]$, which satisfies the "vertical" symmetry condition $g(r, z) = g(r, -z)$, $g(2, -1) = g(2, 1) = 0$. Also, we have that $g(r, z) = 1$ for (r, z) near the boundary of $\mathbf{R}$, and that $g(r, z) > 0$ otherwise. These assumptions are made more precise by specifying that

$$g(r, z) = 1 \quad \text{for} \quad (r - 2)^2 + (|z| - 1)^2 \geq \epsilon_0^2 \tag{44}$$

where $0 < \epsilon_0 \leq 1/4$ is sufficiently small so that the closed ϵ_0-neighborhood of each special point $p_i^{\pm}$ intersects the insertion regions $\mathcal{L}_i^{\pm}$ in the interior of the face. We also require that $2+\epsilon_0 \leq r_e$ where r_e is the exceptional radius defined in (33). Finally, we require that $g(r,z)$ is monotone increasing as a function of the distance $\sqrt{(r-2)^2 + (|z|-1)^2}$ from the special points $(2,-1)$ and $(2,1)$.

As $g(r,z) \geq 0$, the first derivatives of g must vanish at the points $(2,\pm 1)$ and the 2×2 Hessian matrix of second derivatives at these points must be positive *indefinite*. The function g is said to be *non-degenerate* if its Hessian matrix is *positive definite* at the points $(2,\pm 1)$, and the value of $g(r,z)$ is a non-decreasing function of the distance from the points in the ϵ_0-ball around each.

HYPOTHESIS 12.2. *Assume that $f(r,z)$ satisfies the conditions (W1) to (W6) in Section 2, that the condition* (44) *holds and that g is non-degenerate.*

Hypotheses 12.1 and 12.2 are not required for the results in previous sections, though some version of these hypotheses appear to be implicitly assumed by certain conclusions stated in [17, 33].

We next apply these assumptions to the study of the $\mathcal{K}$-orbit of the notched Reeb cylinder $\mathcal{R}'$. First, note that for each $1 \leq r < 3$, if the intersection $\mathcal{C}(r) \cap \mathcal{L}_i^-$ is non-empty, then it is a curve. Hypothesis 12.1.3 implies that each such arc of intersection in $\mathcal{C}(r)$ has the property that, as the z-coordinate increases along the curve, the θ-coordinate decreases for the curve in $\mathcal{L}_1^-$, or increases for the curve in $\mathcal{L}_2^-$.

Consider the intersections of the faces $\mathcal{L}_i^{\pm}$ with the Reeb cylinder $\mathcal{R}$,

$$\gamma' = \mathcal{R} \cap \mathcal{L}_1^- \ , \ \overline{\gamma}' = \mathcal{R} \cap \mathcal{L}_1^+ \quad ; \quad \lambda' = \mathcal{R} \cap \mathcal{L}_2^- \ , \ \overline{\lambda}' = \mathcal{R} \cap \mathcal{L}_2^+ \tag{45}$$

which are arcs transverse to the Ψ_t-flow on $\mathcal{R}$, as illustrated in Figure 18. Label their preimages in $\partial_h^{\pm}\mathbb{W}$ under the insertion maps σ_i by

$$\gamma = \sigma_1^{-1}(\gamma') \ , \ \overline{\gamma} = \sigma_1^{-1}(\overline{\gamma}') \quad ; \quad \lambda = \sigma_2^{-1}(\lambda') \ , \ \overline{\lambda} = \sigma_2^{-1}(\overline{\lambda}'). \tag{46}$$

One endpoint of the curve γ is contained in the boundary $L_1^- \cap \{r = 3\}$ and the other endpoint is the special point $\sigma_1^{-1}(p_1^-) \in L_1^- \cap \{r = 2\}$. Similarly, one endpoint of the curve λ is contained in the boundary $L_2^- \cap \{r = 3\}$ and the other endpoint is the special point $\sigma_2^{-1}(p_2^-) \in L_2^- \cap \{r = 2\}$.

Hypothesis 12.1 implies that both γ and λ are transverse to the cylinders $\{r = r_0\}$ for $2 < r_0 \leq 3$. As the z-coordinate of $x' \in \gamma'$ decreases towards $z = -1$, the radius coordinate r of the corresponding point in γ monotonically decreases to $r = 2$, while the angle coordinate θ monotonically increases towards θ_1 as defined in (K7). For λ', as the z-coordinate of $x' \in \lambda'$ increases towards $z = 1$, the radius of the corresponding point in λ monotonically decreases, while the angle coordinate θ monotonically increases towards θ_2 as defined in (K7). Thus, the graphs of the curves γ and λ in $\partial_h^-\mathbb{W}$ appear as in Figure 23.

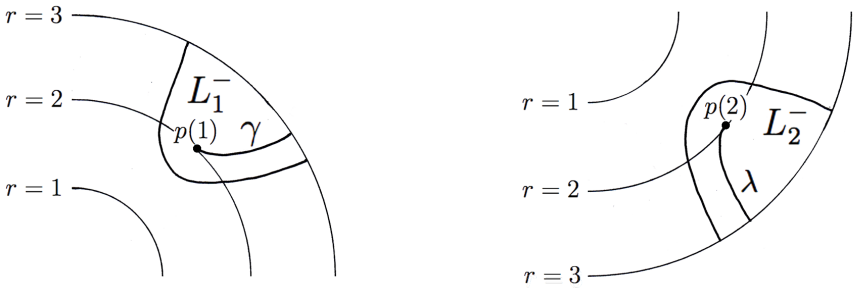

FIGURE 23. The curves γ and λ in $\partial_h^-\mathbb{W}$

LEMMA 12.3. *The curve $\overline{\gamma} \subset L_1^+$ is the facing curve to $\gamma \subset L_1^-$ and $\overline{\lambda} \subset L_2^+$ faces $\lambda \subset L_2^-$. Moreover, for each point $x \in \gamma$ with $r(x) > 2$, the facing point $\overline{x}$ satisfies $x \prec_{\mathcal{K}} \overline{x}$. Similarly, for each point $y \in \lambda$ with $r(y) > 2$, the facing point $\overline{y}$ satisfies $y \prec_{\mathcal{K}} \overline{y}$.*

Proof. The fact that $\overline{\gamma}$ is facing to γ and that $\overline{\lambda}$ is facing to λ, follows from the construction of the insertions σ_i. The assertions $x \prec_{\mathcal{K}} \overline{x}$ for $r(x) > 2$ and $y \prec_{\mathcal{K}} \overline{y}$ for $r(y) > 2$, then follow from Proposition 6.7. □

Let γ be parametrized by $w\colon [0,1] \to \mathbb{W}$, with $r(w(0)) = 3$ and $r(w(1)) = 2$. For $0 \leq \epsilon \leq 1$, define γ^ϵ by $w(\epsilon \cdot s)$ for $0 \leq s \leq 1$, as in (40). Then Lemma 12.3 implies that for $0 < \epsilon < 1$ and $0 \leq s \leq 1$, we have $\gamma^\epsilon(s) \prec_{\mathcal{K}} \overline{\gamma}^\epsilon(s)$. However, the $\mathcal{W}$-orbits of the points $w_1 = w(1)$ and $\overline{w}_1 \equiv w_1$ are both trapped, so cannot satisfy $w_1 \prec_{\mathcal{W}} \overline{w}_1$. Thus, the curves γ and $\overline{\gamma}$ are the horizontal boundary curves in $\partial_h^{\pm}\mathbb{W}$ of the infinite propeller P_γ defined by the Φ_t-flow of γ. Similar conclusions hold for λ, $\overline{\lambda}$ and the propeller P_λ.

Note that in the Definition 11.1 of the infinite propeller P_γ, we formed the union of the propellers P_{γ^ϵ} defined by the curves γ^ϵ for $0 < \epsilon < 1$, with the two trapped orbits $\mathcal{Z}_\gamma$. The $\mathcal{W}$-orbit given by the "long edge" of each P_{γ^ϵ} is a finite $\mathcal{W}$-arc, but as $\epsilon \to 0$ their limit converges to the union $\mathcal{Z}_\gamma$ of infinite orbits. This behavior is reminiscent of the "Moving Leaf Lemma" in [14, 47], which is the key to understanding the orbit behavior in the counter-examples to the *Periodic Orbit Conjecture* [13].

The $\mathcal{K}$-orbits of the curves γ and λ projected to $\mathbb{K}$ have a complicated, hierarchical structure, which we next describe using their Φ_t-flows as the starting model. Define the *notched propellers* of γ and λ by $P'_\gamma = P_\gamma \cap \mathbb{W}'$ and $P'_\lambda = P_\lambda \cap \mathbb{W}'$, respectively. Note that the vertical "transverse" boundary curves for the notches are not included in P'_γ and P'_λ.

For $x \in \tau(\mathcal{R}')$, the level function $n_x(t)$ increases from 0 to 1 when the orbit of x intersects either curve $\tau(\gamma)$ or $\tau(\lambda)$, then drops back to 0 when it exits through the curves $\tau(\overline{\gamma})$ or $\tau(\overline{\lambda})$. Thus, we have

$$\mathfrak{M}_0^0 \;=\; \tau(\mathcal{R}' \;\cup\; \overline{\gamma} \;\cup\; \overline{\lambda}) \tag{47}$$

which is a cylinder, minus two rectangles, embedded in $\mathbb{R}^3$ as a folded eight having two parts that are tangent to the boundary of the notches, as in Figure 24.

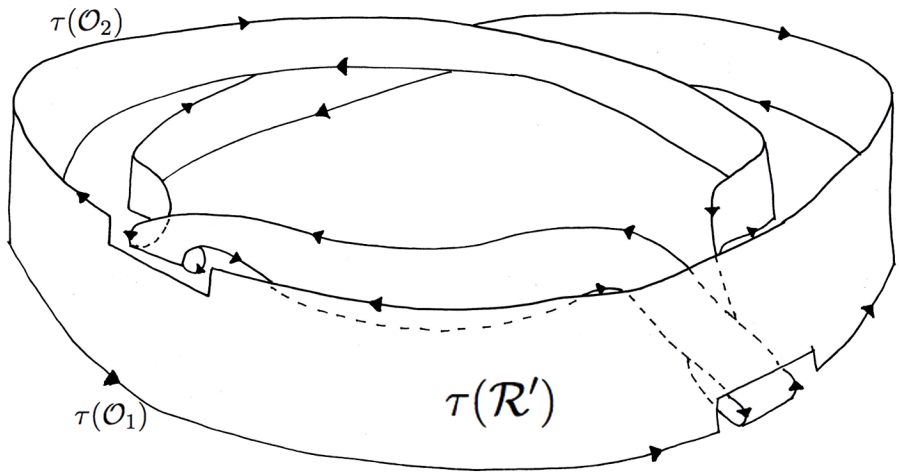

FIGURE 24. Embedding of $\mathcal{R}'$ in $\mathbb{K}$

We comment on the details of Figure 24. Note that the embedding τ of $\mathcal{R}'$ in $\mathbb{K}$ differs from its inclusion in $\mathbb{W}$ as illustrated in Figure 18, as the Reeb cylinder in embedded as a folded figure-eight. The insertions σ_i fold parts of the inner loop in the folded eight and make them tangent to the erased rectangles. This process brings two vertical lines in the cylinder to arcs contained in the erased boundary of the rectangles, covering the middle half of it. The remaining portions on each interval correspond to the cylindrical complement $\mathcal{C} - \mathcal{R}$, and will be considered later in Section 13.

The set $\mathfrak{M}_0^1$ again has a simple intuitive description. It is obtained by attaching the points in $\mathfrak{M}_0$ of level 1 to $\mathfrak{M}_0^0$. The curves $\tau(\gamma)$ or $\tau(\lambda)$ were observed to have level 1, and thus the points in their $\mathcal{W}$-orbits which lie in $\mathbb{W}'$ are also at level 1. In particular, the images $\tau(P'_\gamma)$ and $\tau(P'_\lambda)$ are at level 1, so are contained in $\mathfrak{M}_0^1$.

Each of the infinite propellers $\tau(P'_\gamma)$ and $\tau(P'_\lambda)$ is obtained by removing an infinite sequence of notches from the propellers P_γ and P_λ and then applying τ. There are two types of notches:

(1) an infinite collection of notches, each having a corner containing a point of level 2 in the intersection of the $\mathcal{K}$-orbit of a special point $p_i^\pm$ with the surfaces E_j for $j = 1, 2$;
(2) a finite number, possibly zero, of interior notches corresponding to the intersections of P_γ and P_λ with $\mathcal{D}_j$ for $j = 1, 2$, which do not contain points in the Φ_t-orbit of the special points.

REMARK 12.4. *The intersections of the second type give rise to what we call "bubbles" in the propeller and are discussed in detail later in this section and in Sections 15 and 18.*

The precise shape of propellers depends on the choices made in the construction of the Kuperberg plug. In this section and Section 15 we consider a first type of internal notches and generated bubbles that can arise.

In Section 17 we introduce new hypothesis on the construction that allow to give a more accurate description of the shape of propellers. This analysis is thus postponed until Section 18. One consequence of it, will be another possible situation where internal notches and bubbles arise, as explained at the end of that section.

The construction of the set $\mathfrak{M}_0^2$ uses "gluing" of propellers at higher level to the boundaries of these deletions from the infinite propellers at level 1. In order to give a more precise description of $\mathfrak{M}_0^1$, in preparation for describing the nuances of the construction of $\mathfrak{M}_0^n$ for $n \geq 2$, we develop an indexing system to label these intersections.

Recall from (11) that for $i = 1, 2$, $p_i^\pm = \tau(\mathcal{O}_i \cap \mathcal{L}_i^\pm)$ is called a special point. The corresponding points $\omega_i \in \mathbf{R}_0$ for $i = 1, 2$, as in (27), are used to define the level function along the special orbits. That is, the level function on $\mathfrak{M}_0$ along the $\mathcal{K}$-orbit of ω_i is defined by $n_0(x) = n_{\omega_i}(t_x)$ for $x = \Phi_{t_x}(\omega_i)$. Note that to obtain the full $\mathcal{K}$-orbits of ω_i, it is necessary to consider both their forward and backward orbits.

The first transition point for the forward $\mathcal{K}$-orbit of ω_1 is the entry point $p_1^- \in E_1$ for which $n_0(p_1^-) = 1$. Set $p(1) = \tau^{-1}(p_1^-) \in L_1^-$ and note that $r(p(1)) = 2$. The forward $\mathcal{W}$-orbit of $p(1)$ is trapped in the region $\mathcal{C} \cap \{z < -1\}$ and thus intercepts $\mathcal{L}_1^- \cap \mathcal{C}$ in an infinite sequence of points with increasing z-coordinates between -2 and -1. Label these points $p'(1; 1, \ell)$ for $\ell \geq 0$.

Note that $r(p'(1; 1, \ell)) = 2$ for all $\ell \geq 0$ and we have

$$-2 < z(p'(1; 1, 0)) < \cdots < z(p'(1; 1, \ell)) < z(p'(1; 1, \ell + 1)) < \cdots < -1 \tag{48}$$

where $z(p'(1; 1, \ell)) \to -1$ as $\ell \to \infty$.

Set $p(1; 1, \ell) = \sigma_1^{-1}(p'(1; 1, \ell)) \in L_1^-$ for $\ell \geq 0$. Then $r(p(1; 1, \ell)) > 2$ by the Radius Inequality (K8) and the sequence $p(1; 1, \ell)$ accumulates in L_1^- on $p(1)$ as $\ell \to \infty$. Hence $r(p(1; 1, \ell)) \to 2$ as $\ell \to \infty$. Note that $n_0(\tau(p(1; 1, \ell))) = 2$ for all $\ell \geq 0$.

Similarly, the first transition point for the forward $\mathcal{K}$-orbit of ω_2 is the entry point $p_2^- \in E_2$ with $n_0(p_2^-) = 1$. Set $p(2) = \tau^{-1}(p_2^-) \in L_2^-$ and note that $r(p(2)) = 2$.

The forward $\mathcal{W}$-orbit of $p(2)$ is also trapped in the region $\mathcal{C} \cap \{z < -1\}$ and thus intercepts $\mathcal{L}_1^- \cap \mathcal{C}$ in an infinite sequence of points with increasing z-coordinates also between -2 and -1. Label these points $p'(2; 1, \ell)$ for $\ell \geq 0$.

Note that $r(p'(2; 1, \ell)) = 2$ for all $\ell \geq 0$, and we have

$$-2 < z(p'(2; 1, 0)) < \cdots < z(p'(2; 1, \ell)) < z(p'(2; 1, \ell + 1)) < \cdots < -1 \tag{49}$$

where $z(p'(2; 1, \ell)) \to -1$ as $\ell \to \infty$.

Set $p(2; 1, \ell) = \sigma_1^{-1}(p'(2; 1, \ell)) \in L_1^-$ for $\ell \geq 0$. Again, $r(p(2; 1, \ell)) > 2$ by the Radius Inequality (K8) and the sequence $p(2; 1, \ell)$ also accumulates in L_1^- on $p(1)$ as $\ell \to \infty$. Thus, $r(p(2; 1, \ell)) \to 2$ as $\ell \to \infty$ and $n_0(\tau(p(2; 1, \ell))) = 2$ for all $\ell \geq 0$.

LEMMA 12.5. *The sequences* $\{p'(1;1,\ell) \mid \ell \geq 0\}$ *and* $\{p'(2;1,\ell') \mid \ell' \geq 0\}$ *are* interlaced *on the line segment* $\mathcal{C} \cap \mathcal{L}_1^- \cap \{z < -1\} \subset \mathbb{W}$. *If* $z(p'(1;1,0)) < z(p'(2;1,0))$ *then we have*

$$-2 < \cdots < z(p'(1;1,\ell)) < z(p'(2;1,\ell)) < z(p'(1;1,\ell+1)) < \cdots < -1. \tag{50}$$

The analogous conclusion holds when $z(p'(2;1,0)) < z(p'(1;1,0))$.

Proof. Observe that L_1^- follows L_2^- in the direction of the θ-coordinate in $\mathbb{W}$. Since $p'(1;1,0)$ and $p'(2;1,0)$ are the first intersections of the $\mathcal{W}$-orbit of $p(1)$ and $p(2)$ with $\mathcal{L}_1^-$, we cannot predict which is below. Assuming that $z(p'(1;1,0)) < z(p'(2;1,0))$, the inequality $z(p'(2;1,\ell)) < z(p'(1;1,\ell+1))$, for $\ell \geq 1$, follows from the fact that the Ψ_t-flow preserves the cylinder $\mathcal{C}$ and so preserves the height relationship. The case when $z(p'(2;1,0)) < z(p'(1;1,0))$ follows in the same way. □

Next, consider the backward orbits of the points ω_i, for $i = 1, 2$, which intersect S_i in the points p_i^+ with $\tau^{-1}(p_i^+) \in L_i^+$ and $r(\tau^{-1}(p_i^+)) = 2$. Thus, the backward Wilson orbits of $\tau^{-1}(p_i^+)$ for $i = 1, 2$ are trapped in the region $\mathcal{C} \cap \{z > 1\}$ and so intercept $\mathcal{L}_2^-$ in infinite sequences of points with $r = 2$ and z-coordinates between 1 and 2.

For the backward $\mathcal{W}$-orbit of $\tau^{-1}(p_1^+)$, label these points $p'(1;2,\ell) \in \mathcal{L}_2^-$, for $\ell \geq 0$, with $r(p'(1;2,\ell)) = 2$ and $1 < z(p'(1;2,\ell)) < 2$, where $z(p'(1;2,\ell)) \to 1$ as $\ell \to \infty$.

Set $p(1;2,\ell) = \sigma_2^{-1}(p'(1;2,\ell)) \in L_2^-$. We then have $n_0(\tau(p(1;2,\ell))) = 2$ for $\ell \geq 0$ by formula (13). The Radius Inequality (K8) implies that $r(p(1;2,\ell)) > 2$ and note that the sequence $p(1;2,\ell)$ accumulates on $p(2)$ as $\ell \to \infty$. Thus, $r(p(1;2,\ell)) \to 2$ as $\ell \to \infty$.

Similarly, the backward $\mathcal{W}$-orbit of $\tau^{-1}(p_2^+)$ intercepts $\mathcal{L}_2^- \subset \mathbb{W}$ in a sequence of points with $r = 2$ and z-coordinate between 1 and 2. Label these points $p'(2;2,\ell) \in \mathcal{L}_2^-$, for $\ell \geq 0$. Then $r(p'(2;2,\ell)) = 2$ and $1 < z(p'(2;2,\ell)) < 2$, where $z(p'(2;2,\ell)) \to 1$ as $\ell \to \infty$.

Set $p(2;2,\ell) = \sigma_2^{-1}(p'(2;2,\ell)) \in L_2^-$. Again, we have $n_0(\tau(p(2;2,\ell))) = 2$ for $\ell \geq 0$ by formula (13). Then $r(p(2;2,\ell)) > 2$ by the Radius Inequality (K8) and the sequence $p(2;2,\ell)$ accumulates on $p(2)$ as $\ell \to \infty$. Thus, $r(p(2;2,\ell)) \to 2$ as $\ell \to \infty$.

The analog of Lemma 12.5 follows by the same arguments.

LEMMA 12.6. *The sequences* $\{p'(1;2,\ell) \mid \ell \geq 0\}$ *and* $\{p'(2;2,\ell') \mid \ell' \geq 0\}$ *are* interlaced *on the line segment* $\mathcal{C} \cap \mathcal{L}_2^- \cap \{z > 1\} \subset \mathbb{W}$. *If* $z(p'(1;2,0)) < z(p'(2;2,0))$ *then*

$$1 < \cdots < z(p'(2;2,\ell+1)) < z(p'(1;2,\ell)) < z(p'(2;2,\ell)) < \cdots < 2. \tag{51}$$

The analogous conclusion holds when $z(p'(2;2,0)) < z(p'(1;2,0))$.

REMARK 12.7. *The points* $\tau(p(1;\cdot,\cdot))$ *belong to the* $\mathcal{K}$*-orbit of* ω_1*, the points* $\tau(p(2;\cdot,\cdot))$ *belong to the* $\mathcal{K}$*-orbit of* ω_2*, while the points* $\tau(p(\cdot;1,\cdot)) \in E_1$ *and the points* $\tau(p(\cdot;2,\cdot)) \in E_2$.

Next, we consider in detail the intersections of the propellers P_γ and P_λ with the surfaces $\mathcal{L}_i^-$ for $i = 1, 2$. Recall that $\mathcal{L}_i^-$ was chosen in Section 3 to be transverse to the vector field $\mathcal{W}$ and the insertion $\mathcal{D}_i$ is obtained from the Ψ_t-flow of its points. It follows that the surfaces $\mathcal{L}_i^-$ intersect the propellers P_γ and P_λ transversally, thus each such intersection must be a union of closed line segments whose boundaries are contained in the boundaries of either $\mathcal{L}_i^-$ or in the boundary of the propellers. The intersections of $\mathcal{D}_i$ with a propeller are then obtained as the Ψ_t-flow of each such line segment in $\mathcal{L}_i^-$, until it reaches the facing line segment in $\mathcal{L}_i^+$. We consider the possible cases for the line segments $\mathcal{L}_i^- \cap P_\gamma$. The analysis for the propeller P_λ will be analogous.

Recall that the intersection of P_γ with $\mathbf{R}_0$ is an infinite collection of arcs whose endpoints are on the vertical line $\{r = 2\}$, the lower ones having z-coordinate less than -1 and the upper ones having z-coordinate bigger than 1, as illustrated in Figure 20. The forward Ψ_t-flow of these arcs gives the intersection $\mathcal{L}_i^- \cap P_\gamma$. For $i = 1$, an arc in $\mathcal{L}_1^- \cap P_\gamma$ either has both endpoints on the boundary $\partial\mathcal{L}_1^-$, either has its upper endpoint on $\partial\mathcal{L}_1^-$ and its lower endpoint is a point $p'(1;1,\ell)$ for $\ell \geq 0$. For $i = 2$, an arc in $\mathcal{L}_2^- \cap P_\gamma$ either has both endpoints on the boundary $\partial\mathcal{L}_2^-$, either has its lower endpoint on $\partial\mathcal{L}_2^-$ and its upper endpoint is a point $p'(1;2,\ell)$ for $\ell \geq 0$.

DEFINITION 12.8. *If a segment of $\mathcal{L}_i^- \cap P_\gamma$ has both endpoints on $\partial\mathcal{L}_i^-$, the corresponding intersection of P_γ with $\mathcal{D}_i$ defines a "rectangular notch" in the interior of the propeller, called an* interior notch *for P_γ. If a segment of $\mathcal{L}_i^- \cap P_\gamma$ has an endpoint in the interior of $\mathcal{L}_i^-$, the corresponding intersection of P_γ with $\mathcal{D}_i$ defines a* boundary notch *for P_γ, or sometimes simply as a "notch".*

The surface P'_γ is obtained from P_γ by deleting the interior and boundary notches for $i = 1$ and $i = 2$. This is illustrated in Figure 25.

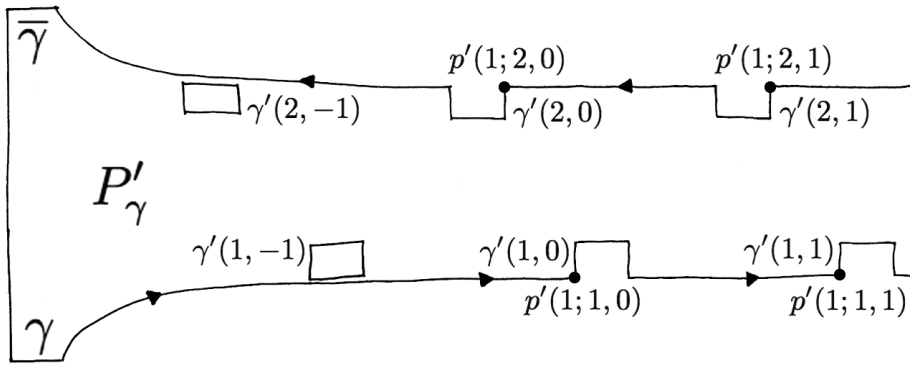

FIGURE 25. Internal and (boundary) notches of P'_γ

For the propeller P_λ formed by the Ψ_t-flow of the curve λ, analogous considerations and notations apply to the connected components of $P_\lambda \cap \mathcal{L}_i^-$ for $i = 1, 2$.

Observe that P'_γ has a boundary notch for each intersection of the $\mathcal{W}$-orbits of $p(1) = \tau^{-1}(p_1^-)$ and $\tau^{-1}(p_1^+)$ with $\mathcal{L}_1^- \cup \mathcal{L}_2^-$. Similarly, P'_λ has a boundary notch for each intersection of the $\mathcal{W}$-orbits of $p(2) = \tau^{-1}(p_2^-)$ and $\tau^{-1}(p_2^+)$ with $\mathcal{L}_1^- \cup \mathcal{L}_2^-$. There are an infinite number of such boundary notches.

In contrast, there are at most finitely many internal notches, since these correspond to the intersections of P'_γ with $\mathcal{L}_1^- \cup \mathcal{L}_2^-$ for which the $\mathcal{W}$-orbits of $p(1) = \tau^{-1}(p_1^-)$ and $\tau^{-1}(p_1^+)$ are away from the insertion region, or to the intersections of P'_λ with $\mathcal{L}_1^- \cup \mathcal{L}_2^-$ for which the $\mathcal{W}$-orbits of $p(2) = \tau^{-1}(p_2^-)$ and $\tau^{-1}(p_2^+)$ are away from the insertion region. Let $-b \geq 0$ denote the number of internal notches, with $b = 0$ if there are no internal notches, so that the $\mathcal{W}$-orbit of $p(1)$ makes at least $|b|$ revolutions in the θ-coordinate, before it intersects the surface $\mathcal{L}_1^-$.

We now describe the set $\mathfrak{M}_0^1$. The images $\tau(P'_\gamma)$ and $\tau(P'_\lambda)$ consist of points of level 1, and the exit boundaries of the notches in these propellers are also at level 1, so all belong to $\mathfrak{M}_0^1$.

We index the notches at level 2 as follows. The segment γ is said to be *based* at its inner endpoint $p(1) = \tau^{-1}(p_1^-) \in L_1^-$ and λ to be *based* at its inner endpoint $p(2) = \tau^{-1}(p_2^-) \in L_2^-$.

Next, introduce labels for the four families of boundary notches which arise. It may help to consider the illustration Figure 25 to keep track of the following definitions.

Let $\gamma'(1,\ell) \subset \mathcal{L}_1^-$ for $b \leq \ell < \infty$ denote the curves corresponding to the intersection of P_γ with $\mathcal{L}_1^-$, where $\gamma'(1,\ell)$ for $b \leq \ell < 0$ denotes an interior curve of the intersection with $\mathcal{L}_1^-$, assuming that such exists. Let $\gamma'(1,\ell)$ for $\ell \geq 0$ denote the boundary curve with lower endpoint $p'(1;1,\ell)$. Set $\gamma(1,\ell) = \sigma_1^{-1}(\gamma'(1,\ell)) \subset L_1^-$. We say that the curve $\gamma(1,\ell)$ for $\ell \geq 0$ is based at the point $p(1;1,\ell)$. For all $x \in \tau(\gamma(1,\ell))$, we have $n_0(x) = 2$ and $r(x) > 2$.

Let $\lambda'(1,\ell) \subset \mathcal{L}_1^-$ for $b \leq \ell < \infty$ denote the curves corresponding to the intersection of P_λ with $\mathcal{L}_1^-$, where $\lambda'(1,\ell)$ for $b \leq \ell < 0$ denotes an interior curve of the intersection with $\mathcal{L}_1^-$, assuming that such exists. Let $\lambda'(1,\ell)$ for $\ell \geq 0$ denote the boundary curve with lower endpoint $p'(2;1,\ell)$. Set $\lambda(1,\ell) = \sigma_1^{-1}(\lambda'(1,\ell)) \subset L_1^-$. We say that the curve $\lambda(1,\ell)$ for $\ell \geq 0$ is based at the point $p(2;1,\ell)$. For all $x \in \tau(\lambda(1,\ell))$, we have $n_0(x) = 2$ and $r(x) > 2$.

Let $\gamma'(2,\ell) \subset \mathcal{L}_2^-$ for $b \le \ell < \infty$ denote the curves corresponding to the intersection of P_γ with $\mathcal{L}_2^-$, where $\gamma'(2,\ell)$ for $b \le \ell < 0$ denotes an interior curve of the intersection with $\mathcal{L}_2^-$, assuming that such exists. Let $\gamma'(2,\ell)$ for $\ell \ge 0$ denote the boundary curve with upper endpoint $p'(1;2,\ell)$. Set $\gamma(2,\ell) = \sigma_2^{-1}(\gamma'(2,\ell)) \subset L_2^-$. We say that the curve $\gamma(2,\ell)$ for $\ell \ge 0$ is based at the point $p(1;2,\ell)$. For all $x \in \tau(\gamma(2,\ell))$, we have $n_0(x) = 2$ and $r(x) > 2$.

Let $\lambda'(2,\ell) \subset \mathcal{L}_2^-$ for $b \le \ell < \infty$ denote the curves corresponding to the intersection of P_λ with $\mathcal{L}_2^-$, where $\lambda'(2,\ell)$ for $b \le \ell < 0$ denotes an interior curve of the intersection with $\mathcal{L}_2^-$, assuming that such exists. Let $\lambda'(2,\ell)$ for $\ell \ge 0$ denote the boundary curve with upper endpoint $p'(2;2,\ell)$. Set $\lambda(2,\ell) = \sigma_2^{-1}(\lambda'(2,\ell)) \subset L_2^-$. We say that the curve $\lambda(2,\ell)$ for $\ell \ge 0$ is based at the point $p(2;2,\ell)$. For all $x \in \tau(\lambda(2,\ell))$, we have $n_0(x) = 2$ and $r(x) > 2$.

Lemmas 12.5 and 12.6 show that the families of points $\{p'(1;i,\ell) \mid \ell \ge 0\}$ and $\{p'(2;i,\ell') \mid \ell' \ge 0\}$ for $i = 1, 2$ are interlaced, so the same holds for the γ and λ curves in $\partial_h^- \mathbb{W}$ and also for the curves with $\ell < 0$. That is, each λ-curve is between two γ-curves, and vice-versa, as illustrated in Figures 26 and 27.

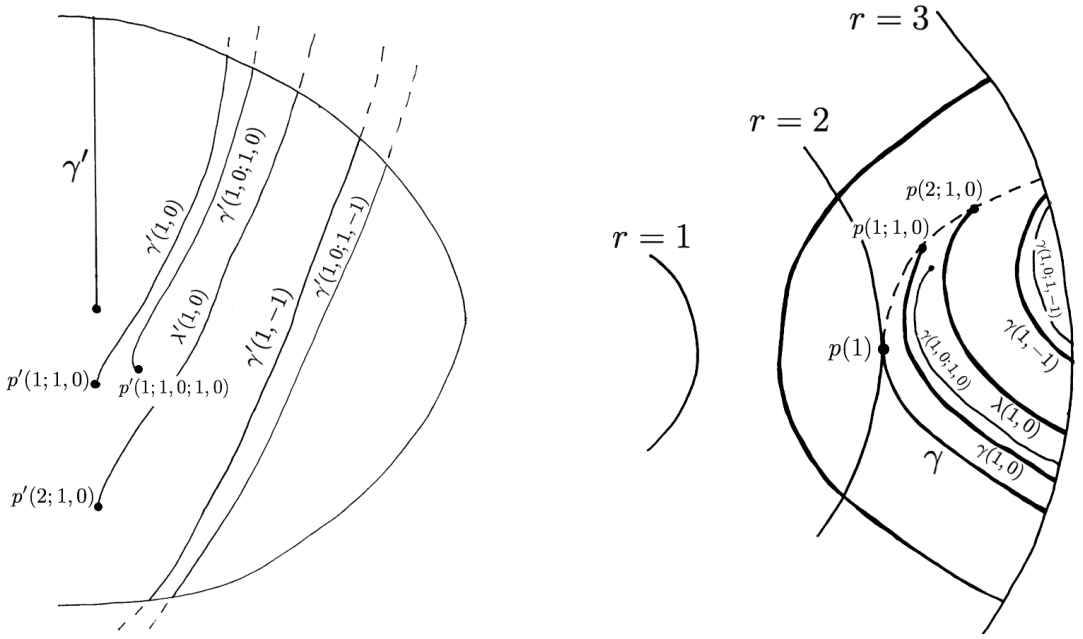

FIGURE 26. Curves of levels 1 and 2, in $\mathcal{L}_1^-$ and in L_1^-

We comment on the details of Figures 26 and 27. The curves in the figures come by pairs, in each pair one curve has level 1 and the other has level 2. We give details for the level 1 curves, that in the left side figures can be distinguished by the fact that one of their endpoints is in the vertical line $\{r = 2\}$. In the left side of Figure 26, the closest curve to γ' is $\gamma'(1,0)$, the boundary of the first boundary notch of P'_γ. The following level 1 curve is $\lambda'(1,0)$ and the next one is $\gamma'(1,-1)$. Observe that b might be -1 for P'_γ and zero for P'_λ, but the number of internal notches is each propeller differs at most by 1. On the right side of Figure 26, the image under σ_1^{-1} of the curves is illustrated. Observe that the curves $\gamma(1,0)$ and $\lambda(1,0)$ have an endpoint in the doted line, that is the image under σ_1^{-1} of the line $\mathcal{C} \cap \{z \le -1\} \cap \mathcal{L}_1^-$. Analogous considerations apply to Figure 27. We give the description of the level 2 curves in this section.

Finally, to complete the description of the level 1 set, note that for $i = 1, 2$, each curve $\tau(\gamma(i,\ell)) \subset E_i$ defines a facing curve $\tau(\overline{\gamma}(i,\ell)) \subset S_i$. These facing curves in S_i are at level 1 again, so belong to $\mathfrak{M}_0^1$. Thus

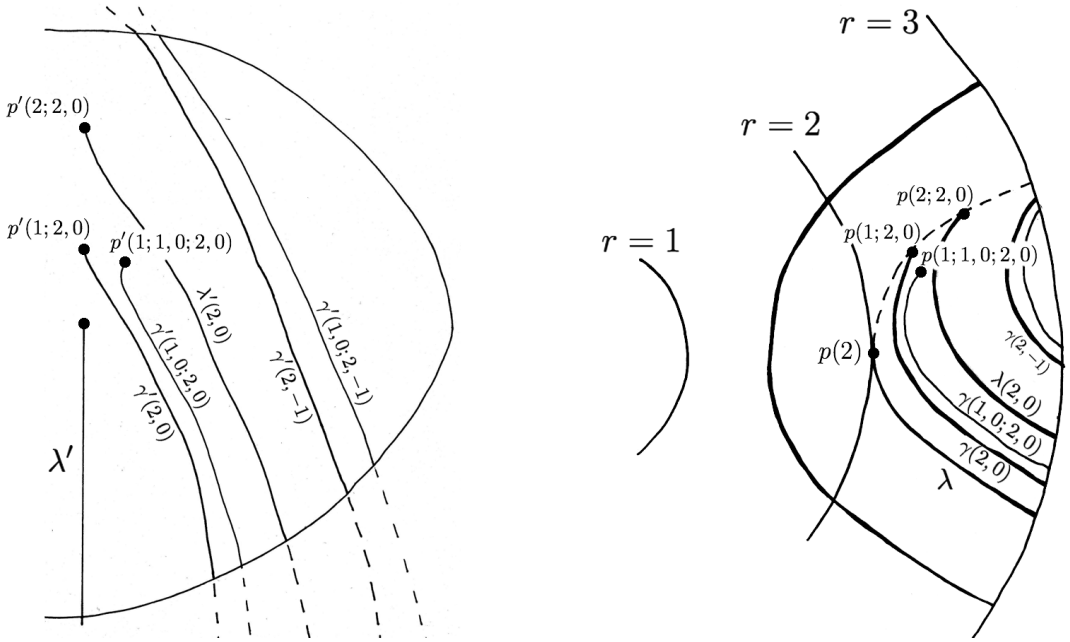

FIGURE 27. Curves of levels 1 and 2, in $\mathcal{L}_2^-$ and in L_2^-

we have

$$\mathfrak{M}_0^1 \;=\; \tau(\mathcal{R}') \;\cup\; \tau(P'_\gamma) \;\cup\; \tau(P'_\lambda) \;\cup \left\{ \bigcup_{\ell \geq b} \bigcup_{i=1,2} \left[\, \tau(\overline{\gamma}(i,\ell)) \;\cup \tau(\overline{\lambda}(i,\ell)) \,\right] \right\} \tag{52}$$

where the propellers and boundary curves are identified via the insertion maps σ_i as appropriate. Observe that in the above, we are assuming that $b \leq 0$ has a constant value for each family of curves. By the interlaced property, the number of internal notches in P'_γ and P'_λ differs at most by one.

For $n \geq 1$, the construction of $\mathfrak{M}_0^{n+1}$ from $\mathfrak{M}_0^n$ follows a procedure similar to the above pattern.

The basic scheme is that for each image under τ of a propeller at level n, the entry curve along each of its notches is a curve at level $n+1$. The Ψ_t-flow of this curve yields a family of propellers at level $n+1$. The resulting propellers at level $n+1$ are contained in the region $r > 2$, so they are finite. We consider the case of $\mathfrak{M}_0^2$ in some detail, to illustrate the general construction of $\mathfrak{M}_0^n$ for $n \geq 2$.

Consider the case $b \leq \ell < 0$ and let $\gamma(1,\ell) = \sigma_1^{-1}(\gamma'(1,\ell)) \subset L_1^-$. All the points on the curve $\gamma(1,\ell)$ have radius greater than 2. Thus by Proposition 6.7 the $\mathcal{K}$-orbit of any point $x \in \tau(\gamma(1,\ell))$ contains the point $\overline{x} \in S_1$ such that $x \equiv \overline{x}$. Let $t_x > 0$ be such that $\Phi_{t_x}(x) = \overline{x}$, then

$$S_{\gamma(1,\ell)} = \{\Phi_t(x) \,|\, x \in \tau(\gamma(1,\ell)),\, 0 \leq t \leq t_x\}, \tag{53}$$

is a compact surface embedded in $\mathbb{K}$. Similarly, we obtain compact surfaces $S_{\lambda(1,\ell)}$, $S_{\gamma(2,\ell)}$ and $S_{\lambda(2,\ell)}$ embedded in $\mathbb{K}$, for $b \leq \ell < 0$.

The surface $S_{\gamma(1,\ell)}$ has points of level 2 and might have points at higher levels, but the level is uniformly bounded above by Proposition 15.4. It contributes to $\mathfrak{M}_0^2$ with a compact set, a bubble, that we describe in detail in Section 15. To simplify the exposition, we assume for the rest of this section that $b = 0$ and thus that the propellers (at any level) do not have internal notches. We discuss the modifications needed to accommodate these internal notches later.

Consider the curve $\gamma(1,\ell) = \sigma_1^{-1}(\gamma'(1,\ell)) \subset L_1^-$ where $\ell \geq 0$. It goes from the outer boundary of $L_1^- \subset \partial_h^- \mathbb{W}$ to the point $p(1;1,\ell)$ with $r(p(1;1,\ell)) > 2$, and all points on the curve $\gamma(1,\ell)$ have radius greater than 2.

Thus, the Ψ_t-flow of the entire curve $\gamma(1,\ell)$ traverses $\mathbb{W}$ in finite time, defining a finite propeller $P_{\gamma(1,\ell)}$ as in Section 11. By (37), the propeller $P_{\gamma(1,\ell)}$ intersects $\mathcal{L}_1^-$ at most $\max_{x\in\gamma(1,\ell)}\Delta(r(x))$ times, for each curve in the collection $\{\gamma(1,\ell)\}_{\ell=0}^{\infty}$. In the same manner, we also obtain finite propellers $P_{\lambda(1,\ell)}$, $P_{\gamma(2,\ell)}$ and $P_{\lambda(2,\ell)}$ for $\ell\geq 0$.

Consider the corresponding four collections of "notched" *finite* propellers

$$\left\{P'_{\gamma(1,\ell))}\right\}_{\ell=0}^{\infty}\ ,\ \left\{P'_{\lambda(1,\ell)}\right\}_{\ell=0}^{\infty}\ ,\ \left\{P'_{\gamma(2,\ell)}\right\}_{\ell=0}^{\infty}\ ,\ \left\{P'_{\lambda(2,\ell)}\right\}_{\ell=0}^{\infty} \tag{54}$$

defined by taking the intersection of the corresponding propellers with $\mathbb{W}'$. Glue these notched propellers to $\mathfrak{M}_0^1$ using σ_1 and σ_2, where the points added with this gluing are level 2 points, hence are contained in $\mathfrak{M}_0^2$.

Each propeller in each of the four infinite collections in (54) yields a family of curves in $\mathcal{L}_1^-$ and another family of curves in $\mathcal{L}_2^-$. Since all the propellers we are considering are finite, the number of curves in the intersection of each propeller with $\mathcal{L}_1^-$ and $\mathcal{L}_2^-$ is finite. Note that the number of notches in a given propeller at level $n\geq 2$ may be zero. Moreover, for $i,j=1,2$ and $\ell\geq 0$, each base point $p(i;j,\ell)$ of the corresponding generating curve has radius greater than 2, so the $\mathcal{W}$-orbit of the labeling points traces out the full boundary of the propeller it defines. This is in contrast to the case with the level 1 propellers, where both forward and backward orbits were required to reach all of the notches. We continue to use the same labeling scheme in levels larger than 1 for the base points of notches corresponding to the intersections with the faces of $\mathcal{L}_1^-$ and $\mathcal{L}_2^-$.

Following the previous scheme, each entry region of a notch of $P'_{\gamma(i_1,\ell_1)}$ and $P'_{\lambda(i_1,\ell_1)}$ defines a curve denoted by $\gamma(i_1,\ell_1;i_2,\ell_2)$ and $\lambda(i_1,\ell_1;i_2,\ell_2)$ for $i_1,i_2=1,2$, where $\ell_1,\ell_2\geq 0$ and ℓ_2 is bounded above by $\max_{x\in\gamma(i_1,\ell_1)}\Delta(r(x))+1<\infty$ or $\max_{x\in\lambda(i_1,\ell_1)}\Delta(r(x))+1<\infty$, accordingly. The index i_2 indicates that the curve is in $\mathcal{L}_{i_2}^-$, while the indices (i_1,ℓ_1) indicate in which notched propeller of level 2 they are contained. Hence, for example, the curve $\gamma(i_1,\ell_1;2,\ell_2)$ is in $\mathcal{L}_2^-$ and belongs to $P'_{\gamma(i_1,\ell_1)}$. Some level 2 curves are represented in Figures 26 and 27. The details of these pictures are considered further in Section 13.

Corresponding to each curve defined by the intersection with an entry face, is the facing curve defined by the intersection with an exit face, denoted by $\overline{\gamma}(i_1,\ell_1;i_2,\ell_2)$ and $\overline{\lambda}(i_1,\ell_1;i_2,\ell_2)$. Then $\mathfrak{M}_0^2$ is obtained by attaching these exit curves to $\mathfrak{M}_0^1$, along with the level 2 finite propellers in (54).

The previous steps are now repeated recursively. Given $\mathfrak{M}_0^n$ for $n\geq 2$, we introduce families of curves defined by the entry curves in the notches of the propellers at level n,

$$\gamma(i_1,\ell_1;i_2,\ell_2;\cdots;i_n,\ell_n)\quad,\quad\lambda(i_1,\ell_1;i_2,\ell_2;\cdots;i_n,\ell_n) \tag{55}$$

and their corresponding facing curves defined by the exit curves, for $i_1,i_2,\ldots,i_n=1,2$ and $\ell_i\geq 0$ which are bounded, except for ℓ_1. The base points of these curves are

$$p(1;i_1,\ell_1;i_2,\ell_2;\cdots;i_n,\ell_n)\text{ and }\ p(2;i_1,\ell_1;i_2,\ell_2;\cdots;i_n,\ell_n),\text{ respectively.}$$

As before, i_n indicates that the curve (or point) is in $\mathcal{L}_{i_n}^-$ and the previous indices $(i_1,\ell_1;i_2,\ell_2;\cdots;i_{n-1},\ell_{n-1})$ indicate the propeller that contains the curve.

The curves in (55) generate finite propellers and the notched finite propellers associated to them. These are hence at level $n+1$. Then $\mathfrak{M}_0^{n+1}$ is obtained from $\mathfrak{M}_0^n$ by attaching the infinite families of finite propellers at level $n+1$ to each of the previously attached propellers in $\mathfrak{M}_0^n$, along with the exit curves at level $n+1$ in these attached propellers. Thus, we obtain the nested compact sets

$$\mathfrak{M}_0^0\subset\mathfrak{M}_0^1\subset\cdots\mathfrak{M}_0^n\subset\mathfrak{M}_0^{n+1}\subset\cdots\subset\mathfrak{M}_0\subset\overline{\mathfrak{M}_0}=\mathfrak{M} \tag{56}$$

Observe that in the construction of $\mathfrak{M}_0^2$ we added 4 countable families of finite propellers, the images under τ of those in (54). In general, in stage n of the construction, we add 2^n countable families of finite propellers, where each propeller is indexed by its base point $p(i_0;i_1,\ell_1;i_2,\ell_2;\cdots;i_{n-1},\ell_{n-1})$ and each family has the indices $i_0,i_1,i_2,\ldots,i_{n-1}$ in common. However, for $(i_0;i_1,\ell_1;i_2,\ell_2;\cdots;i_{n-1})$ fixed, the number of ℓ_{n-1} for which there exists propellers with base curve $\gamma(i_1,\ell_1;i_2,\ell_2;\cdots;i_{n-1},\ell_{n-1})$ if $i_0=1$ or

$\lambda(i_1, \ell_1; i_2, \ell_2; \cdots ; i_{n-1}, \ell_{n-1})$ if $i_0 = 2$, is bounded above by $\Delta(r)$ where r is the maximum radius of the points in the curve $\gamma(i_1, \ell_1; i_2, \ell_2; \cdots ; i_{n-2}, \ell_{n-2})$ or $\lambda(i_1, \ell_1; i_2, \ell_2; \cdots ; i_{n-2}, \ell_{n-2})$, accordingly.

As observed above, the set $\tau(\mathcal{R}')$ is a cylinder, minus two rectangles, embedded as a "folded figure eight" as in Figure 24. One then adds two infinite propellers that wrap around $\tau(\mathcal{R}')$ to obtain $\mathfrak{M}_0^1$. The following steps in the construction add finite propellers to the infinite ones in $\mathfrak{M}_0^1$. The boundary of these finite propellers contain all of the finite *chou-fleurs of Siebenmann*, introduced in [17]. The term "chou-fleur" comes from the diagram of flattened propellers. In fact, if we draw $\mathcal{R}'$ as a rectangle, then we can add the flattened propellers as in Figure 28. The boundary represents $\mathcal{K}$-orbits of the special points p_1^- and p_2^-, and any finite part lying between two facing transition points is a chou-fleur.

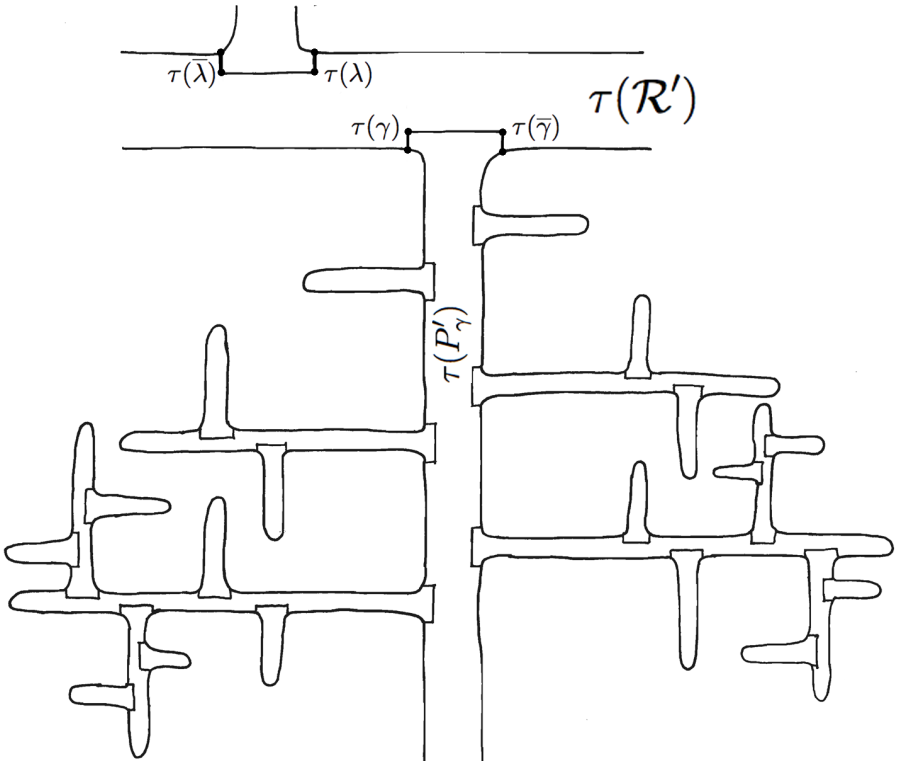

FIGURE 28. Flattened part of $\mathfrak{M}_0$

We comment on the details of Figure 28. The higher horizontal band in Figure 28 represents the notched Reeb cylinder $\mathcal{R}'$ to which the two infinite propellers in $\mathfrak{M}_0^1$ are attached. Part of the infinite propeller $\tau(P'_\gamma)$ is the main vertical branch and only the base of the infinite propeller $\tau(P'_\lambda)$ is pictured in this diagram. The propeller $\tau(P'_\gamma)$ generates by its intersections with the insertions, the finite propellers in $\mathfrak{M}_0^2$, and so on. In $\mathbb{K}$, the width of the infinite propellers is the same as the width of $\mathcal{R}'$. The finite propellers are roughly the same width as the infinite ones, at least for a certain period of time. Hypothesis 12.1, implies that the finite propellers attached to $\tau(P'_\gamma)$ become longer as we move downwards and also that the branching structure gets more and more complicated.

13. Double propellers and pseudogroup dynamics

In this section, we begin our analysis of the dynamics of the Kuperberg flow on $\mathfrak{M}_0$ and the dynamics of the pseudogroup $\mathcal{G}_K$ acting on $\mathbf{R}_0$. A key technique introduced in this section is the the concept of *double propellers*, which are obtained from the $\mathcal{K}$-orbit of special "parabolic" curves in $\partial_h^- \mathbb{W}$. The double propellers

define families of nested topological circles in $\mathbf{R}_0$ which play a fundamental role in the study of the dynamics of the pseudogroup $\mathcal{G}_K$ acting on $\mathbf{R}_0$.

We first introduce the general notion of double propellers in $\mathbb{W}$, then discuss their properties. We then define a labeling system for the double propellers generated by the flow Φ_t, which is based on the labeling system for propellers introduced in the last section. Finally, we consider the intersections of the double propellers with the rectangle $\mathbf{R}_0$, which generates families of nested "ellipses", and introduce a modified labeling system for these curves which corresponds to the action of the generators of the pseudo$\star$group $\mathcal{G}_K^*$ on $\mathbf{R}_0$.

In the following, we assume that the constant $b = 0$, for b as introduced in Section 12 to index the internal notches in the propeller and postpone the discussion of the case $b < 0$ to Section 15.

Consider a smooth curve $\Gamma \subset L_i^-$ parametrized by $u\colon [0,2] \to \partial_h^- \mathbb{W}$, where $u_s \equiv u(s)$, such that:

(1) $r(u_s) \geq 2$ for all $0 \leq s \leq 2$;
(2) $r(u_0) = r(u_2) = 3$, so that both endpoints lie in the boundary $\partial_h^- \mathbb{W} \cap \partial_v \mathbb{W}$;
(3) Γ is topologically transverse to the cylinders $\mathcal{C}(r)$ for $2 \leq r \leq 3$, except at the midpoint u_1.

It then follows that $r(u_s) \geq r(u_1) = 2 + \epsilon$ for all $0 \leq s \leq 2$, and some $\epsilon \geq 0$. See Figure 29 for an illustration in the case when $\epsilon = 0$.

Assume that $\epsilon > 0$, so that $r(u_s) > 2$ for all $0 \leq s \leq 2$, then the $\mathcal{W}$-orbit of each u_s traverses $\mathbb{W}$. Define T_s as the exit time for the $\mathcal{W}$-orbit of u_s. The $\mathcal{W}$-orbits of the points in Γ form a surface embedded in $\mathbb{W}$, whose boundary is contained in the boundary of $\mathbb{W}$, and thus the surface separates $\mathbb{W}$ into two connected components. This surface is denoted P_Γ and called the *double propeller* defined by the Ψ_t-flow of Γ.

Consider the curves $\gamma, \kappa \subset \partial_h^- \mathbb{W}$ obtained by dividing the curve Γ into two segments at the midpoint $s = 1$. Parametrize these curves as follows:

$$\gamma = \Gamma \mid [0,1] \quad , \quad u(s) \text{ for } 0 \leq s \leq 1$$
$$\kappa = \Gamma \mid [1,2] \quad , \quad u(2-s) \text{ for } 0 \leq s \leq 1$$

The orbit $\{\Psi_t(u_1) \mid 0 \leq t \leq T_1\}$ forms the *long boundary* of the propellers P_γ and P_κ generated by the Ψ_t-flow of these curves. Then P_Γ is viewed as the gluing of P_γ and P_κ along the long boundary, which forms a "zipper" joining the two surfaces together, hence the notation "double propeller" for P_Γ. Note that the length of the zipper tends to infinity as $r(u_1) \to 2$.

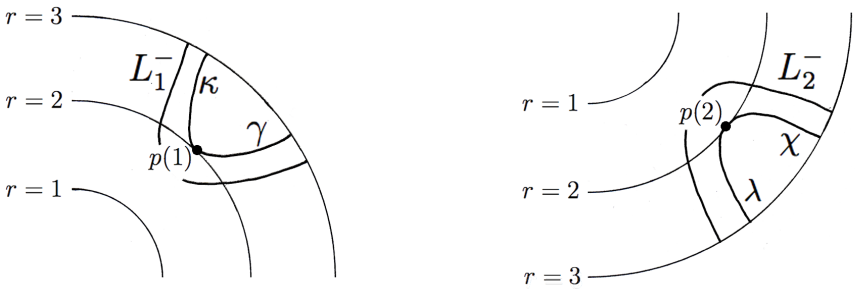

FIGURE 29. The curves $\Gamma = \gamma \cup \kappa$ and $\Lambda = \lambda \cup \chi$ in $\partial_h^- \mathbb{W}$

We comment on the details of Figure 29. Comparing Figure 29 with Figure 23, the γ and λ curves are the first half arcs in Γ and Λ (first in the $\mathbb{S}^1$ direction), while κ and χ are the second half arcs in Γ and Λ, respectively.

If $\epsilon = 0$, define two infinite propellers P_γ and P_κ as in Definition 11.1, and then define $P_\Gamma = P_\gamma \cup P_\kappa$, where the Ψ_t-orbit $\mathcal{Z}_\gamma$ of the midpoint u_1, defined as in (39), is again common to both P_γ and P_κ, and P_Γ is viewed as the gluing of the two propellers along an "infinite zipper".

DEFINITION 13.1. *Let Γ be as above with $r(u_1) = 2$. Let γ^ϵ and κ^ϵ for $0 < \epsilon \leq 1$ be the curves as defined in* (40)*. The* infinite double propeller *is the union:*

$$P_\Gamma \equiv \mathcal{Z}_\gamma \cup \bigcup_{\epsilon>0} \{P_{\gamma^\epsilon} \cup P_{\kappa^\epsilon}\} \tag{57}$$

Observe that $\overline{P_\Gamma} = P_\Gamma \cup \mathcal{R}$ as in Proposition 11.2.

We next apply these ideas to the study of the invariant set $\mathfrak{M}_0$. Recall the curves γ and λ defined by (46) were obtained from the intersection of the Reeb cylinder $\mathcal{R}$ in $\mathbb{W}$ with the entry faces $\mathcal{L}_1^-$ and $\mathcal{L}_2^-$. Now consider the intersections of the *full cylinder* $\mathcal{C} \equiv \{r = 2\}$ with the entry faces $\mathcal{L}_1^-$ and $\mathcal{L}_2^-$, which yields the curves:

$$\Gamma' = \mathcal{C} \cap \mathcal{L}_1^- \subset \mathbb{W} \quad , \quad \Gamma = \sigma_1^{-1}(\Gamma') \subset L_1^- \tag{58}$$

$$\Lambda' = \mathcal{C} \cap \mathcal{L}_2^- \subset \mathbb{W} \quad , \quad \Lambda = \sigma_2^{-1}(\Lambda') \subset L_2^- \tag{59}$$

Hypothesis 12.1 implies that the curves Γ and Λ are topologically transverse to the cylinders $\{r = const.\}$, except at their middle points, where they are tangent to the cylinder $\mathcal{C}$, as in Figure 29. The endpoints of each of the curves Γ and Λ have r-coordinates equal to 3. For the curves γ' and λ' as defined in Section 12, note that $\gamma' = \Gamma' \cap \mathcal{R}$ and $\lambda' = \Lambda' \cap \mathcal{R}$. Also, set

$$\kappa = \sigma_1^{-1}(\Gamma' \cap \{z \leq -1\}) \quad , \quad \chi = \sigma_2^{-1}(\Lambda' \cap \{z \geq 1\}). \tag{60}$$

The graphs of the curves Γ, γ and κ near the special point $\tau^{-1}(p_1^-) \in L_1^-$ are illustrated in Figure 29, as well as the graphs of Λ, λ and χ near the special point $\tau^{-1}(p_2^-) \in L_2^-$.

Let P_Γ and P_Λ be the infinite double propellers associated to these curves by (57). The curves Γ and Λ are disjoint in $\partial_h^- \mathbb{W}$, thus the infinite double propellers P_Γ and P_Λ are disjoint in $\mathbb{W}$. Consider then the notched infinite double propellers,

$$P'_\Gamma = P_\Gamma \cap \mathbb{W}' \qquad \text{and} \qquad P'_\Lambda = P_\Lambda \cap \mathbb{W}'. \tag{61}$$

LEMMA 13.2. *The notched propellers P'_Γ and P'_Λ are tangent to $\mathcal{C}' = \mathcal{C} \cap \mathbb{W}'$ along the $\mathcal{W}$-orbit of the special points $\tau^{-1}(p_1^\pm) \in L_1^\pm$ and $\tau^{-1}(p_2^\pm) \in L_2^\pm$, respectively.*

Proof. The curves Γ, $\overline{\Gamma}$, Λ and $\overline{\Lambda}$ are tangent to the cylinder $\mathcal{C}'$ at their middle points that are the points $\tau^{-1}(p_1^\pm)$ and $\tau^{-1}(p_2^\pm)$, respectively. Hence P'_Γ and P'_Λ are tangent to $\mathcal{C}'$ along the orbits of these points. □

The bases of the propellers P'_Γ and P'_Λ are then "glued" to the notched cylinder $\mathcal{C}'$ using the maps σ_1 and σ_2, respectively. This adds to the notched cylinder $\mathcal{C}'$ two infinitely long "tubes with notched holes" that wrap around $\mathcal{C}'$, accumulating on the notched Reeb cylinder $\mathcal{R}'$. Moreover, the tubes are tangent to $\mathcal{C}'$ along the $\mathcal{W}$-arcs of the special orbits that are in $\mathcal{C}' - \mathcal{R}'$.

Consider the Φ_t-flow of the image $\tau(\mathcal{C}') \subset \mathbb{K}$:

$$\widehat{\mathfrak{M}}_0 \equiv \{\Phi_t(\tau(\mathcal{C}')) \mid -\infty < t < \infty\}. \tag{62}$$

The level function n_0 introduced in Proposition 10.1 extends to a well-defined function on $\widehat{\mathfrak{M}}_0$, using the same method of proof, where $\tau(\mathcal{C}')$ has level 0 by definition. Thus, $\widehat{\mathfrak{M}}_0$ can be decomposed into its level sets:

$$\widehat{\mathfrak{M}}_0^n = \{x \in \widehat{\mathfrak{M}}_0 \mid n_0(x) \leq n\} \ , \ n = 0, 1, 2, \ldots \tag{63}$$

Then $\widehat{\mathfrak{M}}_0^0 = \tau(\mathcal{C}' \cup \overline{\Gamma} \cup \overline{\Lambda})$ as defined above. The set $\widehat{\mathfrak{M}}_0^1$ is obtained by attaching to the notches of $\tau(\mathcal{C}')$ the double infinite propellers $\tau(P'_\Gamma)$ and $\tau(P'_\Lambda)$, as well as part of the boundaries of their notches. In complete analogy with the construction of $\mathfrak{M}_0$, repeat this process recursively for each family of notches, to obtain an embedded surface $\widehat{\mathfrak{M}}_0 \subset \mathbb{K}$. Note that $\mathfrak{M}_0 \subset \widehat{\mathfrak{M}}_0$.

Next, we use the labeling system for $\mathfrak{M}_0$ to describe the intersection of $\widehat{\mathfrak{M}}_0$ with E_1 and E_2. For this section, we keep the assumption $b = 0$ that will be dropped in Section 15. Recall the notation convention of Remark 12.7. The infinite sequence of points $p'(i_0; i_1, \ell_1)$ for $\ell_1 \geq 0$ introduced in Section 12 all lie on

the $\mathcal{W}$-orbits of the points $\tau^{-1}(p_{i_0}^{\pm})$ which are contained in the open "half-cylinders", either $\mathcal{C} \cap \{z < -1\}$ or $\mathcal{C} \cap \{z > 1\}$.

The $\mathcal{K}$-orbits of the points $\tau(p(i_0; i_1, \ell_1))$ for $i_0, i_1 = 1, 2$ and $\ell_1 \geq 0$, yield the families of points labeled as $p(i_0; i_1, \ell_1; i_2, \ell_2; \cdots; i_n, \ell_n)$, which are the basepoints for the curves introduced in Section 12. The double propellers also share these same basepoints, the basepoint of a double propeller is the "middle" point in the curve generating it. We adopt the same notation system.

For $i = 1, 2$, apply σ_i^{-1} to the intersections of P_Γ and P_Λ with the faces $\mathcal{L}_i^-$ to obtain, in $L_1^- \cup L_2^- \subset \partial_h^- \mathbb{W}$, four countable collections of curves, labeled in a manner corresponding to that used for the curves $\gamma(i, \ell)$ and $\lambda(i, \ell)$ in (54). For $\ell \geq 0$, we set:

- $\Gamma(1, \ell) = \gamma(1, \ell) \cup \kappa(1, \ell) \subset L_1^-$, based at $p(1; 1, \ell)$ and corresponding to P_Γ;
- $\Gamma(2, \ell) = \gamma(2, \ell) \cup \kappa(2, \ell) \subset L_2^-$, based at $p(1; 2, \ell)$ and corresponding to P_Γ;
- $\Lambda(1, \ell) = \lambda(1, \ell) \cup \chi(1, \ell) \subset L_1^-$, based at $p(2; 1, \ell)$ and corresponding to P_Λ;
- $\Lambda(2, \ell) = \lambda(2, \ell) \cup \chi(2, \ell) \subset L_2^-$, based at $p(2; 2, \ell)$ and corresponding to P_Λ.

The endpoints of each of the curves $\Gamma(i, \ell)$ and $\Lambda(j, \ell)$ are contained in the boundary of $\partial_h^- \mathbb{W}$, while the midpoints are endpoints for $\gamma(i, \ell)$ and $\kappa(i, \ell)$, or $\lambda(j, \ell)$ and $\chi(j, \ell)$, accordingly.

Note that the curves $\Gamma'(i, \ell)$ and $\Lambda'(i, \ell)$ in the faces $\mathcal{L}_i^-$ are the result of applying the Ψ_t-flow to the curves Γ and Λ. We thus obtain four countable collections of double propellers $P_{\Gamma(i,\ell)}$ and $P_{\Lambda(j,\ell)}$, for $i, j = 1, 2$, and notched double propellers $P'_{\Gamma(i,\ell)}$ and $P'_{\Lambda(j,\ell)}$.

As in Section 12, this creation and labeling of double propellers proceeds recursively, though for levels $n \geq 2$, the propellers obtained are finite as the base curves are contained in the region $r > 2$. There is a nuance that arises with the construction of the corresponding double propellers, however. The curves $\kappa(i_1, \ell_1; i_2, \ell_2; \cdots; i_n, \ell_n) \subset L_{i_n}^-$ and $\gamma(i_1, \ell_1; i_2, \ell_2; \cdots; i_n, \ell_n) \subset L_{i_n}^-$ do not satisfy the radial monotonicity hypothesis. In particular, their intersection point, the "midpoint" u_1 will not be the point where $r(u_s)$ is minimal. However, the κ and γ curves are endpoint isotopic to a curve satisfying the transversality condition, hence the conclusion that the corresponding curve Γ separates the region L_i^- will remain true, so that the double propeller $P_{\Gamma(i_1,\ell_1;\cdots;i_n,\ell_n)}$ is isotopic to a standard double propeller, hence will separate $\mathbb{W}$ into two connected components as well. Similar remarks also hold for the double propeller $P_{\Lambda(i_1,\ell_1;\cdots;i_n,\ell_n)}$, and we label the base curves resulting from the Φ_t-flow:

- $\gamma(i_1, \ell_1; i_2, \ell_2; \cdots; i_n, \ell_n) \subset \Gamma(i_1, \ell_1; i_2, \ell_2; \cdots; i_n, \ell_n) \subset L_{i_n}^-$, which is based at $p(1; i_1, \ell_1; i_2, \ell_2; \cdots; i_n, \ell_n)$;
- $\kappa(i_1, \ell_1; i_2, \ell_2; \cdots; i_n, \ell_n) \subset \Gamma(i_1, \ell_1; i_2, \ell_2; \cdots; i_n, \ell_n) \subset L_{i_n}^-$, which is based at $p(1; i_1, \ell_1; i_2, \ell_2; \cdots; i_n, \ell_n)$;
- $\lambda(i_1, \ell_1; i_2, \ell_2; \cdots; i_n, \ell_n) \subset \Lambda(i_1, \ell_1; i_2, \ell_2; \cdots; i_n, \ell_n) \subset L_{i_n}^-$, which is based at $p(2; i_1, \ell_1; i_2, \ell_2; \cdots; i_n, \ell_n)$;
- $\chi(i_1, \ell_1; i_2, \ell_2; \cdots; i_n, \ell_n) \subset \Lambda(i_1, \ell_1; i_2, \ell_2; \cdots; i_n, \ell_n) \subset L_{i_n}^-$, which is based at $p(2; i_1, \ell_1; i_2, \ell_2; \cdots; i_n, \ell_n)$.

The shape of κ, γ, χ and λ curves will be important in latter sections, and analyzed in Section 18.

There is a tangency relation between double propellers with consecutive levels. Consider the curve $\Gamma \subset L_1^-$ and the curves $\Gamma(1, \ell) \subset L_1^-$. The base point $p'(1; 1, \ell)$ of $\Gamma'(1, \ell) \subset \mathcal{L}_1^-$ has radius equal to 2 and thus belongs to $\mathcal{C} \cap \mathcal{L}_1^-$. Then $p(1; 1, \ell)$ is a point in κ and every $\Gamma(1, \ell)$ curve is tangent to κ at $p(1; 1, \ell)$. Analogously,

- $\Lambda(1, \ell)$ is tangent to κ at $p(2; 1, \ell)$;
- $\Gamma(2, \ell)$ is tangent to χ at $p(1; 2, \ell)$;
- $\Lambda(2, \ell)$ is tangent to χ at $p(2; 2, \ell)$.

Thus the level 2 propellers $P_{\Gamma(i_1,\ell_1)}$ and $P_{\Lambda(i_1,\ell_1)}$ are tangent along the $\mathcal{W}$-orbit of $p(1; i_1, \ell_1)$ and $p(2; i_1, \ell_1)$, respectively, to the level 1 propeller P_Γ if $i_1 = 1$ and P_Λ if $i_1 = 2$. This is illustrated in Figure 30 below.

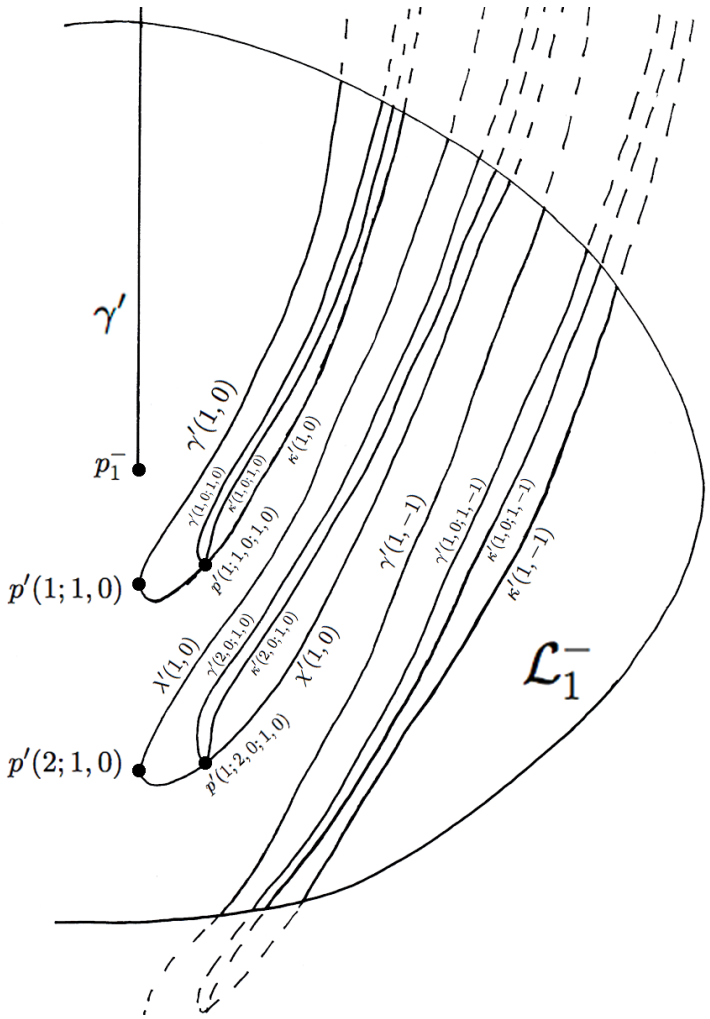

FIGURE 30. Tangencies of level 2 curves with level 1 curves in $\mathcal{L}_1^-$.

In general, a Γ or Λ curve at level n is tangent to a κ or χ curve at level $n-1$, more precisely:

- $\Gamma(1,\ell_1;i_2,\ell_2;\cdots;i_n,\ell_n) \subset L_{i_n}^-$ is tangent to $\kappa(i_2,\ell_2;\cdots;i_n,\ell_n)$ at $p(1;1,\ell_1;i_2,\ell_2;\cdots;i_n,\ell_n)$;
- $\Gamma(2,\ell_1;i_2,\ell_2;\cdots;i_n,\ell_n) \subset L_{i_n}^-$ is tangent to $\chi(i_2,\ell_2;\cdots;i_n,\ell_n)$ at $p(1;2,\ell_1;i_2,\ell_2;\cdots;i_n,\ell_n)$;
- $\Lambda(1,\ell_1;i_2,\ell_2;\cdots;i_n,\ell_n) \subset L_{i_n}^-$ is tangent to $\kappa(i_2,\ell_2;\cdots;i_n,\ell_n)$ at $p(2;1,\ell_1;i_2,\ell_2;\cdots;i_n,\ell_n)$;
- $\Lambda(2,\ell_1;i_2,\ell_2;\cdots;i_n,\ell_n) \subset L_{i_n}^-$ is tangent to $\chi(i_2,\ell_2;\cdots;i_n,\ell_n)$ at $p(2;2,\ell_1;i_2,\ell_2;\cdots;i_n,\ell_n)$.

Recall that the points $p(i_0;i_1,\ell_1)$ converge as $\ell_1 \to \infty$ to $p(i_1)$ as described in Section 12. This type of convergence is repeated at any level. The level n points $p(i_0;i_1,\ell_1;i_2,\ell_2;\cdots;i_n,\ell_n)$ that belong to the curve $\kappa(i_2,\ell_2;\cdots;i_n,\ell_n)$ if $i_1 = 1$ and to the curve $\chi(i_2,\ell_2;\cdots;i_n,\ell_n)$ if $i_1 = 2$, converge to $p(i_1;i_2,\ell_2;\cdots;i_n,\ell_n)$ as $\ell_1 \to \infty$. Observe that the last point is the base point of the κ or χ curve.

We next consider the intersections of the double propeller surfaces with the rectangle $\mathbf{R}_0$. Note that the Ψ_t-flow of a parabolic curve $\Gamma \subset \{r > 2\} \cap \partial_h^- \mathbb{W}$ with endpoints in $\{r = 3\}$ forms a compact surface in $\mathbb{W}$ with boundary contained in $\partial\mathbb{W}$, and the vector field $\mathcal{W}$ is tangent to this surface. Thus, its intersections with the rectangle $\mathbf{R}_0$ are always transverse, so must be a finite union of closed curves. Moreover, the z-symmetry of the vector field $\mathcal{W}$ implies these intersections are symmetric with respect to the horizontal line $\{z = 0\} \cap \mathbf{R}_0$.

In the case of the parabolic curves $\Gamma = \gamma \cup \kappa \subset L_1^-$ and $\Lambda = \lambda \cup \chi \subset L_2^-$, the intersections of the propellers generated by the curves γ and κ with the set $\mathbf{R}_0$ yields a family of arcs, as illustrated in Figure 20. Thus, the intersections with $\mathbf{R}_0$ of the double propeller formed from their Ψ_t-flows yields a family of "thin circles", as illustrated by Figure 31. We call these curves "ellipses" for short.

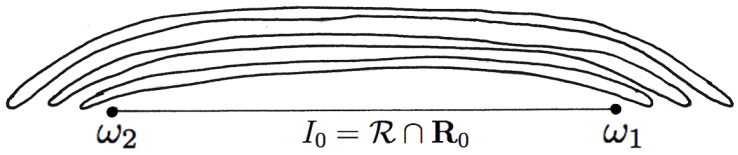

FIGURE 31. Trace of an infinite double propeller in $\mathbf{R}_0$ (viewed sideways)

We next develop a labeling system for the collection of ellipses in $P_\Gamma \cap \mathbf{R}_0$ of the form illustrated in Figure 31. First, introduce the following line segments contained in the intersection $\mathcal{C}_0 \equiv \mathcal{C} \cap \mathbf{R}_0$:

$$I_0 = \{(2, \pi, z) \mid -1 \leq z \leq 1\}, J_0 = \{(2, \pi, z) \mid -2 \leq z \leq -1\}, K_0 = \{(2, \pi, z) \mid 1 \leq z \leq 2\}. \tag{64}$$

$$N_0 = J_0 \cup I_0 \quad , \quad M_0 = I_0 \cup K_0$$

The endpoints of the interval I_0 are the two special points, $\omega_i = \mathcal{O}_i \cap \mathbf{R}_0$, for $i = 1, 2$. The arcs N_0 and M_0 are connected curves in $\mathbf{R}_0$ which contain these special points as midpoints.

Proposition 6.7 implies that the Φ_t-flow of I_0 contains the "notched" Reeb cylinder $\tau(\mathcal{R}')$, thus the Φ_t-flow of I_0 equals $\mathfrak{M}_0$. The Φ_t-flow of $\mathcal{C}_0$ contains the double propellers.

The forward Φ_t-flow of N_0 intersects E_1 in $\tau(\Gamma)$ and generates the embedded double propeller $\tau(P'_\Gamma) \subset \mathbb{K}$. The intersection $\tau(P'_\Gamma) \cap \mathbf{R}_0$ is a countable family of closed curves labeled as $\Gamma_0(\ell)$ that are tangent to J_0 along the forward Φ_t-orbit of ω_1 and to K_0 along the backward Φ_t-orbit of ω_1.

The forward Φ_t-flow of M_0 intersects E_2 in $\tau(\Lambda)$ and generates the embedded double propeller $\tau(P'_\Lambda) \subset \mathbb{K}$. The intersection $\tau(P'_\Lambda) \cap \mathbf{R}_0$ is a countable family of closed curves $\Lambda_0(\ell) \subset \mathbf{R}_0$ that are tangent to J_0 along the forward Φ_t-orbit of ω_2 and to K_0 along the backward Φ_t-orbit of ω_2.

Note that in the above and later, the subscript "0" indicates by convention that a curve is in $\mathbf{R}_0$, and so may be considered as belonging to $\mathbb{W}$ or $\mathbb{K}$, according to the context.

The indexing ℓ of the closed curves $\Gamma_0(\ell)$ and $\Lambda_0(\ell)$ and their images under the Φ_t-flow, involves a subtlety which is analogous to that arising in the proof of Proposition 9.15. It is possible that some of the resulting curves from this flow will intersect in forward time E_1 and E_2, before returning to $\mathbf{R}_0$. Thus, the labeling for curves in these faces as constructed in Section 11 and above, may include some which do not intersect $E_1 \cup E_2$ before returning to $\mathbf{R}_0$. This is the motivation for the following labeling convention.

Let $\Gamma_0(a)$, for $a \leq 0$, denote the first such curve $\Gamma_0(\ell)$ that intersects $\mathbf{R}_0$, whose intersection with the vertical line $\{r = 2\} \subset \mathbf{R}_0$ is composed of the two vertex points $p_0(1; 1, a)$ and $p_0(1; 2, a)$.

Let $\Gamma_0(0)$ be the first such curve for which the $\mathcal{K}$-orbit of its lower vertex point $p_0(1; 1, 0)$ intersects E_1 before intersecting $\mathbf{R}_0$ again. We assume, without loss of generality, that the $\mathcal{K}$-orbit of $p_0(1; 2, 0)$ intersects E_2 before intersecting $\mathbf{R}_0$ again. This symmetry assumption simplifies the labeling system.

REMARK 13.3. *The indexing of the curves starts with a value of $\ell = a$, possibly negative, such that for $a \leq \ell < 0$, the $\mathcal{K}$-orbit of the vertices of the curves $\Gamma_0(\ell)$ do not intercept $E_1 \cup E_2$ in forward time, before returning to $\mathbf{R}_0$. The number of such non-positive indices ℓ is finite, or might be zero. In the latter case, the indexing starts at $\ell = 0$, and it signifies that the forward Φ_t-flow of the vertices of $\Gamma_0(\ell)$ intersects the entry regions E_1 or E_2 in curves $\Gamma(1, \ell)$ or $\Gamma(2, \ell)$, respectively, before intersecting $\mathbf{R}_0$ again. Similar comments apply for the indexing of the Λ_0 curves.*

Observe that $a \leq b \leq 0$ for b as introduced in Section 12. As we assume that $b = 0$, then for $a \leq \ell < 0$, the Φ_t-orbit segment starting at any point of $\Gamma_0(\ell)$ and ending at the corresponding point of $\Gamma_0(\ell + 1)$ will not contain transition points.

Next consider the embedded propellers $\tau(P'_{\Gamma(1,\ell_1)})$ which are the image under τ of compact surfaces traversing $\mathbb{W}$ from the bottom face $\partial_h^-\mathbb{W}$ to the top face $\partial_h^+\mathbb{W}$. They intersect $\mathcal{L}_1^-$ and $\mathcal{L}_2^-$ in finite families of closed curves, denoted by $\Gamma'(1,\ell_1;1,\ell_2)$ and $\Gamma'(1,\ell_1;2,\ell_2)$, and whose inverse image in L_i^- is denoted by $\Gamma(1,\ell_1;i,\ell_2)$, for $i=1,2$ and $\ell_2 \geq 0$. We form the corresponding finite families of closed curves in $\mathbf{R}_0$ denoted by $\Gamma_0(1,\ell_1;\ell_2)$, whose positive Φ_t-flows intersect E_i in the curves $\tau(\Gamma(1,\ell_1;i,\ell_2))$ for $i=1,2$. The index i signifies whether we follow the Φ_t-flow of the curve $\Gamma_0(1,\ell_1;\ell_2)$ in the region $\{z<0\}$ to the surface E_1, or we follow the Φ_t-flow into the region $\{z>0\}$ to the surface E_2.

Similarly, the embedded propellers $\tau(P'_{\Gamma(2,\ell_1)})$ intersect $\mathbf{R}_0$ in finite families of closed curves $\Gamma_0(2,\ell_1;\ell_2)$, as illustrated in Figure 32. The positive Φ_t-flows of these curves in $\mathbf{R}_0$ intersects E_1 and E_2 in curves denoted by $\tau(\Gamma(2,\ell_1;1,\ell_2))$ and $\tau(\Gamma(2,\ell_1;2,\ell_2))$ for $\ell_2 \geq 0$, respectively. These curves define in turn, propellers that intersect $\mathbf{R}_0$ along closed curves, which are recursively defined as:

(1) $\Gamma_0(i_1,\ell_1;i_2,\ell_2;\cdots;i_{n-1},\ell_{n-1};\ell_n) \subset \mathbf{R}_0$ containing the "vertex points" $p_0(1;i_1,\ell_1;i_2,\ell_2;\cdots;i_n,\ell_n)$ for $i_n=1,2$ and with level n;

(2) $\Lambda_0(i_1,\ell_1;i_2,\ell_2;\cdots;i_{n-1},\ell_{n-1};\ell_n) \subset \mathbf{R}_0$ containing the "vertex points" $p_0(2;i_1,\ell_1;i_2,\ell_2;\cdots;i_n,\ell_n)$ for $i_n=1,2$ and with level n.

The points $p_0(i_0;i_1,\ell_1;i_2,\ell_2;\cdots;i_n,\ell_n)$ correspond to the points $p(i_0;i_1,\ell_1;i_2,\ell_2;\cdots;i_n,\ell_n)$ in the same manner as the curves $\Gamma_0(i_1,\ell_1;i_2,\ell_2;\cdots;\ell_n)$ correspond to both

$$\Gamma(i_1,\ell_1;i_2,\ell_2;\cdots;1,\ell_n) \text{ and } \Gamma(i_1,\ell_1;i_2,\ell_2;\cdots;2,\ell_n).$$

We also introduce the curves in $\mathbf{R}_0$:

(1) $\gamma_0(i_1,\ell_1;i_2,\ell_2;\cdots;i_{n-1},\ell_{n-1};\ell_n)$ and $\kappa_0(i_1,\ell_1;i_2,\ell_2;\cdots;i_{n-1},\ell_{n-1};\ell_n)$ contained in $\Gamma_0(i_1,\ell_1;i_2,\ell_2;\cdots;i_{n-1},\ell_{n-1};\ell_n) \subset \mathbf{R}_0$, with $p_0(1;i_1,\ell_1;i_2,\ell_2;\cdots;i_n,\ell_n)$ as common boundary points for $i_n=1,2$;

(2) $\lambda_0(i_1,\ell_1;i_2,\ell_2;\cdots;i_{n-1},\ell_{n-1};\ell_n)$ and $\chi_0(i_1,\ell_1;i_2,\ell_2;\cdots;i_{n-1},\ell_{n-1};\ell_n)$ contained in $\Lambda_0(i_1,\ell_1;i_2,\ell_2;\cdots;i_{n-1},\ell_{n-1};\ell_n) \subset \mathbf{R}_0$, with $p_0(2;i_1,\ell_1;i_2,\ell_2;\cdots;i_n,\ell_n)$ as common boundary points for $i_n=1,2$.

REMARK 13.4. *For points of level at least 2, the number of positive indices ℓ_n such that $p_0(i_0;i_1,\ell_1;\cdots;i_n,\ell_n)$ exists is greater or equal to the number of indices such that the point $p(i_0;i_1,\ell_1;\cdots;i_n,\ell_n)$ exists, since the curves in the the intersection of propellers at level at least 2 get shorter as we approach the tip of the propeller and might not intersect the insertions.*

The γ_0-curves and λ_0-curves are in the Φ_t-flow of I_0, while the κ_0 and χ_0 curves are in the Φ_t-flow of J_0 and K_0, respectively. Each $\Gamma_0(\ell)$ is tangent to J_0 at $p_0(1;1,\ell)$ and to K_0 at $p_0(1;2,\ell)$. Then, we obtain that the Γ_0 curves at level n are tangent to a κ_0 or a χ_0 curve of level $n-1$. Likewise, each Λ_0 curve at level n is tangent to a κ_0 and a χ_0 curve of level $n-1$, as for curves in L_i^-.

Observe that this tangency relation implies that the curves $\Gamma_0(1,\ell_1;\ell_2)$ and $\Lambda_0(1,\ell_1;\ell_2)$ are tangent to $\kappa_0(\ell_2)$ at their vertex points. Hence $\Gamma_0(1,\ell_1;\ell_2)$ and $\Lambda_0(1,\ell_1;\ell_2)$ are inside the region bounded by $\Gamma_0(\ell_2)$, for any $\ell_1 \geq a$. Likewise, $\Gamma_0(2,\ell_1;\ell_2)$ and $\Lambda_0(2,\ell_1;\ell_2)$ are tangent to $\chi_0(\ell_2)$ at their vertex points and lie inside the region bounded by $\Lambda_0(\ell_2)$ for any $\ell_1 \geq a$. Iterating this relation we have that:

- the curves $\Gamma_0(1,\ell_1;i_2,\ell_2;\cdots;\ell_n)$ and $\Lambda_0(1,\ell_1;i_2,\ell_2;\cdots;\ell_n)$ are tangent at their vertex points to $\kappa_0(i_2,\ell_2;\cdots;\ell_n)$ and lie inside the region bounded by $\Gamma_0(i_2,\ell_2;\cdots;\ell_n)$;
- the curves $\Gamma_0(2,\ell_1;i_2,\ell_2;\cdots;\ell_n)$ and $\Lambda_0(2,\ell_1;i_2,\ell_2;\cdots;\ell_n)$ are tangent at their vertex points to $\chi_0(i_2,\ell_2;\cdots;\ell_n)$ and lie inside the region bounded by $\Lambda_0(i_2,\ell_2;\cdots;\ell_n)$.

Thus the Γ_0 and Λ_0 curves form families of nested ellipses. By construction, inside the region bounded by $\Gamma_0(\ell_n)$ are all the Γ_0 and Λ_0 curves whose first i-index is equal to 1 and whose last ℓ-index is equal to ℓ_n. This relation, up to level 3, is illustrated in Figure 32.

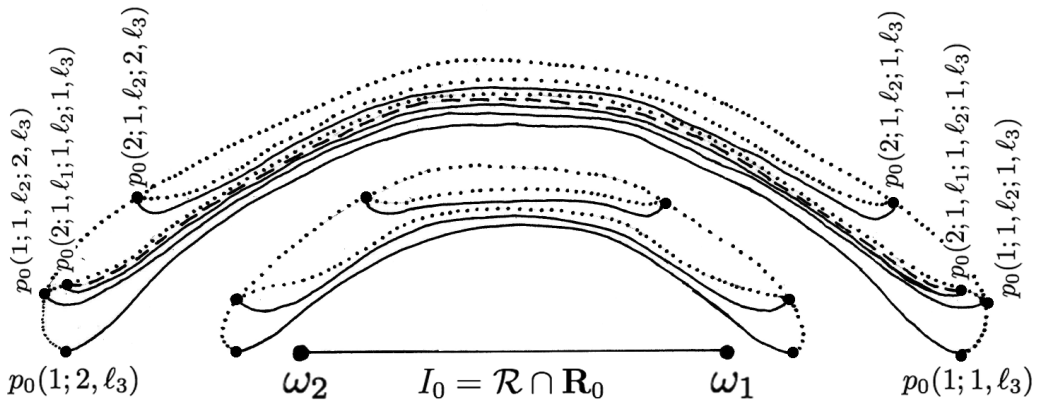

FIGURE 32. Curves in $\mathbf{R}_0$ (viewed sideways). The κ_0 and χ_0 curves of levels 1 and 2 are represented by dotted lines, while the dashed line is a level 3 κ_0-curve.

Thus, the intersection $\widehat{\mathfrak{M}}_0 \cap \mathbf{R}_0$ contains collections of "ellipses" in $\mathbf{R}_0$, indexed as above by their vertex points. We next examine the action of $\mathcal{G}_K^*$ on these collections of ellipses in $\mathbf{R}_0$. The generators $\{\phi_1^{\pm}, \phi_2^{\pm}, \psi\}$ of $\mathcal{G}_K^*$ have domains which are subsets of $\mathbf{R}_0$ that do not contain all of the ellipses themselves, so we define their actions on the ellipses in terms of the actions on the vertex points of these curves. Observe that all these curves are contained in $\mathbf{R}_0 \cap \{r \geq 2\}$. A corollary of the proof of Proposition 9.9 is the following:

LEMMA 13.5. *For each family of curves defined by a member of $\{\Gamma_0, \gamma_0, \kappa_0, \Lambda_0, \lambda_0, \chi_0\}$, and for each $\varphi \in \mathcal{G}_K^*$, the action of φ maps the family of curves to a subset of itself.*

For $n > 1$, recall that the last index ℓ_n for a curve $\Gamma_0(i_1, \ell_1; \cdots; i_{n-1}, \ell_{n-1}; \ell_n)$ is bounded above, with the bound depending on the previous indices, and by abuse of notation, let $\ell'_n = \ell'_n(i_1, \ell_1; \cdots; i_{n-1}, \ell_{n-1})$ denote its maximum value. Recall that there is no restriction on the first index, so $\ell'_1 = \infty$.

Proposition 9.9 implies that each of the sets of points $\{p_0(1; \cdots)\}$ and $\{p_0(2; \cdots)\}$ is invariant, thus the action on these points determines which curve in each of these families is mapped to which curve, and correspondingly, the action on the curves determines the action on these vertices.

We first analyze the action of the map ψ. Recall from Section 9 that the map ψ is obtained from the return map of the Wilson flow to $\mathbf{R}_0$, hence ψ preserves the level function n_0. The intervals I_0, J_0 and K_0 are mapped to themselves, with fixed-points ω_i, for $i = 1, 2$. Consider the open sets in the domain of ψ defined by $U_+ \subset \mathbf{R}_0 \cap \{r \geq 2, z > 0\}$ and $U_- \subset \mathbf{R}_0 \cap \{r \geq 2, z < 0\}$. The set U_- further decomposes into open sets defined by the range of ψ,

$$\psi \colon U_-^- \to U_- \quad , \quad \psi \colon U_-^+ \to \mathbf{R}_0 \cap \{r \geq 2, z \geq 0\}, \tag{65}$$

as illustrated in Figure 33.

The following is a direct consequence of our labeling system:

LEMMA 13.6. *The action ψ on the Γ_0 curves is as follows:*

1. *The map $\psi : U_-^- \to U_-$, sends a subset of the curve $\Gamma_0(i_1, \ell_1; \cdots; i_{n-1}, \ell_{n-1}; \ell_n)$ to a subset of $\Gamma_0(i_1, \ell_1; \cdots; i_{n-1}, \ell_{n-1}; \ell_n + 1)$, for $0 \leq \ell_n < \ell'_n$. For $n = 1$, this operation is always allowed.*
2. *The map $\psi : U_-^+ \to \mathbf{R}_0 \cap \{z \geq 0\}$, sends a subset of the curve $\Gamma_0(i_1, \ell_1; \cdots; i_{n-1}, \ell_{n-1}; \ell_n)$ to a subset of itself.*

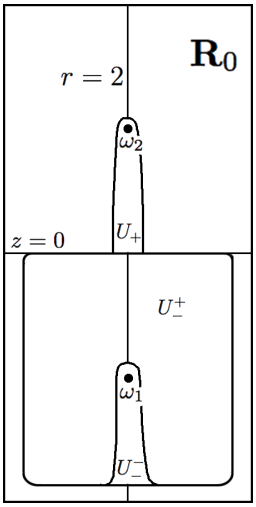

FIGURE 33. Domains of continuity for ψ

(3) The map $\psi : U_+ \to \mathbf{R}_0 \cap \{z \geq 0\}$, sends a subset of the curve $\Gamma_0(i_1, \ell_1; \cdots ; i_{n-1}, \ell_{n-1}; \ell_n)$ to a subset of $\Gamma_0(i_1, \ell_1; \cdots ; i_{n-1}, \ell_{n-1}; \ell_n - 1)$. For every $n \geq 1$, the index ℓ_n is bounded below, hence the map ψ can only be applied to such a curve a finite number of times.

The action on the other families of curves is analogous, but it is slightly different on the base points. The difference is made explicit in Lemma 13.9.1(b).

Next, we analyze the action of the maps $\phi_i^+ \colon U_{\phi_i^+} \to \mathbf{R}_0$ for $i = 1, 2$. The domain $U_{\phi_i^+}$ consists of points $x \in \mathbf{R}_0$ whose forward $\mathcal{K}$-orbit intercepts the face E_i and then continues on to intercept $\mathbf{R}_0$ again, hence the level is increased by one under these maps. Hypothesis (K3) on the embeddings σ_i implies that their domains $U_{\phi_i^+} \subset \mathbf{R}_0$ satisfy

$$U_{\phi_1^+} \subset \mathbf{R}_0 \cap \{z < 0\} \quad , \quad U_{\phi_2^+} \subset \mathbf{R}_0 \cap \{z > 0\} \tag{66}$$

and that their ranges satisfy

$$\phi_1^+(U_{\phi_1^+}) = V_{\phi_1^+} \subset \mathbf{R}_0 \cap \{z < 0\} \quad , \quad \phi_2^+(U_{\phi_2^+}) = V_{\phi_2^+} \subset \mathbf{R}_0 \cap \{z < 0\}, \tag{67}$$

as represented in Figure 17. Then (67) and the definition of the indexing system yields:

LEMMA 13.7. *For $i = 1, 2$, the map ϕ_i^+ sends a subset of $\Gamma_0(i_1, \ell_1; \cdots ; i_{n-1}, \ell_{n-1}; \ell_n)$ for $\ell_n \geq 0$ to a subset of $\Gamma_0(i_1, \ell_1; \cdots ; i_{n-1}, \ell_{n-1}; i, \ell_n; a)$ where $a \leq 0$ is the first index such that the curve $\Gamma_0(a)$ exists.*

Note that ϕ_i^+ sends any point in $U_{\phi_i^+} \cap \{r \geq 2\}$ to a point that is contained in the closed region bounded by the curve $\Gamma_0(a)$ if $i = 1$ and by $\Lambda_0(a)$ if $i = 2$.

We comment on Figure 34, it is useful to compare it to Figure 28. The horizontal upper band represents the Reeb cylinder $\tau(\mathcal{R}')$. The transverse lines to the cylinder and propellers represent their intersections with the rectangle $\mathbf{R}_0$. Since only $\tau(P'_\gamma)$ and its ramifications are illustrated, these lines correspond to γ_0-curves.

The generator ψ preserves level, hence it moves points along propellers. The points in $\tau(\mathcal{R}') \cap \mathbf{R}_0$ are ψ-invariant. For points in the left side boundary of $\tau(P'_\gamma)$, the action of ψ pushes them downwards to the following γ_0-curve, while for points in the right side boundary $\tau(P'_\gamma)$ it moves points upwards. The maps ϕ_i^+ add 1 to the level, so they correspond to jumping to the first curve at higher level. For example, for the curve $\gamma_0(0)$, ϕ_1^+ moves points to $\gamma_0(1, 0; 0)$ and ϕ_2^+ moves points to $\gamma_0(2, 0; 0)$. Observe that the meaning of "first" curve is in the direction of the flow, that runs in opposite directions near the boundaries of $\tau(P'_\gamma)$. The actions of ϕ_i^- are also illustrated.

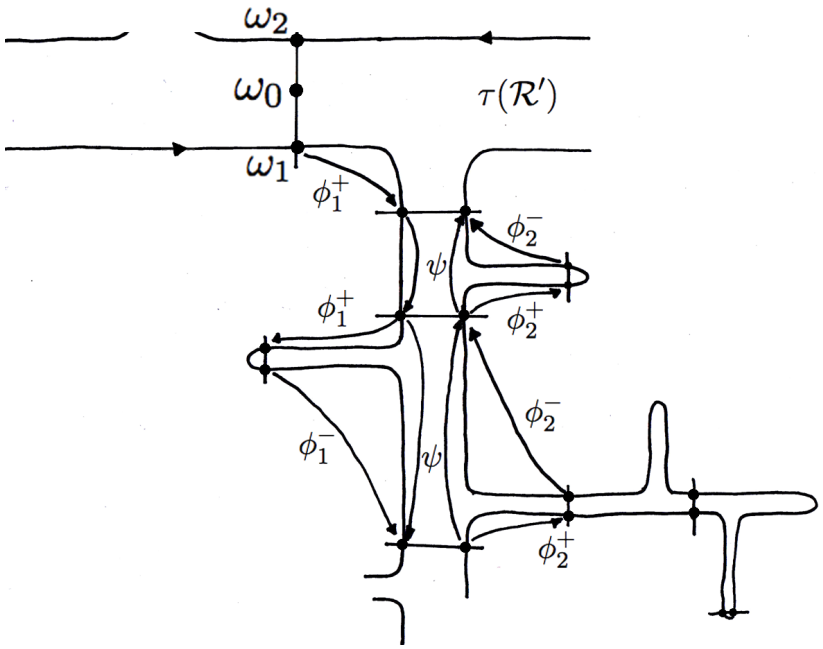

FIGURE 34. Intersection of flattened $\mathfrak{M}_0$ with $\mathbf{R}_0$ with the action of the generators of $\mathcal{G}_K^*$

The action of a general element $\varphi \in \mathcal{G}_K^*$ on a curve in one of the families $\{\Gamma_0, \gamma_0, \kappa_0, \Lambda_0, \lambda_0, \chi_0\}$, can be quite complicated and will be considered further in Section 21. For now, consider the simplest case of iterations of the map ϕ_1^+. The image $\phi_1^+(N_0 \cap U_{\phi_1^+}) \subset \mathbf{R}_0$ is a parabolic curve, twisting upwards as illustrated on the right side of Figure 35. If the image curve $\phi_1^+(N_0 \cap U_{\phi_1^+})$ is again (partially) contained in the domain of ϕ_1^+, then we can consider its (restricted) image under ϕ_1^+ and repeat this process inductively as long as it is defined. This yields a family of parabolic curves, as illustrated on the right side of Figure 35, which shows the image $\phi_1^+(I_0 \cap U_{\phi_1^+})$ on the left-hand-side and three iterations of this map applied to N_0 on the right-hand-side.

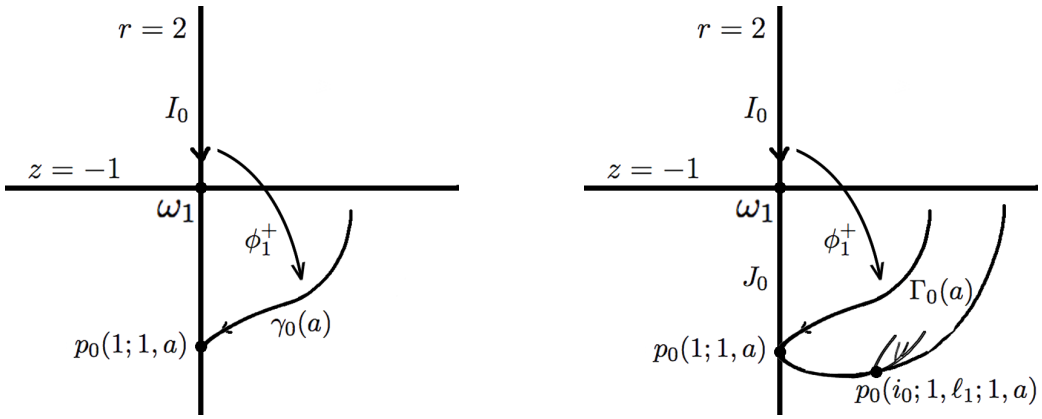

FIGURE 35. The image under ϕ_1^+ of I_0 and $N_0 = I_0 \cup J_0$

The iterates of ψ map $\Gamma_0(i_1, \ell_1; \cdots; i_{n-1}, \ell_{n-1}; a)$ to any $\Gamma_0(i_1, \ell_1; \cdots; i_{n-1}, \ell_{n-1}; \ell_n)$. That is, the action of ψ generates the family $\Gamma_0(i_1, \ell_1; \cdots; i_{n-1}, \ell_{n-1}; \ell_n)$ from $\Gamma_0(i_1, \ell_1; \cdots; i_{n-1}, \ell_{n-1}; a)$.

Finally, we analyze the action of the maps $\phi_i^- : U_{\phi_i^-} \to \mathbf{R}_0$ for $i = 1, 2$, which are defined using the Φ_t-flow. The domain $U_{\phi_i^-}$ consists of points $x \in \mathbf{R}_0$ whose forward $\mathcal{K}$-orbit intercepts the face S_i and then continues

on to intercept $\mathbf{R}_0$ again. Hence, the level is decreased by 1 under these maps, and $U_{\phi_i^-} \subset \mathbf{R}_0 \cap \{z > 0\}$ for $i = 1, 2$.

LEMMA 13.8. *For $i = 1, 2$ and $n \geq 2$, $(\phi_i^-)^{-1}$ maps a subset of $\Gamma_0(i_1, \ell_1; \cdots ; i_{n-1}, \ell_{n-1}; \ell_n)$ to a subset of $\Gamma_0(i_1, \ell_1; \cdots ; i_{n-1}, \ell_{n-1}; i, \ell_n - 1; a)$, where a is defined as in Lemma 13.7. Hence, ϕ_i^- is only defined on the curves $\Gamma_0(i_1, \ell_1; \cdots ; i, \ell_{n-1}; a)$.*

We now comment on the behavior of the points $p_0(i_0; i_1, \ell_1; \cdots ; i_n, \ell_n)$. The points $p'(i_0; 1, \ell)$ are in $\mathcal{L}_1^-$ for $\ell \geq 0$, with $r(p'(i_0; 1, \ell)) = 2$ and $z(p'(i_0; 1, \ell)) < -1$. Thus, $p(i_0; 1, \ell) \in \kappa \subset \Gamma \subset L_1^-$ and $p_0(i_0; 1, \ell) \in J_0$. Since $p_0(i_0; 1, \ell) \to \omega_1$ as $\ell \to \infty$, for ℓ large enough, the points belong to $U_{\phi_1^+}$.

If $p_0(i_0; 1, \ell_1) \in U_{\phi_1^+}$, Lemma 13.7 implies that $\phi_1^+(p_0(i_0; 1, \ell_1)) = p_0(i_0; 1, \ell_1; 1, a)$ that belongs to the curve $\kappa_0(a) \cap \{z \leq 0\}$. Thus the points $p_0(i_0; 1, \ell_1; 1, a)$ accumulate on $p_0(1; 1, a) = \phi_1^+(\omega_1)$ as $\ell_1 \to \infty$. Observe that $p_0(1; 1, a)$ is the vertex point of the curve $\kappa_0(a)$.

Analogously, the points $p_0(i_0; 1, \ell_1; 2, a)$ belong to the curve $\kappa_0(a)$ and accumulate on $p_0(1; 2, a)$, the other vertex point of $\kappa_0(a)$, as $\ell_1 \to \infty$. The points $p_0(i_0; 2, \ell_1; i_2, a)$ belong to the curve $\chi_0(a)$ and accumulate on $p_0(2; i_2, a)$ as $\ell_1 \to \infty$.

Lemmas 13.6 and 13.8 are interpreted in terms of points in the following way.

LEMMA 13.9. *The maps ψ, ϕ_1^+ and ϕ_2^+ act on p_0 points as follow:*

1. *For the map ψ we have the three following possibilities:*
   - (a) *For $1 \leq \ell_n < \ell_n'$, $\psi : U_-^- \to U_-$ maps $p_0(i_0; i_1, \ell_1; \cdots ; 1, \ell_n)$ to $p_0(i_0, i_1, \ell_1; \cdots ; 1, \ell_n + 1)$. For $n = 1$, this operation is always allowed.*
   - (b) *$\psi : U_-^+ \to \mathbf{R}_0 \cap \{z \geq 0\}$ maps $p_0(i_0; i_1, \ell_1; \cdots ; 1, \ell_n)$ to $p_0(i_0; i_1, \ell_1; \cdots ; 2, \ell_n)$.*
   - (c) *$\psi : U_+ \to \mathbf{R}_0 \cap \{z \geq 0\}$ maps $p_0(i_0; i_1, \ell_1; \cdots ; 2, \ell_n)$ to $p_0(i_0; i_1, \ell_1; \cdots ; 2, \ell_n - 1)$. For every $n \geq 1$, the index ℓ_n is bounded below by a, hence the map ψ can only be applied to such a curve a finite number of times.*
2. *ϕ_1^+ maps a point $p_0(i_0; i_1, \ell_1; \cdots ; 1, \ell_n)$ in its domain to $p_0(i_0; i_1, \ell_1; \cdots ; 1, \ell_n; 1, a)$.*
3. *ϕ_2^+ maps a point $p_0(i_0; i_1, \ell_1; \cdots ; 2, \ell_n)$ in its domain to $p_0(i_0; i_1, \ell_1; \cdots ; 2, \ell_n; 1, a)$.*

We have the following consequences of the above results.

LEMMA 13.10. *Every point $p_0(i_0; i_1, \ell_1; \cdots ; i_n, \ell_n)$ is an accumulation point of the set of p_0 points.*

Proof. The points $p_0(i_0; 1, \ell_1; \cdots ; i_n, \ell_n)$ lie in the curve $\kappa_0(i_2, \ell_2; \cdots ; i_{n-1}, \ell_{n-1}; \ell_n)$, and as $\ell_1 \to \infty$ they accumulate on the point $p_0(1; i_2, \ell_2; \cdots ; i_{n-1}, \ell_{n-1}; i_n, \ell_n)$.

Also, the points $p_0(i_0; 2, \ell_1; \cdots ; i_n, \ell_n)$ lie in the curve $\chi_0(i_2, \ell_2; \cdots ; i_{n-1}, \ell_{n-1}; \ell_n)$, and as $\ell_1 \to \infty$ they accumulate on the point $p_0(2; i_2, \ell_2; \cdots ; i_{n-1}, \ell_{n-1}; i_n, \ell_n)$. □

14. Normal forms and tree structure of $\mathfrak{M}_0$

A major theme of this work is to use the pseudogroup $\mathcal{G}_K$ generated by the map $\widehat{\Phi}$ acting on $X = \mathbf{R}_0$, as defined in Definition 9.4, to study the dynamics of the flow Φ_t. The results of Section 13 interpret the local action of $\mathcal{G}_K$ in terms of the propellers introduced in Section 12. The application of these two concepts associated to Φ_t will be made throughout the remaining sections, and many of the results we establish often rely on highly technical arguments, with various nuances. In this section, we pause to give a broader overview of how these concepts, of pseudogroups and propellers, are related. To this end, we introduce a "tree structure" on the space $\mathfrak{M}_0$ as defined in (34) and illustrated in Figure 28. Then in Proposition 14.3 we give an algebraic "normal form" for elements of the pseudo⋆group $\mathcal{G}_K^*$. These two results are closely related, as we explain

below. Finally, in Proposition 14.5 we estimate the number of normal forms as a function of the word length, and show that this function has subexponential growth. This is an intrinsic property of the flow Φ_t.

We first construct the tree $\mathbf{T}_\Phi \subset \mathfrak{M}_0$. Recall that the level decomposition of $\mathfrak{M}_0$ in (56) expresses the space as a union of propellers, and each propeller is defined by the Ψ_t-flow of a curve segment in the face $\partial_h^- \mathbb{W}'$. Each propeller then intersects the center annulus $\{z = 0\} = \tau(\mathcal{A})$. There is a nuance in this picture, as each propeller in the decomposition of $\mathfrak{M}_0$ may give rise to "bubbles" which correspond to double propellers of uniformly bounded complexity attached on the interior of the given propeller, as in (53). This will be discussed in Section 15 and is illustrated in Figure 41. As they do not influence the dynamics of the flow Φ_t, they do not appear in Figure 36.

In the surface $\mathfrak{M}_0$, the intersection of each propeller with the annulus $\{z = 0\}$ forms an embedded "center line segment". Define $\mathbf{T}'_\Phi = \mathcal{A} \cap \mathfrak{M}_0$ which consists of the union of these embedded line segments. Let $\mathbf{T}''_\Phi \subset \mathbf{T}'_\Phi$ consist of the line segments in simple propellers. The connected tree $\mathbf{T}_\Phi$ is formed by adding continuous curve segments in $\mathfrak{M}_0$ joining the line segments in $\mathbf{T}''_\Phi$, as is illustrated in Figure 36.

Define the center line $\mathcal{T} = \{z = 0\} \cap \mathbf{R}_0$, and set $\mathfrak{C}'_0 = \mathcal{T} \cap \mathfrak{M}_0$ and $\mathfrak{C}' = \mathfrak{M} \cap \mathcal{T}$. We will show in Proposition 19.4 that $\mathfrak{C}'$ is a Cantor set, and observe there that it has a decomposition into two disjoint Cantor sets, $\mathfrak{C}' = \mathfrak{C} \cup \mathfrak{C}^1$. The points in the dense subset $\mathfrak{C}^1_0 = \mathfrak{M}_0 \cap \mathfrak{C}^1_0$ of $\mathfrak{C}^1$ correspond to the intersections of the double propellers in bubbles with $\mathcal{T}$, while the points in the dense subset $\mathfrak{C}_0 = \mathfrak{M}_0 \cap \mathfrak{C}$ of $\mathfrak{C}$ correspond to the intersections of γ_0 or λ_0 curves with $\mathcal{T}$. The "fat dots" in Figure 36 correspond to the points contained in the set $\mathfrak{C}_0$, and the lines through the dots represent the intersection with $\mathbf{R}_0$,

The basepoint $\omega_0 = \mathcal{T} \cap \tau(\mathcal{R}')$ is contained in the core annulus $\mathcal{R} = \tau(\mathcal{R}') \subset \mathfrak{M}_0$, illustrated in the picture as the top horizontal strip, which lies at level 0. There is one edge containing ω_0, the top horizontal line in Figure 36, which corresponds to $\tau(\mathcal{R}' \cap \mathcal{A})$ and defines a loop containing ω_0. Thus, strictly speaking, $\mathbf{T}_\Phi$ is a tree provided the loop containing ω_0 is erased.

Recall that the pseudo⋆group $\mathcal{G}^*_K$ denotes the collection of all maps formed by compositions of the maps $\{Id, \phi_1^+, \phi_1^-, \phi_2^+, \phi_2^-, \psi\}$ and their restrictions to open subsets in their domains. The action of these generators on the endpoints of the γ_0 and λ_0 curves in $\mathbf{R}_0$ formed by the intersection $\mathfrak{M}_0 \cap \mathbf{R}_0$ were discussed in Section 13. Note that each such curve intersects the line $\mathcal{T}$ in a point of $\mathfrak{C}_0$, and the actions of the generators $\{\psi, \phi_1^+, \phi_2^+\}$ and their inverses have simple interpretations as actions on the vertices of $\mathbf{T}_\Phi$. We introduce the notation $\{\overline{\psi}, \overline{\phi}_1, \overline{\phi}_2\}$ for the induced action on vertices. Later, in Section 21, we consider the pseudo⋆group $\mathcal{G}_{\mathfrak{M}}$ generated by these actions in detail.

First, the action of $\overline{\psi}$ fixes the basepoint ω_0, and can be thought of as flowing in a loop around the horizontal line in the core annulus $\mathcal{R}'$. The action of $\overline{\psi}$ on points in $\mathfrak{C}_0$, corresponding to γ_0 curves in $\mathbf{R}_0$, is determined by the action of $\psi \colon U_- \to U_-$ as described in Lemma 13.6. We have:

$$\overline{\psi} \,:\, \gamma_0(i_1, \ell_1; \cdots ; i_{n-1}, \ell_{n-1}; \ell_n) \cap \mathcal{T} \;\mapsto\; \gamma_0(i_1, \ell_1; \cdots ; i_{n-1}, \ell_{n-1}; \ell_n + 1) \cap \mathcal{T}. \tag{68}$$

Since $\overline{\psi}$ does not change the level, we conclude that $\overline{\psi}$ moves a point in $\mathfrak{C}_0$ to the "next point" along the line segment in $\mathbf{T}''_\Phi$ containing it. Here, "next" means moving in the positive θ direction along the propeller, hence making one turn around the circle $\mathcal{S} = \{r = 2 \;\&\; z = 0\}$ in $\mathbb{K}$. Thus for $\xi \in \mathfrak{C}_0$ in the domain of the mapping $\overline{\psi}$, we have $r(\overline{\psi}(\xi)) < r(\xi)$ if $\xi \neq \omega_0$. The action of the map $\overline{\psi}$ on the points $\xi \in \mathfrak{C}_0$ defined by λ_0 curves is analogous.

We next show that the paths connecting different level points, which were added to the segments in $\mathbf{T}''_\Phi$ to form $\mathbf{T}_\Phi$, correspond to the actions of the elements $\overline{\phi}_k$ for $k = 1, 2$, analogous to the action of ϕ_k^+. Then by Lemma 13.7 we have that:

$$\overline{\phi}_k \,:\, \gamma_0(i_1, \ell_1; \cdots ; i_{n-1}, \ell_{n-1}; \ell_n) \cap \mathcal{T} \;\mapsto\; \gamma_0(i_1, \ell_1; \cdots ; i_{n-1}, \ell_{n-1}; k, \ell_n; a) \cap \mathcal{T} \tag{69}$$

where $\ell_n \geq 0$ as the curve must intersect the surface E_k in a boundary notch, and $a \leq 0$ is the first index such that the corresponding curve in $\mathbf{R}_0$ exists, as explained in Remark 13.3. A similar result holds for the action of $\overline{\phi}_k$ on λ_0 curves. Note that both maps $\overline{\phi}_1$ and $\overline{\phi}_2$ increase the level function by 1.

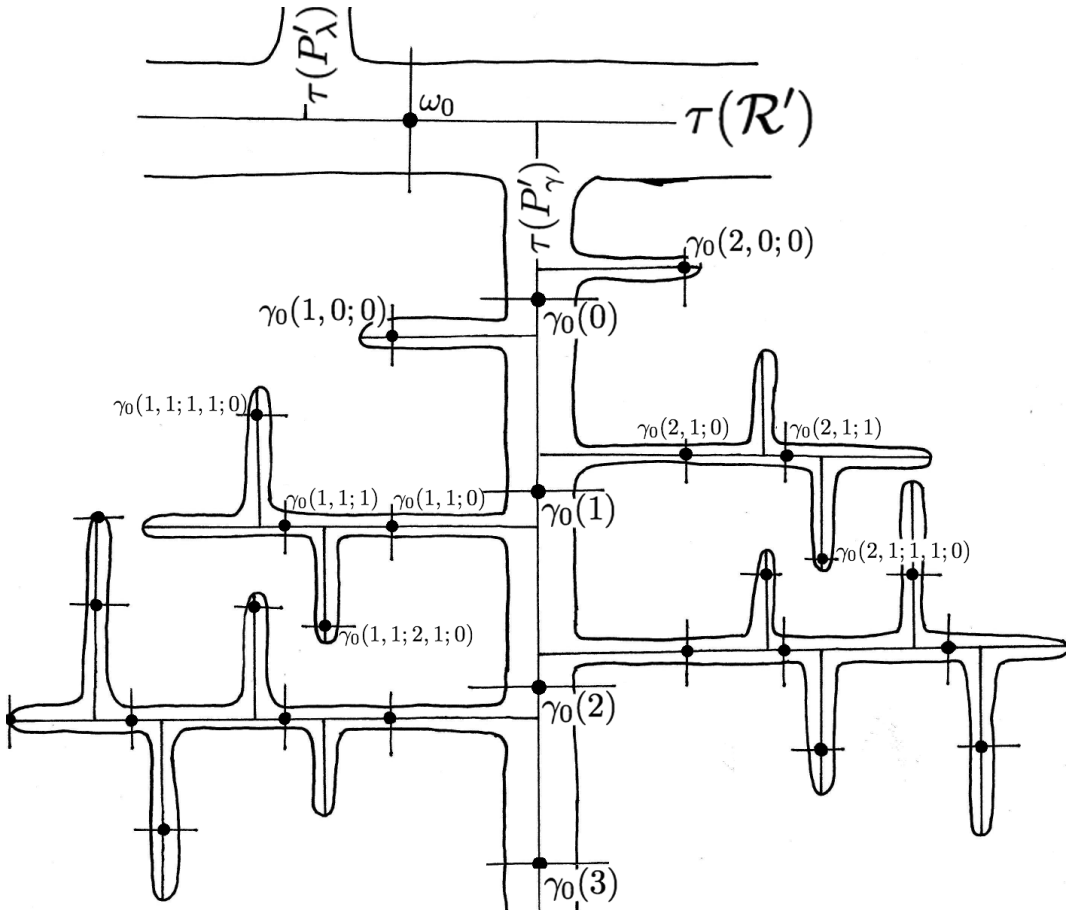

FIGURE 36. $\mathfrak{M}_0$ with the embedded tree $\mathbf{T}_\Phi$

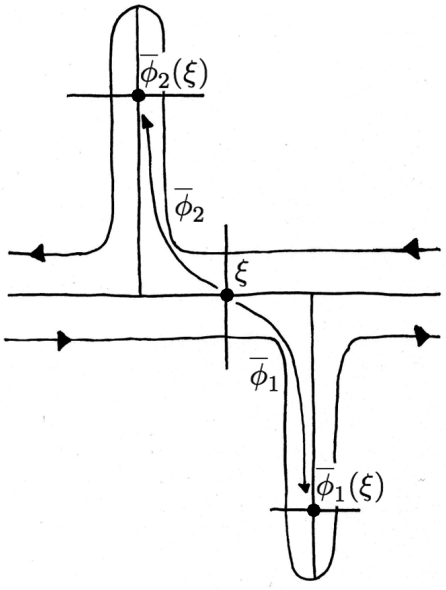

FIGURE 37. The action of $\overline{\phi}_k$

The map $\overline{\phi}_1$ acts on ω_0 via the insertion ϕ_1^+ acting on the point $\omega_1 = (2, \pi, -1)$ to yield $p_0(1; 1, a) = \phi_1^+(\omega_1)$ which corresponds to the first vertex $\overline{\phi}_1(\omega_0)$ at level 1. Graphically, the action of $\overline{\phi}_1$ is to "turn the corner" to the right. This results in adding a curved segment to $\mathbf{T}''_\Phi$ between ω_0 and the point $\overline{\phi}_1(\omega_0)$ in the downward propeller.

The map $\overline{\phi}_2$ acts on ω_0 via the insertion ϕ_2^+ acting on the point $\omega_2 = (2, \pi, 1)$ to yield $p_0(2; 1, a) = \phi_2^+(\omega_2)$ which corresponds to the first vertex $\overline{\phi}_2(\omega_0)$ at level 1. Graphically, the action of $\overline{\phi}_2$ is to "turn the corner" to the left. This results in adding a curved segment to $\mathbf{T}''_\Phi$ between ω_0 and the point $\overline{\phi}_2(\omega_0)$ in the upward propeller.

Note that the remaining vertices in $\mathbf{T}_\Phi$ at level 1 which descend the vertical main propeller $\tau(P_\gamma)$ in Figure 36 correspond to the points $\overline{\psi}^\ell \circ \overline{\phi}_1(\omega_0)$. The points $\overline{\psi}^\ell \circ \overline{\phi}_2(\omega_0)$, also at level 1, ascend on the propeller $\tau(P_\lambda)$ above the core annulus, and are not pictured in Figure 36.

The remaining vertices of the tree $\mathbf{T}_\Phi$ are at level at least 2. The actions of the maps $\{\overline{\psi}, \overline{\phi}_1, \overline{\phi}_2\}$ on these vertices follows the rules above as defined by (68) and (69). The action of $\overline{\psi}$ is translation along the line in $\mathbf{T}''_\Phi$ containing it, while the actions of the maps $\overline{\phi}_1$ and $\overline{\phi}_2$ turn the corner into the propeller at the next higher level, to the right or left accordingly. Accordingly, as mentioned in the definition of $\mathbf{T}_\Phi$ above, we add a curved segment to $\mathbf{T}''_\Phi$ between the vertex ξ and $\overline{\phi}_k(\xi)$, whenever $\overline{\phi}_k(\xi)$ is defined.

We next consider the structure of the pseudo⋆group $\mathcal{G}_K^*$. The analog results for the pseudogroup generated by $\{\overline{\psi}, \overline{\phi}_1, \overline{\phi}_2\}$ are studied in Section 21. The collection

$$\mathcal{G}_K^{(1)} = \{Id, (\psi)^{\pm 1}, (\phi_1^+)^{\pm 1}, (\phi_1^-)^{\pm 1}, (\phi_2^+)^{\pm 1}, (\phi_2^-)^{\pm 1}\} \tag{70}$$

is a symmetric generating set for the pseudo⋆group $\mathcal{G}_K^*$. Let $\mathcal{G}_K^{(n)} \subset \mathcal{G}_K^*$ be the collection of maps defined by the restrictions of compositions of at most n elements of $\mathcal{G}_K^{(1)}$. The "word metric" on $\mathcal{G}_K^*$ is defined by setting $\|\varphi\| \leq n$ if $\varphi \in \mathcal{G}_X^{(n)}$.

Recall that $\mathfrak{M}_0$ is invariant under the flow Φ_t and so each $x \in \mathfrak{M}_0$ has infinite orbit. Set $\mathfrak{M}_{\mathbf{R}_0} = \mathfrak{M} \cap \mathbf{R}_0$. We use the level function defined in Section 10 to show that the words for the restricted action $\mathcal{G}_K^*|\mathfrak{M}_{\mathbf{R}_0}$ have a normal form. First, we define:

DEFINITION 14.1. *A word in $\mathcal{G}_K^*$ is said to be* monotone (increasing) *if it has the form*

$$\varphi \;=\; \psi^{\ell_m} \circ \phi_{i_m}^+ \circ \cdots \circ \psi^{\ell_2} \circ \phi_{i_2}^+ \circ \psi^{\ell_1} \circ \phi_{i_1}^+ \circ \psi^{\ell_0} \tag{71}$$

where each $i_\ell = 1, 2$, each $\ell_k \geq 0$. Let $\mathcal{M}(n)$ be the set of monotone words of length at most n, with $\mathcal{M}(0) = \{Id\}$. Then let $\mathcal{M}(\infty)$ be the union of all collections $\mathcal{M}(n)$ for $n \geq 0$.

Observe that for $\varphi \in \mathcal{M}(\infty)$ as in (71), its length satisfies $\|\varphi\| = m + \ell_0 + \ell_1 + \cdots + \ell_m$.

Also, note that the collection of maps $\mathcal{M}(\infty) \subset \mathcal{G}_K^*$ forms a monoid, as composition of maps of the form (71) is again of that form, assuming that the composition has non-empty domain.

REMARK 14.2. *Observe that if the level along the action of a word in $\mathcal{G}_K^*$ is monotone increasing, the word is written as a composition of the maps ϕ_i^+, $(\phi_i^-)^{-1}$ and ψ, for $i = 1, 2$. By Lemma 13.8, the action of $(\phi_i^-)^{-1}$ can be replaced by $\phi^k \circ \phi_i^+ \circ \psi^{-1}$ for some $k > 0$. The word obtained by this substitution is still monotone increasing in level.*

Even if the substitution made the expression of an element in $\mathcal{G}_K^*$ longer, the counting method below does not consider this nuance and the estimation on the number of monotone words is thus an estimation of words along which the level is monotone increasing.

PROPOSITION 14.3. *Let $\varphi \in \mathcal{G}_K^*$ with $\|\varphi\| \leq n$ and $Dom(\varphi) \cap \mathfrak{M}_{\mathbf{R}_0} \neq \emptyset$. Then there exists a factorization $\varphi = \varphi^+ \circ \varphi^-$, where $\varphi^+ \in \mathcal{M}(n')$ and $(\varphi^-)^{-1} \in \mathcal{M}(n'')$ for integers n', n'' with $n' + n'' \leq n$. Moreover, we have $Dom(\varphi) \subset Dom(\varphi^+ \circ \varphi^-)$. The factorization $\varphi = \varphi^+ \circ \varphi^-$ is said to be the* normal form *for the word φ.*

Proof. By hypothesis we have that $\varphi = \varphi_k \circ \cdots \circ \varphi_1$ for some $k \leq n$ and $\varphi_\ell \in \mathcal{G}_K^{(1)}$ for every $1 \leq \ell \leq k$. Since $\mathfrak{M}$ is the closure of $\mathfrak{M}_0$, and we assume that $Dom(\varphi) \cap \mathfrak{M}_{\mathbf{R}_0} \neq \emptyset$, there exists a point $\xi_0 \in Dom(\varphi) \cap \mathfrak{M}_0 \cap \mathbf{R}_0$. Set $\xi_\ell = \varphi_\ell \circ \cdots \circ \varphi_1(\xi_0)$.

The idea behind the proof is best described in terms of the tree $\mathbf{T}_\Phi$ illustrated in Figure 36. Given $\xi_0 \in \mathfrak{M}_0 \cap \mathbf{R}_0$ there exist a unique point $x \in \mathcal{R}' \cap \mathbf{R}_0$ such that $\Phi_t(x) = \xi_0$ for some $t > 0$. The $\mathcal{K}$-orbit segment $[x, \xi_0]_\mathcal{K}$ is a path in $\mathfrak{M}_0$ so can be deformed into a path in the tree $\mathbf{T}_\Phi$ from ω_0 to the closest endpoint of the γ_0 or λ_0 curve containing ξ_0. This tree path define a unique monotone word $\varphi_{\xi_0} \in \mathcal{G}_K^*$ such that $\varphi_{\xi_0}(x) = \xi_0$. Analogously, there exist a unique monotone word $\varphi_{\xi_k} \in \mathcal{G}_K^*$ and a unique point $y \in \mathcal{R}' \cap \mathbf{R}_0$ such that $\varphi_{\xi_k}(y) = \xi_k$. The expression we are looking for is then the simplified word obtained from $\varphi_{\xi_k} \circ (\varphi_{\xi_0})^{-1}$, that is a product of a monotone word with the inverse of another monotone word.

Let us start the proof. By Proposition 10.1 the level function $n_0 : \mathfrak{M}_0 \to \mathbb{N}$ is well defined. Let $n_*(\varphi, \xi_0) = \min\{n_0(\xi_\ell) \mid 0 \leq \ell \leq k\}$ and $n^*(\varphi, \xi_0) = \max\{n_0(\xi_\ell) \mid 0 \leq \ell \leq k\}$. We consider the following cases:

(1) $n_0(\xi_0) \leq n_0(\xi_k)$ and $n_0(\xi_0) = n_*(\varphi, \xi_0)$.
(2) $n_0(\xi_0) \leq n_0(\xi_k)$ and $n_0(\xi_0) > n_*(\varphi, \xi_0)$.
(3) $n_0(\xi_0) > n_0(\xi_k)$ and $n_0(\xi_k) = n_*(\varphi, \xi_0)$.
(4) $n_0(\xi_0) > n_0(\xi_k)$ and $n_0(\xi_k) > n_*(\varphi, \xi_0)$.

Consider case (1), for which the plot of the function appears as in Figure 38. Let $\ell_1 \geq 0$ be the least index such that there exists $\ell_2 > \ell_1$ with $n_0(\xi_{\ell_1}) = n_0(\xi_{\ell_2})$ and $n_0(\xi_\ell) > n_0(\xi_{\ell_1})$ for all $\ell_1 < \ell < \ell_2$. By Proposition 5.5 combined with Lemma 13.9, we can replace the subword $\varphi_{\ell_2} \circ \varphi_{\ell_2 - 1} \circ \cdots \circ \varphi_{\ell_1}$ by the map ψ, thus changing a non-monotone subword of the expression of φ by ψ. The new word has length less than n and, since the domain of ψ contains the domain of the other generators in $\mathcal{G}_K^{(1)}$, its domain contains the domain of φ. Repeating this process a finite number of times we obtain a monotone word φ^+, and putting $\varphi^- = Id$ we obtain the conclusion of Proposition 14.3.

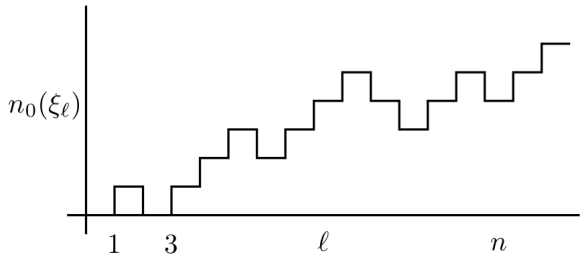

FIGURE 38. Plot of the level function $n_0(\xi_\ell)$

The subword substitution operations in the proof of case (1) above have alternate interpretations. In terms of the sample graph of the level function in Figure 38, we are replacing any parts of the graph which are not increasing with a horizontal line, which corresponds to substituting in some power of the generator ψ^ℓ for the subword. In terms of the tree $\mathbf{T}_\Phi$ in Figure 36, we are following a path that takes a short-cut across the base of each propeller, so that the resulting path follows a curve whose distance from the root is monotonically increasing.

For case (2), let ℓ_* be the first index for which $n_0(\xi_{\ell_*}) = n_*(\varphi, \xi_0)$. We can apply the method of the first case from ξ_0 to ξ_{ℓ_*}, to change φ for a word of the form $\varphi_k \circ \cdots \circ \varphi_{\ell_*+1} \circ \varphi_*$ with $(\varphi_*)^{-1}$ monotone. The word $\varphi_k \circ \cdots \circ \varphi_{\ell_*+1}$ satisfies the hypothesis of the first case and hence can be expressed as a monotone word. This concludes the second case.

In terms of the tree $\mathbf{T}_\Phi$, the point ξ_{ℓ_*} corresponds to a vertex point in the tree which is the closest to the root vertex in the path in $\mathfrak{M}_0$ between ξ_0 and ξ_k.

We are left with the cases where $n_0(\xi_0) > n_0(\xi_k)$. In case (3), let $\ell_* \leq k$ be the first index for which $n_0(\xi_{\ell_*}) = n_*(\varphi, \xi_0)$. As in case (2), we can change the expression of φ for $\varphi_k \circ \cdots \circ \varphi_{\ell_*+1} \circ \varphi_*$ with $(\varphi_*)^{-1}$

monotone. Since $n_*(\varphi, \xi_0) = n_0(\xi_k)$, Proposition 5.5 implies that the word $\varphi_k \circ \cdots \circ \varphi_{\ell_*+1}$ can be replaced by a certain number of consecutive ψ-maps, the number being less or equal to $k - \ell_*$. Thus φ can be expressed as the inverse of a monotone word and the conclusion follows.

The proof for case (4) is analogous to that of case (2). □

We next develop an estimate for the cardinality of the set $\mathcal{M}(n)$ as a function of n. This will be used in later sections when we consider various entropy invariants of the flow Φ_t.

For $\varphi \in \mathcal{M}(n)$ with $\|\varphi\| = n$, assume that φ has the normal form (71). Let $\xi_0 \in \mathfrak{M}_0 \cap Dom(\varphi)$, then let ξ_ℓ for $0 < \ell \leq n$ denote the images of ξ_0 under the partial products of the factors in (71). Note that $r(\xi_{\ell+1}) \geq r(\xi_\ell)$, with equality if $\xi_{\ell+1} = \psi(\xi_\ell)$, and with strict inequality if $\xi_{\ell+1} = \phi_j^+(\xi_\ell)$ and $\xi_\ell \neq \omega_j$ for $j = 1, 2$.

Observe that in the case where $\xi_{\ell+1} = \phi_j^+(\xi_\ell)$, the point ξ_ℓ must lie in the domain of ϕ_j^+. Since $r(\xi_\ell) \geq 2$, if $j = 2$ and $\xi_\ell = \psi^i(\xi_{\ell-i})$, then $i > 0$ must be sufficiently large so that the orbit transverses bottom half of the rectangle $\mathbf{R}_0$ in order to enter the domain of ϕ_2^+. By definition (37), the integer $\Delta(r) = \lfloor \Theta(r)/2\pi \rfloor$ is the number of intersections for the Wilson flow to reach the line $\{z = 0\} \cap \mathbf{R}_0$, where $\Delta(r) \to \infty$ as $r \to 2$. Thus, $i > \Delta(r)$ where $r = r(\xi_{\ell-i})$.

LEMMA 14.4. *For each $b \geq 1$, there exists integers $N_b > 0$ and $L_b > 0$ such that for $\varphi \in \mathcal{M}(n)$ of the normal form (71) with $\ell_0 = 0$, $\ell_1 \leq b$ and sub-index m equaling the number of insertion maps in φ, then $m \leq N_b$ and each $\ell_k \leq L_b$ for $1 \leq k \leq b$. Moreover, $N_b \to \infty$ as $b \to \infty$.*

Proof. The assumption that no factor in (71) is a map ϕ_j^- for $j = 1, 2$ implies that the action of φ on $\mathbf{R}_0$ can be described in terms of the action of the generators $\{\psi, \phi_1^+, \phi_2^+\}$ on the families of nested ellipses in $\mathbf{R}_0$ given by the intersection of $\widehat{\mathfrak{M}}_0 \cap \mathbf{R}_0$. This is described in Lemmas 13.5, 13.6, 13.7 and 13.9. The assumption $\ell_0 = 0$ implies that φ begins with the action of $\phi_{i_1}^+$ and thus the special point $\omega_{i_1} \in Dom(\varphi)$.

Recall that the function $N(r)$ for $r > 2$ was defined in Lemma 6.1, and is the maximum increase in the level function along the orbit of $\mathcal{K}$ starting at an entry point ξ with $r(\xi) = r$. As shown in Section 6, the function $N(r) \to \infty$ as $r \to 2$. We are given $b \geq 1$, so set

$$\rho_b = \min\{r(\phi_{i_2}^+ \circ \psi^{\ell_1} \circ \phi_{i_1}^+(\xi)) \mid \xi \in Dom(\varphi) \text{ and } 0 \leq \ell_1 \leq b\} > 2 \ . \tag{72}$$

Then $N(\rho_b)$ is the maximal increase in the level function starting from the point $\phi_{i_2}^+ \circ \psi^{\ell_1} \circ \phi_{i_1}^+(\xi)$, and thus $m \leq N(\rho_b) + 2$. Set $N_b = N(\rho_b) + 2$. Note that $N_b \to \infty$ as $b \to \infty$.

Let $T_b > 0$ be such that for all $x \in \partial_h^- \mathbb{W}$ with $\rho_b \leq r(x) \leq 3$, then the Wilson flow $\Psi_t(x)$ exits $\partial_h^+ \mathbb{W}$ with $t \leq T_b$. Then L_b can be taken to be the greatest integer less than $T_b/4\pi$. □

We use Lemma 14.4 to obtain an estimate on the growth of the function $\#\mathcal{M}(n)$.

PROPOSITION 14.5. *For each $b \geq 1$, there is a polynomial function $P_b(n)$ of n such that the cardinality of the set $\mathcal{M}(n)$ satisfies*

$$\#\mathcal{M}(n) \leq P_b(n) \cdot 2^{(n/b)}. \tag{73}$$

Proof. For $\varphi \in \mathcal{M}(n)$ with $\|\varphi\| = n$, assume that φ has the normal form (71).

For the given value of b, let $i(\varphi, b) \geq 1$ be the index such that $\ell_i \geq b$ for all $1 \leq i < i(\varphi, b)$, and $\ell_i < b$ for $i = i(\varphi, b)$. Factor $\varphi = \varphi^{(b)} \cdot \varphi_{(b)}$ where $\varphi^{(b)}$ starts with the map $\phi_{i_{i(\varphi,b)}}^+$ and $\varphi_{(b)}$ starts with the map ψ^{ℓ_0}.

Let $k(\varphi, b)$ denote the number of factors in $\varphi^{(b)}$ of the form ϕ_i^+. By Lemma 14.4, $0 \leq k(\varphi, b) \leq N_b$. We have $\|\varphi^{(b)}\| \leq n$, so the indices of the factors of the form ϕ_i^+ appearing in $\varphi^{(b)}$ gives a choice of $k(\varphi, b)$ indices out of the maximum of n possibilities, and for each choice of index, let $i = 1, 2$. Thus, the number of such

words has an upper bound $\binom{n}{k} \cdot 2^k$ for $k = k(\varphi, b)$. Then set

$$B'(n,b) = \binom{n}{0} \cdot 2^0 + \binom{n}{1} \cdot 2^1 + \cdots + \binom{n}{N_b} \cdot 2^{N_b} \tag{74}$$

Observe that $B'(n,b)$ is a polynomial function of n of degree at most N_b. It follows that $B'(n,b)$ is an upper bound on the number of possible words $\varphi^{(b)}$ which can arise for $\varphi \in \mathcal{M}(n)$ and the given value of b.

Next, consider the number of possible choices for the words $\varphi_{(b)}$ which can arise. For $p = i(\varphi, b) - 1$, we then can write

$$\varphi_{(b)} \;=\; \psi^{\ell_p} \circ \phi^+_{i_p} \circ \psi^{\ell_{p-1}} \circ \cdots \circ \psi^{\ell_1} \circ \phi^+_{i_1} \circ \psi^{\ell_0} \tag{75}$$

where each index $\ell_i > b$ for $1 \leq i \leq p$, and so $p \leq n/(b+1) < n/b$. Observe that for $1 \leq k \leq p$, there are at most 2^p possible choices of i_k, so the number of such choices is bounded above by $2^{(n/b)}$.

The placement of the terms $\phi^+_{i_k}$, or equally the choices of the values $\ell_i \geq b$, is given by a more complicated choice function. Observe that $b \leq \ell_0 \leq n$, and $b \leq \ell_1 \leq n - \ell_0 - 1 \leq n - b - 1$. Thus, there are at most $n - 2b$ possible values for ℓ_1. Next, we have $b \leq \ell_2 \leq n - \ell_0 - \ell_1 - 2 \leq n - 2b - 2$, so that there are at most $n - 3b - 1$ possible values for ℓ_2. We continue in this way up to the choice of ℓ_p. The number of possible choices of the indices $(\ell_0, \ell_1, \ldots, \ell_p)$ is then bounded above by the products of the maximal number of values for each ℓ_i for $0 \leq i \leq p$, so is a polynomial in n of degree at most $p + 1$, which we denote by $B''(n,b)$. Set

$$P_b(n) = B'(n,b) \cdot B''(n,b) \tag{76}$$

The estimate (73) follows. □

COROLLARY 14.6. *The function $n \mapsto \#\mathcal{M}(n)$ has subexponential growth. That is, we have*

$$\lim_{n \to \infty} \frac{\ln(\#\mathcal{M}(n))}{n} = 0. \tag{77}$$

Proof. For each $b \geq 1$, the estimate (73) implies that the limit in (77) is bounded above by $\ln(2)/b$ hence equals 0. □

15. Internal notches and bubbles

In this section, we analyze the properties of the "bubbles" that arise when the interior of a propeller intersects an insertion region, resulting in an internal notch, as discussed in Section 12 and illustrated in Figure 25. Recall that an internal notch in a propeller P_γ is a rectangular hole whose boundary is disjoint from the boundary of P_γ. The Φ_t-flow of an internal notch generates a compact surface, as defined by (53) and called a "bubble". A key result of this section is that the bubbles obtained from internal notches all admit a uniform bound on their complexity: the difference of level between any two points in a bubble is uniformly bounded. This is shown in Proposition 15.4.

Assume that the construction of the plug $\mathbb{K}$ and the flow $\mathcal{K}$ satisfies Hypotheses 12.1 and 12.2.

In Sections 12 and 13, the orbits of the special points $p_1^\pm$ and $p_2^\pm$ were used to label the boundary notches of the propellers P'_γ, P'_λ, P'_Γ and P'_Λ, that are bounded by $\mathcal{W}$-arcs spaced along the edges of the propellers. A propeller formed from any of these four families and at any level $n \geq 1$, might also have internal notches as described in Section 12. In this section, we give an analogous labeling for the internal notches and bubbles of the propellers P'_γ and P'_λ, which then also applies to the double propellers P'_Γ and P'_Λ.

First, recall the data that is given. The curve $\gamma' = \mathcal{R} \cap \mathcal{L}_1^-$ denotes the intersection of the face $\mathcal{L}_1^-$ with the Reeb cylinder $\mathcal{R}$, as in (45) and $\overline{\gamma}' = \mathcal{R} \cap \mathcal{L}_1^+$ is its facing curve. Define $\gamma = \sigma_1^{-1}(\gamma') \subset L_1^- \subset \partial_h^- \mathbb{W}$ with facing curve $\overline{\gamma} = \sigma_1^{-1}(\overline{\gamma}') \subset L_1^+ \subset \partial_h^+ \mathbb{W}$. The curve $\kappa' \subset \mathcal{L}_1^-$ is the intersection of the Ψ_t-flow of the interval J_0 with $\mathcal{L}_1^-$ and $\kappa = \sigma_1^{-1}(\kappa') \subset L_1^-$, as illustrated in Figure 29.

The curve $\lambda' = \mathcal{R} \cap \mathcal{L}_2^-$, denotes the intersection of the face $\mathcal{L}_2^-$ with the Reeb cylinder $\mathcal{R}$, as in (45) and $\overline{\lambda}' = \mathcal{R} \cap \mathcal{L}_2^+$ is its facing curve. Define $\lambda = \sigma_2^{-1}(\lambda') \subset L_2^- \subset \partial_h^- \mathbb{W}$ with facing curve $\overline{\lambda} = \sigma_2^{-1}(\overline{\lambda}') \subset L_2^+ \subset \partial_h^+ \mathbb{W}$. The curve $\chi' \subset \mathcal{L}_2^-$ is the intersection of the Ψ_t-flow of the interval K_0 with $\mathcal{L}_2^-$ and $\chi = \sigma_1^{-1}(\chi') \subset L_2^-$, again as illustrated in Figure 29.

Consider first the propeller $P_\gamma \subset \mathbb{W}$ generated by the Φ_t-flow of γ, and let $P'_\gamma = P_\gamma \cap \mathbb{W}'$ be the notched propeller. The intersection of P'_γ with $\mathbf{R}_0$ consists of an infinite family of arcs with lower endpoints in the vertical line segment J_0 that accumulate on ω_1 and upper endpoints that accumulate on ω_2, as in Figure 20. This implies, as observed in Section 12, that P'_γ has an infinite number of (boundary) notches and a finite number $|b| \geq 0$ of internal notches. We assume for the rest of this section that $b < 0$ and investigate the properties of the bubbles which result from their Φ_t-flows.

Let $\gamma'(i,\ell) \subset \mathcal{L}_i^-$ for $b \leq \ell < 0$ denote the intersection of the boundaries of the internal notches of P'_γ with $\mathcal{L}_i^-$. Observe that both endpoints of such a curve are contained in the boundary $\partial \mathcal{L}_i^-$, as for the curve $\gamma'(1,-1)$ in Figure 26 and the the curve $\gamma'(2,-1)$ in Figure 27. The Ψ_t-flow of each $\gamma'(i,\ell)$, from $\mathcal{L}_i^-$ to $\mathcal{L}_i^+$, defines a rectangular region in the interior of P_γ.

Set $\gamma(i,\ell) = \sigma_i^{-1}(\gamma'(i,\ell)) \subset L_i^-$ and parametrize $\gamma(i,\ell)$ by $\gamma_{(i,\ell)} : [0,2] \to L_i^-$ in such a way that:

- $2 < r(\gamma_{(i,\ell)}(1)) \leq r(\gamma_{(i,\ell)}(s))$ for every $s \in [0,2]$;
- $r(\gamma_{(i,\ell)}(0)) = r(\gamma_{(i,\ell)}(2)) = 3$, so both endpoints lie in the boundary $\partial_h^- \mathbb{W} \cap \partial_v \mathbb{W}$.

Analogously define $\lambda(i,\ell) \subset L_i^-$ for $b \leq \ell < 0$. Since the γ and λ curves are interlaced the number of internal notches in P'_γ is equal to ± 1 the number of internal notches in P'_λ. To simplify the notation, we assume that there is the same number of internal notches in P'_λ and P'_γ.

PROPOSITION 15.1. *There exists $r_b > 2$ such that for any $b \leq \ell < 0$ and $i = 1, 2$, then $r(x') \geq r_b$ for all $x' \in \gamma(i,\ell)$ and all $x' \in \lambda(i,\ell)$.*

Proof. For a curve $\zeta\colon [0,1] \to \mathbb{W}$, set $r(\zeta) = \min\{r(\zeta(s)) \mid 0 \leq s \leq 1\}$. Then set

$$r_b = \min\{r(\kappa(1,0)), r(\kappa(2,0)), r(\chi(1,0)), r(\chi(2,0))\} > 2. \tag{78}$$

Consider first the case $\gamma(1,\ell)$ for $b \leq \ell < 0$. Recall that $p(1;1,0) \in \kappa$ is the endpoint of the curve $\gamma(1,0) \subset L_1^-$ and satisfies $r(p(1;1,0)) > 2$. Define a curve $\Upsilon(\kappa,1) \subset L_1^-$ with endpoints in $\{r = 3\}$ which first follows the path $\kappa(1,0)$ from its endpoint in $\{r = 3\}$ to its endpoint $p(1;1,0)$, then follows the curve κ back to its boundary point in $\{r = 3\}$. This is illustrated in Figure 39. Note that $\Upsilon(\kappa,1)$ divides L_1^- into two topological discs and consider the closure $D(\kappa,1)$ of the disk contained in the region $r > 2$. The radius function restricted to $D(\kappa,1)$ has a minimum value greater or equal to r_b.

Note that for $b \leq \ell < 0$, we have $\gamma(1,\ell) \subset D(\kappa,1)$ and hence $r(\gamma(1,\ell)) \geq r_b$.

The radius estimate for the cases $\gamma(2,\ell)$, $\lambda(1,\ell)$ and $\lambda(2,\ell)$ follow in the similar manner, using the corresponding curves $\Upsilon(\kappa,2)$, $\Upsilon(\chi,1)$ or $\Upsilon(\chi,2)$. □

In what follows, we restrict our attention to the surfaces derived from the Ψ_t-flow of the curves $\gamma(1,\ell)$ for $b \leq \ell < 0$, which form the "bubbles" in the propeller P_γ. An analogous discussion applies to the curves $\gamma(2,\ell)$, $\lambda(1,\ell)$ and $\lambda(2,\ell)$.

The endpoints of $\gamma(1,\ell_1)$ are contained in $\partial_v \mathbb{W}$ and thus their $\mathcal{W}$-orbits escape through $\partial_v^+ \mathbb{W}$ without intersecting $\mathbf{R}_0$. Thus, the intersection $P_{\gamma(1,\ell_1)} \cap \mathbf{R}_0$ is a finite family of circles contained in the region $r \geq r(\gamma_{(1,\ell_1)}(1)) > r_b$. The number of circles is bounded by $\Delta(r(\gamma_{(1,\ell_1)}(1))) + 1$, where Δ is defined by (37). The number of circles thus admits the uniform upper bound $\Delta(r_b) + 1$.

Since $\gamma(1,\ell_1)$ is contained in the region of L_1^- bounded by the curve $\Upsilon(\kappa,1)$ introduced in the proof of Proposition 15.1, thus is in the region of L_1^- bounded by Γ. The circles formed by the intersection $P_{\gamma(1,\ell_1)} \cap \mathbf{R}_0$ lie in the discs bounded by a certain $\Gamma_0(\ell_2)$, for $\ell_2 \geq a$. Assuming that $P_{\gamma(1,\ell_1)} \cap \mathbf{R}_0$ is non-empty, the first curve in the intersection is in the region of $\mathbf{R}_0$ bounded by $\Gamma_0(a)$, with a as in Remark 13.3 and the following

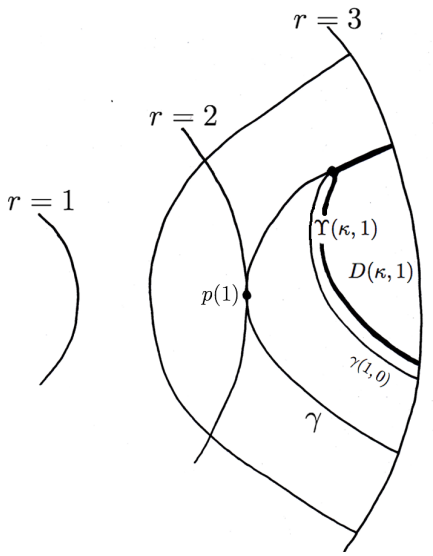

FIGURE 39. The curve $\Upsilon(\gamma, 1)$ and the disc $D(\kappa, 1)$ in L_1^-

curves are obtained by applying the Wilson map $\psi \in \mathcal{G}_K$. Thus if the intersection is formed by n curves, the first one is in the region bounded by $\Gamma_0(a)$, the second one in the region bounded by $\Gamma_0(a+1)$ and the kth curve is in the region bounded by $\Gamma_0(a+k)$, for $0 \leq k \leq n$.

We extend the labeling to $P_{\gamma(1,\ell_1)} \cap \mathbf{R}_0$ by naming the curves in the intersection $\gamma_0(1, \ell_1; \ell_2)$, for $a \leq \ell_2 \leq a+n$, in such a way that $\gamma_0(1, \ell_1; \ell_2)$ is contained in the disc bounded by $\Gamma_0(\ell_2)$. Observe that ℓ_1 is negative and that the connected component of $P_{\gamma(1,\ell_1)} \cap \mathbf{R}_0$ closer to the boundary $r = 3$ of $\mathbf{R}_0$ is denoted by $\gamma_0(1, \ell_1; a)$. This convention agrees with the labeling system introduced in the previous sections. Analogously we have:

- The curves in the intersection $P_{\lambda(1,\ell_1)} \cap \mathbf{R}_0$ are labeled $\lambda_0(1, \ell_1; \ell_2)$ and are contained in regions bounded by Γ_0 curves. Thus $\lambda_0(1, \ell_1; \ell_2)$ lies inside the region bounded by $\Gamma_0(\ell_2)$.
- The curves in the intersection $P_{\gamma(2,\ell_1)} \cap \mathbf{R}_0$ are labeled $\gamma_0(2, \ell_1; \ell_2)$ and are contained in regions bounded by Λ_0 curves. Thus $\gamma_0(2, \ell_1; \ell_2)$ lies inside the region bounded by $\Lambda_0(\ell_2)$.
- The curves in the intersection $P_{\lambda(2,\ell_1)} \cap \mathbf{R}_0$ are labeled $\lambda_0(2, \ell_1; \ell_2)$ and are contained in regions bounded by Λ_0 curves. Thus $\lambda_0(2, \ell_1; \ell_2)$ lies inside the region bounded by $\Lambda_0(\ell_2)$.

For the notched propellers $P'_{\gamma(i,\ell_1)}$ and $P'_{\lambda(i,\ell_1)}$, for $i = 1, 2$ and $b \leq \ell_1 < 0$, obtained by intersecting the corresponding propeller with $\mathbb{W}'$, their images $\tau(P'_{\gamma(i,\ell_1)})$ and $\tau(P'_{\lambda(i,\ell_1)})$ form part of $\mathfrak{M}_0$.

We now describe the compact surfaces $S_{\gamma(1,\ell_1)} \subset \mathbb{K}$ for $b \leq \ell_1 < 0$ introduced in (53). Consider the notched propellers $P'_{\gamma(1,\ell_1)} = P_{\gamma(1,\ell_1)} \cap \mathbb{W}'$ for $b \leq \ell_1 < 0$. If $P_{\gamma(1,\ell_1)} \cap \mathcal{L}_1^-$ is non-empty, let $\gamma'(1, \ell_1; 1, \ell_2)$ be the curves in the intersection. Observe that ℓ_2 admits finitely many possible values, at most $\Delta(r_b) + 1 < \infty$. In the same way if $P_{\gamma(1,\ell_1)} \cap \mathcal{L}_2^-$ is non-empty, let $\gamma'(1, \ell_1; 2, \ell_2)$ be the curves in the intersection. Observe that ℓ_2 admits finitely many possible values, at most $\Delta(r_b) + 1 < \infty$. Since $\gamma_0(1, \ell_1; 1, b-1) \subset \mathbf{R}_0$ is the region bounded by $\Gamma_0(b-1) = \gamma_0(b-1) \cup \kappa_0(b-1)$, the $\mathcal{K}$-orbits of points in $\gamma_0(1, \ell_1; 1, b-1)$ come back to $\mathbf{R}_0$ before hitting the insertions. Hence the first curve in $P_{\gamma(1,\ell_1)} \cap \mathcal{L}_1^-$ is either $\gamma(1, \ell_1; 1, b)$ or $\gamma(1, \ell_1; 1, b+1)$.

Consider now the curves $\gamma(1, \ell_1; 1, \ell_2) = \sigma_1^{-1}(\gamma'(1, \ell_1; 1, \ell_2)) \in L_1^-$ with $b \leq \ell_1 < 0$ and $b \leq \ell_2$. Two possible situations arise, as illustrated in Figure 40:

- $\gamma'(1, \ell_1; 1, \ell_2)$ contains a point of the $\mathcal{W}$-orbit of $\gamma_{(1,\ell_1)}(1)$. In this case the curve is an arc with endpoints in $\partial\mathcal{L}_1^-$. Thus $\gamma(1, \ell_1; 1, \ell_2)$ generates a finite double propeller $P_{\gamma(1,\ell_1;1,\ell_2)} \subset \mathbb{W}$. The Radius Inequality implies that the minimum radius along $\gamma(1, \ell_1; 1, \ell_2)$ is strictly bigger than $r(\gamma_{(1,\ell_1)}(1)) > r_b$,

and thus the number of circles in $P_{\gamma(1,\ell_1;1,\ell_2)} \cap \mathbf{R}_0$ is less or equal that the number of circles in the intersection $P_{\gamma(1,\ell_1)} \cap \mathbf{R}_0$.

- $\gamma'(1,\ell_1;1,\ell_2)$ does not contains points in the $\mathcal{W}$-orbit of $\gamma_{(1,\ell_1)}(1)$ and thus it is formed by the union of two connected components, each being an arc with endpoints in $\partial\mathcal{L}_1^-$. In this case we obtain from $\gamma(1,\ell_1;1,\ell_2)$ two double finite propellers whose union we denote by $P_{\gamma(1,\ell_1;1,\ell_2)} \subset \mathbb{W}$. Observe that the Radius Inequality implies that the minimum radius along any component of $\gamma(1,\ell_1;1,\ell_2)$ is strictly bigger than $r(\gamma_{(1,\ell_1)}(1)) > r_b$, and thus the number of circles in $P_{\gamma(1,\ell_1;1,\ell_2)} \cap \mathbf{R}_0$ is less or equal that twice the number of circles in the intersection $P_{\gamma(1,\ell_1)} \cap \mathbf{R}_0$.

The construction terminates if $P_{\gamma(1,\ell_1;1,\ell_2)} \cap \mathcal{L}_i^- = \emptyset$ for $i = 1, 2$; otherwise, it continues in a recursive manner.

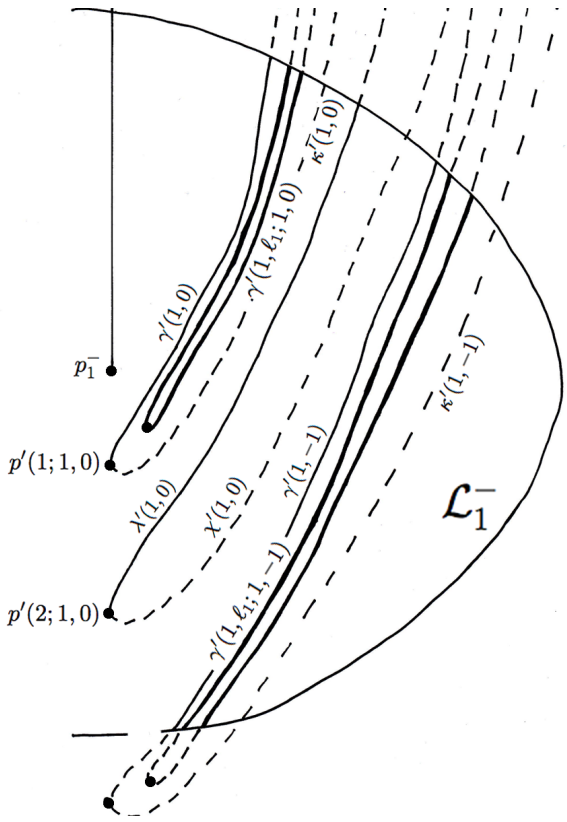

FIGURE 40. Possible intersections of $P_{\gamma(1,\ell_1)}$ with $\mathcal{L}_1^-$ for $b \leq \ell_1 < 0$

We comment on the details of Figure 40. There are two Γ' curves, with the corresponding κ' in dotted lines, and one Λ' curve, with the corresponding χ' in dotted lines. These are level 1 curves. At level two, two curves in the intersection $P_{\gamma(1,\ell_1)} \cap \mathcal{L}_1^-$ are illustrated: $\gamma'(1,\ell_1;1,0)$ with one connected component, and $\gamma'(1,\ell_1;1,-1)$ formed of the union of two connected components. These curves are contained in the regions of $\mathcal{L}_1^-$ bounded by $\Gamma'(1,0)$ and $\Gamma'(1,-1)$, respectively.

Analogous considerations apply to the curves $\gamma(1,\ell_1;2,\ell_2)$ thus we obtain two families of level 3 propellers $P_{\gamma(1,\ell_1;i_2,\ell_2)}$ for $i_2 = 1, 2$ and $b \leq \ell_1 < 0$ that are part of $S_{\gamma(1,\ell_1)}$. Let $P'_{\gamma(1,\ell_1;i_2,\ell_2)} = P_{\gamma(1,\ell_1;i_2,\ell_2)} \cap \mathbb{W}'$. Observe that $\tau(P'_{\gamma(1,\ell_1;i_2,\ell_2)}) \subset S_{\gamma(1,\ell_1)}$. Thus for $b \leq \ell_1 < 0$,

$$\bigcup_{i_2=1,2} \bigcup_{\ell_2} \tau(P'_{\gamma(1,\ell_1;i_2,\ell_2)}) \subset S_{\gamma(1,\ell_1)}, \tag{79}$$

where the union is taken over all the possible values of ℓ_2, once i_2 is given.

LEMMA 15.2. *There exists $N > 0$ such that for any $x \in S_{\gamma(1,\ell_1)}$ with $x \notin \overline{\gamma}(1,\ell_1)$, then $2 \leq n_0(x) \leq N+1$.*

Proof. The boundary of $S_{\gamma(1,\ell_1)}$ is composed by $\tau(\gamma(1,\ell_1)) \subset E_1$, the facing curve $\tau(\overline{\gamma}(1,\ell_1)) \subset S_1$ and the two $\mathcal{K}$-orbit segments going from the endpoints of the entry curve to the endpoints of the facing exit curve. Since $r(\gamma_{(1,\ell_1)}(1)) > 2$ and $\gamma(1,\ell_1)$ is a level 2 curve, then for any $x \in S_{\gamma(1,\ell_1)}$ we know that $n_0(x) \geq 2$.

Consider now $\gamma(1,0)$. Since $r(\gamma_{(1,0)}(1)) > r_b > 2$, the $\mathcal{K}$-orbit of every point in $\tau(\gamma(1,0))$ passes through the facing point, and thus attains a maximum level $N+1$. Thus $n_0(x) \leq N+1$. □

This implies that the construction process above terminates after at most N steps. Thus $S_{\gamma(1,\ell_1)}$ is the union of

$$\bigcup_{1 \leq n \leq N+1} \tau(P'_{\gamma(1,\ell_1;i_2,\ell_2;\cdots;i_n,\ell_n)}),$$

for any combinations of indices, $(i_2,\ell_2;\cdots;i_n,\ell_n)$, where $b \leq \ell_1 < 0$.

In a similar way we obtain the compact surfaces $S_{\gamma(2,\ell)}$, $S_{\lambda(1,\ell)}$ and $S_{\lambda(2,\ell)}$. We call these surfaces the level 2 bubbles in $\mathfrak{M}_0$, since they are associated to a level 2 curve.

Recall that in (52) the set $\mathfrak{M}_0^1$ was described for any value of b. The construction of $\mathfrak{M}_0^{n+1}$ from $\mathfrak{M}_0^n$, for $n \geq 1$, follows the lines of the construction of $\mathfrak{M}_0^1$ from $\mathfrak{M}_0^0 = \tau(\mathcal{R}')$. To obtain $\mathfrak{M}_0^2$ we have to add the level 2 points in the $\mathcal{K}$-orbits of points in $\gamma(i,\ell)$ and $\lambda(i,\ell)$ for $i = 1,2$ and $b \leq \ell$ and unbounded. The case $\ell \geq 0$ was described in Section 12, here we consider the case $b \leq \ell < 0$ and $i = 1,2$, thus the level 2 points in the bubbles $S_{\gamma(i,\ell)}$, $S_{\lambda(i,\ell)}$. If $b \neq 0$, we add to the set $\mathfrak{M}_0^1$ described in Section 12 the notched propellers $\tau(P'_{\gamma(i,\ell_1)})$ and $\tau(P'_{\lambda(i,\ell_1)})$ for $i = 1,2$ and $b \leq \ell_1 < 0$ and the finite collection of exit curves $\tau(\overline{\gamma}(i_1,\ell_1;i_2,\ell_2))$ and $\tau(\overline{\lambda}(i_1,\ell_1;i_2,\ell_2))$.

REMARK 15.3. *The propeller $P_{\gamma(i_1,\ell_1)}$ with $\ell_1 \geq 0$ might also have internal notches, that is the intersection $P_{\gamma(i_1,\ell_1)} \cap \mathcal{L}_{i_2}^-$, for $i_2 = 1,2$, might have curves that are arcs having both endpoints in $\partial\mathcal{L}_{i_2}^-$. In this case we denote these curves by $\gamma(i_1,\ell_1;i_2,\ell_2)$ with $\ell_2 < 0$ and $\ell_1 \geq 0$. Again, such a curve generates a level 3 bubble $S_{\gamma(i_1,\ell_1;i_2,\ell_2)}$ that is part of $\mathfrak{M}_0$.*

In general a propeller $P_{\gamma(i_1,\ell_1;\cdots;i_n,\ell_n)}$ forms part of a bubble if at least one of the indices is negative. Assuming that ℓ_k is the first negative index, then $P_{\gamma(i_1,\ell_1;\cdots;i_n,\ell_n)} \subset S_{\gamma(i_1,\ell_1;\cdots;i_k,\ell_k)}$, that is a level $k+1$ bubble.

The following result generalizes the above discussion to higher level bubbles.

PROPOSITION 15.4. *Let $\gamma'(i_1,\ell_1;\cdots;i_n,\ell_n) \subset \mathcal{L}_{i_n}^-$ be any curve in the construction of $\mathfrak{M}_0$ with at least one negative index. Let $\ell_k < 0$ be the first negative index. Then*

1. *$\gamma(i_1,\ell_1;\cdots;i_n,\ell_n) = \sigma_{i_n}^{-1}(\gamma'(i_1,\ell_1;\cdots;i_n,\ell_n))$ generates a finite double propeller or a pair of finite double propellers. Each propeller intersects $\mathbf{R}_0$ along at most K closed curves, for a fixed number K;*
2. *for every $x \in S_{\gamma(i_1,\ell_1;\cdots;i_n,\ell_n)}$ we have that $n+1 \leq n_0(x) \leq N+n$, for N as in Lemma 15.2.*

Proof. For the first conclusion, observe that $\gamma(i_1,\ell_1;\cdots;1,\ell_n)$ lies in the region $D(\kappa,1) \cup D(\chi,1) \subset L_1^-$ described in the proof of Proposition 15.1, and $\gamma(i_1,\ell_1;\cdots;2,\ell_n)$ lies in the analogous region $D(\kappa,2) \cup D(\chi,2) \subset L_2^-$. Thus the number of circles in the intersection of $P_{\gamma(i_1,\ell_1;\cdots;i_n,\ell_n)}$ with $\mathbf{R}_0$ is uniformly bounded by $\Delta(r_b)+1$.

The second conclusion follows from the arguments above and the proof of Lemma 15.2. □

Observe that if $b \neq 0$ the double propellers P_Γ and P_Λ will also have internal notches, that is notches that are not intersecting the orbits of ω_1 or ω_2, accordingly. Thus they will generate bubbles in the same manner as the simple propellers P_γ and P_λ did.

We consider the case of P_Γ in some detail. The intersection $P_\Gamma \cap \mathcal{L}_1^-$ consists of the curves $\Gamma(1,\ell_1)$ for $b \leq \ell_1$ and unbounded. For $b \leq \ell_1 < 0$ the curve $\Gamma(1,\ell_1)$ consists of two connected components each having its two endpoints in $\partial\mathcal{L}_1^-$, one that corresponds to $\gamma(1,\ell_1)$ and the other one $\kappa(1,\ell_1)$ that belongs to $P_\kappa \cap \mathcal{L}_1^-$. Thus $\Gamma(1,\ell_1)$ is the disjoint union of $\gamma(1,\ell_1)$ and $\kappa(1,\ell_1)$, when $b \leq \ell_1 < 0$. The curves $\gamma(1,\ell_1)$ generate

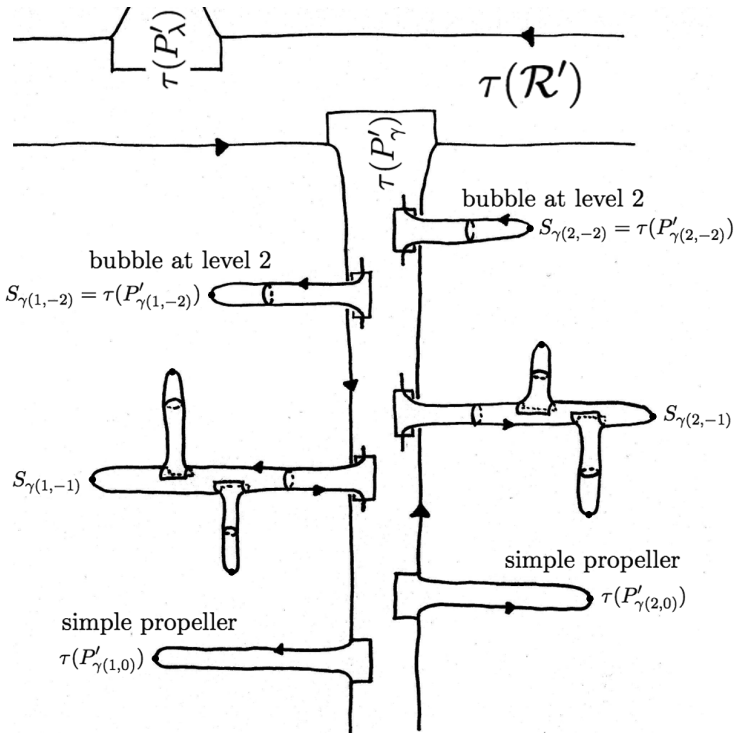

FIGURE 41. Flattened part of $\mathfrak{M}_0$ with bubbles

the bubbles $S_{\gamma(1,\ell_1)}$ that form part of $\widehat{\mathfrak{M}}_0$ as defined in (62). Analogously, the curves $\kappa(1,\ell_1)$ generate the bubbles $S_{\kappa(1,\ell_1)}$ that form part of $\widehat{\mathfrak{M}}_0$. The results above apply without any changes to the bubbles $S_{\kappa(1,\ell_1)}$. Let $S_{\Gamma(1,\ell_1)} = S_{\gamma(1,\ell_1)} \cup S_{\kappa(1,\ell_1)} \subset \widehat{\mathfrak{M}}_0$.

16. Wandering points and propellers

The open set of wandering points $\mathfrak{W} \subset \mathfrak{M}$ for the flow Φ_t was defined by (24) in Section 8, as a union of the four classes:

$$\mathfrak{W} \;=\; \mathfrak{W}^0 \cup \mathfrak{W}^+ \cup \mathfrak{W}^- \cup \mathfrak{W}^\infty$$

where $\mathfrak{W}^0$ consist of all finite orbits, $\mathfrak{W}^+$ is contained in the set of forward trapped orbits, $\mathfrak{W}^-$ is contained in the set of backward trapped orbits, and $\mathfrak{W}^\infty$ is contained in the infinite orbits.

For example, $\mathfrak{W}$ contains the orbits of all points in the region $\{r < 2\}$ by Proposition 8.7. The orbits of points in $\mathfrak{W}^\infty$ exhibit the most subtle dynamical properties of the four classes. Here is the main result of the section:

THEOREM 16.1. *Let $x \notin \mathfrak{M}$, then $x \in \mathfrak{W}$.*

The proof of this result requires the introduction of new classes of double propellers which are used to describe the orbits of points $x \in \mathbf{R}_0$ which satisfy $r(x) \geq 2$. Recall that a key point in the proofs of Propositions 7.5 and 7.6 was to analyze the orbits which intersect an entry region E_i in the sets $\tau(\mathcal{E}_i^{-,+})$, as illustrated in Figure 14, which consist of points that are mapped from the region $\{r > 2\}$ to the region $\{r < 2\}$ by the insertion maps σ_i. The corresponding regions $\sigma_i^{-1}(\mathcal{E}_i^{-,+}) \subset L_i^-$ for $i = 1, 2$ are bounded by what we call "$G - L$" curves. We construct the propellers generated by these curves and consider their intersections with the rectangle $\mathbf{R}_0$, generating families of "$G_0 - L_0$" curves. These curves divide the region $\mathbf{R}_0 \cap \{r \geq 2\}$ according to their dynamical behavior, and the regions thus defined are used to encode the trapped wandering

orbits for Φ_t. One important application of this method is Proposition 16.10, which implies that there are no trapped wandering orbits which are strictly contained in the region $\{r > 2\}$.

We introduce the curves $G \subset L_1^-$ and $L \subset L_2^-$, starting with the curve G. Recall from Section 3 that the boundary of L_i^- is composed of two arcs, α_i and α_i', as illustrated in Figure 5, with α_i contained in the boundary of $\partial_h^- \mathbb{W}$. The curve G starts at one of the points in the intersection $\alpha_1 \cap \alpha_1'$, following an arc in α_1' to the first point with r-coordinate equal to 2, then follows the arc $L_1^- \cap \{r = 2\}$, and finally follows the curve α_1' to the other point in $\alpha_1 \cap \alpha_1'$. Thus, the curve G, as illustrated in Figure 42, is composed of three smooth arcs, where the first and last are contained in α_1' and satisfy the radial monotonicity assumption in Section 11, and the middle arc lies on a segment of the circle $\{r = 2\}$, so is tangent in its interior to the curve Γ at $\sigma_1^{-1}(p_1^-)$ as illustrated in Figure 42. Note that G bounds a region in L_1^- that contains the pre-image of the set $\mathcal{E}_1^{-,+}$ under the insertion map σ_1. We define the curve $L \subset L_2^-$ using the curve α_2' in the analogous manner, with details omitted.

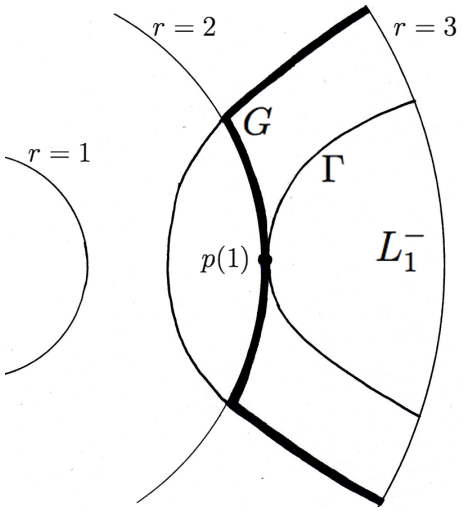

FIGURE 42. The curve G in L_1^-

Next, we form two infinite propellers by considering the flow under $\mathcal{W}$ of the curves G and L, as for the curves Γ and Λ in Section 11. The Ψ_t-flow of the middle arc in G is an infinite strip which spirals around the cylinder $\mathcal{C} = \{r = 2\}$ in the region $\{-2 \leq z < -1\}$, and contains the spiraling curve $\mathcal{Z}_\gamma^- = \{\Psi_t(\sigma_1^{-1}(p_1^-)) \mid t \geq 0\}$ in the interior of the strip. Let $\overline{G} \subset L_1^+$ be the facing curve to G, then similar observations apply to the reverse Ψ_t-flow of $\overline{G}$ and the spiraling curve $\mathcal{Z}_\gamma^+ = \{\Psi_t(\sigma_1^{-1}(p_1^+)) \mid t \leq 0\}$. The Ψ_t-flow of the two arcs of G which are contained in α_1' generate two infinite propellers. Form the infinite double propeller $P_G \subset \mathbb{W}$ from the union of these two propellers and the two infinite strips. Then P_G contains $\mathcal{Z}_\gamma = \mathcal{Z}_\gamma^- \cup \mathcal{Z}_\gamma^+$ defined in (39).

Let P_L be the infinite double propeller corresponding to L defined in the same way, which then contains $\mathcal{Z}_\lambda = \mathcal{Z}_\lambda^- \cup \mathcal{Z}_\lambda^+$. As the curves G and L are disjoint, the propellers P_G and P_L are also disjoint. We then have the analogous result to Proposition 11.2.

PROPOSITION 16.2. *The closures $\overline{P}_G$ and $\overline{P}_L$ of the infinite propellers P_G and P_L contain the Reeb cylinder $\mathcal{R}$, and we have*

$$\overline{P}_G \;=\; P_G \;\cup\; \mathcal{R} \;,\; \overline{P}_L \;=\; P_L \;\cup\; \mathcal{R}. \tag{80}$$

Proof. Let $\{x_n \in P_G \mid n = 1, 2, \ldots\}$ converge to a point x_*. If $r(x_*) > 2$, then we can assume that $r(x_n) > 2$ and as the Wilson flow preserves the radius coordinate r, there is a corresponding sequence of points $\{y_n \in \alpha_1' \cap G \subset L_1 \mid n = 1, 2, \ldots\}$, with $r(y_n) = r(x_n)$ and y_n, x_n in the same $\mathcal{W}$-orbit. Then $r(y_n) \to r(x_*) > 2$, so $x_* \in P_G$. In the case that $r(x_*) = 2$, then the sequence $\{y_n\}$ converges is either in G or in $\overline{G}$. Assuming it

belongs to G, it converges to a point in $G \cap \{r = 2\}$. The forward Wilson flow of these points converge to the periodic orbit $\mathcal{O}_1$. Then the points x_n converge to a point in the cylinder $\mathcal{R}$, so $x_* \in \mathcal{R}$. A similar argument holds for the backward Wilson flow of the facing curve $\overline{\alpha_i'}$, for which the inner endpoints limit on the periodic orbit $\mathcal{O}_2$.

The analysis of the closure of the propeller P_L proceeds similarly. □

Observe that G divides $\partial_h^-\mathbb{W}$ into two open regions. Let $\mathcal{U}$ denote the region in the complement of G which is contained in L_1^-, so that points in $\mathcal{U}$ have r-coordinate bigger than 2. Let U denote the open region in $\mathbb{W}$ obtained from the Ψ_t-flow of $\mathcal{U}$ from L_1^- to L_1^+. It follows that P_G is contained in the closure of U, and so $\overline{P_G} \subset \overline{U}$. Since Γ is contained in the closure of $\mathcal{U}$ and $\Gamma \setminus \{\sigma_1^{-1}(p_1^-)\}$ is contained in $\mathcal{U}$, we conclude that $P_\Gamma - \mathcal{Z}_\gamma \subset U$ as well. We say that the double propeller P_G *envelops* the double propeller P_Γ.

Similarly, let $\mathcal{V}$ denote the region in the complement of L which is contained in L_2^-, so that points in $\mathcal{V}$ have r-coordinate bigger than 2. Let V denote the open region in $\mathbb{W}$ obtained from the Ψ_t-flow of $\mathcal{V}$ from L_2^- to L_2^+. Then P_L is contained in the closure of V, and $\overline{P_L} \subset \overline{V}$. Correspondingly, we say that P_L envelops P_Λ.

Next, consider the notched double propellers

$$P_G' = P_G \cap \mathbb{W}' \qquad \text{and} \qquad P_L' = P_L \cap \mathbb{W}'.$$

Since $\mathcal{Z}_\gamma \subset P_G$, the propeller P_G' intersects $\mathcal{L}_1^-$ infinitely many times, once for each intersection of the $\mathcal{W}$-orbit of the special point $\sigma_1^{-1}(p_1^-)$ with $\mathcal{L}_1^-$. In the same way, P_G intersects $\mathcal{L}_2^-$ infinitely many times.

For each $i = 1, 2$, the intersections $P_G \cap \mathcal{L}_i^-$ and $P_L \cap \mathcal{L}_i^-$ form two infinite collections of curves $G'(i, \ell)$ and $L'(i, \ell)$, respectively, for $b \leq \ell$ and unbounded. Apply σ_i^{-1} to these curves, to obtain in $L_1^- \cup L_2^- \subset \partial_h^-\mathbb{W}$, four countable collections of curves labeled, for $\ell \geq b$, as illustrated in Figure 43:

- $G(1, \ell)$ tangent at $p(1; 1, \ell)$ to $\Gamma(1, \ell)$ in L_1^-;
- $L(1, \ell)$ tangent at $p(2; 1, \ell)$ to $\Lambda(1, \ell)$ in L_1^-;
- $G(2, \ell)$ tangent at $p(1; 2, \ell)$ to $\Gamma(2, \ell)$ in L_2^-;
- $L(2, \ell)$ tangent at $p(2; 2, \ell)$ to $\Lambda(2, \ell)$ in L_2^-.

For $b \leq \ell < 0$ as introduced in Section 12 and illustrated in Figure 40, the curves $G'(i, \ell)$ and $L'(i, \ell)$ have two connected components, which follows from the discussion in Section 15. As in Proposition 15.4.1 the bubbles generated by these curves have uniformly bounded level difference, and thus do not change the discussion below. Thus, without loss of generality we assume for the rest of the section that $b = 0$.

Observe that since the Ψ_t-flow of the middle arc in G spirals around the cylinder $\mathcal{C} \cap \{z < -1\}$, it intersects the interval J_0 defined in (64) in a sequence of closed intervals. Hence each curve $G(1, \ell)$ contains a closed arc contained in $\kappa \subset \Gamma$, for κ as defined in (60). In the same way, each curve $L(1, \ell)$ has an arc in κ. Similarly, each of the curves $G(2, \ell)$ and $L(2, \ell)$ intersects $\chi \subset \Lambda$ along a closed arc.

The endpoints of each one of the $G(i, \ell)$ and $L(i, \ell)$ curves are contained in the boundary of $\partial_h^-\mathbb{W}$, while the middle arcs are in κ or χ, accordingly. By flowing these curves in $\mathbb{W}$, we obtain four countable collections of finite double propellers, denoted by $P_{G(i,\ell)}$ and $P_{L(i,\ell)}$. The curves $G(i, \ell)$ and $L(i, \ell)$ do not satisfy the radial monotonicity assumption in Section 11. However, the two arcs that are not contained in κ or χ, are endpoint isotopic to a curve satisfying the transversality condition, hence the conclusion that each of the curves $G(i, \ell)$ and $L(i, \ell)$ separates the region L_i^- into two open regions remains true. The finite double propellers $P_{G(i,\ell)}$ and $P_{L(i,\ell)}$ are isotopic to a standard finite double propeller and separate $\mathbb{W}$ into two connected components.

Continue the above process recursively, to obtain collections of curves

- $G(i_1, \ell_1; i_2, \ell_2; \cdots; i_n, \ell_n) \subset L_{i_n}^- \subset \partial_h^-\mathbb{W}$, tangent to $\Gamma(i_1, \ell_1; i_2, \ell_2; \cdots; i_n, \ell_n)$ at $p(1; i_1, \ell_1; i_2, \ell_2; \cdots; i_n, \ell_n)$;

- $L(i_1, \ell_1; i_2, \ell_2; \cdots; i_n, \ell_n) \subset L_{i_n}^- \subset \partial_h^-\mathbb{W}$ tangent to $\Lambda(i_1, \ell_1; i_2, \ell_2; \cdots; i_n, \ell_n)$ at $p(2; i_1, \ell_1; i_2, \ell_2; \cdots; i_n, \ell_n)$.

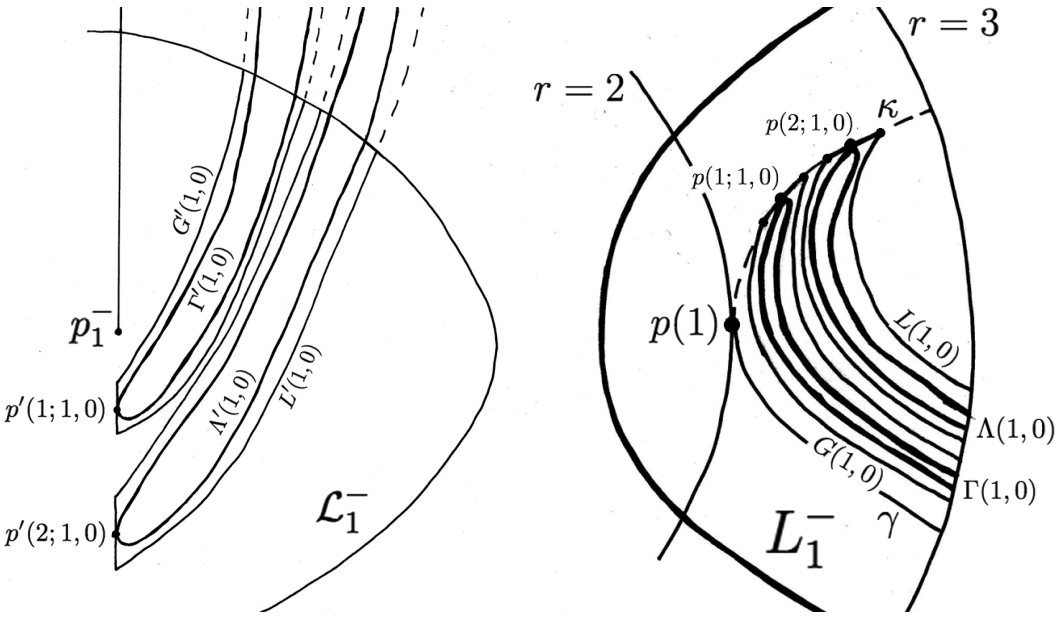

(A) $\Gamma'(1,0) \subset G'(1,0)$ and $\Lambda'(1,0) \subset L'(1,0)$ (B) $\Gamma(1,0) \subset G(1,0)$ and $\Lambda(1,0) \subset L(1,0)$

FIGURE 43. G and L curves at level 1 in the regions $\mathcal{L}_1^-$ and L_1^-

Let $P'_{G(i_1,\ell_1;i_2,\ell_2;\cdots;i_n,\ell_n)} \subset \mathbb{W}'$ and $P'_{L(i_1,\ell_1;i_2,\ell_2;\cdots;i_n,\ell_n)} \subset \mathbb{W}'$ be the corresponding notched propellers.

We next discuss topological properties of the families of propellers formed from the G and L curves. Recall that the points $p(1;i_1,\ell_1;i_2,\ell_2;\cdots;i_n,\ell_n)$ divide the parabolic Γ-curves in two arcs,

$$\Gamma(i_1,\ell_1;i_2,\ell_2;\cdots;i_n,\ell_n) \;=\; \gamma(i_1,\ell_1;i_2,\ell_2;\cdots;i_n,\ell_n) \;\cup\; \kappa(i_1,\ell_1;i_2,\ell_2;\cdots;i_n,\ell_n).$$

The level n curve $\Gamma(i_1,\ell_1;i_2,\ell_2;\cdots;i_n,\ell_n)$ is tangent at $p(1;i_1,\ell_1;i_2,\ell_2;\cdots;i_n,\ell_n)$ to a level $n-1$ curve. For $i_1 = 1$, it is tangent to the curve $\Gamma(i_2,\ell_2;\cdots;i_n,\ell_n)$ and

$$p(1;i_1,\ell_1;i_2,\ell_2;\cdots;i_n,\ell_n) \text{ belongs to } \kappa(i_2,\ell_2;\cdots;i_n,\ell_n).$$

For $i_1 = 2$ the curve $\Gamma(i_1,\ell_1;i_2,\ell_2;\cdots;i_n,\ell_n)$ is tangent to the curve $\Lambda(i_2,\ell_2;\cdots;i_n,\ell_n)$ and

$$p(1;i_1,\ell_1;i_2,\ell_2;\cdots;i_n,\ell_n) \text{ belongs to } \chi(i_2,\ell_2;\cdots;i_n,\ell_n).$$

Thus:

- $p(1;1,\ell_1;i_2,\ell_2;\cdots;i_n,\ell_n)$ and $p(2;1,\ell_1;i_2,\ell_2;\cdots;i_n,\ell_n)$ lie in $\kappa(i_2,\ell_2;\cdots;i_n,\ell_n)$ for any ℓ_1;
- $p(1;2,\ell_1;i_2,\ell_2;\cdots;i_n,\ell_n)$ and $p(2;2,\ell_1;i_2,\ell_2;\cdots;i_n,\ell_n)$ lie in $\chi(i_2,\ell_2;\cdots;i_n,\ell_n)$ for any ℓ_1.

LEMMA 16.3. *Any two distinct G and L curves of the collection above, contained in $L_1^- \cup L_2^-$, are disjoint.*

Proof. The curve Γ divides L_1^- in two regions, one of which is contained in $\mathcal{U}$ and its closure contains all the $G(1,\ell)$ and $L(1,\ell)$ curves. The closure of this region intersects G only at the special point $\sigma_1^{-1}(p_1^-)$. Hence, G is disjoint from all $G(1,\ell)$ and $L(1,\ell)$. In the same way, L is disjoint from all $G(2,\ell)$ and $L(2,\ell)$. Then proceed inductively, to obtain that any two different curves in the collection of G and L curves are disjoint. □

We now consider the intersection of the notched propellers

$$P'_{G(i_1,\ell_1;i_2,\ell_2;\cdots;i_n,\ell_n)} \quad , \quad P'_{L(i_1,\ell_1;i_2,\ell_2;\cdots;i_n,\ell_n)}$$

with the rectangle $\mathbf{R}_0$. Following the notation convention developed in Section 13, the intersections $P'_G \cap \mathbf{R}_0$ and $P'_L \cap \mathbf{R}_0$ yield countable collections of closed curves, labeled $G_0(\ell)$ and $L_0(\ell)$, as illustrated in Figure 44. Observe that for each $\ell \geq a$, where $a \leq 0$ was defined in Remark 13.3, the curve $G_0(\ell)$ contains a segment of

J_0, a segment of K_0, and is tangent at the two points $p_0(1;i,\ell)$ to the curve $\Gamma_0(\ell)$ for $i=1,2$. In the same way, each $L_0(\ell)$ contains a segment of J_0, a segment of K_0 and is tangent at the two points $p_0(2;i,\ell)$ to the curve $\Lambda_0(\ell)$ for $i=1,2$.

Each $G_0(\ell)$ curve divides $\mathbf{R}_0$ in two open connected regions, one of which contains $\Gamma_0(\ell)$ and is contained in $U\cap\mathbf{R}_0$. We call this region the interior of $G_0(\ell)$ and we denote it by $\mathcal{U}_0(\ell)$. Analogously, the interior of each $L_0(\ell)$ curve is denoted by $\mathcal{V}_0(\ell)$.

As in the previous section, we define families of G_0 and L_0 curves in $\mathbf{R}_0\cap\{r\geq 2\}$ recursively.

Recall that U denotes the interior region of $P_G\subset\mathbb{W}$, so that $\mathcal{U}$ as defined previously satisfies $\mathcal{U}=U\cap\partial_h^-\mathbb{W}\subset L_1^-$. Also, V denotes the interior region of $P_L\subset\mathbb{W}$, so that $\mathcal{V}$ as defined previously satisfies $\mathcal{V}=V\cap\partial_h^-\mathbb{W}\subset L_2^-$.

In a corresponding manner, for the families of G and L curves, let $U(i_1,\ell_1,\cdots,i_n,\ell_n)$ denote the interior region of $P_{G(i_1,\ell_1,\cdots,i_n,\ell_n)}\subset\mathbb{W}$, and $V(i_1,\ell_1,\cdots,i_n,\ell_n)$ denote the interior region of $P_{L(i_1,\ell_1,\cdots,i_n,\ell_n)}\subset\mathbb{W}$. Then we define open regions in $\partial_h^-\mathbb{W}$ as follows:

$$\mathcal{U}(i_1,\ell_1;\cdots;i_n,\ell_n) = U(i_1,\ell_1;\cdots;i_n,\ell_n)\cap\partial_h^-\mathbb{W} \tag{81}$$

$$\mathcal{V}(i_1,\ell_1;\cdots;i_n,\ell_n) = V(i_1,\ell_1;\cdots;i_n,\ell_n)\cap\partial_h^-\mathbb{W}. \tag{82}$$

The intersection of the regions $U(i_1,\ell_1;\cdots;i_n,\ell_n)$ and $V(i_1,\ell_1;\cdots;i_n,\ell_n)$ with $\mathbf{R}_0$ form two finite collections of connected open regions, which are indexed as follows:

$$\mathcal{U}_0(i_1,\ell_1;\cdots;i_n,\ell_n;\ell_{n+1}) \subset \tau(U(i_1,\ell_1;\cdots;i_n,\ell_n)\cap\mathbf{R}_0)\ ,\ \ell_{n+1}\geq a \tag{83}$$

$$\mathcal{V}_0(i_1,\ell_1;\cdots;i_n,\ell_n;\ell_{n+1}) \subset \tau(V(i_1,\ell_1;\cdots;i_n,\ell_n)\cap\mathbf{R}_0)\ ,\ \ell_{n+1}\geq a, \tag{84}$$

which extends the notation convention introduced above for $\mathcal{U}_0(\ell)$ and $\mathcal{V}_0(\ell)$. Observe that the index ℓ_{n+1} admits finitely many values since the boundary propellers $P_{G(i_1,\ell_1;\cdots;i_n,\ell_n)}$ and $P_{L(i_1,\ell_1;\cdots;i_n,\ell_n)}$ are finite.

The forward Ψ_t-flow of the region in (83) to $\mathcal{L}_1^-$ yields the region $\sigma_1(\mathcal{U}(i_1,\ell_1;\cdots;i_n,\ell_n;1,\ell_{n+1}))\subset\mathcal{L}_1^-$, and its forward Ψ_t-flow to $\mathcal{L}_2^-$ yields the region $\sigma_2(\mathcal{U}(i_1,\ell_1;\cdots;i_n,\ell_n;2,\ell_{n+1}))\subset\mathcal{L}_2^-$. Similar comments apply to the regions in (84).

Recall from Lemma 16.3 that the collection of all G and L curves in $\partial_h^-\mathbb{W}$ are disjoint. This implies a containment property between their interior regions:

LEMMA 16.4. *Suppose that either*

- $\mathcal{U}_0(i_1,\ell_1;\cdots;i_n,\ell_n;\ell_{n+1})\cap\mathcal{U}_0(i'_1,\ell'_1;\cdots;i'_{n'},\ell'_{n'};\ell'_{n'+1})\neq\emptyset$,
- $\mathcal{U}_0(i_1,\ell_1;\cdots;i_n,\ell_n;\ell_{n+1})\cap\mathcal{V}_0(i'_1,\ell'_1;\cdots;i'_{n'},\ell'_{n'};\ell'_{n'+1})\neq\emptyset$,
- $\mathcal{V}_0(i_1,\ell_1;\cdots;i_n,\ell_n;\ell_{n+1})\cap\mathcal{V}_0(i'_1,\ell'_1;\cdots;i'_{n'},\ell'_{n'};\ell'_{n'+1})\neq\emptyset$,

then $n\neq n'$ and $\ell_{n+1}=\ell'_{n'+1}$.

If $n'>n$, let $n'=n+m$. Then $\mathcal{U}_0(i'_1,\ell'_1;\cdots;i'_{n'},\ell'_{n'};\ell_{n+1})$ is contained in

- $\mathcal{U}_0(i_1,\ell_1;\cdots;i_n,\ell_n;\ell_{n+1})$ *if $i_{n'-n}=1$ and for any $1\leq k\leq n$*

$$i_k=i'_{k+m}=i'_{(n'-n)+k} \text{ and } \ell_k=\ell'_{k+m}=\ell'_{(n'-n)+k}\ . \tag{85}$$

- $\mathcal{V}_0(i_1,\ell_1;\cdots;i_n,\ell_n;\ell_{n+1})$ *if $i_{n'-n}=2$ and for any $1\leq k\leq n$*

$$i_k=i'_{k+m}=i'_{(n'-n)+k} \text{ and } \ell_k=\ell'_{k+m}=\ell'_{(n'-n)+k}\ . \tag{86}$$

The same conclusions hold for $\mathcal{V}_0(i'_1,\ell'_1;\cdots;i'_{n'},\ell'_{n'};\ell_{n+1})$.

Proof. The boundaries of the $\mathcal{U}_0$ and $\mathcal{V}_0$ regions are disjoint by Lemma 16.3, so the inclusion of one into the other follows, if the regions are not disjoint. The identities (85) and (86) involving the indices follow from the construction of the curves. □

We describe two cases to illustrate the conclusion of Lemma 16.4.

• For $i_1 = i_2 = 1$, the region $\mathcal{U}_0(1, \ell_1; 1, \ell_2; \cdots ; \ell_n)$ is contained in $\mathcal{U}_0(1, \ell_2; \cdots ; \ell_n)$ and $\mathcal{U}_0(i_3, \ell_3; \cdots ; \ell_n)$.

• For $i_1 = 2, i_2 = 1$, the region $\mathcal{U}_0(2, \ell_1; 1, \ell_2; \cdots ; \ell_n)$ is contained in $\mathcal{V}_0(1, \ell_2; \cdots ; \ell_n)$ and $\mathcal{U}_0(i_3, \ell_3; \cdots ; \ell_n)$.

Observe that each propeller $P_{G(i_1,\ell_1;\cdots;i_n,\ell_n)}$ envelops the propeller $P_{\Gamma(i_1,\ell_1;\cdots;i_n,\ell_n)}$. This yields a nested relation between the regions bounded by the G_0 and L_0 curves, and the Γ_0 and Λ_0 curves in $\mathbf{R}_0$. This is illustrated in Figure 44, and we describe the relation in two special cases.

• The region $\mathcal{U}_0(i_1, \ell_1; i_2, \ell_2; \cdots ; \ell_n)$ contains the curve $\Gamma_0(i_1, \ell_1; i_2, \ell_2; \cdots ; \ell_n)$ in its interior, and the intersection of the two associated curves consists of the points

$$G_0(i_1, \ell_1; i_2, \ell_2; \cdots ; \ell_n) \cap \Gamma_0(i_1, \ell_1; i_2, \ell_2; \cdots ; \ell_n) = p_0(1; i_1, \ell_1; i_2, \ell_2; \cdots ; i_n, \ell_n) \ , \ i_n = 1, 2.$$

For $i_1 = 1$, the curve $G_0(1, \ell_1; i_2, \ell_2; \cdots ; \ell_n)$ intersects $\kappa_0(i_2, \ell_2; \cdots ; \ell_n)$ in two closed arcs, one containing $p_0(1; 1, \ell_1; i_2, \ell_2; \cdots ; 1, \ell_n)$ and the other containing $p_0(1; 1, \ell_1; i_2, \ell_2; \cdots ; 2, \ell_n)$.

For $i_1 = 2$, the curve $G_0(2, \ell_1; i_2, \ell_2; \cdots ; \ell_n)$ intersects $\chi_0(i_2, \ell_2; \cdots ; \ell_n)$ in two closed arcs, one containing $p_0(1; 2, \ell_1; i_2, \ell_2; \cdots ; 1, \ell_n)$ and the other containing $p_0(1; 2, \ell_1; i_2, \ell_2; \cdots ; 2, \ell_n)$.

• The region $\mathcal{V}_0(i_1, \ell_1; i_2, \ell_2; \cdots ; \ell_n)$ contains the curve $\Lambda_0(i_1, \ell_1; i_2, \ell_2; \cdots ; \ell_n)$ in its interior, and the intersection of the two associated curves consists of the points

$$L_0(i_1, \ell_1; i_2, \ell_2; \cdots ; \ell_n) \cap \Lambda_0(i_1, \ell_1; i_2, \ell_2; \cdots ; \ell_n) = p_0(2; i_1, \ell_1; i_2, \ell_2; \cdots ; i_n, \ell_n) \ , \ i_n = 1, 2$$

For $i_1 = 1$, the curve $L_0(1, \ell_1; i_2, \ell_2; \cdots ; \ell_n)$ intersects $\kappa_0(i_2, \ell_2; \cdots ; \ell_n)$ in two closed arcs, one containing $p_0(2; 1, \ell_1; i_2, \ell_2; \cdots ; 1, \ell_n)$ and the other containing $p_0(2; 1, \ell_1; i_2, \ell_2; \cdots ; 2, \ell_n)$.

For $i_1 = 2$, the curve $L_0(2, \ell_1; i_2, \ell_2; \cdots ; \ell_n)$ intersects $\chi_0(i_2, \ell_2; \cdots ; \ell_n)$ in two closed arcs, one containing $p_0(2; 2, \ell_1; i_2, \ell_2; \cdots ; 1, \ell_n)$ and the other containing $p_0(2; 2, \ell_1; i_2, \ell_2; \cdots ; 2, \ell_n)$.

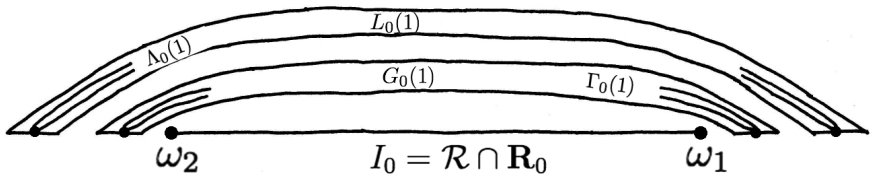

FIGURE 44. Endparts of Γ_0 and Λ_0 curves inside G_0 and L_0 curves in $\mathbf{R}_0$ (viewed sideways)

With these preparations, we can make the following definition for the points in $\mathbf{R}_0$ with $r(x) > 2$, which extends the notion of "level" for those points not contained in $\mathfrak{M}$. Recall that $\mathfrak{M}_{\mathbf{R}_0} = \mathfrak{M} \cap \mathbf{R}_0$.

DEFINITION 16.5. *Let $x \in \mathbf{R}_0$ with $r(x) > 2$, and $x \notin \mathfrak{M}_{\mathbf{R}_0}$. Say that x has* level at least n*, and write $L(x) \geq n$, if either there exists an open region $\mathcal{U}_0$ or $\mathcal{V}_0$ of level n such that x is contained in the closure of either such regions:*

$$x \in \overline{\mathcal{U}_0(i_1, \ell_1; \cdots ; i_{n-1}, \ell_{n-1}; \ell_n)} \quad \text{or} \quad x \in \overline{\mathcal{V}_0(i_1, \ell_1; \cdots ; i_{n-1}, \ell_{n-1}; \ell_n)}.$$

The level *of x is the greatest $n \geq 1$ such that $L(x) \geq n$. If $L(x) \geq n$ for all n, then x is said to have infinite level, and otherwise has finite level. If x is not contained in any such region, set $L(x) = 0$.*

The following is a key property of the level.

PROPOSITION 16.6. *Let $x \in \mathbf{R}_0$ with $r(x) > 2$, and $x \notin \mathfrak{M}_{\mathbf{R}_0}$. Then x has finite level.*

Proof. Let $\mathfrak{G}_0$ denote the union of the G_0-curves in $\mathbf{R}_0$, and $\mathfrak{L}_0$ the union of the L_0-curves. Recall that $\mathfrak{M}$ is the closure of $\mathfrak{M}_0$ which is the union of all γ_0 and λ_0 curves in $\mathbf{R}_0$.

Set $\mathfrak{Y} = \mathfrak{M}_{\mathbf{R}_0} \cup \mathfrak{G}_0 \cup \mathfrak{L}_0$. The set $\mathfrak{Y}$ is bounded in $\mathbf{R}_0$ so its closure is compact, but more is true.

LEMMA 16.7. *The set $\mathfrak{Y}$ is closed, hence is compact.*

Proof. By Proposition 16.2, the limit of curves $G_0(\ell)$ and $L_0(\ell)$ as $\ell \to \infty$ is contained in $\mathfrak{Y}$. Thus, for a fixed index $(i_1, *; i_2, \ell_2; \cdots ; \ell_n)$, the limit of curves $G_0(i_1, \ell_1; i_2, \ell_2; \cdots ; \ell_n)$ or $L_0(i_1, \ell_1; i_2, \ell_2; \cdots ; \ell_n)$ as $\ell_1 \to \infty$ is contained in $\mathfrak{Y}$.

Given a sequence of points in $\mathfrak{Y}$ which are contained in G_0 or L_0 curves with indices $(i_1, \ell_1; i_2, \ell_2; \cdots ; \ell_n)$ where the degree n tends to infinity, we observe that the sequence must be nested by Lemma 16.4, and each interior region $\mathcal{U}_0(i_1, \ell_1; i_2, \ell_2; \cdots ; \ell_n)$ or $\mathcal{V}_0(i_1, \ell_1; i_2, \ell_2; \cdots ; \ell_n)$ contains a corresponding γ_0 or λ_0 arc which is contained in $\mathfrak{M}_0$ hence in $\mathfrak{Y}$. It follows that any convergent sequence of points in $\mathfrak{G}_0$ or $\mathfrak{L}_0$ of this form must have limit in the set $\mathfrak{M}$. □

Let $\epsilon > 0$ be chosen small enough, so that $\epsilon < d_{\mathbf{R}_0}(x, \mathfrak{M}_{\mathbf{R}_0})$ for the metric $d_{\mathbf{R}_0}$ defined in Section 9. That is, the distance from every point of $\mathfrak{M}_{\mathbf{R}_0}$ to x is greater than ϵ. Let

$$\mathcal{U}_0(\mathfrak{M}, \epsilon) = \{y \in \mathbf{R}_0 \mid d_{\mathbf{R}_0}(y, \mathfrak{M}_{\mathbf{R}_0}) < \epsilon\}$$

Recall that the G_0 and L_0 curves in $\mathbf{R}_0$ are disjoint closed curves by Lemma 16.3, so for each index there exists an $\epsilon_* > 0$ (where we abuse notation and do not indicate the precise index on ϵ_*) so that each of the sets

$$\mathcal{U}_0(i_1, \ell_1; i_2, \ell_2; \cdots ; \ell_n, \epsilon_*) = \{y \in \mathbf{R}_0 \mid d_{\mathbf{R}_0}(y, G_0(i_1, \ell_1; i_2, \ell_2; \cdots ; \ell_n)) < \epsilon_*\} \tag{87}$$

$$\mathcal{V}_0(i_1, \ell_1; i_2, \ell_2; \cdots ; \ell_n, \epsilon_*) = \{y \in \mathbf{R}_0 \mid d_{\mathbf{R}_0}(y, L_0(i_1, \ell_1; i_2, \ell_2; \cdots ; \ell_n)) < \epsilon_*\} \tag{88}$$

contains exactly one G_0 or L_0 curve. We comment on these definitions.

Observe that the curve $G_0(i_1, \ell_1; i_2, \ell_2; \cdots ; \ell_n)$ contains the points $p_0(1; i_1, \ell_1; i_2, \ell_2; \cdots ; i_n, \ell_n)$ for $i_n = 1, 2$. Since the curves $G_0(1, \ell; i_1, \ell_1; i_2, \ell_2; \cdots ; \ell_n)$ limit as $\ell \to \infty$ to $\gamma_0(i_1, \ell_1; i_2, \ell_2; \cdots ; \ell_n)$, for ℓ big enough the open set $\mathcal{U}_0(i_1, \ell_1; i_2, \ell_2; \cdots ; \ell_n, \epsilon_*)$ intersects these curves, but it does not contains them, as illustrated in Figure 45.

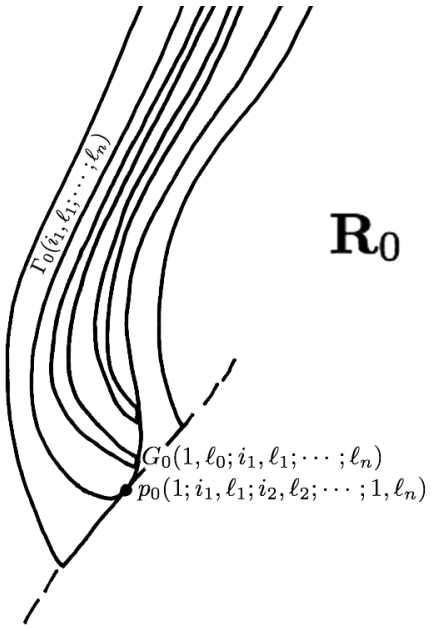

FIGURE 45. Lower part of $\Gamma_0(i_1, \ell_1; i_2, \ell_2; \cdots ; \ell_n)$ inside region bounded by $G_0(i_1, \ell_1; i_2, \ell_2; \cdots ; \ell_n)$

Form an open covering of $\mathfrak{Y}$ which consists of the open neighborhood $\mathcal{U}_0(\mathfrak{M}, \epsilon)$ of $\mathfrak{M}_{\mathbf{R}_0}$, and all open sets of the form (87) and (88). Then by Lemma 16.7, there is a finite subcovering, which must consist of $\mathcal{U}_0(\mathfrak{M}, \epsilon)$ and a finite collection of open sets of the form (87) and (88). It follows that for all but a finite number of

exceptions, the G_0 and L_0 curves are contained in $\mathcal{U}_0(\mathfrak{M}, \epsilon)$, and thus the closures of their interiors are also contained in $\mathcal{U}_0(\mathfrak{M}, \epsilon)$. As $x \notin \mathcal{U}_0(\mathfrak{M}, \epsilon)$, there are only a finite number of G_0 or L_0 curves whose interior closures contain x. If $L(x) \neq 0$, then $L(x)$ is the maximum value of the level for all such interior regions which contain x, which is finite. □

We next use the constructions and results above to describe the dynamical properties of the Φ_t-orbits of points $x \in \mathbf{R}_0$ with $r(x) \geq 2$ and $x \notin \mathfrak{M}_{\mathbf{R}_0}$. First, recall that the map $\tau \colon \mathbb{W}' \to \mathbb{K}$ identifies the surfaces L_i^- and $\mathcal{L}_i^-$ via the map σ_i, to yield the entry region E_i, for $i = 1, 2$. The map σ_i sends α_i' to the arc $\beta_i' \subset \partial_h^- \mathbb{W} \setminus (L_1^- \cup L_2^-)$. The points in $\sigma_1(G \cap \alpha_1')$ and $\sigma_2(L \cap \alpha_2')$ are technically secondary entry points of $\mathbb{K}$ as defined in Section 4, but can also be considered as primary entry points as they lie in the closure of the primary entry points. The two arcs $\sigma_1(G \cap \{r = 2\})$ and $\sigma_2(L \cap \{r = 2\})$ are exactly the secondary entry points in E_1 and E_2, respectively, whose r-coordinate is equal to 2. The forward orbit of these points has r-coordinate bigger or equal to 2 by Corollary 7.3.

PROPOSITION 16.8. *Suppose that $x \in \mathbf{R}_0$ is not in the $\mathcal{K}$-orbit of ω_1 or ω_2, and is contained in a L_0 or G_0 curve, so that for some index $\{i_1, \ell_1; \cdots; \ell_n\}$ we have*

$$x \in G_0(i_1, \ell_1; \cdots; \ell_n) \text{ or } x \in L_0(i_1, \ell_1; \cdots; \ell_n) \ .$$

(1) If $x \notin \kappa_0(i_2, \ell_2; \cdots; \ell_n) \cup \chi_0(i_2, \ell_2; \cdots; \ell_n) \cup J_0 \cup K_0$, then there exists $t, t' \in \mathbb{R}$ such that $\Phi_t(x) \in \tau(\beta_j' \times \{2\})$ and $\Phi_{t'}(x) \in \tau(\beta_j' \times \{-2\})$, for $j = 1$ or 2. Hence the orbit of x escapes $\mathbb{K}$ in positive and negative time.

(2) If $x \in \kappa_0(i_2, \ell_2; \cdots; \ell_n) \cup \chi_0(i_2, \ell_2; \cdots; \ell_n) \cup J_0 \cup K_0$, then there exists $t \in \mathbb{R}$ such that $y = \Phi_t(x)$ is a transition point with $\rho_x(t) = 2$. If y is a secondary entry point, its forward orbit limits to ω_1, while if y is a secondary exit point its backward orbit limits to ω_2.

Proof. We consider the case where $x \in G_0(i_1, \ell_1; \cdots; \ell_n)$, with the case $x \in L_0(i_1, \ell_1; \cdots; \ell_n)$ being analogous.

If $n = 1$, then x is contained in one of the curves $G_0(\ell_1)$, as illustrated in Figure 44. Let $x' = \tau^{-1}(x) \in G_0(\ell_1) \subset \mathbf{R}_0$, then flow backwards in $\mathbb{W}$, to obtain a point $x'_{-1} \in G$, where G is illustrated in Figure 42. As x does not lie on the flow of the special points, the point x'_{-1} lies either on the curve $G \cap \alpha_1'$ with $r(x'_{-1}) > 2$ or in $G \cap \{r = 2\}$. The first case corresponds to (1) and we have that x'_{-1} is a secondary entry point on the boundary of the primary entry points. It follows that the backward Φ_t-orbit of $x_{-1} = \tau(x'_{-1})$ escapes $\mathbb{K}$ in finite time. By Proposition 6.7 the forward Φ_t-orbit of x_{-1} passes through the facing point $\overline{x_{-1}} \in \tau(\beta_1' \times \{2\})$ and thus the forward orbit exits $\mathbb{K}$ as claimed. The second case corresponds to (2) and x_{-1} is the secondary entry point y, whose forward orbit limits to ω_1 by Proposition 7.1.

Next, assume that $n \geq 2$, then $r(x) > 2$. Since $x \in G_0(i_1, \ell_1; \cdots; \ell_n)$ it belongs to the propeller $\tau(P'_{G(i_1, \ell_1; \cdots; i_{n-1}, \ell_{n-1})})$. Then $x' = \tau^{-1}(x)$ is in the propeller $P_{G(i_1, \ell_1; \cdots; i_{n-1}, \ell_{n-1})}$. Flow x' backwards in $\mathbb{W}$, to obtain a point $x'_{-1} \in L_{i_{n-1}}^-$ that belongs to the curve $G(i_1, \ell_1; \cdots; i_{n-1}, \ell_{n-1})$. By Proposition 6.7, $x_{-1} = \tau(x'_{-1})$ is a secondary entry point in the $\mathcal{K}$-orbit of x.

The point x_{-1} can be identified with a point $x^0_{-1} \in G_0(i_1, \ell_1; \cdots; \ell_{n-1})$: consider x_{-1} and flow it backwards from $E_{i_{n-1}}$ to $\mathbf{R}_0$. Then $r(x^0_{-1}) \geq 2$, and repeat the process inductively to obtain $x'_{-(n-1)} \in G(i_1, \ell_1) \in L_{i_1}^-$ and $x^0_{-(n-1)} \in G_0(\ell_1)$. We have two possible situations:

(1) If $r(x^0_{-(n-1)}) > 2$, we have that $x^0_{-(n-1)} \in G_0(\ell_1) \setminus (J_0 \cup K_0)$ and

$$x \in G_0(i_1, \ell_1; \cdots; \ell_n) \setminus [\kappa_0(i_2, \ell_2; \cdots; \ell_n) \cup \chi_0(i_2, \ell_2; \cdots; \ell_n) \cup J_0 \cup K_0] \, .$$

Then the $\mathcal{W}$-orbit of $\tau^{-1}(x^0_{-(n-1)})$ is finite and intersects $\partial_h^- \mathbb{W}$ in a point x'_{-n} contained in $G \cap \alpha_1'$. Thus $\sigma_1(x'_{-n})$ is in the boundary of the primary entry points of $\mathbb{K}$, implying that the orbit of x escapes in negative time. Since $r(\sigma_1(x'_{-n})) > 2$, the orbit of x escapes in forward time.

(2) If $r(x^0_{-(n-1)}) = 2$, then either $z(x^0_{-(n-1)}) < -1$ or $z(x^0_{-(n-1)}) > 1$ and

$$x \in G_0(i_1, \ell_1; \cdots; \ell_n) \cap [\kappa_0(i_2, \ell_2; \cdots; \ell_n) \cup \chi_0(i_2, \ell_2; \cdots; \ell_n) \cup J_0 \cup K_0] .$$

Assume first that $z(x^0_{-(n-1)}) < -1$, or equivalently that $x^0_{-(n-1)} \in J_0$. Consider the point $\tau^{-1}(x^0_{-(n-1)})$ and flow it backwards in $\mathbb{W}$. We obtain an entry point x'_{-n} in $G \cap \{r = 2\}$ and $\sigma_1(x'_{-n})$ is a secondary entry point with r-coordinate equal to 2 in the $\mathcal{K}$-orbit of x. By Proposition 7.1 its forward $\mathcal{K}$-orbit accumulates on ω_1.

If on the contrary $z(x^0_{-(n-1)}) > 1$, or equivalently that $x^0_{-(n-1)} \in K_0$, consider the point $\tau^{-1}(x^0_{-(n-1)})$ and flow it forward in $\mathbb{W}$. We obtain an exit point x'_{-n} in $\overline{G} \cap \{r = 2\}$ and $\sigma_1(x'_{-n})$ is a secondary exit point with r-coordinate equal to 2 in the $\mathcal{K}$-orbit of x. By Proposition 7.1 its backward $\mathcal{K}$-orbit accumulates on ω_2. □

We next investigate the behavior of the $\mathcal{K}$-orbit of points in $\mathbf{R}_0$ with r-coordinate bigger than 2 that do not belong to $\mathfrak{Y}$.

PROPOSITION 16.9. *Let $x \in \mathbf{R}_0$ with $r(x) > 2$, assume that $x \notin \mathfrak{Y}$. Let $0 \le L(x) < \infty$ be the level of x, as in Definition 16.5. Then we have the following possibilities:*

(1) Let $L(x) = 0$, so that x is outside every G_0 and every L_0 curve, then $\rho_x(t) > 2$ for all t, and the orbit of x escapes $\mathbb{K}$ in positive and negative time.

(2) Let $L(x) = n > 0$, so that x is contained in an open $\mathcal{U}_0$ or $\mathcal{V}_0$ region of level n, and assume that x is also in the interior of the corresponding Γ_0 or Λ_0 curve whose vertex lies on the boundary of the region. Then $\rho_x(t) > 2$ for all t, and the orbit of x escapes $\mathbb{K}$ in positive and negative time.

(3) Let $L(x) = n > 0$, and assume that x lies in the interior of $\mathcal{U}_0(i_1, \ell_1; i_2, \ell_2; \cdots; \ell_n)$ and in the exterior of $\Gamma_0(i_1, \ell_1; i_2, \ell_2; \cdots; \ell_n)$, then there exist $s < 0$ such that $\Phi_s(x)$ is a secondary entry point, and for $\epsilon > 0$ sufficiently small we have $\rho_x(s - \epsilon) < 2$.

(4) Let $L(x) = n > 0$, and assume that x lies in the interior of $\mathcal{V}_0(i_1, \ell_1; i_2, \ell_2; \cdots; \ell_n)$ and in the exterior of $\Lambda_0(i_1, \ell_1; i_2, \ell_2; \cdots; \ell_n)$, then there exist $s < 0$ such that $\Phi_s(x)$ is a secondary entry point, and for $\epsilon > 0$ sufficiently small we have $\rho_x(s - \epsilon) < 2$.

Proof. Let $x' \in \mathbf{R}_0 \subset \mathbb{W}$ such that $x = \tau(x')$. By assumption, $r(x') > 2$ thus its Wilson orbit contains an entry point $x'_{-1} \in \partial_h^- \mathbb{W}$ with $r(x'_{-1}) = r(x) > 2$. Then Proposition 6.7 implies that $\tau(x'_{-1}) = x_{-1}$ is in the $\mathcal{K}$-orbit of x. If x_{-1} is a secondary entry point, we find $x^0_{-1} \in \mathbf{R}_0$ by flowing x_{-1} backwards. If $r(x^0_{-1}) > 2$ we can repeat this process for as long as these conditions are satisfied. This reverse flow process stops when either x_{-n} is a primary entry point, or $r(x^0_{-n}) \le 2$.

We now analyze the four cases in the theorem:

(1) Since x is outside every G_0 and every L_0 curve, $x'_{-1} \in \partial_h^- \mathbb{W} \setminus (L_1^- \cup L_2^-)$ and hence x_{-1} is a primary entry point in the $\mathcal{K}$-orbit of x with $r(x_{-1}) = r(x) > 2$. Then Proposition 6.5 implies that $\rho_x(t) > 2$ for all t, and that the orbit of x escapes $\mathbb{K}$ in positive and negative time.

(2) We discuss the case where x is contained in a $\mathcal{U}_0$ region. The alternate case where x is contained in a $\mathcal{V}_0$ region follows similarly. The assumption that $L(x) = n$, and that x does not belong to any G_0 or L_0 curve, implies there is a unique region with $x \in \mathcal{U}_0(i_1, \ell_1; i_2, \ell_2; \cdots; \ell_n)$. It follows that x is contained in the interior of the curve $\Gamma_0(i_1, \ell_1; i_2, \ell_2; \cdots; \ell_n)$, which is a connected component of the intersection of $\tau(P'_{\Gamma(i_1, \ell_1; i_2, \ell_2; \cdots; i_{n-1}, \ell_{n-1})}) \cap \mathbf{R}_0$. It then follows that the point x'_{-1} constructed above lies inside the region bounded by the curve $\Gamma(i_1, \ell_1; i_2, \ell_2; \cdots; i_{n-1}, \ell_{n-1}) \subset L^-_{i_{n-1}}$. Thus, x^0_{-1} is in the interior of $\Gamma_0(i_1, \ell_1; i_2, \ell_2; \cdots; \ell_{n-1})$, and we have that $r(x^0_{-1}) > 2$.

We repeat the process recursively $n-1$ times, to obtain $x^0_{-(n-1)} \in \mathbf{R}_0$ with $r(x^0_{-(n-1)}) > 2$ and contained in the interior of $\Gamma_0(\ell_1)$. The assumption that $L(x) = n$ implies that $x^0_{-(n-1)}$ lies in the exterior of each $G_0(1,k;\ell_1)$ and $L_0(1,k;\ell_1)$ curve, for any $a \leq k < \infty$.

The backward $\mathcal{W}$-orbit of $x^0_{-(n-1)}$ yields the entry point $x'_{-n} \in \partial_h^- \mathbb{W}$. Observe that $r(x'_{-n}) > 2$ since the Wilson flow preserves the radius, and x'_{-n} is in the region inside Γ. Hence $\tau(x'_{-n}) \in E_1 \cap \{r > 2\}$ and the backward $\mathcal{K}$-orbit of this point to $\mathbf{R}_0$ yields the point x^0_{-n}. Then $r(x^0_{-n}) > 2$ and x^0_{-n} is outside every G_0 and L_0 curve, so by case (1) we conclude that $\rho_x(t) > 2$ for all t, and the orbit of x escapes $\mathbb{K}$ in positive and negative time.

(3) Since $G_0(i_1,\ell_1;i_2,\ell_2;\cdots;\ell_n)$ is in the intersection of $\tau(P'_{G(i_1,\ell_1;i_2,\ell_2;\cdots;i_{n-1},\ell_{n-1})})$ and $\mathbf{R}_0$, the point $x'_{-1} \in L^-_{i_{n-1}}$ is in the region between the curves

$$G(i_1,\ell_1;i_2,\ell_2;\cdots;i_{n-1},\ell_{n-1}) \quad \text{and} \quad \Gamma(i_1,\ell_1;i_2,\ell_2;\cdots;i_{n-1},\ell_{n-1}).$$

Thus, x^0_{-1} is in the region between the curves

$$G_0(i_1,\ell_1;i_2,\ell_2;\cdots;\ell_{n-1}) \quad \text{and} \quad \Gamma_0(i_1,\ell_1;i_2,\ell_2;\cdots;\ell_{n-1}),$$

from which it follows that $r(x^0_{-1}) > 2$.

We repeat the process recursively $n-1$ times to obtain $x^0_{-(n-1)} \in \mathbf{R}_0$ in the region between the curves $G_0(\ell_1)$ and $\Gamma_0(\ell_1)$. Then $r(x^0_{-(n-1)}) > 2$ and the entry point x'_{-n} of its $\mathcal{W}$-orbit has radius bigger than 2. Moreover, since $G_0(\ell_1)$ is in the intersection of the propeller $\tau(P'_G)$ and $\mathbf{R}_0$, we conclude that $x'_{-n} \in \mathcal{U} \subset L^-_1$. Analogously, x'_{-n} is outside the curve $\Gamma \subset L^-_1$. Hence x_{-n} is a secondary entry point with $r(x_{-n}) > 2$. Then by the definition of the curve Γ, for $\epsilon > 0$ small $\Phi_{-\epsilon}(x_{-n})$ has r-coordinate less than 2. Since x_{-n} is in the backward $\mathcal{K}$-orbit of x, there exists $s < 0$ be such that $\Phi_s(x) = x_{-n}$ and the conclusion follows.

(4) The proof of this case proceeds exactly as for case (3). □

We next give applications of the properties of $G-L$ curves as developed in this section, to the study of the trapped orbits of points $x \in \mathbb{K}$ in the complement of the compact subspace $\mathfrak{M}$.

PROPOSITION 16.10. *Let $x \in \mathbb{K}$ such that $x \notin \mathfrak{M}$ and $\rho_x(t) > 2$ for all t. Then the orbit of x escapes $\mathbb{K}$ in positive and negative time.*

Proof. Let $x \in \mathbb{K}$ with $x \notin \mathfrak{M}$ and $r(x) > 2$. If the forward $\mathcal{K}$-orbit of x exits $\mathbb{K}$ through an exit point z, by hypothesis $r(z) > 2$. Hence the $\mathcal{K}$-orbit of x escapes $\mathbb{K}$ in positive and negative time by Proposition 6.5. Thus, we need to consider the case where the forward $\mathcal{K}$-orbit of x is trapped.

Now assume that the forward $\mathcal{K}$-orbit of x is trapped, then Proposition 7.9 implies that there exists a subsequence $\{x_{\ell_i} \mid i = 1,2,\ldots\} \subset \mathbf{R}_0$ such that $\lim_{i\to\infty} r(x'_{\ell_i}) = 2$. Hence we can assume that the forward $\mathcal{K}$-orbit of x intersects $\mathbf{R}_0$ in a point x_1 with $r(x_1) > 2$ and arbitrarily close to 2.

By hypothesis, $x \notin \mathfrak{M}$ which implies that $x_1 \notin \mathfrak{M}_{\mathbf{R}_0}$, so there exists $\epsilon > 0$ such that the open ball $B_{\mathbf{R}_0}(x_1,\epsilon) \subset \mathbf{R}_0$ about x_1 is disjoint from $\mathfrak{M}_{\mathbf{R}_0}$, and hence is disjoint from every γ_0 and λ_0 curve. Moreover, since $\rho_x(t) > 2$ for all t, then we can choose ϵ such that $B_{\mathbf{R}_0}(x_1,\epsilon)$ is disjoint from every Γ_0 and Λ_0 curve.

Then x_1 satisfies either the hypothesis of Proposition 16.8.1, the hypothesis of Proposition 16.9.1, or the hypothesis of Proposition 16.9.2. In any case, the $\mathcal{K}$-orbit of x_1 escapes $\mathbb{K}$ in positive and negative time, contradicting the assumption that the forward $\mathcal{K}$-orbit of x is trapped. □

Recall that the Matsumoto region for a Matsumoto constant $\delta_M > 0$, as defined in Definition 7.4, is the set $\mathcal{U}(\delta_M) = \tau(\{y' \in \mathbb{W} \mid 2 - \delta_M < r(y') < 2\}) \subset \mathbb{K}$. We use the above results to describe the intersection of the Φ_t-flow of the Matsumoto region $\mathcal{U}(\delta_M)$ with the rectangle $\mathbf{R}_0$, in terms of the G_0 and L_0 curves introduced above.

PROPOSITION 16.11. *Suppose that $x \in \mathcal{U}(\delta_M) \subset \mathbb{K}$ is a secondary entry point, with $y' \in (\mathcal{L}_1^- \cup \mathcal{L}_2^-)$ and $x' \in (L_1^- \cup L_2^-)$ such that $\tau(y') = \tau(x') = x$. Assume that $2 - \delta_M < r(y') < 2$ and $r(x') > 2$.*

1. *If $z(y') < -1$, then the forward orbit of x is trapped, and the points in the the intersection of its forward orbit and $\mathbf{R}_0 \cap \{r \geq 2\}$ are in the regions between $G_0(i_1, \ell_1; \cdots; \ell_n)$ and $\kappa_0(i_1, \ell_1; \cdots; \ell_n)$, for any collection of indices.*
2. *If $z(y') > 1$, then the backward orbit of x is trapped and the points in the the intersection of its backward orbit and $\mathbf{R}_0 \cap \{r \geq 2\}$ are in the regions between $L_0(i_1, \ell_1; \cdots; \ell_n)$ and $\chi_0(i_1, \ell_1; \cdots; \ell_n)$, for any collection of indices.*
3. *If $-1 < z(y') < 1$, then the orbit of x is an infinite orbit and the points in the the intersection of its orbit and $\mathbf{R}_0 \cap \{r \geq 2\}$ are in the regions between $L_0(i_1, \ell_1; \cdots; \ell_n)$ and $\lambda_0(i_1, \ell_1; \cdots; \ell_n)$, or in the regions between $G_0(i_1, \ell_1; \cdots; \ell_n)$ and $\gamma_0(i_1, \ell_1; \cdots; \ell_n)$, for any collection of indices.*

Proof. The first conclusion in each item above, that the orbit of x is trapped, follows from the corresponding case of Proposition 7.5. For the other claims, we analyze cases as follows.

(1) If $z(y') < -1$, then x' is in the open region of L_1^- bounded by G and κ. The conclusion then follows by Proposition 16.9.3.

(2) If $z(y') > 1$, then x' is in the open region of L_2^- bounded by L and χ. The conclusion then follows by Proposition 16.9.4.

(3) The case $z(y') = 0$ is impossible for a secondary entry point, by the assumptions on the insertion maps. If $-1 < z(y') < 0$, then x' is in the open region of L_1^- bounded by G and γ. If $0 < z(y') < 1$, then $x' \in L_2^-$ in the open region bounded by L and λ. The conclusion then follows by Propositions 16.9.3 and 16.9.4. □

We conclude this section with the proof of Theorem 16.1. Recall that we assume $x \notin \mathfrak{M}$.

First, if x is a primary entry or exit point, then $x \in \mathfrak{W}$ by Lemma 8.5. In particular, $x \in \mathfrak{W}$ for every x whose $\mathcal{K}$-orbit is finite. Thus, we need only consider the case for x such that its $\mathcal{K}$-orbit is infinite. We analyze cases, based on the behavior of the radius function $\rho_x(t) = r(\Phi_t(x))$.

If x satisfies $\rho_x(t) > 2$ for all $t \in \mathbb{R}$, then x has finite orbit by Proposition 16.10, so $x \in \mathfrak{W}$.

If $\rho_x(t) < 2$ for some $t \in \mathbb{R}$, then x is wandering by Proposition 8.7 and hence $x \in \mathfrak{W}$.

The final case to consider is when x is an infinite orbit with $\rho_x(t) \geq 2$ for all t. Then there is a point $y \in \mathbf{R}_0$ on the orbit of x, with $r(y) = 2$. As $y \notin \mathfrak{M}$, it must lie in the interior of one of the segments J_0 or K_0 in (64). Choose an open neighborhood $U(y, \epsilon)$ for $\epsilon > 0$ sufficiently small, which is disjoint from $\mathfrak{M}$.

If y does not lie in one of the G_0 or L_0 curves, as illustrated in Figure 42, then we can assume that $U(y, \epsilon)$ is disjoint from these curves. Consider the cases for the orbit of $z \in U(y, \epsilon) \cap \mathbf{R}_0$. If $r(z) < 2$ then z is wandering by Proposition 8.7. For $r(z) \geq 2$, then the point z is outside any G_0 or L_0 curve. Proposition 16.9.1 implies that the $\mathcal{K}$-orbit of z is finite. Thus, $y \in \mathfrak{W}$ and hence $x \in \mathfrak{W}$.

If y is contained in one of the G_0 or L_0 curves, it is in a level 1 curve. For $z \in U(y, \epsilon) \cap \mathbf{R}_0$ we need only consider the case when $r(z) \geq 2$. If $r(z) = 2$ then Proposition 16.8.2 implies its $\mathcal{W}$-orbit is asymptotic to a special point ω_i. If $r(z) > 2$, then either z is in $\mathcal{U}_0(\ell)$ and outside $\Gamma_0(\ell)$ for some ℓ, or z is in $\mathcal{V}_0(\ell)$ and outside $\Lambda_0(\ell)$ for some ℓ, thus Proposition 16.9.3 or 16.9.4 applies. Then the orbit of z has points with r-coordinate less than 2 and thus is a wandering point by Proposition 8.7.

This covers the possible cases, showing that $\mathbb{K} - \mathfrak{M} \subset \mathfrak{W}$, which is the assertion of Theorem 16.1.

In the next section, we give a condition that implies no points of $\mathfrak{M}$ are wandering, hence $\mathbb{K} - \mathfrak{M} = \mathfrak{W}$.

17. The minimal set for generic flows

The construction of the flow Φ_t on the Kuperberg plug $\mathbb{K}$ involves various choices, in particular the choice of the vector field $\mathcal{W}$ on $\mathbb{W}$ satisfying the hypotheses in Section 2, and the choice of the insertions σ_i satisfying the hypotheses in Section 3. For any such choice, the Φ_t-flow preserves the compact set $\mathfrak{M}$ defined by the closure of the orbits of the Reeb cylinder $\mathcal{R}$. In this section, we consider an additional regularity hypothesis on the insertion maps σ_i, which is a uniform version of Hypothesis 12.1, and is used to estimate the behavior of the flow Φ_t near the special orbits of Φ_t.

We say that Φ_t is *generic* if it satisfies the hypotheses in Definition 17.3. The main result of this section is then:

THEOREM 17.1. *If the flow Φ_t is generic, then $\Sigma = \mathfrak{M}$.*

The proof of Theorem 17.1 will occupy the remainder of this section, and requires a detailed metric analysis of the orbit structure of the Ψ_t-flow near the Reeb cylinder $\mathcal{R}$, which is used to obtain estimates on the Φ_t-flow near the special orbits.

The equality $\Sigma = \mathfrak{M}$ has been previously observed in special cases. Ghys gave an argument in [17, Théorème, p. 302] that this conclusion holds for certain generic classes of insertions. The Kuperbergs constructed in [27], an example using polynomial vector fields for which they sketch the proof of that $\Sigma = \mathfrak{M}$. Our result, which is motivated by these examples, yields this conclusion in more generality. The proof makes full use of the body of techniques developed in this paper, and especially of the properties of the system of double propellers constructed in Section 13. For the more general case of the construction of flows on $\mathbb{K}$ which do not satisfy the generic regularity hypotheses, it seems possible that the inclusion $\Sigma \subset \mathfrak{M}$ may be proper, as was discussed in [27], in which case, the minimal set Σ will be a "Denjoy-type" invariant set for a flow on a surface lamination.

The additional hypotheses is formulated using the notation of Hypothesis 12.1 on the insertion maps σ_i for $i = 1, 2$. The projection along the z-coordinate in $\mathbb{W}$ is denoted by $\pi_z(r, \theta, z) = (r, \theta, -2)$, and we assume that σ_i restricted to the face, $\sigma_i \colon L_i^- \to \mathbb{W}$, has image transverse to the vertical fibers of π_z. This condition is implicit in the illustrations Figures 6, 8 and 9. Given this assumption, there is a well-defined inverse map $\vartheta_i = (\pi_z \circ \sigma_i)^{-1} \colon \mathfrak{D}_i \to L_i^-$ with domain $\mathfrak{D}_i \subset \partial_h^- \mathbb{W}$, which we recall was given in coordinates in (43) by

$$\vartheta_i(r', \theta', -2) = (R_{i,r'}(\theta'), \Theta_{i,r'}(\theta'), -2) = (r(\vartheta_i(r', \theta', -2)), \theta(\vartheta_i(r', \theta', -2)), -2) \, . \tag{89}$$

Also, recall that Hypothesis 12.1.4 assumes that $R_{i,2}(\theta') = r(\vartheta_i(2, \theta', -2))$ has non-vanishing derivative, except at θ_i' defined by $\vartheta_i(2, \theta_i', -2) = (2, \theta_i, -2)$, and that $\epsilon_0 > 0$ is the constant defined after the property (44).

For $i = 1, 2$, consider the curves $\gamma_{i,r}(\theta) = \vartheta_i(r, \theta, -2)$, defined for $1 \leq r \leq 3$ and θ such that $(r, \theta, -2) \in \mathfrak{D}_i$. The transversality assumption on σ_i implies that each curve $\gamma_{i,r}$ is non-singular; that is, $\frac{d}{d\theta}\gamma_{i,r}(\theta) \neq 0$. We impose a hypothesis on the shape of these curves for values of the coordinate r near 2, which implies that they have parabolic shape, up to second order.

HYPOTHESIS 17.2. *For $i = 1, 2$, $2 \leq r_0 \leq 2 + \epsilon_0$ and $\theta_i - \epsilon_0 \leq \theta \leq \theta_i + \epsilon_0$, assume that*

$$\frac{d}{d\theta}\Theta_{i,r_0}(\theta) > 0 \quad , \quad \frac{d^2}{d\theta^2}R_{i,r_0}(\theta) > 0 \quad , \quad \frac{d}{d\theta}R_{i,r_0}(\theta_i') = 0 \tag{90}$$

where θ_i' satisfies $\vartheta_i(2, \theta_i', -2) = (2, \theta_i, -2)$. Thus for $2 \leq r_0 \leq 2 + \epsilon_0$, the graph of $R_{i,r_0}(\theta')$ is parabolic with vertex $\theta' = \theta_i'$.

Note that (90) is a consequence of Hypothesis 12.1 when $r_0 = 2$.

DEFINITION 17.3. *A Kuperberg flow Φ_t is* generic *if the construction of $\mathbb{K}$ and $\mathcal{K}$ satisfies Hypotheses 12.1, 12.2 and 17.2. That is, the singularities for the vanishing of the vertical vector field $\mathcal{W}$ are of quadratic type, and the insertion yields a quadratic-type radius function near the special points.*

Recall from Proposition 2.1 that for each point $x \in \mathcal{R}$ with $-1 < z(x) < 1$, its $\mathcal{W}$-orbit is forward asymptotic to the periodic orbit $\mathcal{O}_2$ and backward asymptotic to the periodic orbit $\mathcal{O}_1$. The periodic orbits intersect $\mathbf{R}_0$

in the points $\omega_i = \mathcal{O}_i \cap \mathbf{R}_0$ for $i = 1, 2$. Also, recall from (64) that $I_0 = \mathcal{R} \cap \mathbf{R}_0 = \{(2, \pi, z) \mid -1 \leq z \leq 1\}$ is the line segment in $\mathbf{R}_0$ between ω_1 and ω_2. Recall that the action of the generator $\psi \in \mathcal{G}_K^*$ defined by the Wilson flow preserves I_0, and for $\xi \in I_0$ with $-1 < z(\xi) < 1$ we have $z(\xi) < z(\psi(\xi))$. Then set

$$I_\xi = \{(2, \pi, z) \mid z(\xi) < z \leq z(\psi(\xi))\}\,. \tag{91}$$

LEMMA 17.4. *Let $\xi \in I_0$ with $-1 < z(\xi) < z(\psi(\xi)) < 0$ and suppose that $I_\xi \subset \Sigma$, then $\Sigma = \mathfrak{M}$.*

Proof. The hypotheses imply that I_ξ is a fundamental domain for the Ψ_t-flow on the interior of $\mathcal{R}$. That is, the $\mathcal{W}$-orbit of each interior point $x \in \mathcal{R}$ intersects the interval I_ξ. If $I_\xi \subset \Sigma$ then $\mathcal{R}' \subset \Sigma$, and hence $\mathfrak{M}_0 \subset \Sigma$. As $\mathfrak{M}_0$ is dense in $\mathfrak{M}$, the conclusion follows. □

The strategy of the proof of Theorem 17.1 is to show that for some $\xi \in I_0$ sufficiently close to ω_1, the $\mathcal{K}$-orbit of ω_1 contains I_ξ in its closure. To this end, we establish some estimates on the orbit under $\mathcal{G}_K^*$ of $\xi \in \mathbf{R}_0$ with $2 \leq r(\xi) < 2 + \delta$ where $\delta > 0$ is sufficiently small.

We first obtain estimates for the metric behavior of the orbits of the Wilson generator $\psi \in \mathcal{G}_K^*$. Recall the functions f and g chosen in Section 2, which are constant in the coordinate θ, with

$$\mathcal{W} = g(r, \theta, z)\frac{\partial}{\partial z} + f(r, \theta, z)\frac{\partial}{\partial \theta}\ . \tag{92}$$

Hypothesis 12.2 and condition (44) imply there exists constants A_g, B_g, C_g such that the quadratic form $Q_g(u, v) = A_g \cdot u^2 + 2B_g \cdot uv + C_g \cdot v^2$ defined by the Hessian of g at ω_1 is positive definite. As a consequence, for $Q_0(r, z) = (r - 2)^2 + (z + 1)^2$, there exists $D_g > 0$ such that

$$|g(r, \theta, z) - Q_g(r - 2, z + 1)| \ \leq\ D_g \cdot (|r - 2|^3 + |z + 1|^3) \quad \text{for } Q_0(r, z) \leq \epsilon_0^2 \tag{93}$$

where ϵ_0 is the constant defined in (44). The condition (93) implies that for (r, z) sufficiently close to $(2, -1)$, the error term on the right-hand-side can be made arbitrarily small relative to the distance squared $Q_0(r, z)$ from the special point $(2, -1)$. We also observe that (93) implies there exists constants $0 < \lambda_1 \leq \lambda_2$ such that

$$\lambda_1 \cdot Q_0(r, z) \leq g(r, \theta, z) \leq \lambda_2 \cdot Q_0(r, z) \quad \text{for } Q_0(r, z) \leq \epsilon_0^2. \tag{94}$$

Next, consider the action of the maps ψ^ℓ for $\ell > 0$. Let $\xi \in \mathbf{R}_0$ with $2 \leq r(\xi) \leq 2 + \epsilon_0$ and $-7/4 \leq z(\xi) \leq -1/4$, such that $\psi(\xi)$ is defined and $z(\psi(\xi)) < 0$. Let $T(\xi) > 0$ be defined by $\psi(\xi) = \Psi_{T(\xi)}(\xi)$. Then the z-coordinate of $\psi(\xi)$ is given by

$$z(\psi(\xi)) - z(\xi) \ =\ \int_0^{T(\xi)} g(\Psi_s(\xi))\ ds \ \geq\ 0. \tag{95}$$

If $\xi \neq \omega_1$ then $g(\Psi_s(\xi))$ is positive along the orbit segment for $0 \leq s \leq T(\xi)$, hence $z(\psi(\xi)) - z(\xi) > 0$.

Note that if the orbit of $x \in \mathbb{W}$ avoids the ϵ_0-tube around the periodic orbits $\mathcal{O}_i$ then $g \equiv 1$ along the orbit, so the z-coordinate along the orbit increases at constant rate 1. As the cylinder $\mathcal{C}$ has height 4, this means that such an orbit traverses an angle of at most 4, hence it does not complete a full turn around the cylinder $\mathcal{C}$. In particular, for $\xi \in \mathbf{R}_0$ with $r(\xi) \geq 2 + \epsilon_0$ and $z(\xi) < 0$ with ψ defined at ξ, this implies the $\mathcal{W}$-orbit crosses the annulus $\mathcal{A}$ where $z = 0$, then returns to intercept $\mathbf{R}_0$ with $z(\psi(\xi)) > 0$. On the other hand, for $\xi \in \mathbf{R}_0$ with $2 < r(\xi) < 2 + \delta$ for $\delta \ll \epsilon_0$ and $z(\xi) < -1$, the $\mathcal{W}$-orbit traverses a region near $\mathcal{O}_1$ where the slope is close to 0, and hence repeatedly traverses the rectangle, with the number of revolutions increasing as $\delta \to 0$. In particular, for such ξ, the powers $\psi^\ell(\xi)$ form a sequence of points in the vertical line $r = r(\xi)$ with increasing z-coordinates, as has been noted previously, especially in the proofs of Propositions 7.5 and 7.6.

We next combine (93) with (95) to obtain metric estimates on the orbit of ω_1 under the action of $\mathcal{G}_K^*$. Recall that the first transition point for the forward orbit of ω_1 is the special entry point $p_1^- = \tau(\mathcal{L}_1^- \cap \mathcal{O}_1)$ with $r(p_1^-) = 2$, as illustrated in Figure 16. Section 12 introduced the alternate notation $p'(1) = p_1^- \in E_1$ and $p(1) = \tau^{-1}(p'(1)) \in L_1^-$, where $r(p(1)) = 2$ by the Radius Inequality.

The forward $\mathcal{W}$-orbit of $p(1)$ is trapped in the region $\mathcal{C} \cap \{z < -1\}$, and thus intercepts $\mathcal{L}_1^- \cap \mathcal{C}$ in an infinite sequence of points with increasing z-coordinates between -2 and -1. For all $\ell \geq b$, these points

are labeled $p'(1;1,\ell) \in \mathcal{L}_1^-$, where $r(p'(1;1,\ell)) = 2$ and $z(p'(1;1,\ell)) < z(p'(1;1,\ell+1)) < -1$. Moreover, $z(p'(1;1,\ell)) \to -1$ as $\ell \to \infty$.

For each $\ell \geq 0$, set $p(1;1,\ell) = \sigma_1^{-1}(p'(1;1,\ell)) \in L_1^-$ then $r(p(1;1,\ell)) > 2$. Note that $r(p(1;1,\ell)) \to 2$ as $\ell \to \infty$, and the sequence $p(1;1,\ell)$ accumulates on $p(1)$ in L_1^-.

Recall from Section 13 that corresponding to the sequence $\{p'(1;1,\ell) \mid \ell \geq 0\} \subset \mathcal{L}_1^-$ is a sequence $\{p_0(1;1,\ell) \mid \ell \geq 0\} \subset \mathbf{R}_0$ where $p_0(1;1,\ell)$ is the point in $\mathbf{R}_0$ whose forward $\mathcal{W}$-orbit has $p'(1;1,\ell)$ as its first transition point. Thus, $r(p_0(1;1,\ell)) = 2$, and $p_0(1;1,\ell+1) = \psi(p_0(1;1,\ell))$ for $\ell \geq 1$, with $z(p_0(1;1,\ell)) \to -1$ (see Figure 46). Define $0 < t_1 < t_2 < \cdots$ such that $\Psi_{t_\ell}(p_0(1;1,0)) = p_0(1;1,\ell)$.

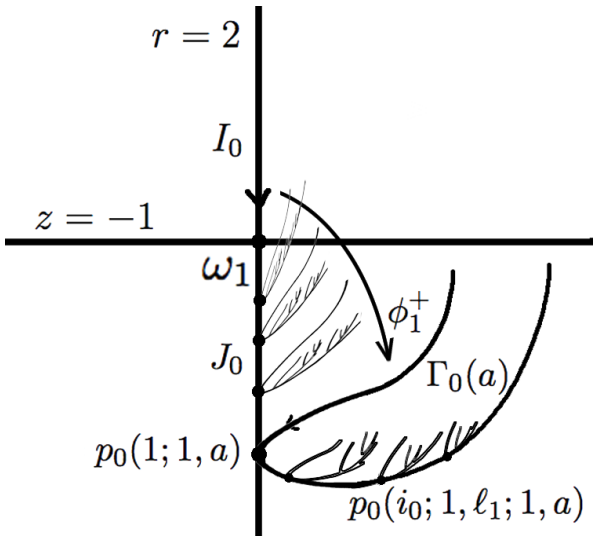

FIGURE 46. Iterations of Γ_0 and Λ_0 in $\mathbf{R}_0$ under $\mathcal{G}_K^*$

LEMMA 17.5. *There exists constants $C_2, C_3 > 0$ such that for all $\ell \geq \ell_0$, where $\ell_0 > 0$ is such that $z(p_0(1;1,\ell_0)) > -(1+\epsilon_0)$, then we have:*

$$\frac{-1}{4\pi\lambda_1\ell + C_2} < z(p_0(1;1,\ell+1)) + 1 \leq \frac{-1}{4\pi\lambda_2\ell + C_3}. \tag{96}$$

Moreover, for the constants $\lambda_1 \leq \lambda_2$ introduced in (94)*, there exists constants $C_4, C_5, C_6 > 0$ such that for all $\ell \geq \ell_0$,*

$$\frac{C_4}{(4\pi\lambda_1\ell)^2 + C_5} \leq z(p_0(1;1,\ell+1)) - z(p_0(1;1,\ell)) \leq \frac{C_4}{(4\pi\lambda_2\ell)^2 + C_6}. \tag{97}$$

Proof. Note that $z(p_0(1;1,\ell_0)) > -(1+\epsilon_0)$ implies the $\mathcal{W}$-orbit of $p_0(1;1,\ell_0)$ satisfies

$$-(1+\epsilon_0) < z(\Psi_t(p_0(1;1,\ell_0))) < -1 \text{ for all } t \geq 0,$$

and thus $f(\Psi_t(p_0(1;1,\ell_0))) = 1$. It then follows from (92) that $t_\ell = t_{\ell_0} + 4\pi(\ell - \ell_0)$ for all $\ell \geq \ell_0$.

Set $z(t) = z(\Psi_t(p_0(1;1,\ell_0)))$ for $t \geq 0$, so that $-(1+\epsilon_0) < z_0 = z(p_0(1;1,\ell_0)) < -1$. Then we have

$$\lambda_1 \cdot (1+z(t))^2 \;\leq\; \frac{dz}{dt} \;\leq\; \lambda_2 \cdot (1+z(t))^2 \;. \tag{98}$$

As $z(0) = z_0$ set $C_1 = -1/(z_0+1) > 0$ then we have

$$\frac{-1}{\lambda_1 t + C_1} \;\leq\; z(t) + 1 \;\leq\; \frac{-1}{\lambda_2 t + C_1} \;. \tag{99}$$

Substitute $t_\ell = t_{\ell_0} + 4\pi(\ell - \ell_0)$ into (99) and collect constants to obtain (96).

The estimate (97) follows by subtracting terms in (96) for ℓ and $\ell+1$, and gathering constants. Alternately, one can use the formula (94) and the estimate (93) to obtain (97). □

The estimates in Lemma 17.5 have counterparts for $\xi \in I_0$ with $-1 < z(\xi) < 0$ for which $z(\psi(\xi)) < -1+\epsilon_0$. In particular, the length of the interval I_ξ defined in (91) has quadratic upper and lower bound estimates as a function of $|z(\xi)+1|$.

We next obtain a more precise estimate than (93) for the restriction of $g(2,\theta_0,z)$ to the line I_0.

Note that for some $\lambda_1 \leq \lambda_g \leq \lambda_2$, the Taylor expansion for $g(2,\theta_0,z)$ gives the approximation $g(2,\theta_0,z) = \lambda_g(z+1)^2 + O(|z+1|^3)$. Next, choose a scale $0 < \epsilon_3 < \epsilon_0/2$ sufficiently small so that this approximation is strong enough to control the dynamics of the Ψ_t-flow near the cylinder $\mathcal{C}$.

DEFINITION 17.6. *Let* $0 < \epsilon_3 \leq \min\{\epsilon_0/2, 1/100, 1/(300\lambda_g)\}$ *be such that*

$$|g(2,\theta_0,z) - \lambda_g(z+1)^2| \ \leq \ \frac{\lambda_g(z+1)^2}{100} \quad \text{for } |z+1| \leq \epsilon_3 \ . \tag{100}$$

As a consequence, we have

$$.99 \cdot \lambda_g(z+1)^2 \leq g(2,\theta_0,z) \leq 1.01 \cdot \lambda_g(z+1)^2 \quad \text{for } |z+1| \leq \epsilon_3 \ . \tag{101}$$

A key point is that we can now choose a $\delta_3 > 0$ so that a weaker form of the estimate (101) holds for some neighborhood of a fundamental domain I_ξ in I_0 as defined by (91). Let $0 < \delta_3 < \epsilon_0/2$ be such that the following two estimates hold:

$$|r-2| \leq \delta_3 \text{ and } |z+1| \leq \epsilon_3 \quad \Longrightarrow \quad 0 \ \leq \ g(r,\theta_0,z) \ \leq \ 1.02 \cdot \lambda_g(\epsilon_3)^2 \tag{102}$$

$$|r-2| \leq \delta_3 \text{ and } \epsilon_3/4 \leq z+1 \leq \epsilon_3 \quad \Longrightarrow \quad .98 \cdot \lambda_g(z+1)^2 \leq g(r,\theta_0,z) \leq 1.02 \cdot \lambda_g(z+1)^2 \tag{103}$$

Note that the assumption that g is non-degenerate in Hypothesis 12.2 and the estimate (94) implies that for ϵ_3 sufficiently small, there exists a constant $C_g > 0$ such that $\delta_3 = \epsilon_3/C_g$.

We next introduce the "target box", which is key to the proof of Theorem 17.1,

$$R_0(\delta_3,\epsilon_3) = \{(r,z) \in \mathbf{R}_0 \mid |r-2| \leq \delta_3 \ , \ \epsilon_3/4 \leq z+1 \leq \epsilon_3\} \ . \tag{104}$$

DEFINITION 17.7. *We say that* $\xi \in \mathbf{R}_0$ *and* $\ell > 0$ *satisfy* Condition $R(\delta_3,\epsilon_3,\ell)$ *if*

$$z(\xi) < -1 \ , \ 2 < r(\xi) \leq 2+\delta_3 \tag{105}$$

$$\epsilon_3/3 < z(\psi^\ell(\xi)) + 1 < z(\psi^{\ell+1}(\xi)) + 1 < \epsilon_3/2 \ . \tag{106}$$

We then have an analog for $r > 2$ of Proposition 7.5.

LEMMA 17.8. *For* δ_3, ϵ_3 *as above and* $\xi \in \mathbf{R}_0$ *satisfying* (105)*, there exists* $\ell > 0$ *such that* (106) *is satisfied.*

Proof. As $z(\xi) < -1$ is assumed, there is a unique $t_1 > 0$ so that $z(\Psi_{t_1}(\xi)) = -1 + \epsilon_3/4$, and let $t_2 \geq t_1$ be the first subsequent time for which $\Psi_{t_2}(\xi) \in \mathbf{R}_0$. Note that $t_2 - t_1 \leq 2\pi\, r(\xi) < 6\pi$, and so by (95) and (102) and Definition 17.6, we obtain

$$z(\Psi_{t_2}(\xi)) - z(\Psi_{t_1}(\xi)) \ \leq \ 6\pi \cdot 1.02 \cdot \lambda_g(\epsilon_3)^2 \ \leq \ \epsilon_3 \cdot 20/300 = \epsilon_3/15 < \epsilon_3/12 \tag{107}$$

so that $z(\Psi_{t_2}(\xi)) + 1 < \epsilon_3/3$. The same estimates as in (107) show that

$$z(\psi^{\ell+1}(\Psi_{t_2}(\xi))) - z(\psi^\ell(\Psi_{t_2}(\xi))) \leq \epsilon_3/15 < \epsilon_3/12$$

for all $\ell > 0$ for which $z(\psi^\ell(\Psi_{t_2}(\xi))) + 1 < \epsilon_3/2$. The estimate (106) then follows. □

The last metric estimate required for the action of ψ, and a key point in the proof of Theorem 17.1, is to obtain estimates on the dependence of $z(\psi^\ell(\xi))$ for small changes of $\xi \in \mathbf{R}_0$. We first estimate $z(\psi^\ell(\xi+\Delta z)) - z(\psi^\ell(\xi))$ for $\ell > 0$, where Δz represents a small vertical increment.

Recall that the Wilson flow Ψ_t is rotationally invariant, and for $x_1 = (r_1, \theta_1, z_1)$ we adopt the notation $R_{\theta'}(x_1) = x_1 + \theta' = (r_1, \theta_1 + \theta', z_1)$, so that the rotation invariance becomes $\Psi_t(x_1 + \theta') = \Psi_t(x_1) + \theta'$.

LEMMA 17.9. *Let $x_1 = (r_1, \theta_1, z_1)$ with $-7/4 \leq z_1 \leq -5/4$ and $|r_1 - 2| \leq \epsilon_0$, so that $f(x) = g(x) = 1$ for x sufficiently close to x_1. For Δz sufficiently small, set $x_1' = x_1 + \Delta z = (r_1, \theta_1, z_1 + \Delta z)$. For $t \geq 0$, set $y_1 = \Psi_t(x_1)$, then*

$$z(\Psi_t(x_1')) - z(\Psi_t(x_1)) \;\approx\; g(y_1) \cdot \Delta z \tag{108}$$

Proof. Let s_1 be defined by $z(\Psi_{s_1}(x_1')) = z(x_1)$. As the slope of the vector field $\mathcal{W}$ near x_1 is $g(x_1)/f(x_1) = 1$, we have $s_1 = -\Delta z$, and hence $\theta(\Psi_{s_1}(x_1')) = \theta_1 - \Delta z$. Thus, $x_1 = R_{s_1}(\Psi_{s_1}(x_1'))$ and so

$$z\left(\Psi_t(x_1')\right) = z\left(\Psi_t(\Psi_{-s_1}(R_{-s_1}(x_1)))\right) = z\left(R_{-s_1}(\Psi_{-s_1}(\Psi_t(x_1)))\right) = z\left(\Psi_{-s_1}(y_1)\right) \tag{109}$$

The slope of $\mathcal{W}$ at y_1 is $g(y_1)$ as $f(y_1) = 1$, so that $z\left(\Psi_{-s_1}(y_1)\right) \approx z(y_1) + g(y_1) \cdot \Delta z$, which yields (108). □

In the case where $x_1 = \xi \in \mathbf{R}_0$ and Ψ_t is the map defining ψ^ℓ, then the estimate (108) can be made precise. For $\ell \geq 0$, set $\xi_\ell = \psi^\ell(\xi)$. Define $T(\xi_0, \ell) > 0$ by $\psi^\ell(\xi) = \Psi_{T(\xi,\ell)}(\xi)$.

COROLLARY 17.10. *Let $\xi_0 \in \mathbf{R}_0$ with $-7/4 \leq z(\xi_0) \leq -1 - \epsilon_0$ and $\ell > 0$ satisfy* Condition $R(\delta_3, \epsilon_3, \ell)$. *Then for Δz sufficiently small so that $\xi_0' = \xi_0 + \Delta z$ again satisfies* Condition $R(\delta_3, \epsilon_3, \ell)$, *we have*

$$|z(\psi^\ell(\xi_0')) - z(\psi^\ell(\xi_0))| \leq 1.02 \cdot \lambda_g(\epsilon_3)^2 \cdot \Delta z \tag{110}$$

Proof. The point ξ_0 satisfies the conditions of Lemma 17.9, and then use (103) in the proof. □

We next develop an estimate for $z(\psi^\ell(\xi_0')) - z(\psi^\ell(\xi_0))$, where $\xi_0' = \xi_0 + \Delta r$.

Assume that $\xi_0 \in \mathbf{R}_0$ with $-7/4 \leq z(\xi_0) \leq -1 - \epsilon_0$ and $\ell > 0$ satisfy condition $R(\delta_3, \epsilon_3, \ell)$. Also assume that Δr is sufficiently small so that $\xi_0' = \xi_0 + \Delta r$ again satisfies condition $R(\delta_3, \epsilon_3, \ell)$.

Then the z-coordinate $z(\Psi_t(\xi_0))$ increases at constant rate 1 in the region $\{z \leq -1 - \epsilon_0\}$, and subsequently increases at a possibly slower rate in the region $\{-1 - \epsilon_0 < z < -1 + \epsilon_0\}$. The $\mathcal{W}$-orbit segment $\{\Psi_t(\xi_0) \mid 0 \leq t \leq T(\xi_0, \ell)\}$ is geometrically a "coiled spring" in $\mathbb{W}$ which wraps ℓ-times around the cylinder $\{r = r(\xi)\}$, with the coils most "tightly spaced" near the periodic orbit $\mathcal{O}_1$. If $\Delta r > 0$ then the orbit $\{\Psi_t(\xi_0') \mid 0 \leq t \leq T(\xi_0', \ell)\}$ is slightly less tightly spaced, so the ends of the orbit segment are spaced further apart. More precisely, we have

$$z(\psi^\ell(\xi_0)) = z(\xi_0) \;+\; \int_0^{T(\xi_0,\ell)} g(\Psi_s(\xi_0))\; ds \tag{111}$$

Obtaining a sharp estimate for $z(\psi^\ell(\xi_0')) - z(\psi^\ell(\xi_0))$ requires estimating this integral as Δr varies in the expression $r(\xi_0') = r(\xi_0) + \Delta r$, and this requires more detailed estimates of the integrand $g(\Psi_s(\xi_0))$ than is given. However, a sufficient estimate can be obtained by noting that $z(\psi^\ell(\xi_0))$ is a smooth function with bounded derivatives on any compact set $K \subset \mathbf{R}_0$ contained in the domain of ψ^ℓ. For $0 < \delta_4 < \delta_3$, define:

$$K(\epsilon_3, \delta_3, \delta_4) \;=\; \{(r, z) \mid -2 \leq z \leq -1 - \epsilon_3 \text{ and } 2 + \delta_4 \leq r \leq 2 + \delta_3\} \tag{112}$$

which is a compact set contained in the domain of ψ^ℓ. Then for the function g chosen, define:

$$M(g, \ell, \epsilon_3, \delta_3, \delta_4) \;=\; \max\left\{ \frac{\partial\{z(\psi^\ell(r, z))\}}{\partial r} \mid (r, z) \in K(\epsilon_3, \delta_3, \delta_4) \right\} \tag{113}$$

Then by the Mean Value Theorem, we have:

LEMMA 17.11. *Let $\xi_0 \in \mathbf{R}_0$ and Δr be such that $\xi_0, \xi_0' \in K(\epsilon_3, \delta_3, \delta_4)$, where $\xi_0' = \xi_0 + \Delta r$. Then*

$$\left|z(\psi^\ell(\xi_0')) - z(\psi^\ell(\xi_0))\right| \;\leq\; M(g, \ell, \epsilon_3, \delta_3, \delta_4) \cdot \Delta r \tag{114}$$

The idea of the proof of Theorem 17.1, is to show that for $\epsilon_3 > 0$ as in Definition 17.6, and for any δ_3 satisfying (102) and (103), the orbits of ω_1 under $\mathcal{G}_K^*$ yields a set of points which have dense z-coordinates in a rectangle defined by (103). As δ_3 can be chosen arbitrarily small, this implies that the closure of the orbit of ω_1 contains a fundamental domain for the Ψ_t-flow on $\mathcal{R}$ as in (91), so the claim that $\Sigma = \mathfrak{M}$ follows from Lemma 17.4. The derivations of the estimates used in the proof of these statements depend fundamentally on Hypothesis 17.2.

The $\mathcal{K}$-orbit of $\omega_1 \in \mathbf{R}_0$ defines the sequence of points $\{p'(1;1,\ell) \mid \ell \geq 0\} \subset \mathcal{L}_1^-$ for $\ell \geq 0$, and corresponding points $\{p_0(1;1,\ell) \mid \ell \geq 0\} \subset \mathbf{R}_0$ with $r(p_0(1;1,\ell)) = 2$ and $z(p_0(1;1,\ell)) \to -1$, where the convergence of $z(p_0(1;1,\ell))$ is estimated by Lemma 17.5.

Assume that $a = b = 0$ for a and b as defined in Sections 13 and 12, respectively. For each $\ell \geq 0$, we then have the curve $\kappa_0(\ell) \subset \mathbf{R}_0$ with lower endpoint $p_0(1;1,\ell)$. For $\ell = 0$, the lower part of the curve $\kappa_0(0)$ is the image of the segment $J_0 \subset \mathbf{R}_0$ under the map $\phi_1^+ \in \mathcal{G}_K^*$, and $\kappa_0(\ell)$ is the image of $\kappa_0(0)$ under the map ψ^ℓ for $\ell \geq 0$.

The curve $\kappa_0(0)$ is "parabolic" by Hypothesis 17.2. That is, the r-coordinate of the graph is approximated by a quadratic function of the z-coordinate, for z near $p_0(1;1,0)$. In particular, the r-value of points on $\kappa_0(0)$ increases as $-(1+z)$ increases for $z \leq -1$. As the map ψ preserves the radius coordinate, the same monotonicity property is true for each of the curves $\kappa_0(\ell)$, as illustrated in the graphs in Figure 32.

Note that the image under the map ϕ_1^+ of the points $\{p_0(1;1,\ell) \mid \ell \geq 0\}$ yields a sequence of points $p_0(1;1,\ell;1,0) \subset \kappa_0(0)$ for which $r(p_0(1;1,\ell;1,0)) > 2$ and $p_0(1;1,\ell;1,0) \to p_0(1;1,0)$ as $\ell \to \infty$. Thus $r(p_0(1;1,\ell;1,0)) \to 2$ as $\ell \to \infty$.

Choose $m_1 > 0$ such that $r(p_0(1;1,m_1;1,0)) < 2 + \delta_3$. By Lemma 17.8, there exists $\ell_1 > 0$ such that

$$\epsilon_3/3 < z(p_0(1;1,m_1;1,\ell_1)) + 1 < z(p_0(1;1,m_1;1,\ell_1+1)) + 1 < \epsilon_3/2 \ , \tag{115}$$

since $p_0(1;1,m_1;1,\ell_1) = \psi^{\ell_1}(p_0(1;1,m_1;1,0))$.

Choose $n_1 > m_1$ such that $r(p_0(1;1,n_1;1,0)) \leq r(p_0(1;1,m_1;1,\ell_1))$, and set $\delta_4 = r(p_0(1;1,n_1;1,0)) - 2$.

Observe that the r-coordinate along the curve $\kappa_0(0)$ between $p_0(1;1,n_1;1,0)$ and $p_0(1;1,m_1;1,0)$ is monotone increasing by Hypothesis 17.2, hence have r values ranging between $2+\delta_4$ and $2+\delta_3$. We next select a collection of sequences of points in the $\mathcal{G}_K^*$-orbit of ω_1 which are sufficiently closely spaced, and which "shadow" this curve segment. Applying the map ψ^{ℓ_1} will then yield a collection of points in the region $R_0(\delta_3, \epsilon_3)$ which have arbitrarily dense z-coordinates.

Introduce the constant

$$\mu = 2 \cdot \max\ \left\{M(g, \ell_1, \epsilon_3, \delta_3, \delta_4)\ ,\ 1.02 \cdot \lambda_g(\epsilon_3)^2\right\} \tag{116}$$

where $M(g, \ell_1, \epsilon_3, \delta_3, \delta_4)$ is defined by 113, and the second term is introduced in 110. Then $\mu > 2$, and for $N \geq 2$, set

$$\epsilon_N = \frac{z(p_0(1;1,m_1;1,\ell_1+1)) - z(p_0(1;1,m_1;1,\ell_1))}{N} < 1/8 \quad , \quad \delta_N = \epsilon_N/\mu. \tag{117}$$

The image under ϕ_1^+ of the lower part of the parabolic curve $\kappa_0(n_1)$ with lower endpoint $p_0(1;1,n_1)$ is part of the curve $\kappa_0(1,n_1;0)$ with lower endpoint $p_0(1;1,n_1;1,0)$. Thus, the lower part of $\kappa_0(1,n_1;0)$ is the image of the interval J_0 under the composition $\phi_1^+ \circ \psi^{n_1} \circ \phi_1^+$. Applying this map to the sequence $p_0(1;1,\ell) = \psi^\ell(p_0(1;1,0))$ yields a collection of points on the curve $\kappa_0(1,n_1;0)$ which converge to $p_0(1;1,n_1;1,0)$, as in Figure 47. By Lemma 17.5, there exists $n_2 > 0$ so that for the collection

$$O(\delta_N; n_1, n_2) = \left\{\phi_1^+ \circ \psi^{n_1} \circ \phi_1^+ \circ \psi^\ell(p_0(1;1,0)) \mid \ell \geq n_2\right\} \subset \kappa_0(1,n_1;0), \tag{118}$$

the differences of both the z and r-values of successive points for $\ell, \ell+1 \geq n_2$ are bounded above by δ_N. By making n_2 bigger, we can assume that the point $p_0(1;1,n_2;1,n_1;1,0)$ has the largest r-coordinate for all points in $O(\delta_N; n_1, n_2)$.

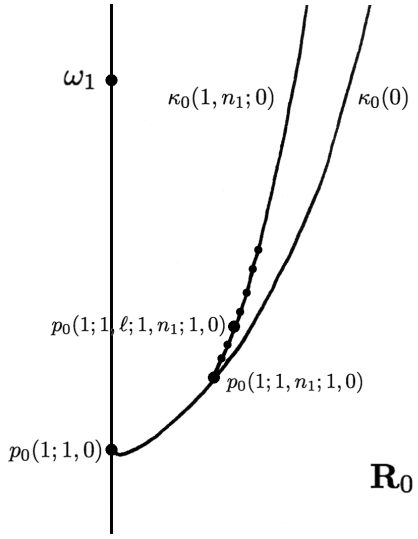

FIGURE 47. The points $p_0(1; 1, \ell; 1, n_1; 1, 0)$ in the curve $\kappa_0(1, n_1; 0)$ in $\mathbf{R}_0$

We now proceed inductively. Assume that the integers $\{n_1, n_2, \dots n_k\}$ have been chosen, with associated sets $O(\delta_N; n_1, n_2, \dots, n_i) \subset \mathcal{G}_K^*(\omega_1)$ for $i \leq k$, so that $p_0(1; 1, n_i; 1, n_{i-1}; \dots; 1, n_1; 1, 0)$ satisfies that

$$r(p_0(1; 1, n_i; 1, n_{i-1}; \dots; 1, n_1; 1, 0))$$

is the maximum of the r-values for all points in $O(\delta_N; n_1, n_2, \dots, n_i)$.

Suppose that $r(p_0(1; 1, n_k; 1, n_{k-1}; \dots; 1, n_1; 1, 0)) < r(p_0(1; 1, m_1; 1, 0))$, then the previous points chosen lie inside the region defined by the region bounded by the parabola $\Gamma_0(1, n_1; 0)$ and the region $\{r \leq r(p_0(1; 1, m_1; 1, 0))\}$ which lies inside the ϵ_0-ball in $\mathbf{R}_0$ about ω_1. Thus, we can continue the above process, and choose n_{k+1} as follows. The curve $\kappa_0(1, n_k; 1, n_{k-1}; \dots; 1, n_1; 0)$ with lower endpoint $p_0(1; 1, n_k; 1, n_{k-1}; \cdots; 1, 0)$ is the image of J_0 under the composition of maps

$$\phi_1^+ \circ \psi^{n_1} \circ \phi_1^+ \circ \psi^{n_2} \circ \phi_1 \circ \cdots \circ \psi^{n_k} \circ \phi_1^+ \tag{119}$$

Thus, applying the map in (119) to the sequence $\{p_0(1; 1, \ell) \mid \ell \geq 0\}$ yields a collection of points on the curve $\kappa_0(1, n_k; \dots; 1, n_1; 0)$ which converge to $p_0(1; 1, n_k; 1, n_{k-1}; \cdots; 1, 0)$. Then by Lemma 17.5, there exists $n_{k+1} > 0$ so that for the collection

$$\begin{aligned} & O(\delta_N; n_1, n_2, \dots, n_{k+1}) \\ &= \left\{\phi_1^+ \circ \psi^{n_1} \circ \phi_1^+ \circ \psi^{n_2} \circ \phi_1 \circ \cdots \circ \psi^{n_k} \circ \phi_1^+(p_0(1; 1, \ell)) \mid \ell \geq n_{k+1}\right\} \end{aligned} \tag{120}$$

which is contained in the curve $\kappa_0(1, n_k; \dots; 1, n_1; 0)$, the differences of both the z and r-values of successive points for $\ell, \ell + 1 \geq n_{k+1}$ are bounded above by δ_N. We can assume that $r(p_0(1; 1, n_{k+1}; 1, n_k; \cdots; 1, n_1; 0))$ is the maximum of the r-values for all points in $O(\delta_N; n_1, n_2, \dots, n_{k+1})$.

The collections of points defined by (120) are contained in the region bounded by the parabola $\Gamma_0(1, n_1; 0)$. Hypothesis 17.2 implies the composite functions in (119) have non-zero derivatives which are bounded away from zero for points in the region $\delta_4 \leq r(\xi) \leq \delta_3$ and $z(\xi) \leq -1 - \epsilon_0$. If $r(p_0(1; 1, n_{k+1}; 1, n_k; \cdots; 1, n_1; 0) < r(p_0(1; 1, m_1; 1, 0))$ then the κ_0 curve with lower endpoint at $p_0(1; 1, n_{k+1}; 1, n_k; \cdots; 1, n_1; 0)$ is defined, and so we can repeat the process to increase $r(p_0(1; 1, n_{k+1}; 1, n_k; \cdots; 1, n_1; 0))$, unless

$$r(p_0(1; 1, n_{k+1}; 1, n_k; \cdots; 1, n_1; 0)) \geq r(p_0(1; 1, m_1; 1, 0)),$$

in which case the inductive selection of points terminates.

Now apply the map ψ^{ℓ_1} to each of the sets $O(\delta_N; n_1, n_2, \dots, n_k)$ to obtain points in the region $R_0(\delta_3, \epsilon_3)$. Then Corollary 17.10 and Lemma 17.11 imply the difference of the z-values of successive points in the sequence

are bounded above by $\mu \cdot \delta_N = \epsilon_N$. Finally, by construction the upper r-value of points in $O(\delta_N; n_1, n_2, \ldots, n_k)$ is approached by the descending r-values of points in $O(\delta_N; n_1, n_2, \ldots, n_{k+1})$.

Thus, the image of $\mathcal{G}_K^*(\omega_1)$ contains points which are in the strip $2 < r \leq 2+\delta_3$ and whose z-values increase from $z(p_0(1;1,m_1;1,\ell_1))$ to $z(p_0(1;1,m_1;1,\ell_1+1))$ in increments at most ϵ_N. As $\delta_3 > 0$ and $N \gg 0$ were arbitrary, this implies the closure of $\mathcal{G}_K^*(\omega_1)$ contains $\mathcal{R}$, as was to be shown to establish Theorem 17.1. □

We conclude with a remark on the proof of Theorem 17.1. The quadratic assumption in Hypothesis 12.2 was not used in any essential way, except to obtain precise estimates on the spacing of the orbits of $\mathcal{W}$. It seems like that a much weaker assumption than this hypothesis should suffice for the proof.

18. Geometry of curves in $\mathbf{R}_0$

The aim of this section is to investigate the geometry of the collection of curves formed by the intersection $\mathfrak{M}_0 \cap \mathbf{R}_0$, thus of γ_0 and λ_0 curves. Up to now, we have only used their topology and the fact that the Γ_0 and Λ_0 curves form families of nested ellipses in $\mathbf{R}_0$. For a generic Kuperberg flow, as defined by Definition 17.3, we obtain estimates on the geometry of these curves, including the following result which has applications in Sections 19 and 22:

THEOREM 18.1. *Let Φ_t be a generic Kuperberg flow on $\mathbb{K}$. Then there exists $L > 0$ such that each connected component of $\mathfrak{M}_0 \cap \mathbf{R}_0$ is a curve with length bounded above by L.*

For γ_0 and λ_0 curves of level 1, the r-coordinate along the lower half of the curve is monotone increasing. If such condition was true for any curve in $\mathfrak{M}_0 \cap \mathbf{R}_0$, the theorem will be trivial. As we explain below this monotonicity condition does not holds for curves at level 2 or higher. To describe how γ_0 and λ_0 curves fold, we introduce a new set of curves, the A_0-curves.

For simplicity, we will restrict our discussion to γ_0 curves. Recall that the union of γ_0 and κ_0 curves gives Γ_0 curves, that at high levels are very thin (as a consequence of the nesting property). Hence the shape of a Γ_0 curve, that is a closed curve, can be seen as the shape of a simple curve. These are the A_0-curves described below.

As mentioned above, the lower half of a γ_0 curve of level at least 2 has no monotone radius. Then, the curve in E_1 generating the corresponding propeller has no monotone radius which implies that the propeller can have internal notches that do not correspond to the ones introduced in Section 12. These new internal notches generate also compact surfaces, to which we refer as bubbles of second type (the bubbles of first type being the ones introduced in Section 15). This phenomena is discussed at the end of this section.

The two aspects we are interested in are the following. First, we show that the lengths of γ_0 and λ_0 curves having one endpoint in the domain of ϕ_1^+ and the other endpoint in the domain of ϕ_2^+ has an upper bound. Observe that such curves admit $2 - 2\epsilon_0$ as a trivial lower bound. Second, these curves are "nice flat" arcs away from their endpoints, in the sense that if we consider a propeller generated by a γ-curve truncated near its tip, the trace that we obtain on the annulus $\mathcal{A} = \{z = 0\}$ will be a spiral that is never tangent to the lines $\{\theta = const\}$.

To prove Theorem 18.1, let us start by analyzing level 1 curves. Recall that the curves $\Gamma_0(\ell)$ for $\ell \geq a$ and unbounded, form the trace of the propeller $\tau(P'_\Gamma)$ on $\mathbf{R}_0$. Hypothesis 12.1 implies that $\Gamma \subset L_1^-$ is a parabolic curve with vertex at $p(1) = \sigma_1^{-1}(p_1^-)$ as illustrated in Figure 29. Thus the curves $\Gamma_0(\ell)$ are tangent to the vertical line $r = 2$ at two points, their vertices, with parabolic shape near these points, as in Figure 31.

The points in $\Gamma_0(\ell) \subset \mathbb{W}$ belong to Wilson orbits that intersect at least $a + \ell$ times $\mathbf{R}_0$, thus orbits that turn at least $a + \ell - 1$ times around the cylinder $\mathcal{C}$ before hitting $\mathcal{A}$. It follows that the radius coordinate along these curves, for $\ell > a$, is bounded above by $2 + \epsilon_0$. Thus the curves are contained in the rectangle $[2, 2+\epsilon_0] \times [-2, 2]$. Moreover, outside the ϵ_0 tube around the periodic orbits $\mathcal{O}_i$, for $i = 1, 2$, we have that $g = 1$ and thus a Wilson orbit intersects at most twice $\mathbf{R}_0$ in this region, once in each direction. Hence the

curves $\Gamma_0(\ell)$ are almost vertical outside the ϵ_0-neighborhood of the points ω_i. These considerations apply to higher level Γ_0-curves.

The problem of describing higher level Γ_0 curves comes from the fact that the curves $\Gamma(i,\ell) \subset L_i^-$ for $i = 1, 2$ do not have monotone radius along $\gamma(i,\ell)$ and the same might apply to the curves $\kappa(i,\ell)$. To illustrate this situation, let us consider the curve $\Gamma_0(\ell)$ for $\ell \geq 0$. The hypothesis $\ell \geq 0$ implies that the positive orbit of its points hit E_1 along $\tau(\Gamma(1,\ell))$, that is tangent to the vertical line $r = 2$. Thus $\Gamma(1,\ell) \in L_1^-$ is tangent to Γ at $p(1;1,\ell)$ and is composed of the union of $\gamma(1,\ell)$ and $\kappa(1,\ell)$. The circle with radius $r = r(p(1;1,\ell))$ is transverse to γ at two points, one being $p(1;1,\ell)$. Thus $\gamma(1,\ell)$ can not have monotone radius, as illustrated in Figure 48.

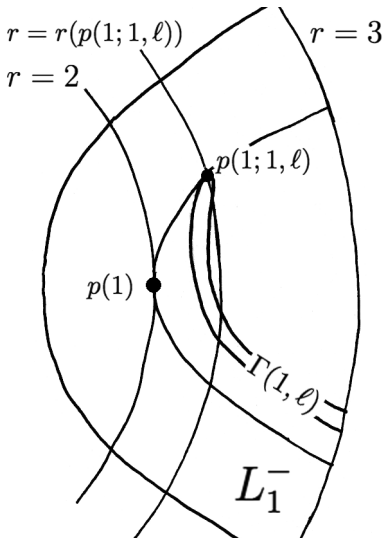

FIGURE 48. Intersection of $\Gamma(1,\ell)$ with the circle $r = r(p(1;1,\ell))$ in L_1^-

Observe that Hypothesis 17.2 implies that a curve in $\mathcal{L}_1^-$ crossing the line $z = -1$ is bended by the inverse of the insertion map σ_1^{-1} at the point with z-coordinate equal to -1. If the original curve is vertical, we obtain a parabolic curve in L_1^-. For example, $\Gamma' \subset \mathcal{L}_1^-$ is the vertical straight line and becomes the parabolic curve $\Gamma \in L_1^-$ with axis $\sigma_1^{-1}(\{z = -1\})$.

Let $A' = \{z = -1\} \subset \mathcal{L}_1^-$, then the curve $A = \sigma_1^{-1}(A') \subset L_1^-$ is a straight line connecting the boundary of $\partial_h^- \mathbb{W}$ to the point $p(1)$ with radius 2. Observe that A is inside the region of L_1^- that is bounded by Γ.

The propeller P_A is an infinite propeller as in Definition 11.1. Consider the notched propeller $P'_A = P_A \cap \mathbb{W}'$ and its image $\tau(P'_A)$ in $\mathbb{K}$. The trace of this propeller on the rectangle $\mathbf{R}_0$ is an infinite family of arcs $A_0(\ell)$, each one of them being in the region of $\mathbf{R}_0$ that is bounded by $\Gamma_0(\ell)$, for the same index ℓ. Since A intersects Γ at the special point $p(1) \in L_1^-$, for each ℓ the curve $A_0(\ell)$ intersects $\Gamma_0(\ell)$ at the two points $p_0(1;1,\ell)$ and $p_0(1;2,\ell)$. Recall that these are the points where $\Gamma_0(\ell)$ is tangent to the vertical line $r = 2$.

From the curve $A \subset L_1^-$ we can construct the infinite family of A-curves and the corresponding A_0-curves in $\mathbf{R}_0$. Observe that a level n curve in the later family is contained in the region of $\mathbf{R}_0$ bounded by a Γ_0-curve at the same level, in fact, by the Γ_0-curve having exactly the same label. We will say that the Γ_0-curve *envelops* the A_0-curve. To be more precise $\Gamma_0(i_1,\ell_1;\cdots;\ell_n)$ envelops $A_0(i_1,\ell_1;\cdots;\ell_n)$ and these two curves intersect at the points $p_0(1;i_1,\ell_1;\cdots;1,\ell_n)$ and $p_0(1;i_1,\ell_1;\cdots;2,\ell_n)$. Finally, observe that at the intersection points the curves are transverse to each other and locally $\Gamma_0(i_1,\ell_1;\cdots;\ell_n)$ has parabolic shape with axis $A_0(i_1,\ell_1;\cdots;\ell_n)$.

As we comment at the beginning of the section we are interested in finding upper bounds to the length of γ_0-curves and describing the end parts of these curves. The length of such curves is approximated by the length of A_0-curves, thus it is enough to find a uniform upper bound to the length of A_0-curves.

We consider next A-curves in detail. Let $A'(i,\ell) \subset \mathcal{L}_i^-$ be the entry curves of the notches of the propeller P'_A and $A(i,\ell) = \sigma_i^{-1}(A'(i,\ell)) \subset L_i^-$, for $i = 1, 2$. Hypothesis 12.2, on the Wilson flow, implies that for $r > 2 + \epsilon_0$ the vertical component of the vector field is equal to 1 and thus the lines $A_0(\ell)$ are steep in this region. Then there exists some positive number B such that for $\ell \geq B$ the curve $A'(1,\ell)$ intersects transversally A'. Let $q'(1;1,\ell)$ be the intersection point. The points in the curve $A'(1,\ell)$ belong to $\mathcal{W}$-orbits that intersect at least $(a+\ell)$-times the rectangle $\mathbf{R}_0$ before intersecting the annulus $\mathcal{A}$ and for $\ell > 0$ the endpoint $p'(1;1,\ell) \in \mathcal{L}_1^-$. The genericity assumptions imply thus that the value of B is small. Assume, without loss of generality, that $B = b$ for b as defined in Section 12.

Thus, for $\ell \geq 0$, $A(1,\ell) \subset L_1^-$ is a curve going from the point $p(1;1,\ell) \in \kappa$ to a point in the boundary of $\partial_h^- \mathbb{W}$ and crossing A at $q(1;1,\ell) = \sigma_1^{-1}(q'(1;1,\ell))$, then $A(1,\ell)$ is folded at the point $q(1;1,\ell)$, as illustrated in Figure 49. Observe that $q(1;1,\ell)$ is not necessarily the point of $A(1,\ell)$ with minimum radius, the point with minimum radius of $A(1,\ell)$ is in the arc between $q(1;1,\ell)$ and $p(1;1,\ell)$.

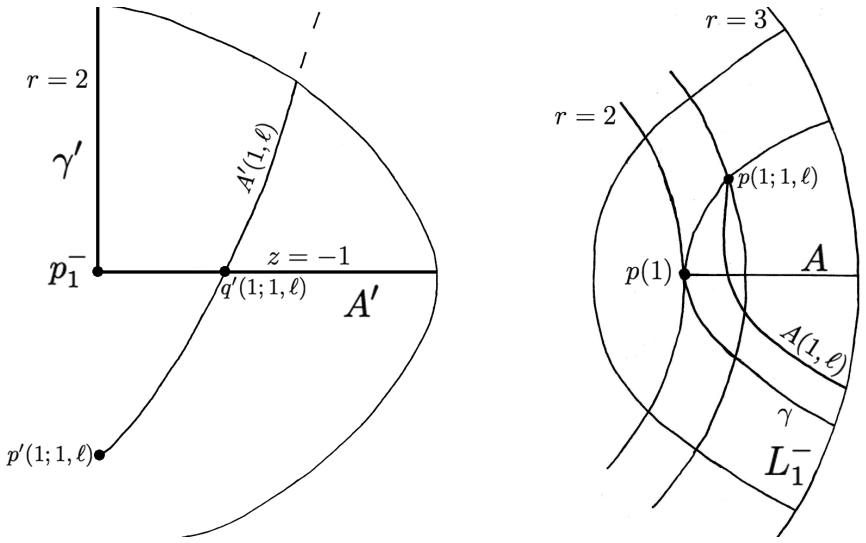

FIGURE 49. Curves A' and $A'(1,\ell)$ in $\mathcal{L}_1^-$ and the corresponding curves in L_1^-

Since A and $A(1,\ell)$ intersect, the propellers P_A and $P_{A(1,\ell)}$ intersect along the $\mathcal{W}$-orbit of the point $q(1;1,\ell)$. Observe that $P_{A(1,\ell)}$ is a finite propeller.

We consider now the intersection of $P_{A(1,\ell_1)}$ with $\mathcal{L}_1^-$, for $\ell_1 \geq b$. Since $P_{A(1,\ell_1)}$ is a finite propeller the intersection consists of finitely many curves $A'(1,\ell_1;1,\ell_2)$ for ℓ_1 fixed and $\ell_2 \geq b$ and bounded. For $\ell_1 \geq 0$ and $\ell_2 \geq 0$, these curves have one endpoint at $p'(1;1,\ell_1;1,\ell_2) \subset \kappa'(1,\ell_2)$ and its other endpoint on the boundary of $\mathcal{L}_1^-$. Moreover $A'(1,\ell_1;1,\ell_2)$ is in the region bounded by $\Gamma'(1,\ell_1;1,\ell_2)$, the later being in the region bounded by $\Gamma'(1,\ell_2)$, by the results of the previous sections. For ℓ_1 big enough and $\ell_2 \geq 0$ the curve $A'(1,\ell_1;1,\ell_2)$ intersects A' and at the intersection the curves are transverse to each other. Let $q'(2;1,\ell_1;1,\ell_2)$ be the intersection point. Observe that $A'(1,\ell_1;1,\ell_2)$ also intersects transversally $A'(1,\ell_2)$ at the point $q'(1;1,\ell_1;1,\ell_2)$ that is in the $\mathcal{W}$-orbit of $q(1;1,\ell_1)$. The points $q'(1;1,\ell_2) = A'(1,\ell_2) \cap A'$ and $q'(2;1,\ell_1;1,\ell_2)$ are on A' and in the region bounded by $\Gamma'(\ell_2)$, as illustrated in Figure 50.

We comment on the assumption ℓ_1 big enough. The curve $A'(1,\ell_1;1,\ell_2)$ intersects A' if its endpoint $p'(1;1,\ell_1;1,\ell_2)$ has z-coordinate smaller than -1, condition that is satisfied for ℓ_1 big enough since the sequence $p'(1;1,\ell_1;1,\ell_2)$ converges to $p'(1;1,\ell_2)$ as $\ell_1 \to \infty$ and $z(p'(1;1,\ell_2)) < -1$ for any $\ell_2 \geq a$. Observe that since we want to describe curves at high levels, we just care for curves with ℓ_1 big. This assumption will be used several times in what follows.

REMARK 18.2. *A_0-curves at level 1 have their lower endpoint below the line $z = -1$, since the lower endpoint belongs to a $\mathcal{W}$-orbit with radius coordinate equal to 2. At higher levels this is not true. However,*

we will only consider A_0-curves whose lower endpoint is below $z = -1$. The reason for this is that a higher level A_0-curve with lower endpoint above $z = -1$ intersects the domain of the map ψ^{-1}. Hence the trace of the propeller containing this A_0-curve has curves whose lower endpoint is below $z = -1$. The latter curve is longer, thus an upper bound to the length of the longer curve suffices.

LEMMA 18.3. *For a generic $\mathbb{K}$ plug, $r(q'(2; 1, \ell_1; 1, \ell_2)) < r(q'(1; 1, \ell_2))$.*

Proof. Observe that

$$r(q'(1; 1, \ell_1; 1, \ell_2)) = r(q(1; 1, \ell_1)) \leq r(p(1; 1, \ell_1)) = r(p'(1; 1, \ell_1; 1, \ell_2),$$

where the two equalities follow since the points are in the same $\mathcal{W}$-orbits and the inequality in the middle follows from Hypothesis 17.2. Thus Hypothesis 12.2 implies that the $\mathcal{W}$-orbit of $p(1; 1, \ell_1)$ climbs faster than the $\mathcal{W}$-orbit of $q(1; 1, \ell_1)$ and thus

$$z(q'(1; 1, \ell_1; 1, \ell_2)) \leq z(p'(1; 1, \ell_1; 1, \ell_2)).$$

For ℓ_1 big enough and ℓ_2 bounded, these two z-coordinates are less than -1. Thus the intersection point of $A'(1, \ell_1; 1, \ell_2)$ and $A'(1, \ell_2)$ has z-coordinate less than -1, implying that $r(q'(2; 1, \ell_1; 1, \ell_2)) < r(q'(1; 1, \ell_2))$. □

Recall that $A'(1, \ell_1; 1, \ell_2)$ intersects transversally $\kappa'(1, \ell_2) \subset \Gamma'(1, \ell_2)$ at the point $p'(1; 1, \ell_1; 1, \ell_2)$. Since the intersection of $A'(1, \ell_1; 1, \ell_2)$ with $A'(1, \ell_2)$ is also transverse, $A'(1, \ell_1; 1, \ell_2)$ bends at the intersection point $q'(1; 1, \ell_1; 1, \ell_2)$. This implies that the curve $\Gamma'(1, \ell_1; 1, \ell_2)$, that envelops $A'(1, \ell_1; 1, \ell_2)$ and is tangent at $p'(1; 1, \ell_1; 1, \ell_2)$ to $\kappa'(1, \ell_2)$, bends at its intersection with $A'(1, \ell_2)$. The intersection between $\Gamma'(1, \ell_1; 1, \ell_2)$ and $A'(1, \ell_2)$ is transverse and consists of one or two points: $\gamma'(1, \ell_1; 1, \ell_2)$ always intersects $A'(1, \ell_2)$ and $\kappa'(1, \ell_1; 1, \ell_2)$ might intersect it to.

Observe that if we fix the index ℓ_2 and we let $\ell_1 \to \infty$, both sequences $q'(1; 1, \ell_1; 1, \ell_2)$ and $p'(1; 1, \ell_1; 1, \ell_2)$ converge to the point $p'(1; 1, \ell_2)$.

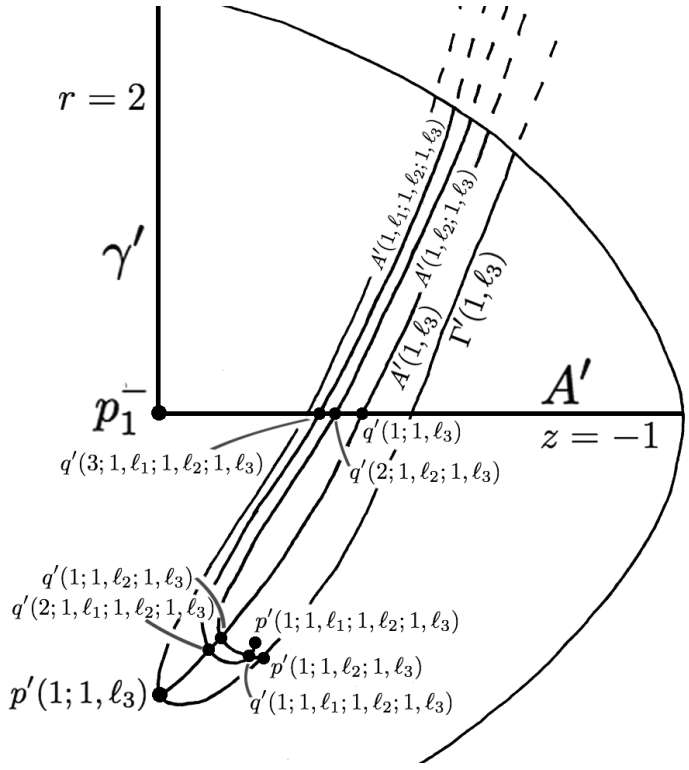

FIGURE 50. Three levels of A'-curves inside the region bounded by $\Gamma'(1, \ell_3)$ in $\mathcal{L}_1^-$

We now iterate the process above, considering only the first insertion for simplicity. The idea is that a level n curve in $\mathcal{L}_1^-$, with ℓ_1-index big enough, intersects a A'-curve at each of the previous levels, and these points are the bending points of the curve.

LEMMA 18.4. *For ℓ_1 sufficiently large, the curve $A'(1,\ell_1;1,\ell_2;\cdots;1,\ell_n)$ intersects A' and the curves $A'(1,\ell_{n-k};\cdots;1,\ell_n)$ for all $1\leq k<n$.*

For $1\leq k<n$, the intersection point of $A'(1,\ell_1;1,\ell_2;\cdots;1,\ell_n)$ with $A'(1,\ell_{n-k};\cdots;1,\ell_n)$ is denoted by $q'(k;1,\ell_1;\cdots;1,\ell_n)$, and the intersection with A' is denoted by $q'(n;1,\ell_1;\cdots;1,\ell_n)$. Observe that the first index in the label of q-points is the difference of levels between the A'-curves that pass through it.

Proof. For ℓ_1 big enough we can assume that the endpoint $p'(1;1,\ell_1;\cdots;1,\ell_n)$ of $A'(1,\ell_1;1,\ell_2;\cdots;1,\ell_n)$ is in $\mathcal{L}_1^-$ and has z-coordinate smaller than -1, thus the curve intersects A'.

We now proceed by induction on n. For $n=1$ the conclusion is straight forward. Assume that the lemma holds up to $n-1$ and consider the case n. For $k=1$ observe that $A'(1,\ell_1;1,\ell_2;\cdots;1,\ell_n)$ intersects $\kappa'(1,\ell_2;\cdots;1,\ell_n)$ at $p'(1;1,\ell_1;\cdots;1,\ell_n)$. Following the proof of Lemma 18.3 we have that

$$r(q'(n;1,\ell_1;\cdots;1,\ell_n))<r(q'(n-1;1,\ell_2;\cdots;1,\ell_n)).$$

Thus at the line $z=-1$ the curve $A'(1,\ell_1;1,\ell_2;\cdots;1,\ell_n)$ is on the left of the curve $A'(1,\ell_2;\cdots;1,\ell_n)$, while near its endpoint it is on the right. These curves intersect.

By hypothesis, the level $n-1$ curve $A'(1,\ell_2;\cdots;1,\ell_n)$ intersects all the curves of smaller levels. The same holds for the curve $\Gamma'(1,\ell_2;\cdots;1,\ell_n)$; that is, $\Gamma'(1,\ell_2;\cdots;1,\ell_n)$ intersects the curves $A'(1,\ell_{n-k};\cdots;1,\ell_n)$ for all $2\leq k<n$. Since $A'(1,\ell_1;1,\ell_2;\cdots;1,\ell_n)$ is in the region bounded by $\Gamma(1,\ell_2;\cdots;1,\ell_n)$, we obtain that it must intersect all the curves $A'(1,\ell_{n-k};\cdots;1,\ell_n)$. □

Now we consider the level 3 case in some detail. For ℓ_1 big enough and ℓ_2 bounded, the curve $A(1,\ell_1;1,\ell_2)=\sigma_1^{-1}(A'(1,\ell_1;1,\ell_2))\subset L_1^-$ intersects transversally:

- $A(1,\ell_2)$ at the point $q(1;1,\ell_1;1,\ell_2)$.
- A at the point $q(2;1,\ell_1;1,\ell_2)$.

Thus the finite propeller $P_{A(1,\ell_1;1,\ell_2)}$ intersects:

- $P_{A(1,\ell_2)}$ along the $\mathcal{W}$-orbit of $q(1;1,\ell_1;1,\ell_2)$.
- P_A along the $\mathcal{W}$-orbit of $q(2;1,\ell_1;1,\ell_2)$.

Consider the trace of $P_{A(1,\ell_1;1,\ell_2)}$ on $\mathcal{L}_1^-$, that forms a finite collection of curves $A'(1,\ell_1;1,\ell_2;1,\ell_3)$ with $\ell_3\geq b$ and bounded. For $\ell_3\geq 0$ we have that:

- $A'(1,\ell_1;1,\ell_2;1,\ell_3)$ is contained in the region bounded by $\Gamma'(1,\ell_1;1,\ell_2;1,\ell_3)$, which is contained in the region bounded by $\Gamma'(1,\ell_2;1,\ell_3)$, that is in the region bounded by $\Gamma'(1,\ell_3)$, by the nesting property.
- $A'(1,\ell_1;1,\ell_2;1,\ell_3)$ intersects $A'(1,\ell_2;1,\ell_3)$ at $q'(1;1,\ell_1;1,\ell_2;1,\ell_3)$; $A'(1,\ell_3)$ at $q'(2;1,\ell_1;1,\ell_2;1,\ell_3)$ and A' at $q'(3;1,\ell_1;1,\ell_2;1,\ell_3)$. Applying the proof of Lemma 18.3 we have that
$$r(q'(3;1,\ell_1;1,\ell_2;1,\ell_3))<r(q'(2;1,\ell_2;1,\ell_3))<r(q'(1;1,\ell_3)).$$

Thus the curve $A'(1,\ell_1;1,\ell_2;1,\ell_3)$ folds twice: once at $q'(1;1,\ell_1;1,\ell_2;1,\ell_3)$ and once at $q'(2;1,\ell_1;1,\ell_2;1,\ell_3)$. We deduce that the corresponding A_0-curve in $\mathbf{R}_0$, $A_0(1,\ell_1;1,\ell_2;\ell_3)$, folds twice near each of its endpoints due to the symmetry condition on the Wilson flow. Recall that $A_0(1,\ell_1;1,\ell_2;\ell_3)\subset\mathbf{R}_0$ is the curve containing points whose forward orbits intersect E_1 along $\tau(A(1,\ell_1;1,\ell_2;1,\ell_3))$.

Iterating this analysis we get that each A'-curve at level n folds $(n-1)$-times, and thus the lower end part of the corresponding A_0-curve coils in a "small" spiral turning in the counter-clockwise direction.

We can now start the proof of Theorem 18.1, that is a direct consequence of the following proposition.

PROPOSITION 18.5. *The length of an A_0-curve is upper bounded by the length of $A_0(a) + D$ for some uniform constant D.*

Proof. As explained in Remark 18.2 we can restrict to curves whose lower endpoint is below $z = -1$. We start by comparing the length of $A_0(1, \ell_1; \ell_2)$ with the length of $A_0(\ell_2)$. The idea is to prove first that

$$\text{length}(A_0(1, \ell_1; \ell_2)) < \text{length}(A_0(\ell_2)) + D,$$

that is clearly upper bounded by the length of $A_0(a) + D$.

The curve $A'(1, \ell_1; 1, \ell_2)$ in $\mathcal{L}_1^-$ can be decomposed into two parts: the one between $p'(1; 1, \ell_1; 1, \ell_2)$ and $q'(1; 1, \ell_1; 1, \ell_2)$ and the rest. Observe that the later part has approximately the same length as the segment of $A'(1, \ell_2)$ that lies above (in the z-direction) the point $q'(1; 1, \ell_1; 1, \ell_2)$. The reason for this is that both curves are in the region bounded by $\Gamma'(1, \ell_2)$ and have no bending points above $q'(1; 1, \ell_1; 1, \ell_2)$.

We can thus bound the length of $A'(1, \ell_1; 1, \ell_2)$ by the sum of the length of $A'(1, \ell_2)$ plus the distance between the points $p'(1; 1, \ell_1; 1, \ell_2)$ and $q'(1; 1, \ell_1; 1, \ell_2)$. We compare the distances in $\mathbf{R}_0$. Translating the discussion above to $\mathbf{R}_0$, we can bound the length of $A_0(1, \ell_1; \ell_2)$ by the sum of the length of $A_0(\ell_2)$ plus twice the distance between $p_0(1; 1, \ell_1; 1, \ell_2)$ and $q_0(1; 1, \ell_1; 1, \ell_2)$. The multiplication by two is due to the symmetry of these curves with respect to the line $\{z = 0\}$. Let $\varphi_{\ell_2} = \psi^{a+\ell_2} \circ \phi_1^+ \in \mathcal{G}_K^*$, then using Lemmas 13.6, 13.7 and 13.9 we obtain

$$d_{\mathbf{R}_0}(p_0(1; 1, \ell_1; 1, \ell_2), q_0(1; 1, \ell_1; 1, \ell_2)) = d_{\mathbf{R}_0}(\varphi_{\ell_2}(p_0(1; 1, \ell_1)), \varphi_{\ell_2}(q_0(1; 1, \ell_1))). \tag{121}$$

The next lemma is the key ingredient in the proof. Recall that $U_{\phi_1^+}$ is the domain of the map ϕ_1^+. Let $\mathcal{D}'(1, \ell)$ be the points in the region bounded by $\Gamma_0(\ell)$ that belong to $U_{\phi_1^+} \cap \{z \leq -1\}$. Define

$$\mathcal{D}(1, \ell) = \{x \in \mathcal{D}'(1, \ell) \,|\, \varphi_\ell(x) \in \mathcal{D}'(1, \ell)\},$$

for $\varphi_\ell = \psi^{(a+\ell)} \circ \phi_1^+$.

LEMMA 18.6. *For a generic Kuperberg plug $\mathbb{K}$, the norm of the differential of $\varphi_\ell = \psi^{(a+\ell)} \circ \phi_1^+$ is less than 1 for points in $\mathcal{D}(1, \ell)$.*

Proof. Observe that $\psi^{-(a+\ell)}(\mathcal{D}(1, \ell))$ is contained in the region of $\mathbf{R}_0$ bounded by $\Gamma_0(a)$. The map ψ preserves the r-coordinate. The map ϕ_1^+ maps $\mathcal{D}(1, \ell)$ to the interior of the region bounded by $\Gamma_0(a)$, and thus

$$\text{Image}(\phi_1^+(\mathcal{D}(1, \ell))) \subset \text{Image}(\psi^{-(a+\ell)}(\mathcal{D}(1, \ell))).$$

For every $\ell' \geq \ell$ such that the region $\mathcal{D}(1, \ell') \neq \emptyset$, we have that

$$\text{Image}(\phi_1^+(\mathcal{D}(1, \ell'))) \subset \text{Image}(\psi^{-(a+\ell)}(\mathcal{D}(1, \ell))).$$

Thus for points in $\mathcal{D}(1, \ell)$ the map ϕ_1^+ contracts distances more than $\psi^{-(a+\ell)}$. Hence, the norm of the differential of ϕ_1^+ is smaller than the norm of the differential of $\psi^{-(a+\ell')}$ for any ℓ' such that $\mathcal{D}(1, \ell')$ is non-empty. Hence, for $\xi \in \mathcal{D}(1, \ell)$ we have that

$$\begin{aligned} \|D\varphi_\ell(\xi)\| &\leq \|D\psi^{(a+\ell)}(\phi_1^+(\xi))\| \times \|D\phi_1^+(\xi)\| \\ &< \|D\psi^{(a+\ell)}(\phi_1^+(\xi))\| \times \|D\psi^{-(a+\ell)}(\psi^{a+\ell} \circ \phi_1^+(\xi))\| \\ &= \|D\psi^{(a+\ell)}(\eta)\| \times \|D\psi^{-(a+\ell)}(\psi^{a+\ell}(\eta))\| = 1. \end{aligned}$$

where $\eta = \phi_1^+(\xi)$. The last equality uses the fact that ψ preserves the r-coordinate. □

Observe that for $\xi \in \mathcal{D}(1, \ell)$ and $\ell' \geq \ell$ we have also that $\|D\varphi_{\ell'}(\xi)\| < 1$, provided $z(\varphi_{\ell'}(\xi)) \leq -1$.

We come back to bounding the length of the level 2 curve $A_0(1, \ell_1; \ell_2)$. From (121) and the previous lemma, we obtain a constant $C < 1$ such that

$$d_{\mathbf{R}_0}(p_0(1; 1, \ell_1; 1, \ell_2), q_0(1; 1, \ell_1; 1, \ell_2)) \leq C\, d_{\mathbf{R}_0}(p_0(1; 1, \ell_1), q_0(1; 1, \ell_1)).$$

Let $a_1 = \max_{\ell_1 \geq 0}\{d_{\mathbf{R}_0}(p_0(1;1,\ell_1), q_0(1;1,\ell_1))\}$ then,

$$\text{length}(A_0(1,\ell_1;\ell_2)) \leq \text{length}(A_0(\ell_2)) + 2Ca_1,$$

concluding the proof of Proposition 18.5 for level 2 curves for any $D \geq 2Ca_1$.

We know consider the level 3 case. Again the curve $A'(1,\ell_1;1,\ell_2;1,\ell_3) \subset \mathcal{L}_1^-$ can be decomposed into two parts: the one between $p'(1;1,\ell_1;1,\ell_2;1,\ell_3)$ and $q'(1;1,\ell_1;1,\ell_2;1,\ell_3)$ and the rest. The later part has approximately the same length as the part of $A'(1,\ell_2;1,\ell_3)$ that lies above the point $q'(1;1,\ell_1;1,\ell_2;1,\ell_3)$. Thus the length of $A'(1,\ell_1;1,\ell_2;1,\ell_3)$ is upper bounded by the length of $A'(1,\ell_2;1,\ell_3)$ plus the distance between the points $p'(1;1,\ell_1;1,\ell_2;1,\ell_3)$ and $q'(1;1,\ell_1;1,\ell_2;1,\ell_3)$.

In $\mathbf{R}_0$, the length of $A_0(1,\ell_1;1,\ell_2;\ell_3)$ is bounded above by the length of $A_0(1,\ell_2;\ell_3)$ plus twice the distance between the points $p_0(1;1,\ell_1;1,\ell_2;1,\ell_3)$ and $q_0(1;1,\ell_1;1,\ell_2;1,\ell_3)$. Observe that for $\varphi_{\ell_3} = \psi^{(a+\ell_3)} \circ \phi_1^+$ we have that $p_0(1;1,\ell_1;1,\ell_2;1,\ell_3) = \varphi_{\ell_3}(p_0(1;1,\ell_1;1;\ell_2))$ and $q_0(1;1,\ell_1;1,\ell_2;1,\ell_3) = \varphi_{\ell_3}(q_0(1;1,\ell_1;1;\ell_2))$. By construction the point $p_0(1;1,\ell_1;1,\ell_2)$ belongs to the curve $\kappa_0(\ell_2) \subset \Gamma_0(\ell_2)$ and $q_0(1;1,\ell_1;1,\ell_2)$ belongs to $A_0(\ell_2)$. Thus these two points are in $\mathcal{D}(1,\ell_2)$. By Lemma 18.6 and $C < 1$ as above, we obtain

$$\begin{aligned} d_{\mathbf{R}_0}\left(p_0(1;1,\ell_1;1,\ell_2;1,\ell_3), q_0(1;1,\ell_1;1,\ell_2;1,\ell_3)\right) &\leq C\, d_{\mathbf{R}_0}(p_0(1;1,\ell_1;1,\ell_2), q_0(1;1,\ell_1;1,\ell_2)) \\ &\leq C^2\, d_{\mathbf{R}_0}(p_0(1;1,\ell_1), q_0(1;1,\ell_1)) \\ &\leq C^2 a_1. \end{aligned}$$

Thus,

$$\begin{aligned} \text{length}(A_0(1,\ell_1;1,\ell_2;\ell_3)) &< \text{length}(A_0(1,\ell_2;\ell_3)) + \\ &\quad +2d_{\mathbf{R}_0}(p_0(1;1,\ell_1;1,\ell_2;1,\ell_3), q_0(1;1,\ell_1;1,\ell_2;1,\ell_3)) \\ &\leq \text{length}(A(\ell_3)) + 2Ca_1 + 2C^2 a_1 \\ &= \text{length}(A(\ell_3)) + 2Ca_1(1+C). \end{aligned}$$

The first inequality follows just by decomposing the lower half of $A_0(1,\ell_1;1,\ell_2;\ell_3)$ it two parts and using the symmetry of this curve with respect to $\{z=0\}$. The second inequality follows from the estimation of the length of level 2 curves and the computation above.

Iterating this argument for level 4 curves we have that

$$\begin{aligned} \text{length}(A_0(1,\ell_1;1,\ell_2;1,\ell_3;\ell_4)) &< \text{length}(A_0(1,\ell_2;1,\ell_3;\ell_4)) + \\ &\quad +2d_{\mathbf{R}_0}(p_0(1;1,\ell_1;1,\ell_2;1,\ell_3;1,\ell_4), q_0(1;1,\ell_1;1,\ell_2;1,\ell_3;1,\ell_4)) \\ &< \text{length}(A_0(\ell_4)) + 2Ca_1(1+C) + \\ &\quad +2Cd_{\mathbf{R}_0}(p_0(1;1,\ell_1;1,\ell_2;1,\ell_3), q_0(1;1,\ell_1;1,\ell_2;1,\ell_3)) \\ &\leq \text{length}(A_0(\ell_4)) + 2Ca_1(1+C) + 2C^3 a_1 \\ &= \text{length}(A_0(\ell_4)) + 2Ca_1(1+C+C^2). \end{aligned}$$

Generalizing to a level n curve, we get

$$\begin{aligned} \text{length}(A_0(1,\ell_1;\cdots;1,\ell_n)) &< \text{length}(A_0(\ell_n)) + 2Ca_1(1+C+\cdots+C^{n-2}) \\ &= \text{length}(A_0(\ell_n)) + 2a_1\left(\frac{C-C^n}{1-C}\right). \end{aligned} \tag{122}$$

The last amount is upper bounded by $\frac{C}{1-C}$, and thus taking $D = max\{2a_1\left(\frac{C}{1-C}\right), 2a_1\}$ we obtain the desired bound. □

This finishes the proof of Theorem 18.1. We can now describe a more accurate picture of the trace on $\mathbf{R}_0$ of a level $n \geq 2$ propeller in $\mathfrak{M}_0$ and thus of the trace of $\mathfrak{M}_0$. In Figure 20 we had made the assumption that the curve generating a finite propeller has monotone radius and thus that the longest $\mathcal{W}$-orbit in the propeller

is the orbit of the endpoint of the curve. As described above, the propellers in $\mathfrak{M}_0$ of level at least 2 are not generated by curves with monotone radius.

Consider a curve $\gamma(i_1, \ell_1; \cdots ; i_n, \ell_n) \subset L^-_{i_n}$ with $n \geq 2$, $i_k = 1, 2$ for $1 \leq k \leq n$ and non monotone radius. Once more, we restrict the discussion to γ-curves for simplicity, but it applies also to λ-curves.

Let $q^\gamma(n; i_1, \ell_1; \cdots ; i_n, \ell_n)$ be the point in $\gamma(i_1, \ell_1; \cdots ; i_n, \ell_n)$ with smaller radius. The trace of the propeller $P_{\gamma(i_1,\ell_1;\cdots;i_n,\ell_n)} \subset \mathbb{W}$ on $\mathbf{R}_0$ consists of at most

$$\Delta(r(q^\gamma(n; i_1, \ell_1; \cdots ; i_n, \ell_n))) + 1$$

curves, one for each intersection of the $\mathcal{W}$-orbit of $q^\gamma(n; i_1, \ell_1; \cdots ; i_n, \ell_n)$ with $\mathbf{R}_0 \cap \{z \leq 0\}$. Call this number $n(q^\gamma(n; i_1, \ell_1; \cdots ; i_n, \ell_n))$. Recall that the $\mathcal{W}$-orbit of $p(1; i_1, \ell_1; \cdots ; i_n, \ell_n)$ intersects $\mathbf{R}_0 \cap \{z \leq 0\}$ in at most $\Delta(r(p(1; i_1, \ell_1; \cdots ; i_n, \ell_n))) + 1$ points. Call this number $n(p(1; i_1, \ell_1; \cdots ; i_n, \ell_n))$. Hence the trace of $P_{\gamma(i_1,\ell_1;\cdots;i_n,\ell_n)}$ on $\mathbf{R}_0$ are the curves $\gamma_0(i_1, \ell_1; \cdots ; i_n, \ell_n; \ell_{n+1})$ with $a \leq \ell_{n+1} \leq n(q^\gamma(n; i_1, \ell_1; \cdots ; i_n, \ell_n))$.

If $n(q^\gamma(n; i_1, \ell_1; \cdots ; i_n, \ell_n)) - n(p(1; i_1, \ell_1; \cdots ; i_n, \ell_n)) = 0$, all the curves in $P_{\gamma(i_1,\ell_1;\cdots;i_n,\ell_n)} \cap \mathbf{R}_0$ are arcs as in Figure 20, except that near the endpoints the arcs coil as explained earlier in this section.

If $n(q^\gamma(n; i_1, \ell_1; \cdots ; i_n, \ell_n)) - n(p(1; i_1, \ell_1; \cdots ; i_n, \ell_n)) > 0$, then for

$$n(p(1; i_1, \ell_1; \cdots ; i_n, \ell_n)) < \ell_{n+1} \leq n(q^\gamma(n; i_1, \ell_1; \cdots ; i_n, \ell_n))$$

the curves $\gamma_0(i_1, \ell_1; \cdots ; i_n, \ell_n; \ell_{n+1})$ are closed, as in Figure 51. The closed curves are contained in the region

$$\{r(q^\gamma(n; i_1, \ell_1; \cdots ; i_n, \ell_n)) \leq r < r(p(1; i_1, \ell_1; \cdots ; i_n, \ell_n))\} \cap \mathbf{R}_0.$$

In conclusion, the trace of $P_{\gamma(i_1,\ell_1;\cdots;i_n,\ell_n)}$ on $\mathbf{R}_0$ can have a non-zero but finite number of closed curves.

We now turn our attention once more to the intersection of $P_{\gamma(i_1,\ell_1;\cdots;i_n,\ell_n)}$ with $\mathcal{L}^-_i$. As explained in Section 12, the intersection consists of a number of internal notches, followed by boundary notches. After the description in this section two new possibilities arise. First, since the radius is non monotone along the curves in $P_{\gamma(i_1,\ell_1;\cdots;i_n,\ell_n)} \cap \mathbf{R}_0$, some of these curves might create internal notches when flowed to $\mathcal{L}^-_i$. Second, the fact that the trace of $P_{\gamma(i_1,\ell_1;\cdots;i_n,\ell_n)}$ on $\mathbf{R}_0$ can have closed curves adds the possibility of having internal notches near the tip of the propeller, as illustrated in Figure 52.

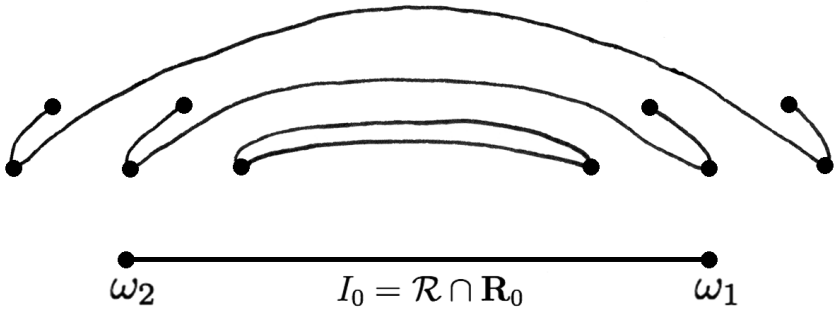

FIGURE 51. Trace of the finite propeller $P_{\gamma(i_1,\ell_1;\cdots;i_n,\ell_n)}$ in $\mathbf{R}_0$ with $n(q^\gamma(n; i_1, \ell_1; \cdots ; i_n, \ell_n)) - n(p(1; i_1, \ell_1; \cdots ; i_n, \ell_n)) = 1$

The two level 1 propellers $\tau(P'_\gamma)$ and $\tau(P'_\lambda)$ in $\mathfrak{M}_0$ are generated by curves with monotone radius. Thus they have a finite number $|b| \geq 0$, maybe zero, of internal notches and an infinite number of (boundary) notches, as described in Section 12. If any, the internal notches generate bubbles as in Section 15.

Consider the case of propellers of level at least 2. Let $P_{\gamma(i_1,\ell_1;\cdots;i_n,\ell_n)}$ be a propeller of level $n + 1 \geq 2$. Let $\gamma'(i_1, \ell_1; \cdots ; i_n, \ell_n; 1, \ell_{n+1}) \subset \mathcal{L}^-_1$ be the curves in the intersection of $P_{\gamma(i_1,\ell_1;\cdots;i_n,\ell_n)}$ with $\mathcal{L}^-_1$ and $\gamma_0(i_1, \ell_1; \cdots ; i_n, \ell_n; \ell_{n+1})$ the corresponding curve in $\mathbf{R}_0$. Internal notches arise when $\gamma'(i_1, \ell_1; \cdots ; i_n, \ell_n; 1, \ell_{n+1})$ has its two endpoints in $\partial\mathcal{L}^-_1$.

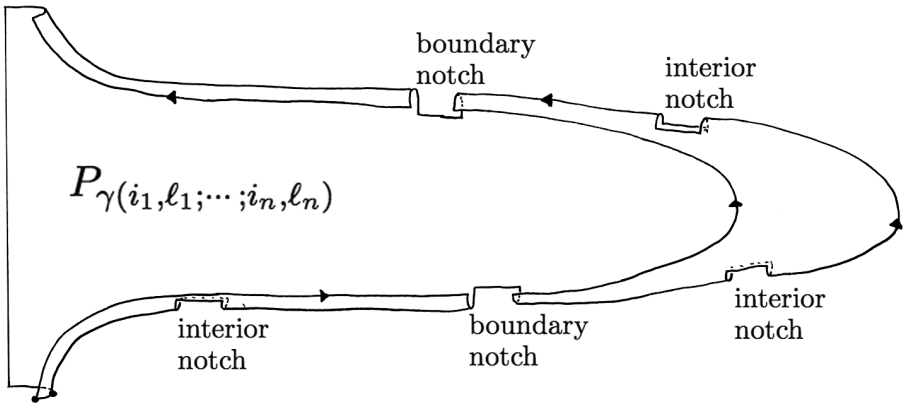

FIGURE 52. Notches with $n(q^\gamma(n;i_1,\ell_1;\cdots;i_n,\ell_n)) - n(p(1;i_1,\ell_1;\cdots;i_n,\ell_n)) = 1$

Assume that this is the case. If the corresponding curve $\gamma_0(i_1,\ell_1;\cdots;i_n,\ell_n;\ell_{n+1}) \subset \mathbf{R}_0$ is not a closed curve, then the forward orbit of its lower endpoint $p_0(1;i_1,\ell_1;\cdots;i_n,\ell_n;1,\ell_{n+1})$ misses $\mathcal{L}_1^-$. Thus the radius coordinate along the curve $\gamma(i_1,\ell_1;\cdots;i_n,\ell_n;1,\ell_{n+1}) \subset L_1^-$ is big, meaning that it is uniformly bounded below. The arguments in Section 15 apply to this case and thus the surface generated by the $\mathcal{K}$-orbits of the points in $\tau(\gamma(i_1,\ell_1;\cdots;i_n,\ell_n;1,\ell_{n+1}))$ is compact and admits a uniform upper bound to the difference of level between points in it. We leave the details to the reader.

For the second case, assume that $\gamma'(i_1,\ell_1;\cdots;i_n,\ell_n;1,\ell_{n+1})$ has its two endpoints in $\partial\mathcal{L}_1^-$ and that the corresponding curve $\gamma_0(i_1,\ell_1;\cdots;i_n,\ell_n;\ell_{n+1}) \subset \mathbf{R}_0$ is a closed curve. This means that

$$n(q^\gamma(n;i_1,\ell_1;\cdots;i_n,\ell_n)) - n(p(1;i_1,\ell_1;\cdots;i_n,\ell_n)) > 0$$

and $n(p(1;i_1,\ell_1;\cdots;i_n,\ell_n)) < \ell_{n+1} \leq n(q^\gamma(n;i_1,\ell_1;\cdots;i_n,\ell_n))$.

LEMMA 18.7. *There exists $r_B > 2$ such that if $n(q^\gamma(n;i_1,\ell_1;\cdots;i_n,\ell_n)) - n(p(1;i_1,\ell_1;\cdots;i_n,\ell_n)) > 0$ the radius coordinate on the curves $\gamma(i_1,\ell_1;\cdots;i_n,\ell_n;1,\ell_{n+1}) \in L_1^-$ with*

$$n(p(1;i_1,\ell_1;\cdots;i_n,\ell_n)) < \ell_{n+1} \leq n(q^\gamma(n;i_1,\ell_1;\cdots;i_n,\ell_n))$$

is bounded below by r_B.

Proof. Observe that the closed curve $\gamma_0(i_1,\ell_1;\cdots;i_n,\ell_n;\ell_{n+1}) \in \mathbf{R}_0$ is contained in the region bounded by $\Gamma_0(i_2,\ell_2;\cdots;\ell_{n+1})$ if $i_1 = 1$ and in the region bounded by $\Lambda_0(i_2,\ell_2;\cdots;\ell_{n+1})$ if $i_1 = 2$. Also, it is far from $\Gamma_0(i_2,\ell_2;\cdots;\ell_{n+1})$ or $\Lambda_0(i_2,\ell_2;\cdots;\ell_{n+1})$ since the point $p_0(i_1;i_2,\ell_2;\cdots;1,\ell_{n+1})$ is in the closure of the endpoints of the curves $\gamma_0(i_1,m;\cdots;i_n,\ell_n;\ell_{n+1})$ that are arcs, for $m > \ell_1$ and unbounded. That is $\gamma_0(i_1,\ell_1;\cdots;\ell_{n+1})$ is separated from $\Gamma_0(i_2,\ell_2;\cdots;\ell_{n+1})$ or $\Lambda_0(i_2,\ell_2;\cdots;\ell_{n+1})$ by the curves $\gamma_0(i_1,m;\cdots;\ell_{n+1})$ and $\lambda_0(i_1,m;\cdots;\ell_{n+1})$ for all $m > \ell_{n+1}$

Assume the conclusion in the lemma is false, then for every $\epsilon > 0$ there exists a curve $\gamma(i_1,\ell_1;\cdots;i_n,\ell_n;1,\ell_{n+1}) \in L_1^-$ with

$$n(p(1;i_1,\ell_1;\cdots;i_n,\ell_n)) < \ell_{n+1} \leq n(q^\gamma(n;i_1,\ell_1;\cdots;i_n,\ell_n))$$

intersecting the ball centered at $p(1)$ of radius ϵ. Equivalently, for every $\epsilon > 0$ there exists a closed curve $\gamma_0(i_1,\ell_1;\cdots;i_n,\ell_n;\ell_{n+1}) \in \mathbf{R}_0$ with

$$n(p(1;i_1,\ell_1;\cdots;i_n,\ell_n)) < \ell_{n+1} \leq n(q^\gamma(n;i_1,\ell_1;\cdots;i_n,\ell_n))$$

intersecting the ball centered at ω_1 of radius ϵ. Thus there is a sequence of closed curves accumulating on ω_1 that belong to the trace of the propellers. This is the contradiction that we needed. □

REMARK 18.8. *An immediate consequence of Lemma 18.7 is that the surfaces given by the $\mathcal{K}$-orbits of the points in $\tau(\gamma(i_1,\ell_1;\cdots;i_n,\ell_n;1,\ell_{n+1}))$, with ℓ_{n+1} satisfying the hypotheses of the lemma, are compact and*

the difference of level between points in them is uniformly bounded as in Proposition 15.4. We refer to these surfaces as bubbles of the second type.

19. Zippered laminations

The notion of an n-dimensional lamination is well-known, and can be summarized as an n-dimensional foliated space which is transversally modeled on a totally disconnected space. In this section, we introduce the notion of *zippered laminations*, which are a type of "stratified" laminations with possibly pathological behavior for the strata. After introducing this and some other preliminary notions, we prove the main result of this section:

THEOREM 19.1. *If Φ_t is a generic Kuperberg flow on $\mathbb{K}$, then $\mathfrak{M}$ is a* zippered lamination.

We begin by recalling the notion of a foliated space [7, 37]. A *continuum* is a non-empty, compact, connected metric space.

DEFINITION 19.2. *A* foliated space of dimension n *is a continuum $\mathfrak{Z}$ with a foliated structure. That is, there exists:*

(1) a separable metric space $\mathfrak{X}$, and a collection of compact subsets $\mathfrak{T}_i \subset \mathfrak{X}$ for $1 \leq i \leq k$;
(2) a finite collection of homeomorphisms (the charts) $\{\varphi_i \colon \mathfrak{T}_i \times [-1,1]^n \to \overline{U}_i \subset \mathfrak{Z} \mid 1 \leq i \leq k\}$;
(3) the "interiors" $\{U_i = \varphi_i(\mathfrak{T}_i \times (-1,1)^n) \mid 1 \leq i \leq k\}$ form an covering for $\mathfrak{Z}$;
(4) the charts $\{\varphi_i \mid 1 \leq i \leq k\}$ satisfy the compatibility condition (123).

Let $\pi_i \colon \overline{U}_i \to \mathfrak{T}_i$ denote the composition of φ_i^{-1} with projection onto the first factor.

For $\xi \in \mathfrak{T}_i$ the set $\mathcal{P}_i(\xi) = \varphi_i(\{\xi\} \times [-1,1]^n) \subset \overline{U}_x$ is called a *plaque* for the coordinate chart φ_i. For $z \in \overline{U}_i$, we adopt the notation $\mathcal{P}_i(z) = \mathcal{P}_i(\pi_i(z))$, so that $z \in \mathcal{P}_i(z)$.

For $\xi \in \mathfrak{T}_i$ the plaque $\mathcal{P}_i(\xi)$ is given the topology so that the restriction $\varphi_i \colon \{\xi\} \times [-1,1]^n \to \mathcal{P}_i(\xi)$ is a homeomorphism, hence $int(\mathcal{P}_i(\xi)) = \varphi_i(\{\xi\} \times (-1,1)^n)$. Then we require, in addition,

$$\text{for all } z \in U_i \cap U_j \ , \ \text{int}(\mathcal{P}_i(z)) \cap \text{int}(\mathcal{P}_j(z)) \text{ is an open subset of both } \mathcal{P}_i(z) \text{ and } \mathcal{P}_j(z) \ . \tag{123}$$

The collection of sets $\mathcal{V} = \{\varphi_i(\{\xi\} \times V) \mid 1 \leq i \leq k \ , \ \xi \in \mathfrak{T}_i \ , \ V \subset (-1,1)^n \text{ open}\}$ forms the basis for the *fine topology* of $\mathfrak{Z}$. The connected components of the fine topology are called leaves, and define the foliation $\mathcal{F}$ of $\mathfrak{Z}$. For $x \in \mathfrak{Z}$, let $L_x \subset \mathfrak{M}$ denote the leaf of $\mathcal{F}$ containing x. The subsets $\mathfrak{T}_i$ of $\mathfrak{X}$ are called the *local transverse models*.

Many of the techniques of foliation theory extend to foliated spaces, including the existence of holonomy transformations defined by "parallel transport" along paths in the leaves, which generate a pseudogroup model for the dynamics of the foliated space. Foliated spaces are considered in greater detail in [37, Chapter 2] and [7, Chapter 11].

An *n-dimensional lamination* is a foliated space $\mathfrak{Z}$ of dimension n, such that the transverse model space $\mathfrak{X}$ is totally disconnected. The leaves of $\mathcal{F}$ are then the path components of $\mathfrak{Z}$.

The definition of a *lamination with boundary* is obtained by modifying the above definition, to allow foliation charts of the form $\varphi_i \colon \mathfrak{T}_i \times ([0,1) \times (-1,1)^{n-1}) \to U_i$. The boundary $\partial\mathfrak{Z}$ then consists of the points which are images under a chart of the chart boundary $\mathfrak{T}_i \times (\{0\} \times (-1,1)^{n-1})$.

The notion of a "zippered lamination" is motivated by our study of the space $\mathfrak{M}$, which is the closure of the non-compact manifold with boundary $\mathfrak{M}_0$. The unusual property of $\mathfrak{M}$ is that the boundary curves of $\mathfrak{M}_0$ are also dense in $\mathfrak{M}$, which is impossible for a usual lamination with boundary. The definition of a zippered lamination below is similar to that of a lamination with boundary, in that each of its leaves is a manifold with boundary, but the boundaries of the leaves do not have to align themselves in a way that they are regularly covered by foliation charts. In place of the covering of $\mathfrak{M}$ by standard foliation coordinate charts as in

Definition 19.2, the definition below covers $\mathfrak{M}$ by foliation coordinate charts whose plaques have varying sizes, and cannot be "standardized" in a continuous manner, though their overlaps do define continuous holonomy transformations.

DEFINITION 19.3. *An* n-dimensional zippered lamination $\mathfrak{Z}$ *is a continuum whose path components are* n*-dimensional manifolds with boundary. Denote the union of the boundaries of the leaves by* $\partial_{\mathcal{F}}\mathfrak{Z}$*, and the complement by* $\mathrm{int}(\mathfrak{Z}) = \mathfrak{Z} - \partial_{\mathcal{F}}\mathfrak{Z}$*. Then we require that* $\mathrm{int}(\mathfrak{Z})$ *is dense in* $\mathfrak{Z}$*, and the following data are given, which satisfies the accompanying conditions: there is given a compact metric space* $\mathfrak{X}$*, and for* $1 \leq i \leq k$*,*

(1) a subset $\mathfrak{T}_i \subset \mathfrak{X}$ *whose closure in* $\mathfrak{X}$ *is totally disconnected;*
(2) a Borel subset $\mathcal{B}_i \subset \mathfrak{T}_i \times [-1,1]^n$*, where for each* $\xi \in \mathfrak{T}_i$ *the slice* $\mathcal{B}_i \cap \{\xi\} \times [-1,1]^n$ *is a compact subset whose interior contains* $\{\xi\} \times \{0\}$*, and is homeomorphic to* $[-1,1]^n$*;*
(3) a homeomorphism $\varphi_i \colon \mathcal{B}_i \to \overline{U}_i \subset \mathfrak{Z}$ *onto its image* $\overline{U}_i$ *with the induced topology from* $\mathfrak{Z}$*;*
(4) the interiors $\{U_i = \mathrm{int}(\overline{U}_i) \mid 1 \leq i \leq k\}$ *form a covering for* $\mathrm{int}(\mathfrak{Z})$*;*
(5) the collection of charts $\{\varphi_i \mid 1 \leq i \leq k\}$ *satisfy the compatibility condition* (123)*.*

The interior $\mathrm{int}(\overline{U}_i)$ for the Borel set $\overline{U}_i$ is defined as the union over the points $\xi \in \mathfrak{T}_i$ of the interiors of the plaques $\mathcal{P}_i(\xi) = \varphi_i(\mathcal{B}_i \cap \{\xi\} \times [-1,1]^n)$ in $\overline{U}_i$.

Note that the Borel property in 19.3.2 allows the plaques $\mathcal{P}_i(\xi_\ell) \subset \mathfrak{Z}$ to degenerate in size for a sequence $\xi_\ell \in \mathfrak{T}_i$ which converge to a point $\xi_* \in \mathfrak{X}$ with $\xi_* \notin \mathfrak{T}_i$. In fact, the limit of such a sequence must then be contained in $\partial_{\mathcal{F}}\mathfrak{Z}$.

The first step in showing that $\mathfrak{M}$ satisfies the conditions of Definition 19.3 is to construct the model spaces $\mathfrak{T}_i$. Recall that $\mathcal{T} = \{z = 0\} \cap \mathbf{R}_0$, and set:

$$\mathfrak{C}'_0 = \mathcal{T} \cap \mathfrak{M}_0 \quad , \quad \mathfrak{C}' = \mathcal{T} \cap \mathfrak{M} \; . \tag{124}$$

The points in $\mathfrak{C}'_0$ are classified according to the properties of the curves in $\mathfrak{M}_0 \cap \mathbf{R}_0$ which define them. The intersection of $\mathcal{T}$ with the Reeb cylinder $\tau(\mathcal{R}')$ defines the point $\omega_0 \in \mathfrak{M}_0 \cap \mathbf{R}_0$ with $r(\omega_0) = 2$. The remaining points in the intersection correspond to the intersections with γ_0 or λ_0 curves, and these can be of two types:

(1) The γ_0 or λ_0 curve is an arc. In the case where the forward orbit of points in such a curve hit the entry regions, the curve corresponds to boundary notches in the propeller, one for each entry region.
(2) The γ_0 or λ_0 curve is a closed curve, hence there are two points in $\mathfrak{C}_0$ corresponding to the same curve. In the case where the forward orbit of points in such a curve hit the entry regions, the curve corresponds to interior notches in the propeller, either one or two for each entry region. These closed curves correspond either to notches generating "bubbles" or to intersections of "bubbles" with $\mathbf{R}_0$ as described in Sections 15 and 18.

Let $\mathfrak{C}^1_0 \subset \mathfrak{C}'_0$ be the intersection points corresponding to closed curves in $\mathfrak{M}_0 \cap \mathbf{R}_0$. Define:

$$\mathfrak{C}_0 = \mathfrak{C}'_0 - \mathfrak{C}^1_0 \qquad , \qquad \mathfrak{C} = \overline{\mathfrak{C}_0}. \tag{125}$$

PROPOSITION 19.4. *The set* $\mathfrak{C}$ *is a perfect and totally disconnected subset of* $\mathfrak{C}'$*.*

Proof. Each point in $\mathfrak{C}_0$ is the intersection of $\mathcal{T}$ with a certain γ_0 or λ_0 curve, and thus is defined by the labeling of the endpoints of this curve as in Section 12. Moreover, the symmetry of the Wilson flow implies that each such γ_0 and λ_0 curve in $\mathfrak{M}_0 \cap \mathbf{R}_0$ intersects $\mathcal{T}$. Thus, a sequence of curves whose intersections with $\mathcal{T}$ defines points in $\mathfrak{C}_0$ which converge, also defines a sequence of converging endpoints, whose corresponding limit curve defines a point in $\mathfrak{M} \cap \mathcal{T}$. Thus, $\mathfrak{C} = \overline{\mathfrak{C}_0} \subset \mathfrak{M} \cap \mathcal{T} = \mathfrak{C}'$. Lemma 13.10 implies that each point of $\mathfrak{C}_0$ is a limit point of the set, hence the closure $\mathfrak{C}$ is a perfect set. It is totally disconnected by the results of Section 16. □

REMARK 19.5. *It can also be proved that* $\mathfrak{C}'$ *is a Cantor set, since any* q^γ *or* q^λ *point is the accumulation point of a sequence of* q^γ *and* q^λ *points of lower level.*

The strategy for constructing foliation charts for $\mathfrak{M}$ using the Cantor set $\mathfrak{C}$ is simple in outline, and we next develop. But there is a nuance that arises near points of $\mathfrak{C}$ corresponding to tips of propellers, that requires covering these "singular points" by a separate construction.

Consider $\xi \in \mathfrak{C} - \mathfrak{C}_0$, then there exists $\{x_k \mid k \geq 1\} \subset \mathfrak{C}_0$ with $x_k \to \xi$. By the results of Section 12, each x_k lies on a propeller curve $\gamma_0(i_1, \ell_1; i_2, \ell_2; \cdots ; \ell_n)$ or $\lambda_0(i_1, \ell_1; i_2, \ell_2; \cdots ; \ell_n)$ where the multi-index depends on k. By passing to a subsequence, we can assume that they are all of the same type, either all γ_0 curves, or all λ_0 curves. Each such curve is then defined by the labeling of its endpoints, denoted simply by $p_0^{i_n}(x_k)$ to shorten the notation introduced in Section 13. That is, $p_0^{i_n}(x_k) = p_0(i_0; i_1, \ell_1; i_2, \ell_2; \cdots ; i_{n-1}, \ell_{n-1}; i_n, \ell_n)$ for $i_n = 1, 2$, where $i_0 = 1$ for a γ_0 curve, and $i_0 = 2$ for a λ_0 curve.

We consider the case where we have a sequence of γ_0 curves. The case for a sequence of λ_0 curves is analogous. As $\mathbf{R}_0$ is compact, we can pass to a subsequence, and assume that the lower endpoints $p_0^1(x_k)$ converge to a point $p_0^1(\xi)$ where $z(p_0^1(\xi)) \leq 0$, and similarly $p_0^2(x_k) \to p_0^2(\xi)$ where $z(p_0^2(\xi)) \geq 0$.

The sequence of endpoints $p_0^1(x_k)$ all lie on the $\mathcal{K}$-orbit of the special point ω_1, so each has a well-defined level by Proposition 10.1. If there is a uniform bound on this level, then the limit must be contained in $\mathfrak{M}_0$ contrary to the choice of ξ. Thus, passing to a subsequence yet again, we can assume that the level $n_0(x_k)$ is monotone increasing.

It then follows that the number n of indices of the sequence $\gamma_0(i_1, \ell_1; i_2, \ell_2; \cdots ; i_n, \ell_n)$ must tend to infinity, and by the results of Section 13, the sequence $\{x_k\}$ defines a nested sequence of ellipses in $\mathbf{R}_0$, each ellipse bounded by the union of the associated γ_0 and κ_0 curves. Moreover, the width of these ellipses must tend to zero. It follows that the intersections of the interiors of these nested ellipses define an arc in $\mathbf{R}_0$, denoted by $[p_0^1(\xi), p_0^2(\xi)]$ where the point $\xi = [p_0^1(\xi), p_0^2(\xi)] \cap \{z = 0\}$.

The arc $[p_0^1(\xi), p_0^2(\xi)]$ is the limit of the boundary γ_0 curves of the nested ellipses, as a point set. Each of these boundary γ_0 curves is an embedded curve with uniformly bounded length by Theorem 18.1. Thus, these curves converge to an immersed curve of finite length. That is, in a generic Kuperberg plug, for $\xi \in \mathfrak{C}$ the curve $[p_0^1(\xi), p_0^2(\xi)]$ has uniformly bounded arclength.

We next repeat these arguments for each of four rectangular sections to $\mathfrak{M}$, defined as follows, and the associated Cantor transversals. Introduce the rectangles

$$\mathbf{T}_i = \{\xi = (r, i \cdot \pi/2, z) \mid \ 1 \leq r \leq 3 \ , \ -2 \leq z \leq 2\} \ , \ 1 \leq i \leq 4 \tag{126}$$

so that $\mathbf{R}_0 = \mathbf{T}_2$. We add a fifth rectangle

$$\mathbf{T}_5 = \{\xi = (r, 3\pi/8, z) \mid \ 1 \leq r \leq 3 \ , \ -2 \leq z \leq 2\}.$$

Each of these rectangles is disjoint from both the regions D_i and their insertions $\mathcal{D}_i$ for $i = 1, 2$ by the choices made in Section 3. It is helpful to review the illustrations in Figures 5 and Figure 8. The key property of these sections that we require, is that for any $\mathcal{K}$ orbit segment $[x, y]_{\mathcal{K}}$ with $x, y \in \mathbf{T}_i$, then either the interior segment $(x, y)_{\mathcal{K}}$ intersects the annulus $\mathcal{A}$, or it must intersect one of the other sections $\mathbf{T}_j$ for $j \neq i$.

For each of $1 \leq i \leq 5$, introduce the set $\mathfrak{C}_{0,i} \subset \mathbf{T}_i \cap \mathcal{A} \cap \mathfrak{M}_0$ consisting of the points that do not belong to a bubble of any type, and correspond to arcs in $\mathbf{T}_i \cap \mathfrak{M}_0$. Note that $\mathfrak{C}_{0,2} = \mathfrak{C}_0$. Define $\mathfrak{C}_i$ to be the closure of $\mathfrak{C}_{0,i}$. We again conclude that each $\xi \in \mathfrak{C}_i$ defines an immersed arc $[p_i^1(\xi), p_i^2(\xi)]$, each of whose length admits a uniform upper bound.

For each $1 \leq i \leq 5$, define functions $S_i^{\pm} \colon \mathfrak{C}_i \to [0, \infty)$ such that for $\xi \in \mathfrak{C}_i$

- $S_i^+(\xi)$ is the length of the arc $[\xi, p_i^2(\xi)] \subset [p_i^1(\xi), p_i^2(\xi)]$ containing ξ as the lower endpoint, where $[\xi, p_i^2(\xi)] \subset \{z \geq 0\}$;
- $S_i^-(\xi)$ is the length of the arc $[p_i^1(\xi), \xi] \subset [p_i^1(\xi), p_i^2(\xi)]$ containing ξ as the upper endpoint, where $[p_i^1(\xi), \xi] \subset \{z \leq 0\}$.

Since $\tau^{-1}(p_i^2(\xi))$ and $\tau^{-1}(p_i^1(\xi))$ belong to the same $\mathcal{W}$-orbit, the symmetry of the Ψ_t-flow implies that $S_i^+(\xi) = S_i^-(\xi)$. Let $S_i(\xi) = S_i^+(\xi)$. Then by the above, for each i, the function $\xi \mapsto S_i(\xi)$ admits a uniform upper bound for all $\xi \in \mathfrak{C}_i$. Let $L_i = \sup\{S_i(\xi) \mid \xi \in \mathfrak{C}_i\}$ denote the upper bound of these lengths for $\xi \in \mathfrak{C}_i$.

The function $S_i(\xi)$ is not continuous, but we note that the proof of (122) shows that for $\epsilon > 0$, there exists N_ϵ which is independent of ξ, such that there exists $x \in \mathfrak{M}_0 \cap \mathfrak{C}_i$ for which the curve σ_x containing x has length $|S_i(x) - S_i(\xi)| < \epsilon$ and moreover, the endpoint $p_i^1(x)$ has level $n \leq N_\epsilon$. It follows that the arclength function $S_i \colon \mathfrak{C}_i \to [0, L_i]$ is the uniform limit of step-functions on $\mathfrak{C}_i$ so is a Borel function of ξ.

Define $\mathfrak{C}_i^+ = \{\xi \in \mathfrak{C}_i \mid S_i^+(\xi) > 0\}$. For $\xi \in \mathfrak{C}_i^+$, let $\gamma_\xi(s)$ denote the parametrization of $[p_i^1(\xi), p_i^2(\xi)]$ by arclength, with $\gamma_\xi(0) = \xi$.

Fix $1 \leq i \leq 5$ and consider a point $\xi \in \mathfrak{C}_i$. The proof of Proposition 9.9 carries over to each of the surfaces $\mathbf{T}_i$, so there exists a constant ν_* such that the set $\mathcal{S}_{i,\xi} = \{s \mid \Phi_s(\xi) \in \mathfrak{M} \cap \mathbf{T}_i\}$ is syndetic for the constant ν_*. Moreover, the constant ν_* can be chosen independent of i and ξ. There is a nuance in the estimation of the return time, ν_* which bounds the return time of a point in $\mathbf{T}_i$ to the same transversal. The return point is contained in $\mathfrak{C}_i' = \mathfrak{M} \cap \mathbf{T}_i$ but not necessarily in the subset $\mathfrak{C}_i$. However, Lemma 15.2, Proposition 15.4 and the discussion in Section 18 imply that there exists a uniform constant which is an upper bound on the length of time any orbit spends in a bubble. That is, the time required to flow across each of the internal notches as illustrated in Figures 25 and 52 has a uniform bound. Thus, replacing ν_* with a fixed multiple of itself, we may assume that ν_* is a syndetic constant for $\mathcal{S}_{i,\xi} = \{s \mid \Phi_s(\xi) \in \mathfrak{C}_i\}$ for each $1 \leq i \leq 5$.

Consider the annulus $\mathcal{A} \subset \mathbb{W}$ and its image $\tau(\mathcal{A})$ in $\mathbb{K}$. For each $\theta \in \mathbb{S}^1$ consider the sets

$$\begin{aligned} \mathbf{R}_\theta &= \{\tau(r, \theta, z) \,|\, (r, \theta, z) \in \mathbb{W}',\, 2 \leq r \leq 3,\, -2 \leq z \leq 2\} \\ \mathcal{T}_\theta &= \{\tau(r, \theta, 0) \,|\, 2 \leq r \leq 3\} \end{aligned}$$

with $\mathcal{T}_\theta \subset \mathbf{R}_\theta$. Observe that for those values of θ for which all the points (r, θ, z) are not in $\mathcal{D}_i$ for $i = 1, 2$, $\mathbf{R}_\theta$ is a rectangle in $\mathbb{K}$. On $\mathcal{T}_\theta$ consider the set of points $\mathfrak{C}_\theta' = \mathcal{T}_\theta \cap \mathfrak{M}_0$. This set contains two types of points: those that belong to a closed curve in $\mathbf{R}_\theta \cap \mathfrak{M}_0$ that we denote by $\mathfrak{C}_\theta^1$ and those that belong to an arc in $\mathbf{R}_\theta \cap \mathfrak{M}_0$. Consider the set $\mathfrak{C}_{0,\theta} = \mathfrak{C}_\theta' - \mathfrak{C}_\theta^1$ and its closure $\mathfrak{C}_\theta$. Observe that $\mathfrak{C}_{0,\pi/2} = \mathfrak{C}_0$. Let $\mathcal{A}_\mathfrak{C}$ be the union over θ of these Cantor sets $\mathfrak{C}_\theta$. Observe that $\mathcal{A}_\mathfrak{C}$ contains the intersection of $\tau(\mathcal{A})$ with all the simple propellers in $\mathfrak{M}_0$.

Let $\mathfrak{M}_{\mathfrak{C}_i} \subset \mathfrak{M} \cap \mathbf{T}_i$ be the path components that contain a point in $\mathfrak{C}_i$ for $1 \leq i \leq 5$, and define $W = \mathfrak{M}_{\mathfrak{C}_1} \cup \cdots \cup \mathfrak{M}_{\mathfrak{C}_5} \cup \mathcal{A}_\mathfrak{C}$ be the union of these closed sets in $\mathbb{K}$. For each i and for $x \in \mathfrak{M}_{\mathfrak{C}_i}$, define $T_i^\pm(x)$, which is the forward and backwards "return time" to W for the flow Φ_t:

$$T_i^+(x) = \inf\{s > 0 \mid \Phi_s(x) \in W\} \quad , \quad T_i^-(x) = \sup\{s < 0 \mid \Phi_s(x) \in W\} \ . \tag{127}$$

For $\xi \in \mathfrak{C}_i$ we have that $|T_i^\pm(\gamma_\xi(s))| < \nu_*$ uniformly. The values of these functions are not necessarily continuous in the variables ξ and s. The discontinuities may arise, for example, when the endpoint of the flow segment starting at $\gamma_\xi(s)$ jumps from a section $\mathbf{T}_j$ to the annulus $\mathcal{A}$.

For each $1 \leq i \leq 5$, define the subsets of $\mathfrak{C}_i^+ \times [-L_i, L_i] \times [-\nu_*, \nu_*]$,

$$\begin{aligned} D_{i,1} &= \{(\xi, s, t) \mid \xi \in \mathfrak{C}_i^+ \ ,\ -S_i(\xi) \leq s \leq 0 \ ,\ T_i^-(\gamma_\xi(s)) \leq t \leq T_i^+(\gamma_\xi(s))\} \\ D_{i,2} &= \{(\xi, s, t) \mid \xi \in \mathfrak{C}_i^+ \ ,\ 0 \leq s \leq S_i(\xi) \ ,\ T_i^-(\gamma_\xi(s)) \leq t \leq T_i^+(\gamma_\xi(s))\} \ . \end{aligned}$$

Let $\epsilon_* > 0$ be sufficiently small so that the ϵ_* neighborhood of W in $\mathbb{K}$ is disjoint from the surfaces E_i and S_j for $1 \leq i, j \leq 2$ as defined in (9). Then for each $1 \leq i \leq 5$, also define

$$\begin{aligned} D_{i,1}^* &= \{(\xi, s, t) \mid \xi \in \mathfrak{C}_i^+ \ ,\ -S_i(\xi) \leq s \leq 0 \ ,\ T_i^-(\gamma_\xi(s)) - \epsilon_* \leq t \leq T_i^+(\gamma_\xi(s)) + \epsilon_*\} \\ D_{i,2}^* &= \{(\xi, s, t) \mid \xi \in \mathfrak{C}_i^+ \ ,\ 0 \leq s \leq S_i(\xi) \ ,\ T_i^-(\gamma_\xi(s)) - \epsilon_* \leq t \leq T_i^+(\gamma_\xi(s)) + \epsilon_*\} \ . \end{aligned}$$

Introduce the continuous maps:

$$\begin{aligned} \varphi_{i,1} \colon D_{i,1}^* \to \mathfrak{M} \quad &, \quad \varphi_{i,1}(\xi, s, t) = \Phi_t(\gamma_\xi(s)) \\ \varphi_{i,2} \colon D_{i,2}^* \to \mathfrak{M} \quad &, \quad \varphi_{i,2}(\xi, s, t) = \Phi_t(\gamma_\xi(s)) \ . \end{aligned}$$

PROPOSITION 19.6. *For each $1 \leq i \leq 5$ and $j = 1, 2$, the map $\varphi_{i,j} \colon D_{i,j}^* \to \mathfrak{M}$ is one-to-one. Moreover, we have*

$$\mathfrak{M} = \bigcup_{1 \leq i \leq 4} \left\{\varphi_{i,1}(D_{i,1}^*) \cup \varphi_{i,2}(D_{i,2}^*)\right\} .$$

Proof. Suppose that $(\xi, s, t) \neq (\xi', s', t') \in D^*_{i,j}$ satisfy $\varphi_{i,j}(\xi, s, t) = \varphi_{i,j}(\xi', s', t')$ for some i, j. Let $x = \gamma_\xi(s)$ and $x' = \gamma_{\xi'}(s')$ then $x' = \Phi_{-t'}(\varphi_{i,j}(\xi, s, t)) = \Phi_{-t'}(\Phi_t(x)) = \Phi_{t-t'}(x)$. Assume without loss of generality that $t - t' > 0$. Then there is a $\mathcal{K}$-orbit segment σ from $x \in \mathbf{T}_i$ to $x' \in \mathbf{T}_i$ whose interior intersects at most once W. Let $x_1, x_2, \ldots$ be the transition points in the forward $\mathcal{K}$-orbit of x. Observe that σ must contain at least one transition point.

Assume first that $\sigma \cap \mathcal{A}_\mathfrak{C}$ is empty. By the choices of $\mathbf{T}_i$, we have that if:

(1) $x \in \mathbf{T}_1 \cap \{z < 0\}$ then $[x, x_1]_\mathcal{K}$ intersects $\mathbf{T}_2 \cap \{z < 0\}$.
(2) $x \in \mathbf{T}_2 \cap \{z < 0\}$ then either $[x, x_1]_\mathcal{K}$ intersects $\mathbf{T}_3 \cap \{z < 0\}$ or x_1 is in E_1.
(3) $x \in \mathbf{T}_3 \cap \{z < 0\}$ then $[x, x_1]_\mathcal{K}$ intersects $\mathbf{T}_4 \cap \{z < 0\}$.
(4) $x \in \mathbf{T}_4 \cap \{z < 0\}$ then $[x, x_1]_\mathcal{K}$ intersects $\mathbf{T}_5 \cap \{z < 0\}$.
(5) $x \in \mathbf{T}_5 \cap \{z < 0\}$ then $[x, x_1]_\mathcal{K}$ intersects $\mathbf{T}_1 \cap \{z < 0\}$.
(6) $x \in \mathbf{T}_1 \cap \{z > 0\}$ then $[x, x_1]_\mathcal{K}$ intersects $\mathbf{T}_5 \cap \{z > 0\}$.
(7) $x \in \mathbf{T}_2 \cap \{z > 0\}$ then either $[x, x_1]_\mathcal{K}$ intersects $\mathbf{T}_1 \cap \{z > 0\}$ or x_1 is in E_2.
(8) $x \in \mathbf{T}_3 \cap \{z > 0\}$ then $[x, x_1]_\mathcal{K}$ intersects $\mathbf{T}_2 \cap \{z > 0\}$.
(9) $x \in \mathbf{T}_4 \cap \{z > 0\}$ then either $[x, x_1]_\mathcal{K}$ intersects $\mathbf{T}_3 \cap \{z > 0\}$ or x_1 is in S_2.
(10) $x \in \mathbf{T}_5 \cap \{z > 0\}$ then either $[x, x_1]_\mathcal{K}$ intersects $\mathbf{T}_4 \cap \{z > 0\}$ or x_1 is in S_1.

If σ intersects W only at its endpoints, in cases (1), (3), (4), (5), (6) and (8) we obtain a contradiction. We next analyze the other four possible cases.

(2) Assume that $x \in \mathbf{T}_2 \cap \{z < 0\}$, then $x_1 \in E_1$. From x_1, the orbit segment σ either continues to a point $y_1 \in \mathbf{T}_5$ or it flows to $x_2 \in S_1$ before intersecting W, with $x_1 \equiv x_2$. In the first case, if $y_1 \in \mathfrak{M}_{\mathfrak{C}_5}$ we obtain a contradiction. If not, $r(x_1) > 2$ and σ contains the point $\overline{x}_1 \in S_1$ such that $x_1 \equiv \overline{x}_1$ (this is the case when σ contains a segment of $\mathcal{K}$-orbit in a bubble). Thus there exists $k \geq 2$ such that $x_k \in S_1$ with $x_1 \equiv x_k$. From x_k the segment σ continues and hits $\mathfrak{M}_{\mathfrak{C}_3} \subset \mathbf{T}_3$, giving us a contradiction. Observe that in the second case we obtain the same contradiction with $k = 2$.
(7) If $x \in \mathbf{T}_2 \cap \{z > 0\}$ then $x_1 \in E_2$. From x_1, the orbit segment σ either continues to a point $y_1 \in \mathbf{T}_4$ or it flows to $x_2 \in S_2$ before intersecting W, with $x_1 \equiv x_2$. In the first case, either $y_1 \in \mathfrak{M}_{\mathfrak{C}_4}$ and we obtain a contradiction, or there exists $k \geq 2$ such that $x_k \in S_2$ with $x_1 \equiv x_k$ and $[x_1, x_k]_\mathcal{K} \cap W = \emptyset$. From x_k the segment σ continues and hits $\mathfrak{M}_{\mathfrak{C}_1} \subset \mathbf{T}_1$, giving us a contradiction. Observe that in the second case we obtain the same contradiction.
(9) If $x \in \mathbf{T}_4 \cap \{z > 0\}$ then $x_1 \in S_2$. From x_1, the orbit segment σ continues to a point $y_1 \in \mathbf{T}_1$. Since x_1 is a secondary exit point, $y_1 \in \mathfrak{M}_{\mathfrak{C}_1}$, a contradiction.
(10) If $x \in \mathbf{T}_5 \cap \{z > 0\}$ then $x_1 \in S_1$. From x_1, the orbit segment σ continues to a point $y_1 \in \mathbf{T}_3$. Since x_1 is a secondary exit point, $y_1 \in \mathfrak{M}_{\mathfrak{C}_3}$, a contradiction.

We are left with the case where the interior of σ intersects W, that we separate in two situations, first when the intersection point is in $W - \mathcal{A}_\mathfrak{C}$ and second when it is in $\mathcal{A}_\mathfrak{C}$. In the first situation, concatenating the cases above, we conclude that there is no $\mathcal{K}$-orbit segment with both endpoints in one of transversals and intersecting $W - \mathcal{A}_\mathfrak{C}$.

In the case where $\sigma \cap \mathcal{A}_\mathfrak{C} \neq \emptyset$, the only possibility for such a segment is to flow from x to a transition point x_1. If $[x_1, x_2]_\mathcal{K}$ does not intersects W, then $x_1 \equiv x_2$ and we can replace it with a short cut. Then, $x \in \mathbf{T}_2$ and, by (2) and (7) above, the arc $[x_2, x_3]_\mathcal{K}$ intersects $W - \mathcal{A}_\mathfrak{C}$. Thus the first intersection point of σ with W is either in $\mathbf{T}_1$ or $\mathbf{T}_3$. A contradiction.

Hence, $[x_1, x_2]_\mathcal{K}$ must intersect $\mathcal{A}_\mathfrak{C}$. Let y be the intersection point. If x_1 is a secondary entry point, then $x_1 \equiv x_2$, $x \in \mathbf{T}_2$ and x' is either in $\mathbf{T}_1$ or $\mathbf{T}_3$. If x_1 is a secondary exit point, then $x \in \mathbf{T}_4 \cap \{z > 0\}$ or $x \in \mathbf{T}_5 \cap \{z > 0\}$. In the first case, $x_1 \in S_2$ and thus has z-coordinate positive. Case (9) above implies that its orbit intersects $W - \mathcal{A}_\mathfrak{C}$ before intersecting $\mathcal{A}_\mathfrak{C}$. In the second case, $x_1 \in S_1$ and by assumption its forward orbit intersects $\mathcal{A}_\mathfrak{C}$ before intersecting the transversal $\mathbf{T}_3$. Then it flows in the negative θ-direction to the transversal $\mathbf{T}_2$, and since x_1 is a secondary exit point, the last intersection point belongs to $\mathfrak{M}_{\mathfrak{C}_2}$. The last contradiction we needed.

Thus, the maps $\varphi_{i,j}$ are homeomorphisms. By definition they cover $\mathfrak{M}$. □

20. Entropy of the flow

A celebrated theorem of Katok [23] on the entropy for C^2-flows on compact 3-manifolds implies that the topological entropy of the Kuperberg flow Φ_t is zero. In this section, we give a geometric proof of this conclusion, based on an analysis of the dynamics of the flow Φ_t restricted to the closed invariant set $\mathfrak{M}$. The key idea is to relate the flow entropy to another type of entropy invariant, which is derived from the pseudogroup dynamics for $\mathcal{G}_K$ acting on the rectangle $\mathbf{R}_0$.

We first prove, in Proposition 20.9, that the entropy of the flow vanishes if the entropy of the return map $\widehat{\Phi}$ vanishes. Then in Proposition 20.13, we relate the entropy of $\widehat{\Phi}$ to the entropy of the pseudo⋆group $\mathcal{G}_K^*$, proving that they are proportional. Finally, in Theorem 20.14, we show that the entropy $h_{GLW}(\mathcal{G}_K^*|\mathfrak{M}_{\mathbf{R}_0})$ of $\mathcal{G}_K^*$ vanishes. The study of the various pseudo⋆group entropies associated to the flow Φ_t reveals the geometrical principles behind the vanishing of its entropy, and provides further insights into the dynamics of this flow.

We define the entropy of the flow Φ_t using a variation of the Bowen formulation of topological entropy [6, 49] for a flow on a compact metric space (X, d_X). The definition we adopt is symmetric in the role of the time variable t. Two points $p, q \in X$ are said to be (φ_t, T, ϵ)-*separated* if

$$d_X(\varphi_t(p), \varphi_t(q)) > \epsilon \quad \text{for some} \quad -T \leq t \leq T \ .$$

A set $E \subset X$ is (φ_t, T, ϵ)-*separated* if all pairs of distinct points in E are (φ_t, T, ϵ)-separated. Let $s(\varphi_t, T, \epsilon)$ be the maximal cardinality of a (φ_t, T, ϵ)-separated set in X. Then the topological entropy is defined by

$$h_{top}(\varphi_t) = \frac{1}{2} \cdot \lim_{\epsilon \to 0} \left\{ \limsup_{T \to \infty} \frac{1}{T} \log(s(\varphi_t, T, \epsilon)) \right\} . \tag{128}$$

Moreover, for a compact space X, the entropy $h_{top}(\varphi_t)$ is independent of the choice of metric d_X.

A relative form of the topological entropy for a flow φ_t can be defined for any subset $Y \subset X$, by requiring that the collection of distinct (φ_t, T, ϵ)-separated points used in the definition (128) be contained in Y. The restricted topological entropy $h_{top}(\varphi_t|Y)$ is bounded above by $h_{top}(\varphi_t)$.

Katok proved in [23, Corollary 4.4] that for a C^2-diffeomorphism of a compact surface, or for a C^2-flow on a compact 3-manifold, its topological entropy is bounded above by the exponent of the rate of growth of its periodic orbits. In particular, Katok's result implies:

THEOREM 20.1 (Katok 1980)**.** *Let $\varphi_t \colon M \to M$ be a C^2-flow on a compact 3-manifold. Suppose that φ_t has no periodic orbits, then $h_{top}(\varphi_t) = 0$.*

Suppose that φ_t is an aperiodic flow obtained by inserting the Kuperberg flow Φ_t on $\mathbb{K}$ into a flow box for some flow on a compact 3-manifold. Then $h_{top}(\varphi_t) = 0$ by Theorem 20.1, and thus we have $h_{top}(\varphi_t|\mathfrak{M}) = 0$ for the flow φ_t restricted to the invariant set $\mathfrak{M}$. By construction, the flows φ_t and Φ_t agree on $\mathfrak{M}$, so that $h_{top}(\Phi_t|\mathfrak{M}) = h_{top}(\varphi_t|\mathfrak{M}) = 0$. That is, the topological entropy vanishes for the restriction of the flow Φ_t to the space $\mathfrak{M}$ with the induced metric. In this section, we give a proof that $h_{top}(\Phi_t|\mathfrak{M}) = 0$ based on the dynamics of the restricted flow $\Phi_t \colon \mathfrak{M} \to \mathfrak{M}$ and the geometry of the invariant set $\mathfrak{M}$.

The idea of our approach to the calculation of $h_{top}(\Phi_t|\mathfrak{M})$, is to consider the return map $\widehat{\Phi}$ on the rectangle $\mathbf{R}_0$, and relate the entropy of the flow Φ_t restricted to $\mathfrak{M}$ with the entropy $h_{top}(\widehat{\Phi}|\mathfrak{M}_{\mathbf{R}_0})$ for $\widehat{\Phi}$ restricted to its invariant set $\mathfrak{M}_{\mathbf{R}_0} = \mathfrak{M} \cap \mathbf{R}_0$. It is standard to relate the entropy of the flow with the entropy of an induced return map to a section to the flow, assuming that the flow is everywhere transverse to the section. However, the flow Φ_t is not everywhere transverse to $\mathbf{R}_0$ as it is tangent to $\mathbf{R}_0$ along its center line $\mathcal{T} = \{z = 0\} \cap \mathbf{R}_0$. As discussed below, these tangencies result in discontinuities for the induced map $\widehat{\Phi}$, which make the relationship between $h_{top}(\Phi_t|\mathfrak{M})$ and the entropy $h_{top}(\widehat{\Phi}|\mathfrak{M}_{\mathbf{R}_0})$ more subtle. We subsequently relate

the entropy $h_{top}(\widehat{\Phi}|\mathfrak{M}_{\mathbf{R}_0})$ with the entropy $h_{GLW}(\mathcal{G}_K^*|\mathfrak{M}_{\mathbf{R}_0})$ for the pseudo$\star$group $\mathcal{G}_K^*$ defined in Definition 9.8, and then show that $h_{GLW}(\mathcal{G}_K^*|\mathfrak{M}_{\mathbf{R}_0}) = 0$.

We first recall the definition of entropy for pseudo$\star$groups as introduced by Ghys, Langevin and Walzcak in [16, Section 2]. Let (X, d_X) be a compact metric space, and $\mathcal{G}_X^{(1)} = \{\varphi_0 = Id, \varphi_1, \varphi_1^{-1}, \ldots, \varphi_k, \varphi_k^{-1}\}$ be a set of local homeomorphisms of X, with their inverses. That is, for each $1 \leq i \leq k$ there are open sets $U_i, V_i \subset X$ such that $\varphi_i \colon U_i \to V_i$ is a homeomorphism. We require that each map φ_i admits an extension to a homeomorphism $\overline{\varphi}_i$ of an open neighborhood of the closure $\overline{U}_i$ of the domain in X. Let $\mathcal{G}_X$ denote the pseudogroup generated by the collection of maps $\mathcal{G}_X^{(1)}$, so that the axioms of Definition 9.3 are satisfied. Let $\mathcal{G}_X^* \subset \mathcal{G}_X$ denote the pseudo$\star$group generated by the compositions of maps in $\mathcal{G}_X^{(1)}$, so that $\mathcal{G}_X$ satisfies conditions (1) to (4) of Definition 9.3, but not necessarily the condition (5). Let $\mathcal{G}_X^{(n)} \subset \mathcal{G}_X^*$ be the collection of maps defined by the restrictions of compositions of at most n elements of $\mathcal{G}_X^{(1)}$.

For $\epsilon > 0$, say that $x, y \in X$ are $(\mathcal{G}_X^*, n, \epsilon)$-*separated* if there exists $\varphi \in \mathcal{G}_X^{(n)}$ such that x, y are in the domain of φ and $d_X(\varphi(x), \varphi(y)) > \epsilon$. In particular, if the identity map is the only element of $\mathcal{G}_X^{(n)}$ which contains both x and y in its domain, then they are $(\mathcal{G}_X^*, n, \epsilon)$-separated if and only if $d_X(x, y) > \epsilon$.

A finite set $E \subset X$ is said to be $(\mathcal{G}_X^*, n, \epsilon)$-*separated* if each distinct pair $x, y \in E$ is $(\mathcal{G}_X^*, n, \epsilon)$-separated. Let $s(\mathcal{G}_X^*, n, \epsilon)$ be the maximal cardinality of a $(\mathcal{G}_X^*, n, \epsilon)$-separated subset of X.

Define the *entropy* of $\mathcal{G}_X^*$ by:

$$h_{GLW}(\mathcal{G}_X^*) \;=\; \lim_{\epsilon \to 0} \left\{ \limsup_{n \to \infty} \frac{1}{n} \ln(s(\mathcal{G}_X^*, n, \epsilon)) \right\}. \tag{129}$$

The property $0 < h_{GLW}(\mathcal{G}_X^*) < \infty$ is independent of the choice of metric on X. Note that the denominator in the expression (129) is the word length n. Thus, $h_{GLW}(\mathcal{G}_X^*)$ differs from other definitions of entropy for group actions which scale by volume growth, rather than length.

A key observation in [16] is that if the generators $\mathcal{G}_X^{(1)}$ are the restrictions of C^1-diffeomorphisms defined on the compact closures of open subsets of a manifold M, then $h_{GLW}(\mathcal{G}_X^*) < \infty$. A discussion of some of the dynamical implications of $h_{GLW}(\mathcal{G}_X^*) > 0$ for C^1-pseudogroups is given in [7, 16, 20, 48].

Given a subset $Y \subset X$, we can restrict consideration to subsets $E \subset Y$ which are $(\mathcal{G}_X^*, n, \epsilon)$-separated. Let $s(\mathcal{G}_X^*, Y, n, \epsilon)$ be the maximal cardinality of such an $(\mathcal{G}_X^*, n, \epsilon)$-separated subset of Y. Define the restricted entropy by

$$h_{GLW}(\mathcal{G}_X^*|Y) \;=\; \lim_{\epsilon \to 0} \left\{ \limsup_{n \to \infty} \frac{1}{n} \ln(s(\mathcal{G}_X^*, Y, n, \epsilon)) \right\} \;\leq\; h_{GLW}(\mathcal{G}_X^*)\ . \tag{130}$$

Before considering the entropy invariants associated to the return map $\widehat{\Phi}$, we consider the points of *discontinuity* for its powers $\widehat{\Phi}^n$, and use this to give a description of the domains of continuity of the maps $\widehat{\Phi}^n$. We restrict to the region $\mathbf{R}_0 \cap \{r \geq 2\}$ which contains the set $\mathfrak{M}_{\mathbf{R}_0}$. In Section 9, the continuity properties for the induced return map $\widehat{\Psi}$ of the Wilson flow were analyzed, which resulted in the description of its domains of continuity in (30). The analysis of the powers of the map $\widehat{\Phi}$ extends this analysis.

Recall that by Condition (K3) in Section 3, the compact annular region $\mathcal{A}(2) = \{(r, \theta, 0) \mid r \geq 2\} \subset \mathcal{A}$ is disjoint from the images of the insertions σ_i for $i = 1, 2$, thus the vector fields $\mathcal{W}$ and $\mathcal{K}$ agree on an open neighborhood of $\mathcal{A}(2)$ and so the flows Ψ_t and Φ_t agree near $\mathcal{A}(2)$ for t near to 0.

Consider a point $\xi_0 \in Dom(\widehat{\Phi}) \cap \{r \geq 2\}$ with $\xi_1 = \widehat{\Phi}(\xi_0)$. Then there exists a $\mathcal{K}$-orbit segment $[\xi_0, \xi_1]_{\mathcal{K}}$ which intersects $\mathbf{R}_0$ only in its endpoints. If the $\mathcal{K}$-flow $\Phi_t(\xi_0)$ intersects $\mathbf{R}_0$ transversally at ξ_1, then there is an open neighborhood in $\mathbf{R}_0$ of ξ_0 consisting of points whose flow is also transverse to $\mathbf{R}_0$ near ξ_1, and thus $\widehat{\Phi}$ is continuous at ξ_0. On the other hand, if the $\mathcal{K}$-flow $\Phi_t(\xi_0)$ intersects $\mathbf{R}_0$ tangentially at ξ_1, then in every open neighborhood of ξ_0 there is some point whose flow does not intersects $\mathbf{R}_0$ near ξ_1, and the map $\widehat{\Phi}$ will be discontinuous at ξ_0. Thus, ξ_0 is a point of discontinuity for $\widehat{\Phi}$ precisely when it is contained in the inverse

image under $\widehat{\Phi}$ of the center line $\mathcal{T} = \{x \in \mathbf{R}_0 \mid z(x) = 0\}$. That is, the set of discontinuities for $\widehat{\Phi}$ is the set $\widehat{\Phi}^{-1}(\mathcal{T})$. Similarly, the set of discontinuities for the inverse map $\widehat{\Phi}^{-1}$ is the set $\widehat{\Phi}(\mathcal{T})$.

These remarks for $\widehat{\Phi}$ generalize to its powers as follows. Let $n > 1$ and $\xi_0 \in Dom(\widehat{\Phi}^n)$, then set $\xi_\ell = \widehat{\Phi}^\ell(\xi_0)$ for $1 \leq \ell \leq n$. If the $\mathcal{K}$-orbit segment $[\xi_0, \xi_n]_{\mathcal{K}}$ intersects $\mathbf{R}_0$ transversally at each point ξ_ℓ then there is an open neighborhood of ξ_0 in $\mathbf{R}_0$ consisting of points whose flow is also transverse to $\mathbf{R}_0$, and thus $\widehat{\Phi}^n$ is continuous at ξ_0. On the other hand, if the $\mathcal{K}$-orbit segment $[\xi_0, \xi_n]_{\mathcal{K}}$ intersects $\mathbf{R}_0$ tangentially at some point ξ_ℓ, that is $\xi_\ell \in \mathcal{T} \subset \mathbf{R}_0$, then in every open neighborhood of ξ_0 there is some point whose flow does not intersects $\mathbf{R}_0$ near ξ_ℓ, and thus ξ_0 is a point of discontinuity for $\widehat{\Phi}^n$. For each integer ℓ, introduce the subset of $Dom(\widehat{\Phi}^\ell)$,

$$\mathcal{L}_\ell = \widehat{\Phi}^{-\ell}(\mathcal{T}) = \widehat{\Phi}^{-\ell}(\mathcal{T} \cap Dom(\widehat{\Phi}^{-\ell})) \ . \tag{131}$$

The above discussion implies that for $n \geq 1$, $\xi \in Dom(\widehat{\Phi}^n)$ is a point of discontinuity for $\widehat{\Phi}^n$ precisely when there exists $1 \leq \ell \leq n$ such that $\xi \in \mathcal{L}_\ell$. The analogous statement also holds for $\xi \in Dom(\widehat{\Phi}^{-n})$ with $n > 0$ and $-n \leq \ell < 0$. For $n \geq 1$, define

$$D^{(n)}(\widehat{\Phi}) = \bigcap_{-n \leq \ell \leq n} \left\{ Dom(\widehat{\Phi}^\ell) - \mathcal{L}_\ell \right\} \ \cap \ \{r \geq 2\} \ . \tag{132}$$

Let $U \subset D^{(n)}(\widehat{\Phi})$ be a connected component, then $\widehat{\Phi}^\ell | U$ is continuous for all $-n \leq \ell \leq n$. Thus, we are interested in the finite collection of domains of continuity,

$$\mathcal{D}^{(n)}_{\mathfrak{M}}(\widehat{\Phi}) = \{U \subset D^{(n)}(\widehat{\Phi}) \mid U \text{ is a connected component of } D^{(n)}(\widehat{\Phi}) \text{ such that } U \cap \mathfrak{M}_{\mathbf{R}_0} \neq \emptyset\}. \tag{133}$$

Corollary 9.14 implies that $\mathfrak{M}_{\mathbf{R}_0} \subset Dom(\widehat{\Phi}^n) \cap Dom(\widehat{\Phi}^{-n})$ for all n. For $U \in \mathcal{D}^{(n)}_{\mathfrak{M}}(\widehat{\Phi})$, let $\overline{U} \subset \mathbf{R}_0$ denote its closure, then we have:

LEMMA 20.2. *For each $n \geq 1$, $\mathfrak{M}_{\mathbf{R}_0} \subset \bigcup \{\overline{U} \mid U \in \mathcal{D}^{(n)}_{\mathfrak{M}}(\widehat{\Phi})\}$.*

The collection $\mathcal{D}^{(n)}_{\mathfrak{M}}(\widehat{\Phi})$ thus gives a decomposition of $\widehat{\Phi}$ into sets on which the function has nice regularity properties. The number of sets in these partitions is an important property of the flow Φ_t.

DEFINITION 20.3. *The* complexity function *of $\widehat{\Phi}$ is defined by $C_\Phi(n) = \#\mathcal{D}^{(n)}_{\mathfrak{M}}(\widehat{\Phi})$. That is, for $n \geq 1$, $C_\Phi(n)$ is the number of connected components of $D^{(n)}(\widehat{\Phi})$.*

We develop a geometric interpretation of the sets $\mathcal{L}_\ell$ and $U \in \mathcal{D}^{(n)}_{\mathfrak{M}}(\widehat{\Phi})$, in terms of the flow Φ_t restricted to the space $\mathfrak{M}_0$. We use this to relate the function $C_\Phi(n)$ to the function $\#\mathcal{M}(n)$, where the collection $\mathcal{M}(n) \subset \mathcal{G}^{(n)}_K$ was defined in Proposition 14.3.

We require some preliminary observations. We first obtain an estimate relating the exponent ℓ and the time T, for the maps $\widehat{\Phi}^\ell$ and the flow Φ_T restricted to $\mathfrak{M}$. It is straightforward to obtain such an estimate for a complete transversal to the flow Φ_t with return times bounded away from zero, but the estimate is more subtle for the return map $\widehat{\Phi}$.

LEMMA 20.4. *There exist $L_\Phi > 0$ so that for $x \in \mathfrak{M}_{\mathbf{R}_0}$, and $T > 0$ such that $\Phi_T(x) \in \mathfrak{M}_{\mathbf{R}_0}$, and $n_x > 0$ for which $\widehat{\Phi}^{2n_x}(x) = \Phi_T(x)$, then $0 < L_\Phi \, n_x \leq T$.*

Proof. We use the properties of the return map $\widehat{\Phi}$ established in Section 9.

Let $x \in \mathfrak{M}_{\mathbf{R}_0}$ with $r(x) \geq 2$, $z(x) < 0$ and $z(\widehat{\Phi}(x)) < 0$. If the $\mathcal{K}$-orbit of x does not intersect an insertion region $\mathcal{L}_i^-$ it must complete a revolution around the core cylinder $\mathcal{C}$ before returning to $\mathbf{R}_0$, hence the segment $[x, \widehat{\Phi}(x)]_{\mathcal{K}}$ has length bounded below by $L'_\Phi = 4\pi$. If the $\mathcal{K}$-orbit of x does intersect an insertion region $\mathcal{L}_i^-$ then the segment $[x, \widehat{\Phi}(x)]_{\mathcal{K}}$ has length at least L''_Φ for some $L''_\Phi > 0$. Let $L_\Phi = \min\{L'_\Phi, L''_\Phi\}$.

In the case where $x \in \mathfrak{M}_{\mathbf{R}_0}$ with $z(x) > 0$ and $z(\widehat{\Phi}(x)) > 0$, then the segment $[x, \widehat{\Phi}(x)]_{\mathcal{K}}$ traverses $\mathbb{K}$ in the clockwise direction, but is otherwise analogous to the case above. We assume that the estimates L'_Φ and L''_Φ also apply in this case.

In the case where $x \in \mathfrak{M}_{\mathbf{R}_0}$ with $z(x) \leq 0$ and $z(\widehat{\Phi}(x)) \geq 0$, then the flow $\Phi_t(x)$ crosses the annulus $\{z = 0\}$. In particular, $\widehat{\Phi}(x) = \psi(x)$ for the map ψ of the pseudogroup $\mathcal{G}_K$. Recall that the action of ψ was described in Lemma 13.6, and we observe that the length of the segment $[x, \widehat{\Phi}(x)]_{\mathcal{K}}$ need not have a positive lower bound. But this segment must be preceded and followed by a segment of the above two types. It follows that the composition $\widehat{\Phi} \circ \widehat{\Phi}$ applied to $x \in \mathfrak{M}_{\mathbf{R}_0}$ is realized by a $\mathcal{K}$-orbit segment of length at least L_Φ, for any $x \in \mathfrak{M}_{\mathbf{R}_0}$.

It follows that $[x, \widehat{\Phi}^{2n_x}(x)]_{\mathcal{K}}$ has length at least $L_\Phi \cdot n_x$. □

Recall that by Propositions 15.1 and 15.4, the constant $r_b > 2$, introduced in Definition (78), provides a lower bound for the radius of points in bubbles of the first type. Also, Lemma 18.7 provides a constant $r_B > 2$ for which bubbles of the second type do not arise. Finally, r_e is the exceptional radius defined in (33). Let $r_u = \min\{r_b, r_B, r_e\}$, so that $2 < r_u \leq r_e$. Observe that the techniques in the proof of Proposition 9.16 apply for any value of the radius upper bound which is less than r_e. In particular, we conclude the following:

PROPOSITION 20.5. *Let $\xi \in \mathbf{R}_0$ have infinite orbit for the flow Φ_t with $r(\xi) < r_u$ and $\rho_\xi(t) \geq 2$ for all t. Then the set $\mathcal{S}^*(\xi, r_u) = \{s \mid \Phi_s(\xi) \in \mathcal{G}_K^*(\xi) \subset \mathbf{R}_0 \ , \ r(\Phi_s(\xi)) < r_u\}$ is syndetic in $\mathbb{R}$ for a constant ν_u^* which is independent of ξ.*

COROLLARY 20.6. *Let $\xi \in \mathfrak{M}_{\mathbf{R}_0} = \mathfrak{M} \cap \mathbf{R}_0$. Then $\mathcal{S}^*(\xi, r_u) = \{s \mid \Phi_s(\xi) \in \mathcal{G}_K^*(\xi) \subset \mathbf{R}_0 \ , \ r(\Phi_s(\xi)) < r_u\}$ is syndetic in $\mathbb{R}$ for the constant ν_u^*.*

Proof. Theorem 8.2 implies that the Φ_t-orbit of ξ contains points arbitrarily close to the special point $\omega_1 \in \mathbf{R}_0$, and thus there exists t such that with $2 \leq r(\Phi_t(\xi)) < r_u$. The claim then follows from Proposition 20.5. □

COROLLARY 20.7. *Let $M_u > 0$ be the greatest integer with $M_u \leq 2\nu_u^*$. For each $x \in \mathfrak{M}_{\mathbf{R}_0}$ there exists $0 < \ell'_x, \ell''_x \leq M_u$ such that $r(\widehat{\Phi}^{\ell'_x}(x)) < r_u$ and $r(\widehat{\Phi}^{-\ell''_x}(x)) < r_u$.*

Proof. This follows from Lemma 20.4 and Corollary 20.6. □

We next characterize the discontinuities of $\widehat{\Phi}^n$ on $\overline{U}$, for $U \in \mathcal{D}^{(n)}_{\mathfrak{M}}(\widehat{\Phi})$. We first reduce this problem to a "standard form". Recall from (64) that the interval $I_0 = \mathcal{R} \cap \mathbf{R}_0$ is the closed vertical segment whose Φ_t-flow generates $\mathfrak{M}_0$, and the intersection of $\mathfrak{M}_0$ with $\mathbf{R}_0$ yields the connected components of $\mathfrak{M}_{\mathbf{R}_0}$. Also, the Φ_t-flows of the closed vertical segments $N_0 = J_0 \cup I_0 \subset \mathbf{R}_0$ and $M_0 = I_0 \cup K_0 \subset \mathbf{R}_0$ generate the double propellers discussed in Section 13. The Φ_t-flows of N_0 and J_0 generate families of nested double propellers, whose intersections with $\mathbf{R}_0$ are the topological circles illustrated in Figures 31, 32 and 40. By the nesting properties of the double propellers, the discontinuities for $\widehat{\Phi}^n$ restricted to $\mathfrak{M}_{\mathbf{R}_0}$ are determined by those for $\widehat{\Phi}^n$ restricted to I_0.

Suppose that $x \in I_0$ is a point of continuity for $\widehat{\Phi}^n$ with $n \geq 1$, so the restriction $\widehat{\Phi}^n$ to I_0 is continuous in an open neighborhood of x. Let $x', x'' \in I_0$ be such that the open connected segment $(x', x'') \subset I_0$ is the maximal open subset of I_0 containing x such that the restriction $\widehat{\Phi}^n|(x', x'')$ is continuous. Set $\mathcal{J}(x, 0) = (x', x'')$. Then for each $z \in \mathcal{J}(x, 0)$ and $w = \widehat{\Phi}^n(z)$, the $\mathcal{K}$-orbit segment $[z, w]_{\mathcal{K}}$ intersects $\mathbf{R}_0$ transversally, while for the endpoints $\{x', x''\}$, the $\mathcal{K}$-orbit segments $[x', \widehat{\Phi}^n(x')]_{\mathcal{K}}$ and $[x'', \widehat{\Phi}^n(x'')]_{\mathcal{K}}$ must each contain a point of tangency with $\mathcal{T}$. The collection of such points of tangency for the flow Φ_t partition I_0 into maximal subintervals on which the restriction of $\widehat{\Phi}^n$ is continuous.

We develop an estimate on the number of intervals of continuity for $\widehat{\Phi}^n$ in I_0, where we consider the case $n > 0$ first. Let $x \in I_0$ be a point of continuity. As $r(x) = 2$, by Corollary 20.7, there exists an infinite sequence $\{0 < \ell_1 < \ell_2 < \cdots\}$ with $(\ell_{i+1} - \ell_i) < M_u$ for all $i \geq 1$, such that for $x_i = \widehat{\Phi}^{\ell_i}(x)$ we have $r(x_i) < r_u$. Set $\mathcal{I}(x, 0) = I_0$, and for $i > 0$ let $\mathcal{I}(x, i) \subset \mathfrak{M}_0 \cap \mathbf{R}_0$ denote the maximal connected component containing x_i. Then $\mathcal{I}(x, i)$ is a simple arc by the choice of r_u. In particular, the endpoints of $\mathcal{I}(x, i)$ are contained in the boundary of $\mathfrak{M}_0$. Let $p_0^1(\mathcal{I}(x, i))$ denote the endpoint of $\mathcal{I}(x, i)$ in the region $\{z < 0\}$, and $p_0^2(\mathcal{I}(x, i))$ denote the endpoint of $\mathcal{I}(x, i)$ in the region $\{z > 0\}$. In particular, $p_0^1(\mathcal{I}(x, 0)) = \omega_1$ and $p_0^2(\mathcal{I}(x, 0)) = \omega_2$ are the special points defined in (27).

For $i > 0$, denote $\mathcal{J}(x,i) = \widehat{\Phi}^{\ell_i}(\mathcal{J}(x,0)) \subset \mathcal{I}(x,i)$. Then $\mathcal{J}(x,i)$ is an open subinterval, disjoint from the center line $\mathcal{T}$. For each $i \geq 0$, if $\mathcal{J}(x,i)$ lies below the line $\mathcal{T}$, let $\zeta_i = p_0^1(\mathcal{I}(x,i)) \in \mathbf{R}_0$ denote the lower endpoint of the interval $\mathcal{I}(x,i)$. If $\mathcal{J}(x,i)$ lies above the line $\mathcal{T}$, then $\zeta_i = p_0^2(\mathcal{I}(x,i)) \in \mathbf{R}_0$ denotes the upper endpoint of the interval $\mathcal{I}(x,\ell)$. Then Proposition 20.5 implies that for each $i \geq 1$ and $n_i = \ell_i - \ell_{i-1}$ the restriction

$$\widehat{\Phi}^{n_i} \colon \mathcal{J}(x,i-1) \to \mathcal{J}(x,i) \tag{134}$$

corresponds to a map $\varphi(x,i) \in \mathcal{G}_K^{(n_i)}$ which maps ζ_{i-1} to ζ_i. Let $\Upsilon(x,i) = \varphi(x,i) \circ \cdots \circ \varphi(x,2) \circ \varphi(x,1) \in \mathcal{G}_K^{(\ell_i)}$.

We next give a geometric interpretation to the maps in $\mathcal{G}_K^*$ defined by the actions (134), in terms of the action of $\mathcal{G}_K^*$ on $\mathbf{T}_\Phi$ defined in Section 14.

The intersection $\mathfrak{M}_0 \cap \mathbf{R}_0$ consists of simple arcs arising from the intersections with propellers, as discussed in Section 12, and double arcs or ellipses which arise from the intersection of $\mathbf{R}_0$ with bubbles in $\mathfrak{M}_0$ as discussed in Section 15. The simple arcs in the intersection of $\mathfrak{M}_0 \cap \mathbf{R}_0$ correspond to transverse line segments to the propellers, as illustrated in Figure 36. The double arcs resulting from the intersections with bubbles are illustrated in Figure 41, but for simplicity are not pictured in Figure 36. In particular, each arc $\mathcal{I}(x,i) \subset \mathfrak{M}_0 \cap \mathbf{R}_0$ is an arc transverse to the flow Φ_t in $\mathfrak{M}_0$.

For each (simple) propeller P_γ or P_λ attached in the level decomposition of $\mathfrak{M}_0$, as described in Section 11, the intersections $P_\gamma \cap \mathcal{A}$ and $P_\lambda \cap \mathcal{A}$ form the center line segments of the propeller, as illustrated in Figure 36. The union of all these lines form the subset $\mathbf{T}''_\Phi \subset \mathbf{T}'_\Phi = \mathfrak{M}_0 \cap \mathcal{A}$, as defined in Section 14. The intersections of $\mathbf{T}''_\Phi$ with $\mathcal{T} = \mathbf{R}_0 \cap \mathcal{A}$ are the vertices in the set $\mathbf{T}''_\Phi$, as illustrated in Figure 36.

For each $i \geq 1$, the map $\varphi(x,i)$ induces a map $\overline{\varphi(x,i)}$ from the vertex of $\mathbf{T}_\Phi$ defined by $\mathcal{I}(x,i-1) \cap \mathcal{T}$ to the vertex defined by $\mathcal{I}(x,i) \cap \mathcal{T}$. Thus the map $\Upsilon(x,i) \colon \mathcal{J}(x,0) \to \mathcal{J}(x,i)$ maps an open set in the simple arc I_0 to an open set in the simple arc $\mathcal{I}(x,i)$. We have $\ell_i = n_1 + \cdots + n_i$ hence $\Upsilon(x,i) = \widehat{\Phi}^{\ell_i} | \mathcal{J}(x,0)$, so that $\mathcal{J}(x,0)$ is contained in the domain of $\widehat{\Phi}^{\ell_i} | I_0$.

We return to the problem of estimating the number of domains of continuity for $\widehat{\Phi}^n | I_0$. Let $x \in I_0$ be a point of continuity, let the indices ℓ_i be defined as above, then let $i_n > 0$ be the least index i such that $\ell_{i_n} \geq n$. Note that $i_n \leq n$, and Corollary 20.6 implies that $\ell_{i_n} \leq n + M_u$.

By Proposition 14.3, $\Upsilon(x,i_n)$ can be written in normal form $\Upsilon(x,i_n) = \varphi^+ \circ \varphi^- \in \mathcal{G}_K^{(\ell_{i_n})}$, where appropriate subwords in $\Upsilon(x,i_n)$ are replaced by shortcuts, or powers of the generator ψ. The interval $\mathcal{I}(x,i_n)$ is thus defined by the word $\varphi^+ \circ \varphi^-$. Proposition 14.5 implies the number of normal forms possible for word length ℓ_{i_n} is bounded by $\#\mathcal{M}(\ell_{i_n}) \leq \#\mathcal{M}(n + M_u)$. By Corollary 14.6, the function $\#\mathcal{M}(n + M_u)$ has subexponential growth as a function of n. It follows that the total number of simple arcs in $\mathfrak{M}_0 \cap \mathbf{R}_0$ which are in the images of the map $\widehat{\Phi}^n | I_0$ is bounded above by $\#\mathcal{M}(n + M_u)$.

Let $x \in I_0$ be a point of continuity, and continuing the notation as above, for $y = \widehat{\Phi}^n(x)$, the $\mathcal{K}$-orbit segment $[x,y]_\mathcal{K}$ is transverse to $\mathbf{R}_0$ at every point of intersection, and the orbit contains a point in each of the sequence of simple arcs $\{\mathcal{I}(x,i) \mid 0 \leq i \leq i_n\}$.

By the choice of the sequence $\{\ell_i\}$, for each $1 \leq i \leq i_n$, the forward $\mathcal{K}$-flow in $\mathfrak{M}_0$ of the points in the interval $\mathcal{J}(x,i-1)$ to the interval $\mathcal{J}(x,i)$ has length at most ν_u^*. Therefore, there is a uniform upper bound M'_u on the number of points $\xi \in \mathcal{J}(x,i-1)$ for which the orbit segment $[\xi, \widehat{\Phi}^{n_i}(\xi)]_\mathcal{K}$ is tangent to $\mathcal{T}$.

Recall that $\{x', x''\} \in \mathcal{I}(x,0)$ are the boundary points of the interval $\mathcal{J}(x,0) \subset \mathcal{I}(x,0)$, and the $\mathcal{K}$-orbit segments $[x', \widehat{\Phi}^n(x')]_\mathcal{K}$ and $[x'', \widehat{\Phi}^n(x'')]_\mathcal{K}$ each contains a point of tangency with $\mathcal{T}$, which must be one of the points of tangency for the Φ_t-flow between $\mathcal{J}(x,i-1)$ and $\mathcal{J}(x,i)$ for some $1 \leq i \leq i_n$. Thus, the number of possible points of tangency with $\mathbf{R}_0$ which can define the lower boundary point x' for $\mathcal{J}(x,0)$ has an upper bound estimate $i_n \cdot M'_u \leq n \cdot M'_u$, and similarly for the upper boundary x''.

Thus, if $\mathcal{J} \subset I_0$ is a maximal domain of continuity for $\widehat{\Phi}^n | I_0$, then there exists a connected component $\mathcal{I}(U,n) \subset \mathfrak{M}_0 \cap \mathbf{R}_0$ for which $\widehat{\Phi}^n(\mathcal{J}) \subset \mathcal{I}(U,n)$. The number of possible such domains is bounded above

by $\#\mathcal{M}(n + M_u)$. Then the number of maximal connected intervals $\mathcal{J} \subset I_0$ for which $\widehat{\Phi}^n(\mathcal{J}) \subset \mathcal{I}(U, n)$ is bounded above by the number of possible endpoints for the domains $\mathcal{J}$, which is bounded above by $(n \cdot M'_u)^2$. It follows that the number of domains of continuity for $\widehat{\Phi}^n$ restricted to I_0 has subexponential growth.

Similar considerations apply to the analysis of $\widehat{\Phi}^{-n}|I_0$, so that the number of domains of continuity for the collection of maps $\{\widehat{\Phi}^\ell|I_0 \mid -n \leq \ell \leq n\}$ is a function of subexponential growth in n. We thus obtain:

PROPOSITION 20.8. *The function $C_\Phi(n)$ has subexponential growth for a generic Kuperberg flow Φ_t.*

We now return to the definition and calculation of the entropy invariants associated with $\widehat{\Phi}$. Recall from Section 9 that $\mathcal{G}_K$ is the pseudogroup generated by $\widehat{\Phi}$ acting on $X = \mathbf{R}_0$.

Let $V_+ = \{x \in Dom(\widehat{\Phi}) \mid z(x) > 0\}$, let V_- be the region of $Dom(\widehat{\Phi})$ which lies below the curve $\mathcal{L}_1$ and let V_0 be the region between V_- and V_+. Then set

$$\widehat{\Phi}_- \equiv \widehat{\Phi}|V_- \quad , \quad \widehat{\Phi}_0 \equiv \widehat{\Phi}|V_0 \quad , \quad \widehat{\Phi}_+ = \widehat{\Phi}|V_+ \, .$$

Let $\mathcal{G}^*_{\widehat{\Phi}} \subset \mathcal{G}_K$ be the pseudo$\star$group defined as in Definition 9.8 by the maps $\{\widehat{\Phi}_-, \widehat{\Phi}_0, \widehat{\Phi}_+\} \subset \mathcal{G}_K$. Also, introduce the symmetric generating set for $\mathcal{G}^*_{\widehat{\Phi}}$,

$$\mathcal{G}^{(1)}_{\widehat{\Phi}} = \{Id, (\widehat{\Phi}_-)^{\pm 1}, (\widehat{\Phi}_0)^{\pm 1}, (\widehat{\Phi}_+)^{\pm 1}\} \, . \tag{135}$$

Then a map $\varphi \in \mathcal{G}^{(n)}_{\widehat{\Phi}}$ is a composition of at most n maps in the collection $\mathcal{G}^{(1)}_{\widehat{\Phi}}$, which by definition of these generating maps is just a composition of $\widehat{\Phi}$, or its inverse, restricted to a connected domain of continuity. In particular, for each open set $U \in \mathcal{D}^{(n)}_{\mathfrak{M}}(\widehat{\Phi})$, and $-n \leq \ell \leq n$, the restriction $\varphi = \widehat{\Phi}^\ell | U \in \mathcal{G}^{(n)}_{\widehat{\Phi}}$.

Recall that $d_{\mathbf{R}_0}$ denotes the metric on $\mathbf{R}_0$ defined in (26), and the metric $d_{\mathbb{K}}$ on $\mathbb{K}$ was defined in Section 4 so that $\mathcal{K}$ has unit length, and thus Φ_t is a unit speed flow.

We restrict the action of $\mathcal{G}^*_{\widehat{\Phi}}$ to the invariant set $\mathfrak{M}_{\mathbf{R}_0} \subset \mathbf{R}_0$. Let $s(\mathcal{G}^*_{\widehat{\Phi}}, \mathfrak{M}_{\mathbf{R}_0}, n, \epsilon)$ be the maximal cardinality of a $(\mathcal{G}^*_{\widehat{\Phi}}, n, \epsilon)$-separated subset of $\mathfrak{M}_{\mathbf{R}_0}$. Define the restricted entropy by

$$h_{GLW}(\mathcal{G}^*_{\widehat{\Phi}}|\mathfrak{M}_{\mathbf{R}_0}) \; = \; \lim_{\epsilon \to 0} \left\{ \limsup_{n \to \infty} \frac{1}{n} \ln(s(\mathcal{G}^*_{\widehat{\Phi}}, \mathfrak{M}_{\mathbf{R}_0}, n, \epsilon)) \right\} \, . \tag{136}$$

Here is the first result.

PROPOSITION 20.9. *$h_{GLW}(\mathcal{G}^*_{\widehat{\Phi}}|\mathfrak{M}_{\mathbf{R}_0}) = 0$ if and only if $h_{top}(\Phi_t|\mathfrak{M}) = 0$.*

Proof. We require some preliminary remarks. As $\mathbf{R}_0$ is compact submanifold of $\mathbb{K}$, there exists a constant $A_1 \geq 1$ so that for $x, y \in \mathbf{R}_0$ we have

$$A_1^{-1} \, d_{\mathbb{K}}(x, y) \; \leq d_{\mathbf{R}_0}(x, y) \leq A_1 \, d_{\mathbb{K}}(x, y). \tag{137}$$

The submanifold $\mathbf{R}_0$ was chosen to be disjoint from the embedded regions $\mathcal{D}_i \subset \mathbb{W}$ for $i = 1, 2$, so there exists some $\epsilon_2 > 0$ so that the ϵ_2-closed neighborhood of $\mathbf{R}_0$ is disjoint from these surfaces. That is, for $i = 1, 2$, we have

$$C_{\mathbb{K}}(\mathbf{R}_0, \epsilon_2) = \{x \in \mathbb{K} \mid d_{\mathbb{K}}(x, \mathbf{R}_0) \leq \epsilon_2\} \quad , \quad C_{\mathbb{K}}(\mathbf{R}_0, \epsilon_2) \cap \mathcal{D}_i = \emptyset.$$

Then the flows Φ_t and Ψ_t agree on the set $C_{\mathbb{K}}(\mathbf{R}_0, \epsilon_2)$.

Define a function $\Delta(\epsilon) > 0$ for $\epsilon > 0$ as follows. For $y \in \mathfrak{M}_{\mathbf{R}_0}$ let $s'_y < 0 < s''_y$ be the minimum and maximum values such that $\{\Phi_t(y) \mid s'_y \leq t \leq s''_y\} \subset C_{\mathbb{K}}(\mathbf{R}_0, \epsilon_2)$. Then for $x \in \mathfrak{M}_{\mathbf{R}_0}$ with $x \neq y$ let $\Delta(x, y, \epsilon_2) = \min\{d_{\mathbb{K}}(x, \Phi_t(y)) \mid s'_y \leq t \leq s''_y\}$. Then $0 < \Delta(x, y, \epsilon_2) \leq d_{\mathbb{K}}(x, y)$, and we set

$$\Delta(\epsilon) = \min\{\Delta(x, y, \epsilon_2) \mid x, y \in \mathfrak{M}_{\mathbf{R}_0} \text{ and } d_{\mathbf{R}_0}(x, y) \geq \epsilon\} \tag{138}$$

Observe that $\Delta(x, y, \epsilon_2)$ is a continuous function of $x \neq y$, and the set $\{(x, y) \mid x, y \in \mathfrak{M}_{\mathbf{R}_0} \text{ and } d_{\mathbf{R}_0}(x, y) \geq \epsilon\}$ is compact, so $0 < \Delta(\epsilon) \leq \epsilon$.

Recall that $\nu_{\mathcal{K}}$ is the constant introduced in Proposition 9.9. As the flow Φ_t is smooth, there exists $A_2 > 1$ such that for $x, y \in \mathfrak{M}$ and $-\nu_{\mathcal{K}} \leq t \leq \nu_{\mathcal{K}}$,

$$A_2^{-1}\, d_{\mathbb{K}}(x,y) \ \leq d_{\mathbb{K}}(\Phi_t(x), \Phi_t(y)) \leq A_2\, d_{\mathbb{K}}(x,y). \tag{139}$$

Now, assume that $h_{GLW}(\mathcal{G}^*_{\widehat{\Phi}}|\mathfrak{M}_{\mathbf{R}_0}) = \lambda > 0$. Then for $0 < \epsilon_3 \leq \epsilon_2$ sufficiently small, and for n sufficiently large, there is a $(\mathcal{G}^*_{\widehat{\Phi}}, n, \epsilon_3)$-separated subset $\widehat{E}_n \subset \mathfrak{M}_{\mathbf{R}_0}$ with cardinality $\#\widehat{E}_n > \exp(n\,\lambda/2)$. Fix n large enough so that this estimate holds.

We have by definition (132) and Lemma 20.2 that for each $0 \leq \ell \leq n$,

$$Dom(\widehat{\Phi}^\ell) \cap \mathfrak{M}_{\mathbf{R}_0} \subset \overline{D^{(\ell)}(\widehat{\Phi})} \cap \mathfrak{M}_{\mathbf{R}_0} \subset \bigcup \left\{ \overline{U} \mid U \in \mathcal{D}^{(\ell)}_{\mathfrak{M}}(\widehat{\Phi}) \right\}.$$

Recall that $C_\Phi(n)$ is the number of connected domains in $\mathcal{D}^{(n)}_{\mathfrak{M}}(\widehat{\Phi})$, so by the Pigeonhole principle, there exists some connected component $U \in \mathcal{D}^{(n)}_{\mathfrak{M}}(\widehat{\Phi})$ such that $\#(\widehat{E}_n \cap \overline{U}) > \exp(n\,\lambda/2)/C_\Phi(n)$. For n sufficiently large, we can assume that $C_\Phi(n) \leq \exp(n\,\lambda/4)$ by Proposition 20.8. Then for such n, set $\widehat{E}'_n = \widehat{E}_n \cap \overline{U}$, and we have that $\#\widehat{E}'_n > \exp(n\,\lambda/4)$. Let $y \neq x$ in $\widehat{E}'_n$, then x and y are (n, ϵ_3)-separated implies there exists $-n \leq \ell_{x,y} \leq n$ such that $d_{\mathbf{R}_0}(\widehat{\Phi}^{\ell_{x,y}}(x), \widehat{\Phi}^{\ell_{x,y}}(y)) > \epsilon_3$.

It may happen that the restricted set $\widehat{E}'_n$ satisfies $\widehat{E}'_n \cap (\overline{U} - U) \neq \emptyset$. That is, there exists $x \in \mathcal{L}_\ell$ for some $-n \leq \ell \leq n$. For such x, there exists $x' \in U$ which is sufficiently close so that the (n, ϵ_3)-separated condition is again satisfied. Thus, by taking a sufficiently small perturbation of each point in $\widehat{E}'_n$, we can assume without loss of generality that $\widehat{E}'_n \subset U$. Recall the definition of A_1 in (137), then for each distinct pair $x, y \in \widehat{E}'_n$ there exists $-n \leq \ell_{x,y} \leq n$ such that

$$d_{\mathbb{K}}(\widehat{\Phi}^{\ell_{x,y}}(x), \widehat{\Phi}^{\ell_{x,y}}(y)) > \epsilon_3/A_1. \tag{140}$$

By Proposition 9.9, the forward and backward return time to $\mathbf{R}_0$ for the $\mathcal{K}$-orbit of any point $x \in \mathfrak{M}_{\mathbf{R}_0}$ is bounded by $\nu_{\mathcal{K}}$. Consequently, for any $x \in \mathfrak{M}$ there exists a least $0 \leq t_x < \nu_{\mathcal{K}}$ such that $\Phi_{t_x}(x) \in \mathfrak{M}_{\mathbf{R}_0}$.

Set $T_n = n\,\nu_{\mathcal{K}}$. For a distinct pair $x, y \in \widehat{E}'_n$ let $-n \leq \ell_{x,y} \leq n$ be as above, and let t_x be the value such that $x' = \Phi_{t_x}(x) = \widehat{\Phi}^{\ell_{x,y}}(x)$, and t_y such that $y' = \Phi_{t_y}(y) = \widehat{\Phi}^{\ell_{x,y}}(y)$. Then $0 < |t_x|, |t_y| \leq \ell_{x,y}\,\nu_{\mathcal{K}} \leq T_n$.

Set $\epsilon_4 = \epsilon_3/A_1$, and $\epsilon_5 = \Delta(\epsilon_4) \leq \epsilon_4$ for the function $\Delta(\epsilon)$ defined by (138).

We claim that the set $\widehat{E}'_n \subset \mathfrak{M}$ is $(\Phi_t, T_n, \epsilon_5)$-separated. If not, then there exists a distinct pair $x, y \in \widehat{E}'_n$ such that $d_{\mathbb{K}}(\Phi_t(x), \Phi_t(y)) \leq \epsilon_5$ for all $-T_n \leq t \leq T_n$, and this holds for $t = t_x$ and $t = t_y$ in particular. It is given that $d_{\mathbb{K}}(x', y') > \epsilon_4$, so by the definition of ϵ_5 and the function $\Delta(\epsilon)$, we have $\Delta(x, y, \epsilon_2) \geq \epsilon_4$. That is, for all t with $s'_y < t < s''_y$ we have that $d_{\mathbb{K}}(x', \Phi_t(y')) \geq \epsilon_4$. If $s'_y < t_1 - t_2 < s''_y$ then this implies that $d_{\mathbb{K}}(\Phi_{t_1}(x), \Phi_{t_1}(y)) \geq \epsilon_4 \geq \epsilon_5$ contrary to assumption. If $s'_y < t_1 - t_2 < s''_y$ is not satisfied, then $\Phi_{t_1}(y) \notin C_{\mathbb{K}}(\mathbf{R}_0, \epsilon_2)$, so that $d_{\mathbb{K}}(\Phi_{t_1}(x), \Phi_{t_1}(y)) \geq \epsilon_2 \geq \epsilon_5$, again contrary to assumption.

It follows that $s(\Phi_t|\mathfrak{M}, T_n, \epsilon_5) \geq \exp(n\,\lambda/4)$.

As T_n is a linear function of n, this implies that $h_{top}(\Phi_t|\mathfrak{M}) > 0$, as was to be shown.

The reverse implication of Proposition 20.9 follows by showing that $h_{GLW}(\mathcal{G}^*_{\widehat{\Phi}}|\mathfrak{M}_{\mathbf{R}_0}) = 0$ implies $h_{top}(\Phi_t|\mathfrak{M}) = 0$. For this purpose, we use an alternate interpretation of the topological entropy $h_{top}(\Phi_t|\mathfrak{M})$, in terms of the minimum cardinality of a (Φ_t, T, ϵ)-spanning set for $\mathfrak{M}$. The properties of spanning sets used to define the entropy of a map are discussed in greater detail in [49, Chapter 7.2].

For $T \geq 0$, introduce the metric $d^T_{\mathbb{K}}$ on $\mathfrak{M}$ where for $x, y \in \mathfrak{M}$,

$$d^T_{\mathbb{K}}(x,y) = \max\left\{ d_{\mathbb{K}}(\Phi_t(x), \Phi_t(y)) \mid -T \leq t \leq T \right\}.$$

A subset $F \subset \mathfrak{M}$ is said to be $(\Phi_t|\mathfrak{M}, T, \epsilon)$-*spanning* if for all $y \in \mathfrak{M}$ there exists $x \in F$ such that $d^T_{\mathbb{K}}(x,y) \leq \epsilon$. Note that for $T' > T$ the metric $d_{T'}$ is finer than d_T, so a $(\Phi_t|\mathfrak{M}, T', \epsilon)$-spanning set F is also a $(\Phi_t|\mathfrak{M}, T, \epsilon)$-spanning set. Let $r(\Phi_t|\mathfrak{M}, T, \epsilon)$ be the minimal cardinality of a $(\Phi_t|\mathfrak{M}, T, \epsilon)$-spanning set in $\mathfrak{M}$.

Then $r(\Phi_t|\mathfrak{M}, T, \epsilon) < \infty$ as $\mathfrak{M}$ is compact, and we have the inequalities $r(\Phi_t|\mathfrak{M}, T', \epsilon) \geq r(\Phi_t|\mathfrak{M}, T, \epsilon)$ for $T' > T$, and $r(\Phi_t|\mathfrak{M}, T, \epsilon') \geq r(\Phi_t|\mathfrak{M}, T, \epsilon)$ for $0 < \epsilon' < \epsilon$. Then we have

$$h_{top}(\Phi_t|\mathfrak{M}) = \lim_{\epsilon \to 0} \left\{ \limsup_{T \to \infty} \frac{1}{T} \log(r(\Phi_t|\mathfrak{M}, T, \epsilon)) \right\}. \tag{141}$$

As an application, we have:

LEMMA 20.10. *Suppose that for all $\lambda > 0$, we have that: for $\epsilon > 0$ sufficiently small and all $T > 0$ sufficiently large, there exists a $(\Phi_t|\mathfrak{M}, T, \epsilon)$-spanning set $F(T, \epsilon) \subset \mathfrak{M}$ with $\# F(T, \epsilon) \leq \exp(T\,\lambda)$. Then $h_{top}(\Phi_t|\mathfrak{M}) = 0$.*

Now, assume that $h_{GLW}(\mathcal{G}^*_{\widehat{\Phi}}|\mathfrak{M}_{\mathbf{R}_0}) = 0$, and let $\lambda > 0$. Then we construct $(\Phi_t|\mathfrak{M}, T, \epsilon)$-spanning sets which have growth rate less than $\exp(T\,\lambda)$. As λ can be chosen arbitrarily small, then Lemma 20.10 implies that $h_{top}(\Phi_t|\mathfrak{M}) = 0$, which completes the proof of Proposition 20.9.

Fix $\lambda > 0$ and $0 < \epsilon < \delta_{\mathcal{K}}$ then set $\epsilon_6 = \epsilon/8$. Then there exists $n_0 > 0$ such that for $n \geq n_0$ we have $s(\mathcal{G}^*_{\widehat{\Phi}}|\mathfrak{M}_{\mathbf{R}_0}, n, \epsilon_6) \leq \exp(n\,\lambda/2)$. Thus, for each $n \geq n_0$ there exists a $(\mathcal{G}^*_{\widehat{\Phi}}, n, \epsilon_6)$-separated subset $\widehat{F}_n \subset \mathfrak{M}_{\mathbf{R}_0}$ with maximal cardinality which satisfies $\#\widehat{F}_n \leq \exp(n\,\lambda/2)$. Then for each pair $x \neq y \in \widehat{F}_n$ there exists $-n \leq \ell_{x,y} \leq n$ such that $x, y \in Dom(\widehat{\Phi}^{\ell_{x,y}})$ and $d_{\mathbf{R}_0}(\widehat{\Phi}^{\ell_{x,y}}(x), \widehat{\Phi}^{\ell_{x,y}}(y)) > \epsilon_6$.

For each $n \geq n_0$, the set $\widehat{F}_n$ was chosen to have maximal cardinality. Thus, for each $y \in \mathfrak{M}_{\mathbf{R}_0}$, there exists $x \in \widehat{F}_n$ such that $d_{\mathbf{R}_0}(\widehat{\Phi}^{\ell}(x), \widehat{\Phi}^{\ell}(y)) \leq \epsilon_6$ for all $-n \leq \ell \leq n$. That is, $\widehat{F}_n$ is $(\widehat{\Phi}|\mathfrak{M}_{\mathbf{R}_0}, n, \epsilon_6)$-spanning.

We consider the restricted set $\widehat{F}_n \cap U$. The set $\widehat{F}_n \subset \mathfrak{M}_{\mathbf{R}_0}$ is $(\mathcal{G}^*_{\widehat{\Phi}}, n, \epsilon_6)$-separated for $\mathfrak{M}_{\mathbf{R}_0}$, hence is $(\widehat{\Phi}|\mathfrak{M}_{\mathbf{R}_0}, n, \epsilon_6)$-spanning for $\mathfrak{M}_{\mathbf{R}_0}$, but this need not imply that $\widehat{F}_n \cap U$ is $(\mathcal{G}^*_{\widehat{\Phi}}, n, \epsilon_6)$-spanning for $\mathfrak{M}_{\mathbf{R}_0} \cap \overline{U}$. If so, then set $\widehat{F}^U_n = \widehat{F}_n \cap U$. Otherwise, if $\widehat{F}_n \cap U$ is not $(\mathcal{G}^*_{\widehat{\Phi}}, n, \epsilon_6)$-spanning for $\mathfrak{M}_{\mathbf{R}_0} \cap \overline{U}$, then we define $\widehat{F}^U_n \subset U$ by adding to the set $\widehat{F}_n \cap U$ sufficiently many points, obtained from ϵ_6-perturbations of points in $\widehat{F}_n - (\widehat{F}_n \cap U)$, so that $\widehat{F}^U_n$ is $(\mathcal{G}^*_{\widehat{\Phi}}, n, \epsilon_6)$-spanning for $\mathfrak{M}_{\mathbf{R}_0} \cap \overline{U}$. This is done as follows. A point $x \in \widehat{F}_n - (\widehat{F}_n \cap U)$ is said to be in the $(\mathcal{G}^*_{\widehat{\Phi}}, n, \epsilon_6)$-shadow of U, if there exists $y_x \in U$ such that $d_{\mathbf{R}_0}(\widehat{\Phi}^{\ell}(x), \widehat{\Phi}^{\ell}(y_x)) \leq \epsilon_6$ for all $-n \leq \ell \leq n$. Then define $\widehat{F}^U_n$ as follows:

$$\widehat{F}^U_n = (\widehat{F}_n \cap U) \cup \{y_x \mid x \in \widehat{F}_n - (\widehat{F}_n \cap U),\ x \text{ is a shadow point for } U\}.$$

Set $\epsilon_7 = 2\epsilon_6 = \epsilon/4$, so that the ϵ_7 ball centered at a point $x \in \mathbf{R}_0$ contains the ϵ_6-ball centered at ζ, for any point ζ in the ϵ_6-ball centered at x. Then by construction, $\widehat{F}^U_n$ is $(\widehat{\Phi}|\mathfrak{M}_{\mathbf{R}_0}, n, \epsilon_7)$-spanning for $\mathfrak{M}_{\mathbf{R}_0} \cap \overline{U}$. Note that $\#\widehat{F}^U_n \leq \#\widehat{F}_n$.

The next step in the proof is to use the flow Φ_t of the sets $\widehat{F}^U_n$, for $U \in \mathcal{D}^{(n)}_{\mathfrak{M}}(\widehat{\Phi})$, to obtain a $(\Phi_t|\mathfrak{M}, T_n, \epsilon)$-spanning set in $\mathfrak{M}$, for appropriate T_n. There is a technical difficulty that arises in this procedure, due to the fact that the return time for the flow to the space $\mathbf{R}_0$ is not constant. We require the following observation, that there is a "modulus of continuity" for the time-change along an orbit, with respect to variations of the initial points for flow segments of Φ_t with bounded lengths.

LEMMA 20.11. *There exists $M_{\mathcal{K}} > 0$ and $\delta_{\mathcal{K}} > 0$ so that for all $0 < \epsilon' < \delta_{\mathcal{K}}$:*

Let $x \in \mathfrak{M}_{\mathbf{R}_0}$ and $|T| \geq 1$ be such that $\xi = \Phi_T(x) \in \mathfrak{M}_{\mathbf{R}_0}$. Let n_x be such that $\xi = \widehat{\Phi}^{n_x}(x)$. For $y, z \in B_{\mathbf{R}_0}(x, \epsilon') \cap \mathfrak{M}_{\mathbf{R}_0}$, assume that $d_{\mathbf{R}_0}(\widehat{\Phi}^{\ell}(x), \widehat{\Phi}^{\ell}(\eta)) < \epsilon'$ for all $0 \leq \ell \leq n_x$, for both $\eta = y$ and $\eta = z$. Let T' be such that $\Phi_{T'}(y) = \widehat{\Phi}^{n_x}(y)$, and T'' be such that $\Phi_{T''}(z) = \widehat{\Phi}^{n_x}(z)$. Then if $d_{\mathbf{R}_0}(y, z) < \epsilon'/(M_{\mathcal{K}}\,|T|)$, we have

$$d_{\mathbb{K}}(\Phi_t(y), \Phi_t(z)) \ \leq \ \epsilon' \quad \text{for all } |t| \leq |T|\ . \tag{142}$$

Proof. The curves $\{\Phi_t(\xi) \mid 0 \leq t \leq T\}$ for $\xi \in \{x, y, z\}$ are integral curves for the vector field $\mathcal{K}$. The idea of the proof is that for appropriately chosen $\delta_{\mathcal{K}}$ the $\mathcal{K}$-orbits segments for y and z are contained in a suitably

small neighborhood of the $\mathcal{K}$-orbit segment for x, chosen so that the length of the vector $\mathcal{K}$ along these curves are uniformly close. It then follows that the return times for y and z are also uniformly close. The details of the proof use standard methods of differential equations, and are left to the reader. □

We use Lemma 20.11 to construct a set $\widehat{F}'_n$ whose points are sufficiently close together, so that the Φ_t flow of $\widehat{F}'_n$ yields a $(\Phi_t|\mathfrak{M}, T'_n, \epsilon)$-spanning set, for a sequence of values T'_n which tend to infinity.

Let $T_n = L_\Phi \cdot n$, and set $\epsilon_8 = \epsilon_7/(2M_\mathcal{K}\, T_n) = \epsilon_7/(2n\, L_\Phi\, M_\mathcal{K})$ for L_Φ as defined in Lemma 20.4 and $M_\mathcal{K}$ as defined in Lemma 20.11. Note that there exists a constant $A_7 > 0$, which depends only on the geometry of $\mathbf{R}_0$, such that the number of points required for an ϵ_8-spanning set of the disk $D_{\mathbf{R}_0}(x, \epsilon_7) \subset \mathbf{R}_0$, *for the metric* $d_{\mathbf{R}_0}$, is bounded above by $A_7\,(\epsilon_7/\epsilon_8)^2 = A_7\,(2n\, L_\Phi\, M_\mathcal{K})^2$.

For each $U \in \mathcal{D}^{(n)}_\mathfrak{M}(\widehat{\Phi})$ and each $x \in \widehat{F}^U_n$, choose an ϵ_8-spanning set for $\mathfrak{M}_{\mathbf{R}_0} \cap D_{\mathbf{R}_0}(x, \epsilon_7) \cap \overline{U}$,

$$S(U, x, \epsilon_8) = \{x(U, x, i) \mid i \in \mathcal{I}(U, x, \epsilon_8)\} \subset \mathfrak{M}_{\mathbf{R}_0} \cap D_{\mathbf{R}_0}(x, \epsilon_7) \cap U \ ,$$

where the index set $\mathcal{I}(U, x, \epsilon_8)$ has cardinality $\#\,\mathcal{I}(U, x, \epsilon_8) \leq A_7\,(2n\, L_\Phi\, M_\mathcal{K})^2$. Then set

$$\widehat{F}'_n = \bigcup_{U \in \mathcal{D}^{(n)}_\mathfrak{M}(\widehat{\Phi})} \bigcup_{x \in \widehat{F}^U_n} S(U, x, \epsilon_8) \ . \tag{143}$$

Observe that $\#\,\widehat{F}'_n \leq C_\Phi(n) \cdot \exp(n\,\lambda/2) \cdot A_7\,(2n\, L_\Phi\, M_\mathcal{K})^2$.

We next construct a set F_n which is contained in the Φ_t-flow of the set $\widehat{F}'_n$, for a sequence of sufficiently small increments of the time parameter. Let M_n be the greatest integer with $M_n \leq T_n/\epsilon_7$, and for each $0 \leq \ell \leq M_n$ set $t_\ell = \ell \cdot \epsilon_7$. Then define

$$F_n = \bigcup_{0 \leq \ell \leq M_n} \Phi_\ell(\widehat{F}'_n) \ \subset \ \mathfrak{M} \ . \tag{144}$$

Observe that

$$\#F_n = M_n \cdot \#\widehat{F}'_n \leq L_\Phi \cdot n/\epsilon_7 \cdot C_\Phi(n) \cdot \exp(n\,\lambda/2) \cdot A_7\,(2n\, L_\Phi\, M_\mathcal{K})^2.$$

Thus, for $n'_0 \geq n_0$ sufficiently large, we have that $n \geq n'_0$ implies that $\#\,\widehat{F}_n \leq \exp(n\,\lambda)$. Set $T'_n = T_n - \nu_\mathcal{K}$.

LEMMA 20.12. *F_n is $(\Phi_t|\mathfrak{M}, T'_n, \epsilon)$-spanning.*

Proof. Let $\eta \in \mathfrak{M}$, then we must show that there exists $\xi \in F_n$ such that

$$d_\mathbb{K}(\Phi_t(\eta), \Phi_t(\xi)) \leq \epsilon \quad \text{for all } -T_n \leq t \leq T_n \ .$$

First, there exists $0 \leq t_\eta < \nu_\mathcal{K}$ such that $y = \Phi_{-t_\eta}(\eta) \in \mathfrak{M}_{\mathbf{R}_0}$. Then there exists $U \in \mathcal{D}^{(n)}_\mathfrak{M}(\widehat{\Phi})$ with $y \in \overline{U}$, and $x \in \widehat{F}^U_n$ for which $d_{\mathbf{R}_0}(\widehat{\Phi}^\ell(x), \widehat{\Phi}^\ell(y)) \leq \epsilon_7$ for all $-n \leq \ell \leq n$. By the choice of the set $N(U, x)$, there exists $z \in N(U, x)$ for which $d_{\mathbf{R}_0}(y, z) \leq \epsilon_8$. Note that $z \in \widehat{F}'_n$.

We may assume that $T_n \geq \nu_\mathcal{K}+1$, as we consider $T_n \to \infty$. Then observe that the hypotheses of Lemma 20.11 are satisfied for $\epsilon' = \epsilon_7$, $T = T_n$, $x \in \widehat{F}_n$ and the pair of points $\{y, z\}$ as above, and so the estimate (142) holds for these points. Thus we have:

$$d_\mathbb{K}(\Phi_t(y), \Phi_t(z)) \ \leq \ \epsilon_7 = \epsilon/4 \quad \text{for all } |t| \leq T_n \ . \tag{145}$$

Choose $0 \leq \ell \leq M_n$ so that $|t_\eta - t_\ell| \leq \epsilon_7$. Then $d_\mathbb{K}(\Phi_{t_\eta}(z), \Phi_{t_\ell}(z)) \leq \epsilon_7$ as the flow Φ_t has unit speed.

Then for $-T'_n \leq t \leq T'_n$, note that $|t + t_\eta| \leq |T_n - \nu_\mathcal{K}| + |\nu_\mathcal{K}| \leq T_n$, so we have the estimates:

$$\begin{aligned} d_\mathbb{K}(\Phi_t(\eta), \Phi_t(\xi)) &= d_\mathbb{K}(\Phi_t \circ \Phi_{t_\eta}(y), \Phi_t \circ \Phi_{t_\ell}(z)) \\ &\leq d_\mathbb{K}(\Phi_{t+t_\eta}(y), \Phi_{t+t_\eta}(z)) + d_\mathbb{K}(\Phi_{t+t_\eta}(z), \Phi_{t+t_\ell}(z)) \\ &\leq \epsilon_7 + \epsilon_7 = \epsilon/2 \ . \end{aligned}$$

as was to be shown. □

Finally, to complete the proof of Proposition 20.9, note that $T_n = L_\Phi \cdot n$ is a linear function of n, so the growth rate of the sets F_n has an exponential bound $\exp(n\,\lambda) = \exp(T_n\,\lambda/L_\Phi)$. As the choice of $\lambda > 0$ was arbitrary, by Lemma 20.10 we conclude that $h_{top}(\Phi_t|\mathfrak{M}) = 0$. □

There is another entropy invariant associated to Φ_t, which is defined in terms of the action of the pseudo⋆group $\mathcal{G}_K^*$ on $\mathbf{R}_0$ introduced in Definition 9.8, and equipped with the symmetric generating set

$$\mathcal{G}_K^{(1)} = \{Id, (\psi)^{\pm 1}, (\phi_1^+)^{\pm 1}, (\phi_1^-)^{\pm 1}, (\phi_2^+)^{\pm 1}, (\phi_2^-)^{\pm 1}\}. \tag{146}$$

Let $h_{GLW}(\mathcal{G}_K^*|\mathfrak{M}_{\mathbf{R}_0})$ denote the pseudogroup entropy associated to the generating set $\mathcal{G}_K^{(1)}$ acting on $\mathfrak{M}_{\mathbf{R}_0}$.

Recall that the map $\psi \in \mathcal{G}_K^{(1)}$ represents the return map for the Wilson flow, and corresponds to the "short-cuts" introduced in Lemma 5.1. This additional generator raises the possibility that the growth rate of $(\mathcal{G}_K^*, n, \epsilon)$-separated points may be greater the growth rate of $(\mathcal{G}_{\widehat{\Phi}}^*, n, \epsilon)$-separated points. On the other hand, the pseudo⋆group $\mathcal{G}_{\widehat{\Phi}}^*$ is the "full pseudogroup" generated by the return map $\widehat{\Phi}$, while the generators for $\mathcal{G}_K^*$ form just a subset of these. We use Proposition 9.16 to compare these growth rates, and prove the following:

PROPOSITION 20.13. *$h_{GLW}(\mathcal{G}_{\widehat{\Phi}}^*|\mathfrak{M}_{\mathbf{R}_0}) > 0$ implies that $h_{GLW}(\mathcal{G}_K^*|\mathfrak{M}_{\mathbf{R}_0}) > 0$.*

Proof. Assume that $h_{GLW}(\mathcal{G}_{\widehat{\Phi}}^*|\mathfrak{M}_{\mathbf{R}_0}) = \lambda > 0$. For $\epsilon > 0$ sufficiently small, and n sufficiently large, let $E_0(n, \epsilon) \subset \mathfrak{M}_{\mathbf{R}_0}$ be a $(\mathcal{G}_{\widehat{\Phi}}^*, n, \epsilon)$-separated set with cardinality $\#E_0(n, \epsilon) \geq \exp(n\,\lambda/2)$. Then for each distinct pair $x, y \in E_0(n, \epsilon)$, there exists $-n \leq \ell_{x,y} \leq n$ such that $d_{\mathbf{R}_0}(\widehat{\Phi}^{\ell_{x,y}}(x), \widehat{\Phi}^{\ell_{x,y}}(y)) > \epsilon$.

By Corollary 20.6, for each $x \in \mathfrak{M}_{\mathbf{R}_0}$, the orbit $\mathcal{G}_K^*(x) \subset \mathfrak{M}_{\mathbf{R}_0}$ is syndetic for the constant ν_u^*. Recall that $M_u > 0$ is the greatest integer with $M_u \leq 2\nu_u^*$ then by Corollary 20.7, there exists $0 \leq m_x \leq M_u$ such that $\widehat{\Phi}^{-m_x}(x) \in \mathcal{G}_K^*(x)$. Also by the proof of Proposition 9.16, there exists $0 \leq \ell_x \leq M_u/2$ such that $r(\widehat{\Phi}^{\ell_x + \ell_{x,y}}(x)) < r_e$. Thus, module changing ℓ_x for $\ell_x + 1$, we can further assume that $|z(\widehat{\Phi}^{\ell_x + \ell_{x,y}}(x))| > \delta$ for some $\delta > 0$ independent of the choice of x and $0 \leq \ell_x \leq M_u$.

For each $x \in E_0(n, \epsilon)$ we have associated two indices, $0 \leq \ell_x \leq M_u$ and $0 \leq m_x \leq M_u$. The total number of pairs $\{\ell_x, m_x\}$ is at most M_u^2, so there exists values $0 \leq \ell' \leq M_u$ and $0 \leq m' \leq M_u$ such that the set

$$E_0(n, \epsilon)(\ell', m') = \{x \in E_0(n, \epsilon) \mid \ell_x = \ell' \text{ and } m_x = m'\}$$

has cardinality at least $\#E_0(n, \epsilon)/M_u^2$. Fix such ℓ', m' and set $E_0'(n, \epsilon) = E_0(n, \epsilon)(\ell', m')$. Set $\mathcal{E}_0'(n, \epsilon) = \widehat{\Phi}^{-m'}(E_0'(n, \epsilon)) \subset \mathfrak{M}_{\mathbf{R}_0}$, which is then $(\mathcal{G}_{\widehat{\Phi}}^*, m' + n, \epsilon)$-separated.

Proposition 9.9 shows that for each $\xi \in \mathfrak{M}_{\mathbf{R}_0}$ and $\eta = \widehat{\Phi}(\xi)$, the $\mathcal{K}$-orbit segment $[\xi, \eta]_{\mathcal{K}}$ has length bounded above by $\nu_{\mathcal{K}}$. Then there is a uniform norm on the derivative $D_\xi \Phi_t \colon T_\xi \mathbb{K} \to T_\eta \mathbb{K}$, so there is a uniform upper bound $M_\Phi \geq 1$ on the norm of the derivative matrix of $D_\xi \widehat{\Phi}$ and on its inverse $(D_\xi \widehat{\Phi})^{-1}$. Thus, for $\xi, \xi' \in \mathfrak{M}_{\mathbf{R}_0} \cap Dom(\widehat{\Phi}^{\ell'})$, we have

$$(M_\Phi)^{-\ell'} \cdot d_{\mathbf{R}_0}(\xi, \xi') \;\leq\; d_{\mathbf{R}_0}(\widehat{\Phi}^{\ell'}(\xi), \widehat{\Phi}^{\ell'}(\xi')) \;\leq\; (M_\Phi)^{\ell'} \cdot d_{\mathbf{R}_0}(\xi, \xi'). \tag{147}$$

For $x \neq y \in E_0'(n, \epsilon)$, set $\xi = \widehat{\Phi}^{-m'}(x) \in \mathcal{E}_0'(n, \epsilon)$ and $\xi' = \widehat{\Phi}^{-m'}(y) \in \mathcal{E}_0'(n, \epsilon)$.

Let $\ell'_{x,y} = \ell_{x,y} + \ell' + m' \leq n + 2M_u$, then by the choice of ℓ' and m', Corollary 20.6 implies the map $\widehat{\Phi}^{\ell'_{x,y}} \in \mathcal{G}_K^{(n+2M_u)}$. Also, we have the estimate

$$d_{\mathbf{R}_0}(\widehat{\Phi}^{\ell'_{x,y}}(\xi), \widehat{\Phi}^{\ell'_{x,y}}(\xi')) = d_{\mathbf{R}_0}(\widehat{\Phi}^{\ell' + \ell_{x,y}}(x), \widehat{\Phi}^{\ell' + \ell_{x,y}}(y)) \geq M_\Phi^{-m'} \cdot d_{\mathbf{R}_0}(\widehat{\Phi}^{\ell_{x,y}}(x), \widehat{\Phi}^{\ell_{x,y}}(y)) > M_\Phi^{-M_u} \cdot \epsilon\ . \tag{148}$$

Set $\epsilon' = M_\Phi^{-M_u} \cdot \epsilon$. Then $\mathcal{E}_0'(n, \epsilon)$ is $(2(n + 2M_u) \cdot \nu_{\mathcal{K}}, \epsilon')$-separated for the action of $\mathcal{G}_K^*$ on $\mathfrak{M}_{\mathbf{R}_0}$.

These estimates hold for a sequence of integers $n \to \infty$, so it follows that $h_{GLW}(\mathcal{G}_K^*|\mathfrak{M}_{\mathbf{R}_0}) \geq \lambda/2 > 0$, as was to be shown. □

The rest of this section is devoted to the study of the entropy invariant $h_{GLW}(\mathcal{G}_K^*|\mathfrak{M}_{\mathbf{R}_0})$. One approach to the study of the restricted entropy $h_{top}(\Phi_t|\mathfrak{M})$ is to calculate the invariant measures for the flow, then estimate the Lyapunov spectrum for the flow on $\mathfrak{M}$ and apply the Margulis-Ruelle Inequality [29, 42] to estimate it from above. To show the entropy $h_{top}(\Phi_t|\mathfrak{M}) = 0$ it then suffices to show that the Lyapunov spectrum must be trivial for any invariant measure, which is done by analyzing the asymptotic properties of the derivative along the flow. In essence, the idea behind the proof of the following result is analogous, in that we obtain uniform estimates for the expansive properties of the dynamics of the pseudo⋆group $\mathcal{G}_K^*$.

THEOREM 20.14. $h_{GLW}(\mathcal{G}_K^*|\mathfrak{M}_{\mathbf{R}_0}) = 0$.

Proof. Assume that $h_{GLW}(\mathcal{G}_K^*|\mathfrak{M}_{\mathbf{R}_0}) = \lambda > 0$. Let $\epsilon > 0$ and $n_\epsilon > 0$ be such that

$$s(\mathcal{G}_K, \mathfrak{M}_{\mathbf{R}_0}, n, \epsilon) > \exp(n\,\lambda/2) \quad \text{for all } n \geq n_\epsilon. \tag{149}$$

Let $E_n \subset \mathfrak{M}_{\mathbf{R}_0}$ be a sequence of $(\mathcal{G}_\Phi^*, n, \epsilon)$-separated sets such that $\#E_n \geq \exp(n\,\lambda/2)$. Actually, it may be necessary to pass to a subsequence $\{n_i \mid i = 1, 2, \ldots\}$ to obtain the estimate (149), but for simplicity of notation, without loss of generality we assume there exists sets E_n for all $n \geq n_\epsilon$ with this property. Then for each pair $\xi \neq \eta \in E_n$, either $d_{\mathbf{R}_0}(\xi, \eta) \geq \epsilon$, or else there exists a word $\varphi \in \mathcal{G}_K^{(n)}$ with $\xi, \eta \in Dom(\varphi)$, and $d_{\mathbf{R}_0}(\varphi(\xi), \varphi(\eta)) \geq \epsilon$. We show this leads to a contradiction.

Recall that the metric $d_{\mathbf{R}_0}$ on $\mathbf{R}_0$ is the usual euclidean flat metric, where its sides have lengths 2×4. Choose m so that

$$\frac{1}{\sqrt{18}} \cdot \exp(n\,\lambda/4) < m < \frac{1}{4} \cdot \exp(n\,\lambda/4),$$

and divide $\mathbf{R}_0$ into $2m \times 4m$ uniform squares with sides of length $\delta = 1/m$ and diameter $\sqrt{2}/m^2$. The number of squares is thus bounded above by $\frac{1}{2} \cdot \exp(n\,\lambda/2)$, so by the Pigeonhole principle, for some square region must contain two distinct points of E_n. Hence, for each n there exists $x_n, y_n \in E_n$ with $d_{\mathbf{R}_0}(x_n, y_n) < \frac{1}{3} \cdot \exp(-n\,\lambda/4)$, and $\varphi_n \in \mathcal{M}(n)$ with $d_{\mathbf{R}_0}(\varphi_n(x_n), \varphi_n(y_n)) > \epsilon$.

For $\xi \in Dom(\varphi_n)$, let $D_\xi(\varphi_n)$ denote the 2×2 Jacobian matrix of first derivatives of φ_n at the point ξ, and let $\|D_\xi(\varphi_n)\|$ denote its matrix norm. Then by the Mean Value Theorem, there exist $w_n \in Dom(\varphi_n)$ in this same square region containing x_n, y_n such that $\|D_{w_n}(\varphi_n)\| \geq \epsilon/3 \cdot \exp(n\,\lambda/4)$. It follows that the norms $\|D_{w_n}(\varphi_n)\|$ grow exponentially as a function of n.

We next show that the uniform norms $\|D_\xi(\varphi)\|$ of the derivative matrices of $\varphi \in \mathcal{G}_K^{(n)}$ admit arbitrarily small exponential bounds as functions of n, which yields a contradiction. We remark that this calculation implies the Lyapunov spectrum of the flow Φ_t for any invariant measure supported on $\mathfrak{M}$ is trivial.

For an invertible matrix A, introduce the "symmetric norm" $|||A||| = \max\{\|A\|, \|A^{-1}\|\}$, where $\|A\|$ is the usual sup-norm on the linear transformation defined by A.

Let $D_\xi(\phi_i^+)$ denote the 2×2 Jacobian matrix of first derivatives of ϕ_i^+ at the point $\xi \in Dom(\phi_i^+)$. Define

$$C(\phi) = \sup\left\{|||D_\xi(\phi_i^+)||| \mid i = 1, 2 \;\&\; \xi \in Dom(\phi_i^+)\right\}. \tag{150}$$

For $b \geq 1$, introduce the upper bound

$$C(\psi, b) \;=\; \sup\;\left\{|||D_\xi(\psi^\ell)||| \mid 0 \leq \ell \leq b \quad \text{and} \quad \xi \in Dom(\psi^\ell)\right\}. \tag{151}$$

As the matrix $D_{\omega_i}(\psi)$ is the identity at the fixed points ω_i for $i = 1, 2$, for $\xi \in \mathbf{R}_0$ with $r(\xi) = 2$, we have that $\lim_{\ell \to \pm\infty} \dfrac{\ln \|D_\xi(\psi^\ell)\|}{|\ell|} = 0$. Thus, for every $\mu > 1$, there exists $n(\psi, \mu) > 0$ such that

$$1 \leq |||D_\xi(\psi^\ell)||| \leq \mu^\ell \quad \text{for } \ell \geq n(\psi, \mu),\ \xi \in Dom(\psi^\ell). \tag{152}$$

Recall from Section 14 the notion of monotone words $\mathcal{M}(n)$ of length at most n in Definition 14.1, and that by Proposition 14.3 every $\varphi \in \mathcal{G}_K^{(n)}$ admits a factorization $\varphi = \varphi^+ \circ \varphi^-$, where $\varphi^+ \in \mathcal{M}(n')$ and

$(\varphi^-)^{-1} \in \mathcal{M}(n'')$ for integers n', n'' with $n' + n'' \leq n$. For $\varphi \in \mathcal{M}(n)$ we use this factorization and the estimates (150), (151), and (152) to obtain a uniform estimate for the norm $|||D(\varphi)|||$ as a function of n.

For $\mu = \exp(\lambda/32)$, choose $b \geq \max\{n(\psi, \mu), (32/\lambda) \cdot \ln(C(\phi))\}$, so that $C(\phi)^{1/b} < \exp(\lambda/32)$. Also, for $\ell \geq b \geq n(\psi, \mu)$, we have $1 \leq |||D_\xi(\psi^\ell)||| \leq \exp(\ell\, \lambda/32)$ for all $\xi \in Dom(\psi^\ell)$.

Given $\varphi \in \mathcal{M}(n)$ recall the product representation in (71). For the b chosen above, there exists $i(\varphi, b) \geq 1$ such that $\ell_i \geq b$ for all $1 \leq i < i(\varphi, b)$, and $\ell_i \leq b$ for $i = i(\varphi, b)$. Write $\varphi = \varphi^{(b)} \cdot \varphi_{(b)}$ where $\varphi^{(b)}$ starts with the map $\phi^+_{i(\varphi,b)}$ and $\varphi_{(b)}$ starts with ψ^{ℓ_0}. Assume that $n \geq \max\{n_\epsilon, n(\psi, \mu)\}$, where n_ϵ was introduced in the paragraph after (149).

The factor $\varphi^{(b)}$ contains at most N_b generators of the form ϕ_i^+, and between each such map is a term ψ^{ℓ_i}, so there are at most $N_b + 1$ such factors with exponents either $\ell_i \leq b$ or $\ell_i > b$. Then

$$|||D(\varphi^{(b)})||| \ \leq \ C(\phi)^{M_b} \cdot C(\psi, b)^{(N_b+1)} \cdot \exp(n\, \lambda/32) \ . \tag{153}$$

The factor $\varphi_{(b)}$ contains at most n/b generators of the form ϕ_i^+, and between each such generator is a term ψ^{ℓ_i} where $\ell_i > b$ by the definition of $\varphi_{(b)}$. Then

$$|||D(\varphi_{(b)})||| \ \leq \ C(\phi)^{n/b} \cdot \exp((n\, \lambda/32) \ \leq \ \exp(n\, \lambda/32) \cdot \exp((n\, \lambda/32) \ = \ \exp(n\, \lambda/16) \ . \tag{154}$$

Combining these estimates, we have:

LEMMA 20.15. *For $\lambda > 0$, let $b \geq \max\{n(\psi, \mu), (32/\lambda) \cdot \ln(C(\phi))\}$. For all $n \geq \max\{n_\epsilon, n(\psi, \mu)\}$, we have*

$$\begin{aligned} \max\{\|D(\varphi)\|, \|D(\varphi)^{-1}\|\} \quad &\leq \quad |||D(\varphi^{(b)})||| \cdot |||D(\varphi_{(b)})||| \\ &\leq \quad \exp(n\, \lambda/32) \cdot \exp(n\, \lambda/16) < \exp(n\, \lambda/8) \ . \end{aligned} \tag{155}$$

Now recall that with the assumption that $h_{GLW}(\mathcal{G}_K|\mathfrak{M}_{\mathbf{R}_0}) = \lambda > 0$, then for each $n \geq n_\epsilon$, there exists $\varphi_n \in \mathcal{M}(n)$ and $w_n \in Dom(\varphi_n)$ such that $\|D_{w_n}(\varphi_n)\| \geq \epsilon \exp(n\, \lambda/4)$. Proposition 14.3 implies that each such word φ_n admits a factorization into a monotone decreasing factor and an increasing factor, each of length at most n. Apply the estimate (155) to both factors to obtain that for n sufficiently large,

$$\|D_{w_n}(\varphi_n)\| < \exp(n\, \lambda/8) \cdot \exp(n\, \lambda/8) = \exp(n\, \lambda/4) \ .$$

For n sufficiently large this yields a contradiction, which completes the proof of Theorem 20.14. □

21. Lamination entropy

The minimal set for a flow is an invariant of topological conjugacy, so represents an "invariant" for the flow. Properties of the minimal set can be used to study and classify the flow as a dynamical system. In the case of a generic Kuperberg flow Φ_t the space $\mathfrak{M}$ is the unique minimal set, and is fundamental for the study of the dynamics of the flow as has been seen in previous sections. In this section, we use the zippered lamination structure of $\mathfrak{M}$ to define invariants for the lamination itself, derived from the holonomy pseudogroup for $\mathfrak{M}$. The invariants studied in this section are "entropy-like". In the next section, we study growth-type invariants for the leaves, and both types of invariants reveal the beautiful subtleties of the class of generic Kuperberg flows.

We first give precise definitions of the maps $\{\overline{\psi}, \overline{\phi}_1, \overline{\phi}_2\}$ introduced in Section 14, and of the pseudo⋆group $\mathcal{G}^*_{\mathfrak{M}}$ they generate. We then study how this pseudo⋆group is associated to the holonomy of the zippered lamination, and compare it with the pseudo⋆group $\mathcal{G}^*_K$ introduced in Section 9. These two pseudo⋆groups are naturally closely related, as the action of $\mathcal{G}^*_K$ on $\mathbf{R}_0$ studied in previous sections induces an action on the families of curves in the intersection $\mathfrak{M} \cap \mathbf{R}_0$ and thus induce maps in $\mathcal{G}^*_{\mathfrak{M}}$ acting on the transverse Cantor set $\mathfrak{C}$ which parametrizes these curves.

A key difference is that $\mathcal{G}^*_{\mathfrak{M}}$ contains maps defined by the holonomy along all paths in the leaves of $\mathfrak{M}$, and not just those paths following a $\mathcal{K}$-orbit. In particular, the short-cut maps, which play a role in the study of

the entropy for the $\mathcal{G}_K^*$ action, arise naturally from the geometry of the leaves of $\mathfrak{M}$. The dynamics of the $\mathcal{G}_{\mathfrak{M}}^*$ action on the transverse Cantor set $\mathfrak{C}$ defined in (125) provides an alternate source of invariants for the dynamics of the flow Φ_t on $\mathfrak{M}$.

The first invariant studied is the entropy $h_{GLW}(\mathcal{G}_{\mathfrak{M}}^*)$ of the action of $\mathcal{G}_K^*$ on the transverse Cantor set $\mathfrak{C} \subset \mathcal{T}$. We relate this entropy to the entropy for the action of the pseudo⋆group $\mathcal{G}_K^*$ on $\mathfrak{M}_{\mathbf{R}_0}$ as studied in the previous section, and prove that $h_{GLW}(\mathcal{G}_{\mathfrak{M}}^*) = 0$ as is naturally expected.

The main result of this section is that there is a non-zero entropy invariant for the pseudo⋆group $\mathcal{G}_{\mathfrak{M}}^*$ which is obtained by considering "lamination slow entropy" $h_{GLW}^{\alpha}(\mathcal{G}_{\mathfrak{M}}^*)$ for $0 < \alpha \leq 1$. We show in Theorem 21.10 that if the insertion maps σ_i used in the construction of $\mathbb{K}$ have "slow growth", as defined in Definition 21.11, then $h_{GLW}^{1/2}(\mathcal{G}_{\mathfrak{M}}^*) > 0$ for growth constant $\alpha = 1/2$. Thus, even though the flow entropy $h_{top}(\Phi_t|\mathfrak{M}) = 0$, there is enough "chaos" in the orbits of Φ_t and hence in the holonomy action of $\mathcal{G}_{\mathfrak{M}}^*$, to imply that it has positive slow entropy. We also note, at the end of the section, how one can obtain $h_{GLW}(\mathcal{G}_{\mathfrak{M}}^*) > 0$ for the usual entropy by modifying properties of the insertions maps σ_i, which gives a new insight into the results of the Kuperbergs in [27, Section 8].

Recall that $\mathcal{T} = \{z = 0\} \cap \mathbf{R}_0$ is the line segment in $\mathbf{R}_0$ transverse to the interiors of most of the leaves of $\mathfrak{M}$, and $\mathfrak{C} \subset \mathcal{T}$ as defined in (125) is a Cantor set by Proposition 19.4. Let $\mathfrak{M}_{\mathfrak{C}} \subset \mathfrak{M}_{\mathbf{R}_0} = \mathfrak{M} \cap \mathbf{R}_0$ be the union of the path components of $\mathfrak{M}_{\mathbf{R}_0}$ that contain a point in $\mathfrak{C}$.

The holonomy pseudogroup $\mathcal{G}_{\mathfrak{M}}$ for the zippered lamination $\mathfrak{M}$ can be defined using a covering of $\mathfrak{M}$ by foliation charts. The proof of Theorem 19.1 introduced the sections $\mathbf{T}_i$ and their associated Cantor sets $\mathfrak{C}_i$ which form the model spaces for the foliation charts constructed there, and so the holonomy defined using this covering produces a pseudogroup. On the other hand, Corollary 9.14 implies that each leaf in $\mathfrak{M}$ intersects the section $\mathbf{R}_0$ so we can alternately define $\mathcal{G}_{\mathfrak{M}}$ using the induced holonomy maps on the space $\mathfrak{M}_{\mathfrak{C}}$ associated to the transverse Cantor set $\mathfrak{C}$. This reduction yields a pseudogroup $\mathcal{G}_{\mathfrak{M}}$ which is most closely related to our previous constructions, so we assume that $\mathcal{G}_{\mathfrak{M}}$ is defined using the space $\mathfrak{C}$. Also, recall that $\mathfrak{M}_0$ is dense in $\mathfrak{M}$ and the intersection $\mathfrak{M}_0 \cap \mathbf{R}_0$ is dense in $\mathfrak{M}_{\mathbf{R}_0}$ so the holonomy maps of $\mathcal{G}_{\mathfrak{M}}$ can be defined by paths in the leaf $\mathfrak{M}_0$ with endpoints in the transversal $\mathfrak{C}$.

Recall the symmetric generating set for the pseudo⋆group $\mathcal{G}_K^*$

$$\mathcal{G}_K^{(1)} = \{Id, (\psi)^{\pm 1}, (\phi_1^+)^{\pm 1}, (\phi_1^-)^{\pm 1}, (\phi_2^+)^{\pm 1}, (\phi_2^-)^{\pm 1}\}$$

which act on the endpoints of the arcs in $\mathfrak{M}_{\mathfrak{C}}$ and so induce actions of the tree $\mathbf{T}_\Phi$ as discussed in Section 14. The vertices of the tree $\mathbf{T}_\Phi$ are points in $\mathfrak{C}_0$ so we get an induced action on $\mathfrak{C}_0$. We formalize the definitions of the local homeomorphisms defined on subsets of $\mathfrak{M}_{\mathfrak{C}}$ induced by these maps. We first note that $\mathfrak{M}_{\mathfrak{C}}$ "fibers" over $\mathfrak{C}$ in the following sense:

LEMMA 21.1. *There exists a continuous map $\pi_{\mathfrak{M}} \colon \mathfrak{M}_{\mathfrak{C}} \to \mathfrak{C}$, such that for $\xi \in \mathfrak{C}$,*

(1) $\pi_{\mathfrak{M}}(\xi) = \xi$;
(2) $\pi_{\mathfrak{M}}(p_0^k(\xi)) = \xi$ for $k = 1, 2$,

where p_0^k for $k = 1, 2$ are the maps introduced in Section 19. The fibers of the map $\pi_{\mathfrak{M}} \colon \mathfrak{M}_{\mathfrak{C}} \to \mathfrak{C}$ are compact intervals $\pi_{\mathfrak{M}}^{-1}(\xi) \subset \mathbf{R}_0$ whose lengths are bounded above.

Proof. For each $\xi \in \mathfrak{C}$ there exists a maximal connected closed arc in $\mathfrak{M}_{\mathfrak{C}}$ intersecting $\mathcal{T}$ at ξ. Let $p_0^1(\xi)$ be the lower endpoint of this arc contained in $\{z \leq 0\}$, and $p_0^2(\xi)$ the upper endpoint of this arc contained in $\{z \geq 0\}$. For $\eta \in \mathfrak{M}_{\mathfrak{C}}$ there is a unique arc with $\eta \in [p_0^1(\xi), p_0^2(\xi)]$, and we set $\pi_{\mathfrak{M}}(\eta) = \xi$. Then properties (1) and (2) follow by definition.

The continuity of the map $\pi_{\mathfrak{M}}$ follows from the proof of Theorem 19.1. The bound on the lengths of the fibers is a consequence of Theorem 18.1. □

For points in the dense subset $\mathfrak{C}_0 \subset \mathfrak{C}$, the definition of $\pi_{\mathfrak{M}}$ is based on the intersections with $\mathcal{T}$ of the families of γ_0 and λ_0 curves in $\mathbf{R}_0$. That is, each $\xi \in \mathfrak{C}_0$ has the form

$$\xi = \gamma_0(i_1, \ell_1; \cdots ; i_{n-1}, \ell_{n-1}; \ell_n) \cap \mathcal{T} \quad \text{or} \quad \xi = \lambda_0(i_1, \ell_1; \cdots ; i_{n-1}, \ell_{n-1}; \ell_n) \cap \mathcal{T}. \tag{156}$$

Each such curve is defined by the labeling of its endpoints denoted by $p_0^1(\xi)$ for the lower endpoint and $p_0^2(\xi)$ for the upper endpoint. Then for $\eta \in \mathfrak{M}_0 \cap \mathbf{R}_0$ in a γ_0 or λ_0 curve which is an arc, the application $\pi_{\mathfrak{M}}$ takes the point η to the intersection with $\mathcal{T}$ of the γ_0 or λ_0 curve which contains it.

The map ϕ_k^+ for $k = 1, 2$ induces maps $\overline{\phi}_k$ with domains defined by

$$Dom(\overline{\phi}_k) \ = \ \left\{\xi \in \mathfrak{C} \mid p_0^k(\xi) \in Dom(\phi_k^+)\right\} \ . \tag{157}$$

The maps are then formally defined by:

$$\begin{aligned} \overline{\phi}_1(\xi) &= \pi_{\mathfrak{M}}(\phi_1^+(p_0^1(\xi))) \text{ for } \xi \in Dom(\overline{\phi}_1) \\ \overline{\phi}_2(\xi) &= \pi_{\mathfrak{M}}(\phi_2^+(p_0^2(\xi))) \text{ for } \xi \in Dom(\overline{\phi}_2) \ . \end{aligned}$$

The map $\overline{\phi}_k$ has inverse $\overline{\phi}_k^{-1}$ defined on the image of $\overline{\phi}_k$. The action of the maps ϕ_k^+ on the γ_0 curves in $\mathfrak{M}_0$ are illustrated in Figure 34, and the action of the induced maps $\overline{\phi}_k$ on the vertices of the tree $\mathbf{T}_\Phi$ are illustrated in Figure 37, as discussed in Section 14. Note that each map $\overline{\phi}_k$ increases the level of the curve in $\mathfrak{M}_{\mathfrak{C}}$ defining a point $\xi \in \mathfrak{C}$ by 1, for $k = 1, 2$.

Next, we define the map $\overline{\psi} \in \mathcal{G}_{\mathfrak{M}}$ induced by the map ψ. Recall from the discussion in Section 9 that the Wilson flow reverses direction at the annulus $\mathcal{A} = \{z = 0\} \subset \mathbb{W}$, and is anti-symmetric with respect to $\mathcal{A}$. Define the domain of $\overline{\psi}$ by

$$Dom(\overline{\psi}) \ = \ \left\{\xi \in \mathfrak{C} \mid z(p_0^1(\xi)) < 0 \ \& \ z(\psi_-(p_0^1(\xi)))leq 0\right\}, \tag{158}$$

for ψ_- as defined in (32). The map $\overline{\psi}$ is then formally defined by:

$$\overline{\psi}(\xi) \quad = \quad \pi_{\mathfrak{M}}(\psi_-(p_0^1(\xi))) \text{ for } \xi \in Dom(\overline{\psi}) \ .$$

The map $\overline{\psi}$ has inverse $\overline{\psi}^{-1}$ defined on the image of $\overline{\psi}$. The action of ψ and its inverse on the γ_0 curves in $\mathfrak{M}_0$, is illustrated in Figure 34 as the vertical maps. The action of the induced map $\overline{\psi}$ on the vertices of the tree $\mathbf{T}_\Phi$ is given by translation along the center lines in $\mathbf{T}''_\Phi$, as discussed in Section 14. Note that the map $\overline{\psi}$ preserves the level.

DEFINITION 21.2. *Let $\mathcal{G}_{\mathfrak{M}}$ be the pseudogroup generated by the collection of maps*

$$\mathcal{G}_{\mathfrak{M}}^{(1)} \equiv \{\overline{Id}, \overline{\psi}, \overline{\psi}^{-1}, \overline{\phi}_1, \overline{\phi}_1^{-1}, \overline{\phi}_2, \overline{\phi}_2^{-1}\} \ . \tag{159}$$

Let $\mathcal{G}_{\mathfrak{M}}^*$ be the pseudo⋆group *formed by the compositions of maps in $\mathcal{G}_{\mathfrak{M}}^{(1)}$ and the restrictions of these compositions to open subsets of their domains in $\mathfrak{C}$.*

REMARK 21.3. *We do not need to consider the maps ϕ_i^-, since for $\xi \in \mathfrak{C}$ such that $p_0^i(\xi) \in Dom((\phi_i^-)^{-1})$ we have that $p_0^i(\xi) \in Dom(\phi_i^+ \circ \psi^{-1})$ and*

$$\pi_{\mathfrak{M}}((\phi_i^-)^{-1}(\xi)) = \pi_{\mathfrak{M}}(\phi_i^+ \circ \psi^{-1}(p_0^i(\xi)).$$

The action of $\mathcal{G}_{\mathfrak{M}}$ on $\mathfrak{C}$ has a geometric model. Identify the points of $\mathfrak{C}_0$ with the vertices of $\mathbf{T}_\Phi$. Then the discussion in Section 14 gives the actions of the generators in (159) on the tree $\mathbf{T}_\Phi$. This remark is the basis for the proof of the following:

PROPOSITION 21.4. *The holonomy pseudogroup $\mathcal{G}_{\mathfrak{M}}$ of $\mathfrak{M}$ is the pseudogroup acting on $\mathfrak{C}$ defined by the holonomy maps associated to leafwise paths in $\mathfrak{M}$.*

Proof. The leaf $\mathfrak{M}_0$ is dense in $\mathfrak{M}$, so it suffices to consider the holonomy associated to a path $\sigma \colon [0, 1] \to \mathfrak{M}_0$ with $\sigma(0), \sigma(1) \in \mathfrak{C}_0$. As each $\xi \in \mathfrak{C}_0$ corresponds to a vertex of $\mathbf{T}_\Phi$, we can assume that the path $\sigma \colon [0, 1] \to \mathbf{T}_\Phi$. Recall from Section 14 that $\mathbf{T}''_\Phi \subset \mathbf{T}'_\Phi = \mathcal{A} \cap \mathfrak{M}_0$ consists of the line segments in $\mathfrak{M} \cap \mathcal{A}$ which are formed by the intersection of $\mathcal{A}$ with the simple propellers in the construction of $\mathfrak{M}_0$. Then $\mathbf{T}_\Phi$ is formed by adding

continuous curve segments in $\mathfrak{M}_0$ joining the line segments in $\mathbf{T}''_\Phi$, as is illustrated in Figure 36. Thus, the edges of the tree $\mathbf{T}_\Phi$ consists of two types, those which belong to $\mathbf{T}''_\Phi$ and the added connecting paths.

If the path σ traverses a connecting segment, then the holonomy map this induces corresponds to the action of one of the maps $\{\overline{\phi}_1, \overline{\phi}_1^{-1}, \overline{\phi}_2, \overline{\phi}_2^{-1}\}$. If the path σ traverses a segment in $\mathbf{T}''_\Phi$, then the holonomy map this induces corresponds to the action of one of the maps $\{\overline{\psi}, \overline{\psi}^{-1}\}$. Thus, the holonomy maps defined by such σ are contained in $\mathcal{G}_{\mathfrak{M}}$.

Conversely, given a word in $\mathcal{G}_{\mathfrak{M}}$ we can associate a path $\sigma\colon [0,1] \to \mathbf{T}_\Phi$ with $\sigma(0), \sigma(1) \in \mathfrak{C}_0$ using the same correspondence of the generators in $\mathcal{G}^{(1)}_{\mathfrak{M}}$ with segments in $\mathbf{T}_\Phi$, so that every word in $\mathcal{G}_{\mathfrak{M}}$ is associated with the holonomy along a leafwise path. □

As noted in Section 14, $\mathbf{T}_\Phi$ is a tree except for the loop based at the basepoint vertex ω_0. Thus, a path $\sigma\colon [0,1] \to \mathbf{T}_\Phi$ is homotopic with endpoints fixed, to a path which is monotone in level. We derive from this remark the existence of normal forms for words in $\mathcal{G}^*_{\mathfrak{M}}$ exactly as in Proposition 14.3.

The word length on $\mathcal{G}^*_{\mathfrak{M}}$ is defined as before, where $\|\overline{\varphi}\| \leq n$ if $\overline{\varphi}$ can be expressed as a composition of at most n maps in $\mathcal{G}^{(1)}_{\mathfrak{M}}$. Also, define monotone words in $\mathcal{G}^*_{\mathfrak{M}}$ in analogy with Definition 14.1:

DEFINITION 21.5. *A word $\overline{\varphi} \in \mathcal{G}^*_{\mathfrak{M}}$ is said to be* monotone increasing *if it is written in the form*

$$\overline{\varphi} = \overline{\psi}^{\ell_m} \circ \overline{\phi}_{j_m} \circ \overline{\psi}^{\ell_{m-1}} \circ \cdots \circ \overline{\phi}_{j_2} \circ \overline{\psi}^{\ell_1} \circ \overline{\phi}_{j_1} \tag{160}$$

where each $j_k = 1, 2$ and $\ell_k \geq 0$. Set $\mathcal{M}_{\mathfrak{M}}(0) = \{\overline{Id}\}$, and define

$$\mathcal{M}_{\mathfrak{M}}(n) \;=\; \{\overline{\varphi} \in \mathcal{G}^*_{\mathfrak{M}} \mid \overline{\varphi} \text{ monotone } \&\; \|\overline{\varphi}\| \leq n\} \quad ; \quad \mathcal{M}_{\mathfrak{M}}(\infty) \;=\; \bigcup_{n \geq 0} \mathcal{M}_{\mathfrak{M}}(n)\ . \tag{161}$$

The proof of the upper bound estimate on the function $\#\mathcal{M}_{\mathfrak{M}}(n)$ in Proposition 14.5 applies verbatim to the function $\#\mathcal{M}_{\mathfrak{M}}(n)$, and we have:

PROPOSITION 21.6. *For each $b \geq 1$, there is a polynomial function $P_b(n)$ of n such that the cardinality of the set $\mathcal{M}_{\mathfrak{M}}(n)$ satisfies*

$$\#\mathcal{M}_{\mathfrak{M}}(n) \leq P_b(n) \cdot 2^{(n/b)}. \tag{162}$$

The following result is analogous to Corollary 14.6, and the proof follows in the same way.

COROLLARY 21.7. *The cardinality of the set $\mathcal{M}_{\mathfrak{M}}(n)$ of monotone words of length at most n in $\mathcal{G}_{\mathfrak{M}}$ satisfies*

$$\lim_{n \to \infty} \frac{\ln(\#\mathcal{M}_{\mathfrak{M}}(n))}{n} = 0. \tag{163}$$

We then have the following result, which is analogous to Proposition 14.3, and follows from Proposition 21.4 and the comments afterwards.

PROPOSITION 21.8. *Let $\overline{\varphi} \in \mathcal{G}^*_{\mathfrak{M}}$ with $\|\overline{\varphi}\| \leq n$. Then there exists a factorization $\overline{\varphi} = \overline{\varphi}^+ \circ \overline{\varphi}^-$, where $\overline{\varphi}^+ \in \mathcal{M}_{\mathfrak{M}}(n')$ and $(\overline{\varphi}^-)^{-1} \in \mathcal{M}_{\mathfrak{M}}(n'')$ for integers n', n'' with $n' + n'' \leq n$. Moreover, we have $Dom(\overline{\varphi}) \subset Dom(\overline{\varphi}^+ \circ \overline{\varphi}^-)$.*

The factorization $\overline{\varphi} = \overline{\varphi}^+ \circ \overline{\varphi}^-$ is said to be the *normal form* for the word $\overline{\varphi}$.

We conclude this discussion of the structure of $\mathcal{G}^*_{\mathfrak{M}}$ with some remarks concerning the relation between the actions of $\mathcal{G}^*_{\mathfrak{M}}$ and $\mathcal{G}^*_K$. First, recall that the domain $D(\widehat{\Psi})^-_-$ of the the induced action of the Wilson map ψ_- contains the segment $J_0 \subset \mathbf{R}_0$ as defined in (64), and ψ_- defines a strict contraction of J_0 to the fixed point ω_1 which is the upper endpoint of J_0. For the γ_0 and λ_0 curves in $\mathbf{R}_0$ with lower endpoint in J_0, the action of ψ_- on these curves induces the map $\overline{\psi}$ which is a strict contraction to $\omega_0 \in \mathfrak{C}$. Thus, the holonomy pseudogroup

$\mathcal{G}_{\mathfrak{M}}$ contains a contracting fixed point, which is just the holonomy along the loop in $\mathbf{T}_\Phi$ containing the point ω_0.

The second remark concerns the action of ψ on the endpoints of curves in $\mathfrak{M}_{\mathfrak{C}}$ and the action of $\overline{\psi}$ on $\mathbf{T}_\Phi$. Let $\xi \in \mathfrak{C}$ be defined by a γ_0 or λ_0 curve in $\mathfrak{M}_{\mathfrak{C}}$ with endpoints $x = p_0^1(\xi)$ and $\overline{x} = p_0^2(\xi)$ where $r(x) = r(\overline{x}) = r_0 > 2$. Let $k_x \geq 0$ be the exponent such that $\overline{x} = \psi^{k_x}(x)$. Then $x_\ell = \psi^\ell(x)$ for $0 \leq \ell \leq k_x$ is a sequence of points with $r(x_\ell) = r_0$ and $z(x_{\ell+1}) > z(x_\ell)$ for $0 \leq \ell < k_x$. Let m_x be the greatest integer with $m_x \leq k_x/2$. By the anti-symmetry of the Wilson flow, we have $z(x_{m_x}) < 0$ and $z(x_{m_x+1}) \geq 0$. That is, the action of ψ on the curves with lower endpoints $\{x_\ell \mid 0 \leq \ell \leq m_x\}$ produces a sequence of curves whose intersections with $\mathcal{T}$ have decreasing radius. For k_x even, the closest curve to I_0 in the sequence, the innermost curve, corresponds to the endpoint x_{m_x}. When k_x is odd, the closest curve degenerates to the single point x_{m_x+1} with $z(x_{m_x+1}) = 0$. The action of ψ on the endpoints $\{x_\ell \mid m_x < \ell < k_x\}$ then reverses this process, where the endpoints x_0 and x_{k_x} correspond to the same curve in $\mathfrak{M}_{\mathfrak{C}}$ and thus the same point in $\mathfrak{C}$.

For the induced map $\overline{\psi} \in \mathcal{G}^*_{\mathfrak{M}}$ acting on $\mathbf{T}_\Phi$, its action on the vertex $\xi \in \mathfrak{C}_0$ corresponding to the γ_0 or λ_0 curve chosen, defines a sequence of vertices $\overline{\psi}^\ell(\xi) = \pi_{\mathfrak{M}}(x_\ell)$ in $\mathbf{T}_\Phi$ tending to the tip of the propeller containing ξ, as in Figure 36. However, if k_x is even, the point ξ_{m_x} is then the furthest point along this sequence, which is closest to the tip of the propeller. If k_x is odd, ξ_{m_x+1} is the furthest point along the sequence. In terms of the normal forms for words in $\mathcal{G}^*_K$ defined in Proposition 14.3 and the normal forms for words in $\mathcal{G}^*_{\mathfrak{M}}$ defined in Proposition 21.8, this implies that a power ψ^ℓ appearing in (71) can collapse to a power $\overline{\psi}^m$ appearing in (160) with $m < \ell$. We will say that the action of $\mathcal{G}^*_{\mathfrak{M}}$ has "leaf short-cuts", which correspond to the holonomy of a path which goes from a point on one side of a propeller, to a point on the opposite side, avoiding the trip that the action of $\mathcal{G}^*_K$ must follow to the extremal end of the propeller, to get to the point on the opposite side.

Finally, note that Hypothesis 12.2 and the structure of the propellers imply that for $\xi \in Dom(\overline{\psi})$ we have $r(\overline{\psi}(\xi)) < r(\xi)$, as $r(\psi_-(p_0^1(\xi))) = r(p_0^1(\xi))$.

We next discuss the entropy associated to the action of the pseudo⋆group $\mathcal{G}^*_{\mathfrak{M}}$ on $\mathfrak{C}$. Let $\mathcal{T} = \mathcal{A} \cap \mathbf{R}_0$ have the metric defined by the radial coordinate r, and endow $\mathfrak{C} \subset \mathcal{T}$ with the restricted metric, denoted by $d_{\mathfrak{C}}$. For $\epsilon > 0$, say that $\xi_1, \xi_2 \in \mathfrak{C}$ are (n, ϵ)-*separated* if there exists $\overline{\varphi} \in \mathcal{G}^{(n)}_{\mathfrak{M}}$ such that ξ_1, ξ_2 are in the domain of $\overline{\varphi}$, and $d_{\mathfrak{C}}(\overline{\varphi}(\xi_1), \overline{\varphi}(\xi_2)) > \epsilon$. A finite set $\mathcal{S} \subset \mathfrak{C}$ is said to be (n, ϵ)-*separated* if each distinct pair $\xi_1, \xi_2 \in \mathcal{S}$ is (n, ϵ)-separated. Let $s(\mathcal{G}^*_{\mathfrak{M}}, n, \epsilon)$ be the maximal cardinality of an (n, ϵ)-separated subset of $\mathfrak{C}$.

Then as in (129), define the entropy of $\mathcal{G}^*_{\mathfrak{M}}$ by:

$$h_{GLW}(\mathcal{G}^*_{\mathfrak{M}}) = \lim_{\epsilon \to 0} \left\{ \limsup_{n \to \infty} \frac{1}{n} \ln(s(\mathcal{G}^*_{\mathfrak{M}}, n, \epsilon)) \right\}. \tag{164}$$

The entropy $h_{GLW}(\mathcal{G}^*_{\mathfrak{M}})$ is closely related to the entropy $h_{GLW}(\mathcal{G}^*_K | \mathfrak{M}_{\mathfrak{C}})$, as the action of $\mathcal{G}^*_K$ on $\mathbf{R}_0$ and $\mathcal{G}^*_{\mathfrak{M}}$ on $\mathfrak{C}$ are "almost intertwined" by the projection map $\pi_{\mathfrak{M}} \colon \mathfrak{M}_{\mathfrak{C}} \to \mathfrak{C}$ defined in Lemma 21.1. The relation between the entropy for a group action under a factor map suggests that $h_{GLW}(\mathcal{G}^*_{\mathfrak{M}})$ should be bounded above by $h_{GLW}(\mathcal{G}^*_K | \mathfrak{M}_{\mathfrak{C}})$, which vanishes by Theorem 20.14.

The standard argument for factor maps used to prove this result does not actually suffice in the situation we consider, as the "leaf short-cuts" in $\mathcal{G}^*_{\mathfrak{M}}$ (discussed above) imply there are actions in $\mathcal{G}^*_K$ which are collapsed by the map $\pi_{\mathfrak{M}}$. We will use instead a more straightforward approach to the estimation of $h_{GLW}(\mathcal{G}^*_{\mathfrak{M}})$ based on the fact that the space $\mathfrak{C}$ is contained in an interval, and the function $\#\mathcal{G}^{(n)}_{\mathfrak{M}}$ has subexponential growth.

THEOREM 21.9. *Let $\mathbb{K}$ be a generic Kuperberg plug, then $h_{GLW}(\mathcal{G}^*_{\mathfrak{M}}) = 0$.*

Proof. Suppose that $h_{GLW}(\mathcal{G}^*_{\mathfrak{M}}) = \lambda > 0$, then there exists $\epsilon > 0$ and a subsequence of sets $\widehat{E}_{n_i} \subset \mathfrak{C}$ which are ϵ-separated by elements of $\mathcal{G}^{(n_i)}_{\mathfrak{M}}$ and $\#\widehat{E}_{n_i} > \exp(n_i \lambda/2)$. We show this yields a contradiction. Fix a choice of $n = n_i$ such that the set $\widehat{E}_n$ satisfies $\#\widehat{E}_n > \exp(n \lambda/2)$ and is ϵ-separated by elements of $\mathcal{G}^{(n)}_{\mathfrak{M}}$.

Then for each pair $\xi \neq \xi' \in \widehat{E}_n$ there exists $\overline{\varphi} \in \mathcal{G}_{\mathfrak{M}}^{(n)}$ such that $d_{\mathfrak{C}}(\overline{\varphi}(\xi), \overline{\varphi}(\xi')) > \epsilon$. We may assume that the word $\overline{\varphi}$ has the normal form $\overline{\varphi} = \overline{\varphi}^+ \circ \overline{\varphi}^-$ where each of $\overline{\varphi}^+$ and $(\overline{\varphi}^-)^{-1}$ is a monotone word as in (160).

Proposition 21.6 and Corollary 21.7 imply that the function $\#\mathcal{G}_{\mathfrak{M}}^{(n)}$ has subexponential growth. It follows that for n sufficiently large, there exists $\overline{\varphi} \in \mathcal{G}_{\mathfrak{M}}^{(n)}$ and a subset $\widehat{E}_{\overline{\varphi}} \subset \widehat{E}_n \cap Dom(\overline{\varphi})$ with $\#\widehat{E}_{\overline{\varphi}} > \exp(n\,\lambda/4)$ and for each $\xi \neq \xi' \in \widehat{E}_{\overline{\varphi}}$ we have $d_{\mathfrak{C}}(\overline{\varphi}(\xi), \overline{\varphi}(\xi')) > \epsilon$.

Thus we conclude that the set $\overline{\varphi}(\widehat{E}_{\overline{\varphi}}) \subset \mathfrak{C} \subset \mathcal{T}$ is ϵ-separated. This is clearly impossible for n sufficiently large, as the length of $\mathcal{T}$ is finite. □

The above proof that $h_{GLW}(\mathcal{G}_{\mathfrak{M}}^*) = 0$ depends fundamentally on the estimate of the growth rate of the reduced word function $\#\mathcal{G}_{\mathfrak{M}}^{(n)}$. This estimation follows from Proposition 21.6, which implies that this function has exponential growth of arbitrarily small exponent, hence must have subexponential growth. This suggests considering a more sensitive entropy-type invariant, which detects growth rates that are subexponential, yet faster than any polynomial function, in order to obtain non-vanishing dynamical invariants of the action of $\mathcal{G}_{\mathfrak{M}}^*$ on $\mathfrak{C}$. It turns out that such invariants exists in the literature.

The *slow entropy* of a map was introduced in the works of Katok and Thouvenot [24] and Cheng and Li [8], and we adapt this idea for the action of $\mathcal{G}_{\mathfrak{M}}^*$. For $0 < \alpha < 1$, define the α-entropy of $\mathcal{G}_{\mathfrak{M}}^*$, or just the slow entropy, by

$$h_{GLW}^{\alpha}(\mathcal{G}_{\mathfrak{M}}^*) \;=\; \lim_{\epsilon \to 0} \left\{ \limsup_{n \to \infty} \frac{1}{n^{\alpha}} \ln(s(\mathcal{G}_{\mathfrak{M}}^*, n, \epsilon)) \right\} \tag{165}$$

where $0 \leq h_{GLW}^{\alpha}(\mathcal{G}_{\mathfrak{M}}^*) \leq \infty$. If $h_{GLW}^{\alpha}(\mathcal{G}_{\mathfrak{M}}^*) > 0$ and $0 < \beta < \alpha$, then $h_{GLW}^{\beta}(\mathcal{G}_{\mathfrak{M}}^*) = \infty$.

Note that for $0 < \alpha < 1$, the function $\exp(n^{\alpha})$ grows faster than any polynomial function, but is slower than any exponential function, so the invariant $h_{GLW}^{\alpha}(\mathcal{G}_{\mathfrak{M}}^*)$ has the right character for measuring the complexity of the dynamics of $\mathcal{G}_{\mathfrak{M}}^*$

The *entropy dimension* for a continuous transformation $T\colon X \to X$ of a compact metric space X was introduced by de Carvalho [10], and studied further by Cheng and Li [8]. We define an analogous invariant for the pseudo⋆group action of $\mathcal{G}_{\mathfrak{M}}^*$ on $\mathfrak{C}$, given by the number $0 \leq D(\mathcal{G}_{\mathfrak{M}}^*) \leq 1$ defined by

$$D(\mathcal{G}_{\mathfrak{M}}^*) = \inf\{\alpha \mid 0 < \alpha \leq 1 \text{ and } h_{GLW}^{\alpha}(\mathcal{G}_{\mathfrak{M}}^*) = 0\}\ . \tag{166}$$

The proof of Theorem 21.9 suggests that to show $h_{GLW}^{\alpha}(\mathcal{G}_{\mathfrak{M}}^*) \neq 0$ for some α, it suffices to estimate the growth rate of the function $\#\mathcal{G}_{\mathfrak{M}}^{(n)}$ more precisely. This, in turn, requires a more precise accounting for what monotone words of the form (160) actually exist in $\mathcal{G}_{\mathfrak{M}}^{(n)}$. This is an extremely difficult question to answer in general, but we next describe further hypotheses on the construction of $\mathbb{K}$, the notion of "slow growth" in Definition 21.11 and "fast growth" in Definition 21.12 below, which makes a lower bound estimate possible. We obtain three results, Theorems 21.10, 21.17 and 21.18 below. Due to the highly technical nature of the proofs and the estimates required, we present in detail only the proof of the following:

THEOREM 21.10. *Let Φ_t be a generic Kuperberg flow. If the insertion maps σ_j have "slow growth" in the sense of Definition 21.11, then $h_{GLW}^{1/2}(\mathcal{G}_{\mathfrak{M}}) > 0$, and thus $1/2 \leq D(\mathcal{G}_{\mathfrak{M}}^*) \leq 1$.*

The strategy of the proof of Theorem 21.10 is to develop an "admissibility criterion" for strings $I = (\ell_1, \ldots, \ell_m)$ and $J = (j_1, \ldots, j_m)$ such that for each admissible pair (I, J), we obtain a point $\xi_{(I,J)} \in \mathfrak{C}_0$ by the expression

$$\xi_{(I,J)} = \overline{\varphi}_{(I,J)}(\omega_0) = \overline{\psi}^{\ell_m} \circ \overline{\phi}_{j_m} \circ \overline{\psi}^{\ell_{m-1}} \circ \cdots \circ \overline{\phi}_{j_2} \circ \overline{\psi}^{\ell_1} \circ \overline{\phi}_{j_1}(\omega_0). \tag{167}$$

Then observe that the images of the maps $\overline{\phi}_j$ on their domains in $\mathfrak{M}_{\mathfrak{C}}$ are contained in the disjoint compact regions bounded by the parabolic curves $\Gamma_0(a)$ or $\Lambda_0(a)$, according to whether $j = 1$ or 2. The parabolic curves $\Gamma_0(a)$ and $\Lambda_0(a)$ define disjoint compact subsets $I(\Gamma_0), I(\Lambda_0) \subset \mathfrak{C}$, where $I(\Gamma_0)$ consists of the points

$\xi \in \mathfrak{C}$ whose corresponding path component in $\mathfrak{M}_{\mathbf{R}_0}$ is contained in the closure of the region bounded by Γ_0, and similarly for $I(\Lambda_0)$. Then choose $\varepsilon_0 > 0$ such that

$$\varepsilon_0 < \inf\{d_{\mathfrak{C}}(\pi_{\mathfrak{M}}(\xi), \pi_{\mathfrak{M}}(\xi')) \mid \xi \in I(\Gamma_0) \ , \ \xi' \in I(\Lambda_0)\} \ . \tag{168}$$

Two points $\xi = \overline{\varphi}_{(I,J)}(\omega_0), \xi' = \overline{\varphi}_{(I',J')}(\omega_0) \in \mathfrak{C}$ where J and J' have $\ell_m = \ell'_m = 0$, and terminate with distinct indices $j_m \neq j'_{m'}$ will then be ε_0-separated in $\mathfrak{C}$. The strategy is then to construct collections of points via formula (167) which are $(\mathcal{G}^*_{\mathfrak{M}}, \varepsilon_0, n)$-separated. The key technical problem is to estimate the number of admissible strings which give rise to $(\mathcal{G}^*_{\mathfrak{M}}, \varepsilon_0, n)$-separated points in this way, using words in $\mathcal{G}^*_K$.

Recall that the difference between $\mathcal{G}^*_{\mathfrak{M}}$ and $\mathcal{G}^*_K$ is that in the former we allow the leaf short-cuts which replace terms ψ^ℓ in (71) with terms $\overline{\psi}^m$ in (160) where $m \leq \ell$. The leaf short-cuts only arise when applying the map ψ repeatedly to a point $\xi \in \mathbf{R}_0$ with $z(\xi) < 0$, such that we eventually have $z(\psi^\ell(\xi)) > 0$. In particular, they do not arise for the orbits $p_0(j; 1, \ell) = \psi^\ell(\phi_j^+(\omega_j))$ for $j = 1, 2$.

Introduce the involution $\iota \colon \mathbf{R}_0 \to \mathbf{R}_0$ defined by $\iota(r, \pi, z) = (r, \pi, -z)$. For a point $\xi \in \mathfrak{C}$, the action of ι switches the endpoints $p_0^1(\xi)$ and $p_0^2(\xi)$ of the γ_0 or λ_0 arc in $\mathbf{R}_0$ through ξ, as in the proof of Lemma 21.1. In particular, ι induces the identity map on $\mathfrak{C}$.

Extend the symmetric generating set in (146) for the pseudo$\star$group $\mathcal{G}^*_K$ by adding the element ι restricted to $\mathfrak{M}_{\mathbf{R}_0}$, to obtain

$$\widehat{\mathcal{G}}^{(1)}_K = \{Id, \iota, (\psi)^{\pm 1}, (\phi_1^+)^{\pm 1}, (\phi_1^-)^{\pm 1}, (\phi_2^+)^{\pm 1}, (\phi_2^-)^{\pm 1}\} \ . \tag{169}$$

Let $\widehat{\mathcal{G}}^*_K$ denote the augmented pseudo$\star$group generated by this set. Then the problem is to obtain criteria for the existence for sufficient numbers of words in $\widehat{\mathcal{G}}^*_K$ that generate $(\mathcal{G}^*_{\mathfrak{M}}, \varepsilon_0, n)$-separated sets in $\mathfrak{C}$ with sufficient growth rates.

The proof that the composition $\overline{\varphi}_{(I,J)}$ in (167) is defined at ω_0 requires technical estimates analogous to those used in the proof of Theorem 17.1. The existence of a point $\xi_{(I,J)}$ is interpreted as a statement about the composition of generators of the pseudogroup $\widehat{\mathcal{G}}^*_K$, which requires a careful analysis of the dynamics of $\widehat{\mathcal{G}}^*_K$ near the special points $\omega_i \in \mathbf{R}_0$. This leads to estimates which give sufficient conditions for (I, J) to be admissible, so that the point $\xi_{(I,J)}$ is well-defined.

For simplicity we assume that $a = 0$, for a as in Remark 13.3.

Observe that for a word $\overline{\varphi}_{(I,J)}$ as in (167), the initial composition $\overline{\psi}^{\ell_1} \circ \overline{\phi}_{j_1}(\omega_0)$ corresponds to a γ_0 or λ_0 curve whose lower endpoint is the point $p_0(j_1; 1, \ell_1) \in J_0$. Then $\pi_{\mathfrak{M}}(\phi^+_{j_2}(p_0(j_1; j_2, \ell_1)))$ must lie in the domain of the remaining factor $\overline{\varphi}_{(I',J')}$ defined by $\overline{\varphi}_{(I,J)} = \overline{\varphi}_{(I',J')} \circ \overline{\phi}_{j_2} \circ \overline{\psi}^{\ell_1} \circ \overline{\phi}_{j_1}$. However, if $j_2 = 2$, it is necessary to apply the involution ι to the point $p_0(j_1; 1, \ell_1)$ to obtain a point in the domain of ϕ_2^+, as will be seen in the subsequent construction of separated sets.

Recall the integer valued function $N(r)$ for $2 < r < 3$ introduced in Section 6, which is defined using the function $\delta(r)$ in (19). The function $N(r)$ is an upper bound on the number of insertion maps that can be applied to a point $\xi \in \mathbf{R}_0$ with $r(\xi) = r$, and $N(r)$ is unbounded as r decreases to $r = 2$. In particular, $N(r)$ for $r = r(\phi^+_{j_2}(p_0(j_1; j_2, \ell_1)))$ provides an upper bound on the number of subsequent maps $\overline{\phi}_{j_k}$ which can appear in the remaining term $\overline{\varphi}_{(I',J')}$ for an admissible word $\overline{\varphi}_{(I,J)}$. Thus, a more precise estimate on the growth rate of the function $N(r)$ for $r > 2$ will yield estimates on the growth rates of sets of (ϵ, n)-separated points for $\mathcal{G}^*_{\mathfrak{M}}$.

The growth rate of the function $N(r)$ for $r > 2$ is closely related to the geometry of the embedding maps ϕ_i^+ for $i = 1, 2$ near the special points $\omega_i \in \mathbf{R}_0$ as defined in (27), which we next consider. We use the assumptions in Hypotheses 12.2 and 17.2 to analyze the properties of the maps ϕ_i^+ on sufficiently small neighborhoods of the points ω_i.

Recall that the first transition point for the forward $\mathcal{K}$-orbit of ω_i is the special entry point $p_i^- \in E_i$ and its backward $\mathcal{K}$-orbit is the special exit point $p_i^+ \in S_i$ as illustrated in Figure 16. For $\epsilon > 0$, define the closed

squares in $\mathbf{R}_0$ centered on the special points ω_i for $i = 1, 2$,

$$S_{\mathbf{R}_0}(\omega_i, \epsilon) = \{(r, \pi, z) \mid |r - 2| \leq \epsilon \text{ and } |z - (-1)^i| \leq \epsilon\} \ ,$$

and let $D_{\mathbf{R}_0}(\omega_i, \epsilon) \subset \mathbf{R}_0$ be the closed ball centered at ω_i with radius ϵ. Then $S_{\mathbf{R}_0}(\omega_i, \epsilon/\sqrt{2}) \subset D_{\mathbf{R}_0}(\omega_i, \epsilon)$.

We next choose $\epsilon_0' > 0$ so that the various generic hypotheses apply to the points in $S_{\mathbf{R}_0}(\omega_i, \epsilon_0')$. Recall that the constant $\epsilon_0 > 0$ was chosen in Hypothesis 12.2 so that the estimate (94) holds for the Wilson vector field $\mathcal{K}$ on the disk $D_{\mathbf{R}_0}(\omega_1, \epsilon_0)$. Recall that for the same ϵ_0, we assumed that Hypothesis 17.2 on the insertion maps σ_i for $i = 1, 2$, holds for $2 \leq r_0 \leq 2 + \epsilon_0$ and $\theta_i - \epsilon_0 \leq \theta \leq \theta_i + \epsilon_0$.

Choose $0 < \epsilon_0' \leq \epsilon_0/\sqrt{2}$ sufficiently small so that $S_{\mathbf{R}_0}(\omega_i, \epsilon_0') \subset Dom(\phi_i^+)$ for $i = 1, 2$.

Moreover, require that the forward Φ_t-flow of $S_{\mathbf{R}_0}(\omega_i, \epsilon_0')$ to the surface E_i is contained in the rectangular domain for Hypothesis 17.2. This automatically holds for the r coordinate, as the flow Φ_t preserves the radius coordinate along these trajectories, but the condition $\theta_i - \epsilon_0 \leq \theta \leq \theta_i + \epsilon_0$ on the image in E_i imposes a restraint on the choice ϵ_0'.

Thus, Hypothesis 12.2 applies for the Wilson return map ψ near ω_i and Hypothesis 17.2 applies for the radial coordinates of the return map ϕ_i^+ near ω_i.

Consider first the map ϕ_1^+. By Hypothesis 12.1, the "parabolic function" $z \mapsto r(\phi_1^+(2, \pi, z))$ has a minimum value 2 at $z = -1$. Then

$$2 = r(\phi_1^+(\omega_1)) \ < \ r(\phi_1^+(r, \pi, z))) \text{ for all } (r, \pi, z) \neq \omega_1 \text{ with } r \geq 2. \tag{170}$$

Moreover, Hypothesis 17.2 implies that the images of the vertical lines $r = c$ for $2 \leq c \leq 2 + \epsilon_0'$ in the neighborhood of ω_1 are mapped by ϕ_1^+ to parabolic curves, so that $z \mapsto r(\phi_1^+(c, \pi, z))$ has a minimum value at a unique value $z = \zeta_1(c)$. Thus the forward orbit of $(c, \phi, \zeta_1(c))$ intersects E_1 in a point with z-coordinate equal to -1. Set $\rho_1(c) = r(\phi_1^+(c, \pi, \zeta_1(c))) > 2$.

For each $2 \leq c \leq 2 + \epsilon_0'$ the function $z \mapsto r(\phi_1^+(c, \pi, z))$ has vertex point $(\zeta_1(c), \rho_1(c))$. The graph of this function near the point $(\zeta_1(c), \rho_1(c))$ has upward parabolic shape, where $\zeta_1(c)$ gives the "offset" of the parabolic vertex along the z-axis.

Hypothesis 17.2 implies that the function $c \mapsto \zeta_1(c)$ is a smooth function of c with $\zeta_1(2) = -1$ and $-1 - \epsilon_0' \leq \zeta_1(c) \leq -1 + \epsilon_0'$. We also have that the function $c \mapsto \rho_1(c)$ is smooth, with $\rho_1(2) = 2$ and $c \mapsto \rho_1(c)$ is strictly increasing for $c > 2$. Moreover, there exists $0 < \alpha_1 \leq \beta_1$ such that for $2 \leq c \leq 2 + \epsilon_0'$ we have the quadratic bounds

$$\rho_1(c) + \alpha_1 \cdot (z - \zeta_1(c))^2 \ \leq \ r(\phi_1^+(c, \pi, z)) \leq \rho_1(c) + \beta_1 \cdot (z - \zeta_1(c))^2 \ . \tag{171}$$

The map ϕ_2^+ near ω_2 admits a similar analysis, yielding functions $c \mapsto \zeta_2(c)$ and $c \mapsto \rho_2(c)$ with the properties $1 - \epsilon_0' \leq \zeta_2(c) \leq 1 + \epsilon_0'$ for $2 \leq c \leq 2 + \epsilon_0'$ and constants $0 < \alpha_2 \leq \beta_2$ for which there is the quadratic estimate

$$\rho_2(r) + \alpha_2 \cdot \ (z - \zeta_2(c))^2 \ \leq \ r(\phi_2^+(r, \pi, z)) \leq \rho_2(r) + \beta_2 \cdot \ (z - \zeta_2(r))^2 \ . \tag{172}$$

Set $\alpha_\Phi = \min\{\alpha_1, \alpha_2\}$ and $\beta_\Phi = \max\{\beta_1, \beta_2\}$.

We also have that the function $c \mapsto \zeta_i(c)$ is smooth with $\zeta_i(2) = (-1)^i$, for $i = 1, 2$, so there exists a constant $\widehat{\zeta} \geq 0$ so that

$$|\zeta_i(c) - (-1)^i| \leq \widehat{\zeta} \cdot |c - 2| \quad \text{for } 2 \leq c \leq 2 + \epsilon_0'. \tag{173}$$

That is, the vertical offset of each parabolic curve $z \mapsto r(\phi_1^+(c, \pi, z))$ has a linear bound as a function of $(c-2)$, for $2 \leq c \leq 2 + \epsilon_0'$.

Recall that we require an estimate on the function $N(r)$ introduced in Section 6, for r near 2, and this is defined in terms of the function $\delta(r)$ defined in (19). Using the normal forms (171) and (172), observe that $\delta(r) = \min\{\rho_1(r), \rho_2(r)\}$ for $2 \leq r \leq 2 + \epsilon_0'$. We introduce two classes for the functions ρ_i which are

determinant in the behavior of the function $N(r)$. Note that each function ρ_i is smooth and strictly increasing, so its derivative $\rho_i'(r) \geq 1$ for all $2 \leq r \leq 2 + \epsilon_0'$.

DEFINITION 21.11. *The insertions σ_j are said to have* slow growth *if the derivatives $\rho_i'(2) = 1$ for $i = 1, 2$. In this case, there exists $C_\rho > 0$ and uniform estimates on $\rho_i(r)$,*

$$r < \rho_i(r) \ \leq \ r + C_\rho \, (r-2)^2 \quad \text{for } 2 < r \leq 2 + \epsilon_0'. \tag{174}$$

DEFINITION 21.12. *The insertions σ_i are said to have* fast growth *if there exists $\lambda > 1$ such that derivatives $\rho_i'(r) \geq \lambda$ for $2 \leq r \leq 2 + \epsilon_0'$ with $i = 1, 2$. In this case, we have the uniform estimate,*

$$\rho_i(r) \ \geq 2 + \lambda \, (r-2) \quad \text{for } 2 \leq r \leq 2 + \epsilon_0'. \tag{175}$$

These two properties of the insertion maps are sufficient to obtain the required estimates on the domains for the maps $\overline{\varphi}_{(I,J)}$ as discussed above. We also require some preliminary estimates which describe the quantitative behavior of the map ψ near the special point ω_1. The derivation of these estimates is similar to those in Section 17, so the arguments are only briefly sketched.

Let $\xi = (r, \pi, z) \in \mathbf{R}_0$. Define times $0 = T_0(\xi) < T_1(\xi) < T_2(\xi) < \cdots$ where $\psi^\ell(\xi) = \Psi_{T_\ell(\xi)}(\xi)$ for $\ell \geq 0$ such that $\psi^\ell(\xi)$ is defined. Then $r(\psi^\ell(\xi)) = r(\xi)$, and by (95) we have

$$z(\psi^{\ell+1}(\xi)) - z(\psi^\ell(\xi)) \ = \ \int_{T_\ell(\xi)}^{T_{\ell+1}(\xi)} g(\Psi_s(\xi)) \, ds. \tag{176}$$

The return time for the flow Ψ_t at ξ is $2\pi \cdot r(\xi)$, so for ξ with $2 \leq r(\xi) \leq 2 + \epsilon_0$, the domain of the integral in (176) satisfies $4\pi \leq T_{\ell+1}(\xi) - T_\ell(\xi) \leq (4 + 2\epsilon_0')\pi$. Moreover, Hypothesis 12.2 implies that $g(r, \theta, z)$ is a non-decreasing function of $r \geq 2$, hence (176) yields

$$z(\psi^\ell(r', \pi, z)) \geq z(\psi^\ell(r, \pi, z)) \quad \text{for } r' > r \geq 2. \tag{177}$$

Recall that $g(\xi) = 1$ if $r(\xi) \geq 2 + \epsilon_0$, so for $\xi \in \mathbf{R}_0$ with $r(\xi) \geq 2 + \epsilon_0$, the orbit $\Psi_t(\xi)$ escapes the plug $\mathbb{W}$ at a time $t = 4 - z(\xi) \leq 6$, hence does not complete a full revolution. Moreover, if $\xi \in \mathbf{R}_0$ satisfies $r(\xi) = 2$ and $-2 \leq z \leq -1 - \epsilon_0$, then $\psi(\xi)$ is defined and satisfies $-(1 + \epsilon_0) < z(\psi(\xi)) < -1$.

In particular, let $\xi_0 = \phi_j^+(\omega_j)$ for $j = 1, 2$, so that $r(\xi_0) = 2$, then we have

$$z(p_0(j; 1, 0)) = z(\psi(\xi_0)) > -(1 + \epsilon_0).$$

We can thus take $\ell_0 = 1$ in Lemma 17.5 so that for $\ell \geq 1$, the estimates (96) and (97) hold for $\psi^\ell(\xi_0) = p_0(j; 1, \ell)$.

LEMMA 21.13. *There exists constants $0 < \mu_1 = 4\pi\lambda_1 \leq 4\pi\lambda_2 < \mu_2$ and $b_0 > 0$ such that for $\ell \geq b_0$, for $j = 1, 2$, the point $p_0(j; 1, \ell)$ satisfies*

$$-1 - 1/(\mu_1 \, \ell) \ < \ z(p_0(j; 1, \ell)) \ < \ -1 - 1/(\mu_2 \, \ell) \ . \tag{178}$$

Proof. Following the notation as in Lemma 17.5, set $\mu_1 = 4\pi\lambda_1$ and choose $4\pi\lambda_2 < \mu_2 < 8\pi\lambda_2$. Then for $b_0 \geq C_3/(\mu_2 - 4\pi\lambda_2)$, (178) follows from (96) of Lemma 17.5. □

Consider next the case where $\xi \in \mathbf{R}_0$ with $-2 \leq z(\xi) < -1$ and $2 < r(\xi) < 2 + \epsilon_0'$. Then the $\mathcal{W}$-orbit $\Psi_t(\xi)$ escapes from $\mathbb{W}$ in finite time, and thus $\psi^\ell(\xi)$ is only defined for a finite range of ℓ, where $\ell \to \infty$ as $r(\xi)$ approaches 2. The next two results give an estimate for the range of ℓ for which $z(\psi^\ell(\xi)) \leq -1 + \epsilon_0'$, using methods analogous to those used in the proofs of Lemmas 17.8, 17.9 and 17.11.

LEMMA 21.14. *There exists constants $U_g > 0$ and $0 < \epsilon_1 < \epsilon_0'$ such that for all $0 < \epsilon \leq \epsilon_1$ and $\xi \in \mathbf{R}_0$ with $z(\xi) \leq -(1 + \epsilon)$ and $2 \leq r(\xi) \leq 2 + \epsilon$, then there exists $\ell_\xi > 0$ so that*

$$-1 - \epsilon \ \leq \ z(\psi^\ell(\xi)) \ \leq \ -1 + \epsilon \quad \text{for all} \quad \ell_\xi \leq \ell \leq \ell_\xi + U_g/\epsilon \ . \tag{179}$$

Proof. Recall from Section 12 that Hypothesis 12.2 and condition (44) imply there exists constants A_g, B_g, C_g such that the quadratic form $Q_g(u,v) = A_g\, u^2 + 2B_g\, uv + C_g\, v^2$ defined by the Hessian of g at ω_1 is positive definite. The remainder term for the quadratic Taylor approximation to $g(r,\theta,z)$ is dominated by a scalar multiple of $d_{\mathbb{W}}(\xi,\mathcal{O}_1)^3$, where $d_{\mathbb{W}}(\xi,\mathcal{O}_1) = \sqrt{(r-2)^2 + (z+1)^2}$ denotes the distance from $\xi = (r,\theta,z)$ to the periodic orbit $\mathcal{O}_1$. As $Q_g(u,v)$ is positive definite, there exists $0 < \epsilon_2 \leq \epsilon_0'$ so that for $\xi = (r,\theta,z)$

$$|g(\xi) - Q_g(r-2, z+1)| \;\leq\; Q_g(r-2,z+1)/4 \quad \text{for} \quad d_{\mathbb{W}}(\xi,\mathcal{O}_1) \leq \epsilon_2. \tag{180}$$

Let λ_2 denote the maximum eigenvalue of the quadratic form Q_g. Then for $0 < \epsilon \leq \epsilon_2/\sqrt{2}$ we have by (180)

$$\max\{g(\xi) \mid \xi = (r,\theta,z)\ ,\ |z+1| \leq \epsilon \text{ and } |r-2| \leq \epsilon\} \;\leq\; 4\lambda_2\, \epsilon^2\ . \tag{181}$$

Let $\epsilon_1 = \min\{\epsilon_2/\sqrt{2}, 1/(24\pi\,\lambda_2)\}$.

Given $0 < \epsilon \leq \epsilon_1$ and $\xi \in \mathbf{R}_0$ with $z(\xi) \leq -(1+\epsilon)$ and $2 \leq r(\xi) \leq 2+\epsilon$, we show (179) holds.

First, note there exist $t_1 \geq 0$ so that $z(\Psi_{t_1}(\xi)) = -(1+\epsilon)$. Let $t_2 \geq t_1$ be the first subsequent time for which $\Psi_{t_2}(\xi) \in \mathbf{R}_0$. Then there exists $\ell_\xi \geq 0$ so that $\Psi_{t_2}(\xi) = \psi^{\ell_\xi}(\xi)$. Set $\xi_* = \Psi_{t_2}(\xi)$.

Note that $z(\xi_*) \geq -(1+\epsilon)$ and $t_2 - t_1 \leq 2\pi\, r(\xi) < 6\pi$, so by (176) and (181) we have

$$0 \;\leq\; z(\Psi_{t_2}(\xi)) - z(\Psi_{t_1}(\xi)) \;<\; 4\lambda_2\,\epsilon^2 \cdot 6\pi \;=\; 24\pi\lambda_2\,\epsilon^2\ . \tag{182}$$

As $z(\Psi_{t_1}(\xi)) = -(1+\epsilon)$ this yields

$$-(1+\epsilon) \;\leq\; z(\xi_*) \;<\; -(1+\epsilon) + 24\pi\lambda_2\,\epsilon^2 \;\leq\; -(1+\epsilon) + \epsilon \;=\; -1$$

The same reasoning yields, for $\ell > 0$ such that $z(\psi^\ell(\xi_*)) \leq -1+\epsilon$, then

$$z(\psi^\ell(\xi_*)) - z(\psi^{\ell-1}(\xi_*)) \;<\; 24\pi\lambda_2\,\epsilon^2 \;\leq\; \epsilon\ . \tag{183}$$

Set $U_g = 1/(24\pi\lambda_2)$. It then follows by applying (183) recursively, that for $\ell \leq U_g/\epsilon$ we have

$$0 < z(\psi^\ell(\xi_*)) - z(\xi_*) \leq \ell \cdot 24\pi\lambda_2\,\epsilon^2 \leq (U_g/\epsilon)\cdot(24\pi\lambda_2\,\epsilon^2) \;=\; \epsilon\ . \tag{184}$$

It follows that for $0 \leq \ell \leq U_g/\epsilon$ we have

$$-(1+\epsilon) \;\leq\; z(\xi_*) \;<\; z(\psi^\ell(\xi_*)) \;\leq\; z(\xi_*) + \epsilon \;\leq\; -1+\epsilon$$

which was to be shown. □

Next, we give a form of density estimate for the flow Φ_t. Recall that for $j = 1, 2$, the function $\zeta_j(c)$ is the "offset" of the vertex of the parabolic graph $z \mapsto \phi_j^+(c,\pi,z)$. The function satisfies $\zeta_j(2) = (-1)^j$ and there is $\widehat{\zeta} > 0$ so that the bounds (173) hold for $j = 1, 2$.

LEMMA 21.15. *Let $0 < \epsilon_1 < \epsilon_0'$ be the constant of Lemma 21.14. Then there exists $L_g > 0$ so that for all $0 < \epsilon \leq \epsilon_1$ and $\xi \in \mathbf{R}_0$ with $-(1+\epsilon) \leq z(\xi) \leq -(1+\epsilon/2)$ and $2 \leq r(\xi) \leq 2 + \min\{1, 1/\widehat{\zeta}\}\cdot\epsilon/2$, then there exists $0 \leq \ell_* \leq L_g/\epsilon$ so that*

$$0 < |z(\psi^{\ell_*}(\xi)) - (-1)^j\, \zeta_j(r(\xi))| \;<\; \epsilon\ . \tag{185}$$

Proof. If $\zeta_1(r(\xi) \leq -1$ or $\zeta_2(r(\xi) \geq 1$, then there is nothing to show. In fact, we need only consider the case where $r_0 = r(\xi)$ is such that $2 < r_0 \leq \epsilon/2 \cdot \min\{1, 1/\widehat{\zeta}\}$ and $-1+\epsilon \leq \zeta_1(r_0) < -1 + \widehat{\zeta}\cdot(r_0 - 2) \leq -1 + \epsilon/2$. It then suffices to estimate the least value of $\ell_* > 0$ such that $\psi^{\ell_*}(\xi) > -1 - \epsilon/2$.

Let λ_1 denote the minimum eigenvalue of the quadratic form Q_g. By (180) there is a lower bound

$$\min\ \{g(\xi) \mid \xi = (r,\theta,z)\ ,\ \epsilon/2 \leq |z+1| \leq \epsilon \text{ and } |r-2| \leq \epsilon\} \;\geq\; \lambda_1\,\epsilon^2/(4\cdot 1.01) \geq \lambda_1\,\epsilon^2/5\ . \tag{186}$$

By (176) and (186), and using that the flow Φ_t has return time at least 4π for $r_0 > 2$, if $-1-\epsilon \leq z(\xi) < z(\psi(\xi)) \leq -1 - \epsilon/2$, then we have

$$0 \;\leq\; z(\psi(\xi)) - z(\xi) \;\geq\; 4\pi\,\lambda_1\,\epsilon^2/5\ . \tag{187}$$

Thus, the least ℓ_* satisfies the estimate $\ell_* \cdot 4\pi\,\lambda_1\,\epsilon^2/5 \leq \epsilon/2$, so for $L_g = 5/(8\pi\,\lambda_1)$ there exists $\ell_* \leq L_g/\epsilon$ such that (185) holds. □

After these preliminary considerations, we return to the proof of Theorem 21.10. We consider monotone words in $\mathcal{G}^*_{\mathfrak{M}}$ of the form (160), and their lifts to monotone words in $\widehat{\mathcal{G}}^*_K$.

We assume that the insertion maps σ_j satisfy Definition 21.11, with C_ρ the constant so that (174) is satisfied. Also, recall $\beta_\Phi = \max\{\beta_1, \beta_2\}$ for the constants β_j as defined by (171), (172), and $\widehat{\zeta} \geq 0$ was defined so that the estimate (173) holds. Then define $C_\Phi = \max\{1, C_\rho, \beta_\Phi\}$.

Let $0 < \epsilon < \min\{\epsilon_1, 1/C_\Phi\}$ for ϵ_1 as defined in Lemma 21.14.

By Lemma 21.13, there exists an integer $b_1 \geq 1$ such that for $\ell \geq b_1$, for $k = 1, 2$, the point $p_0(k; 1, \ell)$ satisfies the estimates in (178). For $m \geq 1$, let $b_m = m\,b_1$. Then $1/(\mu_1\,b_m) \leq \epsilon/m \leq 1/(mC_\Phi)$.

Now consider strings $I = (\ell_1, \ldots, \ell_m)$ and $J = (j_1, \ldots, j_m)$. We develop a criteria for when the point $\xi_{(I,J)} = \overline{\varphi}_{(I,J)}(\omega_0)$ as in (167) is defined. Take $p_0(j_1; 1, 0) = \phi^+_{j_1}(\omega_{j_1})$ for $j_1 = 1, 2$. Assume that $\ell_1 \geq b_m$ and set $(r_1, \pi, z_1) = \psi^{\ell_1}(p_0(j_1; 1, 0)) = p_0(j_1; 1, \ell_1)$. Then $r_1 = 2$ and $z_1 < -1$. Set $\upsilon_1 = |z_1 + 1|$ so that $0 < \upsilon_1 \leq \epsilon/m$ by the choice of ℓ_1.

For $j_2 = 1$, we have $\phi^+_1(p_0(j_1; 1, \ell_1)) = p_0(j_1; 1, \ell_1; 1, 0)$, while for $j_2 = 2$, we use the involution ι to obtain

$$\phi^+_2(\iota(p_0(j_1; 1, \ell_1))) = \phi^+_2(p_0(j_1; 2, \ell_1)) = p_0(j_1; 2, \ell_1; 1, 0).$$

These points are well-defined by the choice of ℓ_1.

Set $r_2 = r(p_0(j_1; j_2, \ell_1; 1, 0))$, then by the quadratic estimates (171) or (172) for $r_1 = 2$ and so $\rho_{j_1}(r_1) = 2$, we have

$$2 + \alpha_\Phi \cdot \upsilon_1^2 \;\leq\; r_2 \leq 2 + \beta_\Phi \cdot \upsilon_1^2 \leq 2 + \beta_\Phi \cdot (\epsilon/m)^2 < 2 + \epsilon/m^2 \tag{188}$$

since $\beta_\Phi\,\epsilon \leq C_\Phi\,\epsilon < 1$. Thus, $r_2 < 2 + \epsilon/m$.

Now set $b'_m = b_m + m\,L_g/\epsilon$ for $L_g = 5/(8\pi\,\lambda_1)$ as defined in Lemma 21.15, so $b'_m \leq m\,\{1/\mu_1 + 5/(8\pi\,\lambda_1)\}/\epsilon$. Then by Lemmas 21.14 and 21.15 applied for ϵ/m we can choose $\ell_2 \leq b'_m$ so that

$$(r_2, \pi, z_2) = p_0(j_1; j_2, \ell_1; 1, \ell_2) = \psi^{\ell_2}(p_0(j_1; j_2, \ell_1; 1, 0))$$

is defined with $|z_2 + 1| \leq \epsilon/m$, and the vertical "offset" along the line $r = r_2$ is given by

$$\upsilon_2 = |z_2 - \zeta_{j_2}(r_2)| \leq \epsilon/m\ . \tag{189}$$

For $j_3 = 1, 2$, we get

$$\begin{aligned} p_0(j_1; j_2, \ell_1; 1, \ell_2; 1, 0) &= \phi^+_1(p_0(j_1; j_2, \ell_1; 1, \ell_2)) \\ p_0(j_1; j_2, \ell_1; 2, \ell_2; 1, 0) &= \phi^+_2(\iota(p_0(j_1; j_2, \ell_1; 1, \ell_2))) \end{aligned}$$

Let $r_3 = r(p_0(j_1; j_2, \ell_1; j_3, \ell_2; 1, 0))$, then by the quadratic estimates (171) or (172), the "slow estimate" (174), and the inductive estimates (188) and (189), we have

$$\begin{aligned} r_3 &\leq \rho_{j_2}(r_2) + \beta_\Phi \cdot \upsilon_2^2 \\ &\leq [r_2 + C_\rho \cdot (r_2 - 2)^2] + [\beta_\Phi \cdot (\epsilon/m)^2] \\ &\leq [2 + \beta_\Phi \cdot (\epsilon/m)^2] + [C_\rho \cdot (\beta_\Phi \cdot (\epsilon/m)^2)^2] + [\beta_\Phi \cdot (\epsilon/m)^2] \\ &= 2 + 2\beta_\Phi \cdot \epsilon^2/m^2 + C_\rho \cdot \beta_\Phi^2 \cdot \epsilon^4/m^4 \\ &\leq 2 + 2\,\epsilon/m^2 + C_\rho \cdot \epsilon^2/m^4 < 2 + 3\,\epsilon/m^2 \end{aligned}$$

where the last inequality follows from $C_\rho \cdot \epsilon^2/m^4 \leq C_\Phi \cdot \epsilon^2/m^4 < \epsilon/m^4 \leq \epsilon/m^2$.

Then by Lemma 21.14 applied for ϵ/m, we can choose $\ell_3 \leq b'_m$ so that

$$(r_3, \pi, z_3) = p_0(j_1; j_2, \ell_1; j_3, \ell_2; 1, \ell_3) = \psi^{\ell_3}(p_0(j_1; j_2, \ell_1; j_3, \ell_2; 1, 0))$$

is defined with $|z_3 + 1| \leq \epsilon/m$, and the vertical "offset" along the line $r = r_3$ is given by

$$\upsilon_3 = |z_3 - \zeta_{j_3}(r_3)| \leq \epsilon/m \ .$$

We continue recursively, assuming the definitions as above for $1 \leq i \leq k$, and that the following inductive assumptions hold for $1 < i \leq k$:

$$\ell_i \leq b'_m \quad , \quad |z_i + 1| < \epsilon/m \quad , \quad 2 \leq r_i \leq \ 2 + (1 + 2i)\, \epsilon/m^2 \quad , \quad \upsilon_i \leq \epsilon/m \tag{190}$$

Also assume that $r_k \leq \min\{1, 1/\widehat{\zeta}\} \cdot \epsilon/2$. Then for $j_{k+1} = 1, 2$, we get

$$\begin{aligned} p_0(j_1; j_2, \ell_1; j_3, \ell_2; \cdots ; 1, \ell_k; 1, 0) &= \phi_1^+(p_0(j_1; j_2, \ell_1; j_3, \ell_2; \cdots ; 1, \ell_k)) \\ p_0(j_1; j_2, \ell_1; j_3, \ell_2; \cdots ; 2, \ell_k; 1, 0) &= \phi_2^+(\iota(p_0(j_1; j_2, \ell_1; j_3, \ell_2; \cdots ; 1, \ell_k))) \end{aligned}$$

and set $r_{k+1} = r(p_0(j_1; j_2, \ell_1; j_3, \ell_2; \cdots ; j_{k+1}, \ell_k; 1, 0))$.

We require one additional assumption and a small calculation to complete the inductive step of the construction. Suppose that $(1+2k) \leq m$, then $C_\rho\, \epsilon < 1$ by choice of ϵ, so $(1+2k) < m/\sqrt{C_\rho\, \epsilon}$. Thus $(1+2k)^2 < m^2/\epsilon C_\rho$ and so $(1 + 2k)^2(\epsilon/m^2) < 1/C_\rho$ which yields $C_\rho((1 + 2k)\epsilon/m^2)^2 < \epsilon/m^2$.

Finally, use the quadratic estimates (171) or (172), the "slow estimate" (174), the inductive estimates (188) and (189), and the small calculation above to obtain

$$\begin{aligned} r_{k+1} &\leq \rho_{j_k}(r_k) + \beta_\Phi \cdot \upsilon_k^2 \\ &\leq [r_k + C_\rho \cdot (r_k - 2)^2] + [\beta_\Phi \cdot (\epsilon/m)^2] \\ &\leq 2 + (1 + 2k)\, \epsilon/m^2 + \epsilon/m^2 + C_\rho((1 + 2k)\epsilon/m^2)^2 \\ &< 2(1 + 2k)\, \epsilon/m^2 + \epsilon/m^2 + \epsilon/m^2 \\ &= 2(1 + 2(k + 1))\, \epsilon/m^2 \end{aligned}$$

Then by Lemma 21.14 applied for ϵ/m, we can choose $\ell_{k+1} \leq b'_m$ so that

$$(r_{k+1}, \pi, z_{k+1}) = p_0(j_1; j_2, \ell_1; j_3, \ell_2; \cdots ; j_{k+1}, \ell_k; 1, \ell_{k+1}) = \psi^{\ell_{k+1}}(p_0(j_1; j_2, \ell_1; j_3, \ell_2; \cdots ; j_{k+1}, \ell_k; 1, 0))$$

is defined with $|z_{k+1} + 1| \leq \epsilon/m$, and the vertical "offset" along the line $r = r_{k+1}$ is given by

$$\upsilon_{k+1} = |z_{k+1} - \zeta_{j_{k+1}}(r_{k+1})| \leq \epsilon/m \ .$$

which completes the recursive step.

We use the constructions above to obtain lower bound estimates on the number $s(\mathcal{G}_{\mathfrak{M}}, n, \varepsilon)$ of (n, ε)-separated words for the action of $\mathcal{G}^*_{\mathfrak{M}}$ on $\mathfrak{C}$.

For $0 < \epsilon < \min\{\epsilon_1, 1/C_\Phi\}$ as before and $\delta = \min\{1, 1/\widehat{\zeta}\} \cdot \epsilon/2$, we construct orbits in the rectangular regions in $\mathbf{R}_0$ centered on the special orbits ω_j for $j = 1, 2$,

$$\left\{(r, \pi, z) \in \mathbf{R}_0 \mid |z - (-1)^j| < \epsilon \ , \ 2 \leq r \leq \delta\right\} \tag{191}$$

As the value of $\epsilon > 0$ tends to 0, the density of such points increases as well, so that one observes the slow entropy of $\mathcal{G}^*_{\mathfrak{M}}$ is concentrated in these regions around the special orbits.

Let $b_1 \geq 1/(\mu_1 \epsilon)$ be such that for all $\ell \geq b_1$, for $j = 1, 2$, the point $p_0(j; 1, \ell)$ satisfies the estimates in (178).

Choose $m \geq 1$, and set $b_m = m\, b_1$. As in Lemma 21.15, let b'_m be the greatest integer satisfying

$$b'_m \ \leq \ b_m + m\, L_g/\epsilon \ \leq \ \{1/\mu_1 + 5/(8\pi\, \lambda_1)\} \cdot m/\epsilon \ .$$

Let k_m be the greatest integer for which $k+1 \leq m/4$, then we have the bound $2(1+2(k_m+1))\, \epsilon/m^2 < \epsilon/m$. So by the recursive procedure above, for $k \leq k_m$ we can realize the point $\xi_{(I,J)} = \overline{\varphi}_{(I,J)}(\omega_0)$ defined by (167), where there are 2^k choices of the string $J = (j_1, \ldots, j_k)$, for a fixed strong $I = (\ell_1, \ldots, \ell_k)$ satisfying $\ell_1 \leq b_m$ and $\ell_i \leq b'_m$ for $1 < i \leq k$. Note that such a word has the length estimate

$$\|\overline{\varphi}_{(I,J)}\| \leq k \cdot b'_m \leq b_1\, k_m^2/4 \ .$$

Recall that ε_0 was defined in (168).

LEMMA 21.16. *For $n \leq b_1\, k^2/4$ we have $s(\mathcal{G}^*_{\mathfrak{M}}, n, \varepsilon_0) \geq 2^k$.*

Proof. Let $J = (j_1, \ldots, j_k)$ and $J' = (j'_1, \ldots, j'_k)$, and let $I = I' = (\ell_1, \ldots, \ell_k)$. Suppose that $J \neq J'$ then let $1 \leq \nu \leq k$ be the greatest integer such that $j_\nu \neq j'_\nu$. Set

$$\overline{\varphi}_{(I,J,\nu)} = \overline{\psi}^{\ell_k} \circ \overline{\phi}_{j_k} \circ \overline{\psi}^{\ell_{k-1}} \circ \overline{\phi}_{j_{k-1}} \circ \cdots \circ \overline{\psi}^{\ell_{\nu+1}} \circ \overline{\phi}_{j_{\nu+1}} \circ \overline{\psi}^{\ell_\nu} \tag{192}$$

where $\|\overline{\varphi}_{(I,J,\nu)}\| \leq \|\varphi_{(I,J)}\|$. Assume that $\xi_{(I,J)} = \varphi_{(I,J)}(\omega_0)$ and $\xi_{(I,J')} = \varphi_{(I,J')}(\omega_0)$ are defined, then

$$\begin{aligned} (\overline{\varphi}_{(I,J,\nu)})^{-1}(\xi_{(I,J)}) &= \overline{\phi}_{j_\nu} \circ \overline{\psi}^{\ell_{\nu-1}} \circ \cdots \circ \overline{\psi}^{\ell_1} \circ \overline{\phi}_{j_1}(\omega_0) \\ (\overline{\varphi}_{(I,J,\nu)})^{-1}(\xi_{(I,J')}) &= \overline{\phi}_{j'_\nu} \circ \overline{\psi}^{\ell_{\nu-1}} \circ \cdots \circ \overline{\psi}^{\ell_1} \circ \overline{\phi}_{j'_1}(\omega_0) \end{aligned}$$

As $j_\nu \neq j'_\nu$ we have $d_{\mathfrak{M}}\left((\overline{\varphi}_{(I,J,\nu)})^{-1}(\xi_{(I,J)}), (\overline{\varphi}_{(I,J,\nu)})^{-1}(\xi_{(I,J')})\right) \geq \varepsilon_0$. Thus the collection of points $\xi_{(I,J)}$ constructed above corresponding to the initial choices of ϵ and b_1 yields a collection of at least 2^k points which are (n, ε_0)-separated for $n \leq b_1\, k^2/4$. □

Then by Lemma 21.16 we have for all $k > 0$ and $n \leq b_1\, k^2/4$ the estimate

$$\frac{\ln(s(\mathcal{G}^*_{\mathfrak{M}}, n, \varepsilon_0))}{\sqrt{n}} \;\geq\; \frac{\ln(2^k)}{\sqrt{b_1\, k^2/4}} \;=\; \frac{2\, \ln(2)}{\sqrt{b_1}}$$

from which we conclude that $h^{1/2}_{GLW}(\mathcal{G}^*_{\mathfrak{M}}) > 0$, completing the proof of Theorem 21.10. □

We conclude this section with two further results concerning the lamination entropy for Kuperberg flows. We only sketch the proofs, which follow the same approach as the proof of Theorem 21.10 above.

THEOREM 21.17. *Let Φ_t be a generic Kuperberg flow. If the insertion maps σ_j have "fast growth" in the sense of Definition 21.12, then the number $s(\mathcal{G}^*_{\mathfrak{M}}, n, \varepsilon_0)$ of $(\mathcal{G}^*_{\mathfrak{M}}, n, \varepsilon_0)$-separated points for the $\mathcal{G}^*_{\mathfrak{M}}$ action on $\mathfrak{C}$ is asymptotically proportional to n.*

Proof. Suppose we are given a finite set $\mathcal{S}_n \subset \mathfrak{C}$ of $(\mathcal{G}^*_{\mathfrak{M}}, n, \varepsilon_0)$–separated points, and the corresponding subset $\mathcal{E}_n = p^1_0(\mathcal{S}_n) \subset \mathfrak{M}_{\mathfrak{C}}$ which is $(\widehat{\mathcal{G}}^*_K, 2n, \varepsilon'_0)$-separated, as in the proof of Theorem 21.10.

Let $\xi_1 \neq \xi_2 \in \mathcal{S}_n$, and suppose that $\overline{\varphi} \in \mathcal{G}^{(n)}_{\mathfrak{M}}$ satisfies $d_{\mathfrak{M}}(\overline{\varphi}(\xi_1), \overline{\varphi}(\xi_2)) \geq \epsilon$. Then set $\eta_i = p^1_0(\xi_i)$ and let $\varphi \in \widehat{\mathcal{G}}^*_K$ be the lifted word which satisfies $d_{\mathbf{R}_0}(\varphi(\eta_1), \varphi(\eta_2)) \geq \epsilon'$. For the purposes of the estimates below, we can assume that $\varphi \in \mathcal{M}(n)$, for $\mathcal{M}(n)$ as in Definition 14.1, and $\eta_1, \eta_2 \in Dom(\varphi)$.

For an analysis of φ as in the proof of Theorem 21.10, we set the offset distances $\upsilon_k = 0$ for all $k \geq 2$, so the lower bound estimates on the values r_k of the $k-th$ image of the special point ω_0 are given by a recursive estimate using the estimates (175) in Definition 21.12. Start with Lemma 21.13 for some point $p_0(j; 1, \ell)$ where $\ell \geq b_0$. Then apply the fast growth estimate (175) to obtain a recursive estimate for r_{k+1} in terms of r_k, which for $k \geq 3$ yields

$$r_k - 2 \;\geq\; \lambda^{k-2}\,(r_2 - 2) \;\geq\; \lambda^{k-2}\,\alpha_\Phi/(\mu_2\,\ell_1)^2. \tag{193}$$

Apply the estimate (193) to φ which is a monotone word ending in $\phi^+_{j_m}$. Assume that $r(\varphi(\eta_i)) \geq 2 + \delta'$, then $2 < r(\eta_i) \leq 2 + (\delta'/\lambda^m)$. Use that $0 < \delta' \leq 1$, then the power ℓ_1 of the initial term ψ of φ satisfies

$$\ell_1 \;\geq\; \sqrt{\lambda^{m-2}\,\alpha_\Phi/\mu_2^2\,\delta'} \;\geq\; \sqrt{\lambda^{m-2}\,\alpha_\Phi/\mu_2^2} \tag{194}$$

so the power ℓ_1 grows exponentially with m, at the rate approximately $\lambda^{m/2}$. Thus, to obtain 2^m words in $\mathcal{M}(n)$ the length of the first segment ψ^{ℓ_1} must be approximately $\lambda^{m/2}$, and we obtain the asymptotic estimate on the word length

$$n \sim m + 1 + \sqrt{1 + \lambda + \lambda^2 + \cdots + \lambda^m} \sim \lambda^{m/2}.$$

That is, the word length required to obtain an (n, ε_0)–separated collection of points grows exponentially if the set of points is assumed to grow exponentially. □

The work [27, Section 8] of Greg and Krystyna Kuperberg introduces piecewise linear (PL) versions of her flows, and studies properties of their minimal sets. Our last result contributes another insight to the dynamical properties of the piecewise-smooth flows. It is based on a simple observation that if the Wilson flow is allowed to have a discontinuity in its defining vector field $\mathcal{W}$ along the periodic orbits, then we can obtain the opposite conclusion to that of Theorem 21.9. The assumption that the Wilson flow is smooth forces the holonomy of Ψ_t along the periodic orbits to be unipotent, and the generic Hypothesis 12.2 yields the estimates in Lemma 21.13 which play a fundamental role above. However, for a piecewise-smooth flow $\mathcal{W}$ the derivative of the transverse holonomy of Ψ_t along the periodic orbits need not equal 1, and in fact can be constructed so that the points ω_i are hyperbolic attracting for the map ψ. It is then a long exercise in the methods of the this section to show:

THEOREM 21.18. *Let Φ_t be a Kuperberg flow constructed from a piecewise-smooth Wilson flow Ψ_t whose holonomy along the periodic orbits is hyperbolic, then $h_{GLW}(\mathcal{G}^*_{\mathfrak{M}}) > 0$.*

Proof. The proof of Theorem 21.9 constructs collections of $(\varepsilon'_0, 2n)$-separated points for the action of the augmented pseudogroup $\widehat{\mathcal{G}}^*_K$ on $\mathfrak{M}_{\mathfrak{C}}$. If the map $\psi \in \mathcal{G}^*_K$ has hyperbolic attracting points ω_i for $i = 1, 2$, then the estimate (178) becomes exponential, which implies that the number of insertions ϕ^+_j that can be realized grows exponentially fast with the length of the initial word ψ^{ℓ_1}. □

The discussion and results of this section suggest two problems to consider.

QUESTION 21.19. *Suppose that Φ_t is a Kuperberg flow with a hyperbolic singularity at the special orbits, as discussed above, so that $h_{GLW}(\mathcal{G}^*_{\mathfrak{M}}) > 0$. Is it also true that $h_{top}(\Phi_t) > 0$ for these flows?*

It seems likely that a careful consideration of the methods of this section will provide an affirmative answer to the above question. The second problem is in regards to the calculations used in the proof of Theorem 21.10.

QUESTION 21.20. *Let Φ_t be a generic Kuperberg flow. If the insertion maps σ_j have "slow growth" in the sense of Definition 21.11, does the flow Φ_t have slow entropy $h^{1/2}_{top}(\Phi_t) > 0$?*

22. Growth of leaves

In this section, we study the growth type of the surface $\mathfrak{M}_0$ considered as a leaf in $\mathfrak{M}$. The growth type is a natural invariant of the flow Φ_t and we will show is closely related to the slow entropy of the pseudo⋆group $\mathcal{G}^*_{\mathfrak{M}}$ introduced in the previous section. This provides a result analogous to Manning's Theorem in [30], that the volume growth rate of the universal cover for a compact manifold M with negative sectional curvature is related to the entropy of the geodesic flow for M.

The idea is to use the construction of the tree $\mathbf{T}_\Phi$ in Section 14, the action of $\mathcal{G}^*_{\mathfrak{M}}$ on $\mathfrak{C}_0$ and the geometry of $\mathfrak{M}_0$ as discussed previously in Sections 14, 18 and 21 to calculate the volume growth function of $\mathfrak{M}_0$ which is defined as follows.

The smoothly embedded zippered lamination $\mathfrak{M} \subset \mathbb{K}$ inherits a Riemannian metric from $\mathbb{K}$, and we let $d_{\mathfrak{M}}$ denote the induced distance function on the *leaves* of $\mathfrak{M}$. The submanifold $\mathfrak{M}_0 \subset \mathbb{K}$ with boundary is given this distance function, and we let $B_{\omega_0}(s) = \{x \in \mathfrak{M}_0 \mid d_{\mathfrak{M}}(\omega_0, x) \leq s\}$ be the closed ball of radius s about the basepoint $\omega_0 = (2, \pi, 0) = \mathcal{R}' \cap \mathcal{T}$. Let $\mathrm{Area}(X)$ denote the Riemannian area of a Borel subset $X \subset \mathfrak{M}_0$. Then $\mathrm{Gr}(\mathfrak{M}_0, s) = \mathrm{Area}(B_{\omega_0}(s))$ is called the *growth function* of $\mathfrak{M}_0$.

Given functions $f_1, f_2 \colon [0, \infty) \to [0, \infty)$ say that $f_1 \lesssim f_2$ if there exists constants $A, B, C > 0$ such that for all $s \geq 0$, we have that $f_2(s) \leq A \cdot f_1(B \cdot s) + C$. Say that $f_1 \sim f_2$ if both $f_1 \lesssim f_2$ and $f_2 \lesssim f_1$ hold. This defines equivalence relation on functions, which defines their *growth type*.

The growth function $\mathrm{Gr}(\mathfrak{M}_0, s)$ for $\mathfrak{M}_0$ depends upon the choice of Riemannian metric on $\mathbb{K}$ and basepoint $\omega_0 \in \mathfrak{M}_0$, however the growth type $[\mathrm{Gr}(\mathfrak{M}_0, s)]$ is independent of these choices, as observed by Milnor [36] for coverings of compact manifolds and Plante [40] for leaves of foliations.

We say that $\mathfrak{M}_0$ has *exponential growth type* if $\mathrm{Gr}(\mathfrak{M}_0, s) \sim \exp(s)$. Note that $\exp(\lambda\, s) \sim \exp(s)$ for any $\lambda > 0$, so there is only one growth class of "exponential type". We say that $\mathfrak{M}_0$ has *nonexponential growth type* if $\mathrm{Gr}(\mathfrak{M}_0, s) \lesssim \exp(s)$ but $\exp(s) \not\lesssim \mathrm{Gr}(\mathfrak{M}_0, s)$. We also have the subclass of nonexponential growth type, where $\mathfrak{M}_0$ has *quasi-polynomial growth type* if there exists $d \geq 0$ such that $\mathrm{Gr}(\mathfrak{M}_0, s) \lesssim s^d$. The growth type of a leaf of a foliation or lamination is an entropy-type invariant of its dynamics, as discussed in [20].

Here is the main result of this section:

THEOREM 22.1. *Let Φ_t be a generic Kuperberg flow. If the insertion maps σ_j have "slow growth" in the sense of Definition 21.11, then the growth type of $\mathfrak{M}_0$ is nonexponential, and satisfies*

$$\exp(\sqrt{s}) \lesssim \mathrm{Gr}(\mathfrak{M}_0, s) \lesssim \exp(s) \tag{195}$$

In particular, $\mathfrak{M}_0$ does not have quasi-polynomial growth type.

Proof. The proof of this result occupies the rest of this section. The first step is to elaborate on the relation between the geometry of the tree $\mathbf{T}_\Phi$ and action of $\mathcal{G}^*_{\mathfrak{M}}$.

Consider the monoid $\mathcal{M}_{\mathfrak{M}}(\infty)$ of monotone words in $\mathcal{G}^*_{\mathfrak{M}}$ as defined in Definition 21.5. The *Cayley graph* of $\mathcal{M}_{\mathfrak{M}}(\infty)$, denoted by $|\mathcal{M}_{\mathfrak{M}}|$, is the graph with:

(1) vertices given by the set $\{\overline{\varphi}(\omega_0) \mid \overline{\varphi} \in \mathcal{M}_{\mathfrak{M}}(\infty)\}$, and
(2) edges given by the actions of the maps $\{\overline{\psi}, \overline{\phi}_1, \overline{\phi}_2\}$ on the vertices.

To be more precise, for $i = 1, 2$, there is an edge $\langle \overline{\phi}_i, \omega_0 \rangle$ joining ω_0 to the vertex $\overline{\phi}_i(\omega_0)$. For $\overline{\varphi} \in \mathcal{M}_{\mathfrak{M}}(n)$ suppose that $\overline{\psi} \circ \overline{\varphi} \in \mathcal{M}_{\mathfrak{M}}(n+1)$ then we have an edge $\langle \overline{\psi}, \overline{\varphi}(\omega_0) \rangle$ joining $\overline{\varphi}(\omega_0)$ to $\overline{\psi} \circ \overline{\varphi}(\omega_0)$. For $\overline{\varphi} \in \mathcal{M}_{\mathfrak{M}}(n)$ and $i = 1, 2$ suppose that $\overline{\phi}_i \circ \overline{\varphi} \in \mathcal{M}_{\mathfrak{M}}(n+1)$ then we have an edge $\langle \overline{\phi}_i, \overline{\varphi}(\omega_0) \rangle$ joining $\overline{\varphi}(\omega_0)$ to $\overline{\phi}_i \circ \overline{\varphi}(\omega_0)$.

All edges of $|\mathcal{M}_{\mathfrak{M}}|$ are assigned length 1 with the standard metric on each, so $|\mathcal{M}_{\mathfrak{M}}|$ becomes a complete metric space. Moreover, each vertex $\overline{\varphi}(\omega_0)$ has valence equal to one plus the number of words in $\{\overline{\psi} \circ \overline{\varphi}, \overline{\phi}_1 \circ \overline{\varphi}, \overline{\phi}_2 \circ \overline{\varphi}\}$ which are well-defined at ω_0.

We compare the geometry of the graph $|\mathcal{M}_{\mathfrak{M}}|$ with that of the tree $\mathbf{T}_\Phi$ introduced in Section 14 and that of the manifold $\mathfrak{M}_0$, using the following standard notion:

DEFINITION 22.2. *A map $f \colon X \to Y$ between metric spaces (X, d_X) and (Y, d_Y) is a* quasi-isometry *is there exists constants $C_f \geq 0$ and $\lambda_f \geq 1$ so that for all $x, x' \in X$ we have*

$$\lambda_f^{-1} \cdot d_Y(f(x), f(x')) - C_f \;\leq\; d_X(x, x') \;\leq\; \lambda_f \cdot d_Y(f(x), f(x')) + C_f \ .$$

Moreover, for all $y \in Y$ there exists $x \in X$ such that $d_Y(y, f(x)) \leq C_f$.

The first comparison is a consequence of our previous observations.

PROPOSITION 22.3. *There is an embedding $\widetilde{\Phi} \colon |\mathcal{M}_{\mathfrak{M}}| \to \mathbf{T}_\Phi$ which is a quasi-isometry.*

Proof. Define $\widetilde{\Phi}$ as follows. The special vertex point ω_0 is sent to basepoint $\omega_0 \in \mathbf{T}_\Phi$ which is pictured in Figure 36 as the point in the upper horizontal strip. The other vertices are mapped to the points of $\mathbf{T}_\Phi$ defined by the intersection with $\mathcal{T}$ of the curve in $\mathbf{R}_0$ defined by the action of $\overline{\varphi}$ on ω_0. For $\overline{\varphi}'$ a generator of $\mathcal{G}^*_{\mathfrak{M}}$, the edge $\langle \overline{\varphi}', \overline{\varphi}(\omega_0) \rangle$ of $|\mathcal{M}_{\mathfrak{M}}|$ is mapped by a constant speed curve to the corresponding branch of $\mathbf{T}_\Phi \subset \mathfrak{M}_0$ connecting the points $\overline{\varphi}(\omega_0)$ and $\overline{\varphi}' \circ \overline{\varphi}(\omega_0)$ that belong to $\mathfrak{C}_0$. We give a uniform estimate on the lengths of these branches of $\mathbf{T}_\Phi$.

LEMMA 22.4. *There exists $0 < L_1 < L_2$ such that for each $\xi, \xi' \in \mathfrak{C}_0$ which are related by the action of a generator $\{\overline{\psi}, \overline{\phi}_1, \overline{\phi}_2\}$ of $\mathcal{G}_{\mathfrak{M}}$, the segment $[\xi, \xi']$ of the tree $\mathbf{T}_\Phi \subset \mathfrak{M}_0$ joining them has length satisfying $L_1 \leq L([\xi, \xi']) \leq L_2$.*

Proof. For the case when $\xi' = \overline{\psi}(\xi)$, it was observed that $4\pi \leq L[\xi, \xi'] \leq 6\pi$. Thus, we need consider the case when $\xi' = \overline{\phi}_k(\xi)$ for $k = 1, 2$. Each point $\xi \in \mathfrak{C}_0$ is joined to the endpoints $\{p_0^1(\xi), p_0^2(\xi)\}$ of the γ_0 or

λ_0 corresponding to it. The segment of $\mathcal{K}$-orbit between $p_0^i(\xi)$ and $\phi_i^+(p_0^i(\xi))$, for $i = 1, 2$, is contained in the concatenation of two $\mathcal{W}$-arcs and thus it is upper and lower bounded as a consequence of Corollary 4.5. Let $L > 0$ be the upper bound and $L' > 0$ be the lower bound.

Taking $L_1 = \min\{L, 4\pi\}$ and $L_2 = \max\{L', 6\pi\}$, the claim follows. □

To complete the proof of Proposition 22.3, note that Lemma 22.4 shows the edges of $\mathbf{T}_\Phi$ have lengths which are uniformly bounded above and below, which implies that $\widetilde{\Phi}$ is a quasi-isometry. □

The proof of Theorem 19.1 shows that every point of $\mathfrak{M}_0$ is a uniformly bounded distance from a point of $\mathbf{T}_\Phi$. Thus, $\mathfrak{C}_0$ is a *net* in $\mathfrak{M}_0$, which implies:

COROLLARY 22.5. *For a generic Kuperberg Plug, the map $\widehat{\Phi}\colon |\mathcal{M}_{\mathfrak{M}}| \to \mathfrak{M}_0$ obtained from the composition of $\widetilde{\Phi}$ with the inclusion $\mathbf{T}_\Phi \subset \mathfrak{M}_0$, is a quasi-isometry. That is, the graph $\mathbf{T}_\Phi$ is a "tree model" for the space $\mathfrak{M}_0$.*

Since, by Corollary 22.5, $|\mathcal{M}_{\mathfrak{M}}|$ is quasi-isometric to $\mathfrak{M}_0$ we have reduced the study of the growth properties of the leaf $\mathfrak{M}_0$ to those of the monoid $\mathcal{M}_{\mathfrak{M}}(\infty)$, so by Corollary 21.7 we have:

PROPOSITION 22.6. *Both $\mathbf{T}_\Phi$ and $\mathfrak{M}_0$ have subexponential growth rates.*

We now return to the proof of Theorem 22.1. By Proposition 22.6 we have $\mathrm{Gr}(\mathfrak{M}_0, s) \lesssim \exp(s)$.

To establish the lower bound $\exp(\sqrt{s}) \lesssim \mathrm{Gr}(\mathfrak{M}_0, s)$, we assume that Φ_t is a generic Kuperberg flow whose insertion maps σ_j have "slow growth". Then the proof of Theorem 21.10 constructs a subset of words in $\mathcal{M}_{\mathfrak{M}}(\infty)$ whose action on the basepoint $\omega_0 \in \mathbf{T}_\Phi$ yields a set of images which grow at the rate $\exp(\sqrt{s})$. In particular, the number of words in $\mathcal{M}_{\mathfrak{M}}(\infty)$ must grow at least this rate, which establishes (195). □

23. Shape of the minimal set

In this section, we consider the topological properties of the minimal set Σ for a generic Kuperberg flow Φ_t. The space Σ is compact and connected, so is a continuum, but its definition in terms of the closure of orbits reveals little about its topological nature. The natural framework for the study of topological properties of spaces such as Σ is using shape theory. For example, Krystyna Kuperberg posed the question whether Σ has stable shape? Stable shape is discussed below, and is about the nicest property one can expect for a minimal set that is not a compact submanifold. Theorem 23.4 below shows that Σ does not have stable shape. This result follows from the equality $\Sigma = \mathfrak{M}$ for a generic flow, and the structure theory for $\mathfrak{M}$ developed in the previous sections of this work.

Shape theory studies the topological properties of a topological space $\mathfrak{Z}$ using a form of Čech homotopy theory. The definition of shape for a space $\mathfrak{Z}$ embedded in the Hilbert cube was introduced by Borsuk [3, 5]. Later developments and results of shape theory are discussed in the texts [12, 31] and the historical essay [32]. We give a brief definition of the shape of a compactum $\mathfrak{Z}$ embedded in a metric space X, following the works of Fox [15], Morita [38] Mardešić [31], and the suggestions of the referee.

DEFINITION 23.1. *A sequence $\mathfrak{U} = \{U_\ell \mid \ell = 1, 2, \ldots\}$ is called a* shape approximation *of $\mathfrak{Z} \subset X$ if:*

(1) each U_ℓ is an open neighborhood of $\mathfrak{Z}$ in X which is homotopy equivalent to a compact polyhedron;
(2) $U_{\ell+1} \subset U_\ell$ for $\ell \geq 1$, and their closures satisfy $\bigcap_{\ell \geq 1} \overline{U}_\ell = \mathfrak{Z}$.

Suppose that X, X' are connected manifolds, that $\mathfrak{U}$ is a shape approximation for the compact subset $\mathfrak{Z} \subset X$, and $\mathfrak{U}'$ is a shape approximation for the compact subset $\mathfrak{Z}' \subset X'$. The compacta $\mathfrak{Z}, \mathfrak{Z}'$ are said to have the same shape if the following conditions are satisfied:

(1) There are an order-preserving map $\phi\colon \mathbb{Z} \to \mathbb{Z}$, and for each $n \geq 1$, a continuous map $f_n\colon U_{\phi(n)} \to U'_n$ such that for any pair $n \leq m$, the restriction $f_n|U_{\phi(m)}$ is homotopic to f_m as maps from $U_{\phi(m)}$ to U'_n.

(2) There are an order-preserving map $\psi\colon \mathbb{Z} \to \mathbb{Z}$, and for each $n \geq 1$, a continuous map $g_n\colon U'_{\psi(n)} \to U_n$ such that for any pair $n \leq m$, the restriction $g_n|U'_{\psi(m)}$ is homotopic to g_m as maps from $U'_{\psi(m)}$ to U_n.

(3) For each $n \geq 1$, there exists $m \geq \max\{n, \phi \circ \psi(n)\}$ such that the restriction of $g_n \circ f_{\psi(n)}$ to U_m is homotopic to the inclusion as maps from U_m to U_n.

(4) For each $n \geq 1$, there exists $m \geq \max\{n, \psi \circ \phi(n)\}$ such that the restriction of $f_n \circ g_{\phi(n)}$ to U'_m is homotopic to the inclusion as maps from U'_m to U'_n.

DEFINITION 23.2. *Let $\mathfrak{Z} \subset X$ be a compact subset of a connected manifold X. Then the* shape of $\mathfrak{Z}$ *is defined to be the equivalence class of a shape approximation of $\mathfrak{Z}$ as above.*

It is a basic fact of shape theory that this definition does not depend upon the choice of shape approximations, and that two homotopic compacta have the same shape. The references [12, 31] give complete details and alternate approaches to defining the shape of a space. A concise overview of some of the key aspects of shape theory for continua embedded in Riemannian manifolds is given in [9, Section 2].

For the purposes of this work, we consider the case where X is a connected compact Riemannian manifold, and $\mathfrak{Z} \subset X$ is an embedded continuum with the induced metric from that on X. The shape of $\mathfrak{Z}$ can then be defined using a shape approximation $\mathfrak{U}$ defined by a descending chain of open ϵ-neighborhoods of $\mathfrak{Z}$ in X, given by $U_\ell = \{x \in X \mid d_X(x, \mathfrak{Z}) < \epsilon_\ell\}$ where we have $0 < \epsilon_{\ell+1} < \epsilon_\ell$ for all $\ell \geq 1$, and $\lim_{\ell \to \infty} \epsilon_\ell = 0$.

DEFINITION 23.3. *A compactum $\mathfrak{Z}$ has* stable shape *if it is* shape equivalent *to a finite polyhedron. That is, there exists a shape approximation $\mathfrak{U}$ such that each inclusion $\iota\colon U_{\ell+1} \hookrightarrow U_\ell$ induces a homotopy equivalence, and U_1 has the homotopy type of a finite polyhedron.*

Some examples of spaces with stable shape are compact manifolds, and more generally finite CW-complexes. A less obvious example is the minimal set for a Denjoy flow on $\mathbb{T}^2$ whose shape is equivalent to the wedge of two circles. In particular, the minimal set of an aperiodic C^1-flow on plugs as constructed by Schweitzer in [43] has stable shape. A result of Krasinkiewicz shows that a continuum embedded in a closed orientable surface is either shape equivalent to a finite wedge of circles, or has the shape of a "Hawaiian earring" [25, 35]. In higher dimensions, Clark and Hunton show in [9] that for an n-dimensional lamination $\mathfrak{Z}$ embedded in an $(n+1)$-dimensional manifold M such that $\mathfrak{Z}$ is an attractor for a smooth diffeomorphism $f\colon M \to M$, and for which the restriction $f\colon \mathfrak{Z} \to \mathfrak{Z}$ is an expanding map on the leaves of $\mathfrak{Z}$, then $\mathfrak{Z}$ has stable shape. In contrast, the results of the previous sections are used to show that the shape properties of the minimal set for a generic Kuperberg flow are not so simple. The first result is the following.

THEOREM 23.4. *The minimal set Σ of a generic Kuperberg flow does not have stable shape.*

We begin the proof of this result after some further discussions of the shape properties of $\mathfrak{M}$.

DEFINITION 23.5. *A compactum $\mathfrak{Z} \subset X$ is said to be* movable in X *if for every neighborhood U of $\mathfrak{Z}$, there exists a neighborhood $U_0 \subset U$ of $\mathfrak{Z}$ such that, for every neighborhood $W \subset U_0$ of $\mathfrak{Z}$, there is a continuous map $\varphi\colon U_0 \times [0,1] \to U$ satisfying the condition $\varphi(x,0) = x$ and $\varphi(x,1) \in W$ for every point $x \in U_0$.*

The notion of a movable compactum was introduced by Borsuk [4], as a generalization of spaces having the shape of an *absolute neighborhood retract* (ANR's), and is an invariant of the shape of $\mathfrak{Z}$. See [9, 12, 31] for further discussions concerning movability. It is a standard result that a compactum $\mathfrak{Z}$ with stable shape is movable. The movable property distinguishes between the shape of a Hawaiian earring and a Vietoris solenoid; the former is movable and the latter is not. It is a more subtle problem to construct compacta which are invariant sets for dynamical systems, which are movable but do not have stable shape, such as given in [46].

Showing the movable property for a space requires the construction of a homotopy retract φ with the properties stated in the definition, whose existence can be difficult to achieve in practice. There is an alternate condition on homology groups, weaker than the movable condition, which is much easier to check.

PROPOSITION 23.6. *Let $\mathfrak{Z}$ be a movable compacta with shape approximation $\mathfrak{U}$. Then the homology groups satisfy the* Mittag-Leffler Condition*: For all $\ell \geq 1$, there exists $p \geq \ell$ such that for any $q \geq p$, the maps on homology groups for $m \geq 1$ induced by the inclusion maps satisfy*

$$Image\{H_m(U_p;\mathbb{Z}) \to H_m(U_\ell;\mathbb{Z})\} = Image\{H_m(U_q;\mathbb{Z}) \to H_m(U_\ell;\mathbb{Z})\} \ . \tag{196}$$

This result is a special case of a more general Mittag-Leffler condition, as discussed in detail in [9]. For example, the above form of the Mittag-Leffler condition can be used to show that the Vietoris solenoid formed from the inverse limit of coverings of the circle is not movable.

We can now state an additional shape property for the minimal set of a generic Kuperberg flow.

THEOREM 23.7. *Let Σ be the minimal set for a generic Kuperberg flow. Then the Mittag-Leffler condition for homology groups is satisfied. That is, given a shape approximation $\mathfrak{U} = \{U_\ell\}$ for Σ, then for any $\ell \geq 1$ there exists $p > \ell$ such that for any $q \geq p$*

$$Image\{H_1(U_p;\mathbb{Z}) \to H_1(U_\ell;\mathbb{Z})\} = Image\{H_1(U_q;\mathbb{Z}) \to H_1(U_\ell;\mathbb{Z})\}. \tag{197}$$

The proof of Theorem 23.7 follows by exhibiting a generating set of homology classes in $H_1(U_p;\mathbb{Z})$ which are represented by closed loops in U_p, and it is shown that the images of these loops in the space U_ℓ become homologous to classes in a fixed 3-dimensional subspace $G_\ell \subset H_1(U_\ell;\mathbb{Z})$, for $p \gg k$ sufficiently large. Moreover, the space G_ℓ is the image of the map on homology induced by the inclusion map. The proof of Theorem 23.4 then follows from the following result.

PROPOSITION 23.8. *Let $\mathfrak{U} = \{U_\ell \mid \ell = 1, 2, \ldots\}$ be a shape approximation of $\mathfrak{Z} \subset X$, such that for $k > 0$*

- *the rank of $H_1(U_k;\mathbb{Z}) \geq 2^k$,*
- *for all $\ell > k$ the rank of the image $H_1(U_\ell;\mathbb{Z}) \to H_1(U_k;\mathbb{Z})$ is 3.*

Assume that for any shape approximation of $\mathfrak{V} = \{V_\ell \mid \ell = 1, 2, \ldots\}$ the rank of the homology groups $H_1(V_\ell;\mathbb{Z})$ is strictly greater than 3, then $\mathfrak{Z}$ does not have stable shape.

Proof. Suppose that $\mathfrak{Z}$ has stable shape, so that there exists a shape approximation $\mathfrak{V} = \{V_\ell \mid \ell = 1, 2, \ldots\}$ such that each inclusion $\iota\colon V_{\ell+1} \hookrightarrow V_\ell$ induces a homotopy equivalence, and thus the inclusion $V_\ell \hookrightarrow V_k$ is a homotopy equivalence for all $\ell \geq k$. Let $3 < n_0 = \text{rank}(H_1(V_1;\mathbb{Z}))$, then $n_0 = \text{rank}(H_1(V_\ell;\mathbb{Z}))$ for all $\ell > 0$. Also, n_0 is the rank of the image of the map $H_1(V_\ell;\mathbb{Z}) \to H_1(V_k;\mathbb{Z})$ for all $\ell \geq k$.

Then, as both $\mathfrak{U}$ and $\mathfrak{V}$ are shape approximations of $\mathfrak{Z}$, there exists k_0, k, ℓ_0 and ℓ such that $V_{k_0} \subset U_k \subset V_{\ell_0} \subset U_\ell$. Thus we obtain the sequence of maps on homology induced by the inclusions:

$$H_1(V_{k_0};\mathbb{Z}) \to H_1(U_k;\mathbb{Z}) \to H_1(V_{\ell_0};\mathbb{Z}) \to H_1(U_\ell;\mathbb{Z}). \tag{198}$$

Then the rank of the image of $H_1(V_{k_0};\mathbb{Z}) \to H_1(U_k;\mathbb{Z})$ must be equal to n_0, and the same holds for the map $H_1(V_{\ell_0};\mathbb{Z}) \to H_1(U_\ell;\mathbb{Z})$. Hence the rank of the image of $H_1(U_k;\mathbb{Z}) \to H_1(U_\ell;\mathbb{Z})$ is equal to $n_0 > 3$ a contradiction. □

The strategy for the proof of Theorem 23.4 is to construct a shape approximation $\mathfrak{U}$ for Σ so that the conditions of Proposition 23.8 are satisfied. This uses the properties of the level function as developed in Sections 10, 12 and 13. We then show in Proposition 23.30 that there is no shape approximation such that the rank of the homology groups is bounded above by 3.

Theorem 17.1 implies that $\Sigma = \mathfrak{M}$ for a generic flow, and thus we analyze the shape properties of $\mathfrak{M}$. As $\mathfrak{M}$ is the closure of $\mathfrak{M}_0$, we have $U_{\mathbb{K}}(\mathfrak{M}, \epsilon) \subset U_{\mathbb{K}}(\mathfrak{M}_0, \epsilon')$ for all $0 < \epsilon < \epsilon'$. Thus, it suffices to consider shape approximations of $\mathfrak{M}_0$.

The space $\mathfrak{M}_0$ retracts to the embedded tree $\mathbf{T}_\Phi \subset \mathfrak{M}_0$ defined in Section 14 and illustrated in Figure 36. In the following, the shape approximation $\{U_k \mid k > 0\}$ for $\mathfrak{M}_0$ is given by sets U_k for $k \geq 0$, where each U_k is an open neighborhood in $\mathbb{K}$ of a compact set $\mathfrak{N}_k$ which is homotopy equivalent to a 1-dimensional complex formed by taking quotients of $\mathbf{T}_\Phi$. Each open neighborhood U_k of $\mathfrak{M}_0$ thus "fuses together" sets of points of the tree $\mathbf{T}_\Phi$, so that the shape approximations to $\mathfrak{M}_0$ are homotopy equivalent to a bouquet of circles formed from paths in $\mathbf{T}_\Phi$ that travel out a branch of $\mathbf{T}_\Phi$ and then are "closed up" via paths in $\mathfrak{N}_k$. The systematic description of the classes in first homology that arise in this way invokes the labeling system for the double propellers developed in Section 13 and the corresponding labels for the vertices of $\mathbf{T}_\Phi$.

First, to fix notation, for $X \subset \mathbb{K}$ and $\epsilon > 0$, set:

- $U_{\mathbb{K}}(X, \epsilon) = \{x \in \mathbb{K} \mid d_{\mathbb{K}}(x, X) < \epsilon\}$ is the *open* ϵ-neighborhood of X in $\mathbb{K}$;
- $C_{\mathbb{K}}(X, \epsilon) = \{x \in \mathbb{K} \mid d_{\mathbb{K}}(x, X) \leq \epsilon\}$ is the *closed* ϵ-neighborhood of X in $\mathbb{K}$.

We now begin the recursive construction of a sequence of compact subsets $\mathfrak{N}_k \subset \mathbb{K}$ for $k \geq 0$, which will be constructed to satisfy the conditions:

(1) $\mathfrak{M} \subset \mathfrak{N}_k$ and $\mathfrak{N}_{k+1} \subset \mathfrak{N}_k$ for all $k \geq 0$;
(2) $\mathfrak{N}_k$ is homotopy equivalent to a finite wedge of circles;
(3) For all $\epsilon > 0$, there exists $k > 0$ such that $\mathfrak{N}_k \subset U_{\mathbb{K}}(\mathfrak{M}_0, \epsilon)$.

It then follows that sufficiently small open neighborhoods of the sets in the collection $\{\mathfrak{N}_k \mid k \geq 0\}$ yield a shape approximation for $\mathfrak{M}$. Moreover, each $\mathfrak{N}_k$ is constructed so that the branches of $\mathbf{T}_\Phi$ above level k are collapsed in the set $\mathfrak{N}_k$ to branches at level k. This critical property is achieved by introducing the notion of "filled double propellers" at level k, which are compact regions in $\mathbb{K}$ which contain all the branches of $\mathbf{T}_\Phi$ with level at least k. This containment property follows from the nesting properties of double propellers, as described in Section 13. Colloquially, these filled propellers can be thought of as a collection of "gloves" which envelop collections of branches of $\mathbf{T}_\Phi$ at level greater than k, grouping them together at the end of a branch at level k. The recursive construction of the sets $\mathfrak{N}_k$ is made precise in the following. We first define $\mathfrak{N}_0$, $\mathfrak{N}_1$ and $\mathfrak{N}_2$, and establish their properties in detail. For the sets $\mathfrak{N}_k$ with $k > 2$, we provide fewer details, as the proofs follow the same outline as for the cases of $\mathfrak{N}_k$ with $k \leq 2$, except as noted. Begin by setting:

$$\mathfrak{N}_0 \ = \ \{x \in \mathbb{K} \mid r(x) \geq 2\} \ \subset \ \mathbb{K}. \tag{199}$$

LEMMA 23.9. *$\mathfrak{N}_0$ is compact.*

Proof. The discontinuities of the radius function $r \colon \mathbb{K} \to [1, 3]$ are contained in the closed subset $\mathcal{T}_{\mathcal{K}} \subset \mathbb{K}$ defined by (10). By the formulation (6) of the Radius Inequality, the radius value increases at a point of discontinuity, hence $\mathfrak{N}_0$ is closed in $\mathbb{K}$, and thus is compact. □

LEMMA 23.10. *The inclusion $\mathfrak{N}_0 \subset \mathbb{K}$ is a homotopy equivalence, and hence $\mathfrak{N}_0$ is homotopy equivalent to a bouquet of three circles.*

Proof. The inclusion $\{x \in \mathbb{W} \mid r(x) \geq 2\} \subset \mathbb{W}$ is a homotopy equivalence, with both spaces retracting to the circle $\{x = (2, \theta, 0) \mid 0 \leq \theta \leq 2\pi\}$. The identification map $\tau \colon \mathbb{W} \to \mathbb{K}$ creates a cross-arc between the circle and itself for each of the insertion maps σ_i, as illustrated in Figure 8. Thus, both spaces are homotopy equivalent to the curve in Figure 53, and so are homotopy equivalent to a bouquet of three circles. □

We fix notation for the generators of $H_1(\mathfrak{N}_0; \mathbb{Z})$ as identified above. Let $[R]$ be the class defined by the loop starting at ω_0 and following the Reeb cylinder around in a counterclockwise direction back to ω_0. For $i = 1, 2$, let $[b_i]$ be the class defined by the straight path from ω_0 to ω_i, then following the cross-arc created by the insertion σ_i and then returning to ω_0. Then $H_1(\mathfrak{N}_0; \mathbb{Z})$ is the group generated by $\{[R], [b_1], [b_2]\}$. Note that the choice of the generators $[b_1]$ and $[b_2]$ have an ambiguity in terms of how the end of the cross-arc is joined to the basepoint ω_0 to close the path. Differing choices of closing paths result in the addition of an integer multiple of $[R]$. We make a choice of these connecting paths, and consider the choice fixed in the following.

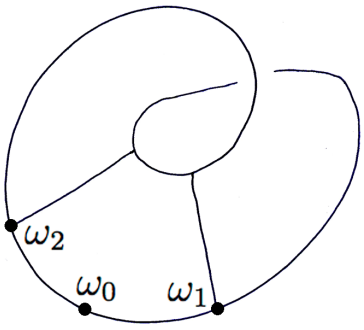

FIGURE 53. Homotopy type of $\mathbb{K}$ and $\mathfrak{N}_0$

Next, we consider the construction of $\mathfrak{N}_1$ which introduces the notion of *filled double propellers*, and also reveals the mechanisms for the change in the topology of the spaces $\mathfrak{N}_k$ as k increases.

Recall the definitions (58) and (59) from Section 13,

$$\Gamma' = \mathcal{C} \cap \mathcal{L}_1^- \subset \mathbb{W} \ , \ \Gamma = \sigma_1^{-1}(\Gamma') \subset L_1^- \quad , \quad \Lambda' = \mathcal{C} \cap \mathcal{L}_2^- \subset \mathbb{W} \ , \ \Lambda = \sigma_2^{-1}(\Lambda') \subset L_2^- .$$

The *filled double propellers at level* 1 are defined as follows. Let $L^-(1) \subset L_1^-$ denote the closure of the interior region bounded by Γ, and $L^-(2) \subset L_2^-$ the closure of interior region bounded by Λ. Analogously, define $L^+(i)$ in the exit region L_i^+ for $i = 1, 2$. The Wilson flow of the curves Γ and Λ generate the infinite double propellers $P_\Gamma, P_\Lambda \subset \mathbb{W}$. Let $D(1) \subset \mathbb{W}$ denote the forward Ψ_t-flow of $L^-(1)$. We call $D(1)$ the filled double propeller associated to Γ. Analogously, let $D(2) \subset \mathbb{W}$ denote the forward Ψ_t-flow of $L^-(2)$, then $D(2)$ is the filled double propeller associated to Λ. Note that $D(1)$ and $D(2)$ are disjoint subsets of $\mathbb{W}$.

Consider the notched Reeb cylinder $\mathcal{R}'$, as illustrated in Figure 18. The filled double propellers in $\mathbb{W}$ do not intersect $\mathcal{R}'$, but they do intersect every neighborhood of it, as the closures of both $D(1)$ and $D(2)$ contain the cylinder $\mathcal{R}$, as discussed in the proof of Proposition 11.2. Also, recall that $\tau(\mathcal{R}') \subset \mathbb{K}$ is the embedded Reeb cylinder, illustrated in Figure 24.

For $\delta > 0$, define the subset of $\mathbb{K}$,

$$C_{\mathbb{K}}^+(\tau(\mathcal{R}'), \delta) \ = \ C_{\mathbb{K}}(\tau(\mathcal{R}'), \delta) \cap \mathfrak{N}_0 \ = \ \{x \in \mathbb{K} \mid d_{\mathbb{K}}(x, \tau(\mathcal{R}')) \leq \delta\} \cap \mathfrak{N}_0 \ . \tag{200}$$

Then $C_{\mathbb{K}}^+(\tau(\mathcal{R}'), \delta)$ is a closed δ-neighborhood of $\tau(\mathcal{R}')$, contained in the compact subset $\mathfrak{N}_0 \subset \mathbb{K}$, hence is compact. Choose δ_1 small enough so that the set $C_{\mathbb{K}}^+(\tau(\mathcal{R}'), \delta_1)$ retracts to $\tau(\mathcal{R}')$. In terms of the illustration Figure 24, we choose δ_1 less than the distance between the insertions and the edges of the gaps, so that $C_{\mathbb{K}}^+(\tau(\mathcal{R}'), \delta_1)$ has no "self-intersections".

For $i = 1, 2$, set $\mathcal{D}(i) = \tau(D(i) \cap \widehat{\mathbb{W}}) \subset \mathbb{K}$, where $\widehat{\mathbb{W}}$ is the closure of $\mathbb{W}'$ as defined in Section 4. Then define:

$$\mathfrak{N}_1 \ = \ C_{\mathbb{K}}^+(\tau(\mathcal{R}'), \delta_1) \ \cup \ \mathcal{D}(1) \ \cup \ \mathcal{D}(2) \ . \tag{201}$$

Thus, $\mathfrak{N}_1$ is obtained by attaching two infinite filled double propellers to $C_{\mathbb{K}}^+(\tau(\mathcal{R}'), \delta_1)$.

LEMMA 23.11. *$\mathfrak{N}_1$ is compact.*

Proof. Consider $\tau^{-1}(C_{\mathbb{K}}^+(\tau(\mathcal{R}'), \delta_1))$ which is a thickened cylinder. For each $i = 1, 2$, the region $D(i)$ is a connected solid spiral turning around $\mathcal{C}$ an infinite number of times, where after a finite number of turns, with the number of times determined by δ_1, the end of the solid region is contained in $\tau^{-1}(C_{\mathbb{K}}^+(\tau(\mathcal{R}'), \delta_1))$. Thus, $D(i) - (D(i) \cap \tau^{-1}(C_{\mathbb{K}}^+(\tau(\mathcal{R}'), \delta_1)))$ has compact closure in $\mathbb{W}$. It follows that $\mathfrak{N}_1$ is the union of the compact set $C_{\mathbb{K}}^+(\tau(\mathcal{R}'), \delta_1)$ with the images under τ of compact subsets of $D(1)$ and $D(2)$, hence is compact. □

LEMMA 23.12. *$\mathfrak{M} \subset \mathfrak{N}_1 \subset \mathfrak{N}_0$.*

Proof. It was shown in Section 12 that $\mathfrak{M}_0$ is the ascending union of the sets $\mathfrak{M}_0^n$ for $n \geq 0$, where $\mathfrak{M}_0^n$ consists of propellers at level at most n. By construction, $\mathfrak{N}_1$ contains the set $\mathfrak{M}_0^1$. It was observed in Section 13 that all of the Γ and Λ curves at level at least 2 in the face $\partial_h^- \mathbb{W}$ are contained in the interiors $L^-(i)$ of the parabolic arcs $\Gamma, \Lambda \subset \partial_h^- \mathbb{W}$. Thus, the double propellers with level at least 2 are contained in the filled propellers $D(1)$ and $D(2)$, hence $\mathfrak{M}_0 \subset \mathfrak{N}_1$. As $\mathfrak{N}_1$ is closed, it also contains $\mathfrak{M}$. □

LEMMA 23.13. *For $\epsilon > 0$ sufficiently small, $U(\mathfrak{N}_1, \epsilon)$ retracts to $\mathfrak{N}_1$.*

Proof. The proof of Lemma 23.11 shows that $\mathfrak{N}_1$ is the union of three compact submanifolds with boundary with corners. Hence, $\mathfrak{N}_1$ is a submanifold with boundary with corners, from which the conclusion follows. □

LEMMA 23.14. $\mathfrak{N}_1$ *has the homotopy type of a finite wedge of circles.*

Proof. For each $i = 1, 2$, attaching $D(i)$ to $\tau^{-1}(C^+_{\mathbb{K}}(\tau(\mathcal{R}'), \delta_1))$ is homotopy equivalent to attaching one endpoint of a line segment to the core circle of the cylinder $\mathcal{R}$. For the image $\mathcal{D}(i) \subset \mathbb{K}$ the other endpoint of the segment is attached to $C^+_{\mathbb{K}}(\tau(\mathcal{R}'), \delta_1)$, resulting in a space with the same homotopy type as $\mathfrak{N}_0$. However, there are additional "handles" formed in the image which are not as immediate to visualize. These result from the intersections of the images $\mathcal{D}(i)$ for $i = 1, 2$ with themselves. That is, while the filled double propellers $D(1), D(2) \subset \mathbb{W}$ are disjoint from each other, their images $\mathcal{D}(1)$ and $\mathcal{D}(2)$ in $\mathbb{K}$ under the quotient map $\tau\colon \mathbb{W} \to \mathbb{K}$ are not disjoint, and this gives rise to additional 1-cycles in $\mathfrak{N}_1$. The loops created by these self intersections are called *exceptional cycles*. While the number of intersections in $\mathbb{K}$ of the filled propellers with themselves will generate an infinite number of homotopy classes of loops, there are at most finitely many homotopy classes of exceptional cycles outside of $C^+_{\mathbb{K}}(\tau(\mathcal{R}'), \delta_1)$. It follows that $\mathfrak{N}_1$ has the homotopy type of a finite wedge of circles. □

Note that the inclusion $\mathfrak{N}_1 \subset \mathfrak{N}_0$ induces a map between homology groups

$$\iota_1\colon H_1(\mathfrak{N}_1; \mathbb{Z}) \to H_1(\mathfrak{N}_0; \mathbb{Z}) \cong \langle [R], [b_1], [b_2] \rangle.$$

We claim that this map is surjective. Since $\mathfrak{N}_1$ contains a neighborhood of $\tau(\mathcal{R}')$, it contains a loop representing the class $[R] \in H_1(\mathfrak{N}_0; \mathbb{Z})$. Consider in $\mathfrak{N}_1$ a loop that starts at ω_0 then goes through the face E_i for $i = 1, 2$, to the first propeller, and after a certain number of turns depending on the value of δ_1, the propeller intersects $C^+_{\mathbb{K}}(\tau(\mathcal{R}'), \delta_1)$. Thus the loop can be closed by passing back to the Reeb cylinder. The image of this loop is $m_i[R] + [b_i]$, for some $m_i > 0$. Hence $[b_1]$ and $[b_2]$ are in the image and ι_1 is surjective.

We next describe in more detail the classes in $H_1(\mathfrak{N}_1; \mathbb{Z})$ generated by intersections and self-intersections of the regions $\mathcal{D}(1)$ and $\mathcal{D}(2)$. We use the labeling of the double propellers from Sections 12 and 13 to index the intersections of these filled propellers. Recall that $\mathcal{D}(1)$ is the interior region of the infinite double propeller $\tau(P'_\Gamma)$, and the propeller $P_\Gamma \subset \mathbb{W}$ intersects $\mathcal{L}_i^-$ along the curves $\Gamma'(i, \ell)$ for $i = 1, 2$ and $\ell \geq b$, with $|b|$ the number of internal notches in the propellers, as defined in Section 13. Analogous observations apply for $\mathcal{D}(2)$ and the infinite double propeller $\tau(P'_\Lambda)$. The curves Γ' and Λ' at levels 1 and 2 are illustrated in Figure 30.

Let $L^-(1; i, \ell) \subset L_i^-$ be the compact region bounded by $\Gamma(i, \ell) = \sigma_i^{-1}(\Gamma'(i, \ell))$. For the exit regions, we have the analogous compact regions $L^+(1; i, \ell) \subset L_i^+$. For Λ-curves, we have the analogous entry and exit compact regions $L^\pm(2; i, \ell) \subset L_i^\pm$.

Consider their images under the map $\tau\colon \mathbb{W} \to \mathbb{K}$ which identifies $L_i^\pm$ and $\mathcal{L}_i^\pm$ with the secondary entry and secondary exit regions. We now analyze the intersections and self-intersections that are created. For $i_0, i_1 = 1, 2$, the regions $\tau(L^-(i_0; i_1, \ell)) \subset \mathcal{D}(i_0)$ are the components of the set $\mathcal{D}(i_0) \cap E_{i_1}$, so by the nesting property of Γ and Λ curves, we have that:

- $\tau(L^\pm(1; 1, \ell)) \subset \tau(L^\pm(1))$ and thus is contained in $\mathcal{D}(1)$;
- $\tau(L^\pm(1; 2, \ell)) \subset \tau(L^\pm(2))$ and thus is contained in $\mathcal{D}(2)$.

Analogously, we have:

- $\tau(L^\pm(2; 1, \ell)) \subset \tau(L^\pm(1))$ and thus is contained in $\mathcal{D}(1)$;

- $\tau(L^{\pm}(2;2,\ell)) \subset \tau(L^{\pm}(2))$ and thus is contained in $\mathcal{D}(2)$.

Thus, $\mathcal{D}(1) \cap \mathcal{D}(2)$ consists of the regions:

- $\tau(L^{\pm}(1;2,\ell)) \subset E_2 \cup S_2$, for $\ell \geq b$ and unbounded;
- $\tau(L^{\pm}(2;1,\ell)) \subset E_1 \cup S_1$, for $\ell \geq b$ and unbounded.

REMARK 23.15. *There exists an index $\ell(\delta_1)$, which tends to infinity as δ_1 tends to zero, such that $\tau(L^{\pm}(i_0;i_1,\ell))$ deforms into $C^+_{\mathbb{K}}(\tau(\mathcal{R}'),\delta_1)$ in $\mathfrak{N}_1$ for $\ell \geq \ell(\delta_1)$. It follows that the number of such intersections which are not deformable in $\mathfrak{N}_1$ to the core $C^+_{\mathbb{K}}(\tau(\mathcal{R}'),\delta_1)$ is finite, and bounded above by $|b| + \ell(\delta_1)$.*

We complete our description of the topology of $\mathfrak{N}_1$ by giving a set of generators for $H_1(\mathfrak{N}_1;\mathbb{Z})$. There are three types of generators: the generator at level 0; the generators that cover the branching of the tree $\mathbf{T}_\Phi$ from level 0 to level 1; and the generators that make one turn around the Reeb cylinder along a level 1 propeller. The branches of $\mathbf{T}_\Phi$ at higher levels are contained in the filled propellers at level 1 and thus do not contribute to the homology of $\mathfrak{N}_1$.

DEFINITION 23.16. *Consider the following generators of $H_1(\mathfrak{N}_1;\mathbb{Z})$:*

(1) The loop $[R]$ corresponding to the fundamental class of the Reeb cylinder.

(2) The exceptional loops $E^1(i_0,i_1)$ at level 1, which are formed as follows. Consider the point $\tau(p(i_0)) \in E_{i_0}$, which we recall is the intersection of the image of the periodic orbit $\mathcal{O}_{i_0}$ of the Wilson plug with the entry face of the corresponding insertion. Recall that $\tau(\gamma(i_1,b))$ is the first curve in the intersection of $\tau(P_\gamma)$ with E_{i_1} and $\tau(\lambda(i_1,b))$ is the first curve in the intersection of $\tau(P_\lambda)$ with E_{i_1}. These curves are illustrated in Figures 26 and 27.

Connect $\tau(p(i_0))$ to a point $\tau(p(i_0;i_1,b)) \in E_{i_1}$ by a path tangent to the propeller $\tau(P_\gamma)$ if $i_0 = 1$, and tangent to $\tau(P_\lambda)$ if $i_0 = 2$. Note that $\tau(p(i_0;i_1,b))$ was not defined before, but for homology purposes we just need a point in $\tau(\gamma(i_1,b))$ if $i_0 = 1$, or in $\tau(\lambda(i_1,b))$ if $i_0 = 2$. Then $\tau(p(i_0;i_1,b)) \in \tau(L^-(i_1)) \subset E_{i_1}$, thus can be connected inside $\mathfrak{N}_1$ to $\tau(p(i_1))$. If $i_1 = i_0$ we obtain a loop, and otherwise close the loop using a path from $\tau(p(i_1))$ to $\tau(p(i_0))$ contained in $\tau(\mathcal{R}')$ (the two possible choices differ by $[R]$). These loops are illustrated in Figure 54. Observe that $E^1(i_0,i_1)$ does not depend on the choice of δ_1 and that there are $2^2 = 4$ such loops.

(3) The loops $T^1(i_0,i_1,i_2;\ell)$ of type (2) at level 1, for $b \leq \ell < \ell(\delta_1)$. Consider a loop which starts by connecting $\tau(p(i_1))$ to $\tau(p(i_0;i_1,\ell))$ by a path contained in E_{i_1}, then goes from $\tau(p(i_0;i_1,\ell))$ to $\tau(p(i_0;i_2,\ell+1)) \in E_{i_2}$ by a path tangent to the corresponding level one propeller (that is, to $\tau(P_\gamma)$ if $i_0 = 1$ and to $\tau(P_\lambda)$ if $i_0 = 2$). This segment makes a full turn around the Reeb cylinder and is contained in a level 1 propeller. Observe that i_2 is not necessarily equal to i_1. Then connect by a path in E_{i_2} the points $\tau(p(i_0;i_2,\ell+1))$ and $\tau(p(i_2))$. If $i_2 = i_1$ we obtain a loop; otherwise close the loop by a path from $\tau(p(i_2))$ to $\tau(p(i_1))$ contained in $\tau(\mathcal{R}')$. These loops are illustrated in Figure 55.

Observe that for $\ell = \ell(\delta_1)-1$, the point $\tau(p(i_0;i_2,\ell+1)) = \tau(p(i_0;i_2,\ell(\delta_1))$ belongs to $C^+_{\mathbb{K}}(\tau(\mathcal{R}'),\delta_1)$ and hence the loop can be closed by a path segment in $C^+_{\mathbb{K}}(\tau(\mathcal{R}'),\delta_1)$ but outside $\mathfrak{M}^1_0 - \tau(\mathcal{R}')$, from the corresponding level one propeller to the Reeb cylinder. Observe that there are $8(|b| + \ell(\delta_1))$ such loops $T^1(i_0,i_1,i_2;\ell)$ that are not homologically trivial or equivalent to $[R]$.

The loops $E^1(i_0,i_1)$ and $T^1(i_0,i_1,i_2;\ell)$ constructed in items (2) and (3) above are based at $\tau(p(i_0))$, and they can be connected to the basepoint ω_0 by a short path in $\tau(\mathcal{R}')$ to obtain pointed loops. We consider the image of these loops in $H_1(\mathfrak{N}_0;\mathbb{Z})$, and express the homology classes they determine in terms of the generators $\{[R],[b_1],[b_2]\}$. As the resulting homology classes do not depend on the basepoint chosen, we do not mention the addition of the basepoint paths again.

We now specify the classes in $H_1(\mathfrak{N}_0;\mathbb{Z})$ determined by the above classes. For $E^1(i_0,i_1)$, the image is $|a-b|\cdot[R]+[b_{i_0}]$, for a as introduced in Section 13. For $T^1(i_0,i_1,i_2;\ell)$ with $b \leq \ell \leq \ell(\delta_1)-1$, the image is simply $[R]$ or $2[R]$ depending on the choice of closing path from $\tau(p(i_2))$ to $\tau(p(i_1))$. All other classes in $H_1(\mathfrak{N}_1,\mathbb{Z})$

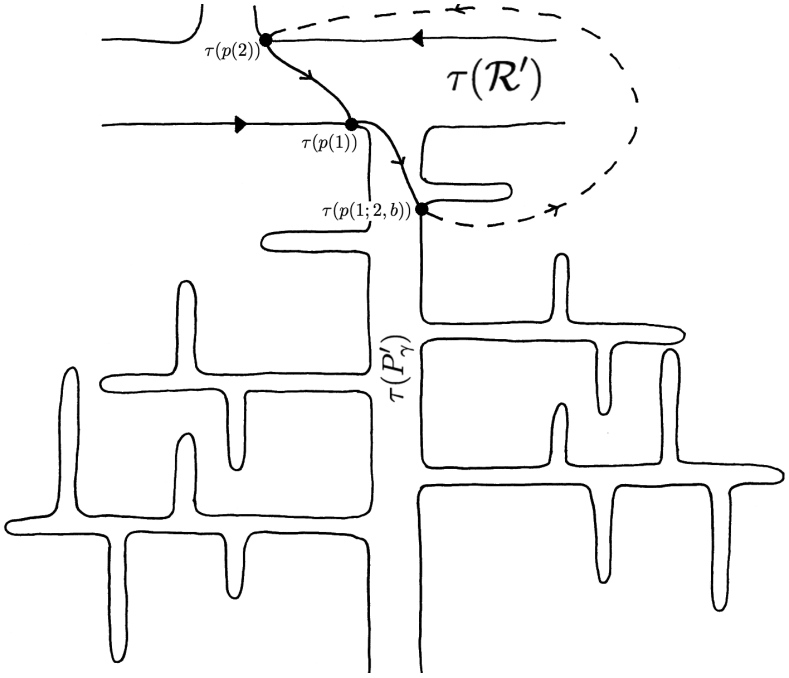

FIGURE 54. The exceptional loop $E^1(i_0, i_1)$ at level $k = 1$.
Solid lines represent paths in the set $\mathfrak{M}_0^1$ and dotted lines represent paths in the intersection of $\mathfrak{N}_1$ with the entry regions E_1 and E_2. Here, $i_0 = 1$ and $i_1 = 2$.

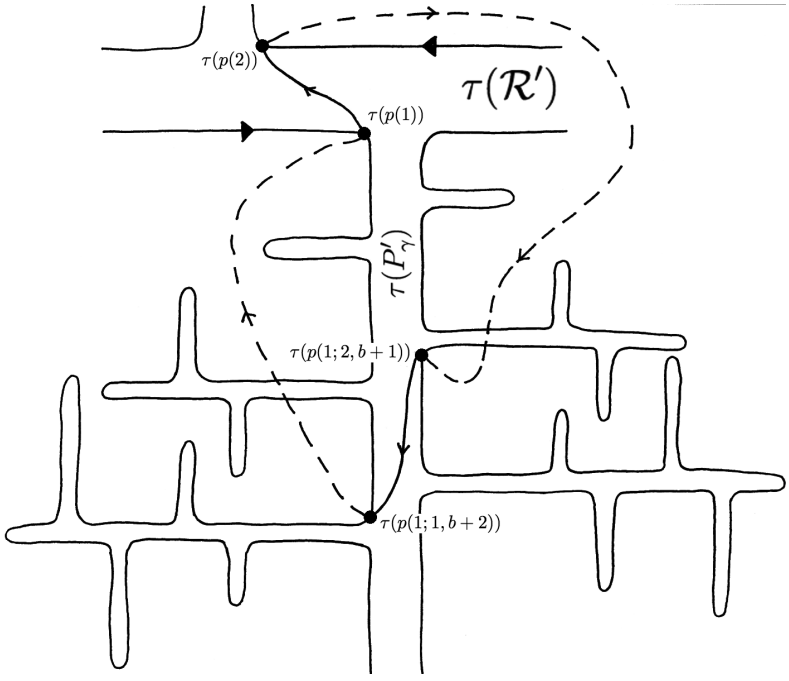

FIGURE 55. The type (2) loop $T^1(i_0, i_1, i_2; \ell)$ at level $k = 1$.
Solid lines represent paths in the set $\mathfrak{M}_0^1$ and dotted lines represent paths in the intersection of $\mathfrak{N}_1$ with the entry regions E_1 and E_2. Here, $i_0 = 1$, $i_1 = 2$, $i_2 = 1$ and $\ell_1 = b + 1$.

are combinations of these classes, as can be seen from geometric considerations. For example, consider the loop generated as in case (2), given by a path starting at $\tau(p(i_0))$ and going to a point $\tau(p(i_0; i_1, \ell_1)) \in E_{i_1}$ for $\ell_1 > b$, by a path tangent to the propeller $\tau(P_\gamma)$ if $i_0 = 1$, , and tangent to $\tau(P_\lambda)$ if $i_0 = 2$. This will be homologous to a class $E^1(i_0, i_1)$ plus a sum of classes $T^1(i_0, i_1, i_2; \ell)$ for $b < \ell \leq \ell_1$.

The construction of the space $\mathfrak{N}_k$ for $k > 1$ is analogous to that of $\mathfrak{N}_1$, and follows an inductive procedure. Assume that the space $\mathfrak{M}_0^{k-1}$ has been constructed. Then $\mathfrak{N}_k$ is defined as a union of a closed 1-sided neighborhood of the space $\mathfrak{M}_0^{k-1}$ with the filled double propellers at level k. Note that the filled double propellers at level $k-1$ in $\mathfrak{N}_{k-1}$ will no longer be contained in $\mathfrak{N}_k$, as they are replaced by filled double propellers at level k. Though it is simple to state the recursive construction of $\mathfrak{N}_k$ in outline, the actual construction becomes increasingly complicated to describe, as it is based on the labeling for components of the filled double propellers given in Section 13. We discuss this process in further detail for level $k = 2$ below.

Recall that the double propellers at level 2 in $\mathbb{W}$ are labeled by their generating curves $\Gamma(i_1, \ell)$ and $\Lambda(i_1, \ell)$ in $L^-_{i_1}$ for $i_1 = 1, 2$ and $\ell \geq b$. For each such curve, we define the filled region $L^-(i_0; i_1, \ell)$ and the corresponding filled double propeller $D(i_0; i_1, \ell)$ at level 2 is given by the Ψ_t-flow of $L^-(i_0; i_1, \ell)$. Regarding this notation, if $i_0 = 1$, then the boundary of $D(i_0; i_1, \ell)$ is $\Gamma(i_1, \ell)$. If $i_0 = 2$, then the boundary of $D(i_0; i_1, \ell)$ is $\Lambda(i_1, \ell)$. As all Γ and Λ curves which generate these double propellers are contained in the region $\{r > 2\} \subset \partial_h^- \mathbb{W}$, each filled double propeller $D(i_0; i_1, \ell)$ is a compact region in $\mathbb{W}$.

Choose $\delta_2 \leq \delta_1/2$ sufficiently small, so that the one-sided closed δ_2-neighborhood of $\mathfrak{M}_0^1$ given by

$$C^+_{\mathbb{K}}(\mathfrak{M}_0^1, \delta_2) = C_{\mathbb{K}}(\mathfrak{M}_0^1, \delta_2) \cap \mathfrak{N}_1 \tag{202}$$

does not contains all the level 2 propellers. Set $\mathcal{D}(i_0; i_1, \ell) = \tau(D(i_0; i_1, \ell) \cap \widehat{\mathbb{W}})$ and define

$$\mathfrak{N}_2 \;=\; C^+_{\mathbb{K}}(\mathfrak{M}_0^1, \delta_2) \;\cup\; \left\{ \bigcup \{ \mathcal{D}(i_0; i_1, \ell) \mid i_0, i_1 = 1, 2 \text{ and } \ell \geq b \} \right\} \;. \tag{203}$$

Thus, $\mathfrak{N}_2$ is obtained by attaching to the set $C^+_{\mathbb{K}}(\tau(\mathcal{R}'), \delta_2)$ a closed 1-sided δ_2-neighborhood of the level 1 propellers to obtain $C^+_{\mathbb{K}}(\mathfrak{M}_0^1, \delta_2)$, and then attaching the filled double propellers at level 2.

We next state versions of Lemmas 23.12 and 23.13 for $\mathfrak{N}_2$ whose proofs follow in the same way.

LEMMA 23.17. $\mathfrak{M} \subset \mathfrak{N}_2 \subset \mathfrak{N}_1$.

LEMMA 23.18. *For $\epsilon > 0$ sufficiently small, $U(\mathfrak{N}_2, \epsilon)$ retracts to $\mathfrak{N}_2$.*

The description of the homology of $\mathfrak{N}_2$ is analogous to the description of $\mathfrak{N}_1$ above, and again uses the labeling of the double propellers from Sections 12 and 13. However, in addition to the exceptional cycles in $\mathfrak{N}_2$ that arise from the intersections and self-intersections of the filled double propellers at level 2, there is an added subtlety in the existence cycles of type (2) at different levels, which occur for the spaces $\mathfrak{N}_k$ when $k \geq 2$, since in these cases the added propellers are no longer infinite.

We begin with some observations, before enumerating a set a generators of $H_1(\mathfrak{N}_2; \mathbb{Z})$. For ℓ large enough, $\mathcal{D}(i_0; i_1, \ell)$ intersects the entry region E_{i_2} for $i_2 = 1, 2$. The intersection $\mathcal{D}(i_0; i_1, \ell) \cap E_{i_2}$ is along the regions bounded by the curves $\tau(\Gamma(i_1, \ell; i_2, \ell'))$ if $i_0 = 1$, and $\tau(\Lambda(i_1, \ell; i_2, \ell'))$ if $i_0 = 2$, where $\ell' \geq b$ and is bounded above. As before, the regions $D(i_0; i_1, \ell)$ are disjoint and contractible in $\mathbb{W}$, but their images $\mathcal{D}(i_0; i_1, \ell)$ may have multiple intersections between them, and also with the neighborhood $C^+_{\mathbb{K}}(\mathfrak{M}_0^1, \delta_2)$, so they are not necessarily contractible.

First define $\ell(\delta_2)$ as in Remark 23.15, so that the curves $\tau(\gamma(i_1, \ell))$ and $\tau(\lambda(i_1, \ell))$ are contained in $C^+_{\mathbb{K}}(\tau(\mathcal{R}'), \delta_2)$ if $\ell \geq \ell(\delta_2)$.

Let $t(i_0; i_1) \geq b$ be the greatest number such that $\mathcal{D}(i_0; i_1, \ell)$ for $\ell = t(i_0; i_1)$ does not intersect E_1, nor E_2. Observe that this phenomena is independent of the choice of δ_2.

We now consider the possible intersections of the filled double propellers at level 2 with $C^+_{\mathbb{K}}(\mathfrak{M}_0^1, \delta_2)$. The filled double propellers $\mathcal{D}(i_0; i_1, \ell)$ get longer as ℓ increases, thus there exist constants

$$\ell(\delta_2; i_0; i_1) > s(\delta_2; i_0; i_1) \geq b \tag{204}$$

such that, for $i_0, i_1 = 1, 2$:

(1) For $b \leq \ell < s(\delta_2; i_0; i_1)$, the filled double propellers $D(i_0; i_1, \ell) \subset \mathbb{W}$ and the pre-image $\tau^{-1}(C^+_{\mathbb{K}}(\mathfrak{M}^1_0, \delta_2))$ are disjoint. If $\ell < t(i_0; i_1)$ then $\mathcal{D}(i_0; i_1, \ell)$ is homotopically trivial and the attachment of $\mathcal{D}(i_0; i_1, \ell)$ to $C^+_{\mathbb{K}}(\mathfrak{M}^1_0, \delta_2)$ does not change the homotopy type.

(2) For $s(\delta_2; i_0; i_1) \leq \ell < \ell(\delta_2; i_0; i_1)$, the filled double propellers $D(i_0; i_1, \ell) \subset \mathbb{W}$ intersect the set $\tau^{-1}(C^+_{\mathbb{K}}(\mathfrak{M}^1_0, \delta_2))$ and $\mathcal{D}(i_0; i_1, \ell)$ does not retract in $\mathfrak{N}_2$ to $C^+_{\mathbb{K}}(\mathfrak{M}^1_0, \delta_2)$. In this case,

$$\mathcal{D}(i_0; i_1, \ell) \, - \, \big(\mathcal{D}(i_0; i_1, \ell) \cap C^+_{\mathbb{K}}(\mathfrak{M}^1_0, \delta_2)\big)$$

is a non-empty submanifold with compact closure, and the finite filled double propeller $\mathcal{D}(i_0; i_1, \ell)$ is such that its base and tip are in $C^+_{\mathbb{K}}(\mathfrak{M}^1_0, \delta_2)$. The attachment of $\mathcal{D}(i_0; i_1, \ell)$ to $C^+_{\mathbb{K}}(\mathfrak{M}^1_0, \delta_2)$ adds a handle.

(3) For $\ell \geq \ell(\delta_2; i_0; i_1)$, the filled double propellers $\mathcal{D}(i_0; i_1, \ell)$ retract in $\mathfrak{N}_2$ to $C^+_{\mathbb{K}}(\mathfrak{M}^1_0, \delta_2)$, and thus adding these propellers does not change the homotopy type of $C^+_{\mathbb{K}}(\mathfrak{M}^1_0, \delta_2)$.

The proof of the following result is analogous to that of Lemmas 23.11 and 23.14.

LEMMA 23.19. *$\mathfrak{N}_2$ is compact and has the homotopy type of a finite wedge of circles.*

The trace of $C^+_{\mathbb{K}}(\mathfrak{M}^1_0, \delta_2)$ on $\mathbf{R}_0$ contains the 1-sided δ_2-neighborhood of $\tau(\mathcal{R}') \cap \mathbf{R}_0$. From (202) we get that this trace contains also the δ_2-neighborhood of the curves $\gamma_0(\ell_1)$, $\lambda_0(\ell_1)$ for $\ell_1 \geq a$ and unbounded. For $\ell_1 \geq b$, the trace of $\mathcal{D}(i_0; i_1, \ell_1)$ is the region bounded by the curves $\Gamma_0(i_1, \ell_1; \ell_2)$ if $i_0 = 1$, and by the curves $\Lambda_0(i_1, \ell_1; \ell_2)$ if $i_0 = 2$, for $\ell_2 \geq a$ and bounded.

Recall from Section 13, that for i_1 and ℓ_2 fixed, the curves $\gamma_0(i_1, \ell_1; \ell_2)$ accumulate on a level 1 curve as $\ell_1 \to \infty$, on $\gamma_0(\ell_2)$ if $i_1 = 1$, and on $\lambda_0(\ell_2)$ if $i_1 = 2$. Analogously, the curves $\lambda_0(i_1, \ell_1; \ell_2)$ accumulate as $\ell_1 \to \infty$, on $\gamma_0(\ell_2)$ if $i_1 = 1$ and on $\lambda_0(\ell_2)$ if $i_1 = 2$. Thus, there exists $\ell'(\delta_2; i_0; i_1)$ such that for every $\ell_1 \geq \ell'(\delta_2; i_0; i_1)$, for $i_0 = 1$ the curve $\Gamma_0(i_1, \ell_1; a)$, and for $i_0 = 2$ the curve $\Lambda_0(i_1, \ell_1; a)$, intersects the 1-sided δ_2-neighborhood of $\gamma_0(a) \cup \lambda_0(a)$.

The index $\ell(\delta_2; i_0; i_1)$ may be required to be chosen larger than $\ell'(\delta_2; i_0; i_1)$ in order that the conditions of case (3) are satisfied: that is, the filled double propeller $D(i_0; i_1, \ell_1) \subset \mathbb{W}$ intersects $\tau^{-1}(C^+_{\mathbb{K}}(\mathfrak{M}^1_0, \delta_2))$ along all its length, and thus $\mathcal{D}(i_0; i_1, \ell_1)$ retracts in $\mathfrak{N}_2$ to $C^+_{\mathbb{K}}(\mathfrak{M}^1_0, \delta_2)$.

We estimate the value of $s(\delta_2; i_0; i_1)$ in (204) above. To simplify the discussion, consider the case $i_0 = 1$. For $\ell_1 < \ell'(\delta_2; 1; i_1) \leq \ell(\delta_2; 1; i_1)$ and δ_2 small, the curve $\Gamma_0(i_1, \ell_1; a)$ is disjoint from the 1-sided δ_2-neighborhood of $\gamma_0(a) \cup \lambda_0(a)$. Take $\ell_1 = \ell'(\delta_2; i_0; i_1) - 1$, then there exists $\ell_2 > a$ such that $\Gamma_0(i_1, \ell_1; \ell_2)$ intersects the 1-sided δ_2-neighborhood of $\gamma_0(\ell_2) \cup \lambda_0(\ell_2)$. Thus the filled double propeller $\mathcal{D}(1; i_1, \ell_1)$ satisfies case (2).

As ℓ_1 decreases, the filled double propellers $\mathcal{D}(1; i_1, \ell_1)$ get shorter, and thus there exists $s'(\delta_2; 1; i_1)$ such that if $\ell_1 < s'(\delta_2; 1; i_1)$, the curves $\Gamma_0(i_1, \ell_1; \ell_2)$ are disjoint from $C^+_{\mathbb{K}}(\mathfrak{M}^1_0, \delta_2)$ for any $\ell_2 \geq a$. In the same way we obtain $s'(\delta_2; 2; i_1)$, and hence $s(\delta_2; i_0; i_1) \leq s'(\delta_2; i_0; i_1)$ such that case (1) is satisfied.

The addition of the propellers $\mathcal{D}(i_0; i_1, \ell)$ in case (2) creates new handles: each propeller retracts to its intersection with the annulus $\mathcal{A}$, thus is an arc whose endpoints are in $C^+_{\mathbb{K}}(\mathfrak{M}^1_0, \delta_2)$ that is not contained in the previous set. As for $\mathfrak{N}_1$, we obtain exceptional cycles in $\mathfrak{N}_2$ that arise from the intersections of the filled propellers at level 2. Thus, the inclusion $\mathfrak{N}_2 \subset \mathfrak{N}_1$ is not a homotopy equivalence for δ_2 sufficiently small.

Before giving the descriptions of the classes of generators for $H_1(\mathfrak{N}_2, \mathbb{Z})$, we make an observation. Consider point $\tau(p(i_0; i_1, \ell)) \in C^+_{\mathbb{K}}(\tau(\mathcal{R}'), \delta_1) \cap E_{i_1}$ at level 1, for $i_1 = 1, 2$, where ℓ is sufficiently large, but such that $\tau(p(i_0; i_1, \ell))$ is not contained in $C^+_{\mathbb{K}}(\tau(\mathcal{R}'), \delta_2)$. The closest level 1 point to $\tau(p(i_0; i_1, \ell))$ is $\tau(p(i_2; i_1, \ell + 1))$ for $i_2 \neq i_0$, since γ and λ curves are interlaced as in (48), (49), (50) and (51). If the δ_2-neighborhood of $\tau(p(i_2; i_1, \ell + 1))$ contains the first point $\tau(p(i_0; i_1, \ell))$, then we can compose these paths to obtain a loop as, as described in item (3) of the list below.

We can now define a set of generators of $H_1(\mathfrak{N}_2;\mathbb{Z})$, which are divided into the following classes: the class $[R]$ at level 0; the ones that cover the branching from level 0 to level 1; the ones that cover the branching from level 1 to level 2; and those that allow to make one turn around the Reeb cylinder along a level 2 propeller.

DEFINITION 23.20. *Consider the following generators of $H_1(\mathfrak{N}_2;\mathbb{Z})$:*

(1) The loop $[R]$ corresponding to the fundamental class of the Reeb cylinder.

(2) The loops $P_1^2(i_0)$ at level 1, which are formed as follows. Observe that the level 1 propellers limit to the Reeb cylinder, so that after $|a|+\ell(\delta_2)$ turns, where $\ell(\delta_2)$ depends on δ_2, the propellers $\tau(P_\gamma)$ and $\tau(P_\lambda)$ intersect $C^+_{\mathbb{K}}(\tau(\mathcal{R}'),\delta_2)$. Consider a loop starting by a segment that connects $\tau(p(i_0))$ to $\tau(p(i_0;i_1,\ell(\delta_2)))\in C^+_{\mathbb{K}}(\tau(\mathcal{R}'),\delta_2)$ and is tangent to $\mathfrak{M}_0^1$. Then connect the last point to $\tau(p(i_1))$ by a path in E_{i_1} and then back to $\tau(p(i_0))$ along the Reeb cylinder. The value of $\ell(\delta_2)$ is the smallest number for which such a loop exists. Observe that the two loops defined by paths

$$\begin{aligned}
&\tau(p(i_0)) \xrightarrow{\text{tangent}} \tau(p(i_0;1,\ell(\delta_2))) \xrightarrow{E_1} \tau(p(1)),\\
&\tau(p(i_0)) \xrightarrow{\text{tangent}} \tau(p(i_0;2,\ell(\delta_2))) \xrightarrow{E_2} \tau(p(2))
\end{aligned}$$

are homologous, since the paths from the level 1 points $\tau(p(i_0;1,\ell(\delta_2)))$ and $\tau(p(i_0;2,\ell(\delta_2)))$ to $\tau(p(1))$, as well as the corresponding level 1 propeller, are contained in the δ_2-neighborhood of the Reeb cylinder.

(3) The one turn loops $S_1^2(i_0,i_1;\ell)$ at level 1, which are formed as follows. Note that if $\tau(p(i_0;i_1,\ell))$ and $\tau(p(i_2;i_1,\ell+1))$ for $i_2\neq i_0$ do not belong to $C^+_{\mathbb{K}}(\tau(\mathcal{R}'),\delta_2)$, there is loop formed by concatenating the path tangent to $\mathfrak{M}_0$ whose endpoints are $\tau(p(i_0;i_1,\ell))$ and $\tau(p(i_2;i_1,\ell+1))$ with the path joining these two points that is contained in $E_{i_1}\cap\mathfrak{N}_2$.

Observe that for ℓ sufficiently large, the points $\tau(p(i_0;i_1,\ell))$ and $\tau(p(i_2;i_1,\ell+1))$ belong to the δ_2-neighborhood of the Reeb cylinder, and thus the loop is homotopic to $P_1^2(i_2)-P_1^2(i_0)+[R]$, as explained in the proof of Proposition 23.21 below.

(4) The exceptional loops $E^2(i_0,i_1,i_2;\ell_1)$ at level 2 , which are formed as follows. As in the case $k=1$, we define $\tau(p(i_0;i_1,\ell_1;i_2,b))$ to be a point in the curve $\tau(\gamma(i_1,\ell_1;i_2,b))$ if $i_0=1$, and in the curve $\tau(\lambda(i_1,\ell_1;i_2,b))$ if $i_0=2$. For $\ell_1\geq t(i_0;i_1)$, consider a path starting at $\tau(p(i_0;i_1,\ell_1))$ and tangent to the corresponding level 2 propeller up to the point $\tau(p(i_0;i_1,\ell_1;i_2,b))\in E_{i_2}$ (that is, tangent to $\tau(P_{\gamma(i_1,\ell_1)})$ if $i_0=1$ and to $\tau(P_{\lambda(i_1,\ell_1)})$ if $i_0=2$). Since $\tau(p(i_0;i_1,\ell_1;i_2,b))$ is contained in the region bounded by $\tau(\Gamma(i_2,b))$ if $i_1=1$ and by $\tau(\Lambda(i_2,b))$ if $i_1=2$, we can connect $\tau(p(i_0;i_1,\ell_1;i_2,b))$ to $\tau(p(i_1;i_2,b))$ by a short segment in $E_{i_2}\cap\mathfrak{N}_2$ (as follows from Lemma 13.10). Finally, connect $\tau(p(i_1;i_2,b))$ to $\tau(p(i_0;i_1,\ell_1))$ by a path tangent to $\mathfrak{M}_0^1$. Observe that for the last step, there is only one possible choice up to multiples of $[R]$, since $\mathfrak{M}_0^1$ retracts to a tree (up to the loop corresponding to the Reeb cylinder). These loops are illustrated in Figure 56.

Observe that for $\ell_1\geq\ell(\delta_2;i_0,i_1)$, these loops retract to $C^+_{\mathbb{K}}(\mathfrak{M}_0^1,\delta_2)$. Thus there are at least $2^3(\ell(\delta_2;i_0,i_1)-t(i_0,i_1))$ such loops that are not homologous to loops in $C^+_{\mathbb{K}}(\mathfrak{M}_0^1,\delta_2)$.

(5) The type (2) loops $T^2(i_0,i_1,i_2,i_3;\ell_1,\ell_2)$ at level 2. Recall that for $\ell_2\geq b$, the point $\tau(p(i_1;i_2,\ell_2))$ lies in the curve $\tau(\Gamma(i_2,\ell_2))$ if $i_1=1$, and in the curve $\tau(\Lambda(i_2,\ell_2))$ if $i_1=2$. Thus, we can connect this point to $\tau(p(i_0;i_1,\ell_1;i_2,\ell_2))$ for any ℓ_1 such that the point exists and for $i_0=1,2$. The connecting path can taken to lie in $E_{i_2}\cap\mathfrak{N}_2$. From $\tau(p(i_0;i_1,\ell_1;i_2,\ell_2))$ take a path tangent to the corresponding propeller to the point $\tau(p(i_0;i_1,\ell_1;i_3,\ell_2+1))$, for $i_3=1,2$. Since $\tau(p(i_0;i_1,\ell_1;i_3,\ell_2+1))\in E_{i_3}$ is in the region bounded by $\tau(\Gamma(i_1,\ell_1;i_3,\ell_2+1))$ or by $\tau(\Lambda(i_1,\ell_1;i_3,\ell_2+1))$, we can connect this point to $\tau(p(i_1;i_3,\ell_2+1))$ by a path in $E_{i_3}\cap\mathfrak{N}_2$ and then back to $\tau(p(i_1;i_2,\ell_2))$ by a path tangent to $\mathfrak{M}_0^1$. These loops are illustrated in Figure 57.

Observe that for $\ell_2\geq\ell(\delta_2;i_0,i_1)$, the paths $T^2(i_0,i_1,i_2,i_3;\ell_1,\ell_2)$ are homologically trivial, as explained in the proof of Proposition 23.21 below.

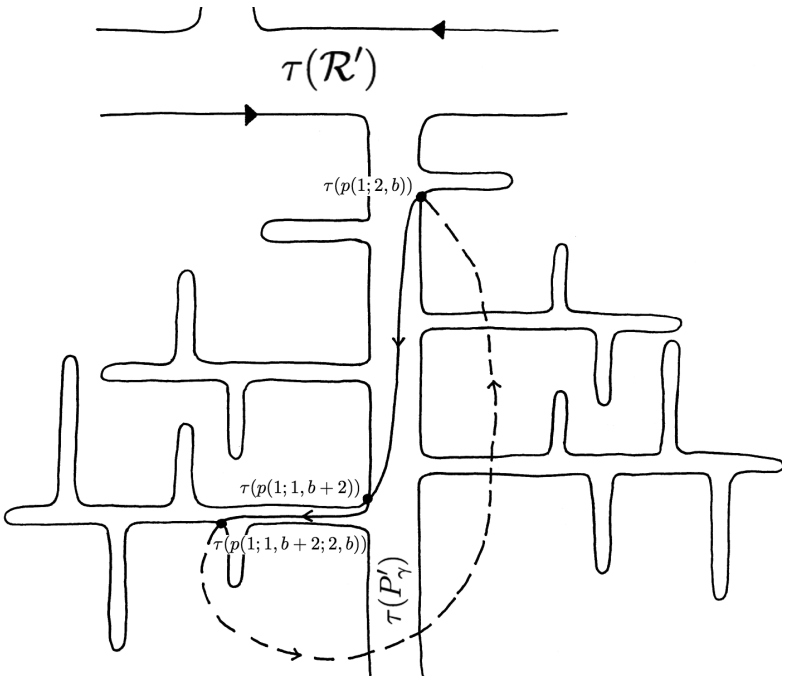

FIGURE 56. The exceptional loop $E(1,1,2;b+2)$ at level $k=2$
Solid lines represent paths in the set $\mathfrak{M}_0^2$ and dotted lines represent paths in the intersection of $\mathfrak{N}_2$ with the entry regions E_1 and E_2. Here, $i_0=1$, $i_1=2$, $i_2=2$ and $\ell_1=b+2$.

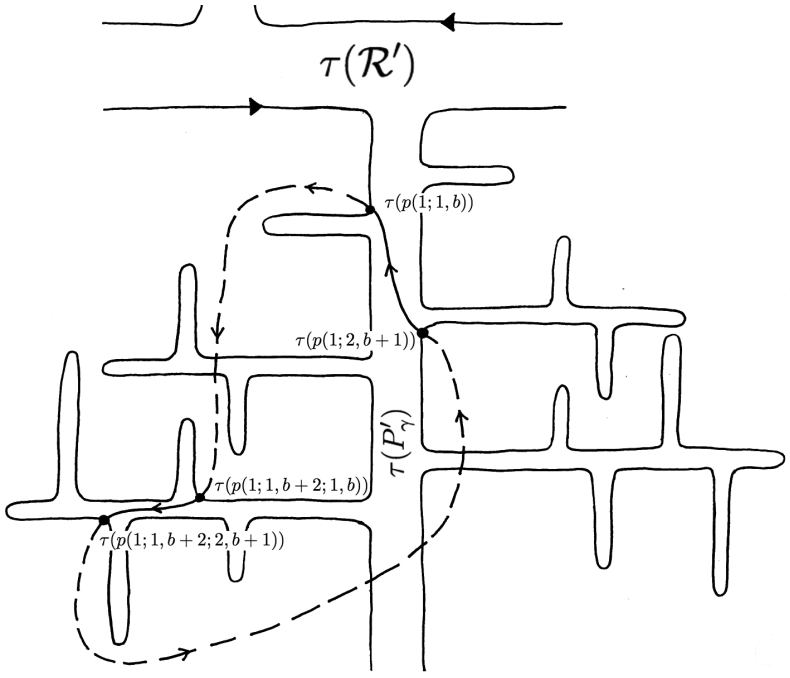

FIGURE 57. The type (2) loop $T^2(1,1,1,2;b+2,b+1)$ at level $k=2$
Solid lines represent paths in the set $\mathfrak{M}_0^2$ and dotted lines represent paths in $\mathfrak{N}_2$ with the entry regions E_1 and E_2. Here, $i_1=1$, $i_2=1$, $i_3=2$, $\ell_1=b+2$ and $\ell_2=b$.

In summary, the set of generators for $H_1(\mathfrak{N}_2;\mathbb{Z})$ are constructed as follows. First, we include the classes generated by the loops in $C^+_{\mathbb{K}}(\mathfrak{M}^1_0,\delta_2)$, that are either at level 0 or level 1. These are the loops described in cases (1), (2) and (3) above. Then we must include the homology classes generated by the exceptional loops which arise from the branching of the level 2 propellers, as described in cases (4) and (5).

PROPOSITION 23.21. *The inclusion $\mathfrak{N}_2 \subset \mathfrak{N}_1$ induces a map*

$$\iota_2 : H_1(\mathfrak{N}_2;\mathbb{Z}) \to H_1(\mathfrak{N}_1;\mathbb{Z})$$

such that:

(1) $\iota_2(P^2_1(i_0)) = T^1(i_0,i_1,i_1;\ell(\delta_2)-1) + T^1(i_0,i_1,i_1;\ell(\delta_2)-2) + \cdots + T^1(i_0,i_1,i_1;b) + E^1(i_0,i_1)$ *for any* i_1*;*

(2) $\iota_2(S^2_1(i_0,i_1;\ell_1))$ *is homologous to*

$$T^1(i_2,i_1,i_1;\ell_1) + \cdots + T^1(i_2,i_1,i_1;b) + E^1(i_2,i_1) - E^1(i_0,i_1) - T^1(i_0,i_1,i_1;b) - \cdots - T^1(i_0,i_1,i_1;\ell_1-1);$$

(3) $\iota_2(E^2(i_0,i_1,i_2;\ell_1)) = T^1(i_0,i_1,i_1;\ell_1-1) + T^1(i_0,i_1,i_1;\ell_1-2) + \cdots + T^1(i_0,i_1,i_1;b) + E^1(i_0,i_1)$*;*

(4) $\iota_2(T^2(i_0,i_1,i_2,i_3;\ell_1,\ell_2))$ *is the trivial element.*

In the proof below, there is a basic technique that is used to investigate the image of the different loops. This operation consist in moving by a homotopy transformation, every path segment tangent to a propeller at level 2, to a path segment tangent to a propeller at level 1, and joining the endpoints of these two segments by paths in the entry regions E_1 and E_2 accordingly. The reason why this is possible, is that the level 1 propellers in $\mathfrak{N}_1$ are filled, and thus contain all path segments tangent to higher level propellers. Once this homotopy operation is performed on a given loop, we then put the resulting deformed loop into "simplest form" and evaluate the resulting homology class.

Proof. Consider first an exceptional loop $E^2(i_0,i_1,i_2;\ell_1)$ of the class (4) which is illustrated in Figure 56. We consider its image in $\mathfrak{N}_1$. Recall that the double propellers at level 1 are filled in $\mathfrak{N}_1$. Consider the segment of $E^2(i_0,i_1,i_2;\ell_1)$ from $\tau(p(i_0;i_1,\ell_1))$ to $\tau(p(i_0;i_1,\ell_1;i_2,b))$ that is tangent to a level 2 propeller, as written in (205) below. Since as $\ell_1 \to \infty$, we have that the points $\tau(p(i_0;i_1,\ell_1))$ limit to $\tau(p(i_1))$, and the points $\tau(p(i_0;i_1,\ell_1;i_2,b))$ limit to $\tau(p(i_1;i_2,b))$. Thus, the tangent path segment at level 2 is homotopic to the union of the segment tangent to $\mathfrak{M}_0$ from $\tau(p(i_1))$ to $\tau(p(i_1;i_2,b))$ and short paths in E_{i_1} and E_{i_2}. The first one of these short paths connects $\tau(p(i_0;i_1,\ell_1))$ to $\tau(p(i_1))$, and the second one connects $\tau(p(i_0;i_1,\ell_1;i_2,b))$ to $\tau(p(i_1;i_2,b))$, and is written in (206) below. We can thus write the loop $E^2(i_0,i_1,i_2;\ell_1)$ in the following way:

$$\tau(p(i_0;i_1,\ell_1)) \xrightarrow{\text{tangent}} \tau(p(i_0;i_1,\ell_1;i_2,b)) \tag{205}$$

$$\xrightarrow{E_{i_2}} \tau(p(i_1;i_2,b)) \tag{206}$$

$$\xrightarrow{\text{tangent}} \tau(p(i_0;i_1,\ell_1)). \tag{207}$$

Then by the previous discussion, this loop is homologous in $\mathfrak{N}_1$ to the loop

$$\tau(p(i_0;i_1,\ell_1)) \xrightarrow{E_{i_1}} \tau(p(i_1)) \xrightarrow{\text{tangent}} \tau(p(i_1;i_2,b)) \xrightarrow{\text{tangent}} \tau(p(i_0;i_1,\ell_1)). \tag{208}$$

Concatenate the two tangential paths to obtain the loop:

$$\tau(p(i_0;i_1,\ell_1)) \xrightarrow{E_{i_1}} \tau(p(i_1)) \xrightarrow{\text{tangent}} \tau(p(i_0;i_1,\ell_1)). \tag{209}$$

Observe that this loop is independent of i_2. Also, if $i_0 \neq i_1$ the segment between $\tau(p(i_1))$ and $\tau(p(i_0;i_1,\ell_1))$ is homotopic to a path segment containing $\tau(p(i_0))$.

The loop $P^2_1(i_0)$ corresponds to the following concatenation

$$\tau(p(i_0)) \xrightarrow{\text{tangent}} \tau(p(i_0;i_1,\ell(\delta_2))) \tag{210}$$

$$\xrightarrow{E_{i_1}} \tau(p(i_1)) \tag{211}$$

$$\xrightarrow{\text{tangent}} \tau(p(i_0)), \tag{212}$$

for any i_1. Thus, in $\mathfrak{N}_1$ the loops $E^2(i_0, i_1, i_2; \ell_1)$ and $P_1^2(i_0)$ are homotopic.

In terms of the generators of $H_1(\mathfrak{N}_1; \mathbb{Z})$, for $\ell_1 \geq b$ we then have

$$\iota_2(E^2(i_0, i_1, i_2; \ell_1)) = T^1(i_0, i_1, i_1; \ell_1 - 1) + T^1(i_0, i_1, i_1; \ell_1 - 2) + \cdots + T^1(i_0, i_1, i_1; b) + E^1(i_0, i_1). \tag{213}$$

It is helpful to consider Figure 56. So while $E^1(i_0, i_1)$ is not necessarily in the image of ι_2, its composition with level 1 loops of type (2) is in the image of ι_2 for each pair (i_0, i_1).

For the loops $P_1^2(i_0)$ at level 1, described in class (2) above, we obtain by similar reasoning that

$$\iota_2(P_1^2(i_0)) = T^1(i_0, i_1, i_1; \ell(\delta_2) - 1) + T^1(i_0, i_1, i_1; \ell(\delta_2) - 2) + \cdots + T^1(i_0, i_1, i_1; b) + E^1(i_0, i_1). \tag{214}$$

Next, consider the one turn loop $S_1^2(i_0, i_1; \ell_1)$, described in class (3) above, that is formed when $\tau(p(i_0; i_1, \ell_1))$ and $\tau(p(i_2; i_1, \ell_1 + 1))$ for $i_2 \neq i_0$ do not belong to $C^+_{\mathbb{K}}(\tau(\mathcal{R}'), \delta_2)$. Schematically, this loop can written as

$$\tau(p(i_0; i_1, \ell_1)) \xrightarrow{\text{tangent}} \tau(p(i_2; i_1, \ell_1 + 1)) \xrightarrow{E_{i_1}} \tau(p(i_0; i_1, \ell_1)). \tag{215}$$

Since $i_2 \neq i_0$ the tangent part of the loop can be written as the concatenation

$$\tau(p(i_0; i_1, \ell_1)) \xrightarrow{\text{tangent}} \tau(p(i_0)) \xrightarrow{\text{tangent}} \tau(p(i_2)) \xrightarrow{\text{tangent}} \tau(p(i_2; i_1, \ell_1 + 1)). \tag{216}$$

If the two endpoints belong to $C^+_{\mathbb{K}}(\tau(\mathcal{R}'), \delta_1)$, we have that $\ell_1 \geq \ell(\delta_1)$. Hence, after inclusion in $\mathfrak{N}_1$, we can further decompose the loop as the concatenation

$$\tau(p(i_0; i_1, \ell_1)) \xrightarrow{\text{tangent}} \tau(p(i_0; i_1, \ell(\delta_1))) \xrightarrow{E_{i_1}} \tau(p(i_1)) \tag{217}$$

$$\xrightarrow{E_{i_1}} \tau(p(i_0; i_1, \ell(\delta_1))) \xrightarrow{\text{tangent}} \tau(p(i_0)) \xrightarrow{\text{tangent}} \tau(p(i_1)) \tag{218}$$

$$\xrightarrow{\text{tangent}} \tau(p(i_2)) \xrightarrow{\text{tangent}} \tau(p(i_2; i_1, \ell(\delta_1))) \xrightarrow{E_{i_1}} \tau(p(i_1)) \tag{219}$$

$$\xrightarrow{E_{i_1}} \tau(p(i_2; i_1, \ell(\delta_1))) \xrightarrow{\text{tangent}} \tau(p(i_2; i_1, \ell_1 + 1)). \tag{220}$$

The paths in the first and last lines (217) and (220) are segments contained in $C^+_{\mathbb{K}}(\tau(\mathcal{R}'), \delta_1)$. The path in the second line (218) corresponds to the loop $-P_1^2(i_0)$, and the path in the third line (219) corresponds to the loop $P_1^2(i_2)$. Let $\approx$ denote homological equivalence, then we conclude

$$\iota_2(S_1^2(i_0, i_1; \ell_1) \approx \iota_2(P_1^2(i_2)) - \iota_2(P_1^2(i_0)) + m[R], \tag{221}$$

for $m = -(\ell_1 - \ell(\delta_1)) + (\ell_1 + 1 - \ell(\delta_1)) = 1$.

If at least one of the endpoints in (216) is not contained in $C^+_{\mathbb{K}}(\tau(\mathcal{R}'), \delta_1)$, then in $\mathfrak{N}_1$ we can express the loop $\iota_2(S_1^2(i_0; i_1, \ell_1)$ as a concatenation of paths:

$$\tau(p(i_0; i_1, \ell_1)) \xrightarrow{\text{tangent}} \tau(p(i_0; i_1, \ell_1 - 1)) \xrightarrow{E_{i_1}} \tau(p(i_1)) \xrightarrow{E_{i_1}} \tau(p(i_0; i_1, \ell_1 - 1)) \tag{222}$$

$$\xrightarrow{\text{tangent}} \tau(p(i_0; i_1, \ell_1 - 2)) \xrightarrow{E_{i_1}} \tau(p(i_1)) \xrightarrow{E_{i_1}} \tau(p(i_0; i_1, \ell_1 - 2)) \tag{223}$$

$$\vdots$$

$$\xrightarrow{\text{tangent}} \tau(p(i_0; i_1, b)) \xrightarrow{\text{tangent}} \tau(p(i_0)) \xrightarrow{\text{tangent}} \tau(p(i_1)) \xrightarrow{E_{i_1}} \tau(p(i_0; i_1, b)) \tag{224}$$

$$\xrightarrow{E_{i_1}} \tau(p(i_1)) \xrightarrow{\text{tangent}} \tau(p(i_2)) \xrightarrow{\text{tangent}} \tau(p(i_2; i_1, \ell_1 + 1)). \tag{225}$$

Then the path in (222) is homotopic to $-T^1(i_0, i_1, i_1; \ell_1 - 1)$ followed by a segment contained in E_{i_1}, from $\tau(p(i_0; i_1, \ell_1))$ to $\tau(p(i_0; i_1, \ell_1 - 1))$. Analogously, the path in line (223) is homotopic to $-T^1(i_0, i_1, i_1; \ell_1 - 2)$ followed by the path egment contained in E_{i_1}, from $\tau(p(i_0; i_1, \ell_1 - 1))$ to $\tau(p(i_0; i_1, \ell_1 - 2))$. Continuing in this way, the path in line (224) is homotopic to $-E^1(i_0, i_1)$ followed by the segment contained in E_{i_1}, from $\tau(p(i_0; i_1, b))$ to $\tau(p(i_1))$. Thus, the path corresponding to the first arrow in (216) is homotopic in $\mathfrak{N}_1$ to

$$-E^1(i_0, i_1) - T^1(i_0, i_1, i_1; b) - \cdots - T^1(i_0, i_1, i_1; \ell_1 - 1). \tag{226}$$

Applying the same argument to the the path corresponding to the last arrow in (216) we conclude that $\iota_2(S_1^2(i_0,i_1;\ell_1))$ is homotopic to

$$T^1(i_2,i_1,i_1;\ell_1)+\cdots+T^1(i_2,i_1,i_1;b)+E^1(i_2,i_1)-E^1(i_0,i_1)-T^1(i_0,i_1,i_1;b)-\cdots-T^1(i_0,i_1,i_1;\ell_1-1). \tag{227}$$

Finally consider a type (2) loop at level 2, $T^2(i_0,i_1,i_2,i_3;\ell_1,\ell_2)$, as described in class (5) above:

$$\tau(p(i_1;i_2,\ell_2)) \xrightarrow{E_{i_2}} \tau(p(i_0;i_1,\ell_1;i_2,\ell_2)) \tag{228}$$

$$\xrightarrow{\text{tangent}} \tau(p(i_0;i_1,\ell_1;i_3,\ell_2+1)) \tag{229}$$

$$\xrightarrow{E_{i_3}} \tau(p(i_1;i_3,\ell_2+1)) \tag{230}$$

$$\xrightarrow{\text{tangent}} \tau(p(i_1;i_2,\ell_2)). \tag{231}$$

In $\mathfrak{N}_1$ the first tangent segment becomes $\tau(p(i_1;i_2,\ell_2)) \xrightarrow{\text{tangent}} \tau(p(i_1;i_3,\ell_2+1))$, and the points $\tau(p(i_1;i_2,\ell_2))$ and $\tau(p(i_1;i_3,\ell_2+1))$ can be joined to $\tau(p(i_2))$ and $\tau(p(i_3))$, respectively, by segments in E_{i_2} and E_{i_3}, respectively, to obtain the path

$$\tau(p(i_1;i_3,\ell_2+1)) \xrightarrow{\text{tangent}} \tau(p(i_1;i_2,\ell_2))$$

at levels 0 and 1. Hence, $i_2(T^2(i_0,i_1,i_2,i_3;\ell_1,\ell_2))$ is the loop

$$\tau(p(i_1;i_2,\ell_2)) \xrightarrow{E_{i_2}} \tau(p(i_1;i_2,\ell_2)) \tag{232}$$

$$\xrightarrow{\text{tangent}} \tau(p(i_1;i_3,\ell_2+1)) \tag{233}$$

$$\xrightarrow{E_{i_3}} \tau(p(i_1;i_3,\ell_2+1)) \tag{234}$$

$$\xrightarrow{\text{tangent}} \tau(p(i_1;i_2,\ell_2)), \tag{235}$$

which yields the trivial class in $H_1(\mathfrak{N}_1,\mathbb{Z})$. This conclusion can be seen in the illustration Figure 57, as the two tangential path components become homotopic, but in reverse directions, when these tangential paths are homotoped to tangential paths in $\mathfrak{N}_1$. □

The construction of $\mathfrak{N}_2$ has an interpretation in terms of the embedded tree $\mathbf{T}_\Phi \subset \mathfrak{M}_0$. The closed set $\mathfrak{N}_2$ defines a closed neighborhood of $\mathfrak{M}_0$ and hence of the embedded tree $\mathbf{T}_\Phi \subset \mathfrak{M}_0$. Topologically, this corresponds to two operations: first attaching, at a suitably large distance from the root point ω_0, the ends of the two level 1 branches to ω_0. Second, selecting a finite number, equal to $\sum_{i_0,i_1} \ell(\delta_2;i_0;i_1) - s(\delta_2;i_0;i_1)$, of level 2 branches whose endparts get identified to a certain point in the level 1 branches. The branches of the tree at higher levels are all collapsed into the filled regions, hence to one of the $\mathcal{D}(i_0;i_1,\ell)$.

We next describe the construction of $\mathfrak{N}_3$, which proceeds in complete analogy with that of $\mathfrak{N}_2$, and so various repetitive details are left to the reader.

For $0<\delta_3<\delta_2/2$, introduce the one-sided closed δ_3-neighborhood of $\mathfrak{M}_0^2$ given by

$$C_{\mathbb{K}}^+(\mathfrak{M}_0^2,\delta_3) = C_{\mathbb{K}}(\mathfrak{M}_0^2,\delta_3)\cap\mathfrak{N}_2. \tag{236}$$

Choose δ_3 sufficiently small, so that $C_{\mathbb{K}}^+(\mathfrak{M}_0^2,\delta_3)$ does not contain all the level 3 propellers.

The double propellers at level 3 are given by the collections

$$\tau(P'_{\Gamma(i_1,\ell_1;i_2,\ell_2)}) \text{ and } \tau(P'_{\Lambda(i_1,\ell_1;i_2,\ell_2)}) \quad \text{for } \ell_1,\ell_2\geq b \text{ and } i_1,i_2=1,2\ . \tag{237}$$

Denote the corresponding filled double propellers in $\mathbb{K}$ by $\mathcal{D}(1;i_1,\ell_1;i_2,\ell_2)$ and $\mathcal{D}(2;i_1,\ell_1;i_2,\ell_2)$, respectively. Observe that the lengths of the double propellers $P'_{\Gamma(i_1,\ell_1;i_2,\ell_2)}$ and $P'_{\Lambda(i_1,\ell_1;i_2,\ell_2)}$ are not bounded above as $\ell_1,\ell_2\to\infty$. Then set:

$$\mathfrak{N}_3 \ = \ C_{\mathbb{K}}^+(\mathfrak{M}_0^2,\delta_3) \ \cup \ \Big\{ \bigcup \{\mathcal{D}(i_0;i_1,\ell_1;i_2,\ell_2) \mid i_0,i_1,i_2=1,2 \ \&\ \ell_1,\ell_2\geq b\} \Big\} \ \subset \ \mathbb{K}. \tag{238}$$

As in the previous analysis of the homotopy types of $\mathfrak{N}_1$ and $\mathfrak{N}_2$, the filled double propellers in (238) have both intersections and self-intersections, so their addition to the space $C^+_{\mathbb{K}}(\mathfrak{M}^2_0, \delta_3)$ adds multiple types of exceptional cycles to the homology of $\mathfrak{N}_3$.

As in the analysis of the homotopy type of $\mathfrak{N}_2$, we define the constant $\ell(\delta_3)$ to be the least integer such that the point $\tau(p(i_0; i_1, \ell(\delta_3)))$ is contained in the δ_3-neighborhood of the Reeb cylinder, and the constants $\ell(\delta_3; i_0, i_1) > s(\delta_3; i_0, i_1) \geq b$ are defined analogously to the level $k = 2$ case (204). Moreover, there are constants $t(i_0; i_1, \ell_1; i_2)$ such that the filled double propellers $\mathcal{D}(i_0; i_1, \ell_1; i_2, \ell)$ intersect the regions E_1 and E_2 for with $\ell \geq t(i_0; i_1, \ell_1; i_2)$, hence they are not homologically trivial. We then have

$$\ell(\delta_3; i_0; i_1, \ell_1; i_2) > s(\delta_3; i_0; i_1, \ell_1; i_2) \geq b \tag{239}$$

and the following conditions are satisfied:

(1) For $b \leq \ell < s(\delta_3; i_0; i_1, \ell_1; i_2)$, the filled double propellers $\mathcal{D}(i_0; i_1, \ell_1; i_2, \ell)$ intersect $C^+_{\mathbb{K}}(\mathfrak{M}^2_0, \delta_3)$ only near their generating curves $P'_{\Gamma(i_1,\ell_1;i_2,\ell_2)}$ and $P'_{\Lambda(i_1,\ell_1;i_2,\ell_2)}$.

(2) For $s(\delta_3; i_0; i_1, \ell_1; i_2) \leq \ell < \ell(\delta_3; i_0; i_1, \ell_1; i_2)$, the filled double propeller $\mathcal{D}(i_0; i_1, \ell_1; i_2, \ell)$ is such that its base and tip are contained in $C^+_{\mathbb{K}}(\mathfrak{M}^2_0, \delta_3)$ and do not retract in $\mathfrak{N}_3$ to $C^+_{\mathbb{K}}(\mathfrak{M}^2_0, \delta_3)$. Thus, each of these propellers adds a handle to $C^+_{\mathbb{K}}(\mathfrak{M}^2_0, \delta_3)$.

(3) For $\ell \geq \ell(\delta_3; i_0; i_1, \ell_1; i_2)$, the attachment of the filled double propellers $\mathcal{D}(i_0; i_1, \ell_1; i_2, \ell)$ does not change the homotopy type of $C^+_{\mathbb{K}}(\mathfrak{M}^2_0, \delta_3)$.

It follows that the analogs of Lemmas 23.17, 23.18 and 23.19 hold for $\mathfrak{N}_3$.

We next describe the image of the map on homology induced by the inclusion. A generating set for $H_1(\mathfrak{N}_3; \mathbb{Z})$ is constructed in an analogous way as before.

DEFINITION 23.22. *Consider the following generators of $H_1(\mathfrak{N}_3; \mathbb{Z})$:*

(1) The loop $[R]$ corresponding to the fundamental class of the Reeb cylinder.

(2) Level 1 and 2 loops.
   (a) Level 1 loops $P^3_1(i_0)$. These are the same as the loops of class (2) generating $H_1(\mathfrak{N}_2; \mathbb{Z})$, represented schematically for $i_1 = 1, 2$, as
   $$\tau(p(i_0)) \xrightarrow{\text{tangent}} \tau(p(i_0; i_1, \ell(\delta_3))) \xrightarrow{E_{i_1}} \tau(p(i_1)) \xrightarrow{\text{tangent}} \tau(p(i_0)).$$
   (b) Level 2 loops $P^3_2(i_0, i_1; \ell_1)$. The level 2 propellers limit to the level 1 propellers, and get longer as the indices $(i_0; i_1, \ell_1)$ increase, for $\ell_1 \geq s(\delta_3; i_0; i_1)$, the propeller $\tau(P_{\gamma(i_1,\ell_1)})$ if $i_0 = 1$, or the propellers $\tau(P_{\lambda(i_1,\ell_1)})$ if $i_0 = 2$, intersect $C^+_{\mathbb{K}}(\mathfrak{M}^1_0, \delta_3)$ near their base and tip, and thus represent handles of $\mathfrak{N}_3$. Then for $s(\delta_3; i_0; i_1) \leq \ell_1 < \ell(\delta_3; i_0, i_1)$, consider the loops starting at $\tau(p(i_0; i_1, \ell_1))$ tangent to $\mathfrak{M}^2_0$ up to the point $\tau(p(i_0; i_1, \ell_1; i_2, \ell_2))$. For ℓ_2 sufficiently large, the point $\tau(p(i_0; i_1, \ell_1; i_2, \ell_2))$ is contained in $C^+_{\mathbb{K}}(\mathfrak{M}^1_0, \delta_3)$, thus we can join this point to $\tau(p(i_1; i_2, \ell_2))$ and then close the loop by a path tangent to $\mathfrak{M}^1_0$.
   The homology class of the loop $P^3_2(i_0, i_1; \ell_1)$ is independent of $i_2 = 1, 2$, as was the case for the analogous level 1 loops. Given (i_0, i_1, ℓ_1), consider the smallest ℓ_2 such that $\tau(p(i_0; i_1, \ell_1; i_2, \ell_2))$ is contained in $C^+_{\mathbb{K}}(\mathfrak{M}^1_0, \delta_3)$ for $i_2 = 1, 2$. Since the part of the level 2 propeller that lies between the points $\tau(p(i_0; i_1, \ell_1; i_2, \ell_2))$ and the tip retracts to $C^+_{\mathbb{K}}(\mathfrak{M}^1_0, \delta_3)$, for any $\ell'_2 > \ell_2$ the loops
   $$\tau(p(i_0; i_1, \ell_1)) \xrightarrow{\text{tangent}} \tau(p(i_0; i_1, \ell_1; i_2, \ell_2)) \xrightarrow{E_{i_2}} \tau(p(i_1; i_2, \ell_2)) \xrightarrow{\text{tangent}} \tau(p(i_0; i_1, \ell_1))$$
   $$\tau(p(i_0; i_1, \ell_1)) \xrightarrow{\text{tangent}} \tau(p(i_0; i_1, \ell_1; i_2, \ell'_2)) \xrightarrow{E_{i_2}} \tau(p(i_1; i_2, \ell'_2)) \xrightarrow{\text{tangent}} \tau(p(i_0; i_1, \ell_1))$$
   are homotopic.

(3) The one turn loops.

(a) Level 1 loops $S^3_1(i_0, i_1; \ell)$. As in the case of the loops of class (3) for $\mathfrak{N}_2$, consider a pair of points $\tau(p(i_0; i_1, \ell))$ and $\tau(p(i_2; i_1, \ell + 1))$ for $i_2 \neq i_0$. By the definition in (236), the two points can be connected by a path in $E_{i_1} \cap \mathfrak{N}_3$ if they belong to

$$C^+_{\mathbb{K}}(\tau(\mathcal{R}'), \delta_2) - C^+_{\mathbb{K}}(\tau(\mathcal{R}'), \delta_3),$$

and the δ_3-neighborhood of $\tau(p(i_2; i_1, \ell + 1))$ contains $\tau(p(i_0; i_1, \ell))$. In this case, there is a loop formed by concatenating the path tangent to $\mathfrak{M}_0$ between the points $\tau(p(i_0; i_1, \ell))$ and $\tau(p(i_2; i_1, \ell + 1))$, with the path joining these two points that is contained in $E_{i_1} \cap \mathfrak{N}_3$.
Observe that for ℓ sufficiently large, the points $\tau(p(i_0; i_1, \ell))$ and $\tau(p(i_2; i_1, \ell + 1))$ belong to the δ_3-neighborhood of the Reeb cylinder, and thus the homology class of the loop $S^3_1(i_0, i_1; \ell)$ is equal to $P^3_1(i_2) - P^3_1(i_0) + [R]$, as explained in the proof of Proposition 23.21.

(b) Level 2 one turn loops $S^3_2(i_0, i_1, i_2; \ell_1, \ell_2)$. For a point $\tau(p(i_0; i_1, \ell_1; i_2, \ell_2))$, the nesting property of the ellipses, as discussed in Section 13, implies that $\tau(p(i_3; i_1, \ell_1 + 1; i_2, \ell_2))$ for $i_3 \neq i_0$ is the closest point at the same level. If the δ_3-neighborhood of $\tau(p(i_3; i_1, \ell_1 + 1; i_2, \ell_2))$ contains $\tau(p(i_0; i_1, \ell_1; i_2, \ell_2))$, then there is loop formed by concatenating the path tangent to $\mathfrak{M}_0$ whose endpoints are $\tau(p(i_0; i_1, \ell_1; i_2, \ell_2))$ and $\tau(p(i_3; i_1, \ell_1+1; i_2, \ell_2))$, with the path contained in $E_{i_2} \cap \mathfrak{N}_3$ joining these two points.
Observe that for ℓ_1 sufficiently large, the points $\tau(p(i_0; i_1, \ell_1; i_2, \ell_2))$ and $\tau(p(i_3; i_1, \ell_1 + 1; i_2, \ell_2))$ belong to the δ_3-neighborhood of $\mathfrak{M}^1_0$ and thus the loop is homotopic to a loop in $C^+_{\mathbb{K}}(\mathfrak{M}^1_0, \delta_3)$.

(4) The exceptional loops $E^3(i_0, i_1, i_2, i_3; \ell_1, \ell_2)$. As in the case of the loops of class (4) for $\mathfrak{N}_2$, let $\tau(p(i_0; i_1, \ell_1; i_2, \ell_2; i_3, b))$ be any point in the curve $\tau(\gamma(i_1, \ell_1; i_2, \ell_2; i_3, b)) \subset E_{i_3}$ if $i_0 = 1$, and in the curve $\tau(\lambda(i_1, \ell_1; i_2, \ell_2; i_3, b)) \subset E_{i_3}$ if $i_0 = 2$. For $\ell_2 \geq t(i_0; i_1, \ell_1; i_2)$, consider a loop starting at $\tau(p(i_0; i_1, \ell_1; i_2, \ell_2))$, then tangent to the corresponding level 3 propeller up to the point $\tau(p(i_0; i_1, \ell_1; i_2, \ell_2; i_3, b)) \in E_{i_3}$, for $i_3 = 1, 2$. Then join this last point to $\tau(p(i_1; i_2, \ell_2; i_3, b))$ by a short segment contained in $E_{i_3} \cap \mathfrak{N}_3$, and return tangent to $\mathfrak{M}^2_0$ to the point $\tau(p(i_0; i_1, \ell_1; i_2, \ell_2))$.
Observe that for $\ell_2 \geq \ell(\delta_3; i_0; i_1, \ell_1; i_2)$ the loops $E^3(i_0, i_1, i_2, i_3; \ell_1, \ell_2)$ are contained in $\mathfrak{M}^2_0$ and thus are homotopic to level 1 and level 2 loops.

(5) The type (2) loops $T^3(i_0, i_1, i_2, i_3, i_4; \ell_1, \ell_2, \ell_3)$ at level 3. For $\ell_3 \geq b$, the point $\tau(p(i_1; i_2, \ell_2; i_3, \ell_3))$ is contained in the curve $\tau(\Gamma(i_2, \ell_2; i_3, \ell_3))$ if $i_1 = 1$, and in the curve $\tau(\Lambda(i_2, \ell_2; i_3, \ell_3))$ if $i_1 = 2$. Thus, we can connect this point to $\tau(p(i_0; i_1, \ell_1; i_2, \ell_2; i_3, \ell_3))$ for any i_0, and for ℓ_1 big enough so that the last point exists. The connecting path can taken to lie in $E_{i_3} \cap \mathfrak{N}_3$. From $\tau(p(i_0; i_1, \ell_1; i_2, \ell_2; i_3, \ell_3))$, take a path tangent to the corresponding level 3 propeller to the point $\tau(p(i_0; i_1, \ell_1; i_2, \ell_2; i_4, \ell_3 + 1))$, for $i_4 = 1, 2$. Since $\tau(p(i_0; i_1, \ell_1; i_2, \ell_2; i_4, \ell_3 + 1)) \in E_{i_4}$ is in the region bounded by $\tau(\Gamma(i_2, \ell_2; i_4, \ell_3 + 1))$ or by $\tau(\Lambda(i_2, \ell_2; i_4, \ell_3 + 1))$, we can connect this point to $\tau(p(i_1; i_2, \ell_2; i_4, \ell_3 + 1))$ by a path in $E_{i_4} \cap \mathfrak{N}_3$ and then back to $\tau(p(i_1; i_2, \ell_2; i_3, \ell_3))$ by a path tangent to $\mathfrak{M}^2_0$.

REMARK 23.23. *The loops in (1), (2a) and (3a) above generate the homology group $H_1(C^+_{\mathbb{K}}(\mathfrak{M}^1_0, \delta_3); \mathbb{Z})$. Adding the loops in (2b) and (3b) in the above listing complete the list of generators for the homology group $H_1(C^+_{\mathbb{K}}(\mathfrak{M}^2_0, \delta_3); \mathbb{Z})$. As in the case of $\mathfrak{N}_2$, the exceptional and type (2) loops are given by the intersections of the filled propellers, in this case at level 3.*

PROPOSITION 23.24. *The inclusion $\mathfrak{N}_3 \subset \mathfrak{N}_2$ induces a map*

$$\iota_3 : H_1(\mathfrak{N}_3; \mathbb{Z}) \to H_1(\mathfrak{N}_2; \mathbb{Z})$$

such that:

(1) $\iota_3(P^3_1(i_0)) = (\ell(\delta_3) - \ell(\delta_2))[R] + P^2_1(i_0)$;
(2) $\iota_3(P^3_2(i_0, i_1; \ell_1))$ is homologous to

$$T^2(i_0, i_1, i_2, i_2; \ell_1, \ell_2 - 1) + T^2(i_0, i_1, i_2, i_2; \ell_1, \ell_2 - 2) + \cdots + T^2(i_0, i_1, i_2, i_2; \ell_1, b) + E^2(i_0, i_1, i_2; \ell_1),$$

for any i_2 and ℓ_2 the minimum possible value so that the loop $P^3_2(i_0, i_1; \ell_1)$ exists.

(3) $\iota_3(S^3_1(i_0;i_1,\ell_1))$ *is homologous to* $\iota_3(P^3_1(i_2)) - \iota_3(P^3_1(i_0)) + [R]$*;*
(4) $\iota_3(S^3_2(i_0,i_1,i_2;\ell_1,\ell_2))$ *is homologous to*

$$\iota_3(-P^3_2(i_0,i_1;\ell_1) - P^3_1(i_0) + P^3_1(i_3) + P^3_2(i_3;i_1,\ell_1+1) + [R]),$$

for $i_3 \neq i_0$ *and up to the sum of type (2) loops at level 2;*
(5) $\iota_3(E^3(i_0,i_1,i_2,i_3;\ell_1,\ell_2))$ *is homologous to*

$$T^2(i_0,i_1,i_2,i_2;\ell_1,\ell_2-1) + T^2(i_0,i_1,i_2,i_2;\ell_1,\ell_2-2) + \cdots + T^2(i_0,i_1,i_2,i_2;\ell_1,b) + E^2(i_0,i_1,i_2;\ell_1);$$

(6) $\iota_3(T^3(i_0,i_1,i_2,i_3,i_4;\ell_1,\ell_2,\ell_3))$ *is the trivial element.*

The idea of the proof is the same as that of Proposition 23.21: given a loop in $\mathfrak{N}_3$ each path segment in the loop that is tangent to a propeller at level 3, can be homotoped in the filled propeller to a path segment tangent to a propeller at level 2, since the propellers at level 2 are filled in $\mathfrak{N}_2$. We then use segments in the faces of the filled propellers in $\mathfrak{N}_2$ to close up the paths into a loop contained in $\mathfrak{N}_2$. The resulting path is then identified up to homology with a combination of the generators for $H_1(\mathfrak{N}_2;\mathbb{Z})$. We sketch the details of the individual cases below.

Proof. There are two immediate cases which proceed exactly as in the proof of Proposition 23.21. The image of a level 1 loop of $\mathfrak{N}_3$ is equal in homology to the addition of the class defined by a level 1 loop in $\mathfrak{N}_2$ with a multiple of $[R]$. We give the details for the level 2 one turn loops, and for the level 2 exceptional loops.

Consider a level 2 loop $P^3_2(i_0,i_1,i_2;\ell_1,\ell_2)$. Assume without loss of generality that $i_0 = 1$. Observe that the loop $P^3_2(i_0,i_1,i_2;\ell_1,\ell_2)$ exists if $\ell_2 \geq s(\delta_3;1;i_1,\ell_1;i_2)$ and that $s(\delta_3;1;i_1,\ell_1;i_2) > s(\delta_2;1;i_1)$. Also, the level 2 propeller $\tau(P_{\gamma(i_1,\ell_1)})$ retracts to $C^+_{\mathbb{K}}(\mathfrak{M}^1_0,\delta_2)$ only if $\ell_2 > \ell(\delta_2;1;i_1)$. We write schematically the loop $P^3_2(1,i_1,i_2;\ell_1,\ell_2)$ as

$$\begin{aligned}\tau(p(i_0;i_1,\ell_1)) &\xrightarrow{\text{tangent}} \tau(p(i_0;i_1,\ell_1;i_2,\ell_2))\\ &\xrightarrow{E_{i_2}} \tau(p(i_1;i_2,\ell_2))\\ &\xrightarrow{\text{tangent}} \tau(p(i_0;i_1,\ell_1)).\end{aligned}$$

Since $\tau(P_{\gamma(i_1,\ell_1)}) \subset \mathcal{D}(1;i_1,\ell_1)$, the loop $P^3_2(1,i_1,i_2;\ell_1,\ell_2)$ is homotopic to the composition of exceptional and type (2) loops in $\mathfrak{N}_2$, so that we obtain

$$\begin{aligned}\iota_3(P^3_2(i_0,i_1,i_2;\ell_1,\ell_2)) \approx\ & T^2(i_0,i_1,i_2,i_2;\ell_1,\ell_2-1) + T^2(i_0,i_1,i_2,i_2;\ell_1,\ell_2-2) + \cdots\\ &+ T^2(i_0,i_1,i_2,i_2;\ell_1,b) + E^2(i_0,i_1,i_2;\ell_1).\end{aligned}$$

Consider now an exceptional loop $E^3(i_0,i_1,i_2,i_3;\ell_1,\ell_2)$. Since the double propellers at level 2 are filled in $\mathfrak{N}_2$, the tangent segment from $\tau(p(i_0;i_1,\ell_1;i_2,\ell_2))$ to $\tau(p(i_0;i_1,\ell_1;i_2,\ell_2;i_3,b))$ can be identified with the segment from $\tau(p(i_1;i_2,\ell_2))$ to $\tau(p(i_1;i_2,\ell_2;i_3,b))$. Hence the image of an exceptional loop becomes

$$\tau(p(i_0;i_1,\ell_1;i_2,\ell_2)) \xrightarrow{E_{i_2}} \tau(p(i_1;i_2,\ell_2)) \tag{240}$$

$$\xrightarrow{\text{tangent}} \tau(p(i_1;i_2,\ell_2;i_3,b)) \tag{241}$$

$$\xrightarrow{\text{tangent}} \tau(p(i_1;i_2,\ell_2)) \tag{242}$$

$$\xrightarrow{\text{tangent}} \tau(p(i_0;i_1,\ell_1;i_2,\ell_2)). \tag{243}$$

This simplifies to $\tau(p(i_0;i_1,\ell_1;i_2,\ell_2)) \xrightarrow{E_{i_2}} \tau(p(i_1;i_2,\ell_2)) \xrightarrow{\text{tangent}} \tau(p(i_0;i_1,\ell_1;i_2,\ell_2))$, from which we obtain

$$\begin{aligned}\iota_3(E^3(i_0,i_1,i_2,i_3;\ell_1,\ell_2)) = & T^2(i_0,i_1,i_2,i_2;\ell_1,\ell_2-1) + T^2(i_0,i_1,i_2,i_2;\ell_1,\ell_2-2) + \cdots\\ &+ T^2(i_0,i_1,i_2,i_2;\ell_1,b) + E^2(i_0,i_1,i_2;\ell_1).\end{aligned}$$

Consider the one turn loop $S_1^3(i_0, i_1; \ell_1)$ that is formed when $\tau(p(i_0; i_1, \ell_1))$ and $\tau(p(i_2; i_1, \ell_1 + 1))$, for $i_2 \neq i_0$, belong to $C^+_{\mathbb{K}}(\tau(\mathcal{R}'), \delta_2) - C^+_{\mathbb{K}}(\tau(\mathcal{R}'), \delta_3)$, thus $\ell_1 \geq \ell(\delta_2)$. Hence, as in the proof of Proposition 23.21 we obtain that $\iota_3(S_1^3(i_0, i_1; \ell_1))$ is homologous to

$$\iota_3(-P_1^3(i_0) + P_1^3(i_3) + [R]).$$

For the level 2 one turn loops, we can express $S_2^3(i_0, i_1, i_2; \ell_1, \ell_2)$ as the concatenation of paths,

$$\tau(p(i_0; i_1, \ell_1; i_2, \ell_2)) \xrightarrow{\text{tangent}} \tau(p(i_0; i_1, \ell_1)) \tag{244}$$

$$\xrightarrow{\text{tangent}} \tau(p(i_0)) \tag{245}$$

$$\xrightarrow{\text{tangent}} \tau(p(i_3; i_1, \ell_1 + 1)) \tag{246}$$

$$\xrightarrow{\text{tangent}} \tau(p(i_3; i_1, \ell_1; i_2, \ell_2)) \tag{247}$$

$$\xrightarrow{E_{i_2}} \tau(p(i_0; i_1, \ell_1; i_2, \ell_2)). \tag{248}$$

In $\mathfrak{N}_2$, the tangent path in (244) is homotopic to

$$-T^2(i_0, i_1, i_2, i_2; \ell_1, \ell_2 - 1) - \cdots - T^2(i_0, i_1, i_2, i_2; \ell_1, b) - E^2(i_0, i_1, i_2; \ell_1),$$

the the tangent path in (245) is homotopic to

$$-(\ell_1 - \ell(\delta_2))[R] - P_1^2(i_0), \tag{249}$$

the the tangent path in (246) is homotopic to

$$(\ell_1 + 1 - \ell(\delta_2))[R] + P_1^2(i_3), \tag{250}$$

and the the tangent path in (247) is homotopic to

$$T^2(i_3, i_1, i_2, i_2; \ell_1 + 1, \ell_2 - 1) + \cdots + T^2(i_3, i_1, i_2, i_2; \ell_1 + 1, b) + E^2(i_3, i_1, i_2; \ell_1 + 1). \tag{251}$$

Thus $\iota_3(S_2^3(i_0, i_1, i_2; \ell_1, \ell_2))$ is homologous to

$$-T^2(i_0, i_1, i_2, i_2; \ell_1, \ell_2 - 1) - \cdots - T^2(i_0, i_1, i_2, i_2; \ell_1, b) - E^2(i_0, i_1, i_2; \ell_1) \tag{252}$$

$$+ [R] - P_1^2(i_0) + P_1^2(i_3) \tag{253}$$

$$+ T^2(i_3, i_1, i_2, i_2; \ell_1 + 1, \ell_2 - 1) + \cdots + T^2(i_3, i_1, i_2, i_2; \ell_1 + 1, b) \tag{254}$$

$$+ E^2(i_3, i_1, i_2; \ell_1 + 1). \tag{255}$$

Analogously to the case of ι_2, the homology class of $T^3(i_0, i_1, i_2, i_3, i_4; \ell_1, \ell_2, \ell_3)$ is trivial. □

In general, for $k > 3$, we consider $\delta_k < \delta_{k-1}/2$ such that $C^+_{\mathbb{K}}(\mathfrak{M}_0^{k-1}, \delta_k) = C_{\mathbb{K}}(\mathfrak{M}_0^{k-1}, \delta_k) \cap \mathfrak{N}_{k-1}$ does not contain all of the propellers at level k.

The space $\mathfrak{N}_k$ is defined by attaching to $C^+_{\mathbb{K}}(\mathfrak{M}_0^{k-1}, \delta_k)$ the collection of filled propellers at level k. As the number of handles in $\mathfrak{N}_{k-1}$ depends on δ_{k-1}, the sets $\mathfrak{N}_{k-1}$ and $C^+_{\mathbb{K}}(\mathfrak{M}_0^{k-1}, \delta_k)$ are not homotopy equivalent for δ_k small enough. Analogous versions of Lemmas 23.17, 23.18 and 23.19 hold for $\mathfrak{N}_k$.

LEMMA 23.25. *The set $\mathfrak{N}_k$ is compact and satisfies:*

(1) $\mathfrak{M} \subset \mathfrak{N}_k \subset \mathfrak{N}_{k-1}$;
(2) For $\epsilon > 0$ sufficiently small, $U(\mathfrak{N}_k, \epsilon)$ retracts to $\mathfrak{N}_k$;
(3) $\mathfrak{N}_k$ has the homotopy type of a finite wedge of circles.

We now generalize the description of the generators of the homology and give a lower bound on the rank of the homology groups $H_1(\mathfrak{N}_k; \mathbb{Z})$.

DEFINITION 23.26. *Consider the following generators of $H_1(\mathfrak{N}_k; \mathbb{Z})$:*

(1) The loop $[R]$ corresponding to the fundamental class of the Reeb cylinder.

(2) Level 1 to $k-1$ loops.
   (a) The level 1 loops $P_1^k(i_0)$ are defined by choosing i_1 then $P_1^k(i_0)$ is the loop:

$$\begin{aligned} \tau(p(i_0)) &\xrightarrow{\text{tangent}} \tau(p(i_0; i_1, \ell(\delta_k))) \\ &\xrightarrow{E_{i_1}} \tau(p(i_1)) \\ &\xrightarrow{\text{tangent}} \tau(p(i_0)). \end{aligned}$$

   (b) For $2 \leq n \leq k-1$, the level n loops $P_n^k(i_0, i_1, \cdots, i_{n-1}; \ell_1, \cdots, \ell_{n-1})$ are defined as:

$$\begin{aligned} \tau(p(i_0; i_1, \ell_1; \cdots; i_{n-1}, \ell_{n-1})) &\xrightarrow{\text{tangent}} \tau(p(i_0; i_1, \ell_1; \cdots; i_n, \ell_n)) \\ &\xrightarrow{E_{i_n}} \tau(p(i_1; i_2, \ell_2; \cdots; i_n, \ell_n)) \\ &\xrightarrow{\text{tangent}} \tau(p(i_0; i_1, \ell_1; \cdots; i_{n-1}, \ell_{n-1})), \end{aligned}$$

   for any i_n and where ℓ_n is the smallest number for which such a loop exist.

(3) The one turn loops at level n for $1 \leq n \leq k-1$, denoted by $S_n^k(i_0, i_1, \cdots, i_n; \ell_1, \cdots, \ell_n)$, is represented schematically as

$$\begin{aligned} \tau(p(i_0; i_1, \ell_1; \cdots; i_n, \ell_n)) &\xrightarrow{\text{tangent}} \tau(p(i_0; i_1, \ell_1 + 1; \cdots; i_n, \ell_n)) \\ &\xrightarrow{E_{i_1}} \tau(p(i_0; i_1, \ell_1; \cdots; i_n, \ell_n)). \end{aligned}$$

(4) The exceptional loops at level k, denoted by $E^k(i_0, i_1, \cdots, i_k; \ell_1, \cdots, \ell_{k-1})$:

$$\begin{aligned} \tau(p(i_0; i_1, \ell_1; \cdots; i_{k-1}, \ell_{k-1})) &\xrightarrow{\text{tangent}} \tau(p(i_0; i_1, \ell_1; \cdots; i_{k-1}, \ell_{k-1}; i_k, b)) \\ &\xrightarrow{E_{i_k}} \tau(p(i_1; i_2, \ell_2; \cdots; i_{k-1}, \ell_{k-1}; i_k, b)) \\ &\xrightarrow{\text{tangent}} \tau(p(i_0; i_1, \ell_1; \cdots; i_{k-1}, \ell_{k-1})). \end{aligned}$$

(5) The type (2) loop at level k, denoted by $T^k(i_0, i_1, \cdots, i_{k+1}; \ell_1, \cdots, \ell_k)$:

$$\begin{aligned} \tau(p(i_1; i_2, \ell_2; \cdots; i_k, \ell_k)) &\xrightarrow{E_{i_k}} \tau(p(i_0; i_1, \ell_1; \cdots; i_k, \ell_k)) \\ &\xrightarrow{\text{tangent}} \tau(p(i_0; i_1, \ell_1; \cdots; i_{k+1}, \ell_k + 1)) \\ &\xrightarrow{E_{i_{k+1}}} \tau(p(i_1; i_2, \ell_2; \cdots; i_{k+1}, \ell_k + 1)) \\ &\xrightarrow{\text{tangent}} \tau(p(i_1; i_2, \ell_2; \cdots; i_k, \ell_k)). \end{aligned}$$

We then have the analog of Proposition 23.24:

PROPOSITION 23.27. *The inclusion $\mathfrak{N}_k \subset \mathfrak{N}_{k-1}$ induces a map*

$$\iota_k : H_1(\mathfrak{N}_k; \mathbb{Z}) \to H_1(\mathfrak{N}_{k-1}; \mathbb{Z})$$

such that:

(1) $\iota_k(P_1^k(i_0)) = (\ell(\delta_k) - \ell(\delta_{k-1}))[R] + P_1^{k-1}(i_0)$*;*
(2) For $2 \leq n \leq k-2$, $\iota_k(P_n^k(i_0, \cdots, i_{n-1}; \ell_1, \cdots, \ell_{n-1}))$ *is homologous to*

$$P_n^{k-1}(i_0, \cdots, i_{n-1}; \ell_1, \cdots, \ell_{n-1}).$$

(3) For level $k-1$, $\iota_k(P_{k-1}^k(i_0, \cdots, i_{k-2}; \ell_1, \cdots, \ell_{k-2}))$ *is homologous to*

$$\begin{aligned} T^{k-1}(i_0, \cdots, i_{k-1}, i_{k-1}; \ell_1, \cdots, \ell_{k-1} - 1) &+ T^{k-1}(i_0, \cdots, i_{k-1}, i_{k-1}; \ell_1, \cdots, \ell_{k-1} - 2) + \cdots \\ &+ T^{k-1}(i_0, \cdots, i_{k-1}, i_{k-1}; \ell_1, \cdots, b) \\ &+ E^{k-1}(i_0, \cdots, i_{k-1}; \ell_1, \cdots, \ell_{k-2}), \end{aligned}$$

for any i_{k-1} *and the minimum possible value of* ℓ_{k-1}*.*

(4) $\iota_k(S_1^k(i_0,i_1;\ell_1)) = -P_1^{k-1}(i_0) + P_1^{k-1}(i_2) + [R]$ *for* $i_2 \neq i_0$.

(5) For $2 \leq n \leq k-1$, *the image of* $S_n^k(i_0,\cdots,i_n;\ell_1,\cdots,\ell_n)$ *is homologous to the image under* ι_k *of*

$$-\sum_{m=1}^{n} P_m^k(i_0,\cdots,i_{m-1};\ell_1,\cdots,\ell_{m-1}) + \sum_{m=1}^{n} P_m^k(i_{n+1},i_1,\cdots,i_{m-1};\ell_1,\cdots,\ell_{m-1}) + [R],$$

for $i_{n+1} \neq i_0$ *and modulo adding some type (2) loops at level* $k-1$.

(6) For the exceptional loops we have

$$\begin{aligned}\iota_k(E^k(i_0,\cdots,i_k;\ell_1,\cdots,\ell_{k-1})) = {} & T^{k-1}(i_0,\cdots,i_{k-1},i_{k-1};\ell_1,\cdots,\ell_{k-1}-1)\\ & + T^{k-1}(i_0,\cdots,i_{k-1},i_{k-1};\ell_1,\cdots,\ell_{k-1}-2)+\cdots\\ & + T^{k-1}(i_0,\cdots,i_{k-1},i_{k-1};\ell_1,\cdots,b)\\ & + E^{k-1}(i_0,\cdots,i_{k-1};\ell_1,\cdots,\ell_{k-2}).\end{aligned}$$

(7) $\iota_k(T^k(i_0,i_1,\cdots,i_{k+1};\ell_1,\cdots,\ell_k))$ *is the trivial element.*

Computing the exact rank of the groups $H_1(\mathfrak{N}_k;\mathbb{Z})$ seems an impossible task, since the values of the ℓ-indices for which the different types of loops exist, and are not trivial, does not appear to follow any simple pattern. In contrast, we can easily give a lower bound.

COROLLARY 23.28. *The rank of* $H_1(\mathfrak{N}_k;\mathbb{Z})$ *is at least* $2^{k+2}-1$.

Proof. We have three distinctive elements in $H_1(\mathfrak{N}_k;\mathbb{Z})$: the classes $[R]$, $P_1^k(1)$ and $P_1^k(2)$. Then for each $2 \leq n \leq k-1$ and each combination $(i_0,i_1,\cdots,i_{n-1})$ of 1's and 2's, there is at least one level n loop. Thus we obtain for each n, 2^n elements in $H_1(\mathfrak{N}_k;\mathbb{Z})$. Observe that the actual number of generators is greater than this. For example, for $n=2$, given (i_0,i_1) then for any ℓ_1 such that $s(\delta_k;i_0,i_1) \leq \ell_1 < \ell(\delta_k;i_0,i_1)$ there is a level 2 loop and we are just counting 1 of these.

The number of exceptional loops is given by the sum of

$$2\left(\ell(\delta_k;i_0;i_1,\ell_1;\cdots;i_{k-1},\ell_{k-2};i_{k-1}) - s(\delta_k;i_0;i_1,\ell_1;\cdots;i_{k-1},\ell_{k-2};i_{k-1})\right)$$

over all possible combinations of these indices. Again, counting two generators ($i_k = 1,2$) for each combination $(i_0,i_1,\cdots,i_{k-1})$ of 1's and 2's, we conclude that there are at least 2^{k+1} loops. Analogously, there are at least 2^k type (2) loops at level k.

We obtain that the rank of $H_1(\mathfrak{N}_k;\mathbb{Z})$ is lower bounded by $1+2+\cdots+2^{k+1} = 2^{k+2}-1$. Observe that we are not counting the one turn loops at any level. □

The objective is to build a shape approximation $\mathfrak{U} = \{U_\ell \,|\, \ell = 1,2,\ldots\}$ of $\mathfrak{M}$ satisfying the hypothesis of Proposition 23.8. That is, we require that for $k > 0$:

- the rank of $H_1(U_k;\mathbb{Z}) \geq 2^k$,
- for all $\ell > k$ the rank of the image $H_1(U_\ell;\mathbb{Z}) \to H_1(U_k;\mathbb{Z})$ is 3.

Observe that taking a sequence ϵ_k of sufficiently small positive numbers and $U_k = U(\mathfrak{N}_k,\epsilon_k)$, then Lemma 23.25 and Corollary 23.28 imply the first condition. In order to satisfy the second condition, we will extract a subsequence of $\mathfrak{N}_{n_k}$ for which the rank of the image $H_1(\mathfrak{N}_{n_{k+1}};\mathbb{Z}) \to H_1(\mathfrak{N}_{n_k};\mathbb{Z})$ is 3. This follows from the following result.

The rank of the image of the map $\iota_\ell^0 : H_1(\mathfrak{N}_\ell;\mathbb{Z}) \to H_1(\mathfrak{N}_0;\mathbb{Z})$ is 3, since the generators $[R]$, $[b_1]$ and $[b_2]$ are in the image and they generate $H_1(\mathfrak{N}_0;\mathbb{Z})$.

As in Remark 23.23, the first homology group of $C_{\mathbb{K}}^+(\mathfrak{M}_0^1,\delta_k)$ is generated by the loops $[R]$, $P_1^k(1)$, $P_1^k(2)$ and the level 1 one turn loops $S_1^k(i_0,i_1;\ell_1)$. Since the rank of $H_1(\mathfrak{N}_0;\mathbb{Z})$ is 3, what the proposition asserts is that given k there is a number ℓ big enough, such that all the homology classes in $\mathfrak{N}_\ell$ are homologous inside $\mathfrak{N}_k$ to loops contained in the δ_k-neighborhood of $\mathfrak{M}_0^1$, and even more in the group generated by $[R]$, $P_1^k(1)$ and $P_1^k(2)$. The idea behind the proof is that if there is a loop in $\mathfrak{N}_\ell$, its image in $\mathfrak{N}_k$ is a loop that travels along

propellers of level at must k. These propellers have to be sufficiently near the core cylinder $\tau(\mathcal{R}')$ to guarantee that they branch up to level ℓ. Thus the image of the loop in $\mathfrak{N}_k$ has to be close to levels 0 and 1, and then are homologous to a combination of the loops $[R]$, $P_1^k(1)$, $P_1^k(2)$. In order to make this assertion precise we need to consider the images of the exceptional loops and the loops at levels n for any $2 \leq n \leq \ell - 1$.

PROPOSITION 23.29. *Given $k \geq 2$ there exists $\ell > k$ such that the image of the map*

$$\iota_\ell^k : H_1(\mathfrak{N}_\ell; \mathbb{Z}) \to H_1(\mathfrak{N}_k; \mathbb{Z}) \tag{256}$$

has rank equal to 3.

Proof. Fix $k \geq 2$ and consider the subgroup G_k of $H_1(\mathfrak{N}_k; \mathbb{Z})$ generated by $[R]$, $P_1^k(1)$ and $P_1^k(2)$. We will find $\ell \gg k$ such that the image of ι_ℓ^k is G_k.

In the following arguments, all the homotopies will be contained in $\mathfrak{N}_k$.

First, observe that case (1) of Proposition 23.27 shows that the map $\iota_i \colon H_1(\mathfrak{N}_i; \mathbb{Z}) \to H_1(\mathfrak{N}_{i-1}; \mathbb{Z})$ satisfies for each $i > k$,

$$\iota_i^{i-1}(P_1^i(i_0)) = (\ell(\delta_i) - \ell(\delta_{i-1}))[R] + P_1^{i-1}(i_0).$$

It then follows by induction, that for any $\ell > k$, the images of the homology classes defined by the level 1 loops, $P_1^\ell(i_0)$ for $i_0 = 1, 2$, are in G_k. Thus, the subgroup G_k is contained in the image of ι_ℓ^k.

Next consider the one turn loops $S_n^k(i_0, \cdots, i_n; \ell_1, \cdots, \ell_n)$ defined in case (3) of Definitions 23.20, 23.22 and 23.26. Case (4) of Proposition 23.27 gives a reductive procedure for reducing the homology classes of the 1 turn loops $S_n^k(i_0, \cdots, i_n; \ell_1, \cdots, \ell_n)$ to some combination of $[R]$ and the classes defined by level n loops, for some $1 \leq n < \ell$. Thus, the one turn loops do not contribute to the rank of the image of ι_ℓ^k for any $\ell > k$.

The Type (2) loops at level ℓ were introduced in case (5) of Definitions 23.20, 23.22 and 23.26. For each $\ell > 1$, it was shown that the images of the homology classes of these loops under the map $\iota_\ell \colon H_1(\mathfrak{N}_\ell; \mathbb{Z}) \to H_1(\mathfrak{N}_{\ell-1}; \mathbb{Z})$ are trivial. Thus, for all $\ell > k$, their images by $\iota_\ell^k \colon H_1(\mathfrak{N}_\ell; \mathbb{Z}) \to H_1(\mathfrak{N}_k; \mathbb{Z})$ are trivial.

Next, we consider the level n loops $P_n^\ell(i_0, \cdots, i_{n-1}; \ell_1, \cdots, \ell_{n-1})$ for $2 \leq n \leq \ell - 1$, as defined in cases (2b) of Definitions 23.22 and 23.26. These are loops defined by paths that go out, possibly a "long" distance, along a propeller at level n, then connect to a path along propellers at a level less than n, and return along the shortest path tangent to $\mathfrak{M}_0$.

Fix n between 2 and $\ell - 1$, and assume without loss of generality that $i_0 = 1$. Let P be a propeller satisfying the two conditions: the tip of the level n propeller $P = \tau(P_{\gamma(i_1, \ell_1; \cdots; i_{n-1}, \ell_{n-1})})$ is contained in $C_{\mathbb{K}}^+(\mathfrak{M}_0^{n-1}, \delta_\ell)$, and P does not retract to this set. Note that these conditions depend on the value of δ_ℓ. Then the loop $P_n^\ell(i_0, \cdots, i_{n-1}; \ell_1, \cdots, \ell_{n-1})$ exists.

Recall from Lemma 13.10 that level n propellers accumulate (as the first ℓ-index goes to infinity) on level $n-1$ propellers, that respectively accumulate on level $n-2$ propellers, and so forth. Assume for a moment that $\ell > k$ is fixed, with the level n propeller as above. Then there exists a positive number $\beta_\ell > \delta_\ell$ such that the propeller P is contained in $C_{\mathbb{K}}^+(\mathfrak{M}_0^1, \beta_\ell)$. Moreover, as ℓ tends to infinity, β_ℓ decreases to zero. Given this observation, we claim that for k fixed, there exists $\ell > k$ such that any propeller P as above is contained in $C_{\mathbb{K}}^+(\mathfrak{M}_0^1, \delta_k)$, as it suffices to take any $\ell > k$ such that $\beta_\ell \leq \delta_k$.

Recall that $P_n^\ell(i_0, \cdots, i_{n-1}; \ell_1, \cdots, \ell_{n-1})$, for $2 \leq n \leq \ell - 1$ is formed by the concatenation of the paths

$$\tau(p(i_0; i_1, \ell_1; \cdots; i_{n-1}, \ell_{n-1})) \xrightarrow{\text{tangent}} \tau(p(i_0; i_1, \ell_1; \cdots; i_{n-1}, \ell_{n-1}; i_n, \ell_n)) \tag{257}$$

$$\xrightarrow{E_{i_n}} \tau(p(i_1; i_2, \ell_2; \cdots; i_n, \ell_n)) \tag{258}$$

$$\xrightarrow{\text{tangent}} p(i_0; i_1, \ell_1; \cdots; i_{n-1}, \ell_{n-1})). \tag{259}$$

The tangent paths (257) and (259) are contained in $C^+_{\mathbb{K}}(\mathfrak{M}^1_0, \delta_k)$, and thus are homotopic to tangent paths contained in propellers at levels 0 and 1. Thus after homotopy, we obtain the loop

$$\tau(p(i_{n-1})) \xrightarrow{\text{tangent}} \tau(p(i_{n-1}; i_n, \ell_n)) \xrightarrow{E_{i_n}} \tau(p(i_n)) \xrightarrow{\text{tangent}} \tau(p(i_{n-1})), \tag{260}$$

that is homologous to a class in G_k.

Now consider the image of the homology classes defined by the exceptional loops $E^\ell(i_0, \cdots, i_\ell; \ell_1, \cdots; \ell_{\ell-1})$ which were introduced in case (4) of Definitions 23.20, 23.22 and 23.26. Recall that such a loop can be described as the composition of paths:

$$\tau(p(i_0; i_1, \ell_1; \cdots; i_{\ell-1}, \ell_{\ell-1})) \xrightarrow{\text{tangent}(\ell)} \tau(p(i_0; i_1, \ell_1; \cdots; i_{\ell-1}, \ell_{\ell-1}; i_\ell, b)) \tag{261}$$

$$\xrightarrow{E_{i_\ell}} \tau(p(i_1; i_2, \ell_2; \cdots; i_{\ell-1}, \ell_{\ell-1}; i_\ell, b)) \tag{262}$$

$$\xrightarrow{\text{tangent}(<\ell)} \tau(p(i_0; i_1, \ell_1; \cdots; i_{\ell-1}, \ell_{\ell-1})). \tag{263}$$

Figure 56 illustrates such a path for the case $k = 2$. The path in (261) starts at a point on a propeller at level $\ell - 1$, entering a propeller at level ℓ and continuing to a point which is the first entry point into a filled propeller. Next, (262) is a short path in the face E_{i_ℓ} to a point at lower level. It then follows the path (263) along propellers at level less than ℓ back to the starting point. A key point, as seen in the analysis below, is that while the path (263) at lower level may be "short" as in Figure 56, it may just as well traverse the tree $\mathbf{T}_\Phi$ from one extreme to another and not be "short".

The level k propellers are filled in $\mathfrak{N}_k$, hence the tangent path segments in (261) and (263) at level greater or equal to k are homotopic to tangent segments at level k. First, the tangent segment (261) is homotopic to

$$\tau(p(i_q; i_{q+1}, \ell_{q+1}; \cdots; i_{\ell-1}, \ell_{\ell-1})) \xrightarrow{\text{tangent}(k)} \tau(p(i_q; i_{q+1}, \ell_{q+1}; \cdots; i_{\ell-1}, \ell_{\ell-1}; i_\ell, b)), \tag{264}$$

for $q = \ell - k$. Note that the result (264) illustrates an important aspect of the homotopy operation moving a path segment from a level ℓ propeller to one at a lower level. This results in the elimination of the initial stages of the labeling; that is, the initial indices $(i_0; i_1, \ell_1; \cdots; i_{q-1}, \ell_{q-1})$ are deleted in (264).

Next, the second tangent segment (263), which is a path

$$\tau(p(i_1; i_2, \ell_2; \cdots; i_{\ell-1}, \ell_{\ell-1}; i_\ell, b)) \xrightarrow{\text{tangent}(<\ell)} \tau(p(i_0; i_1, \ell_1; \cdots; i_{\ell-1}, \ell_{\ell-1})), \tag{265}$$

can be decomposed as a concatenation of segments tangent to propellers at level less than ℓ. This path travels through the tree $\mathbf{T}_\Phi$ to connect the two level $\ell - 1$ endpoints in $\mathfrak{M}^{\ell-1}_0$. We denote the paths at each level as follows, where we note that now the final indices are first being removed in lines (266) to (269), as the path goes to points at successively lower levels. The path then travels along the set $\mathfrak{M}^{k-1}_0$ as indicted in (269). It then continues back up the levels to the path in (271). This process yields the following path which is equivalent to the path (265).

$$\tau(p(i_1; i_2, \ell_2; \cdots; i_\ell, b)) \xrightarrow{\text{tangent}(\ell-1)} \tau(p(i_1; i_2, \ell_2; \cdots; i_{\ell-1}, \ell_{\ell-1})) \tag{266}$$

$$\xrightarrow{\text{tangent}(\ell-2)} \tau(p(i_1; i_2, \ell_2; \cdots; i_{\ell-2}, \ell_{\ell-2})) \tag{267}$$

$$\cdots$$

$$\xrightarrow{\text{tangent}(k=\ell-q)} \tau(p(i_1; i_2, \ell_2; \cdots; i_k, \ell_k)) \tag{268}$$

$$\xrightarrow{\text{tangent}(<k)} \tau(p(i_0; i_1, \ell_1; \cdots; i_{k-1}, \ell_{k-1})) \tag{269}$$

$$\xrightarrow{\text{tangent}(k)} \tau(p(i_0; i_1, \ell_1; \cdots; i_k, \ell_k)) \tag{270}$$

$$\cdots$$

$$\xrightarrow{\text{tangent}(\ell-1)} \tau(p(i_0; i_1, \ell_1; \cdots; i_{\ell-1}, \ell_{\ell-1})). \tag{271}$$

Note that the reduction in level process stops with the paths in level k, as we can no longer move the curves by a homotopy through the unfilled propellers at level less than k. Instead, the curve simply follows the propellers in $\mathfrak{M}_0^k$, as indicated by the path in (269).

Replacing each of the tangential segments above, (266) to (271), with a segment of level at most $k = \ell - q$, we obtain:

$$\tau(p(i_1; i_2, \ell_2; \cdots ; i_\ell, b)) \xrightarrow{E_{i_\ell}} \tau(p(i_q; i_{q+1}, \ell_{q+1}; \cdots ; i_\ell, b)) \tag{272}$$

$$\xrightarrow{\text{tangent}(k)} \tau(p(i_q; i_{q+1}, \ell_{q+1}; \cdots ; i_{\ell-1}, \ell_{\ell-1})) \tag{273}$$

$$\xrightarrow{E_{i_{\ell-1}}} \tau(p(i_{q-1}; i_q, \ell_q; \cdots ; i_{\ell-1}, \ell_{\ell-1})) \tag{274}$$

$$\xrightarrow{\text{tangent}(k)} \tau(p(i_{q-1}; i_q, \ell_q; \cdots ; i_{\ell-2}, \ell_{\ell-2})) \tag{275}$$

$$\cdots$$

$$\xrightarrow{\text{tangent}(k)} \tau(p(i_1; i_2, \ell_2; \cdots ; i_k, \ell_k)) \tag{276}$$

$$\xrightarrow{\text{tangent}(< k)} \tau(p(i_0; i_1, \ell_1; \cdots ; i_{k-1}, \ell_{k-1})) \tag{277}$$

$$\xrightarrow{\text{tangent}(k)} \tau(p(i_0; i_1, \ell_1; \cdots ; i_k, \ell_k)) \tag{278}$$

$$\xrightarrow{E_{i_k}} \tau(p(i_1; i_2, \ell_2; \cdots ; i_k, \ell_k)) \tag{279}$$

$$\cdots$$

$$\xrightarrow{\text{tangent}(k)} \tau(p(i_{q-1}; i_q, \ell_q; \cdots ; i_{\ell-1}, \ell_{\ell-1})). \tag{280}$$

As before, the homotopy operation eliminates the initial indices labeling the endpoints of the path in $\mathfrak{M}_0^\ell$ as the path is moved to a tangential path in a lower level of $\mathfrak{M}_0^k$.

Now observe that if we follow the paths and homotopies indicated in the lines (264) which is homotopic to (261), followed by (262), followed by (272), followed by (273), we obtain a loop:

$$\begin{aligned} \tau(p(i_q; i_{q+1}, \ell_{q+1}; \cdots ; i_{\ell-1}, \ell_{\ell-1})) &\xrightarrow{\text{tangent}(k)} \tau(p(i_q; i_{q+1}, \ell_{q+1}; \cdots ; i_{\ell-1}, \ell_{\ell-1}; i_\ell, b)) \\ &\xrightarrow{E_{i_\ell}} \tau(p(i_1; i_2, \ell_2; \cdots ; i_{\ell-1}, \ell_{\ell-1}; i_\ell, b)) \\ &\xrightarrow{E_{i_\ell}} \tau(p(i_q; i_{q+1}, \ell_{q+1}; \cdots ; i_\ell, b)) \\ &\xrightarrow{\text{tangent}(k)} \tau(p(i_q; i_{q+1}, \ell_{q+1}; \cdots ; i_{\ell-1}, \ell_{\ell-1})) \end{aligned}$$

which is homotopic to the trivial loop, as the first and last tangential paths are inverses of each other.

Thus, the image in $\mathfrak{N}^k$ of the exceptional loop $E^\ell(i_0, \cdots, i_\ell; \ell_1, \cdots ; \ell_{\ell-1})$ defined by the paths in (261), (262) and (263) is homotopic to the loop that starts at the endpoint of (274), then follows (275) up to (280), as indicated in the following:

$$\tau(p(i_{q-1}; i_q, \ell_q; \cdots ; i_{\ell-1}, \ell_{\ell-1})) \xrightarrow{\text{tangent}(k)} \tau(p(i_{q-1}; i_q, \ell_q; \cdots ; i_{\ell-2}, \ell_{\ell-2})) \tag{281}$$

$$\cdots$$

$$\xrightarrow{\text{tangent}(k)} \tau(p(i_1; i_2, \ell_2; \cdots ; i_k, \ell_k)) \tag{282}$$

$$\xrightarrow{\text{tangent}(< k)} \tau(p(i_0; i_1, \ell_1; \cdots ; i_{k-1}, \ell_{k-1})) \tag{283}$$

$$\xrightarrow{\text{tangent}(k)} \tau(p(i_0; i_1, \ell_1; \cdots ; i_k, \ell_k)) \tag{284}$$

$$\xrightarrow{E_{i_k}} \tau(p(i_1; i_2, \ell_2; \cdots ; i_k, \ell_k)) \tag{285}$$

$$\cdots$$

$$\xrightarrow{\text{tangent}(k)} \tau(p(i_{q-1}; i_q, \ell_q; \cdots ; i_{\ell-1}, \ell_{\ell-1})). \tag{286}$$

Now we express the above loop defined by the paths in (281) to (286) in more detail. We rewrite this loop, starting with the segment tangent in (283) to $\mathfrak{M}_0^{k-1}$:

$$\tau(p(i_1;i_2,\ell_2;\cdots;i_k,\ell_k)) \xrightarrow{\text{tangent}(<k)} \tau(p(i_0;i_1,\ell_1;\cdots;i_{k-1},\ell_{k-1})) \tag{287}$$

$$\xrightarrow{\text{tangent}(k)} \tau(p(i_0;i_1,\ell_1;\cdots;i_k,\ell_k)) \tag{288}$$

$$\xrightarrow{E_{i_k}} \tau(p(i_1;i_2,\ell_2;\cdots;i_k,\ell_k)) \tag{289}$$

$$\xrightarrow{\text{tangent}(k)} \tau(p(i_1;i_2,\ell_2;\cdots;i_{k+1},\ell_{k+1})) \tag{290}$$

$$\xrightarrow{E_{i_{k+1}}} \tau(p(i_2;i_3,\ell_3;\cdots;i_{k+1},\ell_{k+1})) \tag{291}$$

$$\vdots$$

$$\xrightarrow{E_{i_{\ell-2}}} \tau(p(i_{q-1};i_q,\ell_q;\cdots;i_{\ell-2},\ell_{\ell-2})) \tag{292}$$

$$\xrightarrow{\text{tangent}(k)} \tau(p(i_{q-1};i_q,\ell_q;\cdots;i_{\ell-1},\ell_{\ell-1})) \tag{293}$$

$$\xrightarrow{\text{tangent}(k)} \tau(p(i_{q-1};i_q,\ell_q;\cdots;i_{\ell-2},\ell_{\ell-2})) \tag{294}$$

$$\xrightarrow{E_{i_{\ell-2}}} \tau(p(i_{q-2};i_{q-1},\ell_{q-1};\cdots;i_{\ell-2},\ell_{\ell-2})) \tag{295}$$

$$\vdots$$

$$\xrightarrow{E_{i_{k+1}}} \tau(p(i_1;i_2,\ell_1;\cdots;i_{k+1},\ell_{k+1})) \tag{296}$$

$$\xrightarrow{\text{tangent}(k)} \tau(p(i_1;i_2,\ell_2;\cdots;i_k,\ell_k)). \tag{297}$$

Observe that the tangent parts in lines (288) to (293) go from a point at level $k-1$ to a point at level k, while the tangent parts in lines (294) to (297) go from a point at level k to a point at level $k-1$

The arrows in lines (293) and (294) represent paths that are tangent to the same propeller, have the same endpoints and opposite directions, hence their concatenation is homotopic to the trivial loop.

Also notice that the arrows in lines (292) and (295) represent paths in $E_{i_{\ell-2}}$ with the same endpoints and opposite directions, hence their concatenation is again homotopic to the trivial loop.

The process continues cancelling pairs of arrows in the representation above, until (296) cancels with (291) and (297) cancels with (290). Hence we are left with the loop:

$$\tau(p(i_1;i_2,\ell_2;\cdots;i_k,\ell_k)) \xrightarrow{\text{tangent}(<k)} \tau(p(i_0;i_1,\ell_1;\cdots;i_{k-1},\ell_{k-1})) \tag{298}$$

$$\xrightarrow{\text{tangent}(k)} \tau(p(i_0;i_1,\ell_1;\cdots;i_k,\ell_k)) \tag{299}$$

$$\xrightarrow{E_{i_k}} \tau(p(i_1;i_2,\ell_2;\cdots;i_k,\ell_k)). \tag{300}$$

The loop defined by the paths in (298), (299) and (300), can then be re-arranged (by moving the first arrow to be last) as the concatenation

$$\tau(p(i_0;i_1,\ell_1;\cdots;i_{k-1},\ell_{k-1})) \xrightarrow{\text{tangent}(k)} \tau(p(i_0;i_1,\ell_1;\cdots;i_k,\ell_k)) \tag{301}$$

$$\xrightarrow{E_{i_k}} \tau(p(i_1;i_2,\ell_2;\cdots;i_k,\ell_k)) \tag{302}$$

$$\xrightarrow{\text{tangent}(<k)} \tau(p(i_0;i_1,\ell_1;\cdots;i_{k-1},\ell_{k-1})). \tag{303}$$

Note that the first maps follows a level k propeller around the cylinder, until the point $\tau(p(i_0;i_1,\ell_1;\cdots;i_k,\ell_k))$, then it closes by going down one level in the face E_{i_k}, then it closes up by following the tree back at levels less than k.

The homology class of the loop defined by (301) to (302) to (303) then equals the class

$$\mathcal{E}(i_0, \cdots, i_k; \ell_1, \cdots, \ell_k) \in H_1(\mathfrak{N}_k; \mathbb{Z}),$$

defined by

$$\begin{aligned}\mathcal{E}(i_0, \cdots, i_k; \ell_1, \cdots, \ell_k) = T^k(i_0, \cdots, i_k, i_k; \ell_1, \cdots, \ell_{k-1}, \ell_k - 1) + T^k(i_0, \cdots, i_k, i_k; \ell_1, \cdots, \ell_{k-1}, \ell_k - 2) \\ + \cdots + T^k(i_0, \cdots, i_k, i_k; \ell_1, \cdots, \ell_{k-1}, b) + E^k(i_0, \cdots, i_k; \ell_1, \cdots, \ell_{k-1}).\end{aligned}$$

It follows that the homology class in $H_1(\mathfrak{N}_k; \mathbb{Z})$ of the exceptional loop $E^\ell(i_0, \cdots, i_\ell; \ell_1, \cdots; \ell_{\ell-1})$ is equal to $\mathcal{E}(i_0, \cdots, i_k; \ell_1, \cdots, \ell_k) \in H_1(\mathfrak{N}_k; \mathbb{Z})$. Observe that the class $\mathcal{E}(i_0, \cdots, i_k; \ell_1, \cdots, \ell_k)$ depends on i_0 and the first k of the double indices defining the loop $E^\ell(i_0, \cdots, i_\ell; \ell_1, \cdots, \ell_{\ell-1})$, but is independent of the indices above k.

For simplicity, now assume that $i_0 = 1$, then the loop defined by (301) to (302) to (303) becomes the level k loop

$$\tau(p(1; i_1, \ell_1; \cdots; i_{k-1}, \ell_{k-1})) \xrightarrow{\text{tangent}(k)} \tau(p(1; i_1, \ell_1; \cdots; i_k, \ell_k)) \tag{304}$$

$$\xrightarrow{E_{i_k}} \tau(p(i_1; i_2, \ell_2; \cdots; i_k, \ell_k)) \tag{305}$$

$$\xrightarrow{\text{tangent}(< k)} \tau(p(1; i_1, \ell_1; \cdots; i_{k-1}, \ell_{k-1})), \tag{306}$$

where the tangent part at level k is along the propeller $\tau(P_{\gamma(i_1, \ell_1; \cdots; i_k, \ell_k)})$.

Recall that we are assuming that the index ℓ is much larger than k.

If we assume that $\ell_k > \ell(\delta_k; i_0; \cdots; i_{k-2}, \ell_{k-2}; i_{k-1})$, then then the loop defined by concatenating the path in (304), followed by (305), followed by (306), is then homotopic to a loop in $C^+_{\mathbb{K}}(\mathfrak{M}^{k-1}_0, \delta_k)$.

Now proceed recursively. If we assume that $\ell_{k-1} > \ell(\delta_k; i_0; \cdots; i_{k-3}, \ell_{k-3}; i_{k-2})$, then the result of the homotopy of the above loop into $C^+_{\mathbb{K}}(\mathfrak{M}^{k-1}_0, \delta_k)$ is then homotopic to a loop in $C^+_{\mathbb{K}}(\mathfrak{M}^{k-2}_0, \delta_k)$.

Continuing in this way, assuming that all the ℓ-indices are large enough, we obtain a homotopy of the loop defined by (304), (305) and (306), to a loop in $C^+_{\mathbb{K}}(\mathfrak{M}^1_0, \delta_k)$. Let $\widetilde{E}(i_0, \cdots, i_k; \ell_1, \cdots, \ell_k)$ denote the loop contained in $C^+_{\mathbb{K}}(\mathfrak{M}^1_0, \delta_k)$ which results from the above homotopies. Then for ℓ sufficiently large, the homology class $\mathcal{E}(i_0, \cdots, i_k; \ell_1, \cdots, \ell_k)$ is defined by the loop $\widetilde{E}(i_0, \cdots, i_k; \ell_1, \cdots, \ell_k)$.

We now claim, that for ℓ sufficiently large, the homology class $\mathcal{E}(i_0, \cdots, i_k; \ell_1, \cdots, \ell_k) \in G_k$.

Observe that the endpoint of line (304), that is the point $\tau(p(1; i_1, \ell_1; i_2.\ell_2; \cdots; i_k, \ell_k))$, can be connected to the level 1 point $\tau(p(i_{k-1}; i_k, \ell_k))$ by a path in E_{i_k} that is inside the set $C^+_{\mathbb{K}}(\mathfrak{M}^1_0, \delta_k)$.

Recall that as ℓ_k increases to infinity, the level 1 points $\tau(p(i_{k-1}; i_k, \ell_k))$ approach the level 0 point $\tau(p(i_k))$.

As the index ℓ is increased, the index ℓ_k also must increase. We may thus assume that ℓ_k is such that $\tau(p(1; i_1, \ell_1; i_2.\ell_2; \cdots; i_k, \ell_k))$ can be connected to the level 0 point $\tau(p(i_k))$ by a path in $E_{i_k} \cap C^+_{\mathbb{K}}(\mathfrak{M}^1_0, \delta_k)$. We choose a value for ℓ so that this condition is satified.

Since the loop $\widetilde{E}(i_0, \cdots, i_k; \ell_1, \cdots, \ell_k)$ is contained in $C^+_{\mathbb{K}}(\mathfrak{M}^1_0, \delta_k)$, the path in line (304) can be homotoped to a path tangent at level 1. The choice of ℓ sufficiently large then implies that $\widetilde{E}(i_0, \cdots, i_k; \ell_1, \cdots, \ell_k)$ is homotopic to the loop

$$\tau(p(i_{k-1})) \xrightarrow{\text{tangent}(1)} \tau(p(i_{k-1}; i_k, \ell_k)) \tag{307}$$

$$\xrightarrow{E_{i_k}} \tau(p(i_k)) \tag{308}$$

$$\xrightarrow{\text{tangent}(0)} \tau(p(i_{k-1})). \tag{309}$$

Thus $\widetilde{E}(i_0, \cdots, i_k; \ell_1, \cdots, \ell_k)$ is homotopic to a loop that travels along a level 1 propeller as in line (307), then jumps back to the Reeb cylinder as in line (308) and then closes by a path contained in the Reeb cylinder as in line (309).

Observe that since line (309) is homotopic to line (306), it might be more complicated than the shortest path from $\tau(p(i_{k-1}))$ to $\tau(p(i_k))$. In any case, the path represented by lines (307) to (309) can be written as the sum $P_1^k(i_{k-1})$ and a certain multiple of $[R]$, thus we get a loop in G_k. □

To define the shape approximation $\mathfrak{U} = \{U_k \mid k = 1, 2, \ldots\}$ satisfying the hypothesis of Proposition 23.8, let $U_1 = U(\mathfrak{N}_2, \epsilon_1)$ for $\epsilon_1 > 0$ small enough such that U_1 retracts to $\mathfrak{N}_2$ (as in Lemma 23.18). By Proposition 23.29 there exists $\ell_2 > 2$ such that the image of $\iota_{\ell_2}^2$ has rank 3. Set $U_2 = U(\mathfrak{N}_{\ell_2}, \epsilon_2)$ for $\epsilon_2 > 0$ small enough such that U_2 retracts to $\mathfrak{N}_{\ell_2}$. Recursively define ℓ_k such that the image of $\iota_{\ell_k}^{\ell_{k-1}}$ has rank 3 and set $U_k = U(\mathfrak{N}_{\ell_k}, \epsilon_k)$ for $\epsilon_k > 0$ small enough such that U_k retracts to $\mathfrak{N}_{\ell_k}$.

The following result finishes the proof of Theorem 23.4.

PROPOSITION 23.30. *There is no shape approximation $\mathfrak{V} = \{V_k \mid k = 1, 2, \ldots\}$ of $\mathfrak{M}$ such that the rank of the homology groups $H_1(V_k, \mathbb{Z})$ is 3 for any k.*

Proof. Let $\mathfrak{V} = \{V_k \mid k = 1, 2, \ldots\}$ be a given shape approximation of $\mathfrak{M}$. Take $k > 0$, then there exists $\epsilon > 0$ depending on k, such that $C^+_{\mathbb{K}}(\mathfrak{M}^1_0, \epsilon) \subset V_k$. The first homology group of $C^+_{\mathbb{K}}(\mathfrak{M}^1_0, \epsilon)$ has at least 3 generators, one corresponding to the Reeb cylinder, and analogous to the class $[R]$ introduced above. The other two generators are associated to paths which travel from the basepoint on the Reeb cylinder, through an entry region, then back down one of the two level 1 propellers back to a neighborhood of the Reeb cylinder. These are analogous to the classes $[b_1]$ and $[b_2]$ introduced before. For k sufficiently large, we can assume that these three generators are also generators of $H_1(V_k, \mathbb{Z})$. Thus, to prove the lemma, it suffices to show that for k sufficiently large, there is at least one more generator of $H_1(V_k, \mathbb{Z})$. As before, let $G_k \subset H_1(V_k; \mathbb{Z})$ be the group generated by the three elements above.

Recall from Section 19 that the connected components of the intersection $\mathfrak{M}_{\mathbf{R}_0} = \mathfrak{M} \cap \mathbf{R}_0$ form a (singular) lamination, and the intersection $\mathfrak{C}' = \mathfrak{M} \cap \mathcal{T}$ with the transversal $\mathcal{T} \subset \mathbf{R}_0$ (introduced in (124)) is a Cantor set. Each V_k is an open set containing $\mathfrak{M}$, thus the set $V_k \cap \mathbf{R}_0$ is a neighborhood of $\mathfrak{M}_{\mathbf{R}_0}$. It follows that for k sufficiently large, the number of connected components of $V_k \cap \mathbf{R}_0$ must tend to infinity. Moreover, given distinct points $x, y \in \mathfrak{C}'$, it follows that for k sufficiently large, the points must be contained in distinct connected components of $V_k \cap \mathbf{R}_0$. Also, let $\gamma_x \subset \mathfrak{M}_{\mathbf{R}_0}$ be the arc-component containing x, and likewise let $\gamma_y \subset \mathfrak{M}_{\mathbf{R}_0}$ be the arc-component containing y. Then for a possibly larger value of k, the compact arcs γ_x and γ_y are contained in distinct connected components of $V_k \cap \mathbf{R}_0$.

For each k, let V_k^0 denote the connected component of $V_k \cap \mathbf{R}_0$ containing the trace $\tau(\mathcal{R}') \cap \mathbf{R}_0$ of the Reeb cylinder. Then for k sufficiently large, V_k^0 does not contain all the level one points $p_0(i_0; i_1, \ell_1)$ in $\mathbf{R}_0$. Even more, let n_k be the largest integer such that for all $a \leq \ell_1 \leq n_k$, the point $p_0(i_0; i_1, \ell_1)$ and the arc-component of $\mathfrak{M}_{\mathbf{R}_0}$ it defines are not contained in V_k^0, for any pair (i_0, i_1).

Recall that $p_0(i_0; 1, \ell)$ denotes the lower endpoint of the curve $\gamma_0(\ell) \subset \mathfrak{M}_{\mathbf{R}_0}$ if $i_0 = 1$, and of $\lambda_0(\ell) \subset \mathfrak{M}_{\mathbf{R}_0}$ if $i_0 = 2$; and $p_0(i_0; 2, \ell)$ is the upper endpoint of the curve $\gamma_0(\ell)$ if $i_0 = 1$, and of $\lambda_0(\ell)$ if $i_0 = 2$.

Let k be sufficiently large so that $n_k > 1$. We set $i_1 = 1$ in the following. For each level 2 point $p_0(1; 1, \ell_1; 1, n_k)$, let $\gamma_0(1, \ell_1; n_k) \subset \mathfrak{M}_{\mathbf{R}_0}$ be the curve with this as lower endpoint. Let V_k^1 be the connected component of $V_k \cap \mathbf{R}_0$ containing the point $p_0(1; 1, n_k)$, and hence the curve $\gamma_0(n_k)$. Note that by our choices, $V_k^0 \cap V_k^1 = \emptyset$. Then for ℓ_1 sufficiently large, we have $\gamma_0(1, \ell_2; n_k) \subset V_k^1$.

Using the notation for paths as above, define the loop $\sigma(\ell_1)$ as

$$\begin{aligned} p_0(1; 1, n_k) &\xrightarrow{\text{tangent}(< 3)} p_0(1; 1, \ell_1; 1, n_k) \\ &\xrightarrow{V_k \cap \mathbf{R}_0} p_0(1; 1, n_k). \end{aligned}$$

Moreover, this path can be chosen so that it is disjoint for the set V_k^0. In terms of the tree $\mathbf{T}_\Phi$, we are choosing a path in a level 2 branch that contains a vertex in $V_k^1 \cap \mathbf{T}_\Phi$ but no vertices in $V_k^0 \cap \mathbf{T}_\Phi$.

Let $[\sigma(\ell_1)] \in H_1(V_k, \mathbb{Z})$ be the homology class of this loop. We claim that it is not contained in G_k, and thus the rank of $H_1(V_k, \mathbb{Z})$ is greater than three as needed. Suppose that $\sigma(\ell_1)$ is homologous to a class in G_k, then there exists a connected singular surface $B \subset V_k$ with boundary, such that $\sigma(\ell_1)$ is one boundary component, and the other boundary component represents a class in G_k. As B is connected, this implies that $V_k^0 \cap V_k^1 \neq \emptyset$, which is a contradiction. □

Note that the above proof of Proposition 23.30 is a particular case of using the Mayer-Vietoris Theorem for the decomposition of V_k as the union of the sets $V_k - (V_k \cap \mathbf{R}_0)$ and the set V_k' which is a small open neighborhood of $V_k \cap \mathbf{R}_0$ in V_k.

We conclude this section with a proof that the Mittag-Leffler Condition in Theorem 23.7 holds for the first homology groups.

Proof of Theorem 23.7. Let $\mathfrak{U} = \{U_\ell\}$ for Σ be a shape approximation of $\mathfrak{M}$. We must show that for any $\ell \geq 1$ there exists $p > \ell$ such that for any $q \geq p$

$$Image\{H_1(U_p; \mathbb{Z}) \to H_1(U_\ell; \mathbb{Z})\} = Image\{H_1(U_q; \mathbb{Z}) \to H_1(U_\ell; \mathbb{Z})\}. \tag{310}$$

Fix $\ell > 0$, and we may assume without loss of generality that $U_\ell \subset \mathfrak{N}_0$. Choose k sufficiently large so that $\mathfrak{N}_k \subset U_\ell$. Then by Proposition 23.29, there exists $m > k$ so that the image of the map $\iota_m^k : H_1(\mathfrak{N}_m; \mathbb{Z}) \to H_1(\mathfrak{N}_k; \mathbb{Z})$ has rank 3. Let $\epsilon > 0$ so that $U(\mathfrak{N}_m, \epsilon)$ retracts to $\mathfrak{N}_m$. Then choose p sufficiently large so that $U_p \subset U(\mathfrak{N}_m, \epsilon)$, then for all $q \geq p$ we have $U_q \subset U_p \subset U(\mathfrak{N}_m, \epsilon)$.

For any such $q \geq p$, there exists some v such that $\mathfrak{N}_v \subset U_q$. Then consider the sequence of homology groups, with maps induced by the inclusions,

$$H_1(\mathfrak{N}_v; \mathbb{Z}) \longrightarrow H_1(U_q; \mathbb{Z}) \longrightarrow H_1(U(\mathfrak{N}_m, \epsilon); \mathbb{Z}) \cong H_1(\mathfrak{N}_m; \mathbb{Z}) \xrightarrow{\iota_m^k} H_1(\mathfrak{N}_k; \mathbb{Z}) \longrightarrow H_1(U_\ell; \mathbb{Z}) \tag{311}$$

The proof of Proposition 23.29 shows that the images of $H_1(\mathfrak{N}_v; \mathbb{Z})$ and $H_1(\mathfrak{N}_m; \mathbb{Z})$ under these maps are both equal to the subgroup $G_k \subset H_1(\mathfrak{N}_k; \mathbb{Z})$, so it follows that the image of $H_1(U_q; \mathbb{Z}) \to H_1(U_\ell; \mathbb{Z})$ equals the image of G_k in $H_1(U_\ell; \mathbb{Z})$. Thus, the image is independent of the choice of $q \geq p$, as was to be shown. □

References

[1] L. Barreira and Ya.B. Pesin, **Lyapunov exponents and smooth ergodic theory**, University Lecture Series. Vol. 23, American Mathematical Society, Providence, RI, 2002.

[2] C. Bonatti, L. Díaz and M. Viana **Dynamics beyond uniform hyperbolicity**, Encyclopaedia of Mathematical Sciences, Vol. 102, Springer-Verlag, Berlin, 2005.

[3] K. Borsuk, *Concerning homotopy properties of compacta*, **Fund. Math.**, 62:223–254, 1968.

[4] K. Borsuk, *On movable compacta*, **Fund. Math.**, 66:137–146, 1969.

[5] K. Borsuk, **Theory of shape**, Monografie Mat., vol. 59, Polish Science Publ., Warszawa, 1975.

[6] R. Bowen, *Entropy for group endomorphisms and homogeneous spaces*, **Trans. Amer. Math. Soc.**, 153:401–414, 1971.

[7] A. Candel and L. Conlon, **Foliations I**, Amer. Math. Soc., Providence, RI, 2000.

[8] W.-C. Cheng and B. Li, *Zero entropy systems*, **J. Stat. Phys.**, 140:1006–1021, 2010.

[9] A. Clark and J. Hunton, *Tiling spaces, codimension one attractors and shape*, **New York J. Math.**, 18:765–796, 2012.

[10] M. de Carvalho, *Entropy dimension of dynamical systems*, **Portugal. Math.**, 54:19–40, 1997.

[11] D. Dou, W. Huang and K.K. Park, *Entropy dimension of topological dynamical systems*, **Trans. Amer. Math. Soc.**, 363:659–680, 2011.

[12] J. Dydak and J. Segal, **Shape theory**, Lecture Notes in Mathematics Vol. 688, Springer, Berlin, 1978.

[13] D.B.A. Epstein, *Periodic flows on 3-manifolds*, **Annals of Math.**, 95:68–82, 1972.

[14] D. B. A. Epstein and E. Vogt, *A counterexample to the periodic orbit conjecture in codimension* 3, **Ann. of Math. (2)**, 108:539–552, 1978.

[15] R.H. Fox, *On shape*, **Fund. Math.**, 74:47–71, 1972.

[16] É. Ghys, R. Langevin, and P. Walczak, *Entropie géométrique des feuilletages*, **Acta Math.**, 160:105–142, 1988.

[17] É Ghys, *Construction de champs de vecteurs sans orbite périodique (d'après Krystyna Kuperberg)*, Séminaire Bourbaki, Vol. 1993/94, Exp. No. 785, **Astérisque**, 227: 283–307, 1995.

[18] M. Handel, *One-dimensional minimal sets and the Seifert conjecture*, **Ann. of Math. (2)**, 111:35–66, 1980.

[19] J.C. Harrison, C^2 *counterexamples to the Seifert conjecture*, **Topology**, 27:249–278, 1988.

[20] S. Hurder, *Lectures on Foliation Dynamics*, **Foliations: Dynamics, Geometry and Topology**, Advanced Courses in Mathematics CRM Barcelona, Springer Basel, 2014.

[21] S. Hurder and A. Rechtman, *Zippered laminations at the boundary of hyperbolicity*, preprint, 2015.

[22] A. Kadlof, *On the shape of pointed compact connected subsets of* E^3, **Fund. Math.**, vol. 115, no. 3:163–193, 1983.

[23] A. Katok, *Lyapunov exponents, entropy and periodic orbits for diffeomorphisms*, **Inst. Hautes Études Sci. Publ. Math.**, 51:137–173, 1980.

[24] A. Katok and J.-P. Thouvenot, *Slow entropy type invariants and smooth realization of commuting measure-preserving transformations*, **Ann. Inst. H. Poincaré Probab. Statist.**, 33:323–338, 1997.

[25] J. Krasinkiewicz, *On pointed* 1*-movability and related notions*, **Fund. Math.**, 114:29–52, 1981.

[26] K. Kuperberg, *A smooth counterexample to the Seifert conjecture*, **Ann. of Math. (2)**, 140:723–732, 1994.

[27] G. Kuperberg and K. Kuperberg, *Generalized counterexamples to the Seifert conjecture*, **Ann. of Math. (2)**, 144:239–268, 1996.

[28] K. Kuperberg, *personal communication*, 2011.

[29] R. Mañé, **Ergodic theory and differentiable dynamics**, Ergebnisse der Mathematik und ihrer Grenzgebiete (3), Springer-Verlag, Berlin, 1987.

[30] A. Manning, *Topological entropy for geodesic flows*, **Ann. of Math. (2)**, 110:567–573, 1979.

[31] S. Mardešić and J. Segal, **Shape theory: The inverse system approach**, North-Holland Math. Library, Vol. 26, North-Holland Publishing Co., Amsterdam, 1982.

[32] S. Mardešić, *Absolute neighborhood retracts and shape theory*, in **History of topology**, pages 241–269, North-Holland Publishing Co., Amsterdam, 1999.

[33] S. Matsumoto, *Kuperberg's* C^∞ *counterexample to the Seifert conjecture*, **Sūgaku**, Mathematical Society of Japan, 47:38–45, 1995. Translation: **Sugaku Expositions**, 11:39–49, 1998, Amer. Math. Soc.

[34] S. Matsumoto, *The unique ergodicity of equicontinuous laminations*, **Hokkaido Math. J.**, 39:389–403, 2010.

[35] D.R. McMillan, Jr., *One-dimensional shape properties and three-manifolds*, in **Studies in topology (Proc. Conf., Univ. North Carolina, Charlotte, N.C.)**, pages 367–381, Academic Press, New York, 1975.

[36] J. Milnor, *Curvature and growth of the fundamental group*, **Jour. Differential Geom.**, 2:1–7, 1968.

[37] C.C. Moore and C. Schochet, **Analysis on Foliated Spaces**, Math. Sci. Res. Inst. Publ. vol. 9, Second Edition, Cambridge University Press, New York, 2006.

[38] K. Morita, *On shapes of topological spaces*, **Fund. Math.**, 86:251–259, 1975.

[39] P.B. Percell and F.W. Wilson, Jr., *Plugging flows*, **Trans. Amer. Math. Soc.**, 233:93–103, 1977.

[40] J. Plante, *Foliations with measure-preserving holonomy*, **Ann. of Math.**, 102:327–361, 1975.

[41] A. Rechtman, *Pièges dans la théorie des feuilletages: exemples et contre-exemples*, **Thèse**, l'Université de Lyon – École Normale Supérieure de Lyon, 2009.

[42] D. Ruelle, *An inequality for the entropy of differentiable maps*, **Bol. Soc. Brasil. Mat.**, 9:83–87, 1978.

[43] P.A. Schweitzer, *Counterexamples to the Seifert conjecture and opening closed leaves of foliations*, **Ann. of Math. (2)**, 100:386–400, 1974.
[44] H. Seifert, *Closed integral curves in* 3*-space and isotopic two-dimensional deformations*, **Proc. Amer. Math. Soc.**, 1:287–302, 1950.
[45] L. Siebenmann, *Le paradigm du serpent: explique les contre-exemples de K. Kuperberg à la conjecture de Seifert*, manuscript privée, décembre, 1997.
[46] P. Šindelářová, *An example on movable approximations of a minimal set in a continuous flow*, **Topology Appl.**, 154:1097–1106, 2007.
[47] D. Sullivan, *A counterexample to the periodic orbit conjecture*, **Inst. Hautes Études Sci. Publ. Math.**, 46:5–14, 1976.
[48] P. Walczak, **Dynamics of foliations, groups and pseudogroups**, Instytut Matematyczny Polskiej Akademii Nauk. Monografie Matematyczne (New Series) [Mathematics Institute of the Polish Academy of Sciences. Mathematical Monographs (New Series)], Vol. 64. Birkhäuser Verlag, Basel, 2004.
[49] P. Walters, **An Introduction to Ergodic Theory**, Graduate Texts in Math. Vol. 79, Springer-Verlag, New York, 1982.
[50] F.W. Wilson, Jr., *On the minimal sets of non-singular vector fields*, **Ann. of Math. (2)**, 84:529–536, 1966.

Steven Hurder, Department of Mathematics, University of Illinois at Chicago, 322 SEO (m/c 249), 851 S. Morgan Street, Chicago, IL 60607-7045

E-mail address: hurder@uic.edu

Ana Rechtman, Institut de Recherche Mathématique Avancée, Université de Strasbourg, 7 rue René Descartes, 67084 Strasbourg, France

E-mail address: rechtman@math.unistra.fr